Efficient Modeling Strategies for Performance-based Building Design Supported by Daylight and Building Energy Simulations

By

Luis Filipe Batista Silveira Dos Santos

A dissertation submitted in partial satisfaction of the

requirements for the degree of

Doctor of Philosophy

in

Architecture

in the

Graduate Division

of the

University of California, Berkeley

Committee in charge:

Professor Luisa Caldas, Chair
Professor Simon Schleicher
Professor Carlo Sequin

Summer 2020

Abstract

Efficient Modeling Strategies for Performance-based Building Design Supported by Daylight and Building Energy Simulations

By

Luis Filipe Batista Silveira Dos Santos

Doctor of Philosophy in Architecture

University of California, Berkeley

Professor Luisa Caldas, Chair

The resources involved in the construction and operation of buildings represent nearly 40% of the global emissions of greenhouse gases (GHG), making the building sector one of the primary contributors to global warming. This reality has led to the creation of many prescriptive regulatory and voluntary programs that aim to mitigate the environmental impact of the building sector while ensuring high standards for Indoor Environmental Quality (IEQ), particularly those regarding the thermal and visual comfort of building occupants. Thus, the design of high-performance buildings, i.e., resource- and energy-efficient buildings that yield high levels of IEQ, is a pressing need. This scenario pushes architects to simulate their projects' environmental performance to better support design tasks in a process referred to as *performance-based design*.

This dissertation studies the integration of daylighting and Building Energy Simulation (BES) tools into performance-based design supported by computational design (CD) methods, particularly parametric design and Building Performance Optimization (BPO). The assumption is that the early integration of parametric, BES, and daylighting simulation tools can be highly effective in the design, analysis, and optimization of high-performance buildings.

However, the research argues that the current daylighting and Building Energy Simulation (BES) tools pose critical challenges to that desirable integration, thus hindering the deployment of efficient exploratory design methods such as Parametric Design and Analysis (PDA) and BPO. These challenges arise from limitations regarding (i) tool interoperability, (ii) computationally expensive simulation processes, and (iii) problem and performance goal definition in BPO.

The primary objective of the dissertation is to improve the use of daylighting and BES tools in PDA and BPO. To that end, the research proposes and validates five modeling strategies that directly tackle the limitations mentioned above. The strategies are the following: (i) Strategy A: *Automatically generate valid building geometry for BES*; (ii) Strategy B: *Automatically simplify building geometry for BES*; (iii) Strategy C: *Abstract Complex Fenestration Systems (CFS) for BES*; (iv) Strategy D: *Assess glare potential of indoor spaces using a time and spatial sampling technique*; and (v) Strategy E: *Painting with Light - a novel method for spatially specifying*

daylight goals in BPO.

The research work shows that the strategies address the research problem and current limitations by (i) improving the interoperability between design and BES and daylighting simulation tools (Strategies A, B, and C); (ii) producing quick and adequate feedback on the daylight, thermal, and energy behavior of buildings (Strategies B, C, and D); and (iii) facilitating the spatial definition of performance goals in daylighting BPO workflows (Strategy E). These three important merits of the proposed strategies effectively contribute to improving the efficiency of using daylight and BES tools in the design, analysis, and optimization of high-performance buildings.

Strategies A, B, and C enable the automatic generation of efficient Building Energy Models (BEMs). Strategy A uses advanced planarization techniques to parse any complex curved or double-curved building envelope for EnergyPlus, a state-of-the-art BES. In order to improve calculation times and thus performance feedback, Strategy B simplifies the models generated by Strategy A. The resulting simplified BEMs run significantly faster than equivalent standard BEMs without compromising the quality of simulation output. Strategy C combines co-simulation and linear regression techniques to generate BEM surrogates of sophisticated façade systems, which are easily designed with parametric approaches. The resulting surrogates run quickly and are useful for year-based building energy analysis.

Strategy D provides an alternative method to initial visual comfort studies by reducing the use of computationally expensive simulations required by some building standards (e.g., EN 170377 – Daylight in Buildings). The strategy utilizes easier-to-compute daylight metrics to spatially assess glare potential and identify worst-case scenarios in order to conduct detailed point-in-time glare simulations.

Strategy E implements a painting-style interface that helps designers to spatially specify daylight goals in indoor spaces. Hence, the strategy (i) reduces the difficulty of defining the daylight optimization (or design) problem, (ii) expands the generative potential of goal-oriented design procedures for daylighting design, and (iii) mitigates the gap between standard optimization approaches used in inverse-design and common methods applied in architectural design.

Finally, the dissertation discusses the merits and limitations of each strategy, provides useful guidelines and recommendations for their use in building design, and suggests future directions for further research.

Contents

List of Figures

List of Tables

List of Acronyms

ACO	Ant Colony Optimization
ACH	Air Changes per Hour
aDPG	Annual Daylight Glare Probability
AEC	Architectural, Engineering, and Construction
AIE	Acceptable Illuminance Extent
ANN	Artificial Neural Networks
API	Application Programming Interface
ASE	Annual Sun Exposure
ASHRAE	American Society of Heating, Refrigeration, and Air-Conditioning Engineers
AZ	Arizona
BEM	Building Energy Model
BES	Building Energy Simulation
BIM	Building Information Modeling
BPO	Building Performance Optimization
BPS	Building Performance Simulation
BR	Bass Ratio
BRE	British Building Research Establishment
BREEAM	Building Research Establishment Environment Assessment Methodology
BSDF	Bidirectional Scattering Distribution Functions
CA	California
CAD	Computer Aided-Design
CAMMOE	CAD-centric Attribution Methodology for Multidisciplinary Optimization Environments
CBDM	Climate-based Daylight Modeling
CBECS	U.S. Department of Energy Commercial Buildings Energy Consumption Survey
CD	Computational Design
C_{ds}	Coefficient Matrix for Direct Sun
CFD	Computational Fluid Dynamics
CFS	Complex Fenestration System
CIBSE	Chartered Institute Building Services Engineers
CIE	Commission Internationale de l'Éclairage
COP	Coefficient of Performance
CPU	Central Processing Unit
CTF	Conduction Transfer Functions
CVRMSE	Coefficient of Variation of the Root Mean Square Error
D	Daylight Matrix
DC	Daylight Coefficient
DD	Digital Design
DF	Daylight Factor
DGI	Discomfort Glare Index
DGP	Daylight Glare Probability
DIR	Design Inclusive Research
DoE	Design of Experiments

DSM	Daylight Simulation Models
E	Illuminance
EA	Evolutionary Algorithm
ECM	Energy Conservation Measures
eDGPs	Enhanced Simplified Discomfort Glare Probability
EDT	Early Decay Time
E_h	Horizontal Illuminance
EN	European Norm
ERC	Externally Reflected Light
EUI	Energy Use Intensity
E_V	Vertical Eye Illuminance
$E_{V,Thr}$	Vertical Eye Illuminance Threshold
FAR	Floor Area Ratios
FDM	Finite Difference Method
FN	False-Negative
FOV	Field-of-View
FP	False-Positive
FVM	Finite Volume Method
GA	Genetic Algorithm(s)
gbXML	Green Building Extensible Markup Language
GD	Generative Design
GDS	Generative Design System
GHG	Green House Gases
GIS	Graphical Information Systems
GUI	Graphical User Interface
HDR	High Dynamic Range
HJ	Hooke Jeeves
HM	Harmony Memory
HOY	Hour-of-the-Year
HS	Harmony Search
HVAC	Heating, Ventilation, and Air Conditioning
IACC	Interaural Cross-correlation Coefficient
ICD/ITKE	Institute for Computational Design/Institute of Building Structures and Structural Design
IDA	Iterative Design and Analysis
IDE	Integrated Development Environment
IDM	Integrated Dynamic Model
IEQ	Indoor Environmental Quality
IESNA	Illuminating Engineering Society of North America
IFC	Industry Foundation Classes
ILAS	Ideal Load Air Zone System
IP	Inch-Pound System of Units
IPCC	Intergovernmental Panel on Climate Change
IRC	Internally Reflected Light
KRM	Krigging Regression Models
L	Luminance

LA	Los Angeles
LBNL	Lawrence Berkeley National Laboratory
LCA	Life Cycle Analysis
LCC	Life Cycle Cost
LEED	Leadership in Energy and Environmental Design
LPM	Lumped Parameter Models
LR	Linear Regression
LRCFS	Light Redirecting Complex Fenestration System
MA	Massachusetts
MARS	Multivariate Adaptive Regression Splines
MDO	Multidisciplinary Design Optimization
MGF	Material and Geometry Format
MIS	Multiple Importance Sampling
ML	Machine Learning
MLR	Multiple Linear Regression
MOO	Multiple-objective Optimization
MOPA	Multi-objective Parametric Analysis
NFRC	National Fenestration Rating Council
NMBE	Normalized Mean Bias Error
NSGA-II	Non-dominated Sorting Genetic Algorithm - II
NURBS	Non-Uniform Ratio Basis Spline
NZEB	Net-Zero Energy Buildings
OLS	Ordinary Least Squares
OR	Operations Research
PD	Parametric Design
PDA	Parametric Design and Analysis
PGD	Performance-based Generative Design
PGDS	Performance-based Generative Design System
POV	Point-of-View
PSO	Particle Swarm Optimization
PSOC/HJ	Particle Swarm Optimization Constriction/Hooke Jeeves
PSO-HJ	Particle Swarm Optimization and Hooke Jeeves algorithm
PSOIW	Particle Swarm Optimization using Inertia Weight
PT	Path Tracing
R^2	Coefficient of Determination
R^2adj	Adjusted Coefficient of Determination
RBF	Radial-basis Function
RF	Response Factors
RMSE	Root Mean Square Error
RPBW	Renzo Piano Building Workshop
RTS	Radiant Time Series
S	Sky Matrix
SA	Simulated Annealing
SAEO	Simplex Algorithm of Nelder and Mead with the Extension of O'Neill
SC	Sky Component
sDA	Spatial Daylight Illuminance

SGA	Standard Genetic Algorithm
SHGC	Solar Heat Gain Coefficient
SI	International System of Units
SNN	Sigmoidal Neural Networks
SOO	Single-objective Optimization
SPEA2	Strength Pareto Evolutionary Algorithm 2
SR	Solar Radiation
SSE	Sum of Squares Error
SST	Total Sum of Squares
S_{sun}	Sun Matrix
sUDI	Spatial Useful Daylight Illuminance
SVM	Support Vector Machines
T	Transmission Matrox
TFM	Transfer Function Methods
TMY	Typical Meteorological Year
TS	Tabu Search
UDI	Useful Daylight Illuminance
UK	United Kingdom
UN	United Nations
V	View Matrix
VAV	Variable Air Volume
VLT	Visual Light Transmittance
VPL	Visual Programming Language
VR	Virtual Reality
WWR	Window-to-Wall-Ratio
XML	Extensible Markup Language
XPS	Extruded Polystyrene
ε	Sky Brightness Index

Acknowledgments

If anyone asks me what I took from my Ph.D. journey at Berkeley, I will reply that aside from the academic expertise, the most important were the people I have met. In a sense, Berkeley was my own "Temple of Apollo" since it provided me relevant insights on the old Delphic teaching: *"Gnōthi seauton,"* i.e., *know thy measure*. Collaborating with my mentors and colleagues heightened my sense of self-criticism and taught me the importance of continuously asking questions. Honestly, I *"never walked alone"* in my doctoral journey and this dissertation would not have been possible without the countless interactions that I had with so many brilliant people.

First and foremost, I would like to thank my advisor and mentor, Professor Luisa Caldas, for believing in me. She was the main responsible for my admission to Berkeley. If it wasn't for her support and endorsement, I would likely miss the opportunity to do a Ph.D. in such a thriving intellectual environment. My enthusiasm for research and teaching developed from my interaction with her. She has taught me about intellectual rigor, method, preparedness, and clarity both in research and teaching. Professor Luisa's incredible capacity to bridge and connect different areas of knowledge will always be an inspiration for me. I am most thankful to her for always pushing me to do and be better, and for providing insightful suggestions when I struggled.

I am also thankful to Professor Simon Schleicher for the enthusiasm, precious suggestions, and brainstorming sessions. From him, I re-learned the value of sketching and diagramming as essential exploratory and synthesis research tools. I will miss our sessions where we would sketch and debate "crazy hypotheses" over trace paper.

I am grateful to Professor Carlo Sequin for being always available and for making the hardest and most critical questions. Our discussions taught me about the importance of framing and synthesizing any research endeavor to its essence.

I was also fortunate to work and learn from Professor Susan Ubbelohde. My interaction with Professor Susan expanded my knowledge about architecture, daylight, and energy in buildings. The time that I spent in her firm (Loisos+Ubbelohde) and the interactions I had there with several designers and consultants were crucial in understanding what it takes to bridge academia and the world of design practice.

A special thanks to Professor Brendon Levitt. From him, I have learned the value of communication in design, building performance analysis, and teaching.

To Professor António Leitão, a very special thanks. First, for being always available; second, for being both a fantastic mentor and friend; and third, for the enthusiasm and patience in several research joint ventures. I would like also to thank the several elements of Professor António Leitão research group in INESC-ID, Algorithmic Design for Architecture (ADA), with whom I was so fortunate to work during the course of my doctoral endeavor – Inês Caetano, Inês Pereira, Catarina Belém, and Renata Castelo-Branco.

The support from Pinto-Fialon Scholarships and the Portuguese Studies Program has been essential for my success. I would like to thank Professor Deolinda Adão for all the help, availability, and hard work in assisting Portuguese students at UC Berkeley. With her and Duarte

Pinheiro, I had the privilege to participate in a symposium about art, architecture, and literature that focused on tracing cultural similarities between the Bay Area and Lisbon.

I was fortunate to share my journey with outstanding colleagues, including both Master of Science and Ph.D. students. It is impossible to measure how much I have learned and grew with Antony Kim, Carlos Duarte, Won Hee Ko, Gabriela Vasconcellos, Mohammad Keshavarzi, Jonathan Wolley, Dana Miller, Megan Dawes, Caroline Karmann, Arfa Aijazi, Benjamim Taube, and Valerie Green.

I am also very thankful to the Center for the Built Environment (CBE), including Professors Stefano Schiavon, Gail Brager, and Ed Arens for all the encouragement, and for inviting me to present part of my work in one of the CBE advisory board meetings. Thanks to Patricia Brennecke for all the help.

During my Ph.D. I have found a second family that provided me a strong emotional support and to whom I am forever thankful. To Miguel Heleno, I am immensely grateful for his genuine friendship, advice, and collaboration with the microgrid group at Lawrence Berkeley Lab. From him, I have learned the value of being pragmatic in research, something that I still need to work on. To Catarina Gama for being such a great friend, roommate, and supportive in all difficult moments. The luxury of having a person that everyday listens to you is priceless. To Ana and Cory for all the encouragement, help, laughs, adventures, and friendship. To Osni Marques for all the moments together and culinary experiences. To Elói Pereira for all the conversations, advice, and camaraderie. To Laura Brennan for helping me at the beginning and for being an amazing friend and roommate. To Maria Coelho for all the help in finding a place to live. To Gonçalo Rodrigues for his kindness. To Carlos Oliveira for the trips, musical moments, and for introducing most of the friends that I mentioned. To the Abreu family for “adopting” all of us.

I cannot properly put into words all the love and encouragement of my mother, brothers, and close family, and how hard it was to them (and me) to seldom see me during my doctoral efforts. Finally, I am deeply thankful to my partner, Inês Reis, for fully supporting me in every step of this academic adventure at the shores of a different ocean. Her infinite patience, love, resiliency, care, and motivation were the fuel that pushed me forward.

Institutional acknowledgments

The research work presented in this dissertation was partially supported by the Ph.D. scholarship SFRH/BD//98658/2013, funded by Fundação para a Ciência e a Tecnologia (FCT), Portugal.

Chapter 1:
Introduction

This dissertation studies the integration of whole-building energy and daylighting simulation into architectural design processes supported by computational design methods, particularly parametric design and building performance optimization. The research develops new modeling methods that improve the use of current simulation techniques in the design of resource- and energy-efficient buildings, thus contributing to a more sustainable built environment. This chapter introduces such research by presenting a general overview of the work, its context, objectives, approach, and structure.

Section 1.1 presents the context, relevance, and challenges of designing energy-efficient buildings that are simultaneously thermally and visually comfortable (for a detailed overview of the state-of-the-art, please refer to chapter 2). Section 1.2 then presents the general problem, which is further developed in chapter 3. The general intention, research question, and hypothesis are stated in section 1.3. Section 1.4 presents the research objective. Section 1.5 summarizes the research methodology used in the dissertation. The research methodology and methods are further described in chapter 4. An overview of the contents of the dissertation is presented in section 1.6. Section 1.7 defines key terms used throughout the dissertation. Section 1.8 describes the different means of research dissemination, including scientific contributions, lectures, and workshops based on the investigation conducted in this dissertation. Lastly, section 1.9 presents the awards given to the dissertation research.

1.1 Context, relevance, and challenges

Currently, the demand for energy-efficient, sustainable, *green buildings* is no longer a "trendy" topic but a civilizational necessity. As demonstrated in Abergel et al. (2018), the resources involved in the construction and operation of buildings represent nearly 40% of the global emissions of greenhouse gases (GHG). The emissions caused solely by operating buildings correspond to 28%. The GHG emissions caused by operation primarily consist of using energy in ventilating, cooling, heating, and lighting buildings to ensure a good *indoor environmental quality* (IEQ).

The GHG emissions associated with the building sector make it a critical sector in energy and environmental policy. The last synthesis report of the Intergovernmental Panel on Climate Change (IPCC) clearly states that the building sector is strategic in mitigating GHG emissions (Pachauri et al., 2014). This finding led to the creation and reinforcement of many prescriptive regulatory and voluntary programs to mitigate the environmental impact of the building sector, including national or state building regulations (e.g., California's Title 24), the Building Research Establishment Environment Assessment Methodology (BREEAM), the Living Building Challenge standard (Challenge, 2016), and the Leadership in Energy and Environmental Design (LEED) (USGBC, 2013) building rating system. These programs fostered not only the idea of energy efficiency but also the qualification of buildings in terms of IEQ.

IEQ factors and energy use in a building are strongly correlated. Thermal comfort is one of the main drivers for active heating and cooling of buildings. The demand for mechanically assisted

ventilation in some buildings also requires the use of energy, and the need for adequately lit and visual comfortable spaces affects both shading and lighting in buildings, thus affecting thermal and electric building loads. Despite the interdependence between IEQ and energy use, the deployment of energy conservation measures (ECM) demonstrates that it is possible to simultaneously minimize energy consumption and improve IEQ. Ensuring high IEQ levels in buildings is also essential to generating healthy indoor environments, which, in the case of commercial buildings, are correlated with an increase of building occupant productivity. To that end, several additions to voluntary building rating systems (e.g., LEED), along with standards and norms have been implemented, including WELL building standard (Living LLC, 2013), and the European Norm (EN) 17037 – Daylight in Buildings (CEN, 2019).

The need of designing and operating energy-efficient buildings that provide occupant comfort and a healthy indoor environment has never been more relevant. Early consideration of environmental factors in building design leads to benefits in energy use, GHG reduction, occupant health, and building occupant productivity (Huang and Niu, 2016). The design of resource- and energy-efficient buildings is essential in the global effort to mitigate global warming and ensure a sustainable future for human societies.

This context, driven by the current environmental crisis, is pushing architects to assess the environmental performance of their projects early in the design process as a way to steer the process towards comfortable and energy-efficient building designs. This method of evaluating building performance to support the design process is referred to as *performance-based design* (Oxman, 2008). When applied to environmental performance, performance-based design integrates factors in the following categories: (i) thermal, (ii) visual (light), (iii) air quality, and (iv) acoustics. This dissertation addresses the thermal and visual aspects because they directly affect energy use and GHG emissions of buildings.

Building Performance Simulation (BPS) is essential to performance-based design. BPS is the process of predicting, quantifying, and assessing the performance of a building or a building design, usually through computer simulation. BPS of energy-related phenomena involves solar, thermal, daylight, and airflow modeling and concerns the form, materials, and building systems (e.g., Heating, Ventilation, and Air Conditioning machinery and controls) (Clarke, 2001).

From the several computational tools used to predict thermal-related phenomena, energy use, and daylight in buildings, the dissertation uses EnergyPlus (Crawley et al., 2001) and Radiance (Ward, 1994, 2004b). Radiance and EnergyPlus are state-of-the-art open-source tools for light and whole-building energy simulation, respectively. Both tools are modular, thus often updated and extended, and their reliability has been tested and validated in several studies (Reinhart and Andersen, 2006; Crawley et al., 2008; Tabares-Velasco, Christensen and Bianchi, 2012; McNeil and Lee, 2013; Zhou, Hong and Yan, 2014).

Computer applications such as OpenStudio (Guglielmetti, Macumber and Long, 2011), Ladybug+Honeybee (Roudsari, Pak and Smith, 2013; Mackey et al., 2015), DIVA + Archsim (Jakubiec and Reinhart, 2011) interface EnergyPlus and Radiance with digital design tools, particularly with Computer-based Aided Design (CAD), Building Information Modeling (BIM) programs, and some domain-specific languages that support algorithmic interaction with CAD and BIM programs (e.g., Grasshopper, GHPython, and Dynamo). Those interfaces between design

tools and simulation software largely contribute to the increasing use of daylighting and whole-building energy simulation in building design processes.

Despite the current progress in building standards, regulations, and analysis tools for sustainable design, the report of Abergel et al. (2019) demonstrates that the sector is not on track with the targets set by the Paris Agreement and the United Nations (UN) Sustainable Developments Goals. The report shows an unfavorable evolution of final energy use in buildings and associated GHG emissions: both are increasing instead of decreasing. Although the reasons for this are complex and multivariate, it is reasonable to question whether simulation-based approaches have been adequately used in the design of a more sustainable built environment.

Even with the support of computer simulation, assessing the thermal and daylight performance of a building design is a non-trivial task. Typically, it involves a considerable number of variables with different parameters that often exert conflicting influences. This complexity hinders a direct approach in which the building designer or energy-analyst uses a model-simulate-evaluate loop to iteratively improve the performance of a design candidate. While of potentially significant value to project teams, this iterative process is prohibitively time-consuming, tiresome, and unproductive. The degree of effectiveness of using such a process depends heavily on the designer's knowledge of the problem and expertise with the tools. Even highly qualified building performance analysts have problems using BPS for the following reasons: (i) setting simulations is a tiresome process that is prone to human error, (ii) simulation output is typically highly susceptible to input error, and (iii) specific simulations might be computationally expensive (i.e., slow to run). Considering that most architects and building designers use the standard generate-and-evaluation iterative approach, it is possible to argue that the standard use of simulation as ancillary processes in building design is inefficient and often results in suboptimal designs.

The automation of the generation and evaluation process can mitigate some of the challenges posed by the standard iterative use of simulation in the design of sustainable buildings. Two computational design processes facilitate such automation: *Parametric Design and Analysis* (PDA), and *Building Performance Optimization* (BPO). PDA automates the simulation of several building variations by manipulating a parametric description of a design that is able to generate a wide range of instances. In PDA workflows, the designer can assess and compare a plethora of different design instances and perform a sensitivity analysis to find the key design parameters of specific building performance problems. By facilitating feedback into design workflows, PDA better supports decision making in architectural processes. By automating the search procedure, BPO goes even further in supporting decisions in design. Typically, BPO workflows combine BPS tools, optimization algorithms, and parametric simulation models to automatically search for high performing candidates. The computational tools that combine BPS tools and optimization algorithms to implement BPO methods are called *Performance-driven Generative Design Systems* (PGDS) (Shea, Aish and Gourtovaia, 2005; Caldas, 2008; Oxman, 2008). PGDS supports a method called *goal-oriented design*, in which the design process is inverted: the design problem is defined along with performance goals, and then an optimization algorithm automatically searches the design space for solutions whose performance is close to the pre-defined, user-supplied goals (Monks, Oh and Dorsey, 2000). Chapter 2, section 2.3, provides more details about the integration of simulation tools in performance-based building design, particularly into workflows supported by PDA and BPO/PGDS approaches.

Although PGDS use optimization algorithms to search large design spaces more efficiently, in the case of multi-criteria optimization problems it is often difficult to ensure the finding of optimal solutions or trade-offs. This limitation is primarily caused by the nature of building optimization problems, which in most cases forces the use of optimization approaches supported by heuristic and stochastic processes (for more detail on optimization in performance-based design, please refer to chapter 2, section 2.3.2). Thus, this dissertation considers optimization as the process by which an automatic improvement in building performance is obtained, under certain assumptions and in comparison with an initial base-case.

The BPO search approach is more effective than PDA since it requires both a detailed description of the building performance design problem and the definition of well-defined performance goals to steer the search. By limiting the user's participation in the search process, PGDSs are less prone to bias but also less interactive. Although PDA exploratory processes are less efficient, they enable more user control than PGDS.

Although PDA and BPO promise to effectively support architects in designing high-performance buildings in terms of energy use and IEQ, they are seldom used in practice (Attia et al., 2013; Shi et al., 2016; W. Tian et al., 2018). Thus, the contribution of such approaches in simultaneously reducing building energy use, and consequently GHG emissions, and ensuring high levels of IEQ is still limited.

This dissertation discusses the application, use, and problems of daylighting and whole-building energy simulations in PDA and PGDS workflows. The dissertation argues that current simulation techniques pose critical challenges that hinder an effective deployment of parametric and optimization approaches in the design of energy-efficient, properly daylit, and comfortable buildings. The following section summarizes the general research problem addressed by the investigation.

1.2 General problem

Despite the benefits of using current daylight and *Building Energy Simulation* (BES) to support building design processes, several obstacles prevent their smooth integration into current PDA and BPO workflows. In order to facilitate the deployment of PDA and BPO approaches in performance-based design further research is needed to address such limitations. The general problem of integrating BES and daylight simulation in current computational building design practices can be articulated as follows:

> ***It is difficult to simultaneously use design, whole-building energy, and daylighting simulation tools to study crucial aspects related to the energy, thermal, and daylight performance of buildings. This limitation hampers their deployment and integration in the early phases of building design, analysis, and performance optimization.***

Daylight and whole-building energy simulation feedback is essential in the early phases of building design. The data produced by such simulations supports the design team to examine the following critical aspects: (i) orientation and solar exposure, (ii) overall building form, which determines the building heat loss form-factor (i.e., the ratio between the building's envelope are and its net floor area), (iii) glazing area per orientation, (iv) shading factor and shading types per orientation, (v)

the effectiveness of natural ventilation, (vi) the benefits of a lightweight construction versus a heavyweight construction that provides thermal mass, and most important (vii) the interplay of all of these factors in the environmental performance of buildings. Typically, decisions regarding these aspects occur early in the design process and have a critical impact on the daylight and energy performance of buildings. A poor decision in any of those building parameters is difficult to remedy at later phases and results in additional costs to all stakeholders involved in the process. Moreover, the different building design phases are not "isolated" from each other and admit some overlap. It is common for architects to study specific building details at early design stages, mainly if such details contribute to the overall aesthetic quality of the building. For example, early analyses can help determining the level of permeability of a sophisticated building skin according to solar exposure and self-shading (see chapter 5, section 5.5).

Additionally, early assessments also provide useful information for later design phases (see chapter 6). For example, the early mapping of glare potential in a room can help determine the position, shape, and size of windows in early design phases and the layout of furniture at later ones. Thus, the early integration of daylight and building energy simulation tools in the design process is desirable.

Nevertheless, three types of limitations hinder an efficient use of daylight and BES tools in computational building design practices. The following briefly summarizes them. For more detail about the research problem, related obstacles, causes, and repercussions, please refer to chapter 3, particularly to section 3.3.

Interoperability and data exchange problems between the different tools used in the design and analysis of sustainable buildings constitute the first primary limitation type (Attia et al., 2013; Jones et al., 2013; Negendahl, 2015; Choi and Park, 2016; Dogan, Reinhart and Michalatos, 2016). Fundamental differences in modeling capabilities between design, BES, and daylight simulation programs create a tool "gap" that frustrates architects in the design and optimization of energy-efficient and comfortable buildings. The required mastery of all the tools and modeling procedures involved in the design process demands a high degree of modeling expertise. Moreover, the difference between analysis and design tools also forces architects to switch between different modeling environments or "modes," which often entails redundant tasks that are prone to error (Bazjanac et al., 2011; Attia et al., 2013; Picco, Lollini and Marengo, 2014). The current limitations in integrating simulation and design tools at early design stages are particularly evident in the analysis of complex building forms, particularly those that entail either curved or double-curved surfaces, e.g., free-form buildings (Kovacic et al., 2013; Picco, Lollini and Marengo, 2014; Cemesova, Hopfe and Mcleod, 2015; Chatzivasileiadi, Lila, et al., 2018).

The second kind of obstacle includes limitations related to thermal, energy, and daylight simulation of buildings. These limitations hinder current simulation-based workflows from providing helpful feedback to design processes in useful time (Chatzivasileiadi, Lila, et al., 2018; Jones, Greenberg and Pratt, 2012; Nathaniel L Jones and Reinhart, 2015; Picco and Marengo, 2015; Zuo and Chen, 2010). Simplifying complex simulation models and efficiently using available analysis resources are essential tasks for developing effective simulation workflows that provide quick analyses and adequate building performance information. However, there are few guidelines that help designers to conduct such tasks. Even when specific standards (e.g., EN 17037 – Daylight in Buildings) define modeling recommendations, such guidelines often entail the use of advanced simulations

that not only require a considerable degree of expertise but are also computationally expensive. The lack of guidelines for simplifying simulation workflow hinders the desirable utilization of useful analysis (e.g., glare) at the early stage of building design, thus limiting the potential benefits of using them in design processes.

The third main obstacle consists of adequately defining building performance goals in BPO workflows. Current methods of defining feasible objectives in BPO are non-trivial, particularly to non-experts in optimization such as architects. Planning and defining decision variables, constraint violation, and particularly performance objective arrangement requires a set of unfamiliar techniques to designers (Attia et al., 2013; Shi et al., 2016; W. Tian et al., 2018; Si et al., 2019). The gap between standard design approaches and PGDS has often led designers to poorly define the optimization problem, thus affecting PGDS outcomes. This scenario leads to an unfounded skepticism among designers about optimization results and the usefulness of using PGDS approaches. Additionally, common methods used to define performance goals in BPO fail to adequately capture spatial performance variation, a relevant aspect in daylighting design.

1.3 General intention, research question, and hypothesis

The overall intention of the dissertation is to contribute to the improvement of the design process of high-performance buildings that simultaneously are energy-efficient and yield high IEQ standards, particularly in terms of thermal and visual comfort. Thus, the dissertation aims to answer the following general research question:

> ***How can we improve the design process of high-performance buildings using current digital design and analysis tools?***

The dissertation assumes that the early assessment of the thermal and daylight performance of building designs contributes positively to the deployment of energy-efficient and sustainable architecture. In the Architectural, Engineering, and Construction (AEC) community, it is widely accepted that the use of whole-building energy simulation tools in design is effective in providing support to decision-making processes. The use of simulation has a high potential to successfully inform and steer design processes, thus reducing the likelihood of making poor early decisions in design that are harder or even impossible to correct later (Picco, Lollini and Marengo, 2014).

The dissertation hypothesizes that a better integration of validated BES and daylight analysis tools in PDA and PGDS is critical to improving the use of simulation-driven processes at early-design phases. Facilitating the early use of BES and daylight simulations enables architects to better decide over critical building environmental performance aspects that are difficult (or even impossible) to correct at later stages. As mentioned in section 1.2, design teams can use simulation to examine aspects related to building orientation, form and envelope, materiality, and the articulation of different passive design strategies (e.g., shading, natural ventilation, thermal mass). The early use of simulation also produces useful information for later stages of the design process, thus promoting a smoother transition between the different phases of performance-based building design supported by PDA and PGDS approaches.

The desirable integration of daylighting and BES tools in PDA and PGDS should facilitate modeling tasks, handle all building forms, and provide quick performance feedback either in parametric-based studies or in BPO workflows. The research hypothesis is as follows:

> ***The early integration of parametric, thermal, and daylight simulation tools is highly effective in the design, analysis, and optimization of high-performance buildings if it promotes model interoperability and provides performance feedback in useful time, regardless of the formal complexity of the design***.

1.4 Research objective

The overarching objective of this work is to improve current computational design methods used in the digital design of high-performance buildings, particularly in the early analysis and optimization of their daylight, thermal, and energy performance. The research aims to develop novel approaches that facilitate the use of simulation-driven processes supported by available software in parametric and generative design workflows. Thus, the purpose is neither to develop nor rewrite existing software. The primary goal is to propose and develop new approaches that both extend and improve the use of state-of-the-art, validated, and research-grade daylight and whole-energy simulation tools by architects and other building designers in current digital building design practices.

To achieve the general objective and to be able to investigate the research hypothesis, the dissertation first identifies and discusses the current limitations of using daylight and whole-building energy simulation in the design and optimization of high-performance buildings. It then introduces modeling strategies that aim to overcome the identified limitations and improve the integration of building energy and daylight models in goal-oriented and parametric building design workflows. The following summarizes the research objective:

> ***To devise a set of alternative modeling strategies that improve the use of current thermal and daylight simulation tools in early-stage design workflows based on parametric and building optimization approaches.***

To accomplish this objective, test the research hypothesis, answer the general research question, and address the current gaps and needs found in the literature, the investigation sets three general objectives for the new modeling strategies proposed in this dissertation. These objectives follow:

- *Enable better interoperability between design and simulations.*
- *Generate quick and adequate feedback regarding the energy and daylight performance of buildings at early design stages.*
- *Help architects and other non-experts in BPO to adequately formulate inverse design problems.*

Chapter 3, section 3.4, – *Refining and reframing the main research question and objective* – subdivides the main research question into specific questions that directly address the current limitations found in the literature regarding modeling and analysis processes based on thermal and daylight simulations (see chapter 2 and chapter 3). The resulting research questions support the

refinement of the general objectives set here for the strategies into specific goals and tasks that the proposed modeling approaches must attain. Such concrete goals and research tasks are set in chapter 4, section 4.4, *Modeling Strategies: tackling the main problem and its causes*.

This dissertation presents five modeling strategies for achieving the research goals, labeled from A to E. Strategy A, B, and C focus on improving interoperability between design and BES tools in parametric- and optimization-driven workflows. Strategy B, C, and D aim to generate quick and adequate feedback in design processes based on daylight and whole-building energy simulations. Finally, Strategy E illustrates how to define performance goals in different areas within a spatial structure for inverse-design problems.

In sum, the research entailed in this dissertation aims to formalize new building design analysis methods that contribute to the advancement of the field. As such, the proposed modeling strategies address the research problem and current limitations of using BES and daylight simulation tools in parametric and generative design workflows. Finally, the strategies are open-ended, thus allowing further extension and refinement. The open-ended nature of the work also promotes a broader discussion on challenging current daylight and BES modeling methods in building design.

1.5 General research approach

As discussed in chapter 4 (sections 4.2 and 4.3), the research approach used in this dissertation is based on the framing methodology of *Design Inclusive Research* (DIR) (Horváth, 2007). As such, the investigative tasks performed in this work support multidisciplinary research, integrate knowledge from different disciplines, and aim to generate additional knowledge and methods for problem-solving in building design processes. The adopted methodology used throughout the dissertation is a top-down approach that recursively decomposes the different research challenges into simpler problems that can be tackled by well-defined research tasks. DIR frames the different top-down methodological steps into three phases:

1) Pre-study: this phase defines the research problem and its context and hypothesizes a solution for it. The pre-study phase entails the collection of information about the problem in the form of a literature review, the formulation of a critique that defines current gaps in needs, the specification of focused research questions and objectives, and develops a hypothesis that addresses the gaps that are at the root of the research problem.
2) Design-study: this stage focuses on devising methods and procedures that concretize the hypothesis formulated in the previous phase. It consists of developing and implementing testable prototypes, i.e., the modeling strategies.
3) Post-study: the last phase comprises the testing and validation of the modeling strategy developed and implemented in the design-study step. This phase includes the development of a design-of-experiments (DoE), the production of results, and their analysis and validation. The goal is to discuss the effectiveness of the proposed strategy and identify advantages and limitations.

These methodological steps are applied not only to the entire thesis but to each proposed modeling strategy. Hence, every chapter that presents the modeling strategies has a dedicated literature review section (Related Work), and every strategy has its own set of methods and DoE.

1.6 Outline of the dissertation

The dissertation consists of 8 chapters arranged in three groups: (i) the introductory chapters, (ii) the development and implementation chapters, and (iii) the conclusion chapter. This clustering closely follows the methodological phases described in the previous section.

Chapter 1, 2, 3, and 4 comprise the introductory chapters. Chapter 1, introduces the dissertation by providing an overview of the background of the research, presenting the main research intention, general question, hypothesis, objective, approach, and dissertation structure.

Chapter 2 presents a literature review that provides a detailed background of the topics addressed in this research. The chapter entails two parts. The first focuses on methods and tools used by designers to predict whole-building energy use, thermal performance, and daylighting in indoor spaces. The second gives an overview of the different computational design methods that use BES and daylighting simulations to improve the predicted performance of building designs.

Chapter 3 further develops, contextualizes, and details the current challenges and problems addressed in the dissertation. Based on the information collected and structured in chapter 2, the chapter formulates a critique of the current use of BES and daylighting simulation in PDA and BPO. The discussion entailed in this chapter also refines the primary research question and objective into specific questions and goals that will steer the development and implementation of the proposed modeling strategies.

Chapter 4 discusses in detail the overall research methodology and methods applied in the development of the proposed modeling strategies. The chapter first frames the research methods in the broader context of design research methodologies and then presents the overall structure of the followed methodology and how it relates to the research goals. Finally, it introduces the concept of modeling strategies as methods that address the limitations discussed in chapter 3. The summary of the modeling strategies provided in chapter 4 also relates them to the refined research questions and goals defined in chapter 3.

The development and implementation chapters include chapters 5, 6, and 7. These chapters introduce the five proposed modeling strategies and group them by application type.

Chapter 5 assembles the three modeling strategies that focuses on improving the use of BES in performance-driven building design. They include Strategy A: *Automatically generate valid building geometry for BES*, Strategy B: *Automatically simplify building geometry for BES*, and Strategy C: *Abstract Complex Fenestration Systems (CFS) for BES*. These strategies aim to improve the interoperability between design and analysis tools and feedback in design processes by proposing alternative methods that result in quicker simulations without impairing the quality of simulation output. Because the three strategies are interdependent, the dissertation presents them together and provides a common background.

Chapter 6 presents and discusses Strategy D – *Assess glare potential of indoor spaces using a time and spatial sampling technique*. This strategy aims to better handle advanced daylight simulations that are recently being adopted by norms and daylight standards used in visual comfort assessments (CEN, 2019). Thus, the strategy follows the objective of improving feedback in design by

proposing new analysis methods that help designers to better manage complex simulation techniques at early design phases.

Chapter 7 introduces Strategy E: *Painting with Light – a novel method for spatially specifying daylight goals in Building Performance Optimization (BPO)*. This strategy illustrates the potential for using methods commonly employed by designers to facilitate the definition of BPO problems. The modeling approach also seeks to help designers defining complex building performance targets that comprise temporal and spatial variation, such as daylighting goals.

Finally, chapter 8 constitutes the conclusion chapter of the dissertation. The chapter summarizes the merits and limitations of the proposed strategies, includes guidelines for their use both in practice and in academic research, and presents recommendations for future work.

1.7 Terminology

This section presents a list of essential terms used throughout the dissertation. The purpose is to clearly define and frame them in the scope of this work, facilitate the reading, and promote a better understanding of the several field domain-specific concepts involved in this investigation. The following defines each selected term in alphabetic order.

Building design process:

This term refers to the process of creating a plan that describes a building. Early-stage building design processes refer to the initial parts of the process. After determining the primary building program (i.e., function) in early design stages, the architect spatially arranges its program according to specific spatial requirements. At the initial phases of the building design process, the design team develops several alternatives that also deal with factors other than functional ones, particularly those related to building form and envelope. These factors include orientation, solar incidence, views, daylight, and ventilation, among others.

Building design solution:
A design alternative that is a feasible solution to a specific design brief or problem.

Building Performance Optimization (BPO):
A process that consists of searching for building design solutions with near-optimal performance in a design space (see *design space* definition below). Since the search process is often heuristic-based, it is difficult to ensure that applying BPO will always result in finding optimal solutions. Thus, as previously mentioned, the term *optimal solution* refers to the design solution of improved performance that results from BPO processes under specific boundary conditions. Chapter 2, section 2.3, provides more detail about BPO and its application in the design of high-performance buildings.

Computational Design (CD):
CD is a building design process that takes advantage of the computational capabilities of digital computers (Cagan et al., 2005; Peters, 2013; Humppi, 2015; Oxman, 2017). Thus, it is distinct from digital design (DD) since DD also includes processes that use computers for drafting or other representational issues. Caetano, Santos, and Leitão (2020) specify that CD uses the computational capabilities in design by doing the following:

1) Automating design procedures based on (i) a deduction, i.e., applying a transformation to an element while knowing its outcome (Chokhachian, 2014); (ii) an induction, i.e., extrapolating the required design process to obtain a specific result (Chokhachian, 2014); and (iii) an abstraction, i.e., understanding the essential design features by removing the irrelevant information.
2) Parallelizing design tasks and efficiently managing large amounts of information.
3) Incorporating and propagating changes in a quick and flexible way.
4) Assisting designers in form-finding processes through automated feedback, e.g., mapping simulation results.

For further details about the CD definition the author refers the reader to the ancillary work by Caetano, Santos, and Leitão (2020).

Design space:
The set of all possible feasible building design solutions for a given design brief or problem. Typically, in BPO or parametric building design (see *parametric design* below), the solutions that constitute the design space are the result of the combinatorial interaction of the design variables and input parameters that describe a parametric building model. The dissertation also uses *solution space* as an equivalent term.

High-performance Building:
A high-performance building that simultaneously integrates and optimizes *Energy Conservation Measures* (ECM) with IEQ critical aspects such as thermal and visual comfort. ECM consists primarily of passive design strategies that aim daylight harvesting and the reduction of heating and cooling loads in a building.

Parametric Design (PD):
PD is a process that describes a design symbolically using parameters and, in some cases, rules that constrain and interrelate those parameters (Kolarevic, 2004; Woodbury, 2010; Kensek and Noble, 2014; Marin, Blanchi and Janda, 2015; Yu et al., 2015; Caetano, Santos and Leitão, 2020). The application of PD to building design always entails the modeling of a parametric building model that, through different combinations of its input parameters, is able to generate several instances and variations of the same design. For a complete definition and discussion about PD the author refers the reader to Caetano, Santos, and Leitão (2020).

Performance-based Design:
As defined by Oxman (2008), performance-based design is an approach in which building performance steers the design process. In architecture, performance-based design uses information produced by building simulation to modify architectural form and other design features with the express purpose of improving the performance of a candidate design. In this dissertation, the building performance considerations used to inform design processes result from the thermal, energy, and daylight simulation of buildings.

Performance-based Generative Design Systems (PGDS):
PGDS are computational tools that implement BPO principles. They combine in a single workflow a generative model (e.g., a parametric description of a building), a building simulation program,

and an optimization algorithm to invert typical design workflow in a process called *goal-oriented design* (Monks, Oh and Dorsey, 2000). The inversion of the design workflow consists of first describing the design problem, establishing performance targets, and running the optimization algorithm to search for a solution or solutions that better match the desired performance goals. Chapter 2, section 2.3, further details and describes PGDS.

Strategy:
A set of heuristic modeling procedures developed to facilitate the use and integration of daylight and BES in computational building design workflows. The implementation of a modeling strategy is always a computational tool or workflow.

1.8 Scientific contributions and research dissemination

During the dissertation research project, parts of the work have been published in peer-reviewed scientific journals and the proceedings of international conferences. The author was also invited to present the research work in several public presentations and workshops in architecture and sustainable design consultancy offices. This section summarizes such contributions. Table 1-1 presents the primary list of publications related to the chapters of this dissertation and the modeling strategies proposed in them.

Table 1-1. Relationship between primary scientific contributions, the dissertation chapters, and the proposed modeling strategies. The name of the author is highlighted in bold.

Chapter	Strategy	Publication
5	A	**Santos, L.**, Schleicher, S., Caldas, L. (2017) 'Automation of CAD models to BEM models for performance based goal-oriented design methods,' *Building and Environment*, 112, pp. 144–158. https://doi.org/10.1016/j.buildenv.2016.10.015
	B	**Santos, L**., Schleicher, S., Caldas, L. (2019) 'Automatic Simplification of Complex Building Geometry for Whole-building Energy Simulations,' in *Proceedings of Building Simulation 2019: 16th Conference of IBPSA. Building Simulation 2019: 16th Conference of IBPSA*, Rome, Italy, pp. 2691–2697. https://doi.org/10.26868/25222708.2019.210991
	C	Schleicher, S., **Santos, L.**, Caldas, L. (2018) 'Data-driven shading systems - Application for freeform glass facades,' in *SKINS on Campus. Bridging Industry and Academia in Pursuit of Better Buildings and Urban Habitat. Facades Tectonics 2018 World Congress*, Tectonic Press, Los Angeles, pp. 3–14.

Table continues in the following page

Table 1-1. Relationship between primary scientific contributions, the dissertation chapters, and the proposed modeling strategies. The name of the author is highlighted in bold (continued).

Chapter	Strategy	Publication
6	D	**Santos, L.**, Caldas, L. (2020) 'Assessing the glare potential of side-lit indoor spaces: a simulation-based approach,' *Architectural Science Review.* Taylor & Francis, pp. *1–14*. https://doi.org/10.1080/00038628.2020.1758622 **Santos, L.**, Caldas, L. (2018) 'Assessing the Glare Potential of Complex Fenestration Systems: A Heuristic Approach Based on Spatial and Time Sampling,' in *Passive Low Energy Architecture (PLEA) 2018: Smart and Healthy within the 2-Degree Limit. PLEA 2018*, Hong Kong, pp. 446–451.
7	E	Caldas, L., **Santos, L**. (2016) 'Painting with light: An interactive evolutionary system for daylighting design,' *Building and Environment,* 109, pp. 154–174. https://doi.org/10.1016/j.buildenv.2016.07.023 Caldas, L., **Santos, L.** (2016) 'Painting with Light: A Generative Design System for Daylighting Design,' in *Passive Low Energy Architecture (PLEA) 2016: Cities, Buildings, People: Towards Regenerative Environments. PLEA 2016: 32th International Conference on Passive and Low Energy Architecture*, Los Angeles, CA, pp. 643–639.

Two additional journal papers provided some indirect contributions to this work. Since the main research focus of such publications is tangential to the main research problem addressed by the dissertation, they are not considered primary publications. Table 1-2 presents those papers and contextualizes their contribution to this research work.

Table 1-2. Contributions of ancillary publications to this dissertation. The name of the author is highlighted in bold.

Publication	Contribution
Caetano, I., **Santos, L.**, Leitão, A. (2020) 'Computational design in architecture: Defining parametric, generative, and algorithmic design,' *Frontiers of Architectural Research*, 9, pp. 287–300. https://doi.org/10.1016/j.foar.2019.12.008	The work developed in this article frame the definition of some important domain-specific concepts used in this investigation.
Santos, L., Leitão, A., Caldas, L. (2018) 'A comparison of two light-redirecting fenestration systems using a modified modeling technique for Radiance 3-phase method simulations,' *Solar Energy*, 161, pp. 47–63. https://doi.org/10.1016/j.solener.2017.12.020	Part of the experimental setting of this research and results supported some research tasks performed in chapter 6.

Additionally, the author was invited to present different parts of the work in public lectures in several institutions and offices, and conduct a workshop in an architectural office about certain methods proposed in this work. The following lists such presentations and workshops.

20/6/2019 *Improving the use of building energy simulation in architectural design practice*, in Aarhus University, School of Architecture, Denmark.

3/5/2019 *Parametric Modeling for Sustainable Design Optimization*, in Syracuse University, School of Architecture, NY.

2/25/2019 *Building Modeling for Sustainable Design Practice and Teaching,* in Kent State University, College of Architecture and Environmental Design, OH.

2/11/2019 *Building Modeling for Indoor Environmental Quality,* in University of North Carolina at Charlotte, School of Architecture, NC.

10/18/2018 *Assessing visual comfort. A simulation-based approach for early to intermediary design phases,* in Center for the Built Environment, Industry Advisory Board Meeting, UC Berkeley, Berkeley, CA.

3/ to 5/2018 *Workshop series: Daylight and energy modeling for early design stages,* in ELS architecture + urban design. Berkeley, CA.

2/26/2018 *Modeling for performance-based design based on thermal and daylight simulations,* in ELS architecture + urban design, Berkeley, CA.

9/26/2017 *Improving thermal and daylight modeling for goal-oriented design methods,* in Atelier 10, San Francisco, CA.

1.9 Awards

The work comprised in this dissertation obtain the following awards:

2018 *PLEA 2018: 34th International Conference on Passive and Low Energy Architecture - Merit Award for the paper entitled "Assessing the Glare Potential of Complex Fenestration Systems: A Heuristic Approach Based on Spatial and Time Sampling."*

The research presented in this paper is part of the work presented in chapter 6.

Best doctoral research presentation in Building Science, Technology, and Sustainability at UC Berkeley College of Environmental Design (CED) Circus

Award given by CED to the presentation that summarize the dissertation progress at the end of Spring 2018 term.

2017 *ASHRAE Golden Gate Chapter Eric Thor Andresen Memorial Scholarship*

Award given by ASHRAE Golden Gate Chapter to initial research endeavors and prospectus.

Chapter 2:
State-of-the-Art

2.1 Introduction

This chapter provides an overview of past and ongoing research on the design of high-performance buildings essential to the research presented in this dissertation. Cross (2006) advanced the following three main types of (building) design research: (i) *design epistemology*, which focuses on the actors that execute building design processes; (ii) *design praxeology*, which studies the practices and procedures of designing; and (iii) *design phenomenology*, which concentrates on the design process outcome. Considering that the dissertation's general scope is the architectural design of high-performance buildings supported by computational design methods, the focus is on *design praxeology* in the context of performance-based design of sustainable buildings. Hence, the chapter discusses the thermal, energy, and daylighting simulation of buildings and their subsequent integration in the design process. The main goal is to provide a solid and detailed background for the chapters that follow.

This state-of-the-art report is two parts. The first part gives an overview of the methods and tools that designers use to predict whole-building energy use, thermal performance, and daylighting in indoor spaces. The second part consists of a literature review of the different computational design methods that use computer building simulations to support the design of high-performance buildings. The purpose of this review is to lay down the fundamental concepts and techniques behind daylight, thermal, and building energy simulations and map the different computational approaches to design that attempt to integrate them.

Building energy modeling (BEM) and computer daylight simulations support architectural workflows by calculating several building performance metrics. However, rather than focuses on performance metrics used in sustainable building design, this chapter concentrates on mapping the methods that enable their use in design. For detailed information about the building performance metrics used in this dissertation and commonly applied in the environmental assessment of high-performance buildings, the author refers the reader to Appendix A.

2.2 Predicting energy use and daylighting in buildings using computational methods

This section discusses the current simulation approaches used to predict whole-building energy use and the thermal and daylight behavior of buildings. First, it presents and summarizes the different groups of simulation methods. Then, it reviews the several approaches that computationally describe the physical principles behind heat transfer phenomena and daylighting simulation in buildings. The computational implementation of such physical principles is the core of the simulation tools commonly used by architects and other building designers in the design of high-performance buildings.

2.2.1 Modeling methods for thermal and daylight simulations

The use of computers to predict the thermal, energy, and daylight behavior of buildings is not new. Since the early 1980s, countless Building Energy Simulation (BES) approaches and programs have been developed, improved, and used by designers and researchers within the Architecture, Engineering, and Construction (AEC) community (Crawley et al., 2008). The problem of predicting whole-building energy performance and daylighting involves several factors, including ambient weather conditions, sky conditions, building physical structure, the operation of building systems like lighting and Heating, Ventilation, and Air Conditioning (HVAC) systems, and building occupancy and occupants behavior (Zhao and Magoulès, 2012). Three types of modeling approaches address the challenge of simulating the thermal, energy, and daylight performance of buildings:

Physical modeling methods. Also known as *white-box models*, these methods predict the thermal and daylight behavior of buildings by following and modeling physical principles and laws. In the case of building energy simulation, they model such physical principles through equations that describe heat transfer in a building. Such equations derive from the energy conservation law expressed in equation (2-1):

$$\Phi_{int} + \Phi_{source} = \Phi_{out} + \Phi_{stored} \quad (2\text{-}1)$$

where, Φ_{int} is the heat flux entering the system, Φ_{source} the heat flux originated by an eventual heat source, Φ_{out} the heat flux leaving the system, and Φ_{stored} the heat flow stored in the system. Three heat transfer mechanisms modulate the fluxes in the system: conduction, convection, and radiation.

Daylighting simulation also follows the principle of energy conservation by balancing light flows from one point of a surface to another. Thus, the amount of visible radiant energy that is transmitted, absorbed, and reflected at a particular point in a surface is equal to the incident visible radiant energy that arrives at that point. The physical simulation of daylighting attempts to solve the rendering equation advanced by Kajiya (1986) and its subsequent extensions, including the ones proposed by Wallace et al. (1987), Ward et al. (1988), Kajiya and Kay (1989), Lange (1994), Smith et al. (2008), and several others.

Statistical modeling methods. These methods are also termed as *black-box models* since they are agnostic to any physical principle, law, or even information. These models use Machine Learning (ML) techniques to deduce a prediction function from samples of measured data. Hence, their application is more common to the modeling of existing buildings since they are well adapted either to cases where the building's physical features are unknown or to post-occupancy studies where it is possible to collect a large number of measurements. The advantage of these methods is that they can accurately predict the building's physical behavior with little or no information about building geometry, materiality, or detailed physical phenomena. Their disadvantage is that they require large amounts of measured data, limiting their use in cases where it is difficult to collect data. Thus, the exclusive use of statistical modeling methods in designing new buildings is impractical. The most common techniques include Linear and Multiple Linear Regression (LR/MLR), Artificial Neural Networks (ANN), and Support Vector Machines (SVM). It is possible to combine these methods with stochastic optimization metaheuristics such as Genetic Algorithms (GA). The most common use of GAs in this context is whether to find weighting factors in MLR regressions or ANN or the regularization (C) and deviation (ε) constants in SVM.

Foucquier et al. (2013) summarizes the principles of each statistical modeling method and their applications in the domain of building energy performance prediction.

Hybrid modeling methods. Also called *grey-box models*, these approaches combine white- and black-box models. Grey-box models aim to overcome some of the limitations of both white- and black-box models. White-box models require a description of all building characteristics. Additionally, although heat exchange phenomena are well known, it is difficult to computationally implement them in an efficient manner (e.g., wind flow in a building). Thus, in white-box modeling, it is common to use some modeling assumptions to approximate the physical phenomena for computational convenience. Black-box models have two main limitations: (i) they require large amounts of data, and (ii) their results are difficult to interpret in physical terms. Grey box-models are able to retain part of the physical meaning, therefore facilitating interpretability, and do not require a full description of physical and geometrical input parameters. There are three main applications of hybrid modeling methods: (i) estimating white-box models' physical parameters; (ii) building surrogate models, which are models that learn from data sets, either produced by white-box models or that combine simulated data with measurements, to describe the behavior of a building; (iii) calibrating white-box models, which typically consists of fine-tuning a simulation model to known data. The improvement of white-box modeling approaches commonly involves the use of optimization metaheuristics such as GAs. Typically, GAs search for the simulation parameters that minimize the error of the simulation model output. The work presented by Lauret et al. (2005), Znouda et al.(2007), Yang et al. (2011), and Wang et al. (2016) are good examples of the use of metaheuristic-based search procedures to improve simulation parameters. Regarding simulation calibration, Coakley et al. (2014) and Fabrizio and Monetti (2015) provide a comprehensive review of BES calibration methods. The review includes a summary of the application of ML techniques to automate BEM calibration. Surrogate models, also known as meta-models, find their use in performance-based building design in sensitivity analysis, uncertainty analysis, and in the optimization of predicted building performance. Westermann and Evins (2019) present a thorough literature review on surrogate modeling for sustainable building design. ML techniques used both in simulation calibration and in surrogate modeling include Bayesian techniques, LR/MLR, Multivariate Adaptive Regression Splines (MARS), kriging regression models (KRM), Radial Basis Function (RBF) networks, SVM, and ANNs, such as Sigmoidal Neural Networks (SNN).

Since this dissertation focuses on early-stage building design, the investigation will not discuss the isolated use of statistical techniques prediction metrics. The subsequent discussion focuses on physical modeling methods for the following reasons: (i) white-box modeling is the most used approach in the design of new buildings; (ii) the dissertation aims to improve current modeling methods towards efficient use of whole-building energy and daylight simulations at the early stage of building design; (iii) hybrid modeling approaches for initial stages of building design heavily depends on the data produced by white-box simulations. The following part of this chapter discusses the thermal and daylight physical principles in buildings and their computational implementation in simulation tools.

2.2.2 Physical modeling methods

Given well-defined boundary inputs, white-box models can accurately estimate the daylight and the energy performance of buildings. Since predicting daylight and energy use of buildings using white-box models is a non-trivial task, this section discusses them separately.

Thermal modeling and whole-building energy simulation in the white-box paradigm

BES requires the description of several simulation input boundaries, namely ambient weather, contextual shading geometry, thermal, solar, and optical properties of the building envelope, occupancy patterns, building systems, and system operation protocols. With such information, physical modeling methods can accurately estimate the energy performance of an entire building and of its several components, e.g., physical building components such as walls, slabs, glazing, or of building systems such as lighting and HVAC systems (Clarke, 2001).

When applied to whole-building energy predictions, white-box models use the *zone* or *nodal approach*, which divides the building into different *thermal zones*. Each thermal zone is a homogeneous enclosed volume characterized by uniform state variables (Clarke, 2001; Foucquier et al., 2013; Harish and Kumar, 2016; Hensen and Lamberts, 2019; Spitler, 2019). The assumptions involved in this modeling strategy allow us to describe the thermal zone in terms of a network of nodes. To better visualize such a network and the heat flow paths within the system, Clark (2001) traces a parallel with an electrical system of resistances and capacitances dependent on transient potential differences. The "electrical currents" that flow in such a "circuit" are equivalent to the heat flows between thermal zones and their constituent parts. Thus, a thermal zone, its constructional elements, its contents (e.g., furniture), equipment gains, glazing components, occupants, HVAC system and its components, are nodes characterized by capacitance and the energy flows or connections between them are described by conductance. Each node possesses state variables such as temperature, which is analogous to voltage. Since the state of the nodes is dynamic, the entire system is transient. This means that several nodes respond to different systems inputs (e.g., hourly meteorological conditions, and occupancy or other loads schedules) at different rates as they compete to capture, store, and release energy. Figure 2-1 illustrates the conceptualization of the thermal and energy model as a node network.

The electrical circuit analogy depicts the complexity of the dynamic and transient behavior of heat transfer and energy flow in a building. The resolution of a whole Building Energy Model (BEM) depends heavily on the complexity of the nodal network. Thus, BEM complexity increases with the number of nodes; this includes nodes that represent different thermal zones or nodes that characterize elements that compose each thermal zone. As Clarke (2001) and Spitler (2019) so well demonstrate, the simulation of such systems is far from being a trivial task since it entails the mathematical description and solving of several complex equations types. Additionally, since these equations express interdependent heat transfer processes, it is necessary to apply simultaneous calculation techniques (Clarke, 2001). The modeling of the heat transfer phenomena in BES demands adequate computational implementations of the three heat transfer processes: conduction, convection, and radiation.

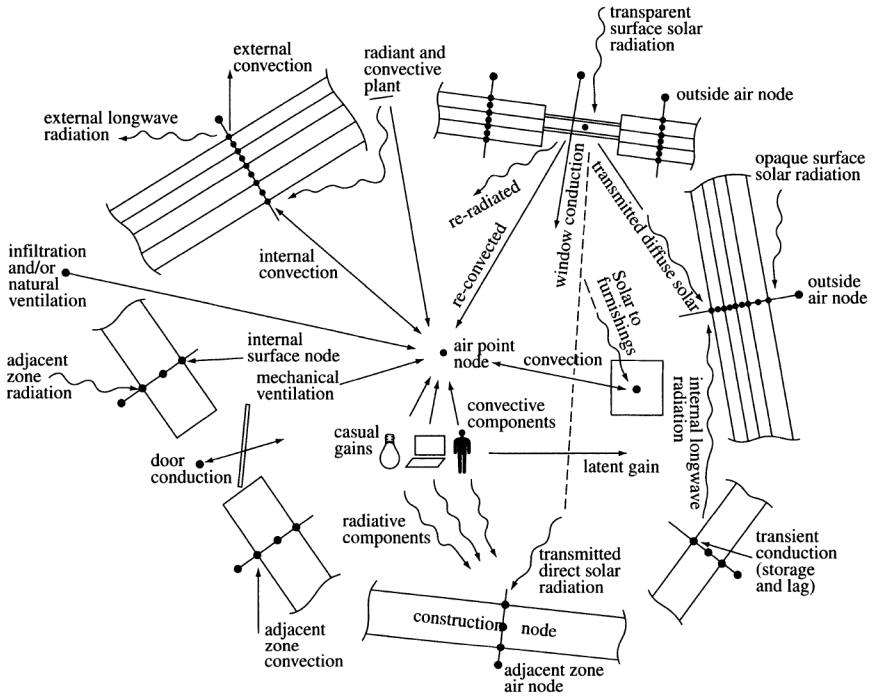

Figure 2-1. A thermal zone described in terms of a network of nodes and flows. Image source: Clarke (2001).

State-of-the-art BES programs such as TRNSYS, Esp-r, EnergyPlus, and IES-VES, accurately model the three heat transfer processes and their interdependencies in the thermal nodal network by using the following main heat and mass transfer mechanisms:

1) ***Transient conduction*** describes how heat flows in a construction element or layer to another building element or construction layer. The thermal resistance and inertia diminish and shift this process in time (Clarke, 2001; Chen, Zhou and Spitler, 2006; Spitler, 2019). Transient conduction is a function of the temperature differential between exposed surfaces. External fluctuations in temperature are the main drivers of this heat transfer mechanism. The thermophysical properties of the materials that modulate the heat transfer by conduction include conductivity, k (W m^{-1}° C^{-1}), density, ρ (kg m^{-3}), and specific heat capacity, C (J kg^{-1} °C^{-1}).

2) ***Surface convection*** expresses the heat exchange between the building surface and the adjacent air layer. Typically, wind triggers external surface convection, whereas natural air movement, caused either by pressure or temperature difference, and forced air movement, originating in a mechanical system, induces internal surface convection. Convection calculations require the computation of the convection coefficient, h_c (W m^{-2} °C^{-1}), which is time-dependent and surface-averaged (Fisher, 1995; Awbi and Hatton, 1999; Clarke, 2001).

3) ***Surface longwave radiation*** describes the radiative heat exchange between different surfaces. In the case of internal surfaces, longwave radiation exchange depends on surface temperatures, emissivities, view factors, and reflection type, i.e., diffuse, specular, or mixed. The zeroth law of thermodynamics determines the heat exchange between surfaces of different temperatures to achieve equilibrium. The modeling of longwave radiation is non-

linear, which poses some computational challenges (Clarke, 2001). External surface longwave radiation models the radiative exchange between the building envelope surfaces, and the sky, surrounding buildings, and ground. Longwave radiation is calculated by considering the following contributing factors: (i) effective sky temperature, (ii) ground temperature, (iii) ambient air temperature, (iv) surrounding building surfaces temperature, (iv) the warming effect caused by incident shortwave radiation, and (v) view factor of each surface of the building envelope with the three parts that compose the immediate outdoor environment – sky, ground, and surrounding buildings (Clarke, 2001).

4) ***Shortwave radiation*** characterizes the impact of solar gains both in the building envelope and in the thermal zone. For that reason, its accurate calculation is paramount in determining cooling loads. The shortwave radiation that arrives at any external surface is partially reflected, absorbed, and transmitted or re-emitted depending on the participating media. In the case of the opaque part of the building envelope, shortwave radiation affects both transient conduction, internal longwave radiation, and convection by increasing the temperature of the inside surface through time (Hussain and Oosthuizen, 2012; Le Dréau and Heiselberg, 2014). Shortwave radiation is responsible for significant temperature differences between exposed surfaces and outdoor dry-bulb air temperature, which in some cases can be as much as 15 to 20˚C (Clarke, 2001). In the case of transparent elements such as glazing, shortwave radiation is partially transmitted and absorbed. The absorption of shortwave radiation raises the glazing assembly temperature, thus affecting transient conduction. This temperature increase will also affect the temperature of the glazed surfaces, thereby affecting convection and longwave radiation heat exchange. The transmitted portion of shortwave radiation quasi-instantaneously impinges internal surfaces in the thermal zone. The internal opaque surfaces that are affected will absorb, reflect, and transmit that energy as an external surface element. Thus, direct shortwave radiation changes the transient conduction, longwave radiation, and convection flows of the affected internal surfaces.

Other factors participate in the heat flow mechanisms described above, including: (i) shading and insolation, (ii) airflow caused by infiltration, natural or mechanical ventilation, (iii) equipment heat gains, (iv) passive solar elements, (v) HVAC systems, (vi) lighting systems, (vii) and the control of any building system that contributes to heat exchange, e.g., dynamic shading, ventilation, equipment, HVAC, and lighting.

There are two main modeling paradigms to numerically model the heat flow in BEM: the *Transfer Function Methods* (TFM) or the *Finite Difference* or *Volume Methods* (FDM/FVM) (Foucquier et al., 2013; Wang and Zhai, 2016).

TFM models the BEM nodal network as systems of linear differential equations with time-invariant parameters (Clarke, 2001; Foucquier et al., 2013; Wang and Zhai, 2016). Such methods involve either the calculation of Response Factors (RF) or Conduction Transfer Functions (CTF) and their coefficients. RFs are a convenient way of presenting dynamic transient time series data in a time-invariant system (Gouda, Danaher and Underwood, 2002; Barrios, Huelsz and Rojas, 2012). The RF primary equation relates the heat flux at one surface of a building element or component to a series of temperature histories at both sides of the component (DOE, 2018). For simplification reasons, the method assumes constant coefficients, although in the real world they

change with temperature fluctuations. While this assumption makes RF methods computationally efficient, it also limits their ability to tackle the so-called building *stiff systems.*

Building stiff systems consists of several differential equations to which certain solving methods, such as RFs, are numerically unstable, unless the step size used in the time series is very small. Building envelope, HVAC systems, fluid flow dynamics, and systems control models are stiff systems (Clarke, 2001). One RF limitation that emerges from its inability to handle stiff equations is adequately model radiant heat transfer (Wang and Zhai, 2016). For example, one of the main limitations of DOE-2 (Winkelmann et al., 1993), a BES program that uses the RF method, is its inability to estimate inner surface long wave radiation heat transfer.

CTF handles stiff systems by replacing the time series terms with flux history terms (DOE, 2018). Despite their computationally efficiency, CTF approaches are able to model any type of heat flow in the building thermal network. Al-Rabghi and Al-Johani (1997) demonstrated that CTF methods can accurately predict conductive heat transfer of different types of building elements such as walls, floors, roofs, and fenestrations. The CTF is the most adopted modeling approach in BES programs because of its robustness and efficiency.

Spitler et al. (1997) advanced the *Radiant Time Series* (RTS), an additional time-invariant heat transfer method for cooling loads calculation, particularly those caused by radiation. RTS uses radiant time-based coefficients to estimate the hourly cooling loads from hourly heat gains. The method uses the heat balance method, a simplified approach to determine thermal loads. Thus, it is less accurate than CTF methods but presents an interesting alternative in cases that prioritize computationally efficiency (Wang and Zhai, 2016).

Unlike TFM, finite difference and volume methods (FDM/FVM) are time-variant and can handle non-linear equation systems. Thus, FDM/FVM avoid approximations of decoupled systems of linear equations (Clarke, 2001). By being non-linear and time-variant, the modeling approaches of these systems are closer to the real-world physics of heat transfer in buildings. Thus, FDM/FVM handle better complex heat flow path interactions of building stiff systems and accommodate time-varying system parameters. Additionally, they are generalizable, making their numerical approach universally applicable to model the thermal interactions and flows in buildings (Clarke, 2001). Despite their accuracy, FDM/FVM approaches are very computationally intensive. Computational Fluid Dynamics (CFD) methods are an example of the application of FVM. CFD is a highly comprehensive thermal transfer modeling technique that allows the detailing of the field flow inside buildings by solving the Navier-Stokes equation (Foucquier et al., 2013). Nevertheless, CFD methods' main disadvantage is their huge computation time (Chronis et al., 2017; W. Tian et al., 2018; Phillips and Soligo, 2019). For that reason, it is uncommon to use CFD methods in early building design phases. In whole-building energy simulations, CFD approaches are usually coupled with standard BES programs in order to improve the accuracy of TFM-based BES tools in cooling and heating calculations (Pan et al., 2010; Zeng et al., 2012; Ascione, Bellia and Capozzoli, 2013; Dols et al., 2015; Alnusairat, Hou and Jones, 2017; Allegrini and Carmeliet, 2018).

The great computationally advantage of using TFM over FDM/FMV is that transfer functions only need a single calculation at simulation initialization. Although TFM does not enable a FVM detailed analysis of flow paths and fields, their predictions are fairly accurate. For that reason,

several BES programs are TFM-based. Popular and validated whole-building energy software such as BLAST (Hittle, 1981), TRNSYS (Trnsys, 2000), EnergyPlus (Crawley et al., 2001), and IES-VE (IES, 2008) use TFM approaches. Different BES comparative studies (Crawley et al., 2008; Wang and Zhai, 2016) show that such programs can fully model all heat transfer processes. Several studies indicate EnergyPlus as one of the most accurate programs in solving heating and cooling loads (Strand et al., 1999; Crawley et al., 2001, 2008).

EnergyPlus is a modular, open-source whole-building energy simulator that uses text-based input/output files. Its modularity supports incremental development. There are several third-party modules and interfaces for EnergyPlus, including Simergy, OpenStudio (Guglielmetti, Macumber and Long, 2011), Design Builder, Archsim (Dogan, Reinhart and Michalatos, 2014), Honeybee (Mackey et al., 2015), Autodesk Insight (Autodesk, 2019). From those interface programs to EnergyPlus, four directly interact either with Computer Aided Design (CAD) or Building Information Modeling (BIM) building design tools. OpenStudio interacts with the CAD platform SketchUp, Archsim and Honeybee with the Non-Uniform Ratio Basis Spline (NURBS) 3D modeling CAD program Rhinoceros, and Autodesk Insight and Honeybee with Revit, a popular BIM application.

ESP-r (Clarke and McLean, 1988) is also an open-source validated whole-building energy simulation software, but unlike EnergyPlus, TRNSY, and IES-VE, it uses the FDM approach to accurately calculate heat flow related phenomena in a building. The FDM approach allows parameter adjustments that are responsive to dynamic boundary conditions and control system signals. ESP-r supports on-demand CFD analysis to detail the flow field of thermal zones in thermal comfort and air quality studies. Nevertheless, ESP-r is primarily targeted at highly skilled building analysts and researchers who have a good understanding of building physics. The program was compiled only for the Linux operating system. Because it is a highly detailed program, does not support different operating systems, and because its use requires a high level of expertise, designers and building energy modelers seldom use ESP-r.

Other alternative methods to the FDM and TFM are the reduced-order *Lumped Parameter Models* (LPM). LPMs can simulate the hourly energy behavior of buildings with a smaller computational cost compared with FDM and TFM (Rumianowski, Brau and Roux, 1989). They implement the "analogous circuit" concept used above to explain BEM nodal models (Foucquier et al., 2013; Wang and Zhai, 2016). First-order LPM fell short in accurately expressing heat transfer flows. However, higher models have been proposed that have improved accuracy without compromising their simplicity or speed (Fraisse et al., 2002; Gouda, Danaher and Underwood, 2002). It is possible to combine LPM with BES programs based on TFM approaches (Martin et al., 2015; Wang and Zhai, 2016). However, LPMs still require a considerable amount of expertise since the user needs to use advanced modular-graphical modeling tools such as Simulink (MathWorks, 2002), or domain-specific programming languages such as Modelica (Fritzson and Engelson, 1998). Thus, building designers, particularly architects, seldom use them.

Regarding the use of a whole-building energy simulation in building design, Clarke (2001) argues that it is more efficient to use a single simulation program throughout the entire design process than to use a progression of tools, from simplified to detailed. Clarke maintains that using a disparity of analysis tools, particularly to simulate similar physical processes, is a problematic

approach since it inevitably entails theoretical and modeling discontinuities as well as pernicious assumptions.

The author of this dissertation agrees with Clarke but adds that BES should be selected as long as the following conditions are met: (i) the tool should be able to model all heat transfer modes accurately, including radiative heat transfer since thermal mass is a critical factor in passive design; (ii) it should support co-simulation as a relevant ancillary process that complements the eventual modeling shortcomings of the used BES program; (iii) the tool needs to, at least partially, interface with design tools such as CAD or BIM programs; and (iv) it should be flexible and, therefore, adaptable to the requirements different design phases, i.e., it should support both simplified and detailed calculations. Such requirements promote the efficient use and integration of BES tools.

Considering the requirements specified for BES selection, this dissertation uses EnergyPlus as the main BES program. Despite some hurdles (see chapter 3 and 5), EnergyPlus fulfills all conditions: (i) it is capable of modeling all heat transfer modes accurately, (ii) there are several modern and well-designed interfaces that support its use through design tools such as CAD and BIM programs (e.g., OpenStudio, Archsim, Honeybee), (iii) detailed simulations such as CFD and daylighting simulation generated by other software can complement EnergyPlus analysis, (iv) several works in early-stage design use this software to predict the thermal and energy behavior of buildings, e.g., the investigations of Anton and Tănase (2016), Konis, Gamas, and Kensek (2016), Qingsong and Fukuda (2016), Negendahl (2015), Asl et al. (2014), and Caldas and Santos (2012).

Daylight simulation in buildings using physical (unbiased) approaches

The daylight simulation of buildings requires the description of a scene that includes the following essential elements: (i) the three-dimensional building geometry of the area to simulate, (ii) the optical material descriptions for all the surfaces in the scene, (iii) and a sky model that quantifies the contribution of direct and diffuse components of daylight emitted by the celestial hemisphere.

Depending on the type of analysis, the user needs to provide additional information. In the case of High Dynamic Range- (HDR) based simulations such as luminance and illuminance point-in-time render or glare analysis, the user needs to specify a point-of-view, also known as a camera. For grid-based simulations, such as point-in-time illuminance, solar irradiance, and annual dynamic daylight analysis, the user needs to specify a grid or an array of sensors. In the case of annual dynamic daylight analysis, also known as *climate-based simulations*, the analysis requires the following information: (i) annual hourly Typical Meteorological Year (TMY) data to build an annual sky using the all-weather Perez sky model (Perez, Seals and Michalsky, 1993), (ii) an occupancy schedule, the control protocol of eventual dynamic shading systems, and (iii) a lighting level threshold (typically an illuminance threshold) (Reinhart, 2019).

Using the input data that describes the scene, physically-based daylighting simulation software is able to predict illuminance- or luminance-related phenomena. Several computational approaches implement different types of light transport models to perform such predictions. This section will discuss the methods currently in use in the digital daylight analysis of buildings, namely the *split flux* method, the several *raytracing* methods, and some hybrid approaches that combine raytracing with other techniques. Other methods like *rasterization* (scanline) (Pineda, 1988), and *radiosity* (Greenberg, Cohen and Torrance, 1986; Immel, Cohen and Greenberg, 1986; Cohen and Wallace, 2012) will not be discussed. Rasterization techniques are commonly used in the animation and

gaming industry and the use of Radiosity in lighting simulation of architectural spaces is in decline (Jakica, 2018).

The split flux method is the simplest physically-based light transport algorithm. The approach computationally implements a manual calculation method established by the British Building Research Establishment (BRE) (Jakica, 2018; Reinhart, 2019). The method divides daylight into three components: (i) the direct Sky Component (SC), (ii) the Externally Reflected Light component (ERC), and (iii) the Internally Reflected Light component (IRC). The approach calculates each component separately and combines them to compute illumination levels. Introduced by Hopkinson, Longmore and Petherbridge (1954), Modest (1982) extends the split flux method and implements it in the SUPERLITE program. Despite being a simplified approach, therefore incapable of fully capturing the daylight phenomena, it computes quickly. For that reason, whole-building energy programs, which do not focus on performing detailed daylight calculations, still use this method. For example, eQUEST-DOE-2 (Hirsch, 2006) and EnergyPlus (Crawley et al., 2001) implement the split flux method to calculate Daylight Factor (DF) in specified light sensors located in thermal zones. Those programs use the DF data to estimate the hourly illuminance levels necessary to compute the thermal zone lighting energy use. Winkelmann and Selkowitz (1984) describe the implementation of the method used in DOE-2. EnergyPlus extends the method implemented in DOE-2 by using a more diverse range of sky models (DOE, 2018). Figure 2-2 depicts the different components of the split flux method.

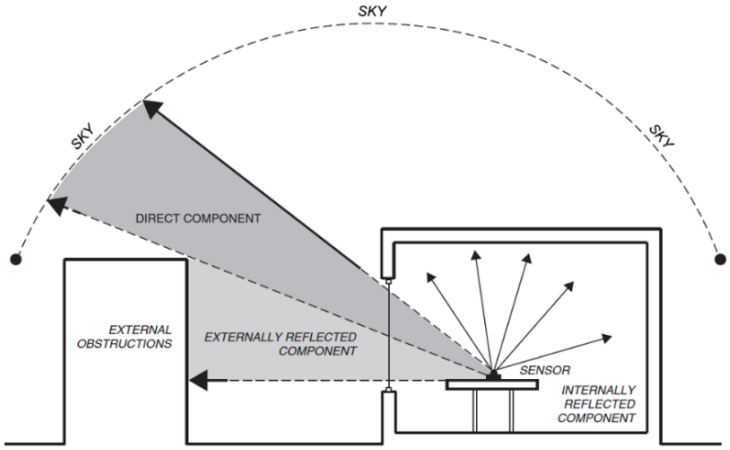

Figure 2-2. The split-flux method calculation components. Image adapted from Reinhart (2019).

Using a technique called *Path Tracing* (PT), Raytracing methods follow the physical principles that determine visible light phenomena (Shirley, 1992). Raytracing calculates light transport by tracing a large number of optic light rays in a scene. Raytracing techniques extend the ray casting algorithm, originally developed to solve intersections of rays within an arbitrary geometry by tracing a ray per pixel. First proposed by Whitted (1979), raytracing later adopted recursive point-sampling techniques to trace the additional rays necessary to calculate global illumination and solve the general rendering equation (Kajiya, 1986). The physical model implemented by raytracing follows energy conservation principles (Pharr, Jakob and Humphreys, 2016), which determine that every recursive light bounce splits a ray into reflected, absorbed, and transmitted components. Light transmission through a material could occur either through refraction, emission, or a combination of both, depending on the participating media. The sum of the components must

be equal to the incident radiosity. Typically, stochastic methods control the ray splitting. However, to avoid expensive computations, current methods use deterministic ancillary approaches to guide stochastic Monte Carlo sampling algorithms (Jakica, 2018). Algorithms that follow this hybrid approach, like the Multiple Importance Sampling (MIS) (Veach and Guibas, 1995) and its extensions (Burke, Ghosh and Heidrich, 2005; Clarberg et al., 2005), have made physically-based rendering computationally feasible nowadays.

There are three main raytracing approaches used in predicting daylight in buildings: *forward, backward,* and *bidirectional raytracing.* In forward raytracing the rays start from the light source. Currently, this method is the most accurate and detailed light transport model since it exactly follows the physical behavior of light. Nevertheless, forward raytracing is computationally expensive since it requires the tracing of millions of ray recursions to achieve smooth and realistic results (Jakica, 2018). For that reason, designers, analysts, and researchers use this method in later design phases and in cases that include optically Complex Fenestration Systems (CFS) that are challenging to simulate (Santos, Leitão and Caldas, 2018). TracePro (Lambda, 1994) is a well-known forward raytracing tool that recently implemented the sun as a light source. However, it is still challenging to use TracePro and other forward raytracing programs as daylighting tools for whole-building analysis (Kolås, 2013). Nevertheless, it is common to use such tools to produce high quality Bidirectional Scattering Distribution Functions (BSDF) that can be used by other simulation techniques.

Backward raytracing techniques trace rays from a point in the scene. In the case of rendering calculations, this point characterizes a camera viewpoint, whereas in grid-based illuminance simulations, this point represents a light sensor (Jakica, 2018). The process begins to emit rays from the point of interest (i.e., a view or light sensor) until the rays either hit a physical object or a light source such as the sun, sky, or a luminaire. The backward tracing process considers all physical interactions caused by reflection and refraction. For example, if a ray hits a surface other than a light source, the luminance of that surface depends on the secondary rays that either bounce back or are partially absorbed and re-emitted from the surface. The optical properties of the surface, typically encoded in material shaders, determine how the ray radiance is absorbed, reflected, refracted, or re-emitted (Reinhart, 2019). Figure 2-3 illustrates the backwards raytracing process.

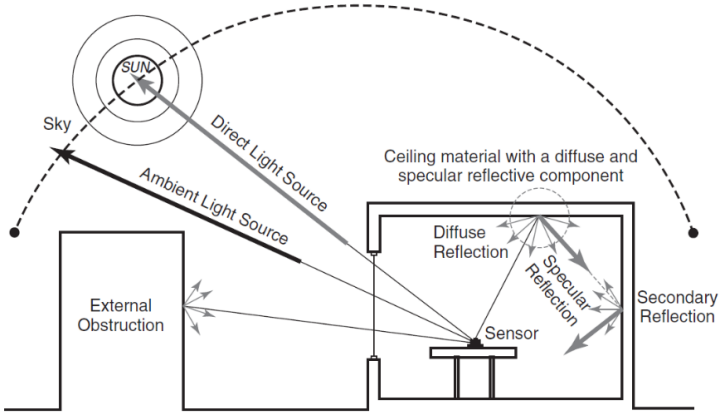

Figure 2-3. The backward raytracing method. Image source: Reinhart (2019).

This light transport model is faster to compute than forward raytracing as it calculates only the rays reaching the view or sensor point.

Radiance (Ward and Rubinstein, 1988; Ward, 1994, 2004b; Ward and Shakespeare, 1998) was one of the first backward raytracing programs, and is the most used daylight simulation engine in research and building analysis (Ochoa, Aries and Hensen, 2012). Radiance outperformed other available lighting simulation programs in several validation and evaluation studies that compared simulation output against measured data (Ubbelohde and Humann, 1998; Crawley et al., 2008; Acosta, Navarro and Sendra, 2011). Ruppertsberg and Bloj (2006) claimed that no widely used rendering software is better than Radiance. The same authors combine spectral rendering methods with Radiance to achieve physically accurate results for visual psychophysicist study. The incremental improvement and extension of Radiance's capabilities led to its being widely regarded as the "golden standard" for lighting simulation (Santos, Leitão and Caldas, 2018). Several authors use this simulation engine as the benchmark program in the validation of other daylighting simulation tools (Reinhart and Breton, 2009; Bellia, Pedace and Fragliasso, 2015; Jones and Reinhart, 2017; Reinhart, 2019). The following discussion focuses on Radiance and Radiance-based tools.

The early applications of Radiance's backward raytracing in predicting daylight in buildings were static, i.e., they reflected a specific sky condition in a scene. Therefore, they mainly consisted of DF and point-in-time calculations such as the calculation of illuminance in a grid of sensor points or luminance-based synthetic HDR images. Such approaches are unable to fully depict the annual variation of daylighting conditions of a specific location. To that end, several authors advanced new methods called *Climate-based Daylight Modeling* (CBDM). CBDMs are annual, dynamic, and climate-based analysis methods that calculate illuminance and luminance times series that result from different daylight conditions derived from TMY data (Nabil and Mardaljevic, 2006; Reinhart, Mardaljevic and Rogers, 2006; Reinhart, 2019). CBDMs enable the calculation of climate-based daylight metrics, including Daylight Autonomy (DA), Useful Daylight Illuminance (UDI), Annual Sun Exposure (ASE), and annual Daylight Glare Probability (aDGP).

Initially, CBDM simulation resulted from the automated repetition of a static simulation under varying sky conditions. However, that process is highly inefficient since it requires extremely long computation times (Reinhart and Herkel, 2000). The Daylight Coefficient (DC) method is a numeric method that speeds up the simulation of annual dynamic light levels. Also known as the *two-phase method*, DC was originally proposed by Tregenza and Watters (1983). Bourgeois, Reinhart, and Ward (2008) advanced a standard for using DC to run CBDM.

The DC method first discretizes the sky model hemisphere into 145 patches (also called *sky segments* or *Tregenza patches*). Then, it computes the contribution of each sky patch to the total illuminance in any arbitrary point inside the building. Figure 2-4 depicts the illuminance (E_α) contributions of a sky patch (S_α) at a specific point and view direction (x) normalized by the luminance (L) and the sky patch angular size (ΔS_α). This normalization result is a daylight coefficient (DC) for that specific sensor point x related to the sky segment S_α. For an annual calculation, the illuminance of a particular sensor node in each time step results from summing up all the 145 multiplications between each sky division luminance and the respective calculated DC.

It is possible to extend the DC concept to luminance, thus allowing the generation of time-series visualizations (Wienold and others, 2007; McNeil and Lee, 2013) essential to annual visual comfort studies. As mentioned in Reinhart (2019) several studies show that Radiance's two-phase method is able to predict annual indoor light levels accurately (Mardaljevic, 2000; Reinhart and Walkenhorst, 2001; Reinhart and Andersen, 2006; Reinhart and Breton, 2009; Sudan, Mistrick and Tiwari, 2017; Brembilla and Mardaljevic, 2019).

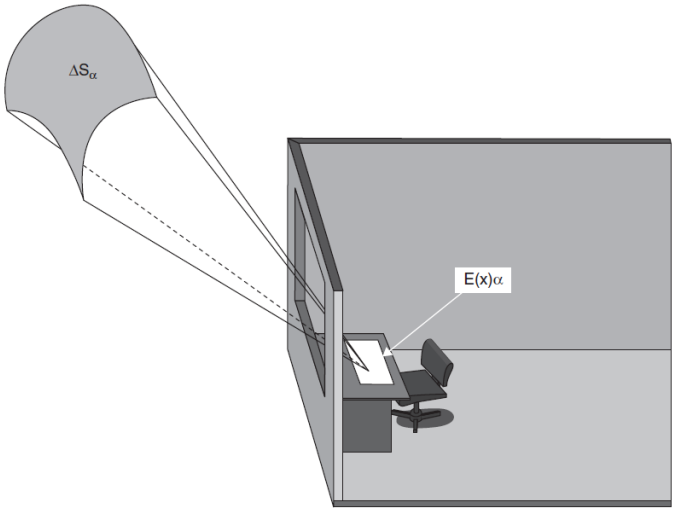

Figure 2-4. Visual definition of the two-phase method showing the several components necessary to compute a daylight coefficient for an indoor point x and a sky patch or segment S_α. Image adapted from Bourgeois et al. (2008).

DAYSIM (Reinhart and Walkenhorst, 2001) and SPOT (Rogers, 2006) are Radiance-based tools that implement the two-phase method for CBDM. An alternative implementation of the two phase method consists of concatenating several Radiance subroutines, a non-trivial task for non-expert Radiance users.

Although backwards raytracing is computationally more efficient than forward raytracing, it is unable to handle complex reflections and refractions of specular surfaces or to properly simulate caustic scattering in transparent materials and participation media (e.g., translucent materials). This shortcoming limits the application of Radiance and Radiance-based tools such as SPOT and DAYSIM to adequately simulate specular light redirecting systems and other types of CFS. The stochastic and probabilistic sampling techniques used in backwards raytracing to find specular reflections of the sun are the reason for this limitation. The probability of using such sampling techniques to find the sun is low when its relative size is small in the overall scene, a situation that often occurs in the study of CFS (McNeil and Lee, 2013).

The introduction to Radiance of bidirectional light transport models extended the program to include some forward raytracing capabilities, thus enabling its use in the simulation of CFS. One of the bidirectional models is *photon mapping*. Schregle (Schregle, 2002, 2003, 2004) implemented a photon map extension to Radiance by pre-processing a photon map using a forward ray tracing technique. Forward raytracing using photon mapping poses a challenge in daylighting simulation since a large number of the photons emitted by the sky and sun do not interact with the interior scene. Schregle (2002, 2003) solved this by using *photon ports* that mapped the visible sky and sun luminance distribution on windows. Using the information stored in the photon ports,

the technique traces photons and stores them in a process called *forward pass* (Figure 2-5). The information produced by the forward pass is then used by the backward raytracing to calculate global illumination (Schregle, 2002; McNeil and Lee, 2013; Jakica, 2018). Initially, this technique did not support annual simulations, and the proposed photon ports could not calculate external inter-reflections. However, the development of progressive photon mapping in Radiance overcomes its initial limitations (Schregle et al., 2015; Schregle, Grobe and Wittkopf, 2015, 2016; Lars O. Grobe, 2019b). EvalDRC (Schregle et al., 2015) is a python-based tool that automates the progressive version of Radiance's photon mapping to fully support CBMDs that include specular CFS (Bauer and Wittkopf, 2015; Kazanasmaz et al., 2016; Grobe, Wittkopf and Kazanasmaz, 2017; Lars O. Grobe, 2019a).

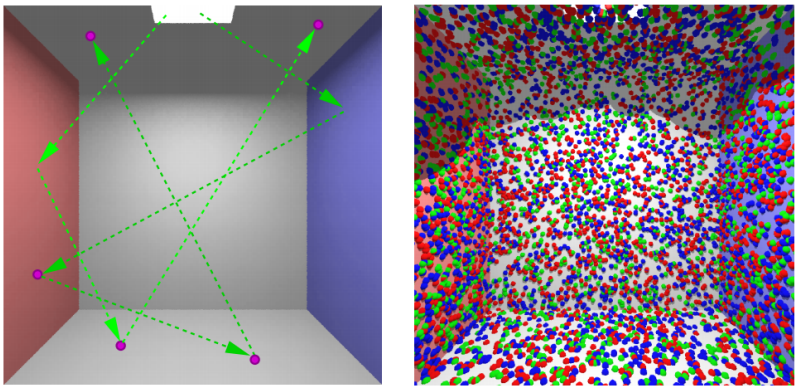

Figure 2-5. Global photon distribution in Radiance's Photon Map approach. Left: individual photon path in the diffuse Cornell box. Dots indicate stored photons. Right: stored photons after the completion of the forward pass. Image source: Schregle (2002).

Another type of approach that addresses Radiance's backward raytracing limitations is the addition of the tool *genBSDF* (Ward, 2010). *genBSDF* enables the generation of bidirectional models of light transport and scattering under the form of BSDF data. This tool overcomes the Radiance's limitation in modeling specular CFS by flipping the convention of source and receiver in Radiance's backwards raytracing architecture, thus operating Radiance as a forward raytracing program (McNeil and Lee, 2013; Geisler-Moroder, Lee and Ward, 2016; Eleanor S. Lee, Geisler-Moroder and Ward, 2018). It is possible to use *genBSDF* output directly with *rtrace* (Ward, 1997) or *rpict* (Ward, 1999) Radiance subroutines to compute illuminance levels in digital light sensors or luminance-based images, respectively. The BSDF data produced by *genBSDF* replaces standard material descriptions of fenestrations like common transparent or participation media materials. However, this use of BSDF data supports only point-in-time calculations. Several modeling methods for Radiance have been developed to use this bidirectional light transport model in annual dynamic daylight calculations. Such modeling approaches use matrix algebra to compute either annual and point-in-time illuminance- and luminance-based metrics. Ward et al. (2011) proposed the 3-phase method and validated it using an inter-modeling approach. The validation consisted of comparing the 3-phase method results against previously validated simulation results generated by Radiance's backwards raytracing method. Later, McNeil and Lee (2013) empirically validated the 3-phase method. The empirical validation consisted of modeling and simulating the LightLouver CFS, a commercially available optical light-redirecting system, and comparing the simulation results against measured data collected over a one-year period outdoor test facility in Berkeley, California.

The 3-phase method extends the DC approach. The modeling approach breaks the luminous energy transport between the sky patches and the interior sensor nodes into three distinct phases, each one simulated independently and stored in a matrix of coefficients: (i) the Daylight matrix (*D*), which describes the way that energy from each Tregenza sky patch arrives into each of the directional Klems patches that subdivide the fenestration (Klems, 1994b, 1994a); (ii) the Transmission matrix (*T*) expressed in the BSDF matrix, which describes the specular and non-specular transmission of the fenestration; (iii) the View matrix (*V*), which characterizes how light that exits the fenestration arrives at the camera or at a grid of sensor nodes. By multiplying the three matrices (*VTD*), a DC is calculated. The annual illuminance ($E_{[annual]}$) or luminance ($L_{[annual]}$) on *V* results from the multiplication of DC by a sky matrix (*S*) that contains the sky patches average luminance for all the hours of the year and correspondent sky conditions (*VTDS*). The calculation of *E* or *L* depends on the Radiance routine that processes the result of the 3-phase method. Equation (2-2) formulates the 3-phase method as follows:

$$E \text{ or } L = V \times T \times D \times S \quad (2\text{-}2)$$

The 5-phase method extends the 3-phase method to closely follow the standard DC modeling approach proposed by Bourgeois, Reinhart, and Ward (2008). Geisler-Moroder et al. (2016) validate the 5-phase method. The validation also showed that this approach outperforms the 3-phase method, particularly in predicting the distribution of direct sunlight (Geisler-Moroder, Lee and Ward, 2016). The approach consists of decoupling the direct solar component from the sky and inter-reflected components of the 3-phase method by adding the following two steps:

1) Computing the direct component (*d*) of the 3-phase method ($V_dTD_dS_{ds}$) and subtracting it from the already computed 3-phase method process.
2) Calculating the direct sun (*ds*) contribution by generating a coefficient matrix for direct sun (C_{ds}) and a sun matrix (S_{sun}) that maps all sun positions and energy in the sky. The final direct sun contribution matrix ($C_{ds}S_{sun}$) results from multiplying C_{ds} and S_{sun}. Finally, the direct sun contribution is added to the previous step.

Figure 2-6 and equation (2-3) summarizes the extension introduced by the 5-phase method to the 3-phase method.

$$E \text{ or } L = VTDS - V_dTD_dS_{ds} + C_{ds}S_{sun} \quad (2\text{-}3)$$

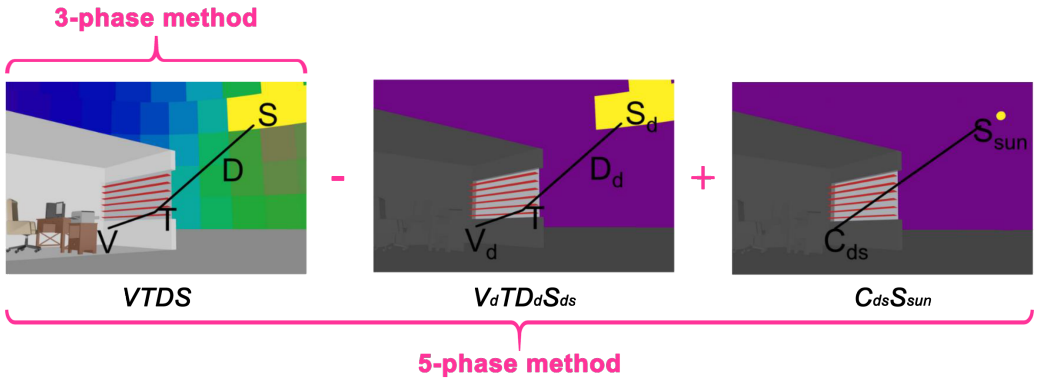

Figure 2-6. Extending the 3-phase to the 5-phase method. Image adapted from Subramaniam (2017).

Photon mapping and the 3- and 5-phase methods require a high degree of expertise. Although they support any kind of daylight simulation, designers need to have programming skills to use them. For that reason, architects default to the two-phase method's front-end applications supported by easy-to-use modern Graphical User Interfaces (GUI), e.g., DIVA for Rhino (Jakubiec and Reinhart, 2011). Typically, designers and building performance analysts limit the use of the 3- or 5-phase and photon mapping methods to cases that demand their application, such as in the study of optical CFS. Additionally, such simulation modeling methods still entail slow run times. For example, parametrically generating custom BSDF data for the 3- or 5-phase methods is still computationally expensive. Nevertheless, if such data is already available, whether through physical measurements or pre-computed BSDF files, the calculations of the 3- or 5-phase methods are reasonably fast to run in current Central Processing Units (CPU) architecture (Zuo et al., 2014).

The use of such powerful simulation techniques would greatly help designers in the early design of sophisticated building skins and architectural screens. Currently, there is still a considerable gap between the ease with which a designer generates a highly complex building skin using modern Visual Programming Languages (VPL), like Grasshopper for Rhino (McNeel and others, 2017), and the difficulty and amount of expertise required to simulate it.

In sum, although Radiance is primarily a backward raytracing engine, it is the benchmark lighting and daylighting simulation tool. This light simulation engine is the most used by architects and building designers to simulate daylight in buildings (Reinhart and Fitz, 2006; Kota and Haberl, 2009; Ochoa, Aries and Hensen, 2012; Jakica, 2018). Daylighting methods based on DC enable Radiance and other Radiance-based tools to perform annual dynamic daylight simulations based on typical meteorological data. Bidirectional ray tracing extensions to Radiance enhanced the software with the necessary forward raytracing capabilities to simulate specular CFS. Additionally, EnergyPlus can use Radiance textual simulation output to improve its ability to determine lighting and thermal loads. For those reasons, the research conducted in this dissertation will use Radiance or Radiance-based tools (e.g., DAYSIM) as the primary support for the development of alternative daylighting analysis and modeling techniques.

2.3 Computational building design supported by daylighting and whole-building energy simulations

As argued in chapter 1, section 1.7, digital computational design consists of using computer algorithmic capabilities to support and develop design. Thus, the use of thermal and daylighting simulations performed by computer programs in the design of high-performance buildings is, in a sense, a computational expression of performance-based design (Oxman, 2008; Zhao and de Angelis, 2019; BuHamdan, Alwisy and Bouferguene, 2020). The information generated by those types of computer simulations provide useful feedback to different building design workflows. The following sections discuss the integration of thermal, whole-building energy, and daylight simulations of buildings in computational design processes. They analyze and debate different workflows, computational methods, and correspondent applications.

2.3.1 Integrating daylighting and building energy simulations in computational building design workflows

The primary goal in using daylight and thermal computer simulations in building design is to assess the current performance status of a design (i.e., evaluate whether the solution complies with pre-established criteria) and move the design process towards a high-performance solution. In other words, architects and other building designers use such simulations to progressively improve the design's thermal, energy, and daylight performance and if possible or desirable, move towards an optimal solution. Building design supported by daylight and whole-building energy simulations can assume three forms: (i) iterative design and analysis (IDA), (ii) parametric design and analysis (PDA), and (iii) performance-based generative design (PGD).

A manual IDA workflow consists of a cycle in which a designer iteratively executes the following tasks: (i) model a building solution, (ii) simulate its thermal, energy, and daylight performance, (iii) analyze the simulation results, and, based on the analysis, (iv) decide whether to confirm the design solution or to refine it by repeating the same process. Although IDA provides useful feedback to the design process, its modeling-simulation-analysis-remodeling cycles are tedious, inefficient, and time-consuming (Zhao and de Angelis, 2019). Moreover, the success of this approach in finding high-performance solutions depends heavily on the designer's knowledge in both using the computational tools involved in the process and processing the simulation output into meaningful information. Figure 2-7 illustrates the IDA process.

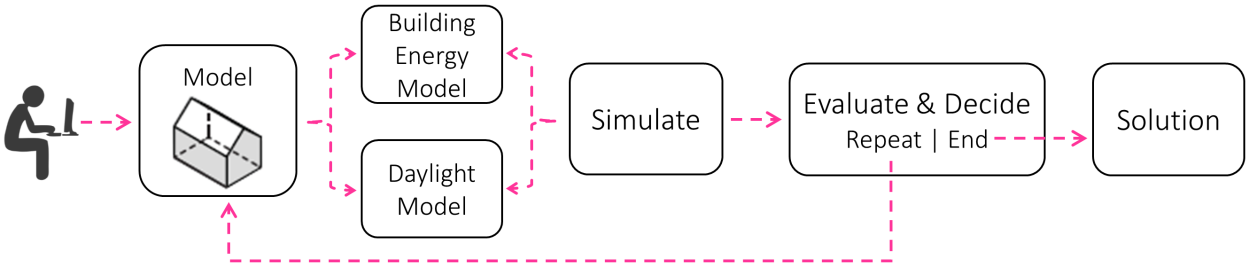

Figure 2-7. The iterative design process of performance-based building design supported by whole-building energy and daylighting simulations. The user needs to manually intervene in every step of the process.

PDA expands the iterative process by automating the modeling and simulation tasks. These types of design workflows combine a parametric model, which describes a design symbolically using parameters (Caetano, Santos and Leitão, 2020), with simulation programs. In this type of modeling process, the parametric model receives parameter inputs, provided either by the user or automatically generated by a script, produces a design instance, and then sends it to the simulation engine, which in turn evaluates it. This enables the prompt generation and evaluation of a plethora of design alternatives (BuHamdan, Alwisy and Bouferguene, 2020) that are part of the design solution space – i.e., the set that encompasses all combinatorial solutions that the parametric model is able to produce. Consequently, PDA increases the probability of finding design solutions that yield acceptable daylight, thermal, and building energy performance.

PDA also supports sensitivity analysis. For a successful sensitivity analysis, the parameters encoded in the parametric model need to express relevant aspects to the thermal and daylighting performance of buildings, e.g., building form and orientation, fenestration geometry, building materials. Sensitivity analyses are essential to understanding the design performance domain and

identifying key design parameters in the overall building performance. They are also beneficial in isolating the model parameters that have a negligible impact on building performance (Menberg, Heo and Choudhary, 2016). Sensitivity analyses are also powerful methods to detect modeling errors, identify poorly modeled components, and improve our understanding of the relationship between model inputs and predicted outputs (Mara and Tarantola, 2008).

PDA sensitivity analysis entails the following steps: (i) determine input parameters variations; (ii) use a parametric model to generate simulation models, (iii) simulate the models, (iv) run sensitivity analysis, and (v) analyze sensitivity analysis methods (Tian, 2013). There are two types of sensitivity analysis, local and global. The local approach studies the effects of uncertain inputs around a base case, whereas global methods measure the influence of the uncertain inputs over the whole design solution space. Although global methods are preferred, local methods are more common since they are faster to perform, do not require specific expertise to use, and produce outputs that are easier to understand by non-experts in building performance analysis (Menberg, Heo and Choudhary, 2016). Global sensitivity analyses include meta-modeling approaches supported by regression-, variance-, and screening-based methods. For detailed information about these methods in energy-efficient building design, the reader can refer to the work of Tian (2013), Nguyen and Reiter (2015), Menberg, Heao, and Chodhary (2016), and Kristensen and Petersen (2016).

PDA approaches are more efficient than IDA workflows in the design of high-performance buildings. They help designers explore the design solution space better and faster, and consequently expand their understanding of key factors to building performance. Nevertheless, PD presents two main limitations. One is that PD does not fully support the search for near-optimal design solutions since it depends on sampling procedures that are either manually defined by the user or supported by an algorithm that randomly samples the solution space. The lack of a guiding principle or a well-defined goal to steer the search makes PDA ill-equipped to efficiently improve a design's predicted performance. Even the automated sampling commonly used in global sensitivities analysis are methods that aim to enhance our knowledge about the design problem, not to search for high performing solutions. The other limitation relates to PD's greatest benefit – promptly generating design variations. It is well-known that human beings have limitations when making decisions about large amounts of information. This limitation is particularly evident if the data available includes several competing factors and conflicting objectives, which is often the case in performance-based building design (March and Simon, 1958; Daru and Snijder, 1997; Zhao and de Angelis, 2019). March and Simon (1958) showed in their economic studies that people can only consider a few decision factors at a time and tend to stop gathering or analyzing information as soon as they feel they have enough to make some sort of decision. Moreover, people are biased in their analysis and decision-making processes. Designers' tendency to stop analysis and search tasks using parametric approaches as soon they hit an acceptable solution leads to a suboptimal use of PDA approaches in performance-based design (Daru and Snijder, 1997).

PGD approaches support more efficient design exploration methods. They integrate optimization techniques, commonly used in the field of Operations Research (OR) to automate and steer the search procedure in the design-analysis workflow. Typically, the computational implementation of PGD methods are tools called *Performance-based Generative Design Systems* (PGDS). PGDS invert the performance-driven design workflow, based on iterative trial-and-error cycles, in a process named *inverse-design* or *goal-oriented design* (Monks, Oh and Dorsey, 2000). The

inversion of the design workflow consists of first describing the design problem (e.g., geometry, materials, variable parameters, and their possible domains and constraints), and then establishing the desired building performance goals. Based on that information, the system will search for a solution that best matches the desired performance criteria in the feasible solution space.

The general search protocol entails the following steps: (i) the PGDS generation module, which typically consists of a parametric building model, produces an initial design solution; (ii) the solution is evaluated by the PGDS evaluation module supported by a simulation software; (iii) an objective function is generated that describes the desired building performance through its minimization or maximization processes the simulation results and returns its output to the PGDS optimization module, typically an optimization metaheuristic (Nguyen, Reiter and Rigo, 2014); (iv) based on the objective function value, the optimization algorithm generates a new design solution using the PGSD generation module, triggering a new cycle. The system repeats this protocol until the optimization process *converges*. The convergence term indicates that the optimization algorithm has reached a final solution. However, because most building optimization processes use heuristic and metaheuristic procedures, convergence does not necessarily mean that the algorithm has found the optimal point (Wetter and Polak, 2004; Nguyen, Reiter and Rigo, 2014). Typically, convergence means that the search hit certain pre-established criteria. For example, a PGDS converges when it executes a fixed number of iterations or, in the case of population-based PGDS (see section 2.3.2 – Metaheuristics), all the solutions generated in a population hit a similarity threshold.

The specific means of generation, evaluation, and selection of design alternatives depends on the optimization algorithm used in the PGDS. Figure 2-8 illustrates the PGDS method applied to the multi-criteria optimization of daylighting and thermal/energy performance of buildings.

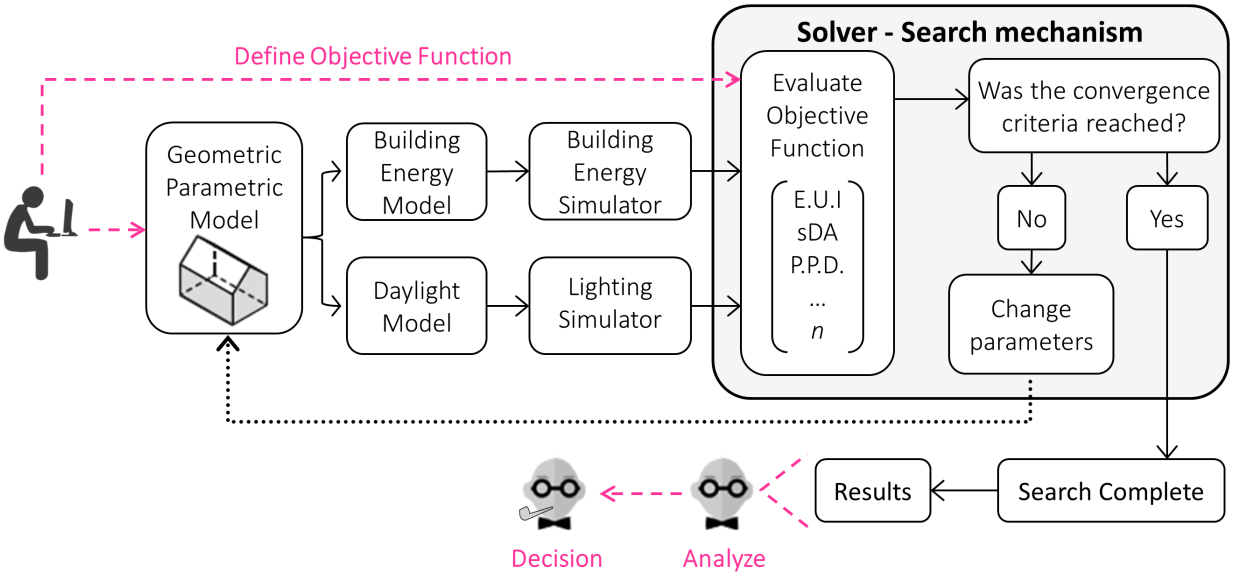

Figure 2-8. Example of a PGDS method supported by daylighting and whole-building energy simulations. The tasks performed by the designer are marked in magenta and consists of the following: (i) defining the parametric geometric and simulation models, (ii) formulating the problem by describing the performance goals and the objective function, (iii) and analyzing and deciding over the results of the automated search. Note that the objective function uses the information provided by different metrics calculated by the simulators – Energy Use Intensity (EUI), spatial Daylight Autonomy (sDA), Percentage of People Dissatisfied (P.P.D) – for illustrative reasons.

Several authors use the term *Building Performance Optimization* (BPO) to describe PGDS workflows. For that reason, this dissertation considers both terms equivalent and uses them interchangeably. Since PGDS are the most advanced and efficient computational design methods in performance-based design, the following sections will briefly summarize optimization techniques and their application in the design of high-performance buildings.

2.3.2 Optimization in performance-based building design

The integration of optimization techniques in goal-oriented building design processes requires the definition of the optimization problem and search algorithm. The modeling of the optimization problem includes the definition of the decision variables, a set of objective or fitness functions to be maximized or minimized, and, depending on the problem, constraints (Wetter and Wright, 2004; Nocedal and Wright, 2006; Belém, 2019).

Equations (2-4) through (2-6) express the generalized mathematical formulation of an optimization problem that either minimizes or maximizes a set of objective functions:

$$\max_{x_n \in S_n}/\min: \quad f_i(x) = f_i(x_1, \dots, x_n), \qquad i = 1, 2, \dots, I \quad (2\text{-}4)$$

$$\text{s.t.:} \quad g_j(x) = g_j(x_1, \dots, x_n) = 0, \qquad j = 1, 2, \dots, J \quad (2\text{-}5)$$

$$h_k(x) = h_k(x_1, \dots, x_n) \leq 0 \vee \geq 0, \qquad k = 1, 2, \dots, K \quad (2\text{-}6)$$

where $f_i(x)$ is the i^{th} objective function of a set of objective functions to be either minimized or maximized. The functions $g_j(x)$ and $h_k(x)$ represent the sets of equality and inequality constraint functions, respectively. The set S_n defines the domain of each design variable, x_n, which can either be *discrete*, *continuous*, or both. When the set of decision variables x contains both discrete and continuous variables, the problem is referred to as *mixed-integer* (Nguyen, Reiter and Rigo, 2014). Objectives and constraints may be interchanged depending on how the problem is defined. If the $f(x)$ set contains only a single objective function, the optimization problem is called *single-objective* and always returns a solution. If the set $f(x)$ contains more than one objective function the problem is then called *multi-objective*. If the set of constraint functions $g(x)$ and $h(x)$ is empty, the optimization problem is *unconstrained*. Otherwise, the optimization problem is *constrained* (Koziel and Yang, 2011).

Continuous optimization problems are easier to solve since they often imply smooth objective functions, a situation which facilitates the prediction of the behavior of the functions around a certain point. In contrast, optimization problems with either discrete or mixed-integer decision variables are more challenging to solve since their objective functions often present irregularities and discontinuities that are difficult to predict (Nguyen, Reiter and Rigo, 2014; Belém, 2019).

In constrained optimization, finding points that satisfy all the constraints is often an ill-defined problem. Since unconstrained optimization does not impose restrictions on the values of the variable, it often poses problems that are easier to solve than constrained ones (Nguyen, Reiter and Rigo, 2014).

Because *Single-Objective Optimization* (SOO) processes evaluate only a single objective function and consequently do not calculate the trade-off front, they are faster and easier to solve than *Multi-Objective Optimization* (MOO) procedures.

Typically, the optimization of energy and daylight simulated performance of buildings is a complex and challenging task since the optimization problems are often mixed-integer, constrained, and multi-objective.

To reduce the complexity of a constrained optimization problem, it is common to transform it into a penalized unconstrained problem, in which values of the penalties values will vary according to the violation degree of the constraints (Coello, 2006; Ehrgott, 2006). The penalty approach to simplifying presents two main drawbacks. The first is that sometimes it is difficult to estimate an adequate penalty value. The second is that the use of penalties might introduce bias to specific optimization algorithms (e.g., evolutionary-based population algorithms), therefore affecting their search process.

Goal-programming (Coello, 2006), also known as the *linear scalarization method* (Coello, 2006; Nguyen, Reiter and Rigo, 2014; Wortmann, 2017; Belém, 2019) is a common technique to reduce a MOO problem to a SOO one. The technique weighs the different objectives and combines them into a single objective function, usually through a summation. A SOO algorithm then optimizes the resulting single-objective function. Despite the complexity reduction, the goal-programming approach can include all the performance aspects involved in the problem. Equation (2-7) illustrates how the goal-programming approach reduces several objective functions into one using weighting factors and a summation. The weight factors (w_i) assigned to each objective function (f_i) represent their relative importance to the designer and must be set during the formulation of the optimization problem.

$$\max_{x_n \in S_n} / \min \sum_{i=1}^{n} w_i f_i(x_1, \dots, x_n), \quad (2\text{-}7)$$

Although goal-programing is more computationally efficient than MOO methods, it presents several limitations to the search and optimization outcome. Determining an adequate distribution of weighting factors is a non-trivial task. It usually depends on the designer's expertise and often it is done *ad hoc*. The problem is more challenging when the different objective functions do not have the same metric or significance (Nguyen, Reiter and Rigo, 2014). Hence, weighting factors inevitably introduce bias in the search process (Coello, 2006; Nguyen, Reiter and Rigo, 2014). Additionally, when dealing with multi-criteria problems with competing factors such as those that involve the thermal and daylight performance of buildings, it is wise to think about the solution's performance in terms of trade-offs.

An approach that adequately addresses the multi-criteria of MOO is *Pareto optimization*. This method uses the concept of Pareto optimality to examine all possible trade-offs to determine the set of *non-dominated* solutions, also called a *Pareto-front*. A solution is a non-dominated one if there is none of the objective functions left that can be improved without worsening the others (Coello, 1999; Caldas and Norford, 2003b). *Multi-criteria decision-making* is the process of selecting a solution from the Pareto-front. This process is non-trivial, as it depends on several

aspects related to the specificity of the problem, such as the significance of objective functions to designers and building investors (Nguyen, Reiter and Rigo, 2014). In cases where the objectives are equally relevant, a common method consists of finding the closest Pareto-front point to the *utopia point*. The utopia point is a fictitious point whose position corresponds to the coordinates of the best solutions in each individual objective. Figure 2-9 presents the selection process based on calculating the Euclidean distance to the utopia point in a minimization dual-objective optimization.

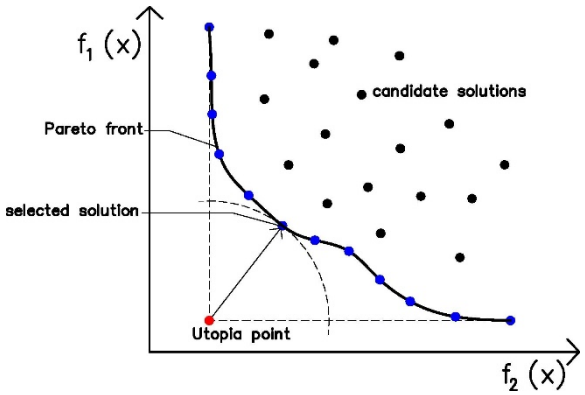

Figure 2-9. The selection of the solution from the Pareto front that is closest to the utopia point. Image source: Nguyen, Reiter, and Rigo (2014).

The efficient handling of mixed-integer or discrete optimization problems depends heavily on the optimization algorithm. Because BPO usually uses simulated data performed by a third-party program (simulator), it is difficult to establish a mathematical relationship between objective function behavior and decision variables or design parameters. The lack of a clear mathematical relationship hampers the collection of essential information about the gradient of the objective function that would greatly facilitate optimization. For this reason, BPO typically uses derivative-free optimization algorithms (Wortmann et al., 2017), also known as global *black-box optimization* algorithms since they do not require any information about the objective function gradient. There are three main types of derivative-free optimization algorithms: (i) direct search, (ii) metaheuristics, and (iii) model-based algorithms. The following paragraphs provide a summary of the different types of derivative-free optimization algorithms.

Direct search

Direct search methods, also known as trajectory search, seek to approach the optimal point by iteratively replacing the current point location (i.e., design solution) in the design space based on rules that determine where the optimization procedure will execute the next trial. The goal is to find a feasible point for which performance cannot be further increased (maximization problem) or decreased (minimization problem). The main difference between the different direct search algorithms is the method used to search for neighboring points, which determines the step-size of the search. The most common search algorithms applied in BPO include Simplex-based methods, such as the Nelder-Mead algorithm, and (ii) Pattern search algorithms such as coordinate search and the Hooke-Jeeves algorithm. For detailed information about the Nelder-Mead, the coordinate search, and the Hooke-Jeeves algorithm, the reader should refer to Nelder and Mead (1965) and Polak and Wetter (2003), respectively.

Metaheuristics

In optimization, a metaheuristic is a high-level procedure designed to find a heuristic that is able to deliver a good solution to an optimization problem. Mostly used in combinatorial optimization, they are problem agnostic and non-deterministic. Thus, it is possible to use a metaheuristic to any search problem. However, they do not guarantee that the search process will find a global optimum. The goal of using metaheuristics is to efficiently sample and steer the search of large design solution spaces towards near-optimal solutions (Blum and Roli, 2003). Optimization metaheuristics are the most prevalent in BPO and include a large number of algorithms. They can be grouped in the *trajectory search*, *stochastic population-based*, and *hybrid algorithms* families (Nguyen, Reiter and Rigo, 2014).

Trajectory search metaheuristics aim to provide sampling methods that prevent the search process from becoming stuck at local optima. These types of algorithms are best suited to handle discrete optimization problems. Simulated Annealing (SA) and Tabu Search (TS) are the most common trajectory search algorithms used in BPO. If the reader is interested in knowing about these algorithms in detail, the author recommends the reading of Brooks and Morgan's (1995) work on SA and Glover and Laguna (2013) on TS.

Natural processes directly inspire stochastic population-based algorithms. Such algorithms are usually based on a rolling population of individuals or agents. There are two main groups of algorithms: population-based metaheuristics based on social or cultural processes, and Evolutionary Algorithms (EA).

Population-based metaheuristics based on social or cultural processes take inspiration from social behavior or production (culture) of animals, insects, and humans. *Particle Swarm Optimization* (PSO), *Ant Colony Optimization* (ACO), and *Harmony Search* (HS) are the most common algorithms in BPO.

Eberhart and Kennedy (1995) modelled PSO after the social behavior of birds flocking or fish schooling. A solution is called a “particle,” and a set of particles is called a “swarm.” PSO begins with a group of random particles and then searches for the optimal point by generating and updating swarms. The algorithm collects the objective function evaluation done by the particles and uses it to update existing swarms and generate new ones. Wetter and Wright (2004) provides a full description of the PSO search process.

ACO (Dorigo, Maniezzo and Colorni, 1996) traces a direct analogy to the process by which ants deposit pheromones on paths to encourage other ants to follow. Similarly to PSO, ACO begins to create agents “nests” (“ants”) in random positions in the design space. The “ants” depart from the “nest” searching for a position in the solution space that yields better fitness values. For each position, they leave a “pheromone” representing a probability value calculated using the objective function. Such marks bias the selection of future nests. For more details about the ACO algorithm the reader should refer to Dorigo, Maniezzo, and Colorni (1996). ACO handles discrete optimization problems well, but it presents some difficulties in continuous search spaces (Song, Chou and Stonham, 1999).

HS (Geem, Kim and Loganathan, 2001) is inspired by the working principles of harmony improvisation in music. Depending on the evaluation of the objective function, HS measures

design solutions in terms of "harmony." It involves the following steps: (i) Initialize a Harmony Memory (HM), i.e., a set of random "harmonies" (design solution performance) produced by a set of "instruments" (decision variables); (ii) Improvise a new harmony from HM by recombining the sounds that each "instrument" produces; (iii) if the new harmony is better than the best harmony in HM, the process replaces the old harmony in HM with the new one; (iv) if the process did not converge, it repeats the cycle from step (ii) (Geem, Kim and Loganathan, 2001). The algorithm maintains a rolling population of best solutions through the several iterations (Evins, 2013). Comprehensive literature reviews by Geem et al. (2001) and Evins (2013) on optimization methods applied to sustainable design provide more details about HS algorithms.

Evolutionary algorithms (EA) are metaheuristics directly inspired by Darwinian concepts. EA methods select high-performance individuals to reproduce new individuals based on their performance fitness. Since EAs are the most prominent approaches in BPO, it is worth presenting a more detailed summary of the EA general search process.

In EA, a chromosome, i.e., a finite length vector of genes that encode the decision variables, represents an "individual," i.e., a design solution. Alleles – i.e., the possible values of a gene – encode each gene (Goldenberg, 1989). A typical evolutionary algorithm generates a new population by using three operators: selection, crossover, and mutation. First, the algorithm randomly generates a series of "individuals" as the initial population. Then the algorithm evaluates their fitness by using the information provided by the objective function for each "individual." The selection of "individuals" for breeding and mutation is executed according to their fitness, meaning that individuals with higher fitness have a higher probability of being selected. The selected "individuals" are then used for inbreeding or mutating to reproduce new individuals that will form the next generation. Inbreeding is performed by the cross-over operator, which randomly selects two parts of the "parents" chromosomes and swaps them. Mutation randomly changes part of an "individual" to generate a new chromosome (Caldas and Norford, 1999). The new population then goes through a new round of selection. The algorithm repeats the process until it converges, which usually occurs when all the individuals of the same population yield the same fitness value or if a limit of generations is reached (Huang and Niu, 2016).

The most popular EA are Genetic Algorithms (GA). GAs use a linear binary data structure, which is usually an array of bits, but other types and structures can be used in the same way. The binary representation facilitates the cross-over operation because the different parts of the chromosome are aligned according to their fixed size. There are several types of GAs, but the most common in BPO are the Non-dominated Sorting Genetic Algorithm II (NSGA-II) (Deb et al., 2002) and the Strength Pareto Evolutionary Algorithm 2 (SPEA-2) (Ziztler, Laumanns and Thiele, 2002), both multi-objective GAs.

Several literature surveys show that GAs, and their modifications, are the most-used search algorithms in BPO. In Evins (2013), 50% of the works cited used GA. Nguyen et al. (2014) reported that in more than 200 BPO studies, 40 used GA followed by 13 PSO studies. Huang and Niu (2016) highlight that slightly more than 60% of the studies included in their review are GA-based. The causes for this popularity are directly related to the nature of the environmental building performance optimization problem based in computer simulations.

The problem of building optimization problems supported by building performance simulation software is discontinuous and multimodal, i.e., with multiple local optima (Wetter and Polak, 2004; 2004). This is for two reasons: (i) when describing the problem, the designer or analyst must sometimes assign discrete values to design parameters (e.g., a list of building materials), which may lead to a disordered and discontinuous output, (ii) the nature of the algorithms used in detailed building simulation engines. For example, discontinuity in EnergyPlus outputs is likely caused by empirically assigned inputs (e.g., wind pressure coefficients) in adaptive solvers with loose precision settings or in iterative solvers that use a convergence criterion, e.g., Warmup Convergence algorithm (EnergyPlus, 2017). In daylight simulations, the discontinuities in the solution space problem can be introduced in the case of small variations of highly specular shading or light redirecting systems. A small deviation of the normal direction of the reflective surfaces affects light bouncing and, therefore, the position of reflected rays of light.

Building energy or daylight simulation programs are also black-box functions in BPO, which makes gradient or derivable information unavailable for several direct search methods based on gradients (Nielsen and Svendsen, 2002), such as gradient-descent or the Discrete Armijo Gradient algorithm available in the GenOpt optimization library (Nguyen, Reiter and Rigo, 2014). The presence of iterative or heuristic solvers or other types of numerical methods typically produces noise in simulation outputs, which also contributes to the presence of discontinuities and many local optima in a BPO problem (Coley and Schukat, 2002).

The discontinuity of the optimization problem makes gradient-free methods less efficient and prone to getting trapped in local minima. Running multiple searches starting at different points is one way to address this. However, due to time limitations, such a process might not be viable in design workflows and yields a high degree of uncertainty: it is hard to determine the number of starting points and their locations that ensure a good search.

The limitations that trajectory search algorithms have in tackling multimodal and discontinuous optimization problems related to building energy and daylight simulation led to the adoption of stochastic population-based optimization algorithms. From those, GAs are the most attractive for several reasons. First, a GA can handle both continuous and discrete variables. BPO typically has both, which hinders, for example, the use of ACO. ACO does not cope well with continuous spaces, which forces the user to discretize continuous variables for a more efficient search, such as in Song et al. (1999). Second, several comparative studies show that GAs are consistently able to find near-optimum solutions to complex problems and do so faster than other metaheuristic methods, i.e., they require less cost function evaluations (Wetter and Wright, 2004; Tuhus-Dubrow and Krarti, 2010; Bichiou and Krarti, 2011). Third, GAs also proved to be robust and capable of delivering different design alternatives with similar performance, such as in the work of Wright and Mourshed (2009), Caldas and Santos (2012), and Wright and Alajmi (2016). Fourth, GAs are becoming more popular among building designers because of the emergence of several interfaces that allow their use in design. For example, MATLAB provides a GA toolbox and is popular among engineers. Architects and designers are beginning to use more goal-oriented design approaches mainly because a popular 3D CAD software, Rhinoceros, allows the use of an SGA, the multi-objective SPEA-2 and NSGA-II through several libraries available in the Grasshopper Visual Programming Language (VPL).

Despite these advantages, GAs, like other population metaheuristics, have some limitations. Although GAs are considered the fastest of all population-based metaheuristics, they still require a considerable number of evaluations to find a high-performance solution. When the process is based on simulations, namely thermal and daylight evaluations, the search typically takes many hours, thus creating an interruption in which the architect/analyst waits for the result. During a design process, which is heavily based on interactive feedback, it is desirable to minimize this intermission. Additionally, despite GAs being rather effective in finding the region of the global optimum they are often unable to conduct a granular search on that area. Hybrid algorithms are more effective in finding the best candidate on the global optimal region (Polak and Wetter, 2003; Wetter and Polak, 2004; Wetter and Wright, 2004).

Hybrid algorithms typically result from the combination of a stochastic population-based algorithm and a gradient-free direct search algorithm. First, the former executes an initial global search; the latter then performs a refined local search around the solution found by the global search. The most used hybrid algorithm is available in the GenOpt software (Wetter, 2000) and combines the PSO global search algorithm with the Hooke-Jeeves pattern search algorithm (PSO-HJ).

Model-based algorithms

The use of model-based algorithms is relatively recent in the field of BPO. These types of search procedures evaluate design candidates in order to build a mathematical approximation of the unknown black-box objective function. The resulting surrogate model guides the search process towards near-optimal solutions (Simpson et al., 2001; Koziel, Ciaurri and Leifsson, 2011; Wortmann, 2018). The purpose of using surrogate models is to speed up the optimization process by avoiding the need to run computationally expensive simulations every time the optimization algorithm queries the objective function or functions. The development of the model-based approaches to BPO directly addresses the search time problem posed by the common use of population-based metaheuristics, particularly GAs.

There are two ways to use surrogate modeling approaches in BPO. The first is to train a model and then replace the original time-intensive simulation with it. Since the surrogate is quicker to evaluate objective function, it supports faster and more extensive searches. The disadvantage of this approach is that its accuracy depends heavily on the number of pre-simulated points necessary to build the surrogate. A large number of samples imply accurate surrogates but negate the speed advantage, whereas smaller samples result in faster but less accurate surrogates whose inaccurate predictions might compromise the optimization outcome (Wortmann, 2018). To overcome this limitation, several researchers employed different strategies to iteratively improve the accuracy of the surrogate model by evaluating and updating it during the optimization process (Hemker et al., 2008; Zhang et al., 2011; Koziel and Leifsson, 2013; Wortmann et al., 2015). Figure 2-10 shows the difference between a standard optimization process (a) that directly uses a simulation program to obtain information about the objective function, a search procedure that first builds a surrogate that replaces the “accurate” simulation (b), and the progressive approach that refines and improves the surrogate during the optimization process (c).

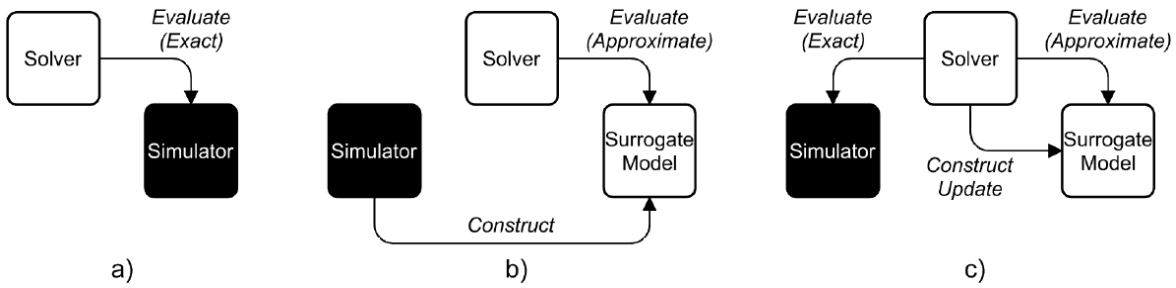

Figure 2-10. Difference between a standard optimization procedure that directly uses the information produced by a simulation engine (a), another that builds *a priori* a surrogate model that replaces the simulation engine in the optimization process (b), and a method that iteratively refines the surrogate model during the optimization process. Image from: Wortmann (2018).

Recent work (Wortmann et al., 2015, 2017; Wortmann, 2018) indicates that model-based methods supported by Radial-basis Functions (RBF) could be better approaches to derivative-free SOO and goal-programming optimization than trajectory search and metaheuristic methods. However, the applications of such model-based methods need to be consistently tested in the solving of multi-criteria BPO problems.

2.3.3 Application of Performance-based Generative Design Systems in sustainable design supported by daylighting and whole-building energy simulations

This section traces an overview of PGDS and BPO application in sustainable building design workflows. Although BPO approaches apply to any discipline involved in the design of high-performance buildings, this section focuses on PGDS fully or partially supported by whole-building energy and daylighting simulations. The literature presents several general reviews of the field (Attia et al., 2013; Nguyen, Reiter and Rigo, 2014; Asadi and Geem, 2015; Huang and Niu, 2016; Shi et al., 2016; Eltaweel and Su, 2017; Longo, Montana and Riva Sanseverino, 2019; Zhao and de Angelis, 2019), demonstrating its increasing scientific relevance to the design research community. The goal of this review is not to provide an extensive and detailed discussion of all the work in BPO and parametric-driven approaches to sustainable design, but to illustrate the evolution of the field and demonstrate its current relevance. To achieve that goal, this chapter entails two parts. The first part discusses the foundational work on BPO approaches to sustainable design. It presents the cutting-edge research conducted at the turning of the twenty-first century that established the field. The second part summarizes the relevant PGDS applications close to and in the present decade, illustrating the field relevance, current approaches, and diversity of applications.

The early years

The adoption of goal-oriented design approaches in energy efficient design is not new. The first attempts date from 1983, when Gero et al. (1983) discussed a simple multi-criteria model to minimize the predicted energy performance of a building. The approach used a mathematical model based on very simplified assumptions to estimate building energy consumption.

However, despite those initial attempts, it was at the turning of the twenty-first century, research related to BPO started to gain more relevance. The development and establishment of sophisticated thermal and lighting simulators such as DOE 2.1, EnergyPlus, and Radiance contributed heavily

to it since they allow the modeling and simulation of a wide range of designs. From those early years, two works on goal-oriented design approaches for sustainable design standout: GenOpt (Wetter, 2000, 2001; Polak and Wetter, 2003; Wetter and Polak, 2004; Wetter and Wright, 2004) and GENE_ARCH (Caldas and Norford, 1999, 2002; Caldas, 2008).

GenOpt is a generic BPO program that can handle any text-based energy simulation software, such as EnergyPlus and Radiance. Wetter (2001) uses GenOpt with EnergyPlus in an optimization experiment that aimed to reduce building energy consumption. GenOpt enables designers to use different optimization algorithms, including GA, direct-search algorithms (e.g., HJ), PSO, and a hybrid optimization technique that combines PSO with HJ. Wetter and Wright (2004) used GenOpt to compare different optimization techniques. The authors reached the conclusion that GA-based approaches are faster in finding high-performing global solutions, but the hybrid PSO-HJ method is more efficient in finding the best performance design.

While the work on GenOpt focused on developing and comparing different search strategies, GENE_ARCH explored the generative potential of PGDS in sustainable architecture. GENE_ARCH is a PGDS for energy-efficient building design that supports SOO and MOO by combining a single-objective GA and a multiple-criteria GA of the Pareto type with DOE2.1 and EnergyPlus (Caldas, 2008). The PGDS was applied to several building energy optimization cases. Caldas and Norford (1999) tested the GENE_ARCH concept in the placing and sizing of windows in an office building. The system aimed to improve the building's thermal and lighting behavior in order to reduce its predicted energy consumption. The same authors also used the system to simultaneously optimize building envelopes and the design and control of HVAC systems (Caldas and Norford, 2003a). The introduction of Pareto-based approaches allowed GENE_ARCH to tackle MOO problems. In Caldas and Norford (2003b), the authors applied the PGDS to the generation of energy-efficient architectural form. The two objectives considered in this work were maximizing daylighting use and minimizing building energy consumption used for conditioning the building. Caldas (2008) fully demonstrated GENE_ARCH capabilities in capturing and manipulating architectural from by applying the generative design system to improve the thermal and daylight performance of a pre-existing building – the O'Porto School of Architecture in Portugal, designed by Pritzker recipient Álvaro Siza Vieira. Caldas and Santos (2012) extended the generative capabilities of GENE_ARCH by combining shape grammars (Stiny, 1980) and GAs linked to energy simulations to the design of energy-efficient Moroccan traditional patio houses. The PGDS was also applied to the optimization of building components. Wang et al. (2016) used GENE_ARCH to select glazing types that promote an energy efficient balance between thermal and daylighting performance, based on a database of the National Fenestration Rating Council (NFRC).

Audioptimization, (Monks, Oh and Dorsey, 2000), and eifForm, (Shea and Cagan, 1997, 1999; Shea, 2000; Shea, Aish and Gourtovaia, 2005) are other PGDS that appeared around the same time as GenOpt and GENE_ARCH. Audioptimization is a PGDS for acoustic-based design and eifForm is a generative design system for structural building design. Although Audioptimization, and eifForm are PGDS applications to building design disciplines that are outside the scope of this dissertation, along with GenOpt and GENE_ARCH they represent the first wave of PGDS, laid down the foundations for subsequent research, and attracted the interest of several researchers in BPO. From those early PGDS, GenOpt and GENE_ARCH are the ones that continue to be further

developed and use, demonstrating the relevance of using generative design approaches to the complex problem of balancing daylighting and energy consumption in buildings.

Recent approaches and applications

Since the early 2000's, several algorithms and methods have been developed, particularly in academia, for building design workflows that are based on daylight, thermal, and energy predicted performance. Nowadays, new programming tools for architectural parametric design (Leitão and Santos, 2011; Celani and Vaz, 2012; Leitão, Santos and Lopes, 2012) are facilitating the integration of BES and daylighting simulation software interfaces (Jakubiec and Reinhart, 2011; Roudsari, Pak and Smith, 2013; Mackey et al., 2015), with optimization algorithms in CAD and BIM environments – e.g., Rhinoceros/Grasshopper (McNeel and others, 2015), Digital Project (Gehry Technologies and others, 2015), and Revit/Dynamo (Keough, 2011; Autodesk, 2020). Thus, the question of using PGDS in the architectural design of sustainable buildings becomes even more relevant.

The current relevance of using computational methods in sustainable building design is also evident in the several general reviews on BPO and PGDS. Attia et al. (2013) review current trends in BPO, and assess the gaps and needs for integrating optimization tools in Net-Zero Energy Buildings (NZEB) design. Asadi and Geem (2014), summarize relevant research applying simulation-based optimization methods to sustainable building design, including a summary of the application of common metaheuristic approaches to different fields of energy-efficient building design. Machairas et al. (2014) present an extensive review of algorithms for building design. Nguyen et al. (2014) focus the discussion on discontinuous multi-modal building optimization problems, the performance and selection of optimization algorithms for building performance, MOO, optimization under uncertainty, and the dissemination of optimization techniques into real-world design challenges. Huang and Niu (2016) analyze the history, current status, and potential of optimal building design supported by building simulated performance. Shi et al. (2016) conduct a literature review on BPO of energy-efficient building design from architects' perspective. The review includes an overview of the origin and development of BPO approaches for minimizing predicted building energy consumption, design objectives and variables in BPO of energy-efficient buildings, whole-building energy simulation engines, the optimization algorithms, and the application of BPO in the design of high-performance buildings. Eltaweel and Su (2017) analyze current parametric design tools in daylighting building design. Longo et al. (2019) review the deployment of optimization techniques to the design and energy retrofitting of buildings. The authors analyze and compare optimization algorithms, common objective functions used in BPO workflows for sustainable design, and discuss the importance of using PGDS approaches to improve the predicted energy use in the life cycle of buildings. Zhao and de Angelis (2019) conducted a general literature review on the use of PGDS in architectural design. The work discusses the use of BPO approaches in the different disciplines that contribute to the design of high-performance buildings, including energy-efficient buildings that benefit from adequate daylighting strategies.

As demonstrated by Longo et al. (2019), the present decade (2010-2020) shows a consistent increase of BPO applied to sustainable building design. This reinforced interest aligns with new governmental directives adopted across the world that establish goals for reducing Greenhouse

Gases (GHG) emissions. Since the building energy use is responsible for significant GHG emissions, the design optimization of energy-efficient buildings has become even more important.

In terms of architectural design strategies, Turrin et al. (2011) discuss the benefits derived from combining parametric modeling and Genetic Algorithms (GAs) to achieve a performance-oriented process in building design. In that work, the authors focus on the key role played by geometry in architecture. Granadeiro et al. (2013) proposed a method to integrate shape grammars and building envelope design using MATLAB and EnergyPlus. As already mentioned, Caldas and Santos (2012) had previously incorporated the generative systems of shape grammars in GENE_ARCH. Approaches that aim specifically at building form and layout include the work of Zhang et al. (2016). In that work, the authors developed a multi-criteria PGDS that optimizes free-form building masses to simultaneously maximize space efficiency (i.e., the ratio between usable space volume and the total volume of the building mass), solar radiation gain, and minimize shape coefficient (i.e., the ratio of the building's area ratio to its inner volume). The work combined a parametric model, implemented using the Visual Programming Language (VPL) Grasshopper, Radiance to perform solar radiation analysis, and a Pareto-based GA.

Konis et al. (2016) applied a MOO framework to improve the predicted performance of passive strategies in the early phases of building design. The proposed PGDS combines parametric building models implemented in Grasshopper, the SPEA-2 algorithm provided by Octopus, an optimization add-on for the Grasshopper environment, with DAYSIM and EnergyPlus. Additionally, the proposed framework is able to automatically model the context of the hypothetical building, given a specific location. To that end, the system uses the CADtoEarth Geographical Information System (GIS). The proposed MOO aims to simultaneously maximize daylight use and minimize building energy consumption. Chapter 7 provides more details about the daylighting metrics used in this work.

Zhang et al. (2017) extended the MOO approach previously proposed in Zhang et al. (2016) to optimize the predicted thermal and daylight performance of a school building in a cold region in China. The work aimed to find the best passive design parameters for each typical spatial configuration of Chinese elementary and high schools. Dino and Üçoluk (2017) presented a MOO approach that combines SOO and MOO in the same workflow. The tool first uses a single-objective GA to generate and optimize near-optimal building layouts according to pre-established formal, topological, and orientation criteria. Then, the system uses a Pareto-based GA to search for different combinations of fenestration positioning and size that promote a good balance between daylighting and thermal building performance.

Regarding decision-making support, Diakaki et al. (2010) propose a multi-objective decision model that aims to simultaneously reduce the predicted building's annual energy consumption, carbon footprint, and initial investment cost. The same authors extended their multi-objective mathematical programming method to select among different energy efficiency measures, considering both energy savings and construction cost. Basbagill et al. (2013; 2014) propose a MOO for reducing the life-cycle environmental impact and cost performance of buildings in conceptual design stages. The authors explore the concept of Multidisciplinary Design Optimization (MDO) already used by Flager et al. (2009) in the multi-objective optimization of a classroom's structural and energy performance. Lin and Gerber (2014b, 2014a) focus on early-stage design decision processes by proposing an MDO framework for concept design that uses a

standard GA for design and performance optimization. The work demonstrates the impact of applying this process to reduce predicted energy use intensity (EUI) at early-stage architectural design, and identifies performance feedback criteria for MDO design and implementation. Welle et al. (2014) developed a CAD-centric Attribution Methodology for Multidisciplinary Optimization Environments (CAMMOE). The proposed method enables designers to improve the accuracy of optimization processes by assisting them in the development and analysis of alternative solutions. In earlier work, Welle et al. (2011) presented ThermalOpt, a BIM-based methodology for multidisciplinary thermal simulation intended for use in MDO environments. Brown and Mueller (2016) also advanced an MDO model for the early design phases supported by structural and building energy analysis. The structural optimization objective was to minimize the amount of steel required, whereas the goal of the energy optimization was to reduce the building's annual energy in terms of lighting, heating, and cooling. The authors used the NSGA-II algorithm to approach the Pareto front over several generations of design alternatives of three types of large steel span structures. The utilized span structures were the following: (i) a trussed arch, (ii) a "PI" structure composed by two columns and a spanning truss, and (iii) an "x-brace" structure, which consists of three-hinged arch cantilevered roof beams composed by a series of vertical struts. Amer et al. (2020) present a new optimization approach named Multi-Objective Parametric Analysis (MOPA). MOPA conducts an exhaustive sensitivity analysis to identify optimum design variables. The authors apply MOPA in a specific, well-defined MOO problem that aimed to reduce construction weight, building energy use, and *Life Cycle Cost* (LCC). The authors found that MOPA could estimate the Pareto much faster than common MOO approaches in specific applications.

Concerning model-based approaches, Asadi et al. (2014) propose a model-based optimization model that combines the fast evaluation of surrogate models developed using Artificial Neural Networks (ANNs) with the optimization power of GAs. The optimization algorithm is able to quantitatively assess and select, from a set of predefined retrofit actions, the most suitable combination of actions in a building retrofit project. The authors applied the optimization method in the energy retrofitting case study of a school building. The goal was to minimize the building's energy consumption, retrofit cost, and thermal discomfort hours. Wortman et al. (2015) propose a new surrogate-based optimization method. The method interpolates and updates a mathematical model that approximates the behavior of the objective function from data generated during the optimization process. The model-based approach combines Radial Basis Functions (RBF) with different metaheuristics and direct-search algorithms. The authors applied their method to optimize the daylighting performance of a mixed-use high-density church in Singapore. They applied the goal-programming approach to simultaneously maximize Useful Daylight Illuminance (UDI) and minimize Daylight Glare Probability (DGP). Research on this model-based approach continued in a series of comparative studies that compare it with common optimization processes (Wortmann et al., 2017; Wortmann, 2019), which eventually led to the development of an optimization tool for the Rhinoceros+Grasshopper environment called Opossum (Wortmann, 2017). Azari et al. (2016) also proposed a model-based optimization procedure by coupling an ANN with a GA to optimize the building envelope with respect to the energy use and life cycle contribution to the environmental impacts of a low-rise office building in Seattle, Washington.

Building energy retrofit studies also use BPO approaches to develop efficient strategies that significantly improve current building energy use. For example, similar to Asadi et al. (2014), Murray et al. (2014) propose a simulation-based optimization approach for the retrofitting of

existing buildings. The BPO approach uses a simplified and quick simulation method based on degree-days derived from the Chartered Institute Building Services Engineers (CIBSE) Guide TM41, Degree Days: Theory and Application, to predict the overall thermal energy consumption of a building. In order to minimize carbon emissions, payback time, and overall energy consumption, the approach consisted of using a GA to optimize a discrete list of decision variables.

BPO applications for energy-efficient design of residential buildings include several works. For example, Fesanghary et al. (2012) developed a multi-objective optimization algorithm that simultaneously tackles energy efficiency, financial cost, and different environmental impacts measured in CO_2 equivalent (CO_2-eq) emissions. Ferrara et al. (2014) describe a simulation-based optimization method to find the cost-optimal level for a nearly zero energy single-family building in France. Xu et al. (2015) developed a systematic methodology to minimize building heating and cooling loads using a combination of experimental design and non-sorting GAs. The experimental design determines an initial ranked list of design parameters. The GA selects near-optimal sets from the evolving list of building design factors.

In façade performance optimization, Schneider and Donath (2013) proposed a PGDS that varies simultaneously the topological and geometric properties of a façade. Wright et al. (2014) presented a MOO approach to optimize fenestrations. The method divides a building façade into several small, regularly spaced cells and uses a multi-objective GA to minimize energy use and initial capital cost. Using MOO, C. Kasinalis et al. (2014) described a framework for assessing the performance of seasonally adaptable façades. Wadgdy and Fathy (2015) propose a parametric approach to optimize solar screens in hot and dry climates. Using a brute force method, i.e., a technique that evaluates all feasible design solutions, the authors optimized different parameters of a louver-based solar screen. Such parameters include Window-to-Wall Ratio (WWR), screen depth ration, louver tilt angle, and screen reflectivity. Futrell et al. (2015a, 2015b) used GenOpt to optimize the thermal and lighting performance of building envelopes. Chapter 7, section 7.2 – Related Work – provides more details about these two works. Hou et al. (2017) proposed an integrated building envelope design workflow that uses the Rhinoceros+Grasshopper platform to control EnergyPlus, DAYSIM, and the MOO algorithm SPEA-2 optimization. Such workflow aimed to simultaneously minimize total annual space thermal loads, envelope construction cost, and maximize UDI in the illuminance range of 100 to 2000 lux. Rodrigues et al. (2018) applied automated sensitivity analysis techniques to generate and simulate large datasets of construction specifications for lightweight building envelopes. The goal was to find the best combination of construction assemblies that are energy-efficient for desert-like climates. The approach uses regression techniques to correlate geometric and construction solutions generated by the system and their energy performance.

In the field of daylighting design, several PGDS approaches have been advanced, including the ones proposed by Torres and Sakamoto (2007), Rakha and Nassar (2010, 2011), Lartigue et al. (2014), the already mentioned works of Futrell et al. (2015a, 2015b) and Wortmann et al. (2015), Caicedo and Pandharipande (2016), Manzan and Clarich (2017), Mangkuto et al. (2018), and Kirimtat et al. (2019). Chapter 7 discusses these works in more detail in section 7.2 – Related Work. The same section of chapter 7 gives special attention to LightSolve (Andersen et al., 2008; Andersen, Gagne and Kleindienst, 2013; Andersen, 2015), a comprehensive, goal-oriented design expert system focused on daylight dynamics that is able to balance solar gains, illumination, and glare levels in buildings over the course of a year.

2.3.4 Application of Parametric Design and Analysis (PDA) and Building Performance Optimization (BPO) approaches in real-world projects

Although PDA and BPO approaches have been more prevalent in academia, there are examples of real-world projects that apply such methods in the design of sustainable buildings. Nevertheless, most of the existing examples refer to high-end buildings designed by well-established and large architectural firms. Typically, such cases involve highly specialized in-house teams, such as BIG Compute in Bjarke Ingels Group (BIG), the sustainable engineering group in Skidmore, Owings, and Merril (SOM), the sustainability team of UN Studio, AEDAS environmental analysis team, Zaha Hadid Computation and Design (co|de) group, and others. The out-sourcing of specialized building consultancy firms, such as Arup, Atelier Ten, Transsolar, Integral Group, Loisos+Ubbelohed, Lam partners, and Thornton Tomasetti, is common as it complements the degree of expertise of design teams in implementing such design workflows.

Despite the fact that PDA approaches are less effective than BPO methods, the former continue to be more used because they require less expertise, and they typically are faster than BPO workflows since they involve fewer performance evaluations. The following discusses selected examples that illustrate different applications of PDA and BPO in the design of sustainable buildings.

Examples of PDA include the collaboration between BIG and Arup that won the National Library in Astana, Kazakhstan competition (BIG, 2009). The project consisted of a Moebius strip with a perforated skin that directly responds to the variations of incident solar irradiation and self-shading. Regarding solar responsive screens, AEDAS (2012) designed a responsive façade system for the Al Bahar Towers (Abu Dhabi). Several parametric explorations supported the design of a sophisticated kinetic shading screen that responds to the different solar and light conditions. Daylight and solar radiation simulations informed the design process. The shading screen applied to the towers can reduce up to 50% of solar gains, thus reducing the energy employed in conditioning spaces.

SOM used similar approaches in the design of the BBVA bank operations in Mexico City (SOM, 2015a). The project involved building energy modeling to support the design of the façade and its shading devices. The exploration and analysis of different design alternatives led to 34% of energy savings compared with initial design attempts and the baseline building that follows ASHRAE standard guidelines (ASHRAE, 2013). SOM utilized sophisticated daylight analysis, including glare evaluations in the extension of the Christ Hospital in Cincinnati, Ohio (SOM, 2015b). The project aimed to achieve high visual and thermal comfort standards and, as a result, obtained LEED Silver accreditation. SOM also uses whole-building energy simulation in PDA workflows. The design of the U.S. Air Force Academy Center for Character and Leadership Development located in Colorado Springs, CO, USA, combined advanced simulation techniques such as Computational Fluid Dynamics (CFD), EnergyPlus BEMs, and Radiance daylighting models to design a high-performance façade and optimize the performance of several building systems (SOM, 2016).

The consultancy firm Loisos+Ubbelohde (L+U) provided comprehensive parametric daylighting analysis, particularly on visual comfort, sun control, and daylight and illumination in the retrofit of Facebook buildings MPK 20 (L+U, 2015) and MPK 21 (L+U, 2018), both located at Menlo Park, CA, USA. Gehry and Partners was the architectural firm responsible for the overall project.

The work used Radiance-based approaches in the design and analysis of skylights, glazing selection, and control of shading devices.

Shigeru Ban architects with Transsolar designed a sophisticated building skin for the free-form building of the Swatch Omega Headquarters, located in Bienne, Switzerland. The design and analysis of the building involve parametric analysis using BEMs, and solar radiation simulations, to achieve an energy-efficient and comfortable building. The building envelope design included selecting high-performance glazing, testing shading devices between glass panels, assessing the thermal resistance of the building envelope, and distributing photovoltaic (PV) panels (Transsolar, 2019).

UN Studio is an architectural firm that uses BPO approaches in the design of sustainable buildings. The firm used multi-objective GAs in the design of a tower for Paris, France, called the *Tour Bioclimatique*. The approach used Rhino+Grasshopper to combine parametric models with the SPEA-2 optimization algorithm in the optimization of the overall shape of the building and the resulting façade system in terms of wind flow, sun angle, and view orientation (UN Studio, 2011). UN Studio used similar methods to optimize the integration and distribution of PV panels and maximize the diversity of the façade using a small number of façade panels (UN Studio, 2013). The design of the Singapore University of Technology and Design utilized a PGDS based on GAs to create a glare-free environment by optimally positioned horizontal shades to reflect and diffuse daylight into the interior spaces (UN Studio, 2015).

From this shortlist of illustrative projects, the only unbuilt projects are the National Library in Astana, Kazakhstan (BIG, 2009), and the Tour Bioclimatique (UN Studio, 2011). These examples show that the PDA and BPO supported by daylight and building energy analysis are becoming a part of the design practice. These examples also suggest that it is a question of time for a broader adoption of PDA and BPO methods supported by daylight and building energy simulations in the design of sustainable buildings. The work presented in this dissertation contributes to facilitating such adoption.

2.4 Concluding remarks

This chapter presented a comprehensive review of the main topics and technical aspects approached by this dissertation. The discussion covered two fields essential to building design that is supported by daylighting and whole-building energy simulations: (i) the simulation of the thermal, energy, and daylighting behavior of buildings using digital tools, and (ii) the integration of such simulation processes in computational design workflows.

The study of current modeling processes for daylight and building energy simulation provides an essential background for specific research tasks conducted in this dissertation, particularly the ones presented in chapters 5 and 6. The work presented in those chapters focuses on developing alternative modeling strategies that either replace, complement, or simplify current simulation-based processes. To better ground the work presented in chapters 5 and 6, this chapter has provided a complete understanding of the fundamental concepts and computational tools that translate light and thermal building physical phenomena. The chapter summarized the main modeling methods that support thermal and daylight simulation, giving particular emphasis to white-box modeling approaches, since they are the most prominent and practicable simulation methods used in early

design phases. The discussion addressed the different requirements and modeling techniques involved in the simulation of heat transfer and light transport in buildings. The review also supported the choice of EnergyPlus and Radiance choice as the main simulation tools for thermal and daylight simulation used in this dissertation. EnergyPlus accurately models all the heat transfer modes (conduction, convection, and radiation) in a building, whereas Radiance is the "gold standard" for daylighting simulation. Both simulation engines are validated and continue to be incrementally updated and extended. Additionally, from the thermal and BES and lighting programs currently available, EnergyPlus and Radiance are the most used by designers and building analysts, primarily because of the several interfaces that enable their use from a CAD and BIM platform.

This chapter also reviewed current methods and practices regarding the integration of BES and daylighting software in computational building design processes. The review identified and defined three main performance-based workflows for sustainable building design: (i) Iterative Design and Analysis (IDA), Parametric Design and Analysis (PDA), and (iii) Performance-based Generative Design (PGD). The discussion summarized the advantages and disadvantages of each workflow, highlighting the benefits of PGD and the subsequent use of Performance-based Generative Design Systems (PGDS) and Building Performance Optimization (BPO). To demonstrate the benefits of using PGDS and BPO and their increasing importance in scientific literature, the chapter provided an overview of the application of PGDS and BPO approaches in the study and design of high-performance buildings. Despite the extensive amount of work found in the literature and the potential benefits that they show in providing useful feedback into design processes, goal-oriented processes are not widely adopted by the building design community, and are thus largely confined to the academic realm (Attia et al., 2013; Shi et al., 2016; W. Tian et al., 2018). The use of PDA and BPO in the design of high-performance buildings in real-world examples is mostly confined to high-end buildings designed by large architectural firms. Even in those cases, the deployment of PDA and BPO workflows often require the involvement of highly specialized teams. The following chapter discusses the current limitations of both simulation processes and goal-oriented design approaches that hamper their wider dissemination and use.

Chapter 3:
Research Problem

3.1 Introduction

The discussion presented in this chapter further develops the general research problem presented in chapter 1, which is as follows:

It is difficult to simultaneously use design, whole-building energy, and daylighting simulation tools to study crucial aspects related to buildings' energy, thermal, and daylight performance. This limitation hampers their deployment and integration in the early phases of building design, analysis, and performance optimization.

The chapter first draws a background, provides an overview of the problem, and describes the current deployment and integration challenges. The investigation then subdivides the main problem into isolated and well-defined issues that are responsible for the current difficulties in the early-stage design of high-performance buildings. Finally, based on the research problem discussion, the work refines the main research question into specific questions and establishes concrete and well-defined goals for hypothesis development.

3.2 Problem overview and background

The recent increase of Building Energy Simulation (BES) programs, daylighting analysis tools, and black-box optimization methods for popular Computer-Aided Design (CAD) and Building Information Modelling (BIM) platforms promotes the deployment of both parametrically-driven or goal-oriented design approaches in the design of high-performance buildings. The literature review in Chapter 2 traced the evolution and consistent rise of such ancillary methods in architectural design and research.

Despite the remarkable advances in adopting energy and daylighting simulation techniques in building design and optimization, some limitations still hinder the widespread use of such approaches at the early design stages. Although parametric-design and Building Performance Optimization (BPO) based on daylight and BES share the same hindrances, the obstacles are more evident in the case of BPO. As a result, goal-oriented design workflows based on simulated daylighting and building energy performance are not yet widely applied by building designers.

Based on a comprehensive review of 165 publications and 28 interviews with practitioners, Attia et al. (2013) determined that 93% of the BPO applications are academic exercises. Three years later, Shi et al. (2016) reported that only 28% of the literature on building energy optimization refers to real-world building design cases, while 66% are on fictitious buildings, i.e., academic exercises. The survey-based review conducted by Tian et al. (2018) confirms the trend by claiming that, although the literature of the last two decades reports more than 30 optimization tools for energy-efficient buildings, goal-oriented design approaches are not yet widely applied by the building design community. The lack of use of performance-based generative design systems is even more acute in the architectural field. A recent comprehensive literature review on applying optimization in the design of high-performance buildings (Longo, Montana and Riva Sanseverino,

2019) confirms what Attia et al. (2013) reported – that the vast majority of BPO work uses tools and techniques unfamiliar to most architects, e.g., MATLAB.

As chapter 2 shows, there is a significant benefit to using either parametric or BPO processes to reduce predicted energy consumption and improve simulated daylighting performance in buildings in the early phases of design development. For example, the work presented by El Daly (2014), Ercan and Elias-Ozkan (2015), and Wagdy and Fathy (2015) illustrates how BPO and parametric approaches supported by BES and daylighting analysis tools effectively helps architects to develop high-performing design solutions. Thus, when designers decide not to use such methods, they are missing an opportunity to efficiently tackle the complex task of designing high-performance buildings – a view shared by a significant number of BPO experts. The survey conducted by Attia et al. (2013) showed a broad consensus among building energy analysts and BPO experts that optimizing simulated building performance should be a standard activity in the design of energy-efficient buildings. Hence, designers and building performance analysts should plan and deploy such processes early in the design process.

Additionally, the design of a high-performance building based on daylighting analysis and BES entails different and often conflicting objectives. However, the literature shows that Single-Objective Optimization (SOO) procedures dominate (Huang and Niu, 2016) and that most Multi-Objective Optimization (MOO) approaches to building envelope design use different measurements provided by a single analysis tool, either a BES or a daylight simulation software. Huan and Niu (2016) show that 62% of multi-objective approaches to BPO use a single analysis tool. The limited use of performance metrics generated by different dedicated simulation tools results from the lack of better interoperability between various computer applications and the high specialization level of academic researchers. For example, a researcher who is an expert on daylight tends to use MOO in the solving of daylighting problems that involve conflicting objectives such as the maximization of daylight availability while minimizing glare.

In sum, the current status of architectural design based on daylighting and building energy performance simulation unveils problems in the following areas:

1) Deployment and impact – despite the increase of BES and daylighting simulation platforms, parametric and generative design workflows supported by such tools are not yet applied by architects or other professionals of the building design community. Most applications are usually research-based and conducted in an academic setting. As a result, despite their potential in improving current performance-based methods, they have limited impact on real-world design scenarios and, consequently, are not used as essential instruments in the improvement of the built environment.
2) Integration of daylighting and energy analysis in early-stage building design workflows – this problem partially relates to the previous one. Most of the work on parametric design and BPO based on daylighting and building energy simulated performance tends to be either daylight- or energy-related. As a result, there are few guidelines for modeling the simultaneous use of both types of analysis in building design.

The following section further explores these problems by presenting and discussing their causes.

3.3 Problem and related obstacles – identifying the main causes

Related work reports several obstacles that hinder the deployment of parametric and goal-oriented design approaches supported by daylighting and building energy simulated performance. Uncertainty of simulation input data and output (Attia et al., 2013), and the lack of user-friendly interfaces for analysis and optimization (Attia et al., 2013; Shi et al., 2016) are some of the reported issues tackled by current research.

Simulation uncertainty is an inherent problem in digital building performance assessments. However, several modeling guidelines aim to reduce uncertainty in building simulation, such as the ones provided in ASHRAE standards and guidelines (ASHRAE, 2002, 2013) – that address building energy modeling (BEM) –, and in IESNA standards (IESNA, 2012), that focus on annual climate-based daylight simulations. Additionally, at the early design stages, designers do not expect entirely accurate and precise predictions, and some deviation is acceptable. High accuracy and precision are only desirable in later design phases and typically demand model calibration. In initial studies, designers are more concerned about quickly obtaining reasonable feedback from several simulations to inform and support decision-making in design.

Regarding user-friendly interfaces, it is undeniable that in recent years, the building performance research and design community have made efforts to deliver easy-to-use tools for architects and other building designers. Ladybug+Honeybee (Roudsari, Pak and Smith, 2013) for Rhino+Grasshopper and Revit+Dynamo, DIVA for Rhino+Grasshopper (Jakubiec and Reinhart, 2011), and OpenStudio (Guglielmetti, Macumber and Long, 2011) for SketchUp are just a few examples of recent software that interface CAD and BIM tools (i.e., Rhino+Grasshopper and Revit+Dynamo) with EnergyPlus (Crawley et al., 2001), a state-of-the-art whole-building energy program, and Radiance (Ward, 1994), a research grade lighting simulation engine. More recently several packages for single and multi-objective optimization became available to architects. Only in the Rhino+Grasshopper ecosystem is it possible to find several optimization algorithms, namely: Simulated Annealing (SA) and Standard Genetic Algorithms (SGA) in Galapagos, Standard Strength Pareto Algorithm 2 (SPEA2) combined with the Hype algorithm in Octopus (Vierlinger, 2018) plug-in, the Non-dominated Sorting Genetic Algorithm II (NSGA-II) delivered by Wallacei (Makki, Showkatbakhsh and Song, 2020), and model-based optimization approaches that combine Machine Learning (ML) techniques with metaheuristics provided by OPOSSUM (Wortmann, 2017), which couples gaussian-regressors based on Radial-basis Function (RBF) with evolutionary-based optimization algorithms.

However, despite the current effort on addressing relevant limitations, there are still fundamental modeling obstacles that hinder both the deployment and integration of daylighting and building energy analysis in BPO and parametric-based architectural design workflows. Based on the discussion in chapter 2, the obstacles reported in three survey-based reviews, and a comprehensive literature review on simulation-based optimization methods for building design (Attia et al., 2013; Nguyen, Reiter and Rigo, 2014; Shi et al., 2016; Z. Tian et al., 2018), it is possible to summarize three types of limitations or obstacles, as follows:

1) **Obstacles in tool interoperability:** poor interoperability between design, simulation, and optimization tools as well as low flexibility of the different models used to share information – i.e., to be fully or partially reused by the various computer applications

involved in the design process – hinders a smooth and desirable integration of daylight and building energy analysis both in parametric and BPO design workflows. This obstacle mainly affects architects, since it forces them to switch between familiar modeling environments and ones that require expertise that frequently they lack, which is inconvenient and error-prone.

2) **Simulation-related obstacles:** daylighting and BEMs are computationally expensive. Therefore, their use results in long calculation times that are incompatible with design times. Model complexity (e.g., multi thermal zone BEM) and the recent demand for the calculation of advanced performance metrics (e.g., daylight glare probability, climate-based metrics) add to this problem. The impact of time-costly simulations is more acute in goal-oriented design since the search process requires a significant number of evaluations.
3) **Limitations in defining design goals and building performance problems:** setting problems on goal-oriented design workflows is a challenging task. Performance-based building design depends heavily on the boundary conditions imposed by the context and the design brief. The context-based nature of performance-based design hampers the development and use of standard approaches in defining and planning optimization procedures in BPO, particularly objective arrangement, variable types, and constraint violation. The definition of optimization problems is more challenging for architects since it involves a set of skills and techniques that are usually alien to them.

The two first obstacles relate to modeling and analysis tasks in both parametric and goal-oriented design workflows. The third limitation focuses on problem formulation in building design processes based on automated search and optimization.

These three obstacles also generate skepticism among architects, particularly early-adopters, about the usefulness of using daylighting and whole-building energy simulations. In the survey conducted by Tian et al. (2018), most of the architects new to simulation and optimization of building energy performance mentioned that, despite the good outcomes provided by BPO approaches, it was unclear if the time spent in using goal-oriented approaches was worthwhile or not. The following discusses each obstacle in detail.

3.3.1 Obstacles in tool interoperability

Lately, the emergence of different tools/plug-ins that interface CAD and BIM tools with daylighting and building energy simulation programs brought the promise of facilitating the use of building performance analysis in architectural design processes. The integration mechanisms proposed by such tools typically assume two forms. The first form consists of Graphical User Interfaces (GUI) that enable both modeling inputs and collect and visualize simulation results. The second is the use of domain-programming languages that enable parametric modeling for building performance simulation in what is referred to in the literature as *Integrated Dynamic Models* (IDM) (Negendahl, 2015).

At the early design stages, designers favor the use of interface tools with GUIs, and the IDM approaches over other methods based on data exchange schemas, such as the Industry Foundation Classes (IFC) (Bazjanac, 2008), and the green building Extensible Markup Language (gbXML) (Roth, 2014). The purpose of such schemas is to automatically parse information from BIM models to simulation tools. Nevertheless, both IFC and gbXML have limitations that prevent their

successful application at the early design stages. IFC typically requires a level of detail and information incompatible with early-stage design; thus, its use is more common in later stages of the design process where parametric or optimization procedures have less impact. Moreover, IFC parsing methods are not fully automated in particular cases, requiring manual modification of some of the data transformation rules (Bazjanac, 2008). Alternatively, some applications use gbXML to handle early-stage building massing models (e.g. Revit + Autodesk 360). However, such applications provide limited control of the automatically created simulation model. For example, they use opaque heuristics to generate missing data required by the simulation, which augments the associated uncertainty. Additionally, both formats only work with BIM software, are difficult to read and consequently debug, and do not embed best modeling practices, making them fallible, error-prone, and extremely sensitive to geometry input. For these reasons, designers, building performance analysts, and researchers prefer the IDM (Negendahl, 2015) or the plug-in approach since they provide better support in terms of modularity, analysis tool diversity, and feedback between tools.

Despite the considerable improvement brought by daylighting and BES plug-ins and IDM approaches, the integration of the different tools is still partial and, in several cases, fragile, primarily because they use design tools as merely geometric modelers for simulation tools. Hence, in the case of early-stage building design based on BES and daylighting simulations, they force users to model three different representations of the same design separately – one that fully describes the solution's geometry and form, another that fits to a BES program, and another tailored for daylight analysis. Separately describing three different models that represent the same entity is redundant, time-consuming, inconvenient, hard-to-manage, and, consequently, error-prone.

In sum, current tools and approaches for early-stage daylighting and energy-efficient design did not fundamentally change modeling procedures towards integration and full interoperability. Thus, although architects currently do not need to switch between different applications, they still need to switch between different modeling modes.

Differences between modeling requirements and capabilities of the tools involved are the main obstacles in finding common ground that will foster better interoperability. One of the main differences relates to data and information requirements. BEM and daylighting models need some information that typically is unknown or uncertain at early-stage design, e.g., material properties, occupancy and other loads schedules, digital sensors, etc. Usually, either the user provides the extra input data while defining the boundary conditions of the simulation, or the tool uses some assumptions to "fill in the blanks." The former is preferable to the latter since it reduces uncertainty.

Another difference, and the one that poses more difficulties, consists of the disparity of general building representation between design and simulation tools, particularly BES programs. BES has specific geometry representation rules and constraints. For example: (i) curved surfaces, thickness are not allowed, (ii) all surfaces need to be planar and convex, the building envelope needs to be closed, (iii) fenestrations needs to be coplanar with their correspondent wall or roof and cannot produce holes in them. These geometric constraints and limitations do not exist in CAD and BIM tools and are radically different from architectural building representation codes, which make them particularly alien to architects. Even simple building designs require an extensive pre-processing

to fit BEM requirements. Moreover, the parsing of single or complex double-curved building surfaces, easily modeled with any CAD or BIM tool, is particularly challenging. Current geometry export methods based on mesh triangulation typically result in inefficient BEMs that are computationally expensive and difficult to debug.

The geometry parsing of a daylight simulation does not pose a significant obstacle since daylight simulations are not as sensitive to geometry. There are few differences between a daylighting and a CAD or BIM model since validated lighting simulation tools include few restrictions such as modeling glazing assemblies as surfaces without thickness and observing some rules for surface direction. The application of those restrictions to a design model is easy to implement. Nevertheless, current CAD- and BIM-based tools and toolkits for daylighting simulation typically force users to create a separate analytical model.

In sum, current tools do not bridge the different modeling approaches and requirements involved in digital design processes based on building energy and daylighting simulations. They often force the designer to model each performance model separately; a task that constrains the generative potential of online feedback between models, entails a significant amount of effort, is inconvenient, and is susceptible to mistakes.

3.3.2 Simulation-related obstacles

The main obstacle of using validated daylighting and BES in early-stage parametric or goal-oriented building design processes is simulation run time. Detailed BEM and building models for daylight simulation might be computationally expensive. Considering that parametric and optimization studies typically require the evaluation of several design alternatives, the calculation time involved might not be feasible for design practices that use parametric or BPO workflows. Survey-based reviews on design and analysis of high-performance buildings show that designers are aware of this obstacle and consider it as a critical aspect that prevents the widespread adoption of goal-oriented design approaches in practice (Attia et al., 2013; Shi et al., 2016; Z. Tian et al., 2018).

BEM and daylighting building simulation models run time is highly sensitive to the type of calculation task and the model's level of detail. Even with current approaches that use different parallelization techniques, simulation run time can range from a couple of seconds to several hours, depending on those two factors.

In the case of early-stage BEM, simulation run time is very susceptible to the number of thermal zones and geometric detail, i.e., polygon mesh density. The higher the number of thermal zones or mesh faces, the longer the simulation. More thermal zones increase the number of heat balance calculations, which involve the complex computation of heat transfer between different zones. Mesh density impacts simulation time superlinearly (Clarke, 2001; Hensen and Lamberts, 2019) because of the necessary view factor calculations for radiative heat transfer. The mesh density issue is relevant in representing curved and double curved building surfaces in BEM. Current tools use simple surface triangulation to automatically parse such surfaces. As a result, they often produce BEMs so detailed that they are impractical to run (see chapter 5, section 5.4).

Daylighting Simulation Models (DSM) are not as susceptible to geometry detail as BEM. The computational complexity of a DSM increases sublinearly with the number of mesh faces (Ward

and Shakespeare, 1998). The computational time complexity of DSM is sensible to analysis type and simulation parameters. The run time of daylighting simulations based on sensor grids, e.g., horizontal illuminance assessments at work plane height (≈ 0.75 m), is highly sensitive to the number of sensors. In grid-based analysis, the computational time complexity increases considerably in the calculation of annual dynamic daylight metrics, also known as *climate-based metrics*. Analyses that depend on the generation of synthetic High Dynamic Range (HDR) images, such as surface luminance-based studies and glare assessments, entail a higher computational overhead when compared with grid-based analysis. DSM are also very susceptible to simulation parameters, particularly those that control ambient calculation of inter-reflected light in a model and consequently provide accuracy to the simulation. Standards for daylighting simulation (IESNA, 2012) and validation and comparative studies (Reinhart and Breton, 2009; McNeil and Lee, 2013; McNeil et al., 2013; Bellia, Pedace and Fragliasso, 2015; Nathaniel L. Jones and Reinhart, 2015; Jones and Reinhart, 2017) recommend specific guidelines to sensor grid size and simulation parameters that often result in computationally expensive DSM. Nevertheless, significant progress has been made in accelerating illuminance grid-based analysis using the Graphical Processing Unit (GPU) architecture (Nathaniel L. Jones and Reinhart, 2015; Nathaniel L Jones and Reinhart, 2015; Jones and Reinhart, 2017).

Presently, there is an increasing demand for annual visual comfort analysis based on HDR images, a computationally expensive simulation type. For example, the European standard EN 17037 – Daylight in Buildings (CEN, 2019) requires the annual assessment of Daylight Glare Probability (DGP) to determine if DGP-threshold values do not exceed a certain fraction of the occupied schedule in specific locations. Annual DGP analysis requires time-series HDR computation to estimate hourly DGP for a particular place and point-of-view (POV). The production of large HDR images arrays increases in orders of magnitude the time complexity of an already computational expensive simulation – a single HDR. The HDR array is also just a sub-product of the computation since the approach deletes it after determining hourly DGP. Moreover, because HDR-based analyses are view dependent, to annually assess the visual comfort of a space, current methods entail the calculation of annual DGP for several POVs in different locations. Considering this, visual comfort analyses, as recommended by standards, are extremely time-consuming and often unfeasible in the early design stages.

Currently, a way to address computationally expensive models is through surrogate models, i.e., an approximate model of the original that attempts to mimic its behavior at reduced computational cost (Nguyen, Reiter and Rigo, 2014). Typically, surrogate models use Machine Learning (ML) techniques that entail the generation of a large data set of full simulations to train an ML method, e.g., a support vector machine, an artificial neural network, etc. Although several works show the usefulness of surrogate modeling (Li et al., 2017; Gou et al., 2018; 2019), particularly in BPO based on simulated performance, building the training data set using simulation is computationally expensive and depends heavily on the complexity of the original simulation model used in the process. Thus, if the surrogate technique uses computationally expensive simulation models, it is likely that the time necessary to build the training data set would make the approach unfeasible. Surrogate methods also increase the degree of uncertainty and perform poorly in optimization problems with sensitive objective functions, i.e., functions where a small deviation from the optimum variables might result in significant degradation of the objective function value (Nguyen, Reiter and Rigo, 2014).

In sum, current modeling approaches for daylighting and whole-building energy simulations are highly susceptible to producing inefficient simulation models that entail unfeasible run times for early-stage parametric and goal-oriented design approaches. In the case of BEM, simulation is highly sensitive to geometric detail. Current methods do not implement efficient geometry simplification procedures, particularly in the parsing of complex (double)curved geometries. Regarding DSM, they are susceptible to critical simulation parameters that determine output quality and analysis types, particularly those involving the computation of large arrays of time-series HDR images, such as the calculation of annual DGP. Finally, although promising, the feasibility of using surrogate modeling approaches based on simulated models in early-design performance optimization depends on the computational complexity of the models used in the generation of the training data set. Thus, even in the deployment of fast and efficient surrogate techniques for building design, it is necessary to address the other problems related to BEM and DSM computational complexity.

3.3.3 Limitations in defining design goals and building performance problem

Goal-oriented approaches to building design that use optimization techniques involve the formulation of an objective function, which the search algorithm needs to minimize (cost function) or maximize (reward function). As discussed in chapter 2, building optimization problems are typically constrained. Still, in most cases, the constraints consist of setting bounds to decision variables, which are relatively easy to define and solve (Si et al., 2019). Regarding dependent variable constraints, BPO typically addresses them using penalty functions (Nguyen, 2013).

Although current digital design tools facilitate the use of black-box optimization in building design (e.g., Galapagos, Wallacei, Octopus for Rhino+Grasshopper), architects still need to define goals, objective functions, and constraints in inverse-design processes – a non-trivial task in certain cases. In general, describing objective functions for optimizing simulated building energy performance is relatively easy since building energy metrics are cumulative, i.e., they use a summation to integrate their temporal variation. Thus, in building energy optimization the most common way to define an objective function is to directly minimize simulation outputs or use a simple function that involves them such as estimated total energy consumption during a specific period and its normalization by unit area – the Energy Use Intensity (EUI). Even in cases involving constraints other than the simple limitation of the range of decision variables, some strategies facilitate the definition of goals and optimization problems. For example, constraining the minimization of predicted building energy consumption with thermal comfort metrics is common (Huang and Niu, 2016; Wright and Alajmi, 2016; Z. Tian et al., 2018). Nevertheless, it is easy to transform this constrained problem into an unconstrained one by either using thermal comfort indices as factors of a penalizing term of a single-objective function, in a process known as *scalarization method* (Coello, 2006; Ehrgott, 2006), or using them in an independent objective-function of a multi-objective optimization problem.

Specifying goals and objective functions in daylighting optimization is a more challenging task. Unlike building energy metrics, which entail only temporal variation, daylight metrics have high spatial variability. The description of spatial granularity and pattern variation of the daylight metric involved in the optimization is a complicated task. As a result, BPO based on daylighting performance tends to oversimplify the target spatial distribution by summarizing it into a single number or target interval. The reduction of the spatial variability of daylight performance often

entails averaging-based processes or measuring areas that meet some illumination criteria. For example, Torres and Sakamoto (2007) averaged annual illuminance averages measured in different observer positions in the design of the fitness function to optimize façade shading elements. Caicedo and Pandharipande (2016) averaged illuminance levels of occupied and unoccupied zones of a typical office space to optimize a lighting system control scheme. Others averaged Useful Daylight Illuminance (UDI) simulated in sensor grids (Zhang et al., 2017; Kirimtat et al., 2019). Despite the valuable contributions of such works, integrating the spatial variability through averaging processes is not recommended since average-based approaches are highly susceptible to the cancelation effect, i.e., when a positive bias compensates a negative one. Averaging daylight metrics is particularly susceptible to the cancelation effect because illuminance levels in daylit spaces vary in one to four orders of magnitude (Reinhart, 2019). A preferable approach is to measure areas that meet specific illumination criteria since such methods are not susceptible to the cancelation effect. For example, climate-based metrics like spatial Daylight Autonomy (sDA) measure the percentage of area that reports an illuminance level equal to or above 300 lux at least for 50% of the considered occupied schedule (IESNA, 2012). Some authors apply the same concept to the different UDI bins and propose spatial UDI (sUDI) (Konis, Gamas and Kensek, 2016; Zhang et al., 2017; Mangkuto, Siregar and Handina, 2018). Although preferable, temporal and zonal daylight metrics such as sDA or sUDI do not enable designers to shape the DA or UDI's annual pattern. Determining spatial patterns for both point-in-time and annual dynamic daylight metrics is crucial in the design of multi-purpose spaces that entail different functional requirements.

In sum, unlike in building energy optimization-based workflows, current approaches of goal definition for generative design methods based on daylighting simulations are ill-defined and fail to capture spatial target variation. Averaging-based processes are highly susceptible to the cancelation effect and, therefore, misleading. Although approaches based on temporal and zonal metrics are preferable, it is difficult to use them to specify the spatial target pattern, limiting the generative potential of goal-oriented design procedures for daylighting in buildings. One possibility to spatially describe goals would be through a weighted polynomial-based objective function. Nevertheless, that task is non-trivial and requires skills such as hyperparameter optimization to fine-tune the different scalars of the polynomial that architects usually do not master.

3.4 Refining and reframing the main research question and objective

Considering the main limitations, obstacles, and their causes, it is possible to subdivide the general question presented in chapter 1 – *How to improve the design process of high-performance buildings using current digital design and analysis tools?* – into four research questions that directly address them. The questions are the following:

1) ***What type of geometric modeling strategies enable a better interoperability between parametric design and Building Energy Simulation (BES) tools?***

2) ***Which modeling and analysis procedures generate quick and adequate feedback on energy and daylight performance of buildings at early design stages?***

3) How can we develop strategies that help architects and other non-experts in optimization to formulate inverse design problems?

4) How effective are the proposed modeling strategies? What are their advantages and limitations?

Solving the main research question involves answering these four questions. The first two questions relate to current modeling and analysis limitations of digital design processes based on whole-building energy and daylighting simulations. The first question directly addresses the problem of interoperability between design, BES, and daylighting simulation tools, particularly regarding geometric modeling and representation of buildings. The second one focuses on surpassing simulation related obstacles in initial parametric and goal-oriented design processes. The third question aims to investigate alternatives to performance target definition in BPO-based workflows. The last is an overarching methodological question necessary to determine the validity and applicability of the proposed modeling strategies.

The first three refined research questions directly inform the formulation of four goals that aim to achieve the general research objective described in chapter 1 – *To devise a set of strategies that improve the use of current thermal and daylight simulation tools in early-stage design workflows based on parametric and building optimization approaches*. Such goals are:

1st Goal - Automatically generate simulation models from an initial building geometry

2nd Goal - Automatically simplify simulation models

3rd Goal - Develop simplified approaches that either replace or reduce the need for computationally expensive simulations

4th Goal - Use familiar techniques known to designers to expedite the definition of performance goals

The first goal addresses the first research question by aiming to improve the interoperability of different building representations, thus shortening the current gap between parametric design tools geometric modeling capabilities and BES software. Achieving this goal will promote a smoother integration of simulation tools in parametric and goal-oriented building design methods. The second and third goals tackle the second research question by seeking the elaboration of methods that expedite simulation feedback in design processes, thus, shortening the difference between simulation and design times. Finally, the fourth goal addresses the third question by focusing on approaches that can facilitate the definition of feasible targets for time-based performance metrics that are difficult to describe in a single zonal index, i.e., metrics that simultaneously include temporal and spatial variation. The last goal appeals to the use of familiar techniques used in architectural design practice to define performance goals spatially as an alternative to more conventional methods purely based on mathematical expressions.

Figure 3-1 maps the refinement of the dissertation's general question and problem into four specific research questions that directly address the problem's causes and obstacles. It also illustrates how these questions inform the particular research goals that are central to this dissertation.

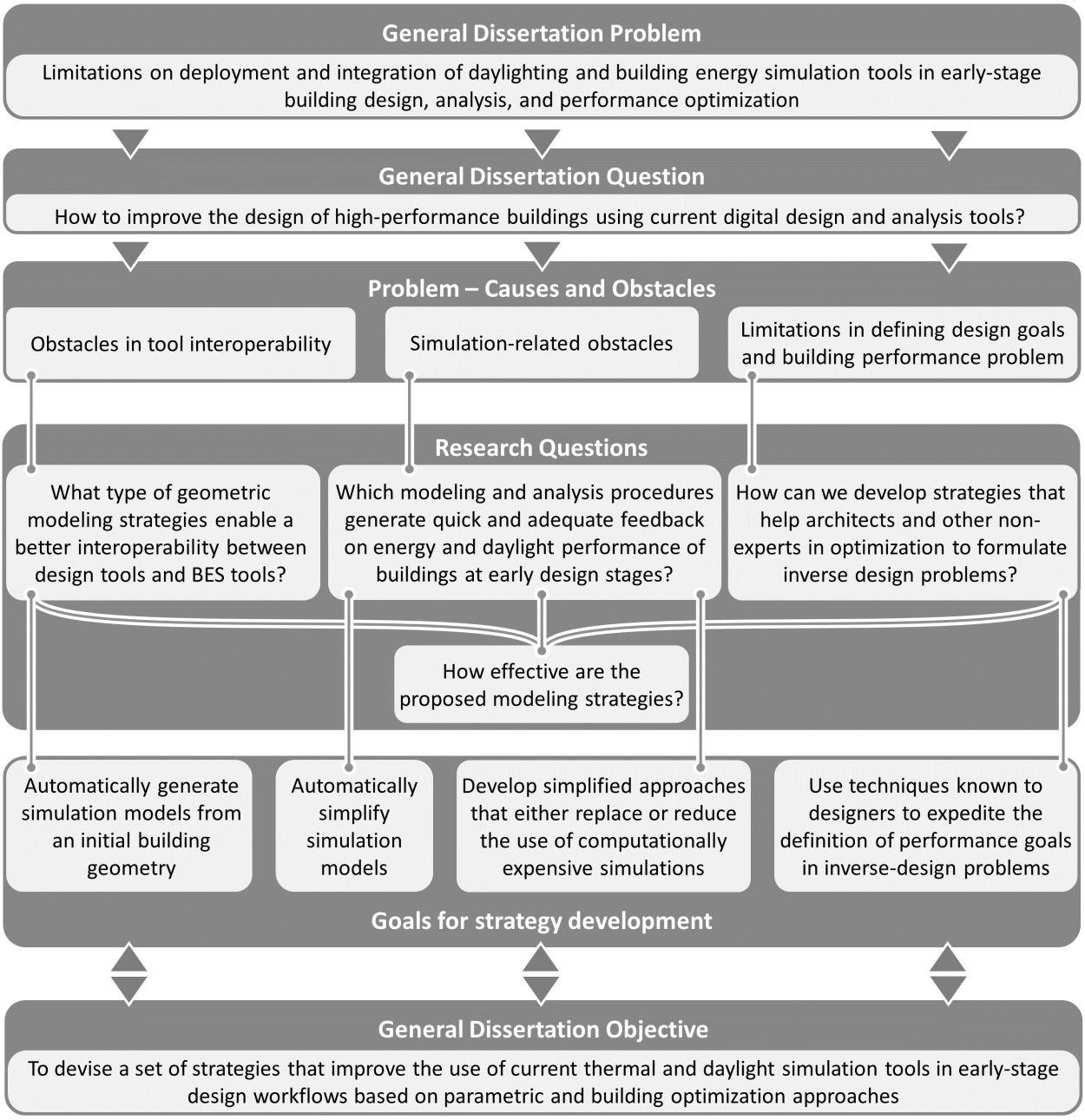

Figure 3-1. Relationship between the general research problem and the specific research questions, goals, and overall objective.

3.5 Concluding remarks

This chapter introduced and discussed in detail the general research problem of this dissertation: to identify, examine, and address current limitations on deployment and integration of daylighting and building energy simulation tools in early-stage building design, analysis, and performance optimization. Based on the existing literature, the work identified and framed three subproblems that contribute to the main one. Such subproblems or main problem causes are as follows: (i) obstacles in tool interoperability, mainly caused by differences in building geometric representation; (ii) simulation-related limitations, particularly the ones related to run time either

caused by computationally expensive simulation models or the maladjustment of advanced simulation and prediction procedures in early-phase parametric and generative design procedures that are based on building performance; (iii) challenges in defining goals and targets for performance-based generative design processes, particularly if they involve the definition of spatially granular objectives.

The discussion of the identified main obstacles led to the refinement of the general research question and definition of four research goals that will steer the formulation of hypotheses to solve each particular problem, answer the specific research questions, and consequently achieve the dissertation's primary objective. The goals are the following : (i) automatically generate simulation models from an initial building geometry; (ii) automatically simplify simulation models; (iii) develop simplified approaches that either replace or reduce the need for computationally expensive simulations; (iv) use familiar techniques known to designers to expedite the definition of performance goals.

The next chapter introduces the methodological approach applied in the development of alternative modeling strategies for parametric and goal-oriented design based on daylight and building energy performance. The different modeling strategies introduced in chapter 4 and developed in chapters 5, 6, and 7 observe the presented research goals, aim to answer the research questions, and achieve the general investigation objective.

Chapter 4:
Research Methodology and Methods

4.1 Introduction

As mentioned in chapter 1, section 1.4. – Research objective – the general objective of this dissertation is to improve current design support methods used in the digital design of high-performance buildings, particularly in the initial analysis and optimization of their daylight, thermal, and energy performance. Hence, the research effort focuses on addressing the main limitations, gaps, needs, and correspondent causes summarized in chapter 3. This chapter introduces and discusses the overall research method applied in the development of dedicated design and analysis approaches that tackle those limitations and, consequently, improve the integration of building energy, thermal, and daylight simulations in early-stage performance-driven design workflows.

The chapter starts by framing the research method in the broader context of design research methodologies. The discussion includes a close examination of the method's objectives, means, structure, and outcomes; thus, it provides a theoretical foundation for the overall approach used and its application. Following the methodological framing, the chapter introduces the general research methodology, presenting its overall structure, discussing its relation to the research goals, and elaborating on its different parts. It then advances by providing specific examples of the use and application of the methodology and introducing modeling, analysis, and validation procedures.

The research methodology introduces the concept of modeling strategies as design and analysis methods that address the limitations discussed in chapter 3.

Finally, the chapter ends by summarizing the advantages and limitations of the proposed research method and discusses how the potential outcomes of its application fulfill the goals of this dissertation.

4.2 Methodological frame

This dissertation's research method positions itself in the overarching family of design research methods, particularly in the Design Inclusive Research (DIR) framing methodology (Keller, 2005; Wensveen, 2005; Horváth, 2007, 2008; Koskinen et al., 2013; Davila Delgado, 2014; Vermeeren, Roto and Väänänen, 2016). At this point, it is helpful to elaborate on the concept of design research and framing methodology.

Design research encompasses a set of methods that bridge basic sciences, such as mathematics and physics, with product development that includes software, industrial design products, or buildings (Overbeeke and Forlizzi, 2006; Davila Delgado, 2014). Hence, design research interfaces fundamental research, applied science, and technology development in the pursuit of designing a specific product or technology (Friedman, 2003; Koskinen et al., 2013). Such type of research fosters short innovation cycles that result from the technological utilization of basic scientific research and provides opportunities to add/generate knowledge that emerges from the development of new technologies (Overbeeke and Forlizzi, 2006; Zimmerman and Forlizzi, 2014). Thus,

scientific research produces knowledge (fundamental research) and means (applied research) for design, and research design synthesizes and contextualizes those otherwise distinct bodies of knowledge for design practice, reshaping their purpose and context (Edelson, 2002; Horváth, 2004, 2007, 2008; Overbeeke and Forlizzi, 2006). Based on this reasoning, design research is both a result of a knowledge transfer from fundamental research to design and also a knowledge enabler, since, as Horváth (2007) argues, it *"extends scientific knowledge with genuine design knowledge."*

Framing methodology (Horváth, 2007; Davila Delgado, 2014; Vermeeren, Roto and Väänänen, 2016) is the process of selecting or developing a research methodology, i.e., a theoretically supporting system of principles, methods, procedures, and practices that facilitates a thinking process. Thus, a framing methodology does not explicitly describe the methods, tasks, and analysis procedures of a research process. It rather specifies a reasoning strategy, a set-up of research actions, and their implementation.

In design research, different framing methodologies express different levels of integration and contextualization (Horváth, 2004, 2007, 2008; Davila Delgado, 2014). Considering that the dissertation aims to develop new modeling and analysis methods for early-stage parametric and goal-oriented design processes, DIR is the adequate framing methodology to structure the research approach. DIR uses design as a research medium and introduces scientific inquiry to either extend, generate, or validate contextualized knowledge. In this dissertation, the integration of the design-like experiments with scientific inquiry aims to develop new models and design methodologies and assess their feasibility and validity.

Generally, DIR encompasses three phases: the pre-study, the design-study, and the post-study. The pre-study includes (i) acquiring knowledge related to the research problem and its context, (ii) formulating a critique based on the existing body of knowledge related to the investigation, (iii) defining research questions that inform an hypothesis that addresses the problem, (iv) set goals for the investigation, and (v) systematizing a set of methods to solve the research problem (Horváth, 2007, 2008; Davila Delgado, 2014). The pre-study phase is essential to the successful development of a design procedure. The literature presents several examples that demonstrate the relevance of pre-design phases in architectural research and practice. The work presented in Lassance (1999) illustrates how to implement a pre-design process as a computational tool. The pre-design tool integrates cognitive representation of different aspects related to the daylighting of selected buildings to aid designers in implementing daylighting design strategies. Elango and Devadas (2014) developed a process to frame a mental model for multi-criteria analysis that shapes a design brief (pre-study) and the analysis procedures (post-study) for a design studio course. Jusselme et al. (2016) proposed a pre-design method that facilitates the integration of sustainable design knowledge at the early design stages. The authors used Life Cycle Assessment (LCA) of buildings, sensitivity analysis methods, and visualization techniques (parallel coordinates) in a computational framework that assesses the LCA impact of different design parameters.

The design-study phase consists in implementing and testing the hypothesis and procedures developed in pre-study. Usually, it consists in defining and executing a Design of Experiments (DoE) by doing the following:

1) Framing the developed research methods and procedures in a specific design problem.

2) Establishing the main design parameters, constraints, assumptions, variables and metrics to measure.
3) Conducting the experiment.
4) Collecting the results or findings.

DIR's post-study is a confirmative stage and typically entails the following actions:

1) Verification of the hypothesis developed in the pre-study phase
2) Internal validation of both research and design methods
3) External validation of the findings, e.g., external validation from the design and scientific community, post-occupancy studies, human-subject experiments, etc.
4) Consolidation of the results by matching them against the existing body of knowledge and if possible generalizing them to other applications (Horváth, 2007).

The literature contains several examples that demonstrate the usefulness of the post-study phase in the assessment and validation of either a built design, a proposal, or a tool. For example, Delgado (2014) conducts internal and external validation of several strategies for structural inverse-design using statistical-based methods that post-process the results of the different experiments. The external validation process used by the author consisted of comparing the effects of different strategies among themselves and against an existing built case. The internal validation consisted of measuring the sensitivity of the different goal-oriented design systems to the variations of key input parameters and system settings. Jones and Reinhart (2019) both internally and externally validated a new daylight simulation technique showing its usefulness in supporting design through a human-subject experiment. Internal validation consisted of assessing the error in simulation output by comparing it with the one produced by current validated approaches. External validation entailed a small human-subject experiment where 40 designers designed two shading devices that aimed to balance glare and daylight availability in an office setting. Chamilothori et al. (2019) present a prediction method for building design that could only be externally validated. The work aims to assess the usefulness of using a Virtual Reality (VR) façade design tool by conducting a within-subject experimental design[1] where 72 participants respond to different façade patterns. These examples show that some of the post-study steps mentioned above are not necessary since their application depends on the scope and research goal. In this dissertation, the post-study phase will adapt to the particularities of each research task and consequent DoE.

Considering that the proposed research seeks to develop new modeling methods that improve the use of validated building energy and daylighting simulation tools in digital design, it will not use experimental-design studies with human subjects as an external validation process. Instead, it will compare the proposed modeling methods to current ones used in research and design practice, a validation process named as inter-program or inter-modeling comparison method (Reinhart, 2019).

[1] A within-subject experimental design, also known as repeated-measures design requires fewer participants and minimizes random noise. In within-subject studies, the same person tests all the conditions of the experiment.

4.3 General Research Methodology

The DIR framing methodology provides a conceptual structure that informs the several methods used in the dissertation's investigation. This section presents the overall methodology and relates it to the different phases and research actions of DIR.

This dissertation adopts a top-down approach to investigate the main research questions and achieve its objectives. Top-down design, also known as design decomposition (Guindon, 1990) or stepwise design (Fricke, 1996) , is a problem-solving method that consists of recursively breaking down an ill-defined problem or system to smaller well-defined sub-problems that are easier to model and solve. In design research the top-down approach focuses both on the problem and on the method used to solve it. Thus, this method is also an investigative approach that provide a complete understanding of the entire problem and its different parts. This type of approach is very common in basic sciences, applied sciences, and other fields of knowledge, such as design. An excellent example of a top-down approach in architectural design is the *parti* approach, which consists of incrementally detailing, refining, and reformulating an initial high-level spatial and formal diagram. In building design research, it is common to use top-down approaches in structuring research steps, methods, and tasks. For example, Chazivasileiadi et al. (2018) proposed a top-down process to solve the adjacencies of complex thermal models automatically.

Given their recursive/iterative nature, it is easy to express top-down research methods as an algorithm. Departing from this analogy, Figure 4-1 depicts a flow chart of the general top-down methodology adopted in this research.

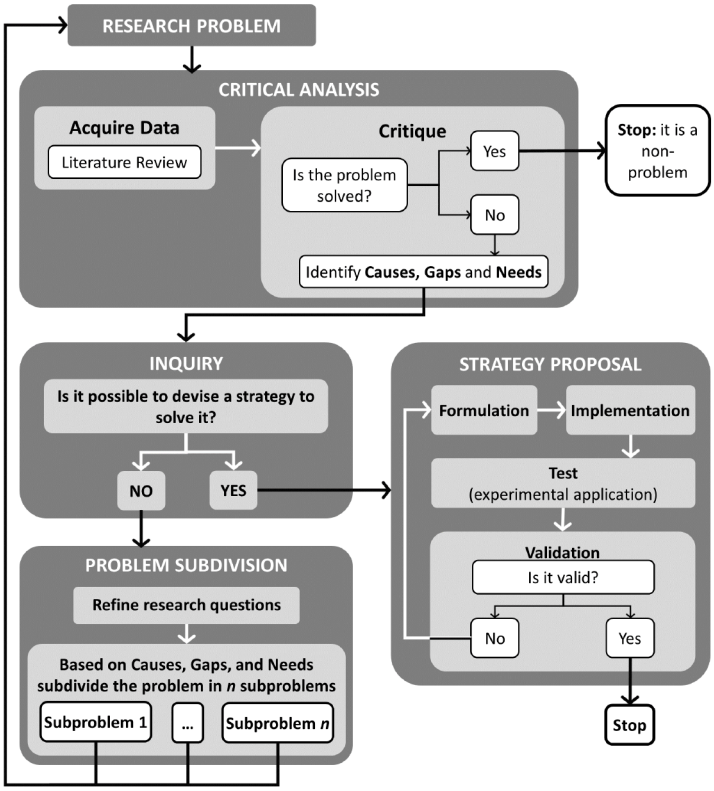

Figure 4-1. Flowchart of the recursive top down approach used as the general method of inquiry in this dissertation.

The algorithmic formulation of the research strategy allows an easy adaptation of its conceptual structure to the different phases of the research. The top-down approach entails the following entwined steps:

1) ***Statement of the research problem*** – i.e., the formulation of the problem to be solved.
2) ***Critical analysis*** – this step is two-fold. The first task consists of collecting existing data and information in the literature to obtain an in-depth knowledge of the problem context, causes, and existing body of work that addresses it. The second involves a critical discussion about the problem to assess whether previous or current work fully solved the problem. If not, the investigation identifies the problem's causes, the existing gaps, and needs.
3) ***Inquiry*** – if the existing body of knowledge does not present a satisfactory solution to the problem, this step assesses whether the problem is well-defined and, consequently, develops a hypothesis for its resolution, i.e., a strategy that tackles it.
4) ***Strategy proposal*** – if the previous step determines that the problem, its causes, and resulting needs are well-defined, the methodology seeks to devise a strategy, i.e., a set of methods and procedures, to address it. Advancing a strategy entails the following tasks: (i) formulate it, i.e., structure it, its goals, methods, and envisioned outcomes, (ii) implement the strategy either as a design method, a heuristic, a computational tool, or a combination of all the previous, (iii) based on a small isolated design example, design an experiment with well-established assumptions, input parameters, output variables, and validation procedures (DoE), execute it and collect the results; (iv) validate the finding using appropriated validation procedures and assumptions. If the results of the experiment are valid and satisfactory, the proposed strategy is a viable solution to the research problem at hand. Otherwise, the methodology pursues to either reformulate or further subdivide the problem.
5) ***Problem subdivision*** – if the inquiry step establishes that the problem is either too complex or ill-defined, the methodology subdivides the problem into smaller problems based on its causes and limitations. For each subproblem, the approach redefines the research questions and repeats the entire process until it produces a satisfactory strategy.

The framing of the presented top-down methodology in DIR is straightforward. All tasks of *Statement of the research problem*, *Critical analysis*, and *Inquiry* are pre-study ones. They define and frame the problem, formulate a critique of the related work, and identify essential gaps and needs. In sum, they assemble the necessary information to define the research goals and the subsequent formulation of a hypothesis that addresses the problem. DIR's design-study frames a considerable part of the *Strategy proposal* step, namely the formulation of the hypothesis in a design or modeling strategy, its consequent implementation, and experimentation. DIR's post-study phase takes place either in the strategy validation tasks or in the *Problem subdivision*. Both comprise confirmative tasks; the former assesses the effectiveness of the proposed strategy in solving the research problem in hands, and the latter confirms the need to re-apply the top-down approach to subdivide the problem into well-defined and solvable subproblems. Additionally, considering that DIR supports the development of research approaches, the proposed methodology concretizes it into a multi-purpose investigative framework that is applicable in different moments of the research.

After this higher-level discussion of the adopted framing methodology and how it shaped a general research approach, the following sections further examine its application to solve the main research problem discussed in chapter 3.

4.4 Modeling Strategies – tackling the main problem and its causes

George E.P. Box's aphorism that *"(...) all models are wrong, but some are useful"* (Box, 1979) acquires a new dimension in the case of architectural design. Because of the context and case-dependent nature of architecture, it is extremely challenging to develop generalized modeling methods for analysis and optimization tasks in performance-based design. However, that does not mean that approximate prediction and optimization methods are not useful in providing feedback to design. Considering this, the dissertation introduces the idea of modeling strategies, i.e., heuristic procedures designed to find a solution to the different research problems or an approximate and reasonable answer to them. Their objective is to achieve the general objective of the dissertation - improve the use of validated thermal, energy, and daylighting simulation in the design of buildings, particularly in cases where existing approaches are insufficient. To that end, they either extend current modeling and simulation approaches or propose different alternatives to them. Nevertheless, because of their heuristic nature, it is likely there are several design instances where the proposed strategies are either insufficient or inadequate.

As discussed in chapter 3, section 3.3, the problem of using daylight and whole-building energy simulation tools in early-stage building design workflows supported by algorithmic, parametric, and optimization tools entail obstacles related both to modeling and analysis tasks and goal definition in inverse-design problems. The modeling and analysis challenges emerge from poor interoperability between design and analysis tools and from the ineffective use of advanced simulation procedures that often result in either computational expensive simulation models or in time-consuming calculations. Regarding target definition tasks in generative design, it is particularly challenging if it involves the description of spatially granular objectives, which are difficult to express in a simple objective or fitness function. To address these obstacles, chapter 3, section 3.4, refined the research question and proposed specific goals that favor tool interoperability, expedite simulation feedback in parametric and generative-design processes, and facilitate the definition of performance targets that include spatial variation in goal-oriented design approaches. Such goals frame the development and implementation of alternative modeling strategies that address the different obstacles and are the following:

1st Goal - Automatically generate simulation models from an initial building geometry.

2nd Goal - Automatically simplify simulation models.

3rd Goal - Develop simplified approaches that either replace or reduce the use of computationally expensive simulations at early-design stages.

4th Goal - Use techniques known to designers to expedite the definition of performance goals in inverse-design problems.

Based on these goals, the work hypothesized five effective modeling methods that directly address the different problem: (i) Strategy A – Automatically generate valid building geometry for Building Energy Simulation (BES); (ii) Strategy B – Automatically simplify building geometry for BES; (iii) Strategy C – Abstract Complex Fenestration Systems (CFS) for BES; (iv) Strategy

D – Assess glare potential of indoor spaces using a time and spatial sampling technique; (v) - Strategy E – Painting with Light - a novel method for spatially specifying daylight goals in Building Performance Optimization (BPO). Strategies A, B, and C focus on BES, D on advanced daylighting analysis of buildings, and E on user-driven methods that promote a better integration of daylighting analysis in BPO.

Figure 4-2 relates the modeling strategies introduced here to the goals set for their development and implementation and correspondent questions discussed in chapter 3. It demonstrates how the proposed methodology refines a set of research questions to well-defined goals that inform the formulation of valid hypotheses for solving the problem – the modeling strategies.

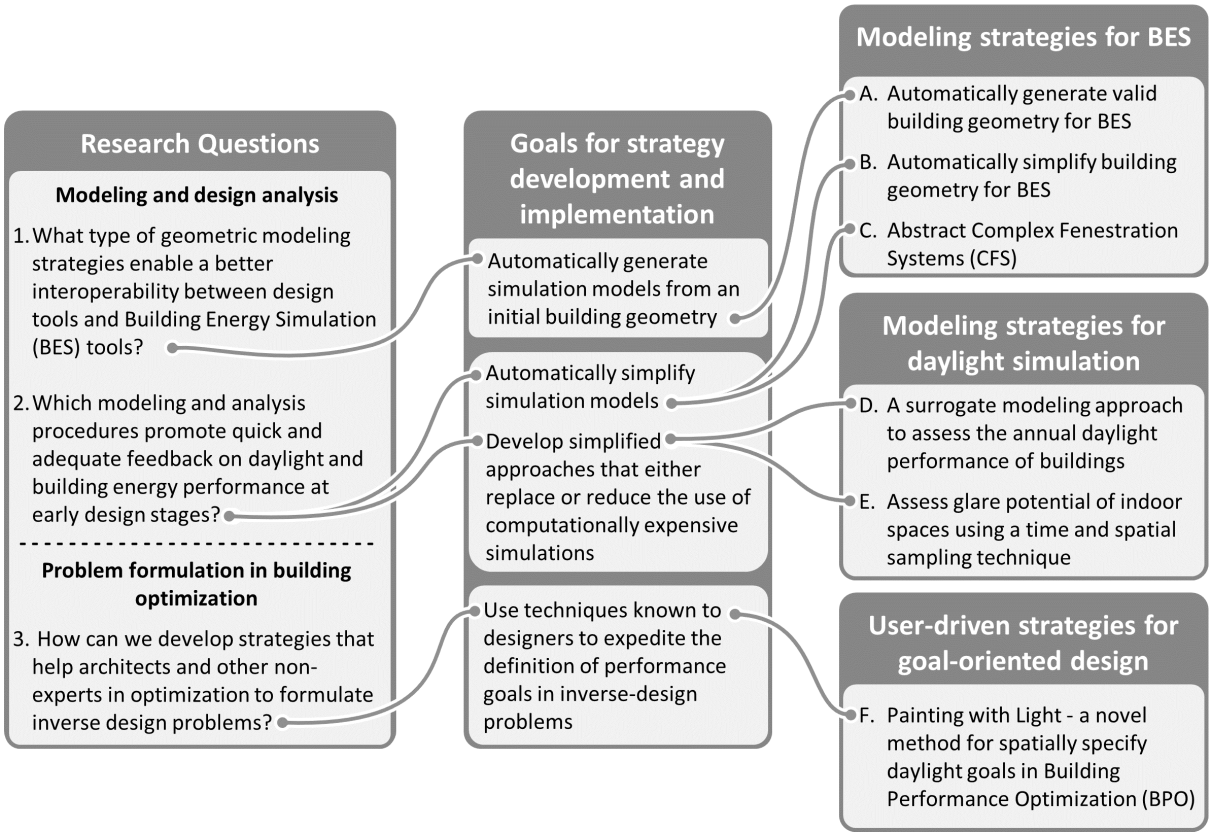

Figure 4-2. Relationship between research questions, goals for strategy development and implementation, both discussed in chapter 3, and the hypothesized strategies introduced in this chapter.

The decomposition of the general research problem into smaller problems (chapter 3), the systematic study of each subproblem, and the development of strategies that addresses them (chapters 5, 6, and 7), directly results from the application of the recursive top-down methodology presented in this chapter. The development of the strategies also re-applies the same methodological approach adjusting it to their requirements, goals, and other particularities. Therefore, each modeling strategy involved a focused literature review to identify gaps and needs – an essential step to design and implement them –, specific sets of methods, and experiments. For that reason, the chapters 5, 6, and 7 have specific related work, methods, and result sections per strategy. The next sections summarize the different modeling strategies.

4.4.1 Modeling strategies for Building Energy Simulation (BES)

Chapter 5 presents a set of strategies to address the problem of interoperability between design and whole-building energy simulation tools. The strategies focus on automatically generating valid, accurate, and efficient geometric descriptions for Building Energy Models (BEM), i.e., geometry surrogates that are faster to run and produce small output deviations in Building Energy Simulation (BES) tools. The main objective is to bridge different computational design and analysis tools in design by (i) shortening the gap of the geometry of design and analysis building models, (ii) avoiding tedious and redundant modeling tasks, and (iii) generating BEMs that provide quick and useful feedback in early-design stages. The resulting strategies are the following:

Strategy A – Automatically generate valid building geometry for BES – using sophisticated algorithms of planarization, the modelling approach generates valid geometric descriptions for BES from an initial building mass.

Strategy B – Automatically simplify building geometry for BES – this strategy extends the previous by automatically simplifying the geometry of complex BEM with one or more thermal zones.

Strategy C – Abstract Complex Fenestration Systems (CFS) for BES – the two previous strategies tackle the issues of representing building form in BES. Strategy C addresses the simplification of complex intricate shading systems and architectural screens explored by architects at early design phases.

The set of modeling strategies for BES realizes the first and second goals envisioned to solve the problem of interoperability between design and whole-building energy tools. Strategy A concretizes the first implementation goal – automatically generate simulation models from an initial building geometry – while Strategy B and C the second one – automatically simplify simulation models. Chapter 5 presents and discusses the above modeling strategies for BES.

4.4.2 A modeling strategy for advanced daylight simulation of buildings

The proposed strategy focuses on addressing the ineffective use of advanced simulation resources in early-stage parametric and generative design based on daylight simulations. As discussed in chapter 3, there is a misalignment between what is required by specific standards in terms of daylight analysis, current simulation approaches that support such analysis, and parametric and generative-driven design processes. Therefore, chapter 6 presents a strategy that expedites expensive computational daylight simulations, particularly those involving climate-based metric calculations for the annual study of glare potential of indoor spaces. The strategy is the following:

Strategy D – Assess glare potential of indoor spaces using a time and spatial sampling technique **–** this approach investigates the potential of using easier-to-compute daylight metrics, such as annual vertical illuminance, to spatially assess indoor visual comfort. The purpose is to substantially reduce the generation and analysis of computationally expensive High Dynamic Range (HDR) images by identifying worst-case scenarios to render point-in-time HDR for detailed Daylight Glare Probability (DGP) calculations. Such a strategy will help designers to conduct detailed glare calculations required by the new European standard for Daylight in Buildings, EN 170377 (CEN, 2019).

Strategy D concretizes the third implementation goal, which tackles the problem of simulation resources misuse in building design and analysis at the early design stages. Chapter 6 describes and discusses in detail the strategy.

4.4.3 A user-driven strategy for goal-oriented design formulation

The last strategy focuses on problem modeling in goal-oriented design rather than on simulation related limitations. It addresses the challenges of modeling optimization problems based on daylight performance metrics. Unlike building energy metrics, which only entail temporal variation, it is difficult to specify and model the spatial variation of daylight targets in a building optimization process. As discussed in chapter 3, this difficulty either promotes the misuse of automated search techniques in the optimization of daylighting in buildings or limits the generative potential of goal-oriented design procedures.

Due to the context-dependent nature of goal-oriented design procedures, the strategy presented in chapter 7 is a proof-of-concept that illustrates the potential of using methods commonly used by designers in defining goal-oriented design processes. The strategy follows here:

> ***Strategy E – Painting with Light - a novel method for spatially specify daylight goals in Building Performance Optimization (BPO)*** – this strategy implements a painting-style interface that helps designers to spatially specify daylight goals in indoor spaces. Its purpose is three-fold: (i) reduce the difficulty of defining the daylight optimization (or design) problem, (ii) expand the generative potential of goal-oriented design procedures for daylighting design, and (iii) reduce the gap between standard optimization approaches used in inverse-design and common methods applied in architectural design.

Strategy E is a good example of how to concretize the fourth development and implementation goal. The modeling approach aims to improve the use of performance-based generative design methods by reducing the gap between commonly used design methods and optimization techniques, particularly in the definition of inverse building design problems. Chapter 7 presents and discusses Strategy E in detail.

4.5 Validation

Validating new modeling and ancillary simulation-based methods for the early building design stages is a challenging task. The dissertation uses two different types of validation procedures – external and internal. The following presents them by first introducing both approaches within the context of the related work and then by discussing their application in the context of this dissertation.

4.5.1 External validation procedures

External validation in building performance simulation frequently aims both to test the accuracy of new simulation methods and to assess whether their application is generalizable and transferable (Matt, Brewer and Sklar, 2010). Frequently, researchers use empirical validation, an external validation method that consists in comparing physical measurements against predictions obtained through simulation with similar boundary conditions to the ones of the physical experiments (Perez et al., 1990; Perez, Seals and Michalsky, 1993; Reinhart and Walkenhorst, 2001; Reinhart and

Andersen, 2006; Reinhart and Breton, 2009; Tabares-Velasco, Christensen and Bianchi, 2012; McNeil and Lee, 2013; Jones and Reinhart, 2017).

Empirical validation often entails calibration, particularly in cases where accuracy is paramount. Since empirical validation uses well-defined experiment settings, it does not ensure that the prediction technique will perform in the same way in different boundary conditions. Thus, the use of a validated simulation tool or method always requires calibration to the characteristics of specific boundaries that frame the analysis problem (Coakley, Raftery and Keane, 2014). In other words, a valid external method does not exclude internal validation. Although it is common to calibrate a prediction procedure to match the output of a validated simulation technique, e.g., surrogate modeling based on statistical learning, usually calibration resorts to physical measurements.

External empirical validation and calibration focus on accuracy and usually involve time-consuming processes such as physical experiments or collection of data in post-occupancy stages. Such methods are often incompatible with design times, requirements, and needs at initial design stages either due to the shortage of time to conduct empirical experiments or to the lack of a well-defined design, i.e., a design that by its evolving nature is incomplete. Hence, external validation based on empirical experiments or physically collected data often happens later in the design process or even after its consummation, i.e., after construction (e.g., post-occupancy studies). As a result, early-stage design based on building performance uses simulation with the available information and seldom confirms simulation results using external empirical validation.

Nevertheless, building performance analysis at initial design phases do not aspire to be entirely accurate; their goal is to provide useful feedback that is accurate enough in the design process. Therefore, accuracy in early-stage building simulations deals more with the ability of the prediction model to properly capture the main dynamics of the phenomena under study than to make very accurate and precise predictions. Thus, the study of the thermal and daylighting performance of buildings at early-design phases demands validated simulation tools that can model all the related physical phenomena.

The external validation of this research aims to assess if the proposed strategies are either valid complements or alternatives to current methods used in the parametric or generative design of high-performance buildings. It consists of comparing the results of the proposed modeling strategies with the ones delivered by the best simulation practices currently used in practice, in a process named as inter-program or inter-modeling approach comparison (Reinhart, 2019). In sum, the research assumes that a modeling strategy is externally valid if employing less effort and using fewer resources delivers similar results provided by the current best practice modeling methods.

Simulation and building performance optimization literature present similar external comparative validation procedures. For example, Dogan and Reinhart (2017) validate the results of a simplified energy modeling tool for urban clusters (Shoeboxer) by comparing its results against the ones of fully detailed multi-zone urban BEM. The first validation of the 3-phase method, an advanced bidirectional raytracing technique for Radiance, consisted of comparing the results produced by the 3-phase method against previously validated results produced by the standard raytracing method used by Radiance – backwards raytracing (Ward et al., 2011). Davila Delgado (2014) validates the proposed modeling strategies for structural analysis and optimization by comparing

them with design calculations used by standard and validated methods. Jones and Reinhart (2017) externally validate a new Radiance-based tool for Graphical Processing Units (GPU) calculation by comparing it with the standard Radiance, compiled to use Central Processing Units (CPU).

This research uses two building simulation tools, EnergyPlus (Crawley et al., 2001) for thermal and whole-building energy analysis, and Radiance (Ward, 1994) and its extensions for daylighting. Both programs are open source, research-grade, and consistently validated. EnergyPlus supports the modeling of all heat transfer modes in buildings (conduction, convection, and radiation), Heating, Ventilating, and Air Conditioned (HVAC) systems, and simplified calculations for natural ventilation and daylighting. Radiance is a synthetic imaging system that fully captures the transient phenomena of daylight, complementing EnergyPlus limitations regarding daylighting. These tools are central in developing the strategies and modeling the benchmark cases used for comparative external validation procedures.

The external validation of Strategy B and C uses EnergyPlus to compare the simulation time and output of the models produced by the strategies with fully detailed BEM modeled using standard practices. Chapter 5 presents in more detail the several experimental results and validation procedures.

Strategy D's external validation (chapter 6) consisted of using DGP data of an external experiment conducted by the author of this dissertation (Santos, Leitão and Caldas, 2018) to determine the vertical illuminance threshold that minimizes the occurrences of False-Positive (FP) and False-Negative (FN) glare events.

The validation procedures of strategies A and E are exclusively internal. The following section summarizes internal validation approaches and presents an overview of the ones applied in each proposed modeling strategy.

4.5.2 Internal validation procedures

Researchers use internal validation to determine to which extent a result supports a cause and effect assertion, considering the problem under study and the amount of collected data. Thus, an internally valid modeling approach is one that proves to be useful and makes sense to its users. It includes three different types of tests (Liu et al., 2011):

1) Theory validity test – this test evaluates if the theory used in the design of the model is sound and if the model makes a valid use of it, i.e., if the model results align with the theoretical framework and system that explain the phenomena that it tries to emulate (Liu et al., 2011).
2) Requirements validity test – examines if the model complies with clearly defined requirements and provides meaningful answers to a well-established research question (Liu et al., 2011).
3) Face validity test – assess if the modeling approach is based on plausible assumptions and if its outcomes “look right” or make sense (Liu et al., 2011).

In performance-based design, the application of internal validity tests aims to assess if a specific process or result supports or provides useful and consistent feedback to a design process. In the

particular case of thermal and daylighting simulations, the theory that describes the related physical phenomena is well known and grounded. Thermal and daylighting simulation approaches are theoretically valid if we can prove or explain their results using physical laws and building physics concepts. For example, the simulation of illuminance (E) due to direct light in a single-window room needs to show a decay pattern that resembles the pattern of the general inverse square law, which determines that E is inversely proportional to the square of the distance from the window. When considering both the direct and indirect components of daylight in the calculation of E, the decay of E might not follow precisely the inverse law behavior because of the indirect contributions caused by interreflections – e.g., cases with light redirecting systems or with surfaces whose reflectance is highly variable.

In building simulation research, the use of consistently validated simulation tools that fully capture the mechanics involved in the simulated phenomena, such as EnergyPlus and Radiance, provides a strong basis for theory validity. Conducting theory validity tests is more relevant in the development of white-box simulation tools. Since this dissertation uses already validated simulation tools, it assumes that the physical phenomena its correctly modeled and that their output is theoretically valid based on several validation studies. EnergyPlus validation studies include Crawley et al. (2001), Zhou et al. Tabares-Velasco et al. (2012), Mateus et al. (2014), Andjelković et al. (2016), Goia et al. (2018), Haves et al. (2019), among several others. Validation studies on Radiance and Radiance-based applications include Reinhart and Walkenhorst (2001), Reinhart and Andersen (2006), McNeill and Lee (2013), Lee et al. (2018), Xuan et al. (2019), Kharvari (2020), and others.

The requirements validity tests assess if the results of a specific modeling strategy are consistent and reasonable. Fulfilling specific requirements in internal validity tests is particularly relevant in stochastic prediction and optimization. It is possible to assess the method's reproducibility by repeating the same experiment several times by measuring the similarity of the results of the different trials. For example, the work presented in (Wetter and Wright, 2004) and in (Wortmann et al., 2017), not only compared several optimization methods in the minimization of energy consumption of particular designs but also measured the variation of optimization outputs of the different analyzed methods. Another example is testing an optimization algorithm in a problem to which the optimal solution is already known. Caldas and Norford (2002) examined whether their goal-oriented design system could find an already known optimal solution previously found using a brute-force method. Similarly, Al-Homoud (2005) used three test functions with known minimum values to assess whether his optimization approach could find such values.

Face validity determines if a method can either provide plausible feedback or generate solutions that improve the predicted performance of a specific design. In other words, if an analysis-based approach delivers results that make sense, then it is valid to use in a design context. The literature presents several examples of this type of internal design validation. Usually, they compare the performance of either a baseline design (also called base-case) or benchmark against the result of the reiterated application of the proposed design method. For example, Shea and Cagan (1999) tested the effectiveness of shape annealing optimization method in truss design, comparing the results against the ones of a standard Warren truss type, the benchmark used by the authors. Caldas (2008) uses a *Generative Design System* (GDS) called GENE_ARCH to explore alternative design solutions that aim to improve the energy performance of Álvaro Siza's School of Architecture at Oporto. In (Pan, Yin and Huang, 2008), the authors internally validated a design process for

energy-efficient data center buildings by comparing different designs produced by their method to an ASHARE 90.1-2004 compliant budget model. Other works, such as (Manzan and Pinto, 2009; Khoroshiltseva, Slanzi and Poli, 2016), validate their proposed goal-oriented design approaches by reporting and analyzing the progress of the optimization procedure, i.e., by assessing whether the optimization progressively approaches towards the desired outcome.

Sensitivity tests are useful internal validation procedures since they can test the three types of internal validity. They consist of systematically varying simulation inputs and study the resulting model's response surface (Feng and Staum, 2017). Consider the already given example of simulating *E* in a single-window room. With sensitivity analysis, it is possible to conduct a theory validity test by varying the distance of the measuring point to the window and examine if the model's *E* predictions observe the inverse square law. A face validity test could involve changing the window size and assessing if *E* values change accordingly. Finally, a requirement validity test might test different Visible Light Transmittance (VLT) and observe the expected impact on *E* values, e.g., assess if a decrease of 10% on VLT corresponds to the same linear reduction on *E*.

In this dissertation, internal validation traverses all proposed strategies. Strategy A (chapter 5) validation only uses a requirement validity test because it serves a single purpose – to automatically generate valid geometries for Building Energy Simulations. The requirement validity test determines whether the geometry created by the proposed approach did not produce severe simulation errors in the EnergyPlus error report. Face validation consists in observing whether the proposed goal-oriented design approach generates alternative solutions that yield better energy performance than an initial base case.

Strategy B (chapter 5) face validation performs a sensitivity analysis to assess the impact of BEM mesh density in simulation time. Considering how EnergyPlus models radiative heat transfer, simulation time should vary super-linearly (e.g., quadratically or exponentially) with the number of BEM faces.

The sensitivity analysis on changing shading factor on Strategy C (chapter 5) experience constitutes a face validity test. Another face validity test used in the assessment of this approach was to measure the reduction in simulation time that resulted from applying the proposed strategy.

In Strategy D (chapter 6), the use of a simple room geometry to test the proposed approach helps in face validation. It is easy determining *a priori* visual discomfort periods on critical points-of-view (POV); thus, facilitating if the proposed modeling approach could produce meaningful and plausible results by checking if it signaled such time events on critical POVs.

In chapter 7, the requirement internal validity test used in Strategy E is similar to the one presented by Caldas and Norford (2002). It consists of feeding the proposed GDS pre-simulated Daylight Factor (DF) data as the desired input goal. Thus, it is possible to assess if the GDS can find similar design solutions to the one that produced the objective function data.

4.5.3 Statistical metrics used in the development and validation of the different strategies

The performance assessment, external, and internal validation of the proposed modeling strategies use several statistical metrics. They measure the quality of the output produced by the different

approaches, particularly in comparison-based validation tasks, and assess their ability to improve feedback in building design, by either reducing computation time or help the finding of better-performing alternatives.

The following describes the statistical indexes used in assessing the quality of a strategy simulated output.

Percentage of error (% error)

Percentage of error (% error) measures the discrepancy between a predicted or measured value (*S*) and a value (*D*) assumed as accurate or correct. It consists of calculating the absolute error, which is the absolute value of the difference between *D* and *S*, dividing it by *D*, resulting in the relative error, and then multiplying it by 100 to obtain the percentage error. Equation (4-1) expresses the calculation of % error used in this dissertation for a given simulation output (ρ):

$$\%\ error\ (\rho) = \frac{|D(\rho) - S(\rho)|}{D(\rho)} \times 100\ (\%) \qquad (4\text{-}1)$$

where, $D(\rho)$ is simulated data that is considered accurate and true, and $S(\rho)$ is the predicted data.

Root Mean Square Error (RMSE)

RMSE is the standard deviation (σ) of a regression prediction error. In other words, it measures the variation or dispersion of the residuals. This metric indicates the level of concentration of measured data points around the best-fit trend line. The dissertation uses RMSE as part of the calculation of more advanced error metrics particularly designed to estimate error in building energy simulation and calibration such as the Coefficient of Variation of Root Mean Square Error (CVRMSE). Equation (4-2) presents the formulation of RMSE:

$$RMSE_{S,D} = \sqrt{\frac{\sum_{I=1}^{N}(S_i - D_i)^2}{N}} \qquad (4\text{-}2)$$

where, D_i is an accurate simulated data point or a correct measurement, S_i is the corresponding prediction, and *N* the data sample size.

Coefficient of Variation of Root Mean Square Error (CVRMSE)

CVRMSE measures the variability of the errors between *S* and *D*. Similar to RMSE, it determines how well a model fits data by analyzing the offsetting errors (residuals). The advantage over RMSE is that CVRMSE is unitless, allowing the comparison of different modeling approaches. Additionally, this index is not susceptible to the cancelation effect, i.e., where a positive bias compensates a negative one. For those reasons, it is one of the most used error metrics in BEM calibration. Equation (4-3) presents the CVRMSE formulation:

$$CVRMSE = \frac{1}{\overline{D}} \cdot \sqrt{\sum_{i=1}^{N} \frac{(D_i - S_i)^2}{N-1}} \times 100\ (\%) \quad (4\text{-}3)$$

where D_i is an accurate data point, S_i is the predicted value, N is the data sample size, and $\overline{D}$ is the mean of the accurate values.

Coefficient of determination (R^2)

R^2 measures how differences in one variable relate to differences in a second variable, i.e., it measures the percentage variation in a y-variable explained by x-variables. Similar to RMSE or CVRMSE, R^2 is an indicator of goodness of fit in regression studies. The higher R^2, the better the fit. It is also useful in determining the likelihood of future events falling within the predicted outcomes. Equation (4-4) determines R^2:

$$R^2 = 1 - \frac{\sum_i (D_i - S_i)^2}{\sum_i (D_i - \overline{D})^2} \quad (4\text{-}4)$$

where, D_i is a correct measurement or simulated data point, S_i is the corresponding predicted value, and $\overline{D}$ is the mean of the accurate values. The fraction numerator is the Sum of Squares Errors (SSE), while the denominator is the total sum of the squares (SST). The dissertation uses R^2 to evaluate the effectiveness of linear regression techniques that uses Ordinary Least Squares (OLS) based on one independent variable or regressor.

Normalized Mean Bias Error (NMBE)

NMBE provides the average of the deviations between forecasts (*S*) and true measurements (*D*) normalized by the mean of D values. Negative values mean over-prediction, while positive values indicate under-prediction. This index is very common in BEM calibration. However, since NMBE is susceptible to the cancelation effect, calibration standards (ASHRAE, 2002) recommend pairing it with CVRMSE. Equation (4-5) describes its calculation:

$$NMBE = \frac{1}{\overline{D}} \cdot \sum_{i=1}^{N} \frac{D_i - S_i}{N} \times 100\ (\%) \quad (4\text{-}5)$$

where D_i is an accurate simulated data point or a correct measurement, S_i is the predicted value, N is the data sample size, and $\overline{D}$ is the mean of the accurate values.

Assessing the usefulness of the proposed modeling strategies requires focusing on two essential aspects. The first is to determine the modeling strategy's ability to reduce simulation time, while the second is to evaluate their capacity in supporting the development of high-performance solutions. To this end, the dissertation used the metrics described below.

Percentage of improvement (% of improvement)

Similar to % of error, this metric measures the relative difference of a particular performance metric between two design solutions. Building energy standards such as (ASHRAE, 2013), use this index to calculate the relative improvement of a design alternative against a benchmark or a baseline design. The only difference between this measurement and % of error is that the numerator does not return an absolute value. Consequently, the resulting value can be either negative or positive. A positive value means that the design instance outperforms the baseline. A negative one indicates that the design alternative performs worse than the base-case. The dissertation uses % of improvement to compare the predicted performance of different design solutions produced by some of the proposed modeling approaches. The ASHRAE 90.1 standard (2013) determines its calculation as follows:

$$\%\ of\ improvement = \frac{D(\rho) - S(\rho)}{D(\rho)} \times 100\% \quad (4\text{-}6)$$

where (ρ) denotes the simulated building performance metric, $D(\rho)$, its value in the baseline case, and $S(\rho)$ in the design alternative.

Simulation time related metrics

Simulation time is a sensible parameter in performance-based design supported by parametric, algorithmic, and goal-oriented approaches. In such cases, simulation feedback should be fast and reliable. Therefore, a way to assess whether alternative modeling techniques are useful is to measure how fast they are to run relative to current simulation methods. In the case of strategies that aim to reduce calculation time, the work compares the simulation time of their resulting models against the runtime of a benchmark model that reflects current best practices. All the time measurements are in seconds (s). The comparison uses two metrics to assess how much run time improvement the proposed strategy attained:

1) Times faster than the baseline case (x times faster), calculated by dividing the simulation time of the baseline case by the run time of the strategy's resulting model.
2) % of simulation time reduction, computed using the % of improvement formulation but using run time of both the benchmark and the modeling strategy cases.

Finally, some experiments conducted in this dissertation use additional indices. For example, in chapter 6 the determination of the illuminance threshold to signal potential glare events involved calculating the percentage of false-positive and false-negative events. Whenever the work introduces a new statistical index, it fully describes it.

4.6 Concluding remarks

This chapter presented and discussed the general methodology used in the dissertation work. Design Inclusive Research (DIR) provides the methodological framework of the top-down methodology used throughout the investigation. The top-down methodology recursively decomposes the different research problems into smaller well-defined problems. The three DIR phases – (i) pre-study, (ii) design-study, (iii) post-study – frame the several methodology tasks.

The pre-study phase entails the *Statement of the research problem*, *Critical Analysis*, and *Inquiry* steps of the general top-down research methodology. Design-study includes a significant part of the *Strategy Proposal*, particularly in devising methods and procedures that implement the formulated hypothesis. The post-study stage comprises the *Strategy Proposal* validation tasks, which assess the effectiveness of the proposed strategy, and the *Problem subdivision* methodological step, which confirms whether it is necessary to re-apply the methodology to further decompose the problem into simpler and solvable subproblems.

The methodology's application to the primary research problem resulted in subdividing the main problem and hypothesizing possible solutions – the modeling strategies. The chapter defines the concept of modeling strategy, frames it in the context of the research questions and objective, sets four goals for strategy development and implementation, and introduces the five modeling strategies proposed in this dissertation.

Strategies A, B, and C focus on improving the interoperability between design and analysis tools as well as the use of the latter in parametric and goal-oriented design processes. Strategy A proposes the automatic generation of valid geometric descriptions for BES from complex (double)curved building masses. Strategy B extends A and aims to improve analysis feedback in building design by automatically simplifying BEM geometry and consequently reducing simulation time. Similarly, Strategy C presents another simplification strategy that addresses the energy modeling of complex architectural screens.

Strategy D aims to improve the deployment and use of advanced daylighting analysis in the early design stages. The strategy advances an ancillary method for visual comfort studies that quickly qualifies entire spaces and supports a more efficient use of detailed glare analysis.

Strategy E proposes a method that helps architects in formulating inverse-design procedures based on daylighting simulations. It facilitates the definition of spatial daylight by employing processes commonly used by designers.

This work uses both external and internal validation procedures. The external validation procedure consists in comparing the simulation output of the proposed modeling strategies with those delivered by standard simulation practices based on research-grade validated software. Strategy B and C use geometrically detailed BEMs as benchmark validation models. Strategy D used external DGP data to determine the accuracy of using vertical illuminance in signaling glare events.

Regarding internal validation, this chapter provided an overview of different approaches and discussed the application of face and requirement-based validity tests in this investigation. The use of validated simulation techniques that fully capture the thermal and daylighting phenomena dynamics in buildings provides theoretical validity to the proposed strategies. A validity test based on requirements determines whether a model is internally valid if it complies with pre-established criteria. In this dissertation, the requirement-based validity tests assess whether: (i) the strategy simulation model runs without generating any errors – Strategy A, B, and C; (ii) the output deviation of the modeling strategies falls into a pre-established range of error – Strategy B, C, and E; (iii) optimization procedures find plausible solutions to a known design problem – Strategy E.

Face validity determines whether a modeling strategy provides useful feedback in digital design processes supported by thermal and daylight simulations. The face validity of this research work examines whether (i) the strategy effectively helps in the generation of better performing designs – Strategy A, C, and E; (ii) the proposed procedure reduces simulation time – Strategy B, C, D; (iii) sensitivity analysis results are plausible – Strategy B and D; and (iv) the strategy's application provides meaningful and expectable feedback in well-defined and easily predictable design scenarios – Strategy D.

The methodological discussion also introduced and defined essential statistical indices that supported the development and validation of the different modeling strategies. Percentage of error (% error), Root Mean Square Error (RMSE), Coefficient of Variation of Root Mean Square Error (CVRMSE), Coefficient of determination (R^2), assess the quality of the strategies simulated output. Percentage of improvement (% of improvement), % of simulation time reduction, and times faster than the baseline case (x faster) are the indices applied in the examination of the usefulness of the proposed strategies either in assisting the design of high-performance buildings or in reducing analysis time during building design.

The proposed top-down methodology provides a flexible investigative framework that can easily adapt to the different research lines pursued in this work. However, it entails two main limitations. First, the general method follows a heuristic process. Thus, it is impossible to determine whether the proposed modeling approaches are optimal, only whether they are valid and improved alternatives to current ones. Second, the validation of the proposed strategies used certain assumptions and particular experimental settings. Thus, their application in design scenarios that comprise significantly different conditions needs to be critically examined.

However, both methodological limitations are acceptable and do not compromise the investigation findings. This dissertation seeks to improve current modeling methods for design processes supported by daylighting and building energy simulations; it does not aspire to develop an ultimate solution to all the modeling issues in the digital design and analysis of high-performance buildings. Therefore, a heuristic approach is acceptable. The second shortcoming, related to validation, is a common hurdle in building simulation. Even sophisticated techniques widely accepted by the building simulation community are susceptible to it. For example, the most advanced sky model used in daylighting simulations, the Perez all-weather sky model (Perez, Seals and Michalsky, 1993), is only based on data collected at Berkeley, CA, and therefore has limited application. Nevertheless, all climate-based simulation techniques use it because of the lack of better alternatives. This work acknowledges that it can only partially generalize its findings. For that reason, it explicitly describes the experiments' boundary conditions and assumptions. Moreover, the purpose of the work is not to provide a universal and closed methodological approach to the problem, but, similar to the Perez all-weather sky example, suggest one whose application is plausible and useful in design analysis tasks, and suitable for further refinement.

Chapter 5:
Modeling Strategies for Building Energy Simulation

5.1 Introduction

The previous chapter presented the general research approach adopted in this dissertation and provided an overview of the different developed strategies to address the causes of the problems identified and discussed in chapter 3. This chapter focuses on the developed strategies that address the existing interoperability limitations between parametric and generative design tools and whole-building energy simulation caused by the current differences in geometric modeling capabilities. The work gives particular attention to the modeling challenges posed in either describing curved or double-curved building surfaces for Building Energy Simulations (BES).

The chapter begins with an analysis of the current state-of-the-art on building geometry modeling techniques that aim to integrate BES in early-stage design workflows. The discussion conducted in section 5.2 – Related Work – focuses on the latest developments of either translating Computer-Aided Design (CAD) or Building Information Modeling (BIM) building models to Building Energy Models (BEM) or describing complex façade systems for early whole-building energy assessments. The main goal is to identify and isolate current limitations, gaps, and needs, which in turn will inform the development of specific modeling strategies that will improve the integration of BES in parametric and generative design workflows.

The literature review identified three main limitations: (i) current interoperability problems in representing complex building geometry in BES tools; (ii) inefficiencies caused by inadequate geometric descriptions in Building Energy Models (BEMs), particularly of (double-) curved building envelopes; (iii) modeling highly sophisticated building skins in early-stage energy performance-driven design workflows.

Section 5.3 presents Strategy A – Automatically generate valid geometry for BES as an answer to the first limitation. This strategy offers a method that mitigates the current gap between the geometric modeling capabilities between design and BES tools. It proposes the automatic parsing of early-stage free-form building geometry, typically modeled using Non-Uniform Ratio Basis Spline (NURBS) based tools, to the more constrained planar mesh face-based BEM geometry. The goal is threefold; (i) to avoid redundant modeling tasks in early stage building energy assessment studies, (ii) to shorten the representational gap between the design model and BEM, and (iii) to automatically generate valid geometric descriptions for BEM from an initial building envelope regardless of its geometric complexity. The application of this strategy in a goal-oriented design experiment confirmed the other two limitations.

Section 5.4 introduces Strategy B: Automatically simplify building geometry for efficient whole-building energy simulations – that directly tackles the second limitation. This strategy extends Strategy A by automatically generating optimized BEM simplifications that are faster to run and do not introduce relevant deviations in simulation output. The goal of producing geometric surrogates to reduce simulation run time is to improve feedback in performance-driven building design processes.

Strategy C: Abstract Complex Fenestration Systems for the early energy assessment of complex building skins (section 5.5), proposes a method that simplifies the modeling of highly sophisticated façade systems for BES. Such complex envelope systems include custom-designed solar control screens, non-planar shading devices, and light redirecting systems, for early whole-building energy performance assessments. Hence, Strategy C aims to shorten the gap between modeling capabilities of design and analysis tools. Current parametric and algorithmic design approaches allow the early development of intricate facades that are challenging to model and simulate using current BES programs. The method introduced by Strategy C facilitates the modeling and simulation of sophisticated building skins.

Finally, the chapter ends with a discussion that frames the advantages and limitations of each strategy, possible ways of integrating them, and suggests areas for future work. Figure 5-1 presents a flow chart that illustrates both the approach used in this chapter and its structure. The flow chart illustrates the adjustment of the top-down methodology approach described in chapter 4 – Research Methodology – to the work presented here.

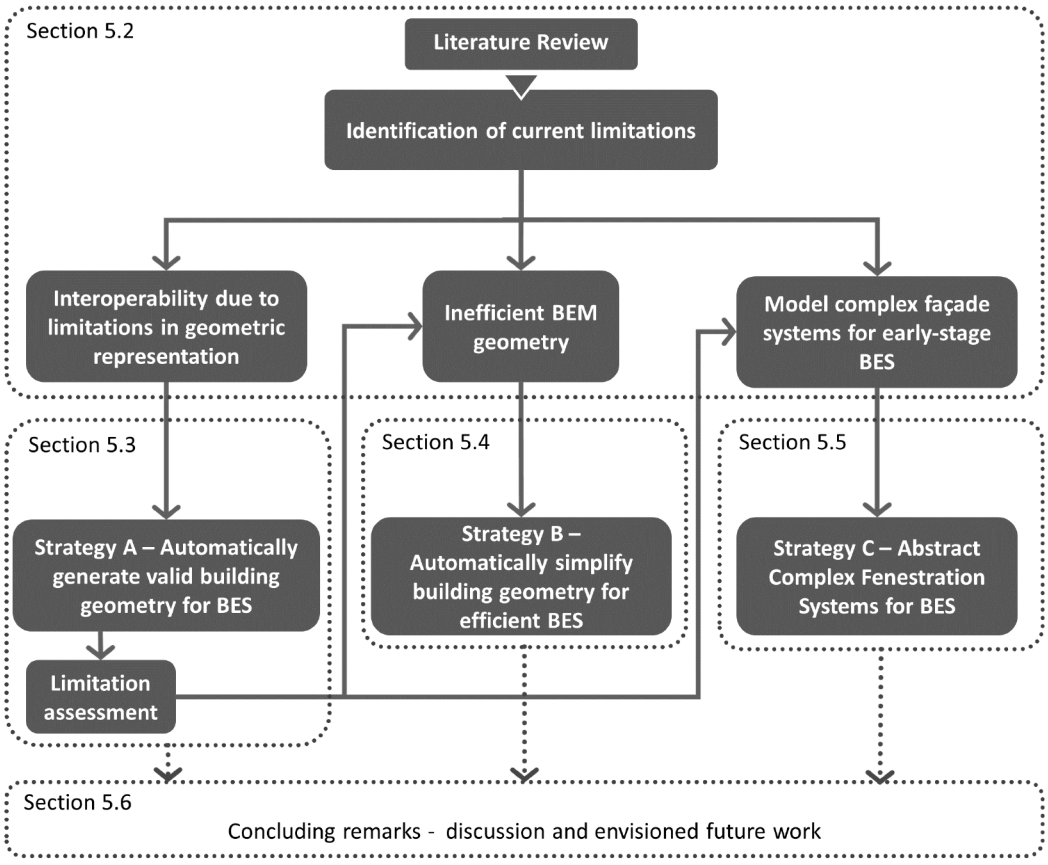

Figure 5-1. General research approach used in this chapter and resulting chapter structure.

The following sections present in detail the analysis of the related literature and describes the different strategies along with their respective methods, experiments, and results.

5.2 Related Work

Recent developments attempt to address to the need to translate CAD and BIM building models to BEM as a way to shorten the geometric modeling gap between design and building energy analysis tools. Several researchers developed methods to automatically or semi-automatically generate valid BEM from digital building models with different degrees of detail that range from conceptual building masses to fully detailed architectural models (Jones et al., 2013; Georgescu and Mezić, 2015; Kensek, 2015; Kim et al., 2015; Dogan, Reinhart and Michalatos, 2016; Jeong and Son, 2016; Lilis, Giannakis and Rovas, 2017). However, the literature on automated BEM inference and simplification focuses primarily on the thermal zoning of massing models according to ASHRAE guidelines (ASHRAE, 2013), such as in Dogan et al. (2016), Dogan and Reinhart (2013, 2017), and Jones et al. (2013), or in sensitivity analysis of simple box-shaped buildings composed by planar surfaces (Amitrano et al., 2014; Picco and Marengo, 2015). Jones et al. (2013), presents a conversion methodology of CAD building models based on extrusions of planar polygons. This work explores ray casting and view factor-based techniques to solve the topological complexity of BEMs. The authors present a method that generates a multi-zone thermal model based on minimal information on internal spatial organization and program. The proposed method automatically executes several modeling tasks that result from the combination of different programmatic volumes or thermal zones such as solving the resulting adjacencies and boundary conditions, and the pairing child-surfaces, i.e., any type of fenestration or vent, with their correspondent parent-surfaces, i.e., the wall, ceiling, or roof to which they belong. Lillis et al. (2017), presents an approach that automates the production of BEMs with simplified thermal zoning from BIM models with well-defined internal spaces. The authors propose a tool that first maps the topological relationship of different spaces and then uses information on orientation, program, HVAC system, and occupancy to automatically merge contiguous similar individual rooms. Despite the significant advances introduced by both works, they do not address either the automatic division of building masses with no interior space layout into thermal zones or complex building envelope geometries.

Dogan et al. (2016) introduced Autozoner, a tool that automatically divides a building mass with undefined interior space boundaries into a multi-zone thermal model. The tool uses ASHRAE 90.1 guidelines for splitting a building plan with no information of its interior layout into perimeter and core zones (ASHRAE, 2013). Autozoner divides the perimeter area into different zones by using cardinal orientation to then iteratively subdivide the resulting zones until all resulting zones are convex. The method successfully processes complicated building floor plans. However, it neither addresses curved geometry nor proposes advanced methods of dividing the perimeter building area in order to capture the impact of self-shading.

Based on the Autozoner experience, Dogan and Reinhart (2017) developed a method called *The Shoeboxer* that automatically simplifies the thermal zoning of urban building clusters. The simplification consists of sampling a set of building volumes into a group of representative simplified "shoebox" BEMs. The sampling technique considers orientation, contextual shading, and incident solar radiation. The tool estimates the energy results of the whole building cluster by first extrapolating the results of each simplified BEM to their respective areas of influence to then aggregate all the extrapolated results. The authors tested the method in several building clusters with different Floor Area Ratios (FAR). Compared with the perimeter and core multi-zone thermal zoning approach of ASHRAE 90.1 Appendix G (ASHRAE, 2013), Shoeboxer's annual energy predictions could be 50 to 296 times faster with low error deviations in simulation output, i.e., with

a Root Mean Square Error (RMSE) of 11% and 20% respectively. This work demonstrates that sampling methods are effective in early-stage design. Nevertheless, the authors apply it only in the analysis of neighborhoods and city blocks composed of simple box-like building volumes. There is still no application of like approaches to large buildings with free-form envelopes.

Other works discuss the viability of geometric simplification of building elements in BES. Pico and Marengo (2015) study the impact of simplifying shading elements, glazed fenestration, and thermal zoning in annual energy simulations. The authors found that, on average, strong simplifications in geometry did not produce relevant differences in energy simulation outputs. Nevertheless, their work also shows that geometric simplifications, particularly on the level of thermal zone definition, can lead to a deviation of ≈ 20 % in simulation output. Amitrano et al. (2014) conducted a similar study that showed that, even in simple shoebox BEM, the inclusion of detailed geometry reduces the uncertainty of energy simulations by 5 to 15%. Although both studies address only simple box-like building envelopes, they show that geometric simplification is acceptable up to a certain point, since oversimplifications significantly increase the degree of uncertainty in thermal and energy analysis.

Regarding the automatic parsing of curved or double-curved building surfaces from a CAD or BIM model to a BEM, current approaches use standard non-adaptive triangulation algorithms. Although they guarantee that all the faces of the model are planar and convex, they limit the control of the geometry density of a model and thus its computational efficiency, and do not guarantee other BES geometric requirements (e.g., the enclosure of thermal zones). Popular front-end tools for thermal and Building Energy Simulation (BES) such as Ladybug/Honeybee (Roudsari, Pak and Smith, 2013) and Autodesk Insight analysis tools (Autodesk, 2019) use this triangulation approach and often produce BEMs that either take too long to simulate or fail to run. Figure 5-2 shows the result of a small experiment, conducted in the context of this dissertation, that anecdotally demonstrates the limitations of current tools in automatically generating either valid or efficient BEMs that run in valuable time. The experiment tested the ability of Autodesk Insight to simulate two building masses produced by a Dynamo (Autodesk, 2020) parametric visual script that generates twisted towers. One (Figure 5-2, left) resulted in time-consuming simulations due to a dense mesh tessellation (left), while the other failed to run (Figure 5-2, right).

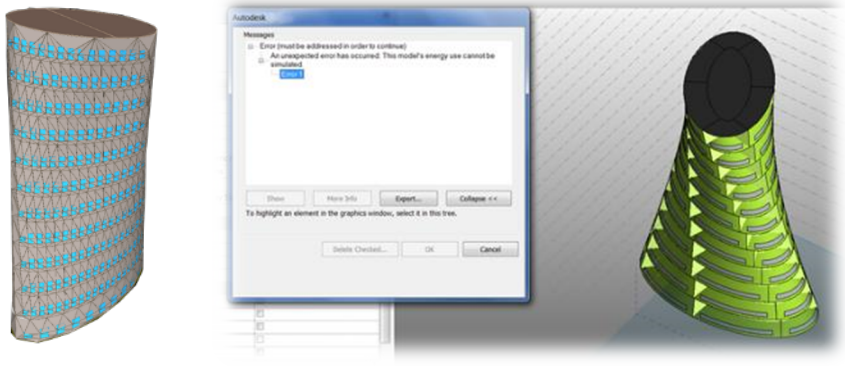

Figure 5-2. Autodesk Insight attempts to automatically parse the geometry of two towers produced by a parametric Dynamo visual script. Left: the BEM highly dense mesh leads to time-consuming simulations in the Autodesk cloud server. Right: a simple twist and the resulting double-curved envelope was impossible to successfully translate to a BEM with a valid geometry description.

Despite the current need for methods that efficiently discretize curved surfaces for BES, the literature that studies the impact on simulation output of simplifying curved or other types of sophisticated building envelope geometry is still limited. Only recently did Chatzivasileiadi et al. (2018) conduct a sensitivity analysis on the discretization of simple curved building envelopes in BES. The authors found that a significant reduction of geometry complexity has a negligible impact on energy simulation output. This work also shows that simulation accuracy deteriorates rapidly below a critical threshold. Despite its valuable contribution, the study focuses primarily on simple extrusions of planar curves. A slightly twisted tower is the only example of a more complex curved building envelope. Moreover, the statistical approach used in the study to measure simulation results deviations lacks the inclusion of essential statistical metrics typically used in hourly-based BES (ASHRAE, 2002), such as the Normalized Mean Bias Error (NMBE) and the Coefficient of Variation of the Root Mean Squared Error (CVRMSE). Thus, the work is unable to provide clear recommendations on techniques for automatically simplifying curved building envelopes that result in efficient thermal and energy simulations.

Efficiently processing curved and double-curved building envelopes in the production of valid BEMs is a challenging problem. Fabricating and assembling curved envelopes typically involve higher financial costs that result both from the required labor, expertise, material, and technological apparatus. The economic impact is more evident in steel and glass construction than in certain types of cast concrete techniques, such as the ones that use metal or polymer-based frameworks. To minimize construction costs and feasibility, it is desirable to discretize curved building surfaces into the smallest number of planar elements, a common research topic in architectural geometry and digital fabrication (Baldassini et al., 2010; Eigensatz et al., 2010; Deng et al., 2015; Pottmann et al., 2015).

Recent developments in architectural geometry and digital fabrication address the discretization problem of curved building surfaces into planar elements by applying quad-mesh quasi-planarization techniques (Sechelmann, Rörig and Bobenko, 2013; Rörig et al., 2015). To obtain a planar quadrilateral subdivision of any given surface, quasi-isothermic algorithms first tessellate an input surface into a triangle mesh. They then use conformal maps of the resulting triangle meshes to generate an S-isothermic quadrilateral mesh. An S-isothermic mesh is a discretization of a surface into planar shapes that are both curvature-aligned and angle-preserving. A quadrilateral mesh is S-isothermic if, and only if: (i) all the quadrilaterals are planar, (ii) all faces have incircles, and (iii) the incircles of adjacent quadrilaterals touch. Figure 5-3 illustrates the concept of a quadrilateral isothermic mesh and how the quasi-isothermic algorithm remeshes a given mesh into a planar quad-mesh. Sechelmann, Rörig, and Bobenko (2013) describe in more depth the algorithmic approach to create S-isothermic quadrilateral meshes.

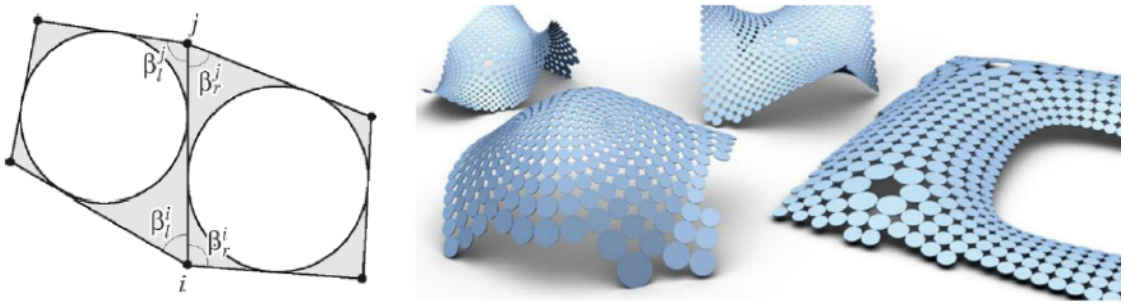

Figure 5-3. S-isotermic and non-isothermic quadrilateral meshes. Left: incircles of a non-S-isothermic quad-mesh. In order to be S-isothermic the incircles of adjacent meshes need to touch. This produces the same ratio on both sides of the edge ij; cot(βi/2)/cot(βj/2) (Sechelmann, Rörig and Bobenko, 2013). Right: examples of S-isothermic quad meshes generated by the algorithm proposed in Sechelman, Rörig, and Bobenko (2013). Images adapted from: Sechelman, Rörig, and Bobenko (2013).

The tools that use quasi-isothermic planarization techniques, such as Kangaroo for Grasshopper (Piker, 2015), allow the user to control the remeshing process of any arbitrary surface into a set of planar and quadrilateral panels. Although such techniques have a direct application in the fields of architectural geometry and digital fabrication, they have great potential to improve the pre-processing of complex curved geometry to produce valid BEMs.

The early design of green buildings includes not only the study of conceptual masses but also the generation of sophisticated building skins. Current algorithmic-based design methods enable the generation of complex and intricate architectural compositions in the design of sophisticated building skins at early design stages. Architects and researchers use such approaches to both conceive and study architectural surfaces with different patterns, levels of porosity, density, and opacity, that adapt to different requirements, such as the geometry of the building envelope or climatic conditions (e.g., solar irradiance). Recently, several researchers have been exploring the potential of parametric-driven tools in the design and optimization of high-performing facades. Tabadkani et al. (2019), used Honeybee and Ladybug, both environmental analysis plugins for Rhinoceros 3D Visual Programming Language (VPL) Grasshopper, to investigate modular and responsive origami-based components for smart façades. The work proposed in (Mahmoud and Elghazi, 2016) presents a similar approach applied to kinetic building envelopes based on the rotation and translation motion of hexagonal components. The authors study the correlation between geometric patterns generated by different states of their dynamic elements and visual comfort in buildings. Zani et al. (2017) combined parametric design tools with a standard Genetic Algorithm (GA) to develop high-performance concrete static shading systems that simultaneously harvest daylight and minimize building energy consumption. Ercan and Elias-Ozkan (2015) present similar work.

Wagdy and Fathy (2015) developed a parametric model that generates louver-based designs based on louver count, depth ratio, tilt angle, and Window-to-Wall Ratio (WWR). Using a brute force approach, the authors simulated all possible solutions via Radiance and EnergyPlus. They found that the louvers depth ratio was the parameter that had the most impact on spatial Daylight Autonomy (sDA) and, consequently, lighting energy end-use. Inspired by the heliotropic response of plants, i.e., the movement of some plants in response to the sun position, Henriques et al. (2012) developed a parametric system that populates canopies with kinetic skylights that dynamically adapt to environmental conditions and internal functional demands. Based on an extensive

parametric study, the work proposes a heuristic that determines in real-time the aperture of the different skylights that provides the required daylight and visual contrast. In Turin et al. (2012), the authors applied a similar approach but extended it to free-form shape roofs of semi-outdoor spaces. The work also used a GA based generative design tool called *ParaGen* to optimize the form of the roof and the orientation, openness, and shading factor of its opening using the ratio between incident solar radiation and Daylight Factor (DF) as the main performance metric.

Nevertheless, the study and design of highly sophisticated building skins using algorithmic, parametric, or generative approaches pose two different types of challenges. The first challenge is the generalization of a method to create parametric façades. Designers often build their parametric models from scratch, a task that, although more efficient than manual modeling, requires effort, programming expertise, and is frequently limited to a specific type of façade element. For example, a program that generates parametric louver systems is unable to produce hexagonal kinetic shading elements. Recent work addresses the generalization for parametric modeling in the context of algorithmic approaches to design. DrAFT (Caetano, Santos and Leitão, 2015; Caetano and Leitão, 2016) is an example of a design tool that expedites the generation and control of parametric façade designs. It provides an algorithmic framework to control key façade aspects such as envelope geometry, façade element's section, size, material, color, and geometric transformation functions. The user can use and combine the different algorithms through functional operators in order to generate any type of façade, easily apply and change different types of façade units, control their distribution, parametric properties, and finally articulate them in any arbitrary building envelope. Figure 5-4 illustrates how DrAFT composes different functional operators to distribute different design elements and control their parametric properties.

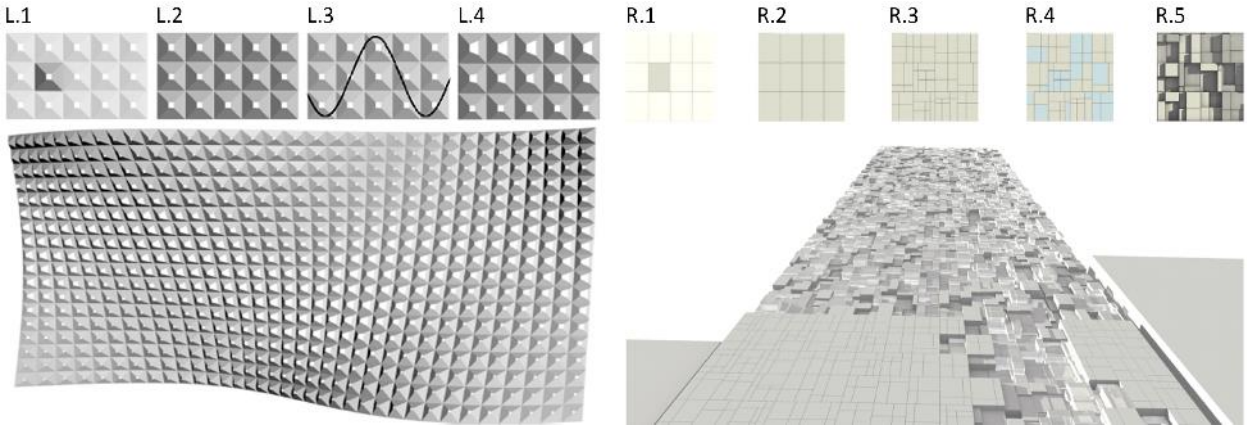

Figure 5-4. Two façade designs produced with DrAFT (Caetano and Leitão, 2016) using a combination of different functional operators. Left: a simple line attractor exercise that controls the opening of a truncated pyramidal building element. It uses the following functions: L1 – function that creates the façade element, L.2 – function that distributes/propagates the element in a regular grid, L.3 – function that sets the smoothness of the attractor curve in controlling the openings of the truncated pyramid elements, L.4 – linear function that sets the range from minimum to maximum aperture for the pyramidal elements. Right: application of DrAFT to model Sheung Wan Hotel in Hong Kong designed by Heatherwick Studio. DrAFT used the following operators: R.1 – function that creates the façade panel, R.2 – function that distributes the panel in a regular-grid, R.3 – function that subdivides the element into irregular patterns, R.4 – function that assigns randomly to each panel glass or metal materials, R.5 – function that assigns random depth-size to the subpanels. Images adapted from: Caetano and Leitão (2016).

The other main challenge in the parametric and generative design of building skins is simulating the impact on energy and daylight performance of sophisticated exterior shades, architectural screens, and other types of Complex Fenestration Systems[2] (CFS) that systems like DrAFT can generate. The modeling of such complex building skins is more cumbersome in thermal and energy simulation because of their geometric limitations and the impact that geometry has on simulation time. Currently, and like daylight simulation, it is possible to use BSDF to describe CFS in BES tools, such as TRNSYS or EnergyPlus, to accurately determine solar gains (LBNL, 2015). Although accurate (Hauer et al., 2019) using BSDF in BES typically results in slow simulations (Petersen et al., 2018), particularly if a BSDF material is applied to discrete parts of the envelope. Additionally, generating BSDF of highly customized parametric façade elements that seamlessly adapt to complex building envelopes is a difficult task that requires a high level of expertise. In daylight and energy building performance studies, there are two ways to generate synthetic BSDF data. One uses WINDOW software (Huizenga et al., 2017) and the other *genBSDF*, a Radiance routine. WINDOW provides BSDF data of some commercially available CFS and allows the synthetic generation of BSDF descriptions of custom CFS based on simple parametric models for even distributed louvers, perforated screens, and glass frit. On the other hand, *genBSDF* generates a BSDF for any type of fenestration geometry given a Radiance scene or a Material and Geometry Format (MGF) file, therefore providing a better support in the analysis of highly customized CFS. Nevertheless, generating BSDF data of custom CFS, either with WINDOW or with *genBSDF*, entails a considerable computational overhead. Moreover, BSDF data describes in detail a specific CFS, thus limiting the desirable exploration of different types of systems and assemblies with similar thermal and optical properties in the early stage of building design. Therefore, despite the recent progress in simulating sophisticated building skins, there is a need to develop simplified approaches that will expedite the assessment of CFS in either parametric or generative design processes.

5.2.1 Discussion

The previous section on related work shows that despite the current progress on combining digital design tools and state-of-the-art BES programs, there are still fundamental limitations in integrating BES in parametric and generative design practice. Such restrictions are more pronounced in the case of representing and analyzing both unconventional building forms and highly sophisticated building skins. As briefly summarized in section 2.1, this literature review unveiled the following limitations and resulting needs:

1) Interoperability problems caused by the difficulty of modeling curved and double-curved building envelopes for BES - the difficulty of current geometry parsing methods to translate free-form surfaces to BES hampers the use of whole-building energy analysis in the early design of free-form buildings. Thus, there is the need for robust methods that effectively

[2] CFS refers to any fenestration assembly that incorporates a non-clear (specular and non-specular) layer in the glazing assembly or in its attachments (e.g., shadings). It includes switchable (smart) glazing, translucent or transparent insulation, solar films, patterned/fritted glass, light redirecting systems based both in nanoparticles and in macroscopic systems such as reflective louvers, non-planar shading systems, etc. The combination of such layers with other shading elements and advanced clear window products (e.g., spectrally selective glazing) promote an efficient use of daylight and reduce the unwanted solar heat gains and potential glare problem associated with the clear window product alone.

discretize any type of building geometry and produce valid BEMs from an initial CAD or BIM massing model.

2) Inefficient building energy simulations caused by BEM geometric descriptions – this limitation is directly related to the previous one. As discussed, when current methods of automatically parsing complex building envelopes are able to produce valid geometric descriptions for BES, the outcome is far from being optimal. Usually, the resulting BEMs entail a considerable computational simulation overhead. Therefore, it is paramount to develop and implement approaches that generate valid and optimized geometric descriptions that promote quick and accurate analysis in current digital design workflows.

3) Difficulty in modeling complex façade systems for early whole-building energy assessments – current parametric, algorithmic, and generative tools allows designers to easily model a wide variety of building skins with intricate shading screens, devices, and other complex façade systems. Although there are ways to model such building skins in BES, the current methods entail a considerable modeling effort, expertise, and usually result in slow simulations, therefore unfit for early analysis. Consequently, architects are unable to fully analyze the impact in whole-building energy performance of advanced façade solutions. In order to reduce the considerable gap that exists between the early design and energy analysis of complex façade systems, it is necessary to find ways that simplify the modeling and early analysis of sophisticated facades in BES.

The following sections describe the different proposed modeling strategies that directly address the limitations and needs described above.

5.3 Strategy A: Automatically generate valid geometry for Building Energy Simulation

This section proposes an automatic and robust method for deriving valid BEMs from fully parametric building models with complex curved or double-curved envelopes. The development and implementation of the proposed modeling method results from a joint research effort between the author of this dissertation and his advisers, published in Santos et al. (2017).

Automatically deriving BEMs from their parametric/architectural counterparts allows designers to directly use energy-based generative design processes without the need for remodeling simulation models, a time-consuming task. Thus, it promotes a smoother integration of BEM either in early-stage parametric or goal-oriented design based on whole-building energy analysis. The proposed automation also aims to reduce the current gap between the geometric representation of a BEM and a conceptual architectural building massing model, thereby strengthening the relationship between them. Reinforcing the relationship between the geometry of the building design model and the BEM fosters a more precise assessment of the impact that specific formal changes have on the thermal and energy building performance.

To achieve this goal, the proposed method uses mesh planarization algorithms to discretize curved or double-curved surfaces into meshes composed by planar quadrilateral faces of enclosed building massing models based on NURBS geometry. The resulting model is an enclosed volume, or a set of enclosed volumes, with surfaces that a BES tool such as EnergyPlus can process. Applying such planarization algorithms minimizes the differences among the geometries of the parametric model

used in the architectural design process and the energy simulation model. In this way, one model can directly inform the next.

Because surface remeshing algorithms are common in digital fabrication, the automated BEM generation approach will support a goal-oriented design approach that focuses both on energy performance and on construction feasibility. The goal-oriented approach uses a standard GA to search for glass frit solutions that reduce the energy consumption of an all-glass building envelope. The resulting generative design system will also adapt the emergent mesh subdivision within pre-defined boundaries and rules that ensure construction feasibility (e.g., maximum glass panel size and deviation from the original surface). Figure 5-5 illustrates the proposed integration of mesh planarization techniques in the goal-oriented design process that aims to reduce building energy use.

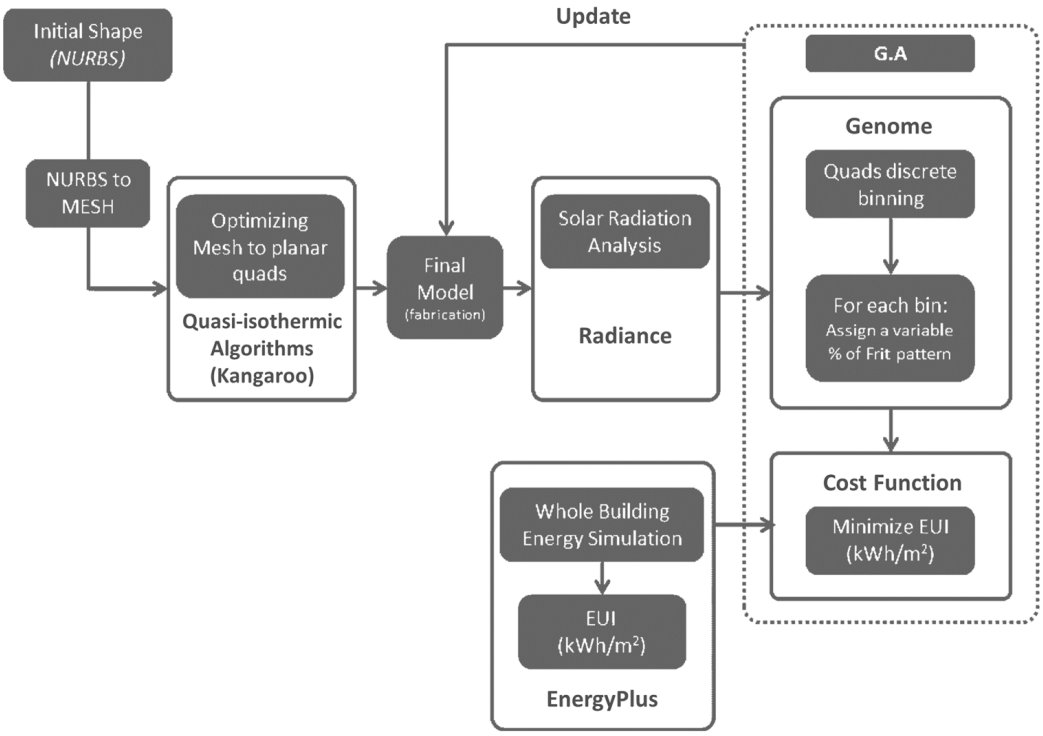

Figure 5-5. Diagram of an energy-based generative design system that uses the proposed discretization method of curved or double-curved building envelopes. From an initial surface, a mesh based on planar quad-meshes is produced both for fabrication and energy simulation. The GA search process will optimize the fritting density of the fabrication model glass panels.

In the proposed goal-oriented design system, planarization algorithms first process an initial freeform geometry. The result is a mesh composed of planar quads with constraints applied to their maximum dimensions. Each planar quad corresponds to a planar glass panel with a maximum size of a standard double glass panel: 3x3 m. The resulting geometry is directly fed to EnergyPlus and Radiance by assigning specific EnergyPlus and Radiance materials to each panel. An irradiance Radiance simulation maps solar radiation on the building envelope. Based on incident solar radiation similarity, the system clusters the façade panels. A Genetic Algorithm (GA) controls the glass frit density assigned to each panel cluster. In this way, the GA searches for the best fritting densities for each solar exposure. Finally, when the GA converges, the resultant glass frit pattern

is remapped on the digital fabrication model. Through this loop, two parameters, construction and building energy consumption, inform a single architectural geometric representation. The following section discusses in detail the methodological approach used in discretizing complex curved building envelopes for valid BEM.

5.3.1 Method for discretizing curved and double-curved building envelopes

The discretization of arbitrarily curved building surfaces entails two steps; (i) panelize the input surface into quadrilateral panels, and (ii) planarize the resulting panels.

The first step consists of a simple algorithm implemented in Rhino/Grasshopper that, given the number of desired panels or specific constraints to the panel dimensions, divides the original surface along its $\vec{u}$ and $\vec{v}$ direction. The discretization process transforms the original surface into a poly-mesh composed of quad-meshes. Finally, the program identifies the largest and smallest panel that resulted from the panelization and outputs their dimensions upon request.

The second step planarizes the quad-panels of the polymesh using algorithms that implement S-isothermic planarization techniques. The proposed tool used Kangaroo Physics 2.0, a dynamic physics simulator for Rhino/Grasshopper that provides access to such algorithms. S-isothermic discretization is a quasi-isothermic remeshing technique; thus, it does not ensure that all the resulting quad-meshes are perfectly planar. Such algorithms only guarantee quasi-planarity, since there are surfaces that are impossible to be subdivided into a set of planar quads. Thus, after the first planarization, the proposed approach tests the planarity of each quad-panel using a dedicated procedure. The planarization test calculates the dot product of the normal vector of the plane created by three points of the quad with the vector formed between two points of the quad. The test always returns a Boolean value; if the result of the dot product is 0 or below the epsilon (ε) that EnergyPlus uses to approximate 0 in vertex coordinates, 1.0^{-8}, the test returns "True"; otherwise, it returns "False." If all the planarity test returns are "True" for all quad-mesh panels, Kangaroo's remeshing settings are validated, and the parsed surface is valid for a BEM. If not, the system reapplies the planarization procedure iteratively until the resulting poly-mesh is fully composed by planar surfaces or it reaches the number of remeshing iterations defined by the user. In the unlikely case that this approach does not generate a fully planar poly-mesh, the system identifies the non-planar quads and subdivides them into triangular planar meshes. Figure 5-6 shows the output from both the panel sizing algorithm and the planarity test executed in an intermediate step of the planarization process of a quad-mesh composed of 120 panels.

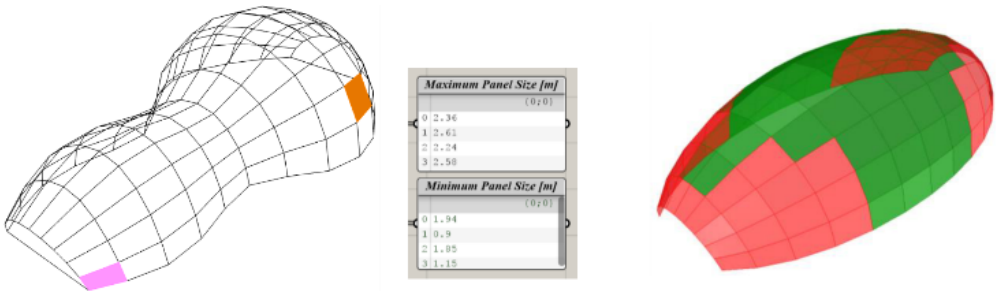

Figure 5-6. Left: the design system identifies the location and the dimensions of the biggest (orange) and smallest (purple) glass panel. In this way, the user can assess the construction feasibility of the surface rationalization. Right: planarity test of an intermediary step of the planarization process. The red color flags non-planar quad-meshes, while the green color indicates planar ones.

5.3.2 Design of experiments

To test and validate the proposed approach, the following section presents the application of the goal-oriented design system to a hypothetical design scenario. The design scenario consists of optimizing the distribution of glass frit densities to minimize building energy consumption in three instances of a parametric glass pavilion. The three pavilions are variations of a semi-ellipsoid shape. This type of spheroid is a good example of a double-curved non-developable quadratic surface commonly used as the starting point in the development of complex building envelopes. In fact, it is possible to find different variations and deformations of ellipsoids and semi-ellipsoids in contemporary architectural production. Figure 5-7 presents a collage that shows different buildings with an overall geometry that is based on a semi-ellipsoid. It shows a wide range of approaches on how to use and adapt this base geometry to different programmatic, structural, and spatial requirements. The Rika Mansueto Library – Figure 5-7, a) – located in Chicago, IL, and the National Wales Botanical Gardens – Figure 5-7, b) – situated at the welsh village of Llanarthney, UK, are examples of grid shell glass canopies that apply the semi-ellipsoid geometry in a more literal way. Foster and Partners (2000) designed the latter canopy while the Chicago based firm Murphy/Jahn Architects designed the former (2011). Figure 5-7, c) and d), presents a deformed egg-shaped building designed by Renzo Piano Building Workshop (RBWP) for the Pathé Foundation in Paris, France, as an example of a deformed variation and a freer application of the ellipsoid base geometry. There are also small-scale buildings such as architectural pods and pavilions that are good examples of derivations of the ellipsoid's double-curvature geometry. Figure 5-7 presents two examples of this type of pavilions: the Cella Bar located in the Azorean island of Pico designed by the joint venture FCC Arquitectura + Paulo Lobo (2015) – Figure 5-7, e) –, and Achim Menges' (2019) proposal for the Pavillion of the German State of Baden-Wuerttemberg in the World EXPO 2020 at Dubai – Figure 5-7, f).

Figure 5-7. Examples of buildings with double curved envelopes formulated either using more direct applications of ellipsoid-based geometries or deformations of it: a) Rika Mansueto Library, Chicago, IL (Murphy/Jahn, 2011); b) National Wales Botanical Gardens, Llanarthney, UK (Foster and Partners, 2000); c) and d) Pathé Foundation, Paris, France (RPBW, 2014); e) Cella bar, Pico, Portugal (FCC Arquitectura, 2015); f) proposal for the World EXPO 2020 Baden-Wuerttemberg German state pavilion (Menges, 2019). All images rights reserved.

The base semi-ellipsoid used in the experiment has a 30 m long primary axis, a 15 m long secondary axis with, and a 7.5m height apex. In each case, the primary axis aligns with the North-South cardinal direction: poles are cut to provide two entrances on the North and South ends. This base geometry constitutes Solution A. Solution B is a deformation of solution A that resulted from the rescaling of the ellipsoid section along the primary axis. The "peanut" shape of this solution promotes self-shading and, consequently, different patterns of solar radiation across the building skin that will cause local variations in glass fritting coverage. Finally, Solution C is the result of the deformation of the main meridians of the ellipsoid. Since it has different curvatures in both directions, it is the most challenging model to parse into a BEM. Figure 5-8 shows the initial NURBS geometry of all the solutions of the case study. Table 5-1 reports the floor area, surface area, volume, and form factor (surface-to-volume ratio) of each pavilion.

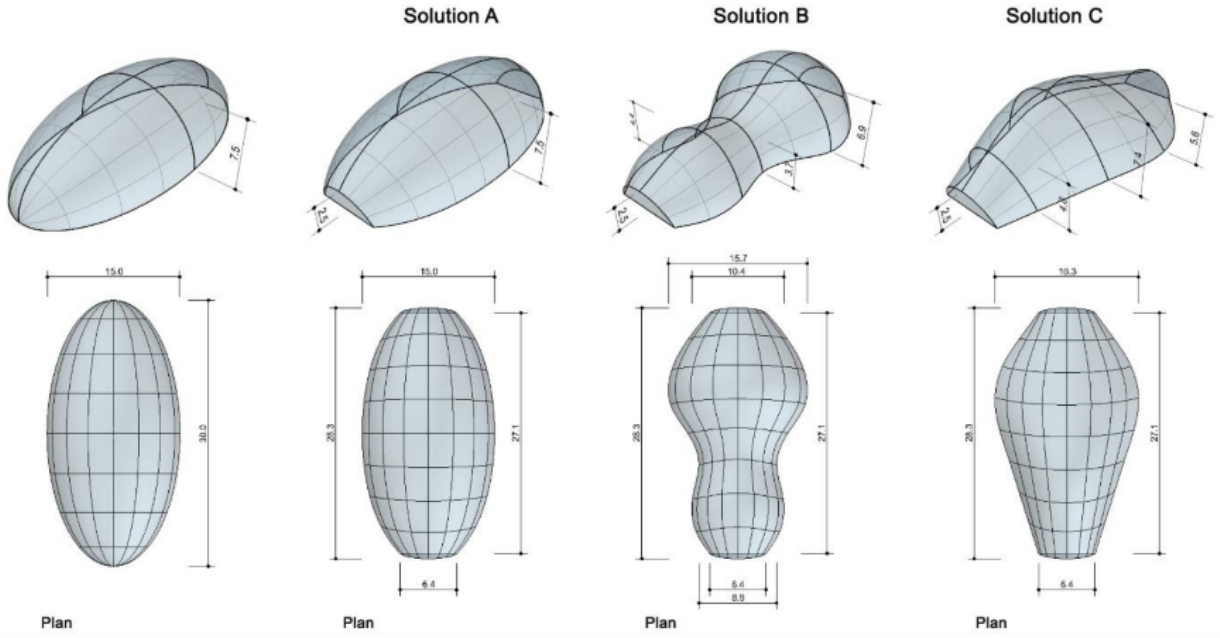

Figure 5-8. The base semi-ellipsoid and the three pavilions derived from it.

Table 5-1. Floor area, volume, surface area, and form factor of each solution.

	Floor Area (m^2)	**Volume** (m^3)	**Surface area** (m^2)	**Form factor**
Solution A	339.5	1646.8	583.2	0.35
Solution B	302.5	1182.6	508.3	0.43
Solution C	321.9	1211.5	497.8	0.41

The system automatically parsed the geometry of the three parametric instances into valid BEMs. Figure 5-9 illustrates both the original surfaces and the resulting planar quad-meshes of applying S-isothermic planarization algorithms available in Kangaroo. They constitute both the construction/fabrication model for the glass panels and the geometric model for EnergyPlus.

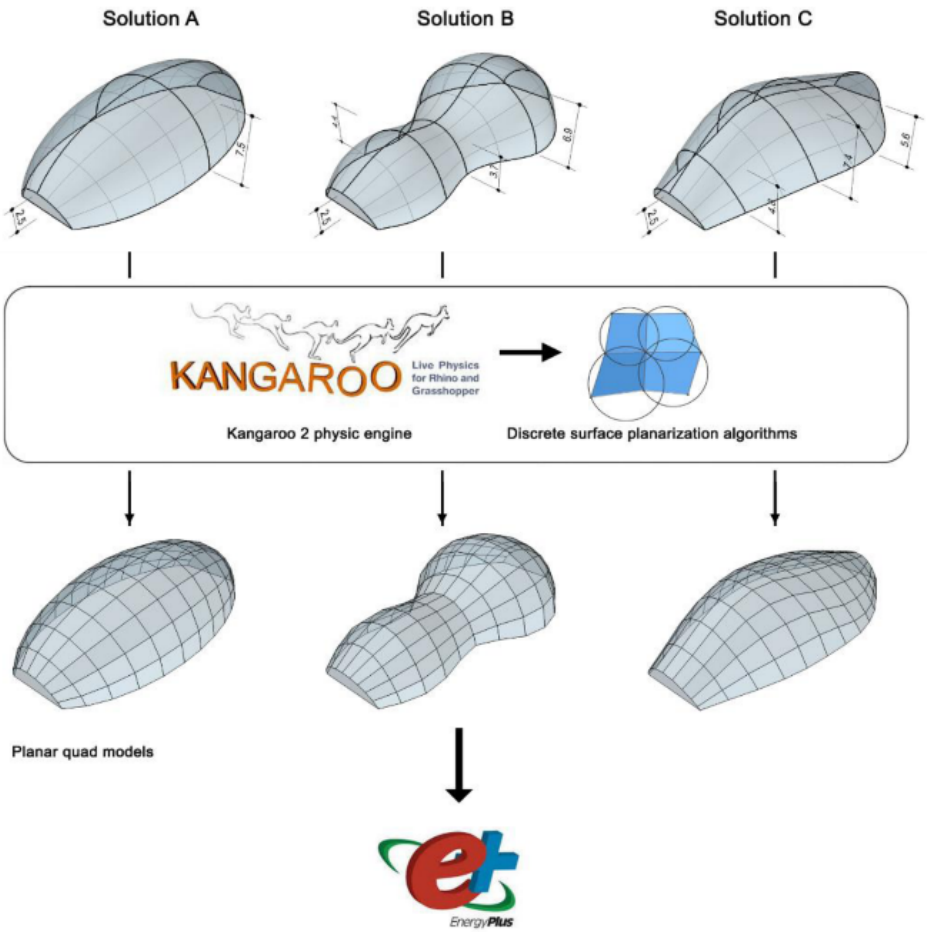

Figure 5-9. Original surfaces and the resulting S-isothermic planar quad-meshes. The processed meshes are ready to be fed to EnergyPlus, a popular thermal and whole-building energy simulation software.

The modeling of parametric glass fritting panels, which can vary their fritting density, is challenging in goal-oriented design processes based on BES. Glass frit panels are Complex Fenestration Systems, which are properly modeled in EnergyPlus using BSDF material descriptions. As mentioned in section 5.2, either synthetically generated BSDF data or BSDF descriptions in BES entails a considerable computational overhead that hampers their use in optimization-based procedures. Thus, in order to reduce the simulation time this work assumes a rough simplification; every glass panel has a scalable centered opaque EnergyPlus shading object with Solar and Visible Reflectance of white ceramic material (≈ 0.7). By scaling every shading object, it was possible to infer the glass frit percentage applied to each glass panel. The system then reprocessed the simplified shades back to the digital fabrication model as fritting patterns through a dedicated set of scripted functions that allows the user to control the size and shape of the glass frit pattern. Figure 5-10 shows a BEM with shading objects equivalent to a fritting density of 60% and their translation to a possible fritting pattern within the digital fabrication model.

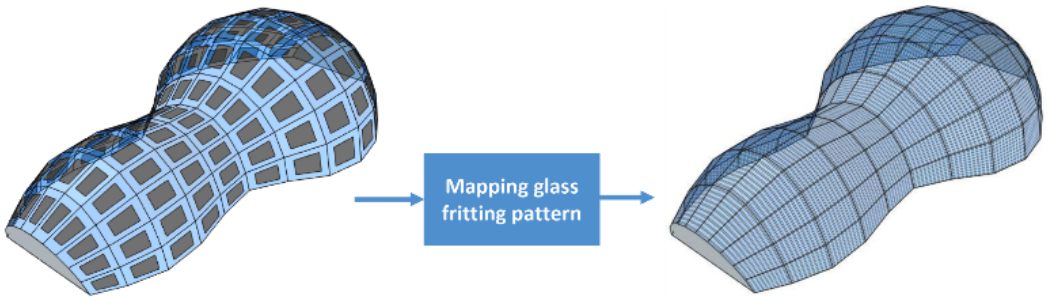

Figure 5-10. EnergyPlus shading objects (60% shading ratio) and their remapping to a possible glass fritting pattern.

After generating a valid BEM by automatically parsing the initial geometry of the pavilions, the system runs energy and solar radiation simulations using EnergyPlus and Radiance, respectively. The location and climatic data used in this experiment refers to the Typical Meteorological Year (TMY) of Logan International Airport, Boston, USA. Although having a cold climate, Boston experiences hot and humid summers; thus, it provides a useful environment to test both winter and summer conditions. Summer thermal performance was of importance because the proposed system aims for solar control optimization, a passive cooling design strategy.

Triple Low-e glazing assemblies, with argon and aluminum frames with thermal breaks, compose the all-glass envelope. This type of glazing was chosen for its high thermal performance, specifically its low thermal conductivity (U-factor), which is appropriate for the climate of Boston. Finally, the ground floor is a heavyweight concrete slab.

To avoid panel-by-panel glass frit density optimization, the system automatically clusters panels according to their irradiance values (kWh/m^2). This dimensionality reduction technique aims to reduce the number of design variables controlled by the GA. Although this strategy constrains the design solution space, it facilitates the search process without losing too much granularity. Thus, before running a whole energy building simulation, an ancillary Radiance simulation determines the cumulative incident solar radiation per panel for a specific selected analysis time period. To conduct this solar analysis, the system places a Radiance sensor node in the area centroid of each panel. Based on the range of solar radiation results, the system groups the different panels into 5 bins. Table 5-2 shows the irradiance binning process for each design alternative. Figure 5-11 pairs the results of annual solar radiation per panel in each design alternative with the result of the clustering process that groups panels with similar solar radiation (SR) or irradiance.

Table 5-2. Solar radiation bins for each pavilion.

	SR: Full range (kWh/m^2)	**Bin I SR: 0-20%** (kWh/m^2)	**Bin II SR: 20-40%** (kWh/m^2)	**Bin III SR: 40-60%** (kWh/m^2)	**Bin IV SR: 60-80%** (kWh/m^2)	**Bin V SR: 80-100%** (kWh/m^2)
Solution A	[417, 1636]	[417, 1636[	[661, 905[	[905, 1148[	[1148, 1392[	[1392, 1636]
Solution B	[593, 1647]	[593, 804[	[804, 1015[	[1015, 1225[	[1225, 1436[	[1436, 1647]
Solution C	[830, 1613]	[830, 987[	[987, 1143[	[1143, 1230[	[1230, 1456[	[1456,1613]

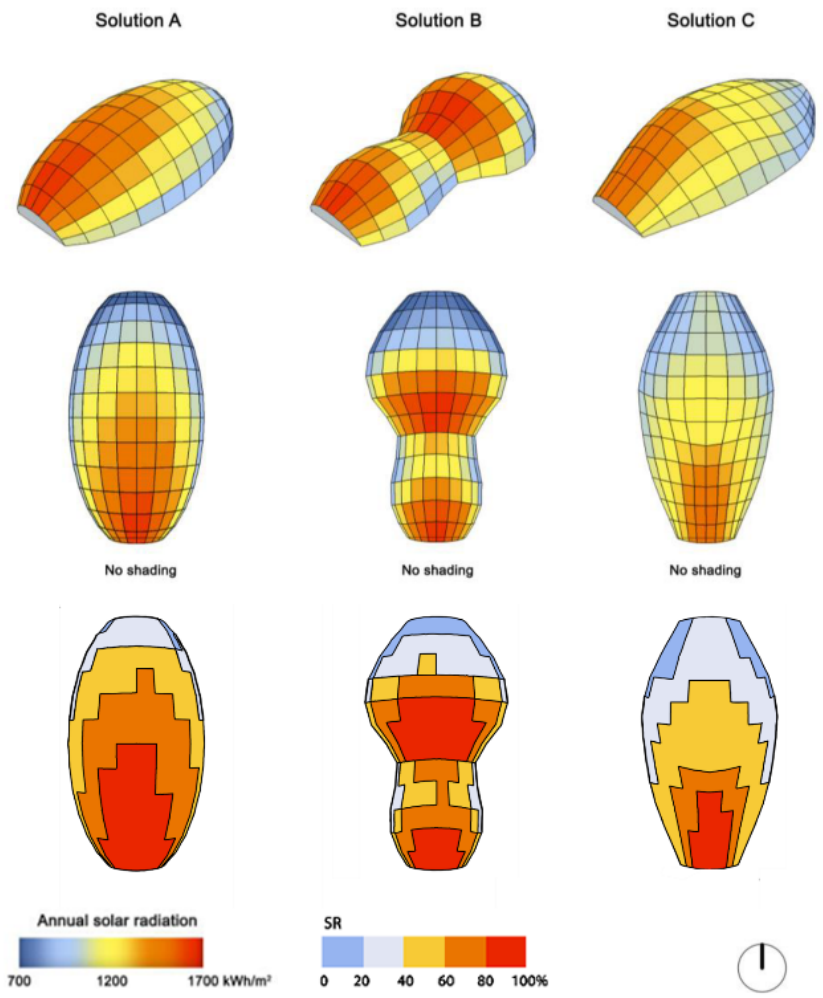

Figure 5-11. Top and middle: annual solar radiation per panel mapped in the three pavilions. Bottom: the five glass panel clusters based on the annual irradiance of Boston, MA.

The percentages of glass fritting coverage in each panel cluster make up the decision variables (x) of the optimization problem. The experiment used Galapagos, a Standard Genetic Algorithm (SGA) available in Grasshopper to minimize energy consumption. The analysis of building energy performance considered three main energy uses: heating, cooling, and lighting. The experiment excluded equipment/process loads because they do not depend on environmental factors or on building envelope characteristics but on the type of equipment and appliances used, as well as on occupancy schedules. Thus, the total building energy consumption is the sum of hourly energy for heating, cooling, and lighting. Considering that the different design alternatives have different areas and volumes, the experiment normalized energy consumption results per area unit, using the Energy Use Intensity (EUI - kWh/m^2) metric, and per volume unit, by modifying the previous metric (EUI(v) - kWh/m^3). In this way, the results of the different solutions are comparable.

EnergyPlus simulated the energy performance of each solution generated by the SGA. The main simulation assumptions and settings were the following: (i) a simplified Variable Air Volume (VAV) HVAC system, the Ideal Loads Air Zone System (ILAS) to calculate sensible cooling and heating loads and energy consumption for space conditioning; (ii) heating setpoint set to 20 ºC and

cooling setpoint set to 26 ºC; (iii) infiltration rate of 0.3 Air Changes per Hour (ACH), which represents an airtight building; (iv) a power density for light fixtures of 11.4 W/m^2 (a typical value for fluorescent light bulbs); and finally, (v) an illuminance setpoint of 300 lux to control the dimmable lighting system used in the model.

Finally, the performance-based design exploration of this experiment included two main tasks:

An annual parametric study of different shading conditions – before setting an automatic optimization procedure for shading/fritting density, the proposed approach generated and simulated three different glass frit coverage scenarios to understand the baseline energy profile of the three pavilions better. The different glass fritting alternatives were as follows: (i) no fritting (base case), (ii) 40% evenly distributed fritting, and (iii) a fritting gradient determined by solar radiation (SR) measurements. Table 5-3 shows the distribution of glass fritting in different glass clusters of the latter glass fritting alternative.

Table 5-3. Distribution of glass frit densities in the different panel clusters with varying fritting gradient, determined by incident solar radiation.

	Bin I	**Bin II**	**Bin III**	**Bin IV**	**Bin V**
% of frit coverage	25	40	55	70	85

By simulating different design solutions with similar areas and volumes, it is possible to assess how form affects solar irradiance and total energy consumption, as well as the impact of different shading schemes in the overall energy profile of each case.

Optimization of shading/fritting percentage for cooling energy consumption – using the lessons learned from the previous task, the proposed generative design system optimized the glass fritting densities in the different clusters to reduce cooling energy. The experiment focuses on cooling energy demand because the shading effect introduced by glass frit is a strategy that mainly reduces solar heat gains. Thus, the cooling period of the year considered for the optimization was May 20th to September 21st, which includes the end of spring and the whole of summer.

5.3.3 Results

The following presents the results of the two-phased experiment.

Parametric study of different shading/glass frit conditions

Figures 5-11, 5-12, and 5-13 illustrate the annual solar radiation analysis for Boston, and the three different glass fritting strategies applied for each design alternative. Figure 5-11 (see section 5.3.2 - Experiment) shows how the geometric differences in tilt, angle, and self-shading patterns generate different irradiance distributions among the three tested forms. Thus, although these tested forms derive from the same archetypical geometry, their annual irradiance distributions are sufficiently diverse to result in mutually unique glass fritting patterns. Figure 5-12 illustrates the resultant patterns given a desired homogeneous glass fritting coverage of 40% per panel. In contrast, Figure 5-13 shows the shading pattern given a gradient glass fritting strategy based on

solar radiation values, where incident radiation acts as an attractor/repeller that controls the frit coverage for each panel cluster.

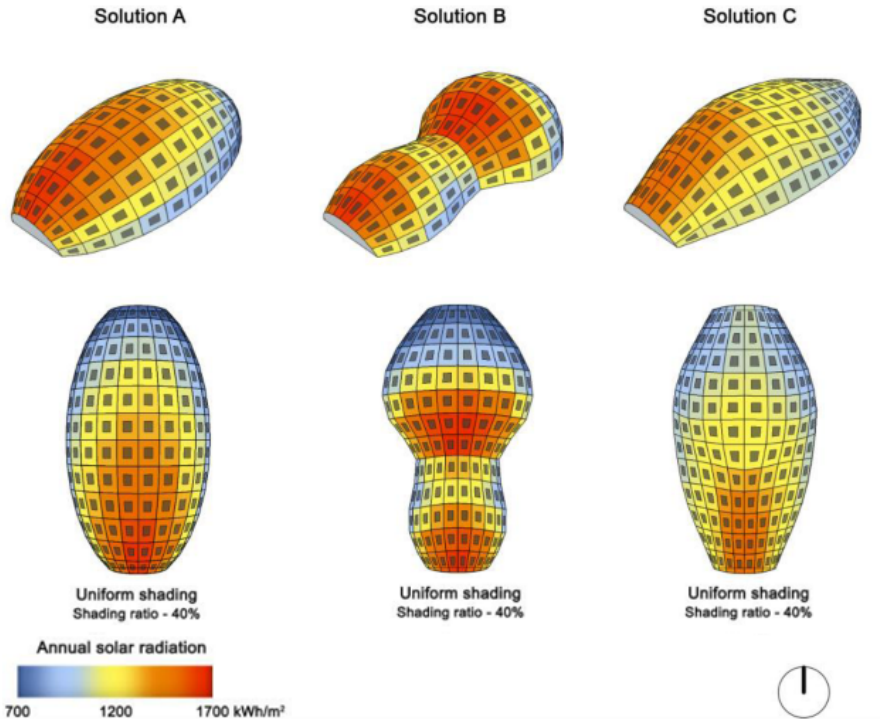

Figure 5-12. The three design alternatives with a homogeneous 40 % glass fritting distribution.

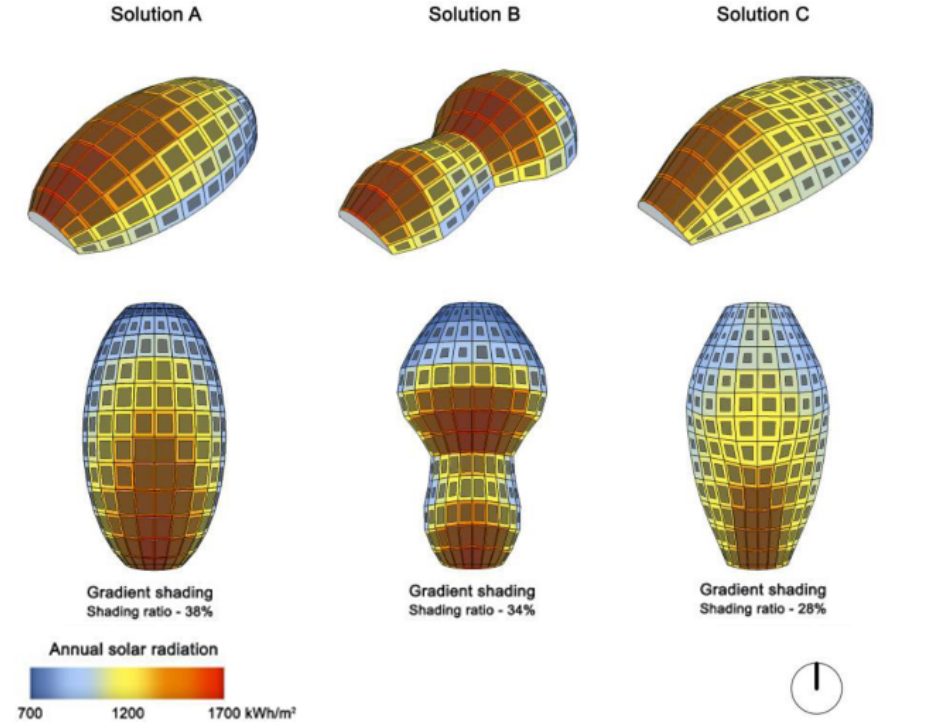

Figure 5-13. The gradient glass fritting solution is modeled with the simplified modeling approach of glass frit coverage composed by quasi-coplanar EnergyPlus shading objects.

Table 5-4 reports both EUI and EUI(v) annual results of each solution. Figures 5-14 and 5-15 present a bar chart that compares the energy performance of the three design alternatives, respectively, in terms of EUI (kWh/m^2) and EUI(v) (kWh/m^3).

Table 5-4. EUI and EUI(v) annual results of the parametric study conducted in each design alternative.

	Solution A			**Solution B**			**Solution C**		
	No shading	40% shading	Gradient shading	No shading	40% shading	Gradient shading	No shading	40% shading	Gradient shading
EUI - kWh/m^2									
Heating	105.1	110.5	128.9	53.6	54.5	64.7	52.8	57.0	62.2
Cooling	29.6	22.2	11.4	49.2	40.5	25.5	45.1	35.2	26.5
Lighting	10.5	10.5	10.7	11.4	11.5	11.6	11.0	12.0	11.1
EUI [total]	145.2	143.3	151.0	114.2	106.5	101.8	108.9	104.3	99.9
EUI(v) - kWh/m^3									
Heating	21.7	22.8	26.6	13.7	13.9	16.6	14.0	15.2	16.5
Cooling	6.1	4.6	2.4	12.6	10.4	6.5	11.97	9.4	7.0
Lighting	2.2	2.2	2.2	2.9	2.9	3.0	2.9	3.2	3.0
EUI(v) [total]	29.9	29.5	31.1	29.2	27.3	26.1	28.9	27.7	26.5

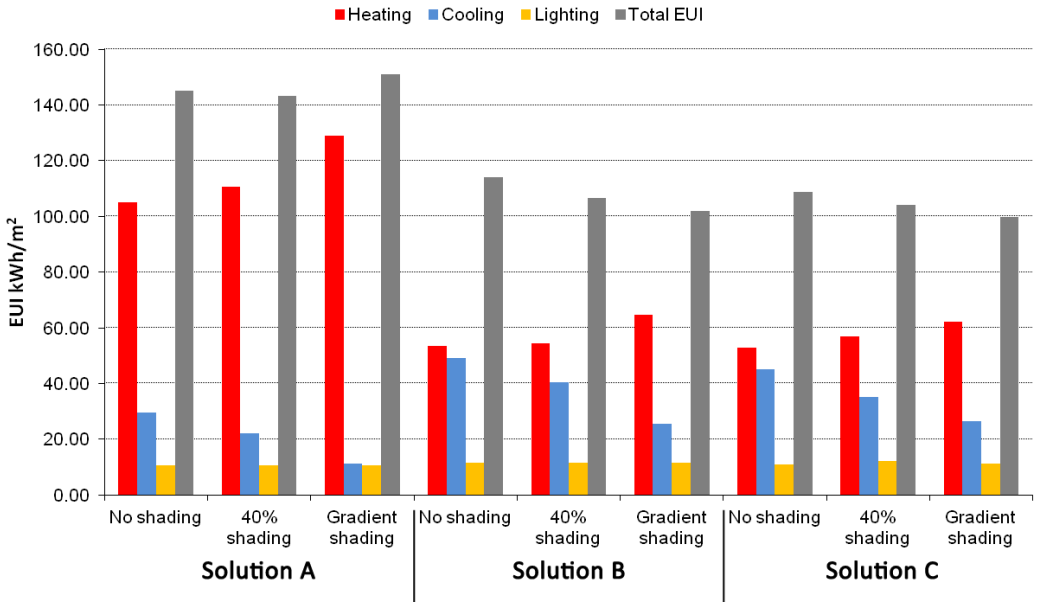

Figure 5-14. Annual EUI (kWh/m^2) of the different design alternatives in the parametric study.

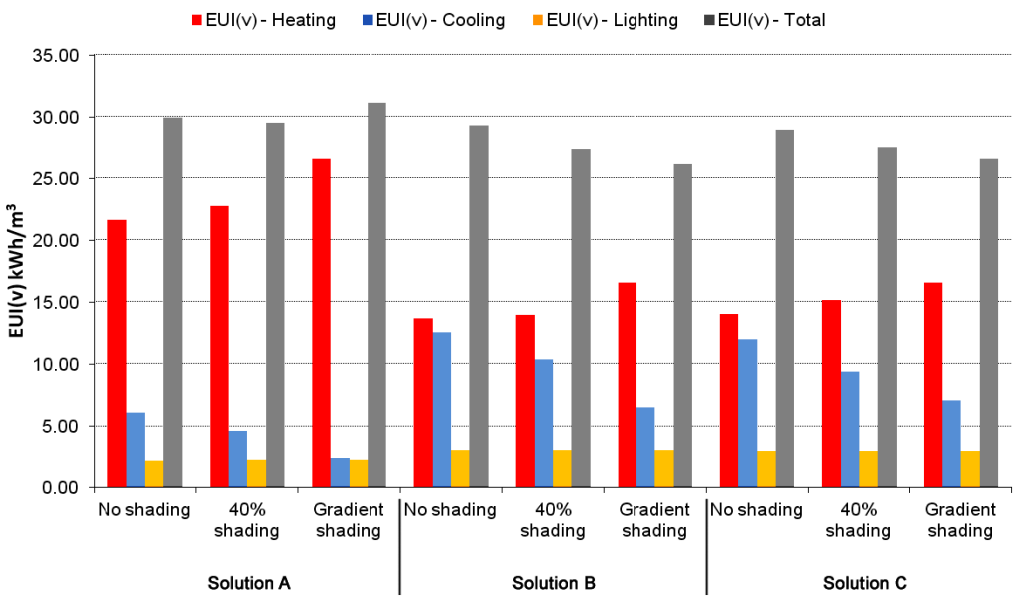

Figure 5-15. Annual EUI(v) (kWh/m^3) of the different design alternatives in the parametric study.

As Table 5-4 and the charts of Figures 5-14 and 5-15 show, solution A has the highest heating energy consumption, which results from the small solar exposure that this solution has on the northern part of its envelope. Solutions A and B have similar irradiance distributions on their north-facing regions; however, solution B compensates for the associated heat losses via two south-facing areas that receive high solar gains. Solution C has the lowest heating energy consumption of the three test cases due to a more uniform solar irradiance distribution, which reduces the contrast between heat losses and gains. In all cases, shading is effective in reducing cooling loads, but it also increases the heating demands. The gradient shading solution is the most effective in reducing cooling energy consumption, thus supporting the intuition that the panels that need more shade are the ones that are more exposed to the sun. The small variation on lighting energy consumption is a direct result of the large glazed area of all solutions, and of the glass fritting strategy blocks the direct sun by diffusing it, thus promoting diffuse light across all solutions. Moreover, the differences between lighting energy consumption are insignificant relative to those of the space conditioning end-uses, i.e., heating and cooling.

Figures 5-14 and 5-15 indicate that the significant reduction of cooling energy consumption provided by the gradient solution is not enough to offset heating demand. From this more holistic perspective, the 40% homogeneous shading solution is slightly more efficient, as indicated by its lower EUI and EUI(v).

This parametric study shows that providing a static system to control solar gains in a specific all-glass building geometry can be effective year-round, even in a climate like Boston. The experiment shows that even a homogeneous 40% shading ratio improves overall energy consumption. This supports the choice to run the optimization cycle for the summer period only to find the best glass frit strategy for reducing cooling loads.

Optimization of glass frit percentage for cooling energy consumption

The second phase of the experiment consisted of conducting two fully automated search procedures using Galapagos' standard GA. The first, Opt#1, does not have restrictions on the parameters that control the glass frit coverage for each group of panels receiving the same irradiance range. In contrast, the second, Opt#2, entails some constraints assigned to those parameters, which minimize shading in panels that are less exposed to solar radiation, thus promoting a gradient shading pattern. Since glass fritting is a design strategy that supports passive cooling through shading and blocking unwanted solar radiation, the optimization period comprises the cooling season in Boston - end of spring, May 20th, to the end of summer, September 21st.

Figures 5-16 and 5-17 show the results of the unconstrained optimization experiment, Opt#1. Figure 5-17 shows the remapping of glass frit coverage ratios, presented in Figure 5-16, to a specific frit pattern. Figures 5-18 and 5-19 show the results of the second optimization experiment, Opt#2.

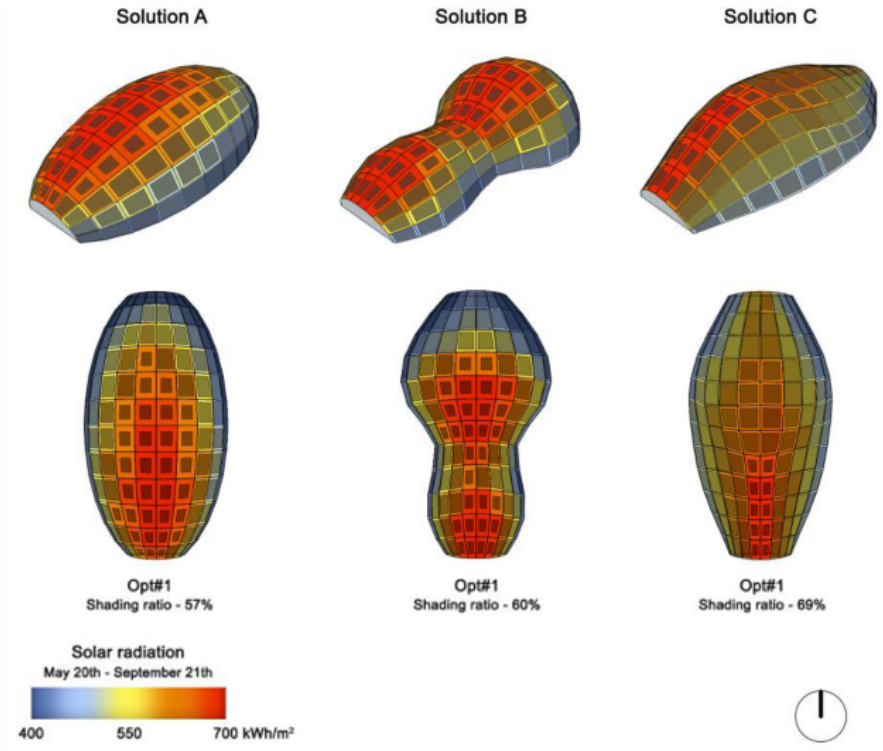

Figure 5-16. The result of the unconstrained optimization experiment Opt#1 using the simplified modeling approach of glass frit coverage composed by quasi-coplanar EnergyPlus shading objects.

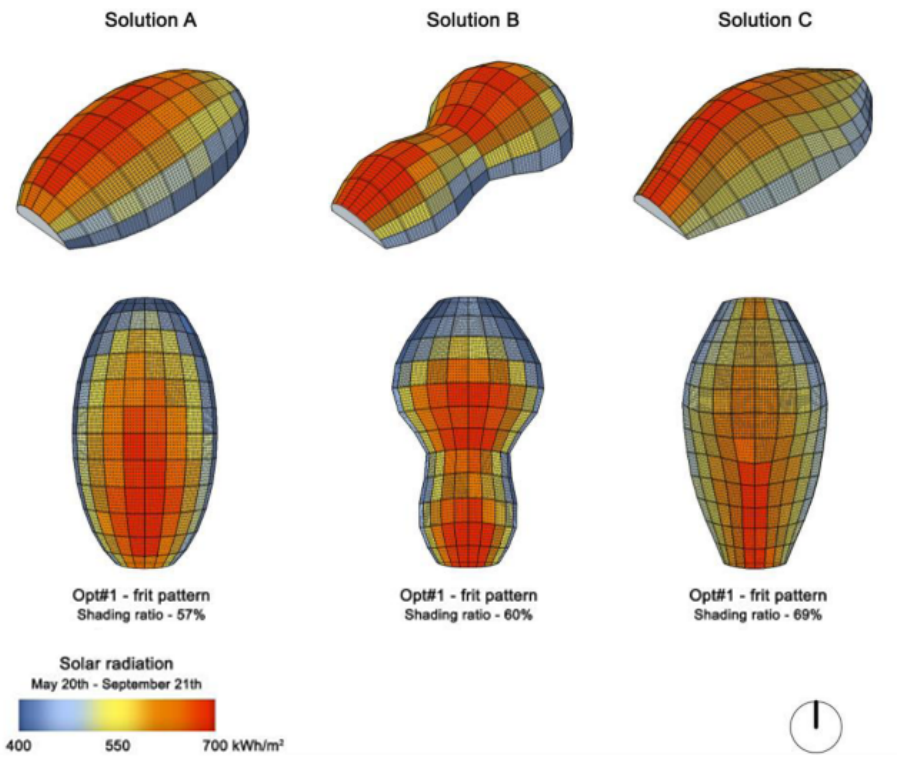

Figure 5-17. Opt#1 resulting shading ratio remapped as a fritting pattern. Shading ratio label indicates the average of the different ratios attributed to each panel cluster.

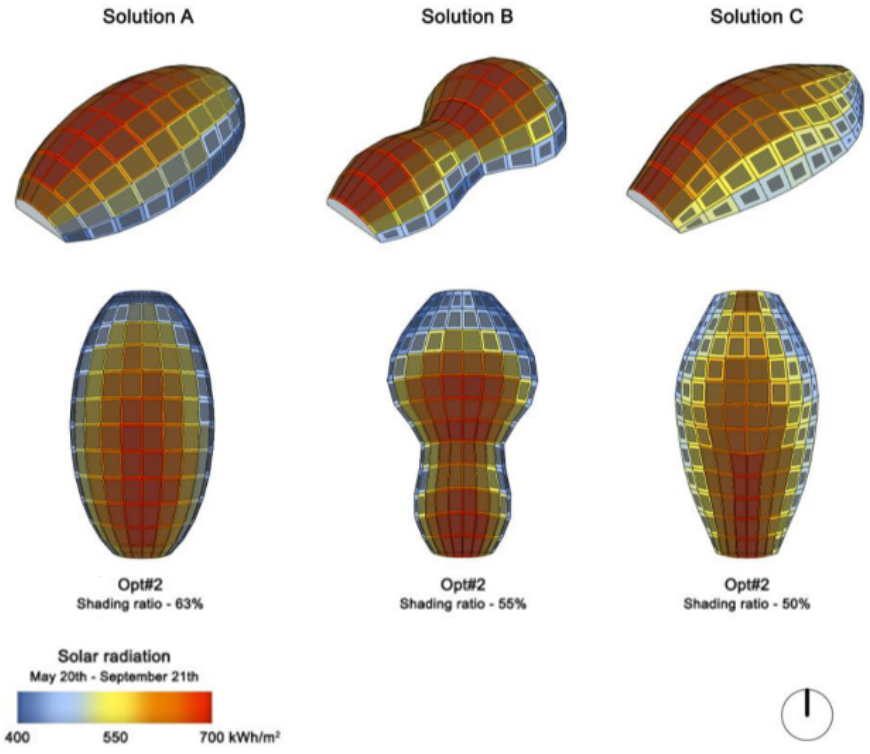

Figure 5-18. The result of the constrained optimization experiment Opt#2 using the simplified modeling approach of glass frit coverage composed by quasi-coplanar EnergyPlus shading objects.

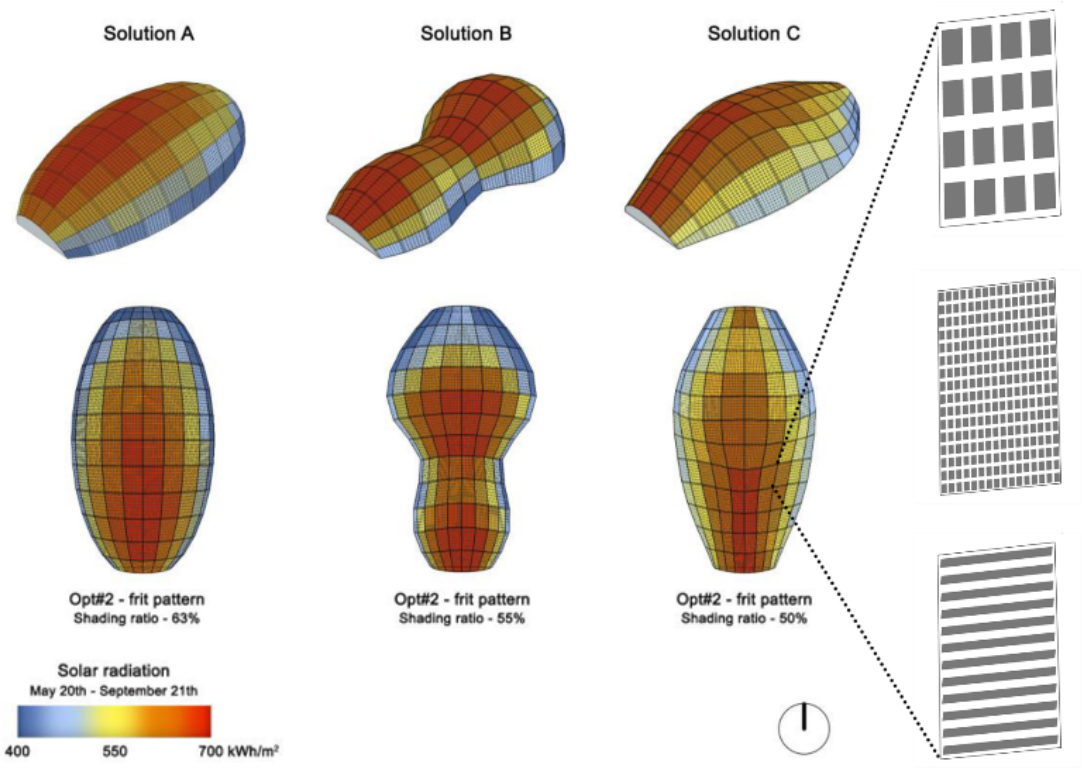

Figure 5-19. Left: Opt#2 resulting shading ratio remapped as a fritting pattern. Shading ratio label indicates the average of the different glass fritting ratios attributed to each panel cluster. Right: Examples of fritting patterns generated with the remapping algorithm. All three options have the same shading ratio, 70%.

Opt#1 recommended solution is counterintuitive because it provides more glass frit to the panels that are less exposed to solar radiation. To reduce cooling loads, the GA blocked the panels with the largest area, except the ones that are more exposed to the sun. This optimization run indicates that the GA probably found a local minimum and that the process needed more guidance. In Opt#2, the constraints imposed on the search lead the GA to find a more expectable solution that places the higher shading ratio in the areas that report higher irradiance values.

Table 5-5, Figure 5-20, and Figure 5-21 compare the energy performance of the three designs for no shading (baseline), Opt#1, and Opt#2 in the period under study. The comparison shows that Opt#2 is extremely effective in reducing cooling loads in Solution A, slightly effective in Solution B and not as effective as Opt#1 in Solution C.

However, the results of solution A and B show that steering the optimization process, through constraints based on preliminary parametric analysis, can lead to better results that are more energy-efficient and closer to the designer's intents. In sum, using a metaheuristic approach based on GA, it is possible to search a considerable large solution space and find efficient design strategies that improve the energy performance of all glazing pavilions in the summer period.

Table 5-5. EUI and EUI(v) of each solution for no shading, Opt#1, and Opt#2.

	Solution A			**Solution B**			**Solution C**		
	No shading	Opt#1	Opt#2	No shading	Opt#1	Opt#2	No shading	Opt#1	Opt#2
EUI - kWh/m²									
Heating	0.37	0.46	0.54	0.08	0.13	0.11	0.07	0.11	0.09
Cooling	24.24	6.59	4.34	34.65	12.05	11.26	32.85	6.47	12.47
Lighting	4.28	4.29	4.41	4.55	4.49	4.58	4.34	4.42	4.46
EUI [total]	28.89	11.33	9.29	39.28	16.66	15.95	37.26	11.00	17.01
EUI(v) - kWh/m³									
Heating	0.08	0.09	0.11	0.02	0.03	0.03	0.02	0.03	0.02
Cooling	5.00	1.36	0.90	8.87	3.08	2.88	8.73	1.72	3.31
Lighting	0.88	0.88	0.91	1.16	1.15	1.17	1.15	1.18	1.18
EUI(v) [total]	5.96	2.34	1.92	10.05	4.26	4.08	9.90	2.92	4.52

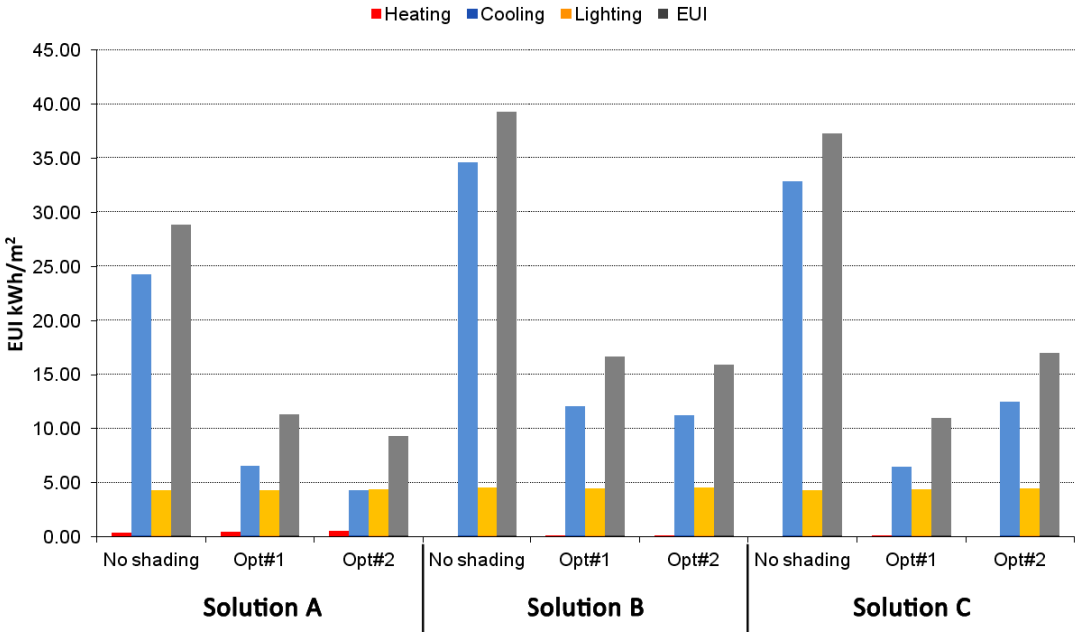

Figure 5-20. Annual EUI of the different design alternatives in the optimization experiment.

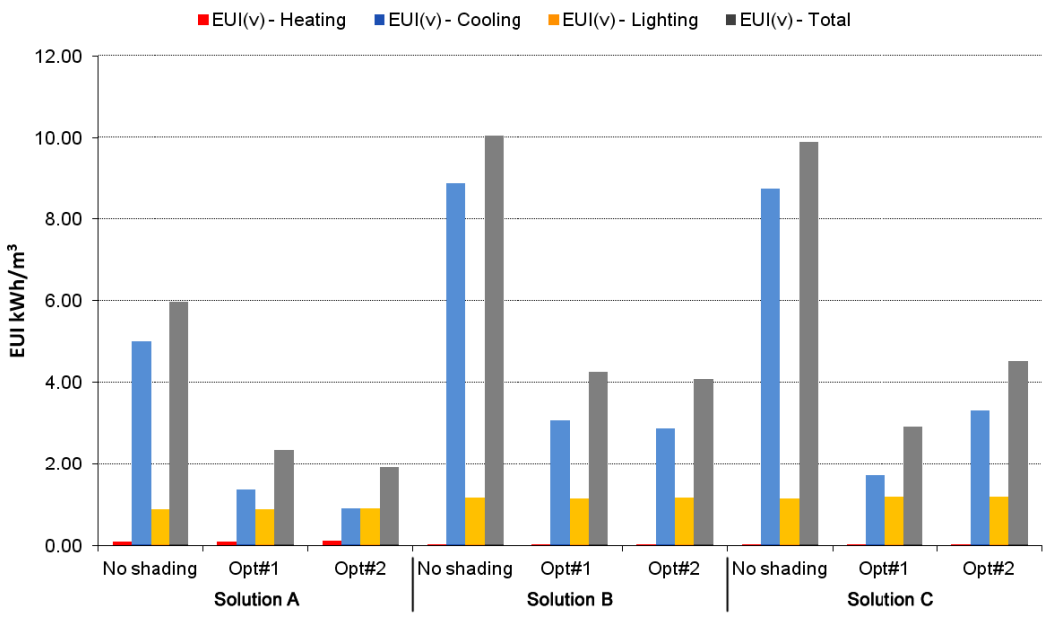

Figure 5-21. Annual EUI(v) (kWh/m^3) of the different design alternatives in the optimization experiment.

5.3.4 Discussion

Both phases of the experiment demonstrated that the optimization of individualized fritting patterns in glass panels requires BEMs with a geometry that captures at least the essential features of the initial models. Thus, they reinforce the usefulness of the adopted strategy in automatically parsing the geometry of a buildable panelized envelope geometry with minimal formal deviations.

The parametric study tested three shading scenarios for each of the following glass fritting solutions: no shading, 40% homogeneous shading for the glass panels, and a gradient shading approach based on incident solar radiation incident over the building envelope. The goal was to test the efficacy of a shading strategy based on a glass frit pattern to reduce annual energy consumption in Boston, Massachusetts. Boston experiences all seasons. The summers are warm to hot and humid, with periods that can exceed 32 ºC, while winters are cold, with freezing temperatures from November through the end of March. Typically, Boston's climate is heating-dominated, but because it also experiences hot and humid summers, cooling loads are relevant in this period. Thus, and considering that this work focused on whole glass pavilions, controlling solar gains is also an important energy conservation measure.

The annual parametric simulations show two different patterns. Table 5-4, Figure 5-14, and Figure 5-15 show that heating loads dominate Solution A, while in Solutions B and C, the difference between heating and cooling loads is much smaller. There are several reasons for this, but it seems that the relationship between surface area and volume plays an important role. Because it has the largest volume of the three, Solution A has the biggest volume of air to heat; simultaneously, it has the largest surface area of the three solutions, which means that it is more sensitive to heat loss. The result is significantly higher heating than cooling loads.

Moreover, because Solution A does not have self-shading and has a more exposed surface area, it also requires a higher percentage of glass frit in the panels of the gradient shading scenario. This

eventually blocks desired solar heat gains in the winter, which also contributes to the relatively high heating loads. That is why the gradient shading scenario is the only one where glass frit is unfavorable. The volumes and surface areas of Solutions B and C are smaller; thus they require a smaller heating load and experience less heat dissipation than solution A. Self-shading and a more even distribution of solar radiation on the envelopes of solutions B and C help distribute a more balanced frit pattern in the gradient shading scenario.

Table 5-6 shows the percentage of improvement (% of improvement) of EUI by adding shading to the glass pavilions. Chapter 4, section 4.5.3, equation (4-7) describes the calculation of % of improvement as proposed in ASHRAE standard 90.1 (ASHRAE, 2013). In this particular case the equation is reformulated as follows (5-1):

$$\%\ of\ improvement = \frac{Base\ Case\ EUI - Alternative\ EUI}{Base\ Case\ EUI} \qquad (5\text{-}1)$$

The results presented in Table 5-6 show that shading through glass frit is an effective year-round passive strategy in all solutions. Even solution A sees a small benefit from 40% homogeneous shading in its glass panels, indicating that glass frit reduces energy consumption in cases with a large glazed exposed surface area even in climates with cold winters. The table also shows that deriving a shading pattern based on solar radiation distributions can be more efficient than using homogeneous shading factors. These results reinforced the need for the second set of tests that aimed to optimize the glass frit in each glass panel cluster.

Table 5-6. Percentage of improvement in energy consumption in the parametric study of different glass fritting coverage. The calculation of percentage of improvement considered two scenarios: (i) 40% homogeneous and the gradient shading against no shading; (ii) gradient shading against 40% homogenous shading.

	% of improvement (Base case: No shading)		**% of improvement** (Base case: 40% homogeneous shading)
	40% homogeneous shading	Gradient	Gradient
Solution A	1%	-4%	-5%
Solution B	7%	11%	4%
Solution C	5%	8%	3%

Because shading is a passive cooling strategy, the optimization experiment aimed to determine the efficacy of glass fritting in reducing cooling energy demand in a whole glass pavilion in Boston. Thus, the period considered in optimization corresponds to Boston's warm months. This phase of the experiment entailed two optimization runs. The first, Opt#1, did not constrain the amount of shading for each panel cluster. Figure 5-16 shows that the shading optimization prioritized panel cluster area rather than the amount of solar radiation incident on the building envelope. To test the quality of the search in Opt#1, a second optimization (Opt#2) imposed a more direct relationship between incident solar radiation and the amount of glass frit.

Table 5-7 compares both Opt#1 and Opt#2 to a non-shaded base case, as well as to each other. The automated search procedure provided by the GA made it possible to considerably reduce the overall energy consumption of the non-shaded base cases.

Table 5-7. Percentage of improvement of energy consumption in the optimization study. The calculation of percentage of improvement considered the following scenarios: (i) Opt#1 and Opt#2 against no shading; (ii) Opt#2 against Opt#1.

	% of improvement (Base case: No shading)		**% of improvement** (Base case: Opt#1)
	Opt#1	Opt#2	Opt#2
Solution A	61%	68%	18%
Solution B	58%	59%	4%
Solution C	71%	54%	-55%

As expected, the optimization produced a considerable improvement in Solution A in both optimization procedures. This improvement is related to the fact that Solution A has the largest surface area and, consequently, the most exposed envelope of the three scenarios. Comparing the two optimization strategies, constraining the search procedure to promote a gradient glass frit pattern based on the solar radiation distribution yields better results in solutions A and B. In solution A, Opt#2 was able to find a solution that is 18% better than the Opt#1. In the case of solution C, Opt#2 found a worst solution than Opt#1, indicating that the success of steering the search by imposing constraints in Opt#2 is closely related to the amount of exposed surface area. Thus, the poor performance of Opt#2 in solution C could be related to that scenario's lower solar radiation variance, which makes this option a less suitable candidate for a gradient-based shading approach.

The different experiments demonstrated the benefit of using goal-oriented methods to understand the complex trade-offs associated with energy-related problems in buildings. Unexpected results from these methods could inform the design process with new perspectives and different solutions to solve specific design problems. The results also indicate that in some cases steering the optimization process by constraining certain design parameters improves the quality of the search. Finally, the experiments also showed how the energy performance approach can inform the physical and aesthetic properties of the building envelope with different densities of fritting patterns.

Despite the robustness of the proposed method in parsing complex double-curved geometry for BES, the resulting integration in a goal-oriented design workflow presents a few drawbacks, some already mentioned and discussed in section 5.2. The main limitations are: (i) efficiency of the search; (ii) slow simulation run times that make it difficult to use the proposed approach at early design phases; (iii) the oversimplification used in modeling a complex glass-frit system might affect the accuracy of the results.

Since the proposed generative design system is search mechanism agnostic, it is possible to improve the efficiency of the search by using a more sophisticated optimization metaheuristic. Thus, addressing the first limitation is not vital. However, the two other limitations are intrinsically related to the geometric modeling of BEMs, a task to tackle up-front. Thus, the following sections of this chapter present two strategies that specifically address those limitations. Section 5.6 - Concluding remarks - discusses in detail Strategy A limitations.

5.4 Strategy B: Automatically simplify building geometry for efficient whole-building energy simulations

The previous section successfully proposed a method that automatically generates valid geometric descriptions of complex building envelopes with a reduced formal gap between the initial geometry and the resulting BEM. This section focuses on extending that method to produce equivalent and more efficient geometric descriptions that result in valid, accurate, and faster whole-building energy simulations. Therefore, this section presents and discusses approaches that automatically simplify the geometry of either single or multi-thermal zone BEM, by using the following two approaches:

1) Reduce the amount of geometry, i.e., the number and density of mesh polygons, particularly in BEM that entail complex (double-) curved building envelopes.
2) Decompose complex multi-zone BEM into simpler, faster to run, sets of representative single thermal zone BEM.

5.4.1 Automatically reducing geometry

Current parametric design tools and visual programming languages for popular CAD/BIM tools (e.g., Dynamo for Revit and Grasshopper for Rhinoceros 3D) are becoming increasingly popular among architects. One of the reasons for this trend is because such tools facilitate the quick development and exploration of building geometries of considerable formal complexity and sophistication at early design phases. Unfortunately, the formal scope of state-of-the-art and validated BEM tools, such as EnergyPlus, mainly focus on simple box-like building geometries. As a result, BES tools can quickly process box-like buildings but have difficulties in providing feedback in useful time if the simulation model mesh includes many polygons. The following work focuses on automatically simplifying BEM geometry. Thus, the goal is to automatically generate geometric surrogates for BES, particularly if the building geometry entails either curved or double-curved surfaces or both. The resulting geometric-surrogates based BEMs are simulation models with coarser geometric representations that capture the essential formal features of a more refined building representation. They are faster to run, and although they sacrifice some accuracy, they do not introduce relevant deviations to simulation output. To pursue the objective of automating the generation of BEMs that have a more efficient geometric description, the following work aims to answer two essential research questions:

1) How to automatically simplify early-stage building models, namely those with single- or double-curved envelopes?
2) How far can this simplification go?

To answer these questions, the following sections of this subchapter present two geometry simplification heuristics for BEMs. The proposed heuristics and subsequent implementation result from a collaborative research effort between the author of this dissertation and his advisers, published in 2019 (Santos, Schleicher and Caldas, 2019). The first is a tessellation procedure that generates a low-poly mesh version of the building's envelope while preserving the original volume. The second proposes a zone sampling technique that reduces a complex multi-zone BEM to its most representative parts. The result is a novel digital tool that automatically simplifies

complex and convoluted building envelopes for BES. Two different experiments tested the proposed method and its computational implementation. The analysis and discussion of the experiments results led to potential modeling recommendations for mesh reduction in BES, particularly at early design stages.

5.4.2 Methods to reduce the geometric complexity of complex building forms for Building Energy Simulations

This work proposes the computational implementation of the two heuristics for automated simplification of complex curved building envelopes in BES. The first heuristic uses the method presented in section 5.3 to tessellate the building's envelope into a simpler low-polygon mesh, composed of planar faces. By dividing the original surface width (u) and length (v) the proposed approach generates an approximated mesh formed by quadrilateral faces, i.e., quads. If planar quads do not entirely compose the resulting mesh, the heuristic remeshes the envelope surface using a quasi-isothermic planarization algorithm (Sechelmann, Rörig and Bobenko, 2013; Rörig et al., 2015). If the planarization step is not successful in planarizing all quads, the heuristic will split the resulting non-planar quads into tri-meshes. The simplification of the building's envelope into a low-poly mesh has a direct impact on the original volume of air of the thermal zone or zones, thus introducing deviations to the heat balance calculation. To avoid volume deviations, our approach automatically scales the simplified thermal model to match the original volume. Equation (5-2) determines the factor of the uniform 3D scaling (S_{factor}) for the x-, y-, and z-directions.

$$S_{factor} = \sqrt[3]{\frac{Original\ Volume}{Simplified\ Volume}} \quad (5\text{-}2)$$

The second proposed approach simplifies multi-zone BEMs by decomposing them into a set of representative single-zone models. The user can manually identify and isolate the sample thermal zones by drawing a polygon over the model or let the system automatically find and isolate the representative thermal parts. Currently, the implemented heuristic uses information regarding orientation, zone program, schedules, loads, and other zone properties such as heating and cooling setpoints to perform this automatic subdivision. After subdividing the BEM into representative single thermal zones (Z_i), the system calculates the original volume of influence of each representative zone (V_{z_i}) and closes the sampled simplified thermal model with adiabatic surfaces. Then, the tool simulates each single thermal zone in parallel and normalizes the simulation outputs in a volume-based Energy Use Intensity (EUI_V), as an alternative to the typical EUI that normalizes energy by unit area. Equation (5-3) is then used to find the energy consumption of any energy end-use of the entire building, which sums the energy consumption of all representative zones Z_i, which in turn result from the multiplication of the correspondent EUI_V by V_{z_i}.

$$Energy\ consumption\ (Z_i) = \sum_{i=1}^{n} V_{z_i} \times EUI_{V(V_{z_i})} \quad (5\text{-}3)$$

The following section presents in detail two experiments that tested the effectiveness of the two simplification approaches in automatically simplifying both single- and multi-thermal zone BEMs.

5.4.3 Design of experiments

Two experiments assessed the performance of the proposed approaches in automatically simplifying BEM in terms of run time and energy simulation output deviation. Both compared the simplified BEM (i.e., a BEM with a coarser geometric resolution) results with the ones from a BEM with a high geometric resolution using the following metrics: simulation time, measured in seconds (s), the Coefficient of Variation of the Root Mean Squared Error (CVRMSE), and Normalized Mean Bias Error (NMBE). In this case, NMBE provides the average of the errors of the BEMs with simplified versions of the building envelope (the simplified models) normalized by the mean of the results of a BEM with a highly detailed envelope representation, the benchmark model. In NMBE, negative values mean over-prediction, while positive values indicate underprediction. Because NMBE is susceptible to the cancelation effect, it needs to be complemented with CVRMSE, a statistical index that is not affected by it. In this experiment, CVRMSE measures the variability of the errors between the benchmark BEM and the different simplified BEMs. Chapter 4, section 4.5.3, equation (4-6) describes NMBE while equation (4-3) CVRMSE.

Table 5-8 presents ASHRAE Guideline 14 (ASHRAE, 2002) acceptability thresholds for CVRMSE and NMBE for hourly building energy simulations. Although these guidelines directly apply in BES calibration studies (i.e., compare BEM results with measured data), this work uses them to study the impact of different geometric resolutions of complex (double-) curved building envelopes in simulation outputs. The assumption is the higher the geometric resolution of a BEM the higher the accuracy of the simulation results. Thus, the benchmark case used to compare different levels of resolution is the BEM with the highest resolution produced by the proposed approach.

Table 5-8. ASHRAE Guideline 14 for whole-building energy simulation calibration criteria.

Data type	NMBE (%)	CVRMSE (%)
Hourly	± 10 %	30 %

EnergyPlus (Crawley et al., 2001) was the whole-building energy software used to conduct all simulations, and Rhinoceros 3D was the CAD modeling software used to generate the initial geometry of the models. The implementation of the proposed BEM simplification methods used both visual and textual programming techniques by combining Grasshopper with Python.

All simulations used TMY data from Oakland's Airport. Table 5-9 presents the thermal and optical properties of the building envelope used in both experiments. The thermal properties of the opaque surfaces align with ASHRAE 90.1 standard (ASHRAE, 2013) recommendations for Oakland's ASHRAE climate zone (iii). Because the specified glazing assembly for climate zone 3 by ASHRAE 90.1 standard has a low VLT, this work uses the thermal, solar, and optical properties of a clear, low-emissivity double-glazed unit. The investigation assumes that such glazing unit balances well thermal and daylight performance. The use of the Façade Design Tool, an online recommendation system for high performing glazed façade systems based on COMFEN analysis software (Hitchcock et al., 2008), supported the selection of the used glazing properties.

Table 5-9. Thermal, solar, and optical properties used in the experiments.

Opaque Surfaces	
Building Element/Surface	R-value ($m^2 \cdot K/W$)
Floors	1.8
Walls	1.95
Roof	1.95
Glazed/Transparent Surfaces	
U value ($W/m^2 \cdot K$)	2.56
Solar Heat Gain Coefficient (SHGC)	0.27
Visible Light Transmittance (VLT)	0.64

Table 5-10 lists the main simulation parameters used in the EnergyPlus simulations, including internal loads, HVAC system properties, thermostat, infiltration and ventilation rates, and daylighting controls.

Table 5-10. EnergyPlus simulation parameters.

Internal Loads	
People (ppl)	0.05 ppl/$m^{2,}$ with a typical office schedule
Lights	11.8 W/m^2, with a typical office schedule and daylight dimming
Equipment	1.95
HVAC System	
Type	2.56
Cooling COP*	0.27
Heating COP*	0.64
Economizer	None
Outdoor Air	0.14 cfm** per person
Thermostat	
Cooling setpoint	26 ºC, with a typical office schedule
Cooling setback	32 ºC
Heating setpoint	21 ºC, with a typical office schedule
Heating setback	18 ºC
Daylight Controls	
Type	Continuous off dimming control with typical office schedule
Minimum Input Power Fraction	0.1
Minimum Light Output Fraction	0.1
Illuminance Setpoint	300 lux
Zone Fraction per daylight sensor	1 / Number of daylight sensors

*Coefficient of Performance | ** cubic feet per minute

The following discusses in more detail the setting of each experiment.

Experiment 1 – reducing mesh density in Building Energy Models

The first experiment assesses the impact of simplifying complex double-curved building envelopes in BES outputs. The goal of this experiment is to find the optimal degree of mesh reduction that improves run time with minimal impact in simulation output. This experiment used the NURBS massing model illustrated in Figure 5-22. This massing model is similar to the peanut-like building of section 5.3 - Solution B. It encloses a single thermal zone that corresponds to a 1700 m^3 double-curved pavilion with a varying depth (7.5 m to 16.8 m), 25 m of length, and height (3.75 m to 8.4 m).

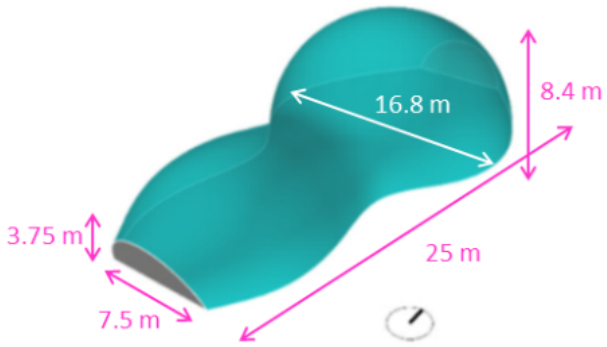

Figure 5-22. Initial massing model composed of Non-Uniform Rational Basis Spline (NURBS) surfaces.

This particular shape was selected for two reasons: first, its double-curved envelope is challenging to model for BES; second, its overall form alludes to some existing free-form built buildings, namely the Landesgartenschau Exhibition Hall pavilion in Stuttgart, Germany (Krieg et al., 2015) and the Sage Gateshead building in London, UK, designed by Foster and Partners (Foster and Partners, 2004), both shown in Figure 5-23.

Figure 5-23. The Landesgartenschau Exhibition Hall pavilion in Stuttgart (left) and the Sage Gateshead building in London (right) inspired the shape of the single thermal zone pavilion presented in Figure 5-22. Left image source: Krieg et al. (2015). Right image from: Foster and Partners (2004).

Using the first geometry simplification heuristic, the proposed method generated 10 different BEM from the initial massing model with varying mesh resolutions, i.e., quad count. All BEM have a Window-to-Wall-Ratio (WWR) of 40%. Initially, the NURBS surface parser available in Honeybee (Roudsari, Pak and Smith, 2013), a popular EnergyPlus and Radiance front-end for

Grasshopper, produce the benchmark energy model, i.e. the high polygon count BEM used to assess the impact of geometry reduction/simplification in simulation output. The Honeybee resulting BEM, shown in Figure 5-24, has 6,278 faces, and it was unable to run in useful time – after 4 hours the energy simulation was still initializing warm-up calculations. This attempt emphasizes the results of the small experiment presented in section 2.1 that used Autodesk Insight to automatically parse the geometry of two curved towers to EnergyPlus. The failed attempt to use existing automatic NURBS surface parsers to BEM reinforces the anecdotal evidence of the difficulty that current tools designed to integrate energy modeling and architectural design have in dealing with complex geometries. As a result, the BEM considered as the comparison benchmark in this experiment was the model generated by our approach with a high mesh polygon count (see Table 5-11).

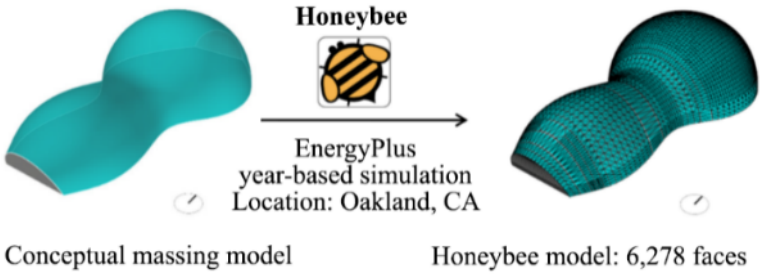

Figure 5-24. Initial massing model (left) and the resulting Honeybee BEM (right). Due to the high polygon mesh count, the BEM was unable to run in EnergyPlus in useful time.

Table 5-11 lists the different simplified models along with the original envelope surface *u* and *v* subdivisions and the resulting main building surfaces (i.e., walls, floors, and roofs) and subsurfaces (i.e., windows and skylights) count. A light gray fill highlights the benchmark BEM (Res10). Figure 5-25 presents an axon of every geometry generated by the proposed simplification method.

Table 5-11. BEMs generated by the proposed approach for the initial massing model.

BEM ID	Envelope subdivisions (*u*, *v*)	Main Surfaces	Subsurfaces
Res01	(4, 4)	26	16
Res02	(6, 6)	52	36
Res03	(8, 8)	86	64
Res04	(10, 10)	126	100
Res05	(12, 12)	178	144
Res06	(14, 14)	236	196
Res07	(16, 16)	298	256
Res08	(18, 18)	376	324
Res09	(20, 20)	457	400
Res10	(22, 22)	543	484

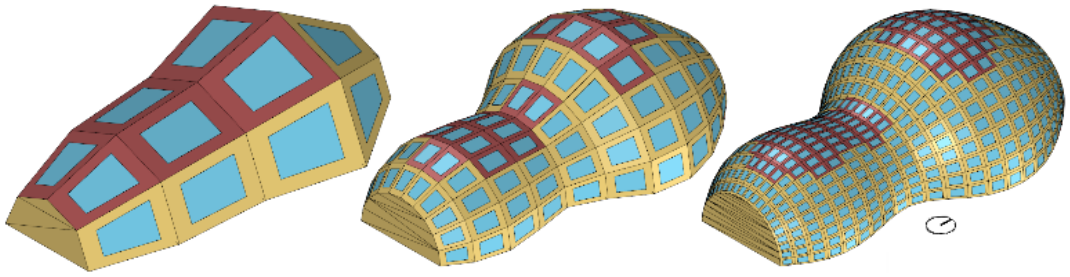

Figure 5-25. BEMs with different levels of geometric resolution generated by the proposed simplification method, from the coarsest one in the left, Res01, an intermediate resolution in the middle, Res04, to the highest resolution in the right, Res10, the BEM considered as the geometric benchmark in this experiment due to its higher polygon count.

Although the approach ensures that the resulting simplified BEM has the same air volume of the benchmark, it is essential to measure the deviations on external surface area, since the heat transfer through the envelope depends on exposed envelope area. Table 5-12 compares relevant envelope surface parameters, including form-factor (i.e., surface-to-volume ratio) and surface area. The approach keeps the deviation very low both in envelope surface area and in form factor, thus minimizing any simulation output errors due to differences in surface area.

Table 5-12. BEMs' form parameters comparison.

BEM ID	**Surface Area** (m^2)	**Surface Area % error** (compared with Res10)	**Form Factor**	**Form Factor % error** (compared with Res10)
Res01	1005.3	5 %	0.592	5 %
Res02	979.1	2 %	0.576	2 %
Res03	970.5	1 %	0.571	1 %
Res04	966.4	1 %	0.568	1 %
Res05	964.3	0 %	0.567	0 %
Res06	962.9	0 %	0.567	0 %
Res07	961.9	0 %	0.566	0 %
Res08	961.3	0 %	0.566	0 %
Res09	960.9	0 %	0.565	0 %
Res10	960.5	N.A.	0.565	N.A.

Table 5-13 assesses the difference between the glazed area considered as a window and as a skylight. The difference between window and skylight is a sensitive modeling point since there are differences in terms of the heat transfer coefficients applied to different tilts of glazed surfaces. The proposed implementation automatically dispatches envelope surfaces either as roofs or walls and consequently as windows or skylights, depending on the tilt angle of the surface. Thus, the proposed method labels outdoor surfaces with a tilt angle between $\geq 60^{o}$ and $\leq 120^{o}$ as walls or windows. The deviation variability presented in Table 5-13 directly results from the application of this rule. Nevertheless, starting from Res03, the deviation error is acceptable for the area assigned to skylights and windows in the simplified models ($\leq |10|\%$).

Table 5-13. BEMs' window and skylight surface area comparison.

BEM ID	**Window Area** (m^2)	**Window Area % error** (compared with Res10)	**Skylight Area** (m^2)	**Skylight Area % error** (compared with Res10)
Res01	149.8	-21 %	87.64	105 %
Res02	176.61	-7 %	57.52	35 %
Res03	194.62	3 %	38.59	-10 %
Res04	188.7	0 %	44.08	3 %
Res05	187.8	-1 %	44.74	5 %
Res06	191.46	1 %	40.9	-4 %
Res07	185.44	-2 %	46.8	9 %
Res08	191.2	1 %	40.95	-4 %
Res09	192.77	2 %	39.33	-8 %
Res10	189.31	N.A.	42.75	N.A.

All the energy models have three equally spaced daylight sensors located along the central North-South axis at 0.8m height. The first experiment compared the simulation time, NMBE and CVRMSE for heating, cooling, lighting, process, and total energy of the benchmark BEM (Res10) against their simplified counterparts.

Experiment 2 – sampling and decomposing multi-zone Building Energy Models

The first experiment tested the effectiveness of the first simplification method, focusing on reducing the overall geometric complexity of single thermal zone models with complex (double-) curved envelopes. The second simplification method extends the first one to BEM with several thermal zone models – multi-zone BEM. Experiment 2 assesses the performance of the second simplification heuristic that decomposes a multi-zone model into simpler and smaller representative single thermal zone models. The aim is to estimate the overall results of a larger BEM by quickly simulating smaller parts of it, thus saving simulation time and reducing the effort in complex modeling tasks. The building geometry used to test this heuristic is a semi-torus mass with a volume of approximately 27,426 m^3, an inner radius of 12 m, an outer radius of 24 m, and a 12 m high arched section (see Figure 5-28 - left). Similarly, to the geometry selection process in the previous experiment, real architectural designs inspired the use of a funnel-like space in this experiment. These types of structures are common both in large commercial buildings with big free-form roof canopies or in small pavilion-like architecture. Figure 5-26 presents two examples of architectural designs that use funnel structures to sustain big continuous canopies that enclose large spaces. In the left, it presents the New Milano Trade Fair, Rho-Pero designed by Studio Fuksas (Studio Fuksas, 2005); in the right the proposal for the New Mexico City airport, designed by a joint venture between Foster and Partners and Fernando Romero Architects (Foster and Partners, 2014). Figure 5-27 depicts the 2010 research pavilion of the Institute for Computational Design/Institute of Building Structures and Structural Design (ICD/ITKE) of the University of Stuttgart that used a semi-torus as its base form.

Figure 5-26. Examples of funnel/torus like structures for large continuous roof canopies. Left: New Milano Trade Fair Rho-Phero. Image from: Studio Fuksas (2005). Right: New Mexico City Airport. Image from: Foster and Partners (2014).

Figure 5-27. The semi-torus shape of 2010 ICD/ITKE research pavilion. Images adapted from: Knippers and Menges (2010).

The semi-torus BEM used in this experiment entails four different thermal zones are physically separated by partition walls with a thermal resistance value (R-value) of 0.39 k.m^2/W.

Figure 5-28 shows the implementation workflow of the second BEM simplification method. First, using the first simplification method, the proposed tool starts to automatically process the curved building envelope of the initial semi-torus mass. Since there is no programmatic differentiation in the original thermal mass and the overall shape is symmetric, the implemented algorithm splits the original mass into four thermal zones that follow orientation and solar exposure. In the context of this experiment, the tool produced two BEMs, one with a dense mesh (Full_High_res) and another with a coarser geometric resolution (Full_Simp_res). The Full_High_res BEM is the benchmark BEM of this experiment, i.e., the reference model used to assess simulation output deviation and run-time improvements. After generating the two multi-zone BEM, the proposed approach further samples each BEM by isolating a representative part of each thermal zone, consequently reducing the initial BEM into a group of four small single-zone models. Thus, the Sample_High_res, the BEM composed by four single thermal zones of high mesh resolution results from sampling the Full_High_res BEM, while Sample_Simp_res results from slicing the Full_Simp_res model. Since each slice represents a portion of the volume of the larger thermal zone, the proposed approach

assumes that there is no heat transfer on the side surfaces of the sampled single-zone models. Thus, the tool caps each single-zone sample with adiabatic surfaces. This is a common procedure in other thermal zone reduction procedures of multi-zone models, such as the use of thermal zone multipliers in EnergyPlus to reduce the redundant analysis of similar thermal zones in high-rise buildings (Big Ladder, 2015). Figure 5-28 colors the adiabatic surfaces in magenta.

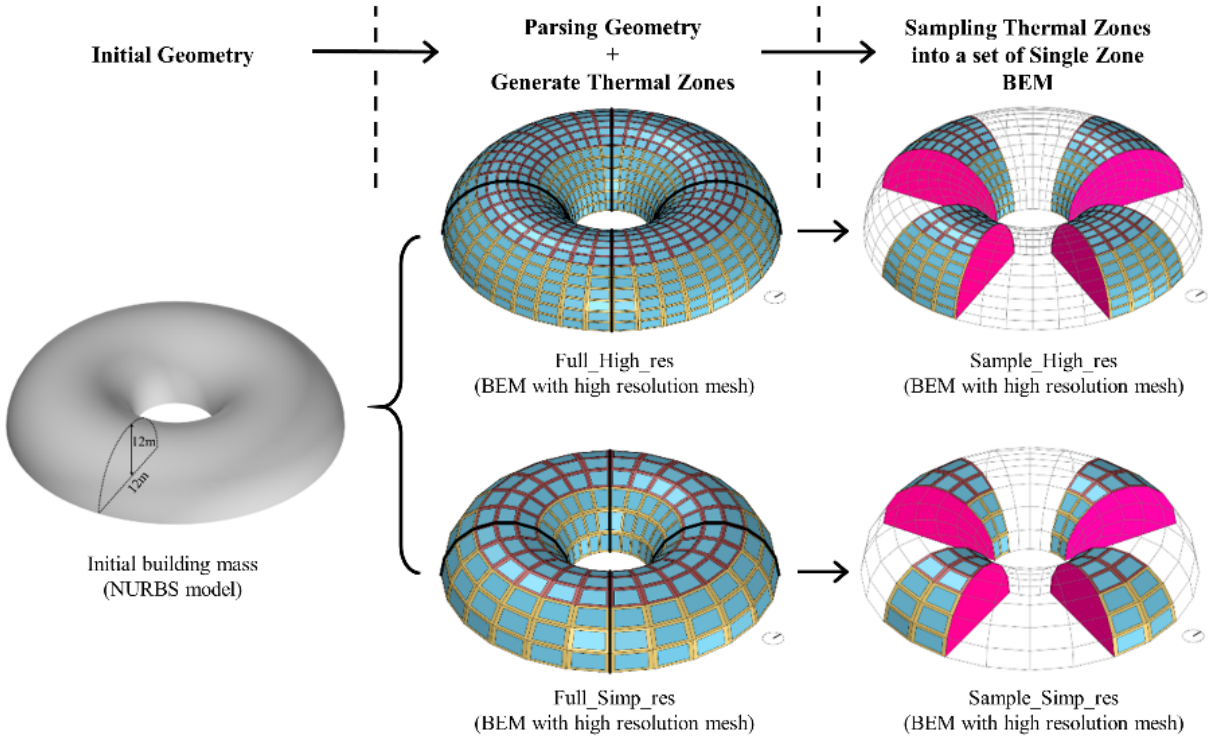

Figure 5-28. Simplification method for multi-zone BEMs applied to a torus shaped building mass. Original semi-torus mass building mass (left), the two generated multi-zone BEMs with different mesh resolutions (center), and the resulting sampled BEMs. The thicker black lines in the two multi-zone BEMs (center) indicate the location of the partition walls that separate the different thermal zones. The magenta colored surfaces in the sampled BEMs (right) represent the location of adiabatic surfaces that resulted from slicing each thermal zone.

Table 5-14 compares the geometry of the different BEMs used in this experiment; Full_High_res, the detailed four thermal zone energy model benchmark, the Sample_High_res, which corresponds to the sampled BEM with a high degree of mess resolution, and Sample_Simp_re, the reduced BEM with a coarser surface subdivision.

Table 5-14. Geometry comparison between the BEMs generated in the second experiment, by the simplification approach for multi-zone BEMs.

BEM ID	Number of Main Surfaces	Number of Sub Surfaces (windows)
Full_High_res	732	480
Sample_High_res	588 (147 per single-zone)	288 (72 per single-zone)
Sample_Simp	156 (39 per single-zone)	72 (18 per single-zone)

The second experiment compared the results of Sample_High_res and Sample_Simp_res against the outputs of the benchmark BEM used in this experiment, Full_High_res.

5.4.4 Results

The following present the results of the two experiments that focused on producing equivalent but simplified geometric descriptions for efficient BES of a building with complex geometry.

Experiment 1 – results of reducing mesh density in BEM

To determine the impact of the discretization degree of complex (double-) curved building envelopes in building energy simulation run time, Figure 5-29 plots the number of main surfaces against simulation time. Using regression analysis, the data show that simulation time tends to grow exponentially with the increase of the number of main surfaces in a BEM. A high coefficient of determination (R^2) of the exponential fit, R^2= 0.92 confirms this trend. Using this regression technique, the implemented tool can reasonably predict the amount of simulation time that a certain degree of simplification entails in this specific case.

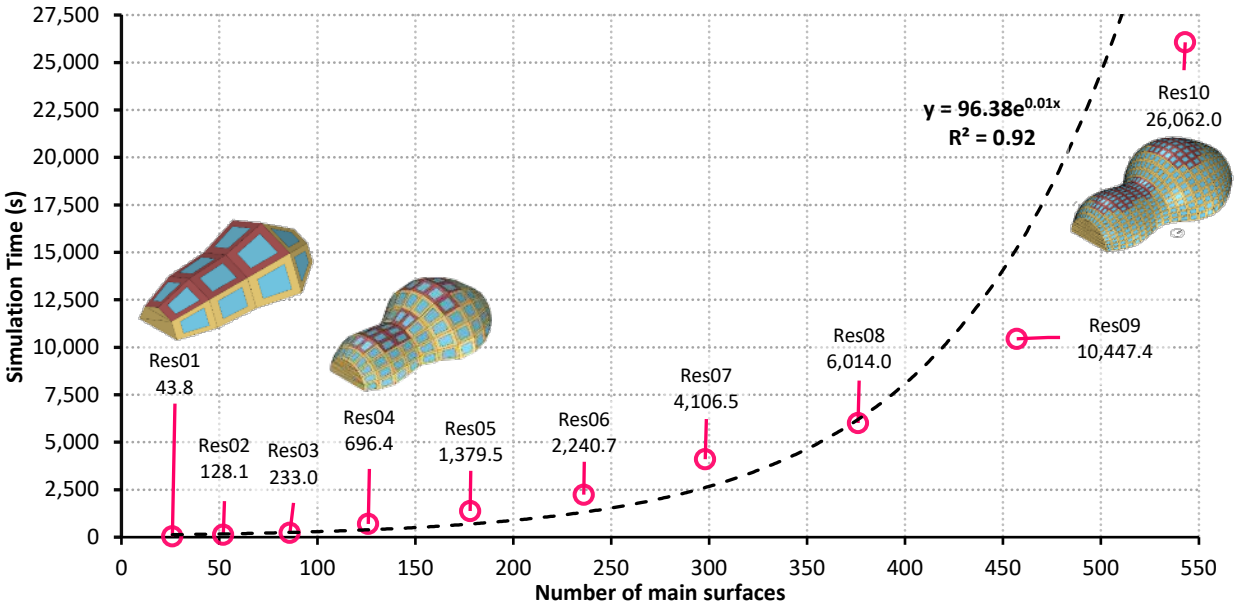

Figure 5-29. The impact of BEM geometry complexity, measured in number of main surfaces, in BES simulation time. Each data point is a BEM generated by the first simplification proposed approach.

Figure 5-30 shows the relation between the geometric complexity of each simplified BEM and simulation output deviation, measured through CVRMSE and NMBE. Those two error statistical indexes are broken down by energy end-use cooling, heating, lighting, process, and total energy – and, as already mentioned in section 5.4.3, they use Res10 as the reference BEM.

Table 5-15 relates the percentage of geometry reduction, simulation speed, CVRMSE, and NMBE of the total estimated building energy consumption for each simplified BEM, relative to the benchmark model (Res10).

Table 5-15. Geometry reduction, relative run speed, and CVRMSE and NMBE of each simplified BEM.

BEM ID	**Geometry reduction**	**CVRMSE** (total energy)	**NMBE** (total energy)	**x faster than Res10**
Res01	95.2%	11.4%	-6.7%	595
Res02	90.4%	4%	-1.3%	204
Res03	84.2%	3.4%	0.1%	112
Res04	76.8%	3%	0.5%	37
Res05	67.2%	2.2%	0.3%	19
Res06	56.5%	1.4%	0.4%	12
Res07	45.1%	1.1%	0.3%	6
Res08	30.8%	1%	0.3%	4
Res09	15.8%	0.6%	0.2%	2.5

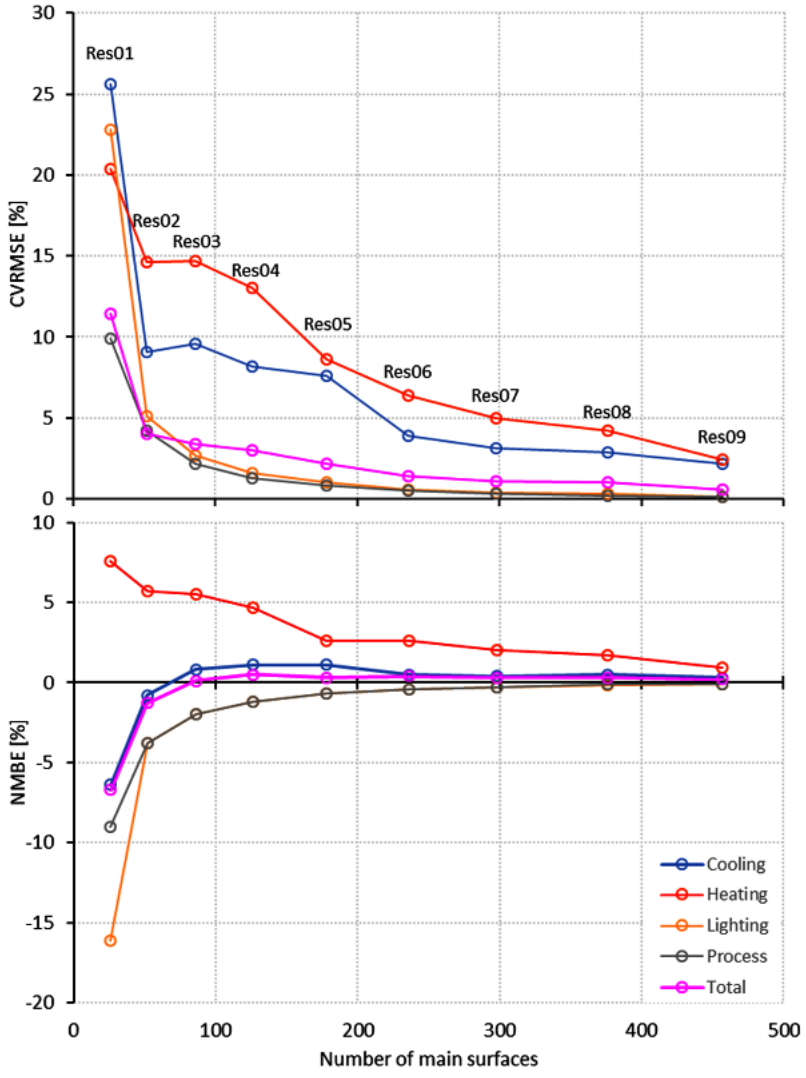

Figure 5-30. Impact of degree of geometry complexity in energy-end use prediction. Top: deviation of hourly annual energy data of each simplified BEM measured in terms of CVRMSE. Bottom: deviation of hourly annual energy data measured of each simplified BEM in terms of NMBE.

Experiment 2 – results of sampling and decomposing multi-zone BEMs

Tables 5-16, 5-17, and Figure 5-31 present the results of the two tests performed in the second experiment: (i) sampling, isolating, and simulating the full multi-zone BEM (Full_High_res) in four detailed samples (Sample_High_res), (ii) further simplification of the geometry of the samples (Sample_Simp_res) by adopting the heuristic used in the first experiment.

Table 5-16 presents the simulation time of the Full_High_res, Sample_High_res, and Sample_Simp. It also lists the percentage of simulation time reduction of the simplified BEMs in comparison with the benchmark BEM - Full_High_res.

Table 5-16. Simulation time of the three BEM approaches and reduction of simulation time of the simplified BEMs, Sample_High_res and Sample_Simp_res.

BEM ID	**Simulation time** (seconds)	**% of simulation time reduction**
Full_High_res	15,407	N.A.
Sample_High_res	644,4	95.8
Sample_Simp_res	89	99.4

Table 5-17 relates both run time and the error deviation in the simulation output of the implemented method of simplifying multi-zone BEM in simulation output deviation. The table presents the CVRMSE and NMBE of total energy and speed improvement of the simplified BEM when compared with the geometry and annual hourly results of the benchmark used in this experiment – Full_High_res.

Table 5-17. Geometry reduction in of the simplified BEM compared with the benchmark BEM used in the second experiment (Full_High_res) and correspondent simulation output deviation measured using CVRMSE, NMBE, and improvement of simulation run time.

BEM ID	**% of geometry reduction**	**CVRMSE** (total energy)	**NMBE** total energy)	**x faster than Full_High_res**
Sample_High_res	20 %	6.4 %	-1.4 %	24
Sample_Simp_res	79 %	7.2 %	-1.7 %	173

Finally, Figure 5-31 presents a full breakdown of the error metrics CVRMSE and NMBE by energy end-use for the two simplified BEMs and how do they relate with the acceptance threshold adopted for those metrics – see Table 5-8.

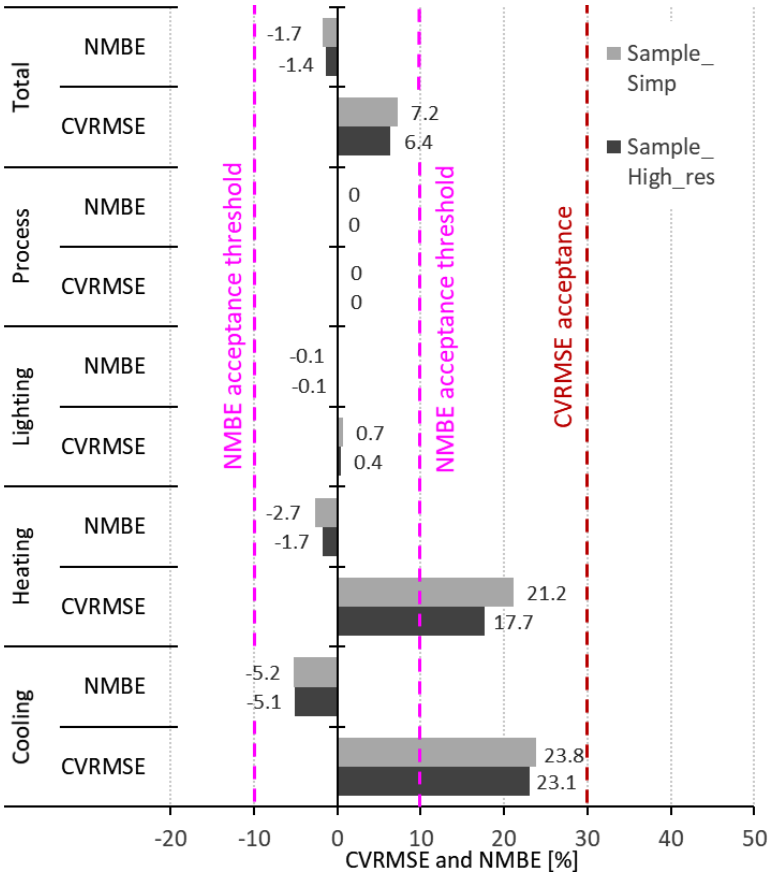

Figure 5-31. CVRMSE and NMBE of the second experiment simplified BEMs per energy end-use. The NMBE acceptance interval is marked in a magenta dashed line and the CVRMSE in a red dashed line.

5.4.5 Discussion

Experiment 1 results indicate an exponential relationship between simulation run time and geometric complexity, measured in terms of the number of quad panels necessary to describe a complex curved envelope in BES. Figure 5-29 clearly shows that small increments in surface subdivision yield a significant impact in simulation time. Additionally, Figure 5-30 demonstrates that high levels of surface discretization are extremely useful in reducing simulation time at a minimal cost in simulation output results. Nevertheless, they also show that extreme simplifications CVRMSE and NMBE rapidly increase. Although the simpler BEM Res01 shows acceptable CVRMSE and NMBE for most of the energy end uses, it presents higher error values when compared with the other simplified BEMs. The deviation is more evident for lighting and heating, indicating that high levels of geometric simplification might fail to fully capture solar-related phenomena such as solar heat gains and daylighting. As a matter of fact, the NMBE of Res01 in lighting is not acceptable (> |10|%). It is plausible to assume that if we increase the level of simplification, for example, to only two $\vec{u}$ and $\vec{v}$ subdivisions of the shell surface, that both heating and lighting would not fulfill the acceptance criteria adopted for CVRMSE and NMBE. This indicates that reducing envelope dominated buildings with complex curved facades to shoebox BEMs is oversimplification that will likely fail in properly model the heat transfer phenomena. Considering the results presented in Figure 5-29, Figure 5-30, and in Table 5-15, we recommend a maximum of ≈ 80% reduction of the original number of polygons that describe in

detail complex building envelopes. Res03 (≈ 84% of geometry reduction) shows an excellent balance between error and simulation time – it ran in 3 min and 53 seconds (112 times faster than Res10) and shows minimal error in total energy consumption; CVRMSE and NMBE is 3.4% and 0.1%, respectively.

The simplification method for larger multi-zone BEM tested in Experiment 2 also presents promising results in significantly improving simulation run time while ensuring accuracy, i.e., minimal impact on simulation results. It shows that sampling a multi-zone model and decomposing it into smaller and simpler single thermal zones generates an efficient proxy of fully detailed, complex multi-zone BEM. The combination of this approach with the building envelope geometry simplification used in the first experiment yield significant improvements in simulation time with minimal output deviations. Sample_Simp_res, the BEM that combines both the thermal zone sampling and surface rationalization approaches, is 7 times faster than Sample_High_res, the BEM that only uses the sampling and decomposition approach. This improvement in run time as a small impact in NMBE (-0.3%) and CVRMSE (+0.8%). Compared with Full_High_res, the benchmark model of this experiment, Sample_Simp is 173 faster to run (1 min and 29 seconds) and reports acceptable CVRMSE and NMBE in terms of total energy; 7.2% (22.8% below the acceptance threshold) and -1.7% (8.3% above the negative range of acceptance threshold) respectively (see Table 5-17).

Figure 5-31 provides a more detailed analysis on the effectiveness of the proposed simplification method for multi-zone BEM by measuring the deviation error in each energy end-use. It shows that all the energy end-uses in Sample_High_res and Sample_Simp are within the acceptance criteria adopted for CVRMSE and NMBE. As expected, the error in process loads is null, since this energy use exclusively depends on surface area and control schedules, and the simplification approach introduced minimal deviations to the original surface area. The error in both Cooling and Heating are similar, indicating that the simplifications can properly capture the overall performance of the highly detailed BEM.

The small difference between Sample_High_res and Sample_Simp in all energy end-uses also indicates that the combination of the two simplification heuristics is feasible, valid, and beneficial to use in the study of multi-zone BEMs with complex curved envelopes, particularly at early design stages where faster whole building energy simulations are desirable.

5.5 Strategy C: Abstract Complex Fenestration Systems for the early energy assessment of complex building skins

Sections 5.3 and 5.4 presented methods to automatically generate valid, accurate, and efficient geometric descriptions of early-stage free-form architectural massing models. However, current parametric and generative design workflows empower architects to quickly explore highly complex patterns of porosity, opacity, and other surface properties in the early design of highly sophisticated building skins. The design and control of Complex Fenestration Systems (CFS) have a direct impact on the energy and daylight performance of buildings, particularly in narrow plan designs. Although current digital tools facilitate the design and automatic propagation of complex and intricate patterns or façade elements, it remains challenging to translate the resulting building skins to a BEM and simulate the impact that they have in whole-building energy.

The design of intricate patterns entails a level of geometric detail that often result in time-consuming or highly specialized BEM modeling tasks (e.g., the use of Bidirectional scattering distribution function) and in computationally intensive simulations that are incompatible with early-stage design times. Moreover, in the case of free-form building geometries, the resulting irregular panelization and formal adjustment of different façade components is even more difficult to model for BES. Thus, designs that combine curved or double-curved building envelopes further add to the difficulty of using current validate whole-energy building simulation tools in the early energy performance of parametric and generative façade solutions. As a result, the energy simulation of such façade systems is unfortunately often moved to a post-design stage, where it has less influence on the building design. In sum, under an environmental perspective, the current gap between design and BES tools limits a sustained and grounded design of highly sophisticated building skins, particularly at early-design stages.

The research presented in this section emerges from collaborative work between the author of this dissertation and his two thesis advisers. The work, published in 2018 (Schleicher, Santos and Caldas, 2018), aims to directly answer the third limitation discussed in sections 2.1 and 5.2 and respond to the current need to quickly evaluate the energy performance of CFS in the context of unconventional building forms.

5.5.1 Goal and general approach

Strategy C aims to improve the integration of whole-energy simulation tools in the early study of CFS used in (double-) curved building envelopes. It proposes a new streamlined performance-driven workflow that avoids complex modeling tasks, accelerates the simulation of BEM that contain CFS, and delivers useful information to steer the early design of highly sophisticated building skins. To achieve this goal, the proposed method combines parametric modeling techniques with whole-building energy simulation based on co-simulation. More precisely, the proposed method improves the data exchange between powerful 3D geometry parametric modelling tools such as Rhinoceros + Grasshopper, with state-of-the-art BES software such as EnergyPlus (Crawley et al., 2001), Radiance (Ward and Rubinstein, 1988), and WINDOW 7.5 (Huizenga et al., 2017). The parametric modeling capabilities of Rhinoceros/Grasshopper allows architects to quickly generate, explore, and compare different building skin designs. EnergyPlus simulates the impact of such designs assisted by irradiance analysis performed by Radiance and a new CFS simplification method based on WINDOW 7.5 single fenestration simulations. The following section explains in more detail the integration of the different tools, the co-simulation method, and the resulting modeling workflow.

5.5.2 Method of abstracting CFS for building energy performance-driven design

The proposed method integrates the different design and simulation tools into a single workflow using the following five steps:

Step 1 – Form-generation and panelization – this step uses the process proposed in section 5.3 to discretize a smooth (double-) curved building envelope, usually represented through a NURBS surface, into a set of planar quad-mesh faces of different sizes, but which are similar in shape and angles. As already discussed, the panelization of an initial arbitrary free-form building envelope into a set of planar meshes is an essential pre-requisite to generating a valid BEM.

Step 2 – Mapping cumulative annual irradiance – based on TMY data of a specific location, the proposed method computes the cumulative annual incident radiation in each façade panel using Radiance. This information is crucial either to a user or an automated optimization system to determine the shading needs of each panel to constrain its overall optical, solar, and thermal properties.

Step 3 – Conversion of the shading geometry of a CFS into simplified thermal, solar, and optical glazing properties – in BEM, it is possible to model a glazed facade panel using two different procedures: (i) a detailed one, which specifies each layer material and component of the fenestration, or (ii) a simplified one, which describes the glazing assembly through conductance (U-factor), Solar Heat Gain Coefficient (SHGC), and Visual Light Transmittance (VLT). Although the detailed modeling of windows delivers more precise results, the simplified description of a glazing system is accurate enough to inform early design stages. Because the goal of the proposed method is to simplify the geometrical features of CFS, it adopts the simplified modeling approach. The proposed method uses WINDOW 7.5 (Huizenga et al., 2017), a validated computer program for calculating window performance indices, to study the impact that different CFS, and their different configurations, have on U-factor, SHGC, and VLT on a standard glazing assembly. The user can either use WINDOW built-in parametric shading devices (e.g., louvers, fins, different shaped perforated screens, and frit ceramic cover) or develop custom shading geometry, transform it into a BSDF WINDOW layer using the Radiance subprogram *genBSDF* (Ward, 2010). The latter requires more expertise and involves demanding calculations when compared with the former. Because the approach advanced here reduces the geometric data of a CFS to simple performance indices, this dissertation refers to this modeling procedure as abstracting CFS to their correspondent performance indices. The proposed method also gathers data that results from testing different fenestration and shading systems to build a surrogate model that links the CFS' geometric features to their correspondent SHGC, VLT, and U-factor. The current implementation of the method uses supervised statistical learning techniques, specifically regression-based approaches, to build a surrogate model that predicts fenestration performance indices from key geometric parameters and vice-versa. The resulting surrogate enables the selection of different CFS solutions of similar performance, thus allowing the optimization of the distribution of the key fenestration performance indices without entailing the *a priori* selection of a specific CFS.

Step 4 – Whole-energy Building Simulation – after abstracting different CFS and their parametric variations to simplified fenestration performance indices, the user or a generative design system can assign different fenestration performance indices for each façade panel. The user or the generative design systems can use the solar radiation results to inform each panel with specific values for SHGC, U-factor, and VLT. After every façade panel has an SHGC, U-value, and VLT, it is possible to assess the overall impact of the CFS strategy in whole-building energy performance by running an EnergyPlus simulation for the desired period.

Step 5 – Re-generating the geometry of the CFS back to the model – based on the correlation between the CFS geometry and fenestration performance indices, it is possible to reverse the process of converting geometric data to a simplified material surrogate to re-create the three-dimensional features of the shading devices in Grasshopper. This visual feedback is helpful for the further development of the facade design. For example, such feedback allows users to compare the solutions visually and fine tune them parametrically.

Figure 5-32 illustrates the integration of the several steps that compose the proposed co-simulation method for abstracting and efficiently modeling CFS for free-form building envelopes at early design stages.

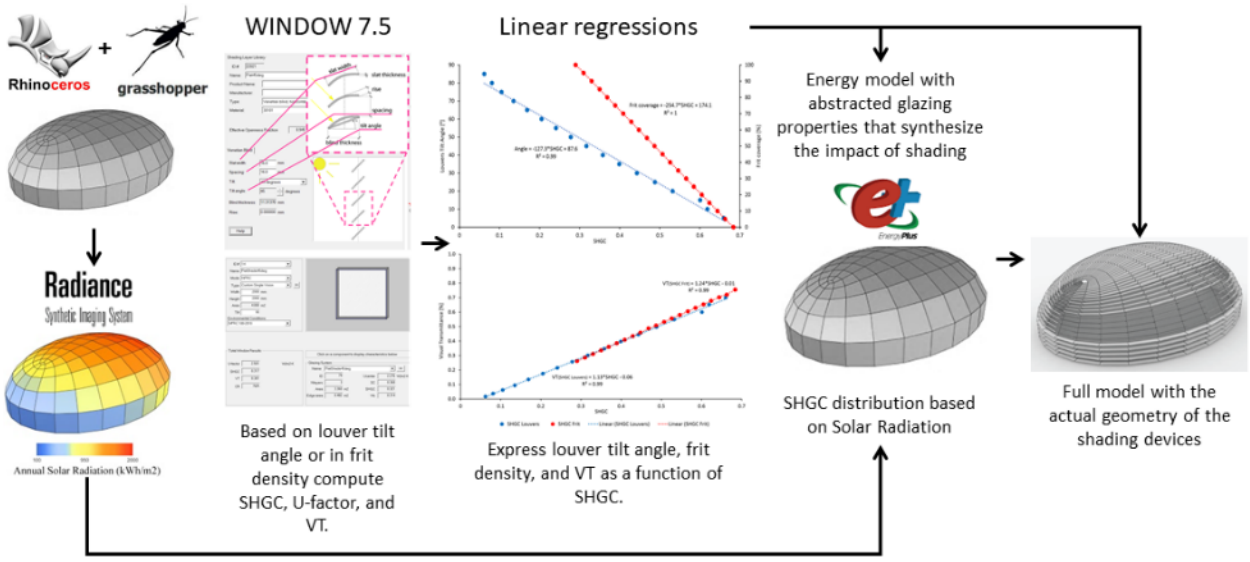

Figure 5-32. Flow-chart of the proposed method of abstracting and simulating CFS in (double-) curved building envelopes.

The computational implementation of the proposed modeling workflow combined textual and visual programming languages – Python and Grasshopper, respectively. The outcome is a prototype of a performance-driven design tool that enables users to explore and assess two different types of CFS. The following sections introduce an experiment that both shows the potential of the proposed modeling method and validates it.

5.5.3 Design of experiment – reducing solar heat gains in a free-form glass enclosed canopy using the new CFS abstraction modeling method

The application of the proposed workflow in a concrete design example illustrates its potential. Thus, the study of different shading systems in a prototypical curved glass façade served as the testbed of the new methodology. The experiment considers the modeling, simplification, and abstraction of two different types of parametric CFS as a proof-of-concept of the proposed modeling method. The first CFS is a glass frit, a surface glass treatment based on silk-screening ceramic frit that reduces solar heat gains and that can assume different types of patterns and density of surface coverage. The second is a non-planar shading system composed of parametric equally spaced louvers that seamlessly adapt to the local curvature of the envelope.

The overall form of the building used in this experiment is a double-curved quadratic surface, a semi-ellipsoid. As mentioned in section 5.3, sphere deformations, as ellipsoids, are common in double-curved free-form architectural envelopes. The glass dome of the Academy Museum of Motion Pictures, in Los Angeles (LA), California, designed by RPBW (2019), served as the starting inspiration point for the glass semi-ellipsoid used in this experiment. Figure 5-33 shows the “soap-bubble” glass canopy, as the architect Renzo Piano calls it, that covers a rooftop venue over the museum’s theater. The dry-warm climate of LA is not a favorable climate for a fully

glazed structure, which makes it a good example of a design that could directly benefit from CFS that mitigate unwanted solar heat gains.

Figure 5-33. The glass dome of the Academy Museum of Motion Pictures by RPBW (2019). This built example and location motivate the experiment conducted in this section. Images adapted from: RPBW (2019).

To be consistent with the previous experiments presented in this chapter, the prototypical building mass used is a semi-ellipsoidal glass building similar to section 5.3 base geometry - Solution A. This form is interesting and challenging because it results from a scale affine transformation of a base hemi-sphere. Hemi-spheres are double-curved quadratic surfaces that can be easily described using only three parameters, length of primary and secondary axis, and apex height.

The first step of the new modeling method for simplifying CFS pre-processes an initial geometry for BES. The panelization in planar quad-meshes used in Strategy A (section 5.3), is based on the conformal mapping approach introduced by Sechelmann et al. (2013). As demonstrated in section 5.3, the panelization approach enables a subdivision of the surface into planar mesh faces of different sizes, but of similar shapes and angles. Figure 5-34 illustrates the process of obtaining the initial semi-ellipsoid shape and the subsequent surface discretization for BES. The generation of the base geometry entailed the following:

1) Using Rhinoceros, the research team first modeled an ellipsoid of 25x18x7 meters, to then subdivide it using the lines of surface curvature. The surface curvature lines are appropriate guidelines for an efficient planarization of this type of quadratic surfaces. The result of this process is a network of lines that follow the curvature of the original surface and divides into quadrilateral patches (see Figure 5-34 – left and center).

2) A simple algorithm detected the intersection points of the network and subdivided the original surface. The modeling process then involved cutting the ellipsoid in half using its equator as the cutting edge. The process preserved the upper part of the ellipsoid (see Figure 5-34 – center and right).

3) The application of quasi-isothermic planarization techniques that enables the generation of simulation models composed of completely planar quad panels. The touching inner circles of

the mesh faces, shown in Figure 5-34 – right, demonstrates the planarity requirement of the proposed envelope discretization.

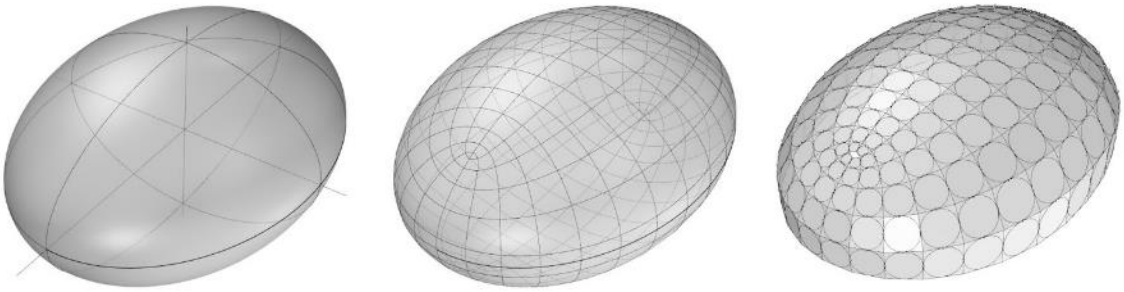

Figure 5-34. Conformal mapping of an ellipsoidal test body and the resulting semi-ellipsoid mesh composed of planar quadrilateral panels. Left: initial ellipsoid modelled as a NURBS surface. Center: ellipsoid's curvature line network. Right: resulting mesh of planar quad panels of the upper part of the ellipsoid.

The primary axis of the emerging structure runs north-south.

The second step of the proposed simplification method consists in assessing the annual cumulative irradiance in each panel. This information will inform either a user or an automated optimization system on the local variance of shading needs that might constrain the optical, solar, and thermal properties of different CFS. Annual solar radiation analysis depends on location. Since this experiment studies new ways to model CFS that reduce solar gains in (double-) curved glass building envelopes, the selected location is Los Angeles, CA; thus, following the motivational example of Figure 5-33. The dry, warm climate of LA (ASHRAE climate zone 3B) is suitable for assessing the impact of passive cooling shading strategies on the energy performance of such large glazed spaces.

Using TMY data (TMY3) collected in Los Angeles International Airport (LAX), the proposed method uses Radiance to calculate the cumulative solar radiation kWh/m^2 on each glass panel. Figure 5-35 shows the irradiance distribution on the entire envelope. As expected, the solar exposure of the individual panels varies, thus indicating that locally adapted shading solutions are better suited to control solar gains. Figure 5-35 color gradient shows an annual solar radiation range that goes from 100 to 2000 kWh/m^2.

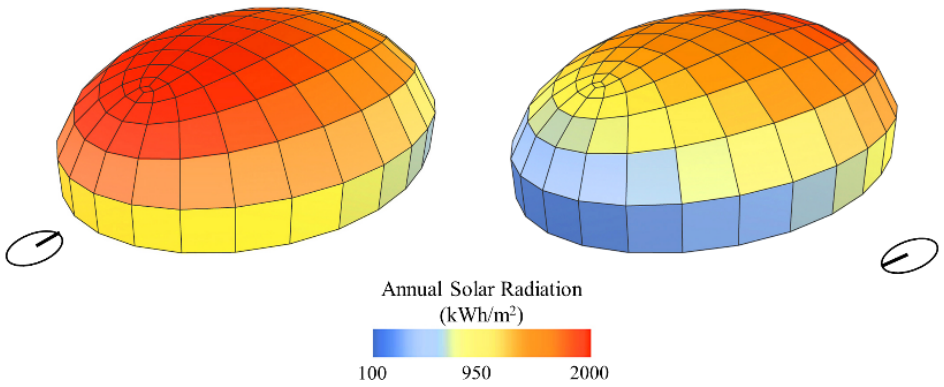

Figure 5-35. Based on the LA TMY file, the proposed workflow uses Radiance to map annual solar radiation on the envelope as seen from south-east (left) and north-west perspective (right).

The third step of the novel workflow uses WINDOW 7.5 to convert the geometry of CFS to an equivalent U-factor, SHGC, and VLT. Since this experiment focuses on simplifying two parametric CFS into simple fenestration performance indices, the application of this step involved a parametric study of different states of both systems and the resulting impact on SHGC, U-factor, and VLT of a standard glazing assembly. The standard glazing assembly is composed of two 6 mm clear glass panes and an air gap of 12 mm and has an SHGC of 0.68, a U-factor of 2.83 W/m^{2}K, and a VLT of 0.76 (76%).

Figure 5-36 provides an example of how a user utilizes WINDOW 7.5 GUI to conduct a parametric study to assess the impact of varying the tilt angle of a louver-based shading system on the overall window assembly performance. The proposed method automates this workflow in particular and similar procedures for other types of planar and non-planar CFS.

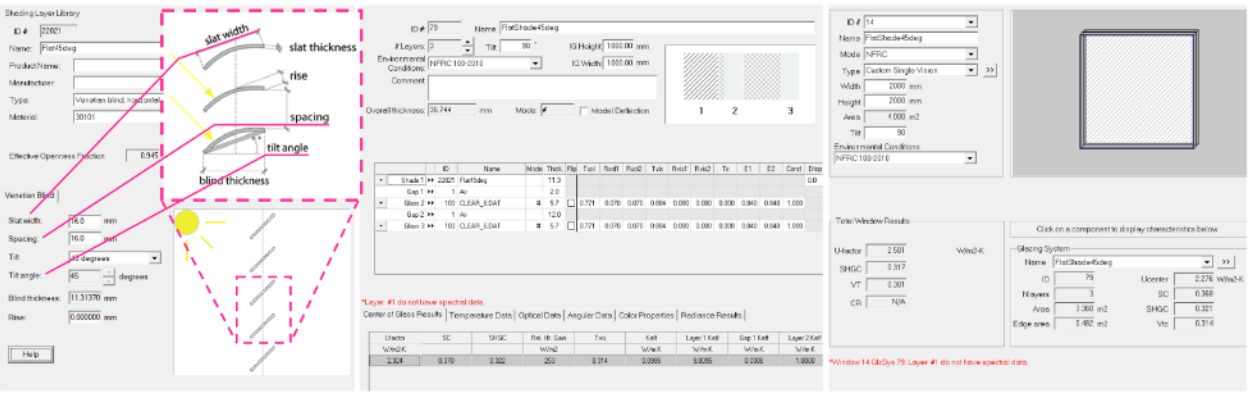

Figure 5-36. WINDOW 7.5 interface. Left: louver editor with slat width, louver spacing, blind tilt angle key parameters highlighted. Center: glazing assembly editor. Right: Window assembly editor with glazing and total window optical, solar, and thermal properties.

The first CFS is a parametric louver-based shading system composed of white-colored metal louvers. The parametric study of different states of the systems maintains a 1:1 ratio between slat spacing and slat width. By preserving this ratio as a constant, it is possible to generate louvers in different sizes and geometry while keeping the same profile solar angle and thus the same overall performance. The parametric study performed on the louver-based system tested the system for various tilt angles in incremental steps of 5º with the axis parallel to the glass plane.

The second CFS, the glass frit-based system, uses a white silk-screening ceramic frit applied directly on the interior surface of the outermost glass pane. The specular and diffuse light distribution data of the used glass frit result from measurements conducted at Lawrence Berkeley National Laboratory (LBNL). The parametric study entailed the analysis of different frit coverage ratios, from 0% (no frit coverage) to 100% (full frit coverage) in incremental steps of 5%.

Based on the results from simulating different instances of the two CFS, the proposed method builds a surrogate model that predicts the different window performance indices based on the variables used in the parametric assessment.

The study results reveal that changing the different parameters of the parametric CFS different CFS did not produce a relevant impact on U-factor. The only registered significant change in U-

factor happens with the addition of external louver-based shades to the standard glazing unit, which resulted in a drop from 2.83 to 2.5 W/m^{2}K. All the other variations of the tilted louvers had a negligible impact. As expected, the adding of frit to the standard base glazing assembly did not change its conductance properties. Therefore, the system kept the U-factor of the base glazing assembly. Hence, the U-factor assumed for all louver variations is 2.5 W/m^2.K while the U-factor of the frit-based assembly is the same of the base assembly, 2.83 W/m^2.K. Considering that there is a fixed U-factor for all states of the two CFS, the implemented workflow used linear regression to build a surrogate model that expresses slat tilt angle, frit coverage, and VLT as a function of SHGC.

Figure 5-37 shows the linear regression models obtained for the louver- and frit-based shading systems. In both cases, the high R^2 values present a strong correlation between the variables, indicating that the model predictions are robust. It is possible to use the resulting linear models to map SHGC, and VLT in the envelope in function of solar radiation, as well as to (re)generate the respective louver and/or frit geometry given a specific SHGC value. The graphs of Figure 5-37 also show that, by applying the parametric approach prescribed in the third step of the proposed modeling method, it is possible to find different CFS that have similar overall solar, thermal, and optical performance. As a result, the method enables architects to consider and compare different shading systems simultaneously – and thus different façade compositions – at early design phases, stages where usually designers are not yet committed to a single type of solution.

Having a surrogate model that abstracts different CFS, and their respective instances, into solar, thermal, and optical indices it is possible to use the resulting information in the BEM to study the impact of different types of skin design strategies on building energy performance.

The fourth step of the proposed workflow uses EnergyPlus to conduct such studies.

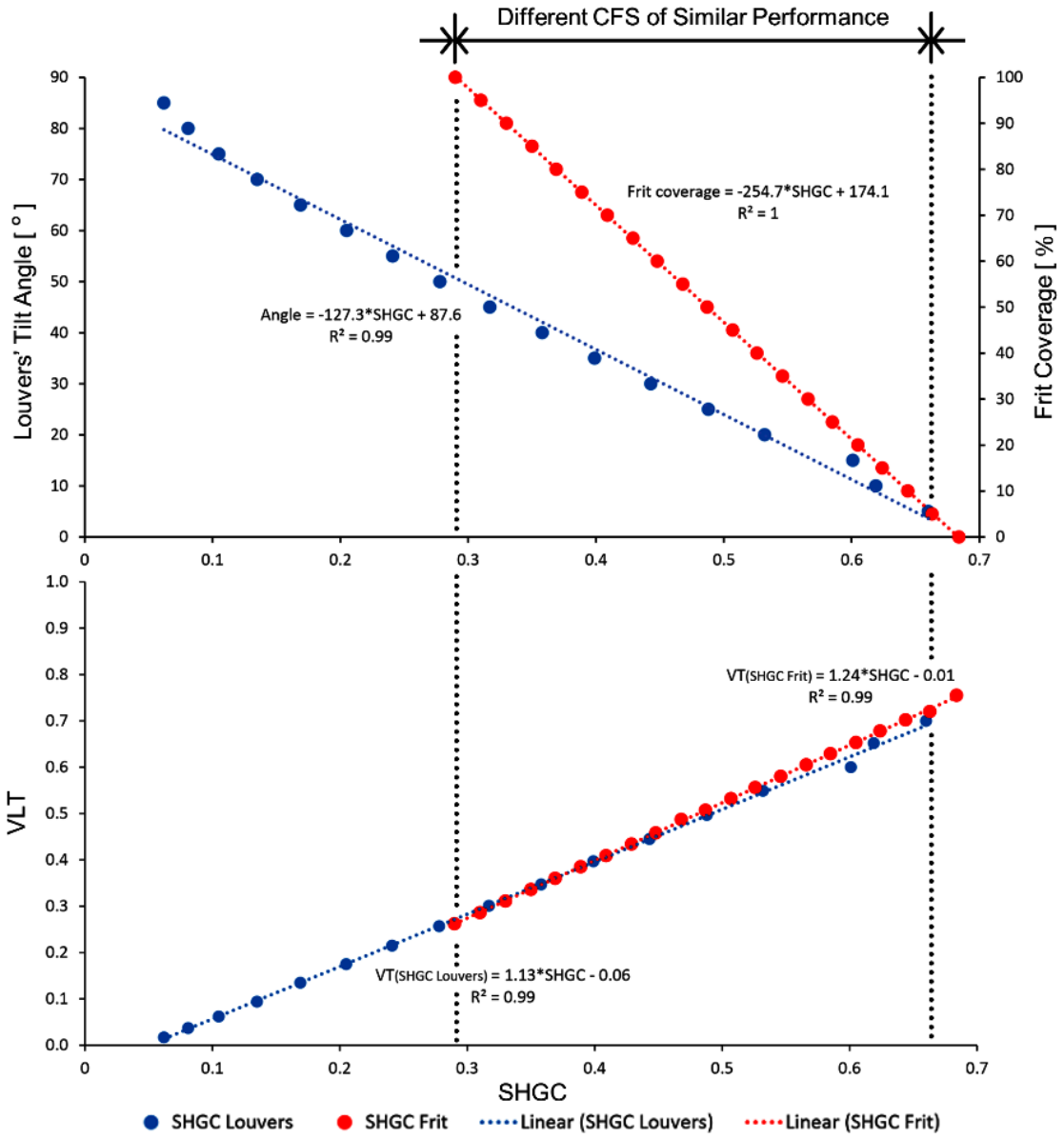

Figure 5-37. Linear regression models for the louver- and frit-based shading systems. Top: the tilt angle of the individual louvers (blue) and frit coverage (red) - measured in percentage of glass surface - expressed as a function of SHGC. Bottom: visual light transmittance (VLT) as a function of SHGC for louver- (blue) and frit-based (red) shading systems. In both graphs, the space between the two dashed lines marks the solution space where the two different CFS have similar optical, solar, and thermal performance.

The experiment applied the method to study and compare the following façade designs:

A. Base Case - No shading and standard glazing.

B. Perpendicular Louvers - all louvers are perpendicular to the glass panel, which corresponds to a tilt angle of 0°.

C. 45° tilted Louvers - the glass panels have louvers with a tilt angle of 45°.

D. SR based Gradient Louvers – the result of the work presented in section 5.3, and published in (Santos, Schleicher and Caldas, 2017), showed that applying a shading density gradient that follows the distribution of Solar Radiation (SR) on the envelope might yield a significant reduction in cooling loads. Thus, for each panel this solution remaps the incident SR to a SHGC value and corresponding tilt angle of the louver. This remapping is based on a linear interpolation, where the highest SR value relates to the lowest SHGC that the louver-based shading system can reach (0.06), and vice versa. In this way, the louvers of the panels with high SR will be more closed than the ones with low SR.

E. 25% Frit Coverage - the envelope has a uniform frit coverage of 25%.

F. 50% Frit Coverage - all panels have a frit coverage of 50%.

G. SR based Gradient Frit - the same logic of SR based Gradient Louvers but applied to the frit-based shading system where the range of SHGC only goes from 0.3 to 0.68.

Figure 5-38 illustrates solutions B through G. Solution A is the base model generated in step 1 and presented in Figure 5-34 – right.

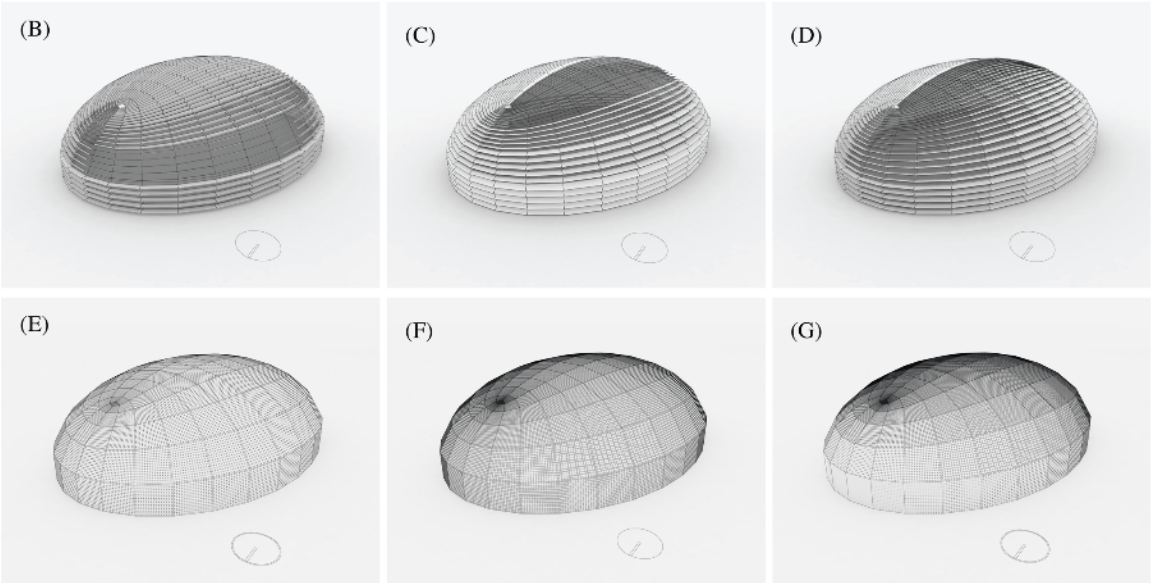

Figure 5-38. Freeform facade with different CFS configurations used in this experiment. The top three pictures show the three louver-based configurations, respectively: Perpendicular louvers (B), 45° tilted louvers (C), and SR based gradient louvers (D). The bottom three images illustrate the three frit-based configurations, respectively: 25% frit coverage (E), 50% frit coverage (F), and SR based gradient frits (G).

All solutions used a single thermal zone BEM with a floor composed of a 200 mm thick concrete slab plus a 120 mm thick Extrude Polystyrene (XPS) insulation board covered with a cement screed. The resulting combined U-factor is 0.28 W/m^2.K. The simulation parameters used in the EnergyPlus simulations, which encompasses internal loads, HVAC system properties, thermostat, infiltration and ventilation rates, and daylighting sensors and controls, are identical to the ones used in section 5.4 and listed in Table 5-10 (page 110). The daylight sensor is in the center of the space located at a typical work plane height, 0.8 m above the floor.

Total annual energy consumption (kWh), total EUI (EUI_{total}) (kWh/m^2) and parceled annual energy consumption and EUI per energy end-use, are the metrics that express the BES results. In this experiment, total energy consumption is considered the sum of heating, cooling, and lighting energy. Since the study focuses on the energy performance of either shading systems or solar glazing surface treatments, other factors like plug loads or fan energy were not included in the total energy calculation. Finally, the comparison of the performance of the different designs uses percentage of improvement (% of improvement) in EUI_{total}, as formulated in ASHRAE 90.1 standard – see chapter 4, section 4.5.3, equation (4-7), or equation (5-1).

The fifth and last step of the proposed method uses the correlation between CFS geometry and the simplified glazing performance indices established in step 3 to re-create the three-dimensional features of the CFS in Rhinoceros + Grasshopper. In this experiment, the implemented workflow uses the SHGC assigned to each panel to automatically generate either a louver-based shading system, given a specific number of louvers or louver width, and different glass frit coverage densities, given a particular pattern. This visual feedback is helpful for the further development of the facade design. For example, it allows architects to compare different solutions for their optical effect and/or fine-tune design alternatives parametrically. Figure 5-39 illustrates how a designer can use this step to parametrically adjust the geometrical characteristics of a louver-based envelope strategy without affecting the overall solar, optical, and thermal properties of the envelope.

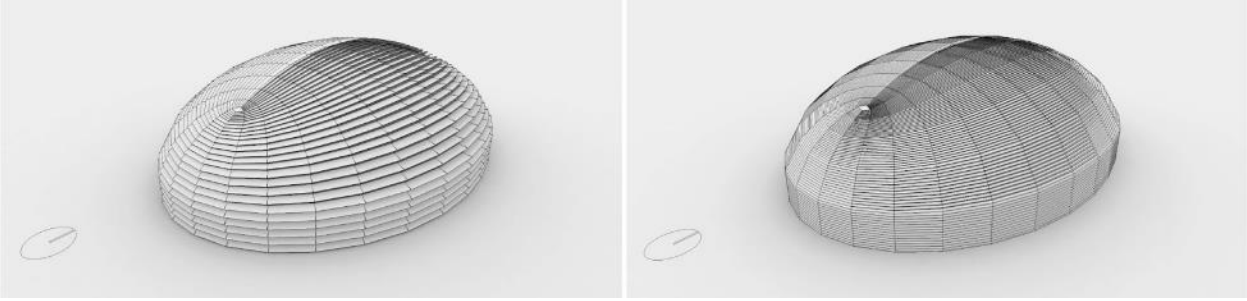

Figure 5-39. The proposed modeling method allows to parametrically modify the geometric features of a selected shading device – for example, from 8 (left) to 14 louvers per panel (right) – without affecting the predefined glazing properties of the panels.

This experiment also includes a validation procedure of the proposed simplification method that consists of comparing the simulation output of two fully detailed re-created solutions, one per CFS type, with their simplified counterparts. Solution C, a louver-based CFS solution, and solution F, a frit-based instance, were the solutions used in the validation process – see Figure 5-38. The validation process is similar to the one used to validate the modeling strategy presented in section 5.4. It uses CVRMSE – chapter 4, section 4.5.3, equation (4-3) –, NMBE - chapter 4, section 4.5.3, equation (4-6) – and the percentage of error (% error) – chapter 4, section 4.5.3, equation (4-1). Although those statistical indexes are commonly used in BES calibration (Coakley, Raftery and Keane, 2014), the proposed validation process adopts them to measure simulation output deviation.

By definition, CVRMSE and NMBE are able to process data series, such as annual hourly simulation data, while % error is only able to analyze single values, in this case post-processed data such as the cumulative energy consumption over a period of time. Thus, this experiment uses CVRMSE and NMBE to measure the deviation in hourly energy simulated data, either for each energy end use or total energy, and % error to assess the difference in EUI_{total}. The acceptance

criteria of CVRMSE and NMBE are set out by ASHRAE Guideline 14 (ASHRAE, 2002) which are 30% and - or + 10% respectively (see Table 5-8, section 5.5.3). The acceptance threshold assumed for % of error is 10%. Finally, to assess the cost-benefit of the proposed method, the study compares the run time of simplified BEM against the one of the detailed BEM.

5.5.4 Results

Table 5-18 shows the summary results of the EnergyPlus simulations for all shading alternatives. Figures 5-40 and 5-41 plot the results of the annual energy performance for each individual façade solution. The chart of Figure 5-40 compares in detail the annual cumulative energy consumption per end-use. Due to the existence of outliers in cooling energy, the graph maps the values in $\log_{10}$ scale. Through the analysis of Table 5-18 and Figure 5-40, it is possible to assess the weight of each energy end-use in the overall energy performance.

Table 5-18. Summary of energy simulation results of each shading design solution.

	Annual Energy Consumption [kWh]				**EUI** [kWh/m^2]			
	Heating	**Cooling**	**Lighting**	**Total**	**Heating**	**Cooling**	**Lighting**	**Total**
Base case (A)	99.1	148, 289.4	1,006.3	149,454.8	0.3	418.1	3	421.4
Perpendicular louvers (B)	55.2	143,128.8	1,066.5	144,250.5	0.2	403.6	3	406.8
45° Tilted louvers (C)	755.7	53,975.3	1,072.5	55,803.5	2.1	152.2	3	157.4
SR-based gradient louvers (D)	1,039.7	42,502.1	1,083	44,624.8	2.9	119.9	3	125.8
25% Frit coverage (E)	205.4	113,307.9	1,066.7	114,580	0.6	319.5	3	323.1
50% Frit coverage (F)	360	93,684.1	1,067.4	95,111.5	1	264.2	3	268.2
SR-based frit coverage (G)	627.6	71,130.3	1,069.3	72,287.2	1.8	200.6	3	205.4

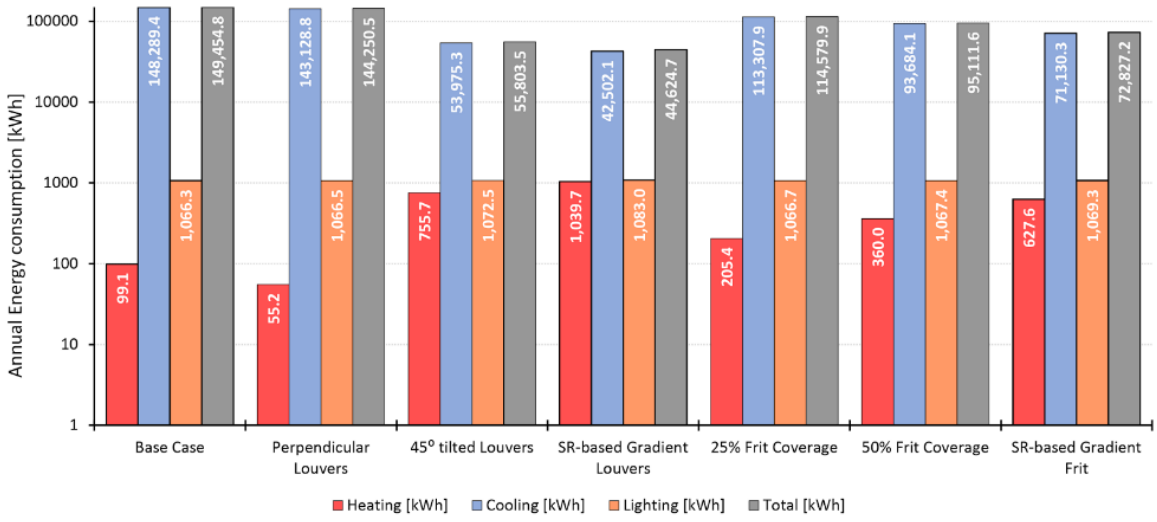

Figure 5-40. Bar chart of annual energy consumption (kWh) for each shading system. Note that the y-axis uses $\log_{10}$ scale.

Figure 5-41 shows the EUI_{total} per façade solution. The magenta dotted line marks the EUI benchmark for the same building type in Los Angeles, California. The benchmark value is from the U.S. Department of Energy Commercial Buildings Energy Consumption Survey (CBECS). Figure 5-42 shows the % of improvement (see chapter 4, section 4.5.3, equation (4-7), or equation (5-1), page 105) in EUI_{total} of each design solution when compared with the base case.

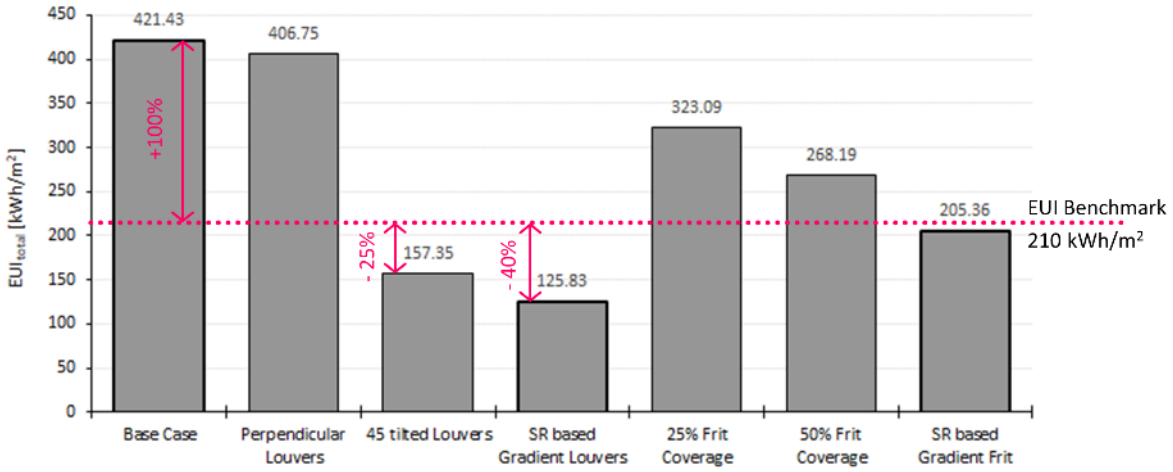

Figure 5-41. Total Energy Use Intensity (EUI) per design alternative. The thicker bar outline highlights the base case and the louver and frit solution that are more energy efficient.

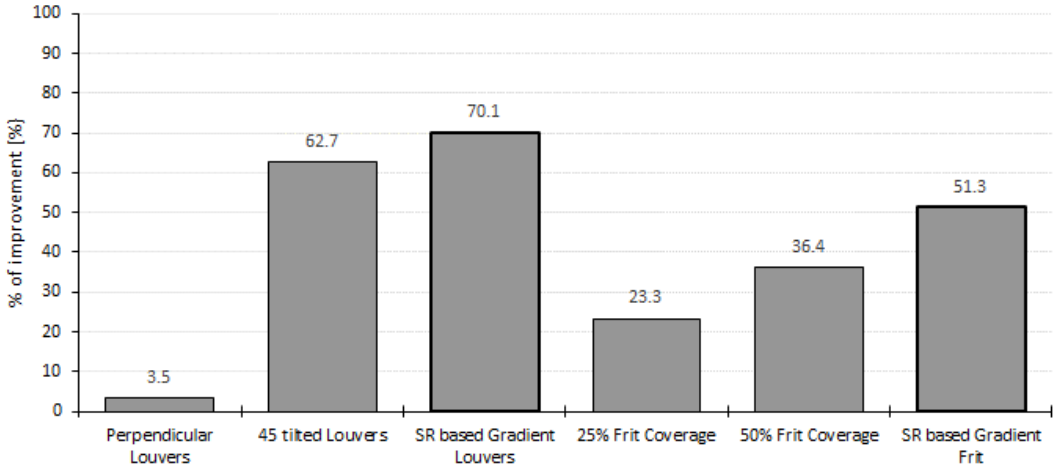

Figure 5-42. Percentage of improvement of each design alternative when compared with the Base Case. The bars with a thicker outline indicate the best performing solution per CFS type.

Figures 5-43 and 5-44 present the validation results. Figure 5-43 maps the simulation output deviation error of the simplified selected models in terms of CVRMSE and NMBE. Figure 5-44 shows the % of error in total EUI and compares the simulation time of the fully detailed energy models with the simplified models.

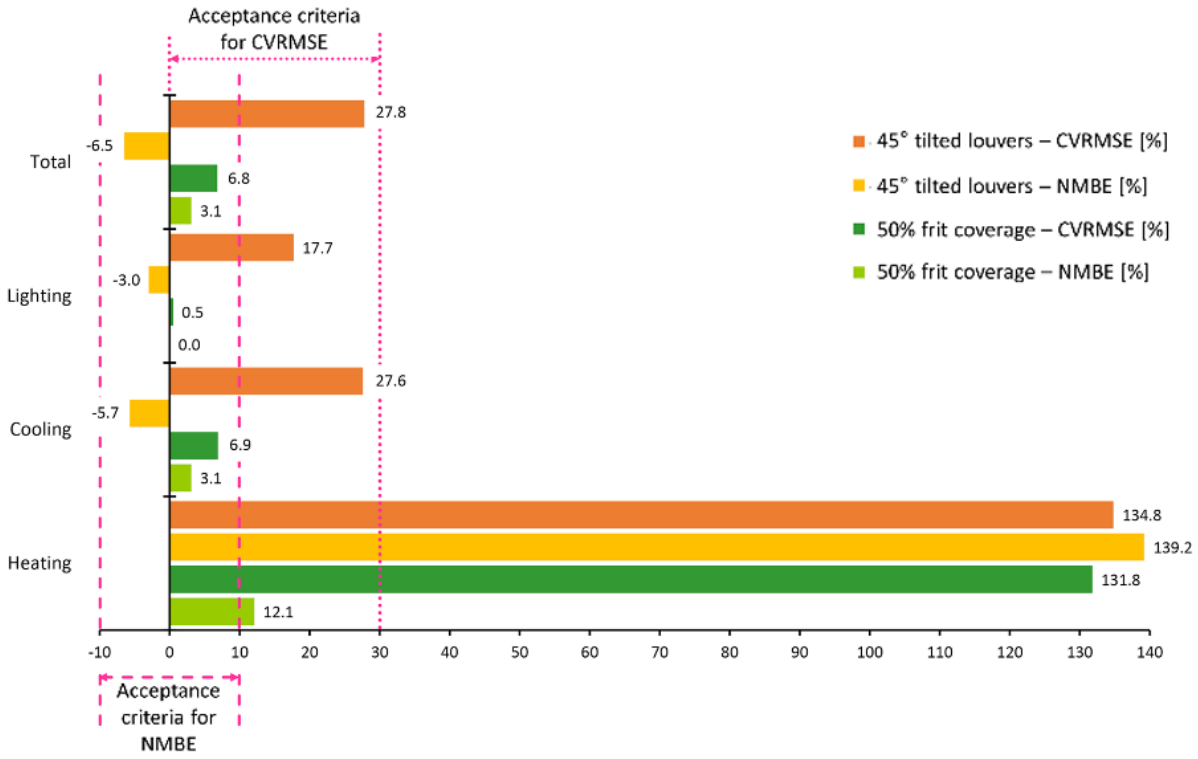

Figure 5-43. Assessment of the error metrics CVRMSE and NMBE of the proposed simplification for the 45° tilted Louvers and 50% Frit Coverage. These two metrics measure the deviation on hourly simulation output for different energy metrics between the simplified BEM and their fully modeled counterparts, i.e., the same solution but with CFS geometry fully modeled. The magenta dotted and dashed lines mark the acceptance thresholds for CVRMSE and NMBE respectively.

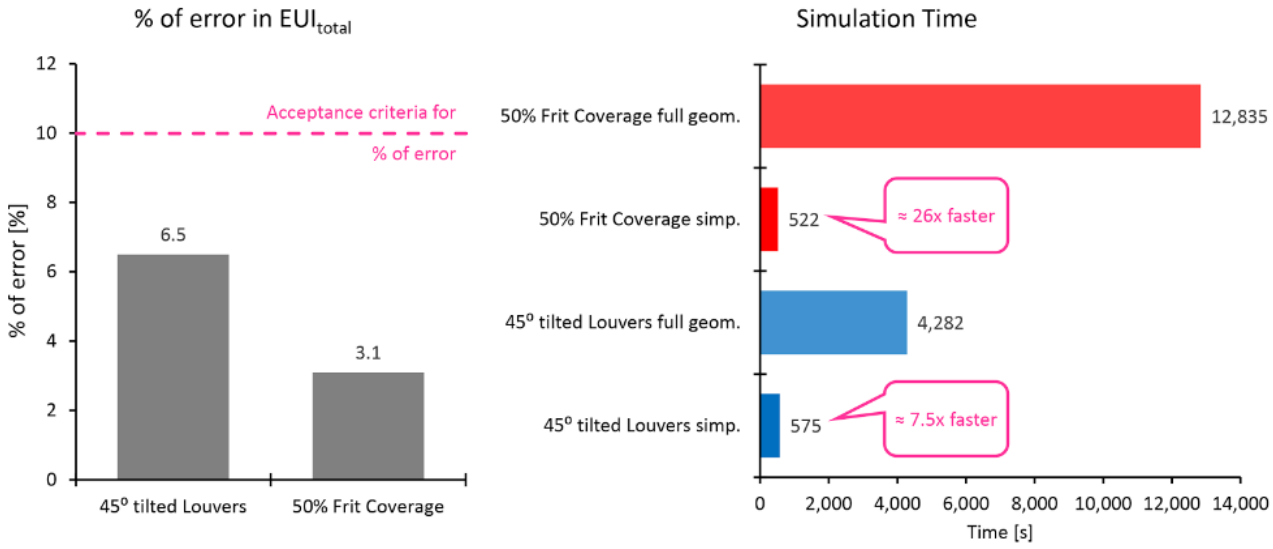

Figure 5-44. Left: Percentage of error in total EUI$_{total}$ between the simplified (simp.) and detailed modeled versions (full geom.) of solutions 45° tilted Louvers and 50% Frit Coverage. Right: comparison of run time of the same solutions.

5.5.5 Discussion

Table 5-18 and Figure 5-40 show that cooling is the most relevant energy end-use. Even in the best performing case (D), cooling still represents more than 95% of the overall energy consumption. The weight of cooling loads in the energy performance of all cases indicates that it is possible to analyze the energy benefits of reducing solar heat gains through shading by analyzing the total energy consumption or the total EUI. As expected, the base case has the worst energy performance because of the overwhelming amount of cooling required to ensure thermal comfort in a fully glazed dome like space located in LA. Figure 5-41 shows that the base case consumes twice as much energy as the benchmark, showing how inefficient this type of structure is for warm climates. Adding perpendicular shades to each panel produces a marginal improvement of only 3.5% (Figure 5-42). The small impact that this shading solution has on reducing SHGC of the standard glazing unit explains the small improvement.

In comparison, a relatively small percentage of frit coverage produces a more significant impact: an improvement of 23.3% for 25% of frit coverage (Figure 5-42). Figures 5-40 and 5-41 show that either increasing the louver tilt angle or the frit coverage yields a positive impact in energy performance. Nevertheless, the effect of incrementally closing the louvers by changing their tilt has a bigger impact on decreasing cooling loads than would be achieved by increasing frit coverage. A close analysis of Figure 5-37 top graph explains this phenomenon: the slope of the linear regression in the louver system is more pronounced than in the frit system, meaning that the tilt angle is more effective in reducing SHGC than frit coverage.

The adaptive shading schemes based on solar radiation present the best results in each shading type, confirming the pattern observed in section 5.3 and by Santos, Schleicher, and Caldas (2017). The SR based Gradient Frit (G) improves the energy performance of the base case in 51.3%, and it is the only frit-based solution that reduces EUI to levels below the benchmark. The SR based Gradient Louvers (D) yielded an outstanding 70.1% improvement relative to the base case, lowering the total EUI from 421.4 kWh/m2 to a reasonable 125.8 kWh/m^2, 40% below the benchmark of assembly buildings in LA. In sum, louver-based shading systems have the highest potential of reducing cooling loads in fully glazed envelopes. If well designed, they could reduce the overall energy consumption of large glazed structures even in non-favorable climates, such as those like that of Los Angeles, to acceptable levels that are significantly below the benchmark. The gradient of louvers based on incident solar radiation is the most effective solution in reducing cooling loads with a relatively small impact on heating and lighting loads.

The validation results show that the proposed simplification modeling method for CFS is effective in both simplifying modeling tasks and is capable of accelerating BES with a low impact in simulation output. Figure 5-43 error results are within the acceptable criteria except for heating. However, heating is of little relevance in the error assessment due to its small weight in the overall energy performance: 1.4% and 0.38% for the louver and frit cases, respectively. The low weight of heating in the overall building energy performance also distorts the error in CVRMSE and NMBE, since any little deviation has more relative impact. The % of error in total EUI is also comfortably below the acceptance threshold. The simplified energy models can run 7.5 to 26 times faster than the detailed models (5-44) indicating that the method promotes useful energy performance feedback in the early design of complex building skins. Finally, the wide range of

simulation acceleration confirms the pattern identified both in the literature and in section 5.4 – the run time of BES is highly sensitive to the number of faces of the energy model.

5.6 Concluding remarks

This chapter presented three different strategies that automate the generation of efficient whole-building energy models, particularly in early-stage building designs of complex geometry that emerge from the use of parametric, generative design tools, and algorithmic approaches. Each strategy aims to address the needs identified in the analysis of the related work, namely:

- To parse the geometry of curved or double-curved parametric building envelopes and sophisticated parametric façade systems for BES.
- To reduce simulation run time of either free-form building masses in order to reduce the gap between simulation and analysis time and design time.
- To facilitate the modeling and simulation of sophisticated custom-designed building skins and CFS at early design stages.

Strategy A addresses the need to accurately translate complex curved or double-curved building surface geometry to a BEM. Strategy B extends A to improve simulation run time by implementing new and valid geometric simplification methods. Strategy C proposes a novel approach that substantially reduces the geometric modeling and simulation effort in energy-related studies of CFS.

Section 5.3 presented and discussed Strategy A. This strategy offers a new modeling method to describe complex building envelopes in BEM for goal-oriented design methods based on BES. It consists of automatically generating valid geometry for BEM from initial parametric descriptions of curved and double-curved building geometry. The proposed approach uses planarization methods, borrowed from the architectural computational geometry and digital fabrication fields, to overcome the current limitations of energy modeling of curved and double curved building envelopes. The integration of such planarization methods allows architects to automatically generate valid BEM geometry from a 3D CAD model, thus avoiding time-consuming manual modeling tasks that are incompatible with fully automated optimization workflows. The proposed approach also allows controlling the discretization of the initial building surfaces and, consequently, the degree of detail of the resulting BEM. The application of Strategy A in the case-study of optimizing glass frit ratios in fully glazed grid shell envelopes was successful in minimizing the gap between the design model and the energy model, optimizing glass frit ratios, and, consequently, reducing predicted whole-building energy consumption. The deployment of the strategy in such a case study also demonstrated how accurate geometric building envelope descriptions are relevant in energy optimization workflows, particularly in the case of free-form buildings. Additionally, the case study showed that optimization of glass frit in double-curved building envelopes requires a geometric description detailed enough to capture self-shading and variable solar radiation distribution patterns. Thus, Strategy A utilization demonstrates that in the energy optimization of building energy use in building with complex (double)curved envelopes, excludes the use of oversimplified approaches based on shoebox BEM.

The integration of the proposed strategy in an inverse design process exemplified the usefulness of using goal-oriented methods in the study of complex trade-offs associated with building-energy related performance. The analysis of unexpected results that emerge from these methods inform the design process with new perspectives and different solutions to solve specific design problems. The experiments indicated that steering the optimization process by constraining specific design parameters can improve the quality of the search. The implemented method also demonstrated how the results of an optimization process could inform the design of different glass-fritting densities and patterns and, consequently, the overall aesthetic properties of the building envelope.

In sum, the integration of Strategy A in a generative-design system prototype proved to be:

- Robust – it was able to parse a diversity of double-curved building geometries to EnergyPlus automatically.
- Adaptable – it allows the user to control the generation of the BEM model and steer the optimization process through the use of constraints.
- Useful – particularly in providing feedback, since it allowed the search mechanism to evaluate valid BEM in order to find design solutions that improve the building energy performance of the base cases in almost 70% (see Table 5-7).

As briefly mentioned in section 5.3.4, although Strategy A is robust, the resulting workflow presents three main limitations: (i) one related to the search process, (ii) another to simulation run time, (iii) and the last to the simplification strategy used in describing CFS, such as glass fritting.

Regarding the first limitation, Opt#1 experiment showed that the GA probably became stuck in a local minimum. The fact that the used GA, Galapagos (SGA), does not scale well along with the increasing number of decision variables might explain the inefficiency of the search. Nevertheless, the use of a Galapagos SGA served as a proof-of-concept that tested the integration of Strategy A in the context of an ecosystem of digital design tools that architects currently use. Hence, it is not a limitation caused by the modeling strategy but rather by the search algorithm. Since Strategy A is agnostic to the optimization algorithm used in the search procedure, it is relatively easy to improve it through the use of more robust optimization evolutionary metaheuristics, such as SPEA2 (Ziztler, Laumanns and Thiele, 2002) or the Nondominated Sorting Genetic Algorithm II (Deb et al., 2002).

The second limitation results from the direct correlation between the number of panels and simulation time: the higher the BEM polygon count, the higher the calculation time of its energy performance. This run time overhead in EnergyPlus is primarily due to view factor calculations for radiant heat transfer computation and the resulting impact on heat balance convergence.

The third limitation emerges as a consequence of the second one. The glass fritting modeling approach is oversimplified to avoid long simulations that hamper the usability of the proposed methodology. The modeling of individual frits would increase the number of mesh faces to an unacceptable (or even unfeasible) run-time horizon. The generation and use of BSDF to describe the different glass frit states would also slow EnergyPlus simulations and consequently burden the optimization with a considerable time overhead. Thus, the proposed simplification intentionally

sacrifices accuracy over speed, considering that some deviation on energy simulation output is acceptable in the context of a workflow that requires the simulation of many design alternatives.

Since Strategy A focuses on parsing complex (double-) curved geometry into a valid mesh representation for BES, the second and third limitations are a direct consequence of its application. Strategy B and C address those limitations by proposing the generation of surrogate geometric representations of both complex building forms and façade systems.

Section 5.4 introduces Strategy B, which both extends Strategy A's scope to multi-zone models and improves the efficiency of the generated BEMs by automatically simplifying their geometric descriptions. Strategy B encompasses and combines two modeling approaches. The first automatically parses any curved enclosed building envelope and generates an equivalent low polygon BEM. The second approach samples a multi-zone BEM to isolate smaller and representative parts of the original model.

The experiments that tested Strategy B modeling approaches confirmed that BES are highly sensitive to the geometry complexity of BEMs. Figure 5-29 shows that simulation run-time increases exponentially with the number of BEM mesh faces. The results also show that BEMs with oversimplified geometries that do not capture the overall building shape are likely to be inadequate surrogates (see Table 5-15 and Figure 5-30). However, it also demonstrated that it is possible to automatically generate simpler and more efficient BEM geometries, i.e., geometric descriptions for BES that result in faster simulations and have minimal impact in simulation output. However, the simplification is only successful if it preserves the volume of each thermal zone and minimizes deviations in envelope surface area.

The results showed that Strategy B can generate simplified and efficient geometric surrogates for either single or multi-zone BEMs. Both experiments showed that the proposed modeling approaches produce BEMs that run faster, with simulation output deviation within the acceptable range assumed both for CVRMSE and NMBE. The sensitivity analysis that tested the first modeling approach (geometry simplification of complex building envelopes) showed that it is possible to reduce by 80% the number of mesh faces in a BEM. The second experiment demonstrated that it is not only possible to decompose a multi-zone BEM into isolated representative single-zone models, but that it is feasible and desirable to reduce their mesh density.

Despite the usefulness of the strategy, three points limit a generalized application of the results and recommendations of the experiments. The first is the HVAC model assumed in both experiments, the simple EnergyPlus Ideal Loads Air System (ILAS). ILAS is a variable-air-volume (VAV) system that is not connected to a central air system, making it a system that supplies cooling and heating air to each zone in just a sufficient amount to meet each zone thermal load. It also assumes a well-mixed air volume for each thermal zone. As a result, the simulations do not capture the typical inefficiencies and losses of a centralized VAV system and thermal stratification. Although the use of such a simplified HVAC system limits the applicability of the results, this simplification is acceptable since this dissertation focuses on the use of BES at early-design stages, and ILAS is a system that designers commonly use in such phases. The second is that both experiments used buildings with narrow plans, making the envelope have a more predominant role in heat exchange. This assumption is also acceptable in the general scope of the research since the dissertation focuses on high-performance buildings, which usually have narrow plans since they

facilitate the implementation of both natural ventilation and passive solar design strategies as essential energy conservation measures. The third point is that both experiments used TMY data from Oakland, CA – ASHRAE climate zone 3C, Warm-Marine. The mild Oakland climate might be smoothing errors, and, consequently, some of the recommendations suggested by the results, such as the level of acceptable geometry reduction, might not be valid. Future work will address this point to assess the applicability of the proposed method results at early-stage parametric and generative design in a wide diversity of climates. The envisioned locations to further test Strategy B will be representative of more extreme climates, e.g., Phoenix, AZ (hot and dry), and Boston, MA, (cold winter and hot and humid summers).

Although the assumptions used in section 5.4 experiments constrain the applicability of the results, the tests showed that Strategy B is effective in automating the description of buildings with complex geometries in the context of BES-based design workflows. Thus, it is especially useful for non-expert energy modelers, such as architects. It also yields a high integration potential in early building energy optimization studies, particularly the ones that use metaheuristics, since the tool can automatically generate valid BEMs that are faster to simulate.

Strategy C also extends the modeling capabilities of Strategy A. It proposes a simplification approach that addresses the generation of efficient geometric descriptions of highly sophisticated façade systems at the early design stages. Such facades systems include CFS that control solar heat gains and mediate light and air in complex free-form building envelopes.

This strategy combines parametric design, surrogate modeling techniques based on statistical-learning, window performance and whole-energy building analysis tools in a single streamlined design workflow. The main innovation that it proposes is using co-simulation to first abstract and simplify the geometric features of CFS into simplified fenestration performance indices, and then use them in the early study and optimization of whole-building energy performance. Since the method abstracts the geometry of façade systems into simplified fenestration performance metrics, it is possible to use it to find formally distinct solutions of similar thermal, solar, and optical performance. This ability makes the method particularly useful in the early design of facades with intricate patterns, phases where architects usually are still evaluating the aesthetic contribution and qualities of different façade strategies and their resulting patterning effects.

The application of the novel method in the design and simulation of louver- and frit-based shading systems for a fully glazed semi-ellipsoid showed that it is possible to select configurations of the two systems that have similar performance. The experiments demonstrated that Strategy C delivers building energy performance results on valuable time and within an acceptable accuracy for either parametric or goal-oriented design processes based on overall building energy performance. The application of Strategy C in a specific design case confirmed an observation that emerged from the Strategy A experiments: static shading façade systems are more effective if annual incident solar radiation simulation data constrains the modulation of either their shading factor or SHGC. The application of Strategy C showed that informing the façade panels with a specific louver tilt or frit coverage based on incident solar radiation is the most effective strategy to improve the energy performance of fully glazed envelopes with static shading devices or high-performance glazing coatings. The experiments also indicate that a more refined study, which would include the hourly variation of solar radiation, may have the potential to inform the design and operation of dynamic shading devices that most likely outperform static shading solutions. This particularly

true for buildings with continuous envelopes that simultaneously face different orientations, as was the case for the semi-ellipsoid glazed covered space used in the Strategy C study.

Although Strategy C presented acceptable errors, particularly in annual EUI_{total}, it is less robust in minimizing simulation output deviations than Strategy B. The models produced by Strategy C showed hourly deviations (measured using CVRMSE and NMBE) outside the acceptability range in the case of predicting heating energy consumption. The other energy end-uses reported acceptable CVRMSE and NMBE values. Nevertheless, the experimental setting might lead to an overestimation of the error measured in heating. Since heating has a minimal weight in the overall energy performance of the case study used in the experiments, any small absolute deviation on it will produce significant relative errors. However, it is also plausible to assume that the proposed simplification is causing such errors. Abstracting complex fenestration assemblies to static performance indices result in a considerable dimensionality reduction. Consequently, such abstraction flattens the granularity of the hourly impact that shading has on building energy performance. However, the loss of information is acceptable at early design phases since quick feedback is desirable, and designers are more concerned with the overall annual performance than with hourly predictions.

Considering annual estimations, the models produced by Strategy C introduce minimal deviations, confirming the usefulness of the method. Nonetheless, it is possible to refine the proposed approach through the development of dynamic SHGC, VLT, and U-factor. Such an approach will model CFS similarly to electrochromic or thermochromic glazing units. Although this refinement will increase simulation run-time, it will allow the detailed assessment of several solutions that emerged through the application of the current strategy. It will also extend the proposed method to analyze dynamic CFS.

In sum, Strategy A enables the automatic generation of valid BEMs for BES of complex free-form building envelopes. Strategy B extends A by allowing the creation of geometric surrogates that simplify the geometry of an initial massing model or refined multi-zone BEM. By preserving essential geometrical properties (e.g., air volume, surface-to-volume ratios, and overall shape), the models produced by Strategy B are computationally more efficient since they run faster and the resulting simplification has a small impact on simulation output. Strategy C also extends A by expanding its scope to the study of complex façade systems that shape the solar, thermal, and optical performance of highly sophisticated building skins. The simplification proposed by Strategy C reduces the geometry of CFS to simple fenestration performance indices – SHGC, VLT, and U-factor. The resulting surrogates are faster to run and deliver useful feedback of acceptable accuracy for early whole-building energy assessments.

Because the modeling Strategies B and C directly derive from Strategy A, it is possible to combine Strategy B and C with A. For example, a complex parametric model could use Strategy A to parse complex double-curved building envelope geometry and Strategy C to study and optimize different shading façade systems. Strategy A can also pre-process the envelope geometry of a massing model that entails different thermal zones. Then, Strategy B can both simplify the initial geometric description produced by Strategy A and sample the multi-zone BEM and decompose it into simpler representative single-zone BEMs.

Considering that Strategy C is more robust in annual estimations and less in hourly predictions,

its combination with Strategy B could produce oversimplified models that, although presumably quicker to run, might deliver inaccurate results because of error accumulation.

Chapter 6:
Modeling Strategies for Advanced Daylight Simulation of Buildings

6.1 Introduction

As mentioned in chapter 3, section 3.3.2, the obstacles to using daylighting simulations in BPO or other parametric building design workflows are primarily related to the demand for advanced, detailed, and computationally expensive simulations to assess glare in indoor spaces.

The examination of glare is essential in assessing visual comfort in buildings since it is a key visual discomfort indicator. Thus, when architects and daylight analysts want to improve the daylight performance of buildings, they aim to simultaneously minimize glare and maximize the use of daylight, which in turn minimizes lighting energy use.

Like thermal comfort, preferred light levels and visual comfort in buildings are subjective; they vary from person to person. Thus, one might argue that glare mitigation should be directly addressed by building occupants. Nevertheless, leaving control of the daylit environment solely in the hands of building occupants is risky, as their behavior is often unpredictable. For example, the building monitoring study conducted by Correia da Silva et al. (2013) presented some cases where glare led building occupants to permanently block light with operable shades despite the limited duration of the phenomena – see section 3.1 in Correia da Silva et al. (2013). This type of behavior has a direct impact on building energy performance since it leads to the undesired increased use of electric light, and, consequently, to higher building energy consumption.

Although shading is an effective strategy to mitigate glare, they may not always be easily accessed or controlled. There may be cases in which several occupants compete for control, or where manual shading devices are too high for occupants to reach.

Moreover, some types of shade may even magnify glare. For example, a building occupant might adjust a highly specular venetian blind system to his or her liking, yet the resulting light reflections might bother another user. The use of micro-perforated light-colored roller blind systems can also increase the discomfort caused by glare. Such shades decrease the intensity of the glare source by diffusing it through their participating media. As a result, the roller shades glow and increase the size of the glare source. Since glare source size is a critical factor in determining visual discomfort, such roller shades might themselves become a glare source, affecting an area than that of the original small bright light source. Finally, if glare is caused by a high contrast ratio of surfaces, the building occupant has a limited range of actions with which to improve the situation.

The previous scenarios show the difficulty of controlling glare using standard shading devices. The assessment of glare thus becomes an important task in designing visually comfortable spaces, either through manipulating building geometry, conceiving and operating shading devices, or selecting building materials.

To address the complexity of visual comfort, several glare metrics were developed. Recent studies (Wienold et al., 2018) reveal that the Daylight Glare Probability (DGP) (Wienold and Christoffersen, 2005, 2006) is the best daylight metric available for estimating glare and visual comfort by measuring the discomfort caused by glare. Like thermal comfort metrics, DGP predicts the expected level of visual discomfort among a large number of people. Nevertheless, the calculation of DGP requires the generation of synthetic High Dynamic Range (HDR) images, which are computationally expensive.

Several efforts have been made to advanced simpler alternatives to DGP. Those alternatives attempt to correlate simpler annual climate-based metrics based on horizontal illuminance (E_h) with visual comfort, such as Useful Daylight Illuminance (UDI) and Annual Sun Exposure (ASE) (IESNA, 2012; Konis, 2014). However, such studies present certain limitations, mainly: (i) annual E_h metrics are unable to either partially or fully capture the glare phenomenon; (ii) they lack generalized consensus in the daylight research community; and (iii) they result in over-constrained guidelines as to what is admissible in terms of direct light.

Thus, the most refined method to assess annual glare induced by daylight still consists of calculating the Daylight Glare Probability index (DGP), using a time series of HDR images for the entire year with the *evalglare* program (Wienold, 2004). The increasing relevance of annual DGP (aDGP) led its adoption by the new European standard EN 17037 – Daylight in Buildings (CEN, 2019) as an essential visual comfort metric. The goal of such adoption is to mitigate visual discomfort as much as possible in design phases by accurately assessing glare. By requiring the analysis of glare and setting acceptability criteria for DGP, the standard promotes the reduction of glare through the following: (i) building form, (ii) orientation and correspondent façade design, (iii) the design of fixed building elements such as windows, static shades, and light redirecting systems, (iv) the selection of building materials, particularly shades and interior building finishes, and (v) an adequate arrangement of the interior spatial layout, particularly regarding furniture.

EN 17037 determines whether a space is visually comfortable or not if hourly DGP-threshold values do not exceed a certain fraction of the annual occupied schedule for specific points-of-view (POV). However, the definition of the POV entails a complex process that depends heavily on the geometry of the building. For that reason, designers and researchers often default to the simplified method presented by the standard that is exclusively based on solar geometry, making it even more rudimentary than the use of E_h based metrics to estimate glare (Paule et al., 2018).

Although annual DGP (aDGP) adequately addresses the temporal aspect of the glare phenomenon, typically its calculation takes a considerable amount of time making its use unfeasible in most building design processes, particularly initial ones. Moreover, because DGP depends on the viewer's location and POV, it cannot qualify an entire space or a zone in terms of visual discomfort or comfort.

Considering that DGP is currently the best available method to predict visual discomfort caused by glare in indoor spaces (Wienold et al., 2018) and that aDGP analyses times are often unfeasible in most building design workflows, two questions emerge:

Is it possible to develop a simplified prediction approach that quickly classifies the visual comfort of an indoor space over an entire year?

The underlying hypothesis of the strategy advanced in this chapter (Strategy D) is that it is possible to use annual vertical illuminance at the eye level (E_V) to generally qualify a space in terms of its visual comfort. The hypothesis also includes using the same E_V data to find critical time events at well-defined POVs and utilizing them in point-in-time DGP analysis. Such detailed DGP analysis would provide granularity and useful detail about critical aspects of worst-case scenarios, including the relative size and position of the circumsolar region in the observer's field-of-view (FOV), reflections, and surface luminance contrast. In sum, the strategy aims to address the following challenging question:

If it is desirable to replace aDGP with point-in-time simulations, when, where, and for which point-of-view should we run point-in-time DGP?

These questions that motivate the development of the strategy proposed in this chapter frame the second dissertation research question specified in chapter 3, section 3.4 to the use of advanced visual comfort analysis in architectural design workflows. The second research question mentioned in chapter 3, section 3.4 states the following: *What modeling and analysis procedures generate quick and adequate feedback on energy and daylight performance of buildings at early design stages?* Consequently, the resulting method satisfies the third development and implementation goal (chapter 3, section 3.4): *Develop simplified approaches that either replace or reduce the need for computationally expensive simulations*.

The work presented in this chapter results from a collaborative effort between the author of this dissertation and his primary advisor, Professor Luisa Caldas. The chapter summarizes two publications, one in a peer-review international conference (Santos and Caldas, 2018), which presentation won a merit award, and the other published in a peer-reviewed scientific journal of the field (Santos and Caldas, 2020).

6.2 Related Work

Wienold and Christoffersen (2005, 2006) introduced DGP, a glare metric expressed in equation (6-1):

$$DGP = 5.87 \cdot 10^{-5} E_V + 0.0918 \cdot log_{10}\left[1 + \sum_{i=1}^{n}\left(\frac{L_{s,i}^2 \cdot \omega_{s,i}}{E_V^{1.87} \cdot P_i^2}\right)\right] + 0.16 \qquad (6\text{-}1)$$

where E_V is the vertical eye illuminance, measured in lux, produced by the light sources at the observer's eye, $L_{s,i}$ is the luminance of a glare source, $\omega_{s,i}$ is the solid angle of the source seen by the observer in steradians (sr), and P_i is the position index that expresses the change in experienced glare relative to the angular displacement of the source (azimuth and elevation) from the observer's line of sight.

The DGP formula is valid within DGP values that range between 0.2 and 0.8 (DGP ∈ [0.2, 0.8]), and for vertical eye illuminance (E_V) above 380 lux. Table 6-1 shows the DGP categories of visual discomfort caused by glare.

Table 6-1. Daylight Glare Probability (DGP) categories.

DGP glare categories	**Probability range** ∈ [0-1]
Imperceptible glare	DGP < 0.35
Perceptible glare	0.35 ≤ DGP < 0.4
Disturbing glare	0.4 ≤ DGP < 0.45
Intolerable glare	DGP ≥ 0.45

The formulation of DGP was a considerable breakthrough because no other glare metric was able to handle large light sources such as the sun and thus address the effect of direct daylight in visual comfort (Suk, Schiler and Kensek, 2013). However, different researchers reported several limitations to DGP, including the following:

1) DGP is less accurate in predicting visual discomfort in glare situations caused by luminance contrast than by high E_V (Kleindienst and Andersen, 2009).
2) The development of the metric used only stable clear skies (Van Den Wymelenberg and Inanici, 2014), thus presenting a higher uncertainty with other types of skies, such as hazy bright ones.
3) DGP is based on a correlational fit of mean data, thus it might either not have the desired granularity or be susceptible to the cancelation effect (Van Den Wymelenberg and Inanici, 2014).
4) DGP model did not perform as expected when tested on data sets of similar experiments (Van Den Wymelenberg, Inanici and Johnson, 2010).

Nevertheless, recent studies showed that DGP is currently the most advanced available method for assessing visual comfort (Jakubiec and Reinhart, 2010; Suk, Schiler and Kensek, 2013; Wienold et al., 2018) outperforming other glare metrics such as the Discomfort Glare Index (DGI) (Hopkinson, 1972; Chauvel et al., 1982).

The simulation of DGP involves the production of a synthetic HDR image and its analysis through the *evalglare* software (Wienold, 2004; Wienold and Christoffersen, 2006). This simulation-based pipeline entails a considerable computational overhead, primarily caused by the generation of full HDR images, a task typically performed through Radiance (Ward, 1994).

To accelerate DGP simulations, Wienold proposed a simplification under the name of *DGPs*, which stands for DGP simplified (Wienold, 2009). Mostly based on E_V, DGPs is faster to calculate than full DGP. Nevertheless, it assumes that no direct sun – or any specular reflection of it – reaches the eye; thus it is not suitable in the glare assessment of indoor spaces that are highly exposed to direct light or in the study of highly specular LRCFS. To deal with these limitations, Wienold proposed the Enhanced Simplified Discomfort Glare Probability (eDGPs) as an alternative that is more accurate than DGPs and faster to simulate than DGP (Wienold, 2009). The eDGPs approach splits the initial definition of DGP into two simplified terms: the first depends on

E_V and the second on the detected glare sources. The first term is easy to calculate while the second requires the computation of a simplified image that renders only the main glare sources, thus neglecting most of the indirect ambient reflections. Although eDGPs is a faster method to predict glare, it is still computationally expensive for annual glare assessments.

Jones and Reinhart (Jones and Reinhart, 2017) used Graphical Processing Unit (GPU) parallelization techniques to accelerate DGP simulations. Although the remarkable improvements in simulation time brought by GPU parallelization, aDGP simulations are still slow for metaheuristic-based optimization studies. This approach also constrains designers and lighting analysts to use specific graphics cards (hardware lock).

Another way to study glare and visual comfort avoiding time-consuming DGP simulations is to correlate annual E_h metrics such as UDI with glare related phenomena. However, there is no consensus about UDI use and its upper illuminance threshold as a proxy to glare and visual discomfort. Mardaljevic et al. (2012) reported some promising correlations between UDI and DGPs, but because the study used DGPs it is difficult to establish a full correlation between E_h and DGP. In a field-based study, Konis (2014) concluded that the use of E_h as an estimator of visual comfort is context-specific and that it is thus necessary to complement E_h analysis with luminance-based assessments. Similarly, Santos, Leitão and Caldas (2018) showed that even using a conservative illuminance threshold (> 2000 lux), UDI is insufficient to accurately assess the glare performance of LRCFSs. ASE is another annual E_h based metric used to assess visual discomfort potential. However, because it considers only direct light, it falls short in assessing the glare performance of more complex fenestration systems, such as LRCFS.

Giovannini et al. (2018) used E_V to predict DGP. Although the work showed a good correlation between the different DGP bins with E_V, the research presents some limitations that constraint the generalization of its results, particularly:

1) It is difficult to validate the results since the authors used DAYSIM (Reinhart and Walkenhorst, 2001) to calculate DGP. For computationally convenience, DAYSIM calculates eDGPs (Wienold, 2009), which uses a simplified HDR to determine the luminance contrast term of DGP, thus being more biased towards E_V.
2) The authors test the approach under the annual sky conditions of a single location.
3) DAYSIM does not support materials described through bidirectional scattering distribution functions (BSDFs). Hence, it is highly questionable if the collected data captures light scattering effects, particularly in the models that used specular materials.

Despite the assumptions and resulting limitations of the work presented by Giovannini et al. (2018), the investigation shows a correlation between E_V and glare discomfort, mainly if the scene includes the sun or its reflections in the viewer's field-of-view (FOV). However, the experiments conducted by Wienold and Christoffersen (2006) showed that using E_V as a predictor of the different levels of visual discomfort yields a considerable deviation error, especially if E_V is high. Based on this discussion, the work presented in this chapter assumes that there is the potential to use E_V only as a binary indicator of glare events (DGP $\geq$ 0.35), not as a predictor of the different DGP categories.

Using simulation to map visual discomfort spatially is a challenging task. Early attempts (Reinhart and Wienold, 2011) used DA and UDI to generate a daylight availability map that marks overlit areas susceptible to glare. Despite its usefulness in early design phases, the approach is susceptible to the limitations that result from using E_h to predict glare. Recently, researchers use either E_V or DGP to spatially assess visual comfort. In Giovannini et al. (2018), the authors used E_V to infer DGP values to color-code a point grid. The use of E_V to extrapolate a DGP value limits a generalized use of the method. Additionally, since the work uses only one view direction, the proposed visualization does not provide any information about different view directions and critical time events.

The work advanced by Zomorodia and Tahsildoost (2019) provides information on critical time events by proposing a spatial DGP index (sDGP) that measures the hourly percentage of space exposed to intolerable glare. Although this metric provides information on critical time events, it reduces spatial information to a percentage. Therefore, sDGP is unable to report critical POVs susceptible to glare. Jones (2019) presents an imageless method to accelerate DGP calculations. The work also advances a new annual glare metric, *glare autonomy*, which is the fraction of occupied hours that a specific POV does not report perceptible glare. This simulation-based approach has two main limitations. First, the method uses the two-phase method, which limits its applicability – for example, it excludes the use of BSDFs and consequently the study and analysis of CFS. Second, the imageless approach considers only the sun and sky contributions to calculate the luminance contrast term of DGP equation, thus excluding any other glare source. Nevertheless, the method maps both point-in-time DGP and glare autonomy into a sensor grid by color-coding different view directions (arrows) per sensor. The resulting tool provides detailed information about glare potential, relevant POVs, but not on critical time events.

Considering the limitations of current metrics and simulation methods, it is reasonable to assume that combining E_V analysis with the calculation of DGP in critical events and POVs is a suitable approach for performing quicker annual visual comfort studies. Additionally, there are few guidelines for selecting appropriate POV and HOY in DGP-based studies. An interactive map that summarizes annual E_V data in different locations can be useful in the selection of POV/HOY pairs for detailed glare analysis.

6.3 Strategy D: Assess glare potential of indoor spaces using a time and spatial sampling technique

In order to answer the research questions stated in section 6.1, this section presents a new simulation-based tool that implements a heuristic approach that explores the relation between glare and E_V previously reported in the literature, particularly in Wienold and Chirstoffersen (2006) and Giovannini et al. (2018). The strategy hypothesis is that it is possible to use annual E_V calculations, which are much simpler and faster to compute than aDGP, in preliminary visual comfort assessments. The heuristic uses E_V specifically to spatially map glare potential and find POV and hour-of-the-year (HOY) pairs that yield high glare potential for further analysis.

To that end, the envisioned modeling strategy consists of a heuristic that samples annual E_V data calculated in a grid of sensors. The proposed heuristic uses an E_V threshold ($E_{V,Thr}$) to label every time event on any POV as susceptible or non-susceptible to glare (DGP $\geq$ 0.35).

The tool then displays preliminary visual comfort information that consists of mapping glare potential over a POV grid and providing the necessary information to conduct more detailed analyses. Such analyses consist of accurate point-time DGP simulations or false-color luminance HDR images for the most critical POVs and HOY pairs. Considering this, the investigation goals are as follows:

1) Find a robust $E_{V,Thr}$ that is able to detect glare events in different types of annual skies in any given location.
2) Propose an interactive computational tool that samples, maps, and visualizes annual E_V data. This tool should deliver preliminary visual comfort assessments and information on critical locations, POVs, and time events to guide the user in more detailed studies, including full point-in-time DGP simulations.
3) The tool should support all types of daylight simulations, including the accurate simulation of specular reflections, which typically are one of the primary causes of glare.

To fully support the simulation of specular reflections and caustics effects, the proposed modeling strategy uses advanced techniques that include forward ray tracing in daylight simulation. Such techniques enable the tool to assess the glare potential of different spaces with different types of fenestrations, including spaces with highly specular Light Redirecting Complex Fenestration Systems (LRCFS). For this reason, the work presented here demonstrates the applicability of the tool in the study of different combinations of 2 different fenestration systems, one consisting of a standard clear double pane glazing and the other of a LRCFS, previously developed and tested by the author of this dissertation in a research done in collaboration with others (Santos, Leitão and Caldas, 2018). The research tests the different combinations of fenestration in a simple scene composed of a common office space with two windows, one facing south and the other west.

6.3.1 Methods

The development and testing of Strategy D entails three parts: (i) use annual E_V data to detect glare events; (ii) develop and implement an heuristic that spatially maps glare potential and queries E_V data to find POV/HOY pairs to conduct full DGP simulations; and (iii) apply the resulting tool in a case study to face validate the proposed approach. The following summarizes the methods used in each part.

Finding an Ev threshold to detect potential glare events

A parametric analysis tested different E_V values to find a robust threshold ($E_{V,Thr}$) that detects potential glare events. Using the results of similar work that attempts to correlate E_V and DGP (Wienold and Christoffersen, 2006; Giovannini et al., 2018), the tested values for $E_{V,Thr}$ range from 2000 to 3500 lux in increments of 50 lux ($E_{V,Thr} \in \mathbb{N}$: {2000,2050,…,3500}). Although the results reported by Giovannini et al. (2018) use a higher $E_{V,Trh}$, the proposed range starts at 2000 lux, based on the empirical work that led to the formulation DGP metric (Wienold and Christoffersen, 2005, 2006). The laboratory human subject experiment conducted in that study found a reasonable linear correlation between E_V and percentage of people disturbed by glare ($R^2 = 0.77$). The same research also showed that as E_V increases, the error of using to predict visual discomfort levels also

increases. Thus, and in contrast to the work of Giovannini et al. (2018), this work uses E_V as a binary marker to identify if a specific POV/HOY pair is susceptible to glare.

The parametric analysis compares different E_V values against full annual DGP results of three POVs in a south-facing small office room. This comparison uses Typical Meteorological Year (TMY) data of three locations that represent different annual sky trends: (i) Phoenix, AZ, USA (33.45º N, 112º W) – a tendentially clear annual sky; (ii) London, UK (51.15º N, 0.18º E) – a location dominated by overcast skies; (iii) Oakland, CA, USA (37.72º N, 122º W) – a good example of an annual mixed sky. The hourly calculation of the *sky clearness index* (ε) supported the selection of these locations. Perez et al. (Perez et al., 1990) define eight ε bins that range from a totally overcast (bin 1) to a completely clear sky (bin 8). Figure 6-1 presents an ε annual hourly heatmap for each location paired with the relative frequency of each ε bin.

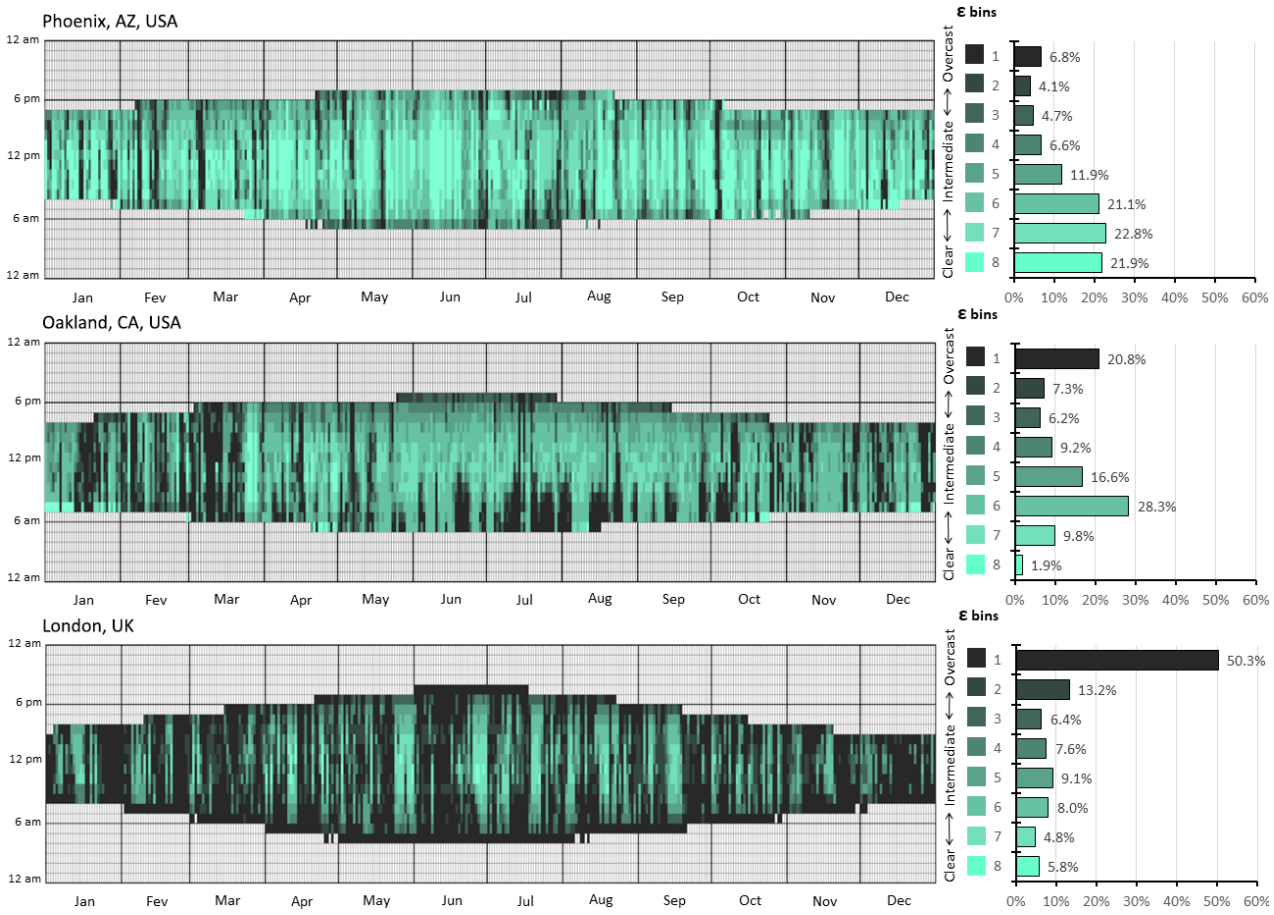

Figure 6-1. Annual sky clearness index, ε, for Phoenix, AZ, USA (top), Oakland, CA, USA (middle), and London, UK (bottom).

Figure 6-1 shows that clear skies dominate Phoenix since the ε bins 6 to 8 represent ≈ 66% of the daytime hours. In London, the bins 1 to 3 represent ≈ 70% of the hourly skies, making this location a good representative of a typical annual overcast sky. In Oakland, the ε bin 6, an intermediate to clear sky condition, yields the highest frequency (28.3%), immediately followed by the overcast condition (bin 1 – 20.8%). The clearer sky conditions (bins 7 to 8) report ≈ 12% of the daylit hours

while intermediate conditions (bin 3 to 6) ≈ 60%. Considering this variability, Oakland is an adequate location to represent an annual mixed sky condition.

Figure 6-2 and Table 6-2 shows the geometry and the optical surface properties of the room model used in this parametric analysis. The room represents a generic space of an enclosed office that is 5 m large, 7 m deep, and 2.7 m high with a 5 x 1.7 m (width x height) south-facing window placed 1 m above the floor. The glass in the window has an overall Visible Light Transmittance (VLT) of 65 %. Figure 6-2 also shows the location of three representative POVs – POV01, POV02, and POV03 – placed at the average eye height of a seated person, 1.3 m. This basic room layout simplifies the identification of the room's daylit and non-daylit zones. Hence, if we consider the rule-of-thumb that specifies that the depth of the daylit zone of a sidelight room is approximately 1.5 times window head height (Reinhart, 2014; Grondzik and Kwok, 2019), POV01 and POV02 are at the middle of the daylit zone. PV01 is centered relative to the window, while PV02 has an eccentric view of it. POV03 is at the back of the room (6 m from the window) and represents a view outside the daylit zone. The aim of selecting three POVs was to determine how well each $E_{V,Thr}$ captures glare events by considering different daylit zones with different surface area weights in the FOV. The authors also used this particular geometry because they had previously used it in a comparative study of LRCFSs (Santos, Leitão and Caldas, 2018), and consequently had some validated aDGP data on it.

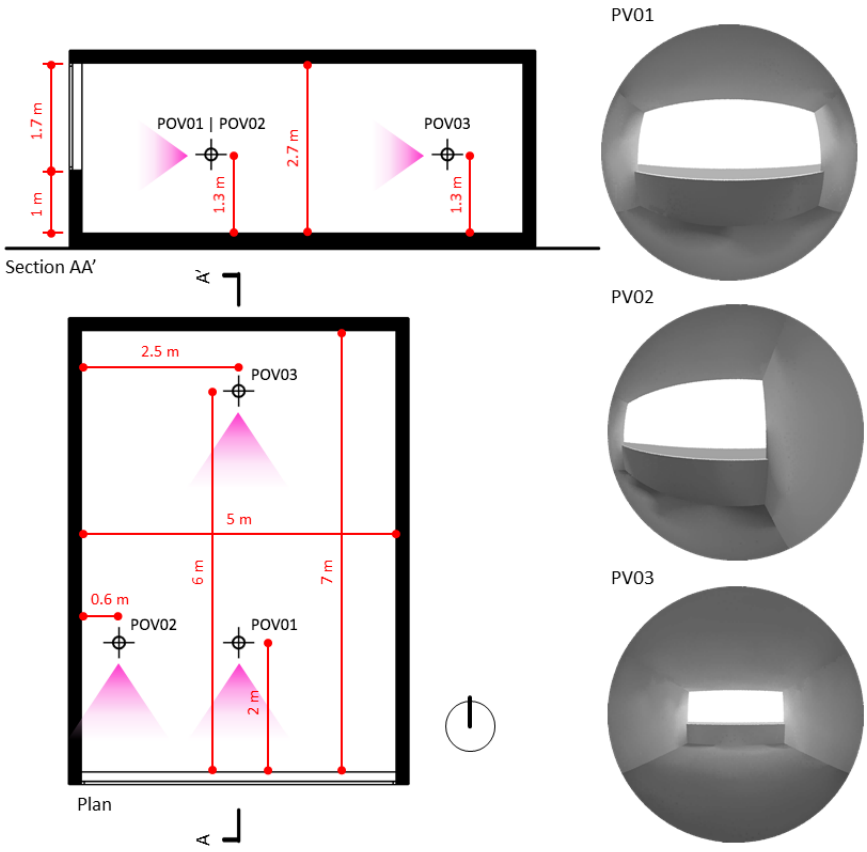

Figure 6-2. The geometry of the room of an enclosed office. Top left: section. Bottom left: plan. Right: pre-visualization of the different views using Radiance's *rvu* routine (Ward, 2004a).

Table 6-2. Optical properties of the different room surfaces used in the $E_{V,Thr}$ assessment experiment.

Surface	Reflectance (%)	Visual Light Transmittance (%)
Outside ground	20	N.A.
Floor	40	N.A.
Ceiling	80	N.A.
Interior Walls	60	N.A.
Exterior Surfaces	35	N.A.
Window glass	N.A.	65

For each POV, $E_{V,Thr}$, and hour of the occupied schedule, the parametric analysis assesses whether the $E_{V,Thr}$ matches the binary condition DGP < 0.35 (no glare event) or DGP (≥ 0.35) calculated using the available aDGP data. Whenever the $E_{V,Thr}$ fails to meet such criteria, the analysis classifies the prediction as a False Positive (FP), i.e., an overestimation, or as a False Negative (FN), i.e., an underestimation. The following functions determine for each hour, *t*, whether an $E_{V,Thr}$ is successful in signaling a glare event or not. Equation (6-2) describes the condition when $E_{V,Thr}$ captures a glare event, equation (6-3) when it reports an FP event, and equation (6-4) when it signals an FN event. The computation of each function always returns a Boolean value.

$$Successful\ estimation\ (t, E_{V,Trh}) = E_V(t) \geq E_{V,Trh} \wedge DGP(t) \geq 0.35 \quad (6\text{-}2)$$

$$FP\left(t, E_{V,Trh}\right) = E_V(t) \geq E_{V,Trh} \wedge DGP(t) < 0.35 \quad (6\text{-}3)$$

$$FN\left(t, E_{V,Trh}\right) = E_V(t) < E_{V,Trh} \wedge DGP(t) \geq 0.35 \quad (6\text{-}4)$$

To test the accuracy of $E_{V,Thr}$ in predicting potential glare events, the parametric analysis uses equation (6-5) to report the percentage of the hourly failed predictions (FP + FN) relative to the total number of hours that reported glare.

$$\%\ of\ failed\ predictions\ \left(E_{V,Trh}\right) = \frac{\sum_{t=1}^{n}(FP(t, E_{V,Trh}) + FN(t, E_{V,Trh}))}{\sum_{t=1}^{n}(DGP(t) \geq 0.35)} \times 100\% \quad (6\text{-}5)$$

The goal is to identify the $E_{V,Thr}$ that minimizes equation (6-5). The sensitivity analysis that supports the determination of the $E_{V,Thr}$ assumes an acceptability threshold for error predictions on an average of 10%. In this way, the adopted $E_{V,Thr}$ would be within the 90% interval of confidence on average.

Strategy description and implementation

The proposed strategy encompasses three phases: simulation, data post-processing, and visualization and querying. Each phase entails several tasks, detailed below.

Phase I – Simulation: initially, the user describes a Radiance scene, including geometry, materials, an analysis sensor grid, and provides TMY data. For each sensor, the implemented heuristic generates an *n* ($n \in \mathbb{N}$: {1, 2, …, 8}) cardinal-based POV, and conducts an annual E_V simulation for each POV.

Phase II - Data post-processing: using $E_{V,Thr}$, the approach begins to process the hourly E_V data of each POV by labeling it as susceptible ($E_V(t) \geq E_{V,Thr}$) or non-susceptible to glare ($E_V(t) < E_{V,Thr}$). Then the procedure calculates the frequency of events susceptible to glare.

Phase III - Visualization and querying: having collected and labeled the E_V data of each POV, the tool spatially maps the glare potential over the sensor grid. The tool generates a radar graph for each sensor that displays the frequencies of potential glare events in each POV for a given analysis period. By default, this period corresponds to the entire year, but the user can set it to monthly or seasonally intervals.

The resulting visualization indicates which POVs are more susceptible to glare. Figure 6-3 describes the visualization output for a sensor. Each radial line corresponds to a POV. The four concentric rings indicate different percentages of the annual daylit hours (i.e., the total number of hours when the sun is up), ranging from 0% (center) to 100% (circumference ring) in incremental steps of 25%. The colored polygon reports the glare potential. The position of the intersection of the polygon with each POV line measures the number of hours that yield glare potential normalized as a percentage of the total number of daylit hours.

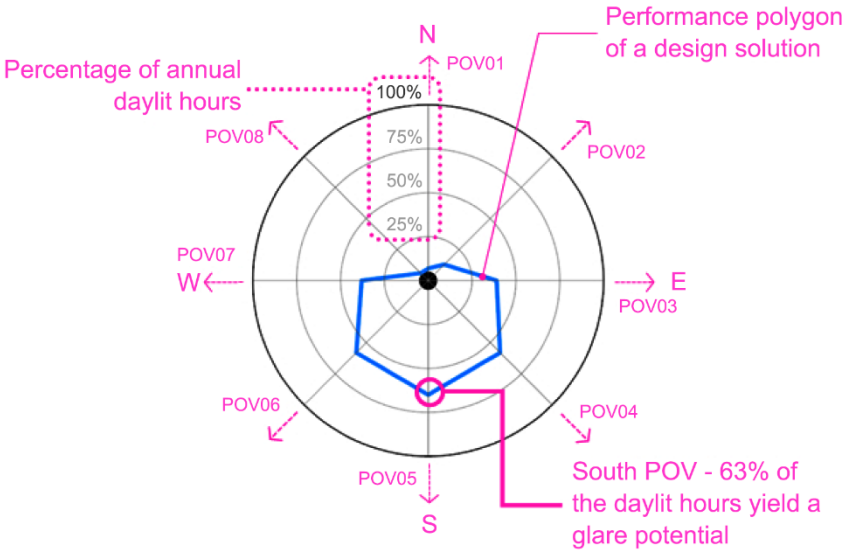

Figure 6-3. Guide to interpret the radar graph output of a given sensor.

Although the user can visualize and query the data of each sensor, the modeling strategy automatically selects the POVs with a frequency whose deviation is within +/- 10% of the maximum frequency. Finally, in each sensor of the analysis grid, the user can select any of the eight POVs to obtain feedback about the period that yields a higher glare potential. Once more, for each selected POV, the strategy heuristic approach automatically identifies the HOY in order to conduct a full point-in-time DGP simulation by finding the hour that yields the highest E_V of the largest set of consecutive pairs day/hour that are susceptible to glare.

Strategy D was computationally implemented in the Rhino+Grasshopper environment as a daylighting analysis tool using the Python programming language. The resulting digital tool uses Radiance's 3-phase method (McNeil and Lee, 2013) to simulate annual E_V. The 3-phase method provides bi-directional raytracing capabilities to Radiance backward raytracing engine, thus

enabling the accurate simulation of highly specular scenes, caustic light effects, and complex fenestration systems (see chapter 2, section 2.2.2 - *Daylight simulation in buildings using physical (unbiased) approaches*). The point-in-time DGP simulations for the selected POV/HOY pairs use Radiance's *rpict* (Ward, 1999) routine to produce the HDR images and *evalglare* to calculate DGP. The system uses Radiance's *gendaylit* (Delaunay, Wienold and Sprenger, 1994) subprogram to generate an accurate Perez all-weather sky given a specific hour, location, and TMY data, thus ensuring that the resulting HDR image reflects the sky condition considered in E_V calculations. Figure 6-4 summarizes the proposed approach modeling phases, and subsequent steps, in a flow diagram.

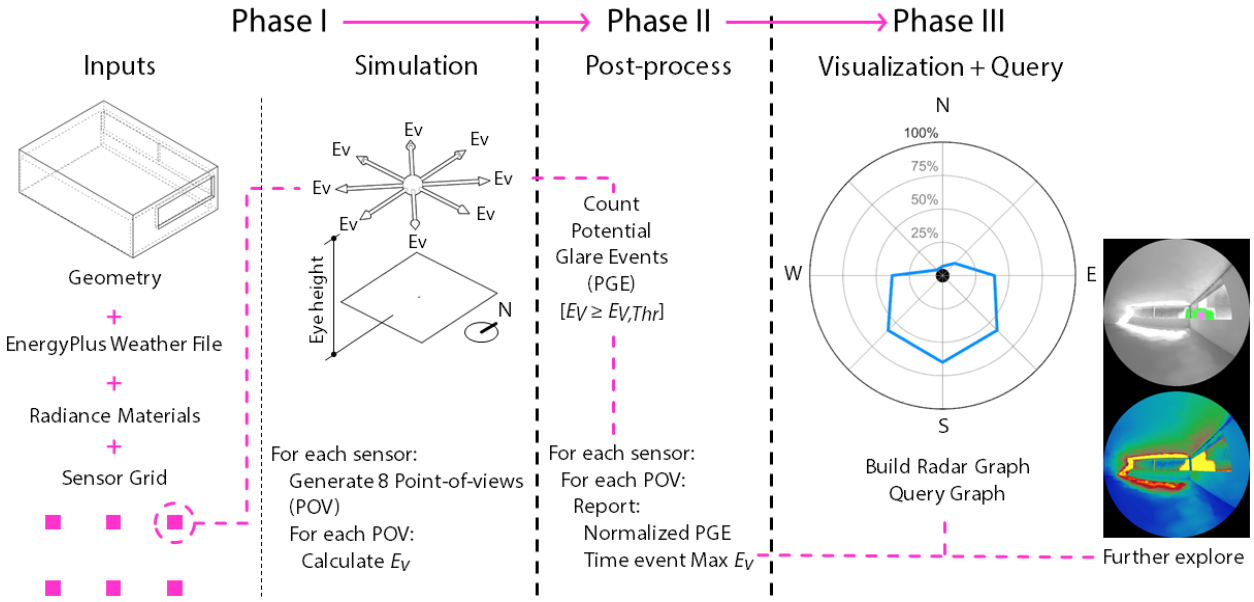

Figure 6-4. Proposed modeling approach to assess annual glare potential using vertical illuminance simulated at eye level (E_V) data.

Design of Experiments – application to a case study

The test and face validation of the proposed modeling strategy consisted of applying the tool to analyze the annual glare potential of an architectural space. To that end, the authors 3D-modeled a hypothetical representative office room of a commercial building in a typical 5 x 7.5 m structural grid. The 9.8 x 7.2 x 2.7 m (width x length x height) room faces both south and west. Compared with the model used in the determination of the $E_{V,Thr}$, the case study model introduces more complexity by adding a challenging window in the FOV, the West window.

After determining the $E_{V,Thr}$ the goal of the case study experiment was to test how the proposed approach copes with different daylight contributions from multiple orientations, a common scenario in design practice. The south and the west façade have windows that start at 1.1 m height and end at the ceiling. A six-point 4.2 x 3.2 x 1.5 m grid defines the spatial location of the different POVs. This grid is centered relative to the room, and its spacing is representative of a typical office layout. The tool generates 8 POVs per point, each one facing a different cardinal direction. The optical properties of the opaque surfaces of the case study model are the same used in the sensitivity analysis (see Table 6-2). Figure 6-5 shows two axonometric views, SE and NW of the

model, whereas Figure 6-6 presents the sensor grid overlaid over a hypothetical office furniture layout marked with a dashed line.

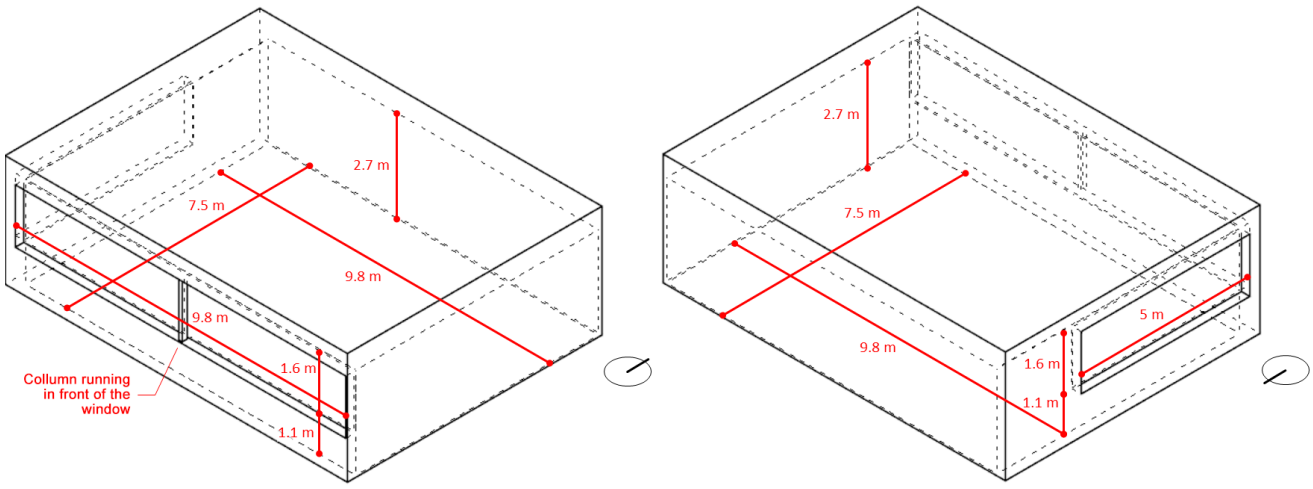

Figure 6-5. Axonometric views of the 3D model of a typical office room used in the experiments that test the proposed modeling strategy. Left: Southeast axonometry. Right: Northwest axonometry.

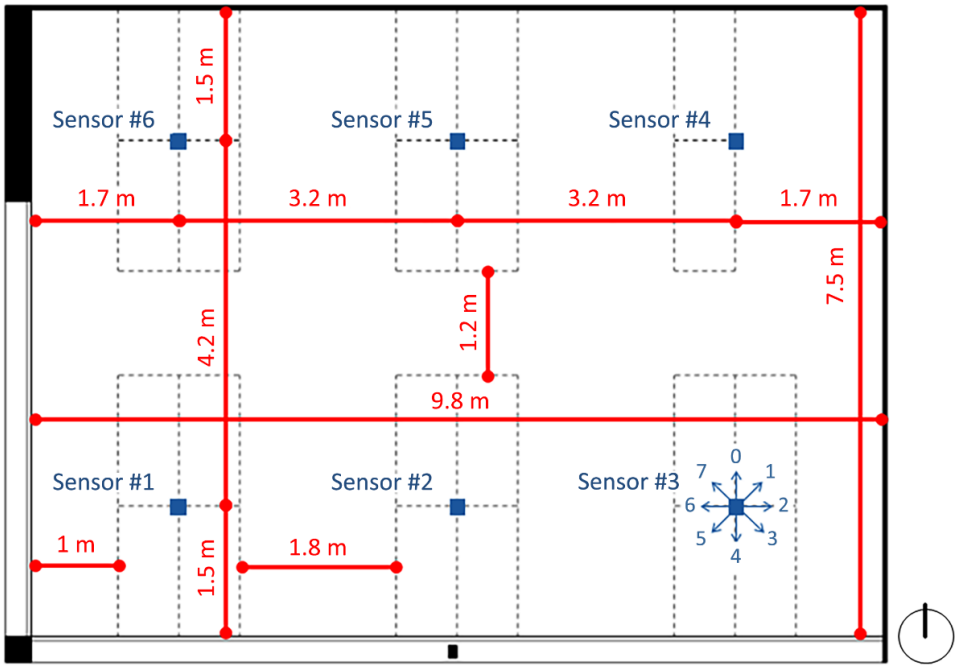

Figure 6-6. Plan of the typical office room used in the experiments that test the proposed modeling strategy. The sensor grid (blue) is placed over a hypothetical room layout (dashed line). Sensor 3 (bottom right) illustrates the 8 POV directions generated in each sensor.

The experiment compares three different fenestration assembly schemes in the model described above at the three locations considered in the determination of $E_{V,Trh}$ – Phoenix, AZ, USA; London, UK; Oakland, CA, USA. The first fenestration scheme (Scheme #1) defines a baseline case. It consists of a double-clear glazing with a VLT of 65% applied in both windows. Scheme #2 combines the double-clear glazing with a glazing assembly composed of a macroscopic LRCFS

optimized to maximize Daylight Factor (DF) levels. The west window received the double-clear glazing assembly, whereas the south window received the LRCFS. The LRCFS is a set of equally spaced highly specular/reflective blinds (99.3% of reflectance) placed between two clear glass panes (VLT of 65%) developed and tested in a comparative study conducted by the dissertation's author in collaboration with other researchers (Santos, Leitão and Caldas, 2018). Figure 6-7 depicts the in-between glass layers light redirecting system. Santos, Leitão, and Caldas (2018) provides more detail about the LRCFS. The third fenestration scheme (Scheme #3) applies the LRCFS to both windows.

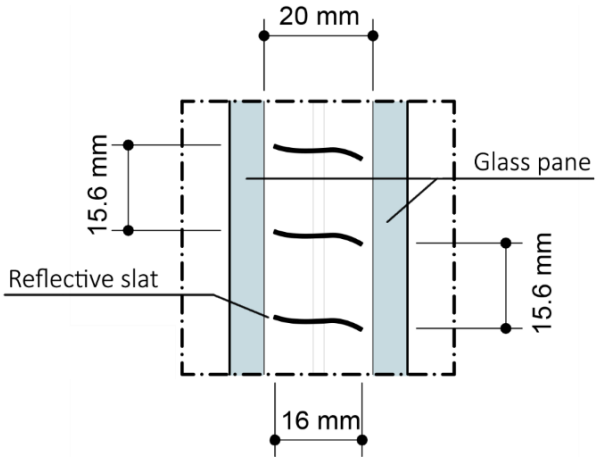

Figure 6-7. Sectional detail of the LRCFS used in the case study application and previously optimized in Santos, Leitão, and Caldas (2018).

The purpose of using different combinations of clear glazing assemblies with LRCFS is to test the flexibility of the proposed modeling strategy in handling both simple and complex fenestration systems. Clear glazing assemblies are often used at the early-stage design process. In contrast, the deployment of CFS are more common in comparative studies conducted by designers to support the selection or development of specific facade products. The use of CFS might significantly impact the overall image of a building. Thus, although the CFS analysis usually occurs at later design phases, it is not unusual to undertake preliminary studies involving CFS at the early stages of the design process.

For each scheme, the proposed tool runs a climate-based annual E_V simulation, visualizes the frequency of events susceptible to glare in each POV, and selects the critical POV/HOY pairs for the different rows of sensors separately, to then run a full DGP analysis. To better compare the results, the tool overlays the resulting radar graphs of the different fenestration schemes.

The simulation parameters used in the 3-phase method annual simulations closely follow the LM-83 standard recommendations (IESNA, 2012). The list below presents the simulation parameters:

- Ambient resolution (-ab) – 6 ambient bounces to guarantee enough accuracy without a substantial computational burden using the 3-phase method.
- Ambient resolution (-ar) – 300, a reasonable number for a point grid calculation with Radiance's subroutine *rtrace* (Ward, 1997) and for a model of that size.

- Ambient divisions (-ad) – 1000, a fair amount of ambient division for a sensor-based simulation.
- Ambient sampling (-as) – 500, typically half of -ad (Ward, 1999).
- Ambient accuracy (-aa) – 0.1.
- Direct threshold (-dt) – 0, to test all light source sampling both in global illumination and shadow calculation (Ward, 1999).

In the case of the DGP HDR-based simulations, Radiance parameters are well above the recommendations provided by manufacturers of commercial LRCFSs (LightLouver LLC, 2010). They keep the same parameter values used in the sensor-based simulation except the -ad parameter, which is set at 50,000. This -ad value ensures an adequate number of ambient divisions to accurately capture specular reflections and inter-reflections originated by the LRCFS (McNeil, 2010).

6.4 Results

The following sections present in detail the parametric analysis results, conducted to determine an appropriate vertical eye illuminance threshold ($E_{V,Trh}$) to detect glare events, as well as, to test the application of the tool to the case study described in section 6.3.1, Design of Experiments – application to a case study.

6.4.1 Determination of the E_V threshold ($E_{V,Trh}$)

Table 6-3 and Figure 6-8 presents the results of the sensitivity analysis that tested the accuracy of different $E_{V,Trh}$ in predicting glare events (DGP ≥ 0.35). Both Table 6-4 data and the scatter plot of Figure 6-8 map the percentage of failed events of each $E_{V,Trh}$ relative to the total number of hours that reported glare (DGP ≥ 0.35).

Table 6-3. Percentage of hours, relative to the total number of glare events (DGP ≥ 0.35), when $E_{V,Trh}$ failed to predict a glare event (DGP ≥ 0.35) either by reporting an FN or an FP. The selected $E_{V,Thr}$ (2300 lux) is highlighted in bold over a gray background.

	Phoenix, AZ, USA Failed predictions [%]			Oakland, CA, USA Failed predictions [%]			London, UK Failed predictions [%]			
$E_{V,Thr}$ [lux]	POV01	POV02	POV03	POV01	POV02	POV03	POV01	POV02	POV03	Average failed predictions [%]
2000	7.7	12.0	26.7	9.4	12.2	16.4	16.5	16.9	5.9	13.7
2050	7.4	11.8	23.0	8.6	11.7	12.6	15.8	15.3	4.1	12.3
2100	6.8	11.3	19.6	7.8	11.2	9.4	15.0	14.3	3.0	10.9
2150	6.3	10.7	15.9	6.7	10.5	6.8	14.0	13.0	3.2	9.7
2200	5.8	10.0	11.7	6.3	9.6	4.7	12.2	12.0	4.7	8.6
2250	5.2	9.5	8.6	5.9	8.7	4.5	11.0	11.4	6.9	8.0
2300	**4.8**	**8.7**	**7.3**	**5.5**	**8.1**	**5.0**	**9.9**	**10.6**	**9.2**	**7.7**
2350	4.4	8.2	8.2	5.3	7.4	5.9	9.1	9.2	13.7	7.9
2400	4.0	7.6	9.9	4.6	6.5	8.9	8.2	8.0	15.9	8.2
2450	3.6	7.0	12.5	4.0	5.9	13.2	7.2	7.4	17.7	8.7
2500	3.2	6.4	16.0	3.6	5.2	16.3	6.0	6.4	20.9	9.3
2550	2.9	5.5	17.8	3.3	4.4	19.7	4.9	5.2	24.2	9.8
2600	2.7	4.9	20.6	2.8	3.5	23.4	3.8	4.4	26.3	10.2

Table continues in the following page.

Table 6-3. Percentage of hours, relative to the total number of glare events (DGP ≥ 0.35), when $E_{V,Trh}$ failed to predict a glare event (DGP ≥ 0.35) either by reporting an FN or an FP. The selected $E_{V,Thr}$ (2300 lux) is highlighted in bold over a gray background (continued).

	Phoenix, AZ, USA Failed predictions [%]			Oakland, CA, USA Failed predictions [%]			London, UK Failed predictions [%]			
$E_{V,Thr}$ [lux]	POV01	POV02	POV03	POV01	POV02	POV03	POV01	POV02	POV03	Average failed predictions [%]
2650	2.2	4.4	22.5	2.0	2.1	26.7	3.1	3.1	28.0	10.5
2700	2.1	4.0	24.0	1.5	1.6	29.3	2.6	2.1	29.2	10.7
2750	1.8	3.7	26.2	1.0	1.3	31.4	2.1	1.9	31.0	11.1
2800	1.3	3.8	28.7	0.8	1.8	33.8	1.6	2.4	33.0	11.9
2850	1.3	3.8	30.8	0.7	2.3	37.4	0.9	3.1	34.7	12.8
2900	1.3	3.7	32.6	0.6	3.2	40.2	0.6	4.0	36.9	13.7
2950	1.7	4.1	33.8	1.0	3.6	42.6	1.0	4.9	39.0	14.6
3000	2.3	4.6	36.2	1.3	4.0	44.5	1.6	5.7	41.7	15.8
3050	2.9	5.1	38.1	2.0	4.6	45.8	2.3	6.6	44.7	16.9
3100	3.2	5.4	40.0	2.6	5.2	47.1	3.1	7.7	46.9	17.9
3150	3.7	5.9	41.4	3.0	5.6	48.1	4.6	8.5	49.0	18.9
3200	4.2	6.3	42.7	3.5	6.2	49.0	5.5	9.2	50.4	19.7
3250	5.0	6.7	43.9	3.8	7.0	50.0	6.2	10.1	52.0	20.5
3300	5.8	7.2	45.8	4.2	7.7	51.3	7.1	10.9	53.3	21.5
3350	6.5	7.6	47.3	4.7	8.7	52.2	8.2	12.0	55.2	22.5
3400	7.0	8.3	49.3	5.6	9.3	53.1	9.2	12.5	57.1	23.5
3450	7.8	9.1	50.3	6.1	10.6	54.3	9.9	13.1	58.3	24.4
3500	8.3	9.5	51.5	6.7	12.4	55.3	11.4	13.7	60.3	25.5

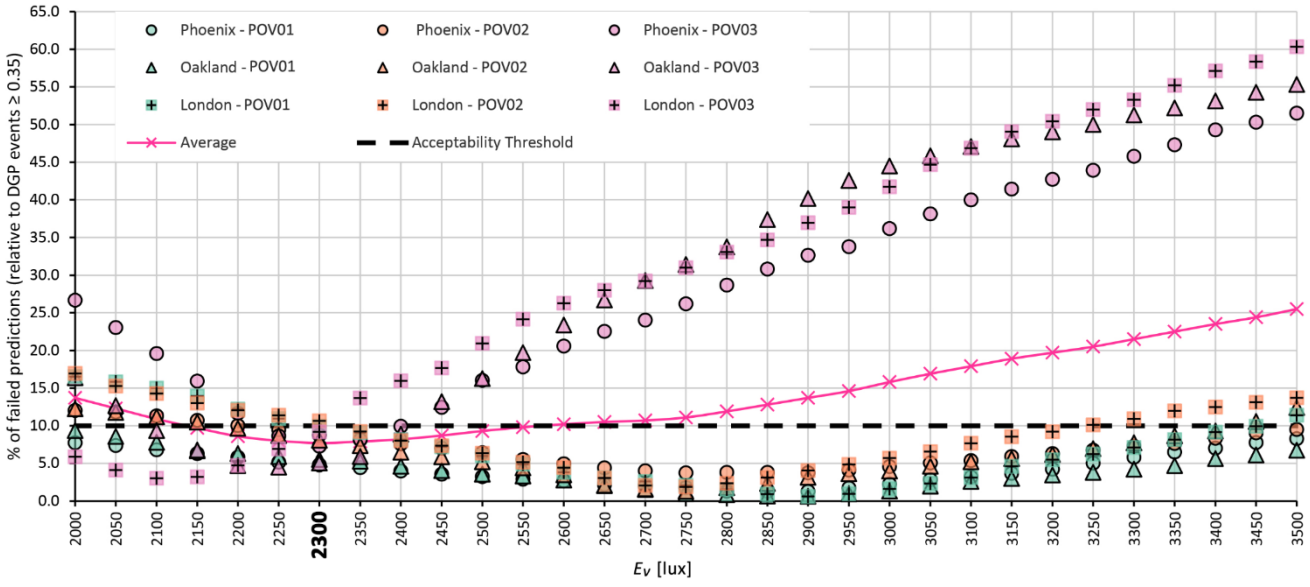

Figure 6-8. Measuring the percentage of failed predictions relative to the DGP events (≥ 0.35) of each $E_{V,Thr}$. The continuous magenta line shows the average error. The black dashed line marks the acceptability error threshold considered in this study (10 %). The adopted $E_{V,Thr}$ is highlighted in bold.

The $E_{V,Thr}$ of 2300 lux is the threshold that reports the minimum of failed predictions on average, 7.7 % in all POVs and locations. The results indicate that higher thresholds ($E_{V,Thr}$ ∈ [2750, 2950 lux]) are more successful in capturing glare events closer to the window (% failed events ∈ [0.6,

4.9]). However, such thresholds fail more often in predicting glare in POVs farther away from the window by frequently signaling FN events. Figure 6-9 illustrates the inability of the best $E_{V,Thr}$ ($E_{V,Thr}$ = 2900 lux) for POV1 and POV2, the POVs closer to the window, in detecting glare events in POV3, the POV located at the back of the room.

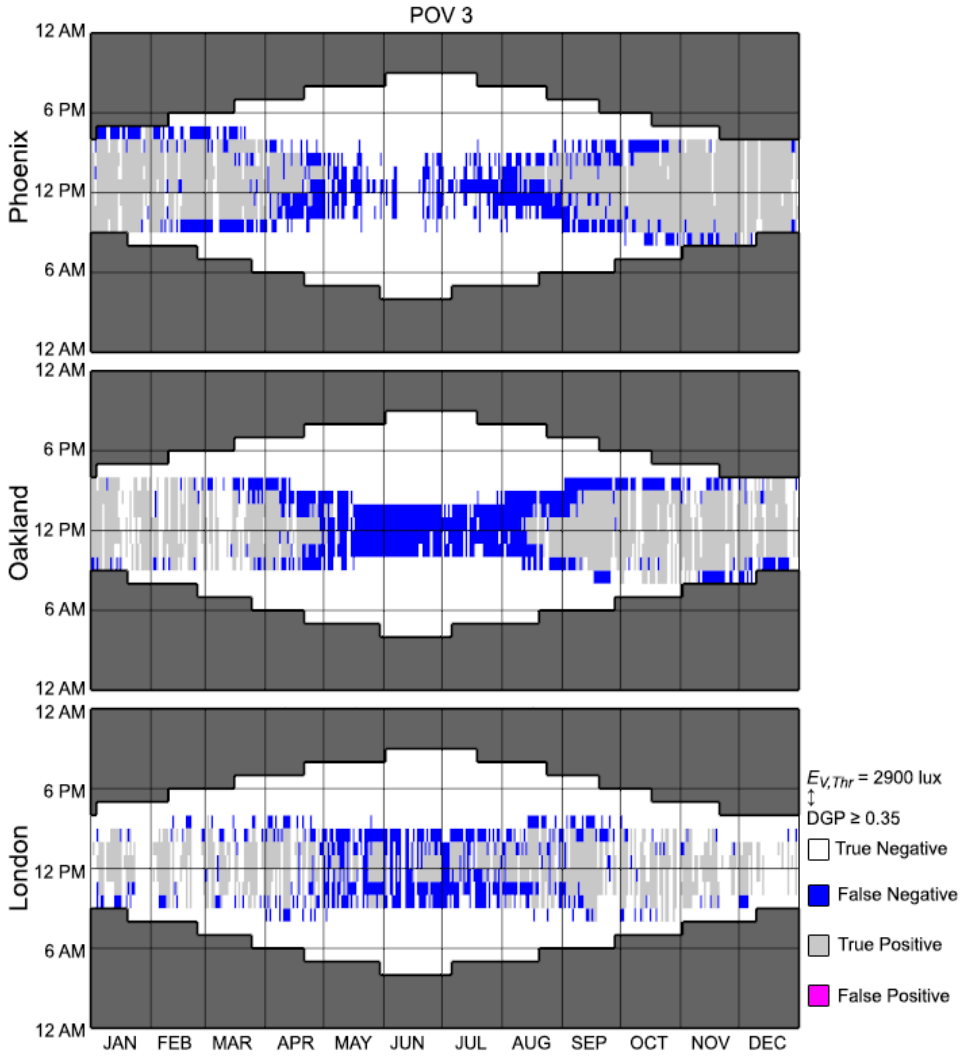

Figure 6-9. Annual hourly heatmap of the performance of the $E_{V,Thr}$ = 2900 lux in detecting glare events in POV03 in Phoenix, AZ, USA (top), Oakland, CA, USA (middle), and London, UK (bottom).

Considering that the goal is to find a single $E_{V,Thr}$ that qualifies any point in space in terms of glare potential, the difference of error trends between different POVs types constrains the selection of a threshold to the 2200 to 2400 lux range ($E_{V,Thr} \in$ [2200, 2400 lux]). Therefore, this work adopted E_V = 2300 lux as the $E_{V,Thr}$ to detect glare events.

Figure 6-10 presents a detailed analysis of the adopted $E_{V,Thr}$ performance at Phoenix, Oakland, and London. If we consider the entire daylit period of the year in each location (4399 hours in Phoenix, 4392 hours in Oakland, and 4400 hours in London), rather than the total number of hours that the aDGP reported a glare event, the percentage of events where $E_{V,Thr}$ failed to predict glare

on average is smaller: 4.4 %. Appendix B breaks down Figure 6-10 heatmaps per location and shows them at a bigger scale to provide more detail. Table 6-4 summarizes the percentage of failed predictions relative to the entire daylit period of the year.

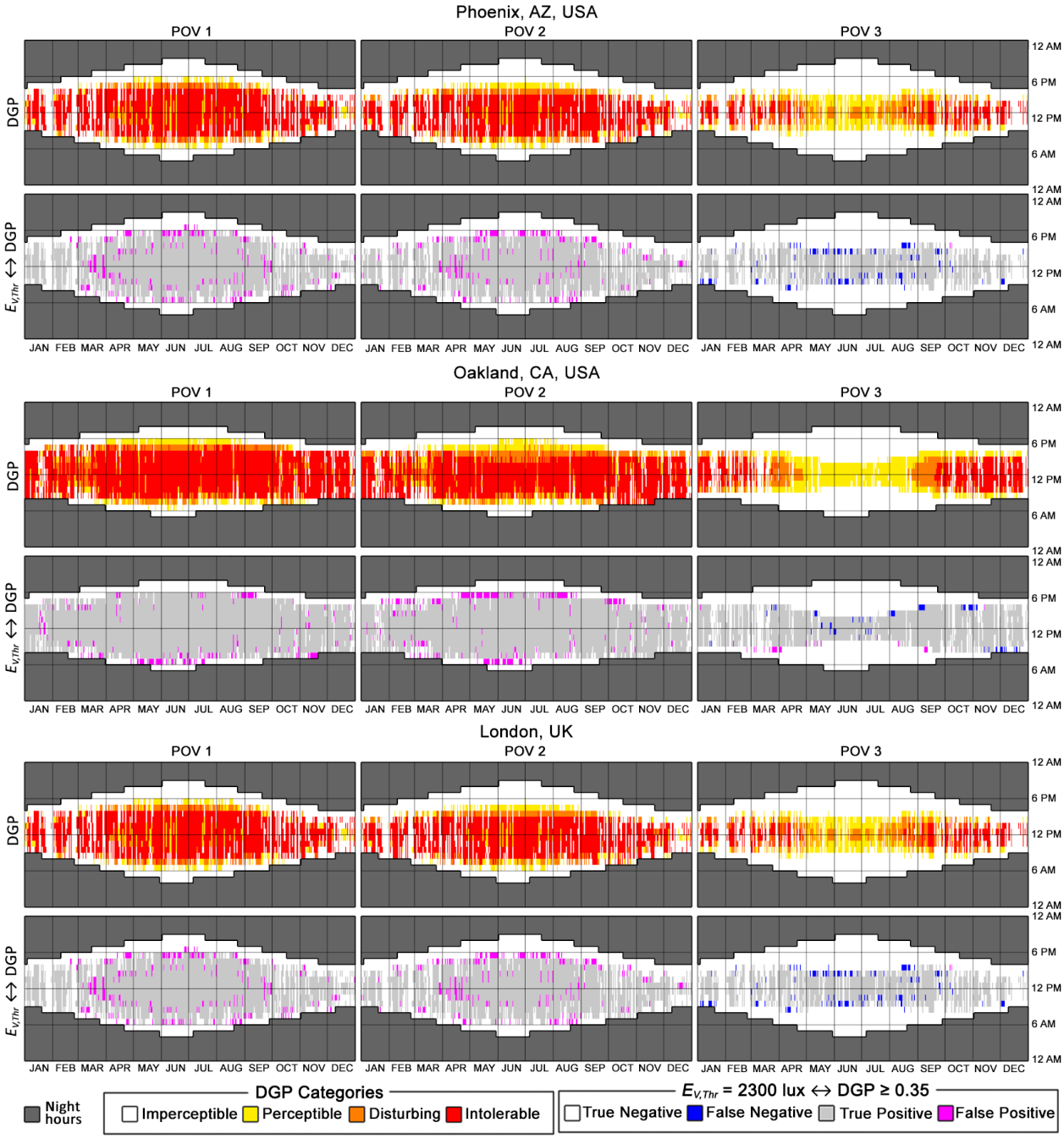

Figure 6-10. Performance of the selected $E_{V,Thr}$ (2300 lux) in detecting glare events in all POVs in Phoenix, AZ, USA (top), Oakland, CA, USA (middle), London, UK (bottom). In each location, the top heatmap visualizes hourly aDGP, while the bottom heatmap maps the failed (FN + FP) and successful hourly events in using $E_{V,Thr}$ = 2300 lux to detect glare events.

Table 6-4. Percentage of failed predictions (FN + FP) of $E_{V,Thr}$ = 2300 lux for each POV, relative to the total number of daylit hours per location.

	Phoenix, AZ, USA Failed predictions [%]	Oakland, CA, USA Failed predictions [%]	London, UK Failed predictions [%]
POV01	3.8	4.1	5.6
POV02	6.5	5.6	5.5
POV03	3.2	2.1	3.0
Average - Failed predictions [%]			4.4

6.4.2 Case study results

Table 6-5 and Figures 6-11 through 6-16 present the results of the application of the proposed modeling strategy to the case study. Figures 6-11 through 6-13 show the visualization output of the proposed computational tool, i.e., the radar graphs per sensor point mapping the frequency of the events susceptible to glare for each POV direction. The frequencies are normalized for the number of daylit hours in each location: 4399 hours in Phoenix, AZ, USA, 4392 hours in Oakland, CA, USA, and 4404 hours in London, UK.

Table 6-5 presents a summary of the relevant information used by the proposed tool in selecting POV/HOY pairs to conduct a full point-in-time DGP simulation. The last row of the table shows the DGP results for each pair POV/HOY selected. Figures 6-14 through 6-16 present the result of using *evalglare* to analyze in detail the selected POV/HOY pairs. The resulting images deliver detailed information about the location of glare sources, the position of the circumsolar region, reflections, and the luminance contrast of the different surfaces.

Table 6-5. Results per sensor of the implemented modeling strategy.

Phoenix, AZ, USA						
	Sensor #2			Sensor #6		
Fenestration Scheme	#1 (Double Clear)	#2 (Mixed)	#3 (Full LRCFS)	#1 (Double Clear)	#2 (Mixed)	#3 (Full LRCFS)
POV [v_x,v_y,v_z]	[0, -1, 0]	[0, -1, 0]	[0, -1, 0]	[0, -1, 0]	[0, -1, 0]	[0, -1, 0]
Date [m/d/h]	1/5/3PM	12/30/2PM	12/30/2PM	11/27/2PM	12/30/2PM	12/30/2PM
E_V [lux]	4057	3982	3752	8008	8468	7965
Frequency [%] ($E_V \geq E_{V,Thr}$)	87%	82%	76%	76%	75%	73%
DGP	1	1	1	0.84	0.81	0.65

Table continues in the following page,

Table 6-5. Results per sensor of the implemented modeling strategy (continued).

Oakland, CA, USA						
	Sensor #2			Sensor #6		
Fenestration Scheme	#1 (Double Clear)	#2 (Mixed)	#3 (Full LRCFS)	#1 (Double Clear)	#2 (Mixed)	#3 (Full LRCFS)
POV [v_x,v_y,v_z]	[0,-1,0]	[0,-1,0]	[0,-1,0]	[0,-1,0]	[0,-1,0]	[0,-1,0]
Date [m/d/h]	11/19/10AM	12/22/2PM	12/22/2PM	12/22/12PM	8/1/1PM	8/1/1PM
E_V [lux]	4339	4755	4302	9974	7858	7828
Frequency [%] ($E_V \geq E_{V,Thr}$)	84%	78%	77%	71%	68%	64%
DGP	1	1	1	0.36	0.44	0.45
London, UK						
	Sensor #2			Sensor #6		
Fenestration Scheme	#1 (Double Clear)	#2 (Mixed)	#3 (Full LRCFS)	#1 (Double Clear)	#2 (Mixed)	#3 (Full LRCFS)
POV [v_x,v_y,v_z]	[0, -1, 0]	[0, -1, 0]	[0, -1, 0]	[0, -1, 0]	[0, -1, 0]	[0, -1, 0]
Date [m/d/h]	1/15/1PM	1/7/2PM	1/21/12PM	1/12/3PM	1/12/3PM	1/12/3PM
E_V [lux]	10403	6986	7878	18599	15538	16840
Frequency [%] ($E_V \geq E_{V,Thr}$)	69%	61%	61%	51%	49%	47%
DGP	1	1	1	1	1	1

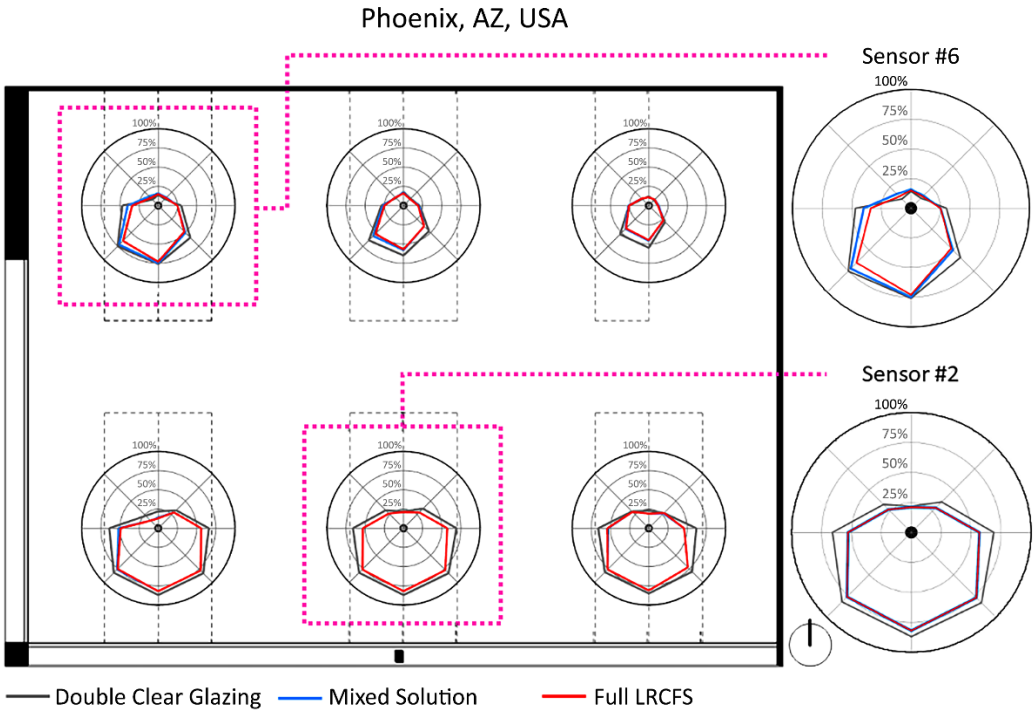

Figure 6-11. Visualization output of the proposed strategy in analyzing the several fenestration schemes applied to the case study model using an annual all-weather Perez sky calculated for Phoenix, AZ, USA.

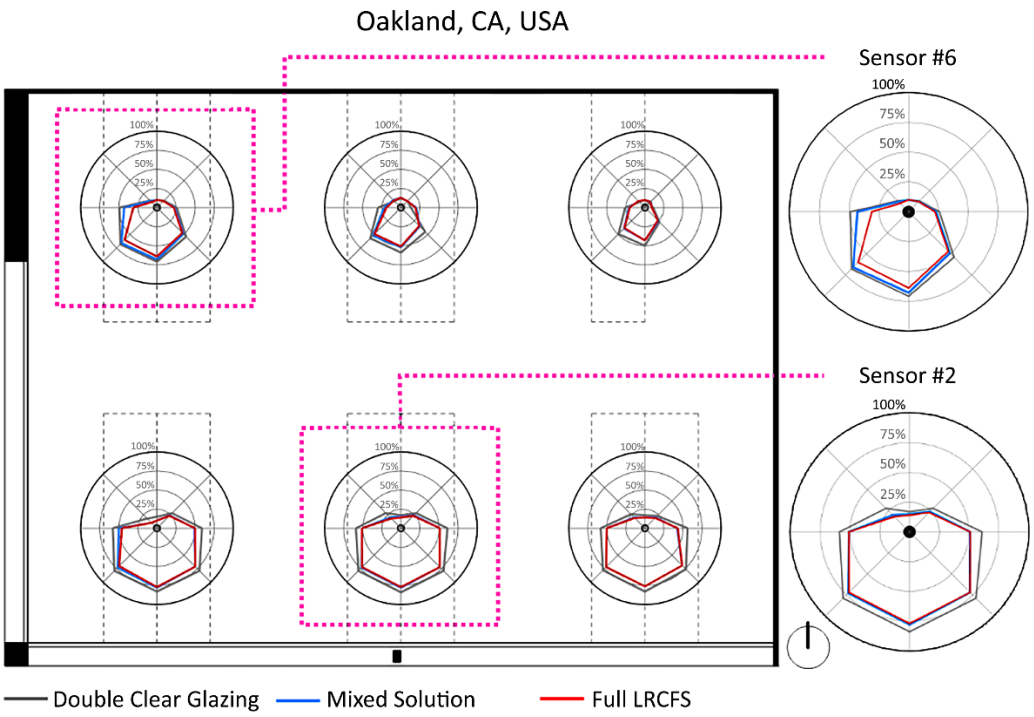

Figure 6-12. Visualization output of the proposed strategy in analyzing the several fenestration schemes applied to the case study model using an annual all-weather Perez sky calculated for Oakland, CA, USA.

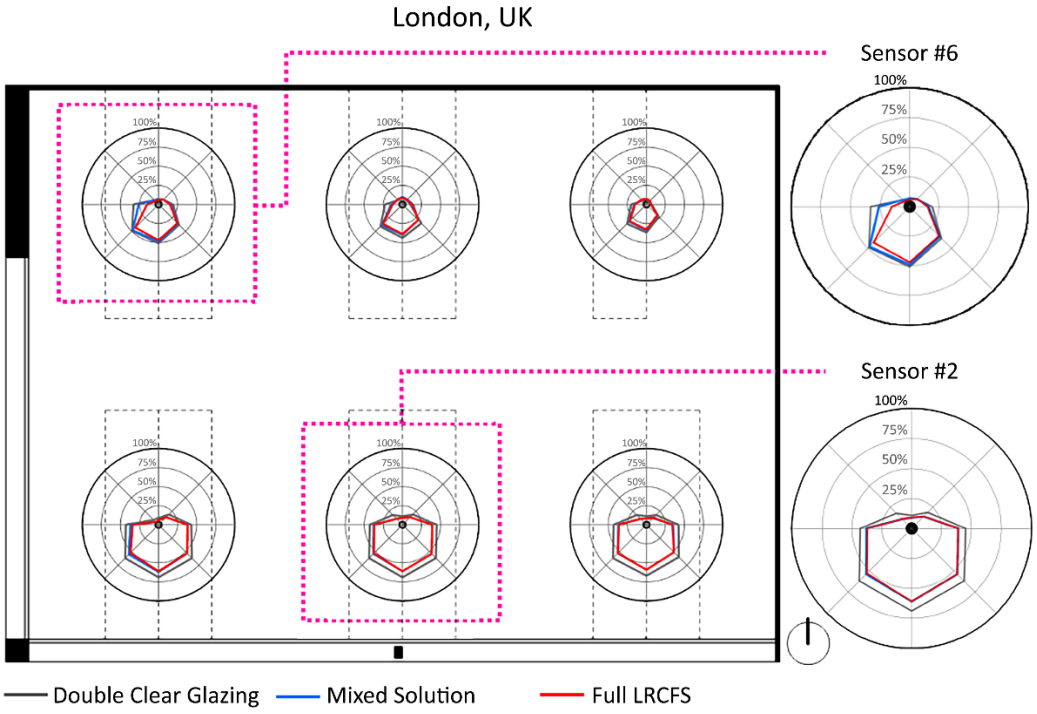

Figure 6-13. Visualization output of the proposed strategy in analyzing the several fenestration schemes applied to the case study model using an annual all-weather Perez sky calculated for London, UK.

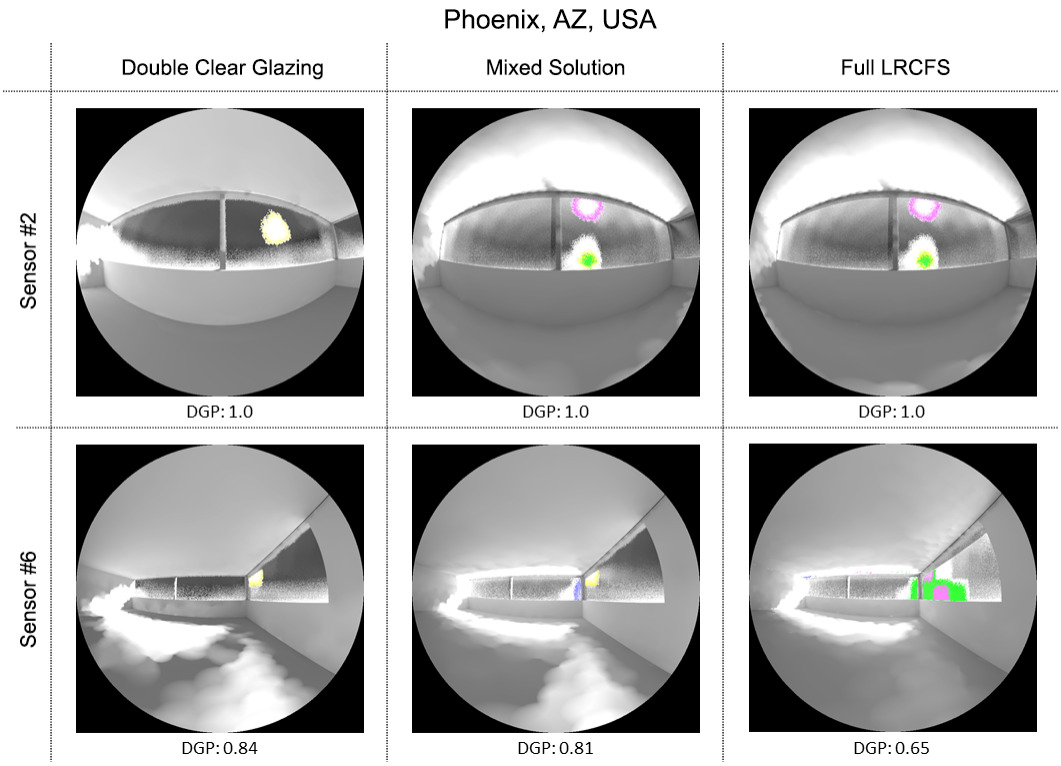

Figure 6-14. Full DGP analysis for the POV/HOY pairs selected by the proposed tool for Phoenix, AZ, USA. The different colored areas in the images represent potential glare sources in the FOV found by *evalglare*.

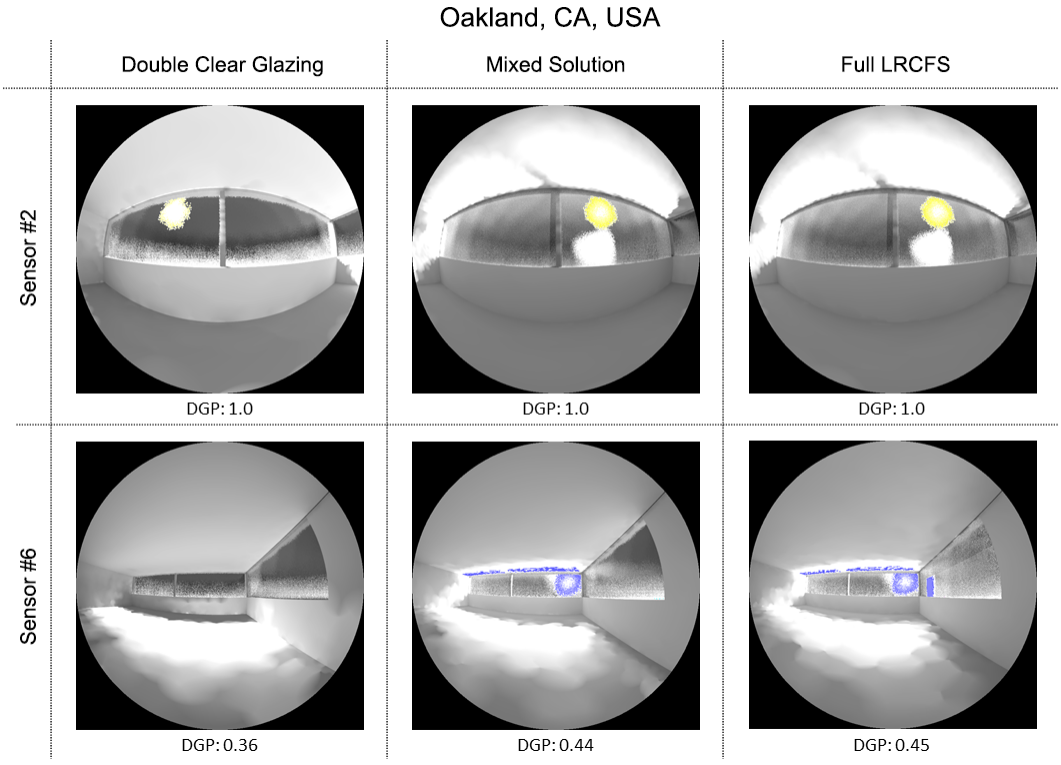

Figure 6-15. Full DGP analysis for the POV/HOY pairs selected by the proposed tool for Oakland, CA, USA. The different colored areas in the images represent potential glare sources in the FOV found by *evalglare*.

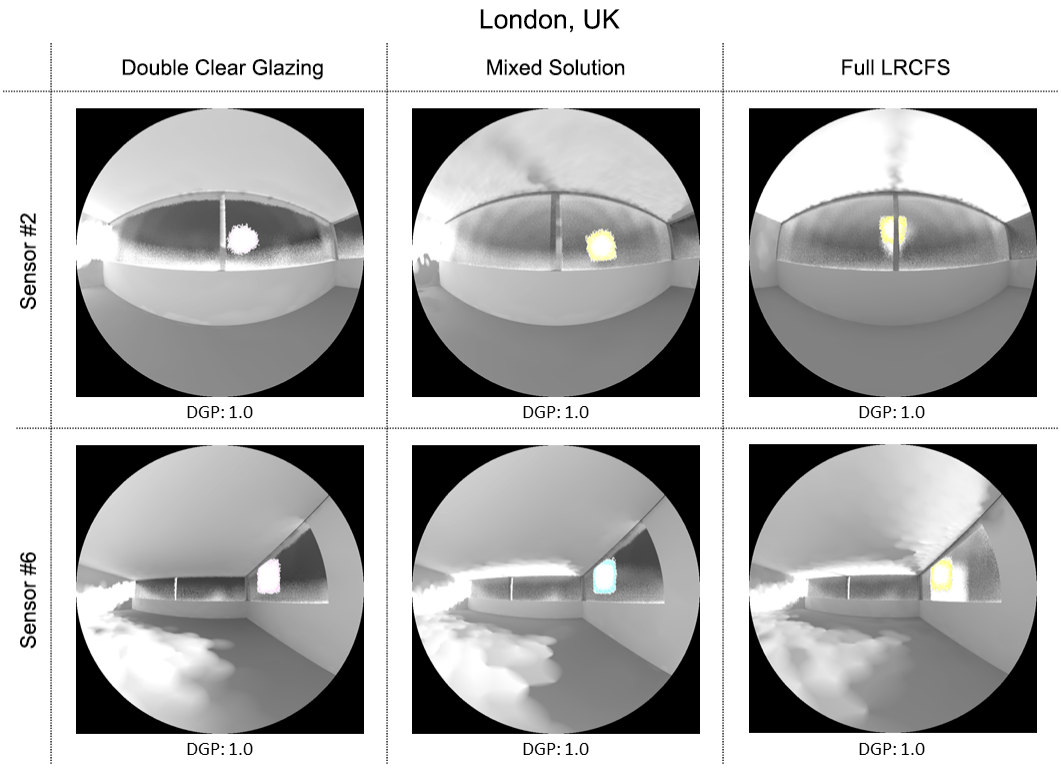

Figure 6-16. Full DGP analysis for the POV/HOY pairs selected by the proposed tool for London, UK, USA. The different colored areas in the images represent potential glare sources in the FOV found by *evalglare*.

6.5 Discussion

The 2300 lux threshold that emerged from the $E_{V,Thr}$ parametric study diverges from the one adopted in Giovaninni et al. (2018) to estimate perceptible glare (DGP ≥ 0.35), which was approximately 3250 lux. Although the goals and assumptions of the two works do not exactly match, the difference between E_V thresholds results from the fact that this work considered POVs that are both inside and outside of the daylit zone, whereas Giovaninni et al. (2018) only used POVs placed within the daylit zone. The results of this experiment show that the success of an E_V threshold depends on spatial location. As Table 6-3 and Figure 6-8 demonstrate, for the two daylit zone POVs, POV01 and POV02, E_V thresholds that are closer to 3000 lux (∈ [2750, 2950 lux]) are fairly accurate in detecting glare events. Their percentage of failed events oscillates in the range between 0.6% and 4.9 % (% of failed events ∈ [0.6, 4.9]). However, these thresholds show a high number of failed predictions in POVs located farther away from the window; locations where DGP is more sensitive to surface luminance contrast due to the lower E_V and the size of glare sources in the viewer's FOV is smaller. In such cases, higher $E_{V,Thr}$ tend to detect more FN events.

Figure 6-8 reveals this trend by showing a lower error variation in POVs within the daylit zone compared with the one reported in PV03, illustrated by the abrupt slope that begins around $E_{V,Thr}$ > 2400 lux. Figure 6-9 confirms that higher vertical eye illuminance thresholds, which are suitable to POVs placed closer to fenestrations, are not effective in signaling glare events in POVs placed outside the daylit zone. The figure shows that the best $E_{V,Thr}$ ($E_{V,Thr}$ = 2900 lux) in the POVs closer to the window, POV01 and POV02, labeled several HOY as FN

($E_V(HOY) < E_{V,Thr} \wedge$ DGP(HOY) ≥ 0.35) in POV03, particularly in hours that bear low sun angles. This analysis supported the adoption of 2300 lux as the $E_{V,Thr}$ for signaling potential glare events, since it yields the minimum of failed predictions on average, considering all locations and POVs. Table 6-4 and Figure 6-10 attest to the good performance of the selected $E_{V,Thr}$, by reporting at the most 6.5% of failed predictions at POV01 under the annual all-weather Perez sky model of Phoenix, AZ.

Although the results support the adoption of a single $E_{V,Thr}$ in the study of glare in side-lit rooms, they also suggest that an adaptive $E_{V,Thr}$, determined in function of the distance between the POV to the main glare sources, would be a suitable approach, particularly in deep and complex plans. Such an adaptive threshold should be higher closer to the windows and lower outside the daylit zone since E_V sensitivity of DGP is higher in the former and lower in the latter. The future development and generalization of an adaptive $E_{V,Thr}$ would require the study of more complex building plans, orientations, and fenestration types.

The proposed modeling strategy used the selected $E_{V,Thr}$ to map glare potential and identify critical events in the room described in Figures 6-5 and 6-6 at three locations that represent different types of annual skies: a location dominated by clear skies, another by mixed skies, and another by overcast skies.

When compared with Phoenix, London has a lower frequency of potential glare events. However, Table 6-5 and Figure 6-13 show that the selected events for London yield both a higher DGP and vertical illuminance levels. The analysis of Figure 13 HDR images indicates that one of the reasons for higher E_V and DGP values is the higher latitude and a more frequent presence of the circumsolar region in the FOV, particularly on the POVs that look at the South quadrant. Oakland results follow a similar trend to Phoenix but with lower DGP values. Sensor #6 reports the lowest DGP value of the select pair POV/HOY – the 22nd of December, 2 pm – 0.36, a value close to the threshold that separates perceptible from imperceptible glare, DGP < 0.35.

Considering the geometry of the model and the sensor grid layout, Figure 13 presents an expected pattern: the south window is the largest daylighting contributor, the northeast corner is the darkest because it is the less exposed, and sensor #6 has an asymmetric distribution of potential glare events due to the impact of the west window. Although sensors #1 and #2 show similar results, the system selected the south direction of the latter because it was the most consistent POV of the three locations, i.e., although all locations reported the same frequency of potential glare events, sensor #2 reported events with higher E_V. The corner column slightly shades sensor #1. In the second row of sensors, the system selected the south direction of sensor #6 as the representative POV because it yields both the higher frequency of potential glare events and the highest E_V. Although the southwest POV of sensor #2 also shows a high glare potential, the size of the south window in the FOV is responsible for making the south POV the most critical. The radar graphs also show the shading effect of adding an LRCFS to the windows. Both the frequencies and illuminances values are lower when the LRCFS is added to the south window. Nevertheless, adding the LRCFS to the west window did not produce a relevant impact on the frequency of events susceptible to visual discomfort. The main reason for the small impact of adding the LRCFS to the west window is that the LRCFS

configuration resulted from an optimization procedure for a south facing window (Santos, Leitão and Caldas, 2018).

Finally, a closer analysis of Figures 6-14, 6-15, 6-16, and the E_V values reported in Table 6-5 shows that the computational implementation of Strategy D captures critical glare events. In those events, however, the circumsolar region has a considerable weight in the FOV, indicating a bias towards low sun angles and clear skies. This bias is a direct consequence of using a single $E_{V,Thr}$ that resulted from an annual analysis that includes different and mixed sky conditions. A further refinement of the strategy should study $E_{V,Thr}$ that only address overcast or hazy skies in periods of the year with higher sun angles (mid-season to summer).

6.6 Concluding Remarks

The work conducted in the development and implementation of Strategy D demonstrates that a proper vertical illuminance (E_V) threshold ($E_{V,Thr}$) can signal hourly glare events (DGP ≥ 0.35). Through the use of such $E_{V,Thr}$, the research demonstrated that it is possible to sample annual E_V data spatially and temporally in order to:

- Conduct preliminary assessments on glare performance in perimetral zones of office spaces.
- Find the relevant POV/HOY pairs to conduct full point-in-time DGP analysis.
- Reduce the number of time-consuming DGP simulations in visual comfort studies.

Although this investigation showed that a single $E_{V,Thr}$ can qualify the glare potential of any location in space, it also indicated that an adaptive $E_{V,Thr}$, i.e., one that responds to the distance between glare sources and the viewer's location, has the potential to be even more accurate in predicting potential glare events. The sensitivity analysis experiment that supported the $E_{V,Thr}$ selection revealed that higher thresholds performed better in the daylit zone of a side-lit room while lower ranges better predicted the occurrence of glare events in locations out of the daylit zone of the room. Future work will address this in order to improve the proposed approach.

There are several examples of the use of E_V as a preliminary indicator for visual discomfort both in the literature and in current simulation approaches. For example, for annual DGP analysis, current tools use the 2-phase method, particularly its implementation in DAYSIM (Reinhart and Walkenhorst, 2001). Such tools use E_V estimations to inform eDGPs calculations in the occupied schedule, usually for a specific POV, to reduce simulation time. Compared with such approaches, the proposed daylighting analysis tool uses E_V to spatially map glare potential over a grid of sensors. Consequently, the proposed strategy addresses current POV-related limitations of annual DGP (aDGP) by simultaneously considering several points in space and different view directions.

Additionally, the tool uses E_V simulated data to automatically identify critical POV and time events to then conduct detailed full DGP analysis, using the three-phase method (McNeil and Lee, 2013). Hence, it avoids the eDGPs and the 2-phase method limitations, particularly those concerning the inability of the former in considering indirect glare sources and of the latter in capturing specular light scattering.

The tool uses E_V to signal where and when to conduct fully detailed DGP analyses that are able to capture the effect of glare sources and accurately describe luminance distribution in a scene. Fully detailed DGP analyses using the 3- or 5-phase method for Radiance, are particularly relevant in the analysis of highly specular complex fenestration systems such as the one used in the case study application. The automatic identification of critical POV and time events proposed by this tool are also important pieces that promote the use of glare simulations in automated daylighting optimization procedures. Future work will explore the use of the proposed tool in the context of optimization of light redirecting complex fenestration systems.

Although the proposed method finds critical events, it shows a bias for low sun angles of bright and clear skies. This bias is a direct result of the procedure used to determine the $E_{V,Thr}$ applied in this investigation. Future work also includes the refinement of the strategy by enabling the detection of events with high glare potential in a wider range of skies. The envisioned refinement could be achieved by either adding or modifying the HOY selection rules or using an adaptive $E_{V,Thr}$ that responds to spatial location and sky type. In this way, future iterations of the tool will be able to find critical events on which the circumsolar region is either not visible or is relatively small in the FOV.

The focus of DGP and E_V studies on the perimetral zone of office spaces limits their application scope. Thus, since the proposed assessment method relies both on E_V and DGP, the application of the results presented here is limited to the examination of side-lit offices perimetral areas. Further research is necessary to determine if E_V and DGP are good indicators for visual discomfort in areas located in deeper zones of buildings. Future developments of the proposed strategy will include ancillary and easy-to-compute metrics such as luminance contrast ratios to complement E_V and DGP analysis in the study of visual discomfort of deeper building areas.

Regarding other building types and programs, it is necessary to conduct further empirical research to determine whether building occupants have different levels of visual adaptation and tolerance and whether E_V and DGP are good indicators of visual comfort. Future improvements of the proposed analysis method will include updating any potential future DGP and E_V future guidelines and thresholds. Moreover, the experiments considered only a limited set of fenestration systems – a clear glazing and a particular LRCFS – and one type of advanced daylight simulation based on daylight coefficients, Radiance's 3-phase method. Thus, to further validate and extend the scope of the proposed approach, future work will address top-lighting strategies, other types of glazing, shading, and light-redirecting systems, and use other advanced daylight simulation methods, including the 5-phase method and dedicated front-forward raytracing approaches based on photon-mapping techniques.

The inclusion of the 5-phase method to the modeling strategy will enable a thorough study of both the direct and diffuse light contribution to visual(dis)comfort. As discussed in chapter 2, section 2.2.2 *–Daylight simulation in buildings using physical (unbiased) approaches*), the 5-phase method decouples the direct solar component from the sky and the inter-reflected solar component, thus facilitating the identification of potential glare events when the circumsolar region is not visible in the FOV. The photon-mapping will allow a better assessment of the

specular effects of LRCFS and better handling of light caustics in the FOV, thus enabling a deeper understanding of their role in evaluating E_V in the perimeter zone.

The research presented in this chapter also shows that Strategy D has a high potential for use in automated search procedures for daylight-based design since it effectively helps to reduce the number of computationally expensive simulations used in annual visual comfort studies.

At early design stages, this strategy supports the arrangement of the different building spaces, the design of the overall building form, façade windows, and static shading devices. At intermediate design phases, the strategy is able to provide useful information for the development of efficient automated shading control protocols, glazing selection, shading devices, light redirecting systems, interior surface materials, and the layout of furniture.

Finally, the strategy presented in this chapter focused on facilitating glare studies in the design of buildings that aim to achieve high visual comfort standards, such as the one set by EN 17037. Nevertheless, it is up to the design team to evaluate the potential constraints to the design process that might result from a heavy emphasis on achieving overall light quality. Although it is desirable to achieve the maximum level of visual comfort in buildings, such achievement should not hinder the overall quality of the design. It is equally recommendable that some agency be provided to building occupants in controlling their immediate daylit environment. As demonstrated in personal comfort systems for thermal comfort (Kim, Schiavon and Brager, 2018; Luo et al., 2018; André, De Vecchi and Lamberts, 2020), a designer should first ensure an overall comfortable environment and then allow, as much as possible, the building occupant to adjust the immediate environment in order to satisfy his or her personal preferences (de Bakker et al., 2018). In the case of visual comfort, this granular control could be achieved by the design of furniture, monitoring and managing occupant feedback to control automated shading systems (Meerbeek et al., 2016), personal control of desk materials selection, and deployment of task lights controlled by the user (de Bakker et al., 2017).

Chapter 7:
User-driven formulation of spatial-based performance goals for generative design systems

7.1 Introduction

As argued in chapter 3, section 3.3.3, formulating optimization problems for goal-oriented design approaches that are based on daylighting simulations is more challenging than in design processes that aim to optimize building energy simulated performance. The primary cause for such difficulty is that daylight performance metrics have a high spatial granularity, i.e., their spatial pattern is highly variable. In fact, some daylight metrics, such as illuminance (*E*), may vary from "tens to ten thousands of lux" in indoor settings (Reinhart, 2019), making them very susceptible to the *cancelation* or *compensation effect*, whereby a high values cancel low ones. Therefore, summation or average-based processes are not adequate to summarize the zonal variation of daylight indices. In contrast, although building energy-related metrics entail temporal variation, it is relatively easy to reduce their temporal transience to a single or a small array of cumulative values. The lower sensitivity of common building energy indices to spatial distribution (e.g., Energy Use Intensity - EUI, energy consumption, unmet load hours, etc.) in a thermal zone facilitates the definition of building energy-related performance goals in design processes that are based on Building Performance Optimization (BPO) workflows.

Considering that light is one of the determining factors that contribute to the spatial quality of buildings and the wellbeing of its occupants (Ozorhon and Uraz, 2014), goal-oriented processes for daylighting design must support the definition of spatial performance target patterns. Enabling designers to specify the spatial distribution of goals in daylighting inverse design problems provides them a better control of the daylight behavior of the search result, an important aspect in cases that aim to integrate diverse lighting environments. The spatial definition of daylight performance targets is particularly helpful in cases where variable light environments are desirable, i.e., scenarios in which the architect aims to promote visual alliesthesia[3]. One of the typical examples of visual alliesthesia in buildings is either the gradual or abrupt transition from dim and more "introspective" spaces to bright and "lively" ones. The Vals spa/baths located on Graubünden, Switzerland, designed by the architect Peter Zumptor is an excellent example of how a thoughtful arrangement of different light environments triggers different experiences in building occupants. Another built example that aims to convey a specific experience through a progression of different light environments is the Leça da Palmeira outdoor swimming pool building, located at Leça da Palmeira, Portugal, and designed by the architect, Álvaro Siza Vieira. The visitor or the user of that swimming pool is first exposed to a bright outdoor environment, then to different spaces that include locker rooms and showers with variable light qualities, and finally to the bright environment of the pools located at the shores of the Atlantic Ocean.

[3]Alliesthesia is a psychophysiological phenomenon that describes the relationship between the environmental stimuli and the internal subjective perception of pleasure or displeasure by the subject exposed to that stimuli (Parkinson and De Dear, 2015).

Another case where the spatial definition of daylight targets is useful is when architects desire to design a building form that expresses the variable light environments that the building comprises. Recent pavilion-like structures are good examples of buildings that formally express their light environments. Examples include the Serpentine temporary gallery designed by Bjarke Ingels Group, the Sclera and Genesis pavilions designed by Adjaye Associates, and the Crematorium in Kakamigahara (Gifu, Japan) designed by Toyo Ito and Associates, which wavy roof responds both to structural requirements and to the required light levels of different building functions – see Figure 7-8, right. Although these examples did not use a BPO approach to daylighting design, they would benefit from a spatial definition of daylight targets if they were to be designed using a goal-oriented design method.

To better support goal-oriented design of diverse daylit environments, this chapter focuses on discussing generative design approaches to daylighting design and proposes a new modeling method that supports the spatial definition of daylight performance targets.

Following the top-down investigative method described in chapter 4, section 4.3, the chapter begins with a summarized literature review that traces the evolution of goal-oriented design approaches in daylighting design. Such approaches includes systems that use optimization algorithms as search mechanisms, expert systems (Aronson, Liang and MacCarthy, 2005; Shu-Hsien Liao, 2005), and interactive Graphical User Interfaces (GUI) for performance target specification as viable alternatives to conventional methods that mathematically formulate objective functions. The objective of the literature review is to frame the development and implementation of the strategy and assess current needs by analyzing existing limitations that prevent an easier deployment of goal-oriented design methods in daylighting design. After the literature review, the chapter introduces Strategy E and its computational implementation: the performance-based generative design system (PGDS) Painting with Light. The research tasks, development, implementation, and calibration of the proposed PGDS are fully described in the Design of Experiments (DoE) section. The chapter then presents and discusses the results. Finally, it summarizes the findings discussed in this chapter, the advantages and limitations of Painting with Light, and future directions for the research.

The work presented in this chapter is part of a larger research project led by the primary adviser of the author of this dissertation, Professor Luisa Caldas, which evolved to be a part of this dissertation investigation. The dissertation's author contributed both to the conceptualization of the proposed PGDS and substantially to its development and implementation. Thus, this chapter results from a joint research effort between the author and his primary adviser, published in Caldas and Santos (2016). The present chapter extends and updates the content of that publication.

7.2 Related Work

The development of computational tools capable of predicting daylight in buildings has allowed designers to apply building simulation tools to optimize predicted building performance, including daylighting in buildings. Johnson et al. (1984), presents one of the earliest works that involve daylight estimations to minimize building energy consumption, particularly through the optimization of glazing assemblies. The authors used the DOE-2.1B Building Energy Simulation (BES) program, which contains a simplified daylighting prediction model, to run an extensive parametric study that involved several combinations of wall and fenestration properties. Most of

the earlier works on optimizing the daylight performance include iterative simulation and the indirect optimization of daylighting in buildings by considering it in the calculation of the energy needs of a building, such as in the works of Sullivan et al. (1992) and Hayter et al. (1999).

At the turn of the twenty-first century, several researchers began to integrate different optimization metaheuristics to fully automate the search in building performance optimization. However, in the early years of research in goal-oriented building design, most approaches used daylight prediction only indirectly in the optimization process. Peippo et al. (1999) implemented a direct search algorithm to minimize building cost and energy. The authors considered daylight simulations in the calculation of energy demands. Wetter proposed GenOpt (2000) as a generic BPO program that allows coupling with any building simulation software such as DOE-2 or EnergyPlus. The work presented by Wetter (2001) exemplifies the coupling of GenOpt with EnergyPlus to minimize building energy consumption, which considered the contribution of daylight in the calculation of lighting building energy use.

GENE_ARCH (Caldas and Norford, 2002) is a generative design system that combines Genetic Algorithms (GA) and EnergyPlus in the design of energy-efficient buildings. Similarly to GenOpt, GENE_ARCH uses DOE2.1 and EnergyPlus to calculate the daylight contribution in the overall building energy performance. In Caldas (2008), the author uses GENE_ARCH in a Multi-Objective Optimization (MOO) that includes daylight and thermal performance. The formulation of both objectives results in estimating building energy use. The daylighting goal consists of minimizing lighting energy consumption, while the thermal goal was to reduce heating and cooling loads of the O'Porto School of Architecture, designed by the architect Siza Vieira. Nevertheless, the work is an early example of the use of refined daylight analysis, including point-in-time illuminance distribution and sun penetration, as a post-analysis step.

The emergence of toolkits that facilitate the use of detailed daylight simulations and advanced metrics that describe the annual daylight performance of buildings has enabled designers to explore goal-oriented design methods that directly use advanced annual daylighting performance metrics. Torres and Sakamoto (2007) averaged annual illuminance averages measured in different observer positions in the design of the fitness function to optimize façade shading elements.

Andersen et al. (2008) propose LightSolve, an interactive goal-oriented expert system for daylighting design. With this tool LightSolve, the user is able to draw areas of interest and set goals for annual periods determined by time-segmentation, a method that splits the year into a small number of periods and averages their daylight illumination levels (Kleindienst, Bodart and Andersen, 2008). The work describes a holistic view on daylighting performance based on five "good daylighting" goals, calling for goal-based design decision support with non-deterministic feedback loops. Andersen et al. (2013) further extended LightSolve's expert system to a more comprehensive analysis and daylighting design tool that balances illumination, glare and solar gains over a year. The authors validated the system in a user study focused on early design stages. The last LightSolve development extended the approach to include both perceptual, visual (comfort), and non-visual physiological (health) approaches to daylighting (Andersen, 2015).

Rakha and Nassar (2010, 2011) combined Radiance and LUA scripting language to create a generic tool for the generation of curvilinear ceiling forms, using a criteria applied to the daylight uniformity ratio metric. The daylight uniformity ratio results by dividing the maximum *E* by the

minimum *E* found in a sensor grid given a specific sky condition, location, and time. The authors used the CIE clear sky with sun in Cairo, Egypt, at noon.

Manzan (2014) used the GA of modeFrontier (Bäck, 2005) – a proprietary Multidisciplinary Design Optimization (MDO) framework – to optimize primary energy consumption that includes artificial lighting, heating, and cooling. Radiance (Ward, 1994) and DAYSIM (Reinhart and Walkenhorst, 2001) were the daylighting programs used to calculate the annual building daylighting performance using climate-based daylight metrics. The authors used the data generated by the daylight simulation process as input to the BES program used in this research, ESP-r (Strachan, Kokogiannakis and Macdonald, 2008), to accurately determine the energy consumption of the building's lighting system. Similarly to Caldas (2008), the author used the climate-based daylight simulation data to analyze in more detail the performance of the solutions optimized for energy consumption by the approach. Later, Manzan and Clarich (2017) further extended the approach by advancing a new search procedure – FAST – applied to a slightly different design that adds dynamic exterior shading control but has the same performance goals.

Lartigue et al. (2014) developed a methodology for optimizing the building's envelope to minimize heating and cooling loads and maximize daylight. The method uses Daysim climate-based calculations to estimate lighting loads. In order to control the lighting, the system compares annual hourly illuminance data to a threshold. The search procedure couples an Artificial Neural Network (ANN), to reduce the calculation time of computationally expensive cost functions, with GenOpt.

Futrell et al. (2015b) proposed a method for building design to minimize predicted lighting loads by combining GenOpt with Radiance simulations. The latter determines the building daylighting performance using dynamic climate-based lighting simulations. The work compared four optimization algorithms implemented in GenOpt: (i) Simplex Algorithm of Nelder and Mead with the Extension of O'Neill (SAEO), (ii) Hooke Jeeves (HJ), (iii) Particle Swarm Optimization using Inertia Weight (PSOIW), (iv) and a hybrid PSO Constriction/Hooke Jeeves (PSOC/HJ) algorithm. Later, the same authors proposed a bi-objective optimization of building enclosures, both for thermal and daylighting performance (Futrell, Ozelkan and Brentrup, 2015a). In this work, the authors considered annual daylighting performance as an independent objective. They advanced a normalized daylighting objective that sums annual hourly daylighting scores normalized by the number of the horizontal sensor nodes and the total hours of the occupied schedule. The hourly score assigned to each sensor node depends on whether *E* observes a specified criterion or not.

Wortman et al. (2015), used surrogate modeling approaches that use Radial Basis Functions (RBF) kernel methods to interpolate a mathematical model from simulated Useful Daylight Illuminance (UDI) and annual Daylight Glare Probability (aDGP). The authors applied the goal programming method (Coello, 1999; Aköz and Petrovic, 2007; Biswas and Pal, 2019) to combine both UDI and aDGP in a single objective function. The surrogate model replaces expensive daylight simulations during the optimization of a perforated architectural screen that aims to maximize UDI and minimize aDGP.

Caicedo and Pandharipande (2016) averaged illuminance levels of occupied and unoccupied zones of a typical office space to optimize a lighting system control scheme. Konis et al. (2016), applied a different strategy, which avoids cumulative or averaging processes on daylight studies. Utilizing the spatial daylight autonomy (sDA) concept, the authors advanced a new zonal and annual metric,

spatial UDI (sUDI) – a climate-based index that applies the sDA concept to UDI. The work aimed to simultaneously maximize the sUDI of a specific illuminance range (300 to 3000 lux) and minimize building energy use of typical commercial buildings. The authors implemented the goal-oriented design approach in Rhino Grasshopper and used Octopus Pareto GA – the Strength Pareto Evolutionary Algorithm 2 (SPEA2) (Ziztler, Laumanns and Thiele, 2002) – in the MOO exercise. Zhang et al. (2017) and Mangkuto et al. (2018) use a similar approach, although Zhang et al. (2017) also considered UDI averages of a grid of sensors in the search process. Kirimtat et al. (2019) also averaged the UDI calculated in a sensor grid in a MOO of amorphous shading devices that aim to reduce the total energy consumption and maximize UDI of an office room.

With the exception of LightSolve (Andersen et al., 2008; Andersen, Gagne and Kleindienst, 2013; Andersen, 2015), all the goal-oriented design approaches above fail both in including the spatial variation of the daylight phenomena and in proposing more accessible means for non-experts in optimization to set performance targets. A large part of the literature work includes daylight simulations only as a necessary step to control and calculate the energy of a building's lighting system, such as the works proposed by Johnson et al. (1984), Sullivan et al. (1992), Hayter et al. (1999), Peippo et al. (1999), Wetter (2001), Caldas and Norford (2002), Caldas (2008), Manzan (2014), Lartigue et al. (2014), Futrell (2015b), Manzan (2017), and Caicedo and Pandharipande (2016). In such cases, the formulation of performance goals is straightforward since it consists of minimizing the simulated lighting energy end-use in a building. Of the authors that directly optimize daylight metrics, a significant number use cumulative and average-based processes to reduce the spatial dimension of daylight simulation data, such as Rakha and Nassar (2010, 2011), (Futrell, Ozelkan and Brentrup, 2015a), Wortman et al. (2015), Zhang et al. (2017) – in a part of the work, and Kirimtat et al. (2019). As previously mentioned, daylight in buildings is highly susceptible to the compensation effect, which increases the risk of misguiding optimization processes that averages or aggregates daylight simulated data. To reduce such risk, some researchers use specific normalization or weighting processes (Futrell, Ozelkan and Brentrup, 2015a; Wortmann et al., 2015), a non-trivial task that involves time-consuming trial-and-error processes and requires expertise that most architects do not have. Thus, zonal-based assessments such as sDA and sUDI are preferable to averaging or cumulative based methods. However, only few works fully adopt that approach, such as the ones presented by: Konis et al. (2016), Zhang et al. (2017) – partially, and Mangkuto et al. (2018). Although the measurement of areas that meet an illumination criterion is less biased than averaging illumination predictions, it does not fully support the spatial distribution of daylighting performance targets.

Despite the current variety and application of goal-oriented approaches in building performance-based design, only a few advanced visual interfaces that use interactive brushing and linking techniques (Becker and Cleveland, 1987) for target setting in automated search processes, namely: Audioptimization (Monks, Oh and Dorsey, 2000), for acoustic design, and LightSolve (Andersen et al., 2008; Andersen, Gagne and Kleindienst, 2013; Andersen, 2015), for lighting and daylighting design.

Audioptimization (Monks, Oh and Dorsey, 2000) is a PGDS for acoustic design. The workflow proposed by this system encompasses two stages. In the first, the user describes a parametric model of the space to optimize, including both its fixed characteristics and the discrete geometric and material variables to be optimized, and their respective minimum and maximum ranges. This description defines the solution space of the design problem, i.e., all the geometric and material

combinations possible. In the second stage the user sets the goals for different acoustic metrics (interaural cross-correlation coefficient, early decay time, bass ratio, and sound strength/level) by painting them in different spatial elements. Figure 7-1 shows Audioptimization's goal specification visual interface and illustrates how to paint objectives with it.

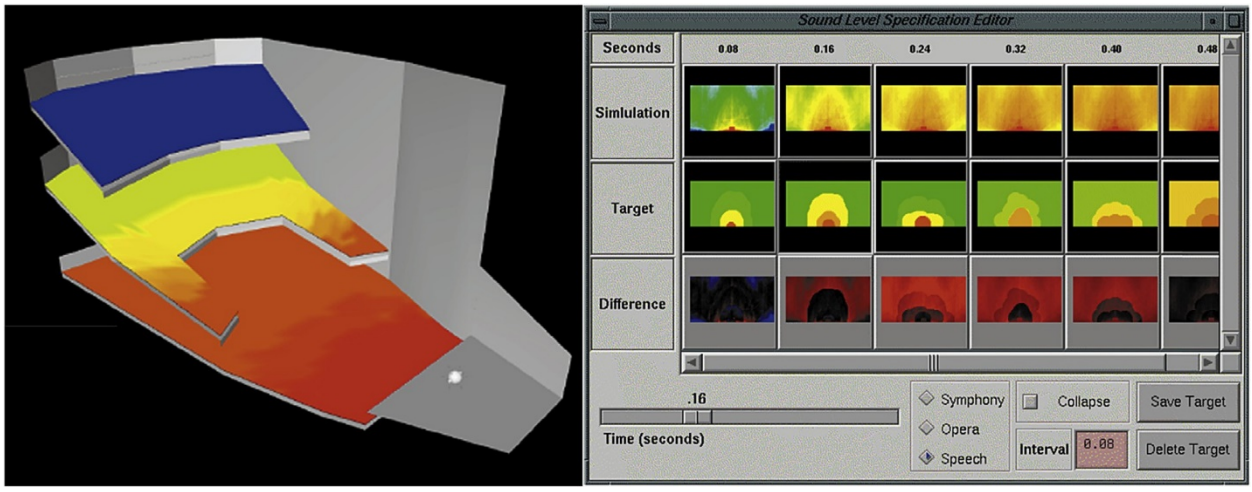

Figure 7-1. Painting objectives through Audioptimization's visual interface. Left: sound level painted goals in different surfaces for 80 ms. Right: sound level specification editor for a specific surface. Top row shows the current sound level simulation; the middle row shows the painted targets for this particular metric; and the bottom row shows the difference heatmap between the two. Images adapted from: Monks et al. (2000).

After describing both the design problem and the desired acoustic targets, Audioptimization searches the solution space for a high performance solution by combining two search procedures: Simulated Annealing (SA) for a more global search, and steepest descent (a gradient-based optimization algorithm) for a more refined search around the global minimum found by SA.

Audioptimization has an advanced visual interface that allows the user to paint objectives through brushing and linking techniques. The generation of a difference heatmap (Δ heatmap) between desired performance targets and the results of the optimized solutions is useful in quality assessment tasks. The Δ heatmap visualization contributes to the understanding of the design problem by assessing: (i) to what degree the system met the spatial performance patterns set; (ii) the feasibility of painted goals; (iii) the constraint levels applied to the design problem, i.e., whether the design problem is over or under-constrained.

The tool also supports point-in-space measurements through the use of positional glyphs. A glyph is a cylinder that positions a listener in space, and it conveys the difference between target and actual simulation value of three different acoustic metrics as follows:

1) Interaural Cross-correlation Coefficient (IACC) through the offset shell region not covered by the actual result. Ideally, this difference shell would be absent.
2) Early Decay Time (EDT), represented as a cone on top of the listener cylinder icon. The radius of the cone indicates absolute difference and the color shows whether the result is higher than (red) or lower than (blue) its target. Ideally, the radius of the cone would be the smallest possible or zero.

3) Bass Ratio (BR) difference, represented by a ring between result and target values, with the same EDT color code. Like the other metrics, the ring would be absent in an ideal scenario.

However, these diagnostic techniques are purely visual and only convey the difference between the desired targets and simulated performance. Advanced analysis with sophisticated statistical error metrics typically used in building performance simulation, such as percentage error (% error), Coefficient of Variation of the Root Mean Square Error (CVRMSE), and Normalized Mean Bias Error (NMBE), could be automatically provided by the system in order to support better decision making processes.

LightSolve (Andersen et al., 2008; Andersen, Gagne and Kleindienst, 2013; Andersen, 2015) is an interactive goal-oriented design tool that integrates into a single workflow several daylighting considerations such as daily and seasonal variations, illumination, and visual comfort. LightSolve design workflow supports a bidirectional interaction between user inputs, and system outputs through three primary interfaces: (i) geometry and material editor; (ii) a set of selection tools for specifying horizontal workplane sensors, views and times of interest from a temporal map; and finally (iii) the performance target interface, which allows the user to alter the current design goals by specifying a range of desirable or acceptable values for the daylight metric under study.

Figure 7-2 shows the LightSolve interface and how it enables the user to assess the linked relation between performance and renders interactively. If the current design does not meet all the designer's goals, LightSolve will propose effective changes to improve its daylight performance through a search mechanism that computationally implements a set of "expert rules." This "expert system" is based on a Design of Experiments (DoE) approach. Thus, unlike other PGDS such as Audioptimization (Monks, Oh and Dorsey, 2000), eifForm (Shea, Aish and Gourtovaia, 2005), GenOpt (Wetter, 2000), and GENE_ARCH (Caldas and Norford, 2002; Caldas, 2008; Caldas and Santos, 2012), LightSolve's goal-oriented design workflow does not aim to find a global or even a local optimum but attempts to predict the effectiveness of specific design changes on the daylighting improvement of a current design status. In a sense it acts as a "virtual design assistant."

LightSolve has a detailed and sophisticated interface that supports sensor point workplane grids, goal-based illuminance temporal maps displayed alongside interactive renderings, and a triangular color scale specially developed to assess goal compliance (Kleindienst and Andersen, 2012). Different daylight metrics, such as Acceptable Illuminance Extent (AIE) (Andersen, Gagne and Kleindienst, 2013), are also incorporated. While previous versions of the tool (Andersen et al., 2008) only allowed users to assign a threshold value to a given geometrical surface, the target definition the current target definition consists of defining a minimum and maximum illuminance value to different workplane sensor points, thus allowing the definition of spatial daylighting patterns. In terms of outputs, LightSolve is now more focused on time-mapped visualizations of daylight performance combined with sequential rendering visualizations.

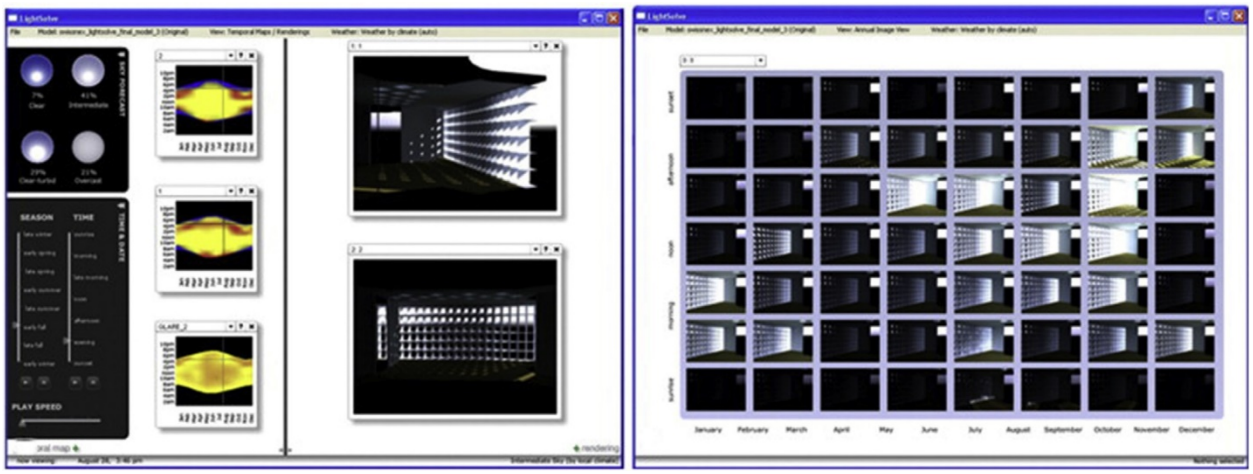

Figure 7-2. LightSolve interface. Left: time-varied daylight performance displayed in temporal maps interactively linked to renders of the space under study. Right: annual image map showing renderings over time. Images adapted from: Andersen et al. (2013).

Outside the building performance field, some computer graphics tools have been using interactive approaches to steer image-editing software solvers. An example is the Interactive Digital Photomontage tool (Agarwala et al., 2004). From an initial set of color-coded images of the same scene, the user defines a goal image by painting a series of strokes in one image using the designated color associated with the other source images. Then, the tool creates a composite image that approximates the desired objective using two main techniques: (i) graph-cut optimization, to find the best possible seams to cut the various source images; (ii) gradient-domain fusion, to remove any visible artifacts that might remain after the joining of image seams. Figure 7-3 illustrates the Interactive Digital Photomontage workflow by exemplifying how the user selects and paints the objectives over an image, the relation between the targets set for each part of the goal-image and the initial set of images, and the final composite image generated by the tool.

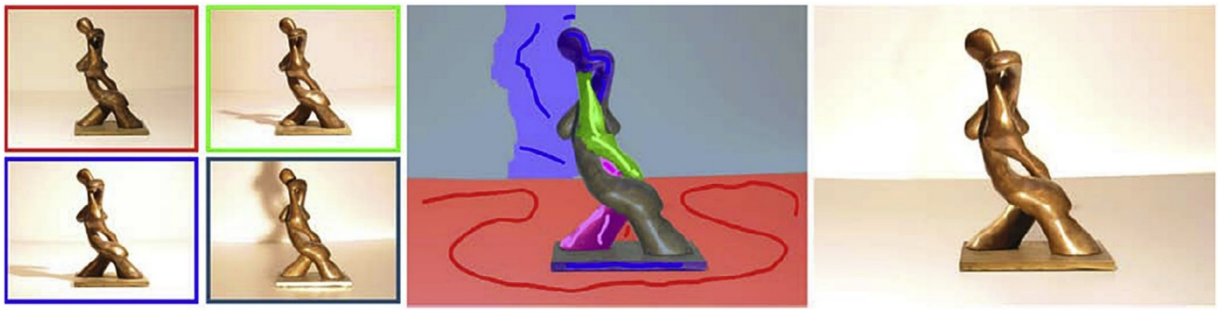

Figure 7-3. Example of the Interactive Digital Photomontage workflow. Left: the initial source image set. The colors around each image represents an objective associated with each specific image to be painted on one of the source images. For example, red represents the maximum luminance objective, while blue is the minimum luminance objective. Middle: one of the source images painted with the different image-objective goals. Right: the final composite image found by the Interactive Digital Photomontage solver. Images adapted from: Agarwala et al.(2004).

In sum, the few approaches that support the spatial definition of performance targets in performance-based generative design systems are either limited in their scope or in their analysis methods. The Interactive Digital Photomontage tool (Agarwala et al., 2004) advances a Graphical

User Interface (GUI) that allows users to set different goals for combining and composing images. Although the work is outside of the building performance field, it provides a conceptual example of how a user can interactively set targets for a goal-oriented tool using intuitive visual methods. Although Audioptimization (Monks, Oh and Dorsey, 2000) is an acoustic PGDS, it supports a visual interface that allows users to spatially specify performance targets. However, the diagnostic methods supported by the tool consist only of visual difference maps, thus lacking essential error metrics to assess the output quality of the search, such as the Root of Mean Square Errors, CVRMSE, NMBE, percentage of error (% error), among others. LightSolve (Andersen et al., 2008; Andersen, Gagne and Kleindienst, 2013; Andersen, 2015) is the only goal-oriented design tool that enables the visual specification of performance targets for daylighting design. Despite LightSolve's significant contribution, it constrains the designer to use time-mapped visualizations, complex triangular color scales to assess the quality of the solution provided by the expert system, and seldom-used annual dynamic daylight metrics. LightSolve also has limited search capabilities since its search mechanism is based only upon a Design of Experiments and not on optimization algorithms. Additionally, the tool also does not include essential statistical indices to assess the quality of the solutions that emerge from the interaction between user and the program. Finally, both Audioptimization and LightSolve are stand-alone applications. Although they support the export-import of geometry with CAD applications, they are not modular and do not follow the *Interface Dynamic Models* (IDM) "toolkit" paradigm preferred by designers in the deployment of parametric and goal-oriented design approaches (Negendahl, 2015). IDM is a modular approach to parametric and generative design that allows designers to custom tailor modeling approaches that best fit their needs. IDM combines a programming language, typically a visual one, a CAD or a Building Information Modelling (BIM) tool, simulation software, and, in inverse design, a library of optimization algorithms.

Considering the current limitations of goal-oriented approaches in allowing the specification of daylight spatial target patterns there is a need to develop a modeling strategy that enables designers to easily define spatial daylight targets for inverse daylighting design. Additionally, the computational implementation of the strategy approach should favor modularity and aim for full integration into current digital design "ecosystems" that enable the use of design tools, simulation software, and optimization algorithms.

7.3 Strategy E: Painting with Light – a novel method for spatially specifying daylight goals in Building Performance Optimization

Strategy E focuses on providing a feasible answer to the third research question specified in chapter 3, section 3.4 – *How to develop strategies that help architects and other non-experts in optimization to formulate inverse design problems?* Consequently, it aims to achieve the fourth development and implementation goal defined in the same chapter and section – *Use familiar techniques known to designers to expedite the definition of performance goals*. Hence, the main objective is to address the problem of setting performance targets for daylighting-based goal-oriented design approaches by proposing an initial, proof-of-concept interactive interface in the Rhino environment – Painting with Light. The integration of Painting with Light with Rhino favors the implementation of the IDM concept (Negendahl, 2015) by allowing access and integration of the following components: (i) advanced 3D modeling tools; (ii) Grasshopper's – a Visual Programming Language (VPL) for Rhino – built-in functions and methods for parametric/generative design; (iii) dedicated interfaces for lighting simulation with Radiance and

DAYSIM (Reinhart and Walkenhorst, 2001), such as DIVA (Jakubiec and Reinhart, 2011); and finally (iv) evolutionary solvers for search and optimization, such as Galapagos, which uses a Standard Genetic Algorithm (SGA) and Octopus, which can perform multi-criteria optimization using SPEA2 (Ziztler, Laumanns and Thiele, 2002).

The proposed interface aims to facilitate a performance target description using painting-style processes that use brushing and linking techniques. A painting-style interface will allow designers to easily set performance goals and define their spatial distribution to building performance-based problems. By promoting the draw of colored regions, the proposed interface better approximates the methods commonly used by designers in their workflows, thus being more intuitive and easier to use.

Finally, this work aims to address some of the limitations found in previous research (Monks, Oh and Dorsey, 2000; Andersen et al., 2008; Andersen, Gagne and Kleindienst, 2013) by implementing a visual performance target editor that adequately addresses the spatial resolution and pattern variation of the daylight problem, and supports any grid-based daylight metric, namely, Daylight Factor (DF) (Hopkinson, Petherbridge and Longmore, 1966), point-in-time illuminance (*E*) and climate-based metrics such as Daylight Autonomy (DA) (Reinhart, Mardaljevic and Rogers, 2006), Annual Sun Exposure (ASE) (IESNA, 2012), and Useful Daylight Illuminance (UDI) (Nabil and Mardaljevic, 2006).

7.3.1 Method for specifying performance targets in goal-oriented design using user-driven painting-like techniques

The development of Strategy E includes the computational implementation of the Painting with Light tool in Rhino using Grasshopper visual programming language (VPL) and Integrated Development Environment (IDE), and GHPython (Piacentino, 2011; Cuvilliers, 2017), a Python library and interpreter for Grasshopper. The interface allows designers to use typical CAD drawing techniques to color the performance targets for the space under study. The painting process entails two steps: (i) define areas with a specific color/performance target by drawing enclosed areas with closed polylines or Non-Uniform Rational Basis Splines (NURBS) curves; and (ii) use sliders to control the degree and strength of light decay from the drawn areas. The system automatically groups the sensor nodes by color, and consequently, by performance target value.

Figure 7-4 shows how a designer uses closed polylines or NURBS curves to paint the space and link the sensor nodes to a specific performance target. The image on the left shows how the user draws closed NURBS curves to specify the area with the highest performance target value. The image on the right demonstrates how the user can repaint goals by either redrawing the NURBS curves that represent lighting boundaries or by manipulating the curves control points.

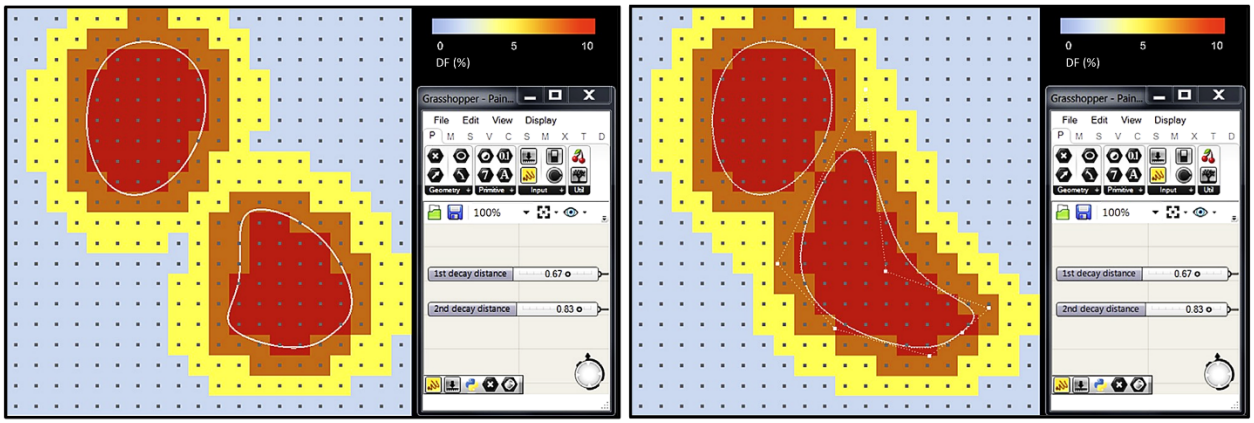

Figure 7-4. Painting performance targets using and manipulating closed NURBS curves over a grid of lighting sensors. Left: the user draws the area of that correspondents to the highest DF target value. In this particular case, the highest DF admitted is 10 %, since it corresponds to high light levels (Grondzik and Kwok, 2019). Right: the user repaints the performance targets by manually manipulating the NURBS curve control points.

Figure 7-5 illustrates how to control the desired light decay (left) and how to adjust performance target values by changing the numeric range of the color scale (right) using sliders specially designed for those purposes. As Figure 7-4 and Figure 7-5 show, the assignment of targets is discrete, i.e., each color represents a range of performance values.

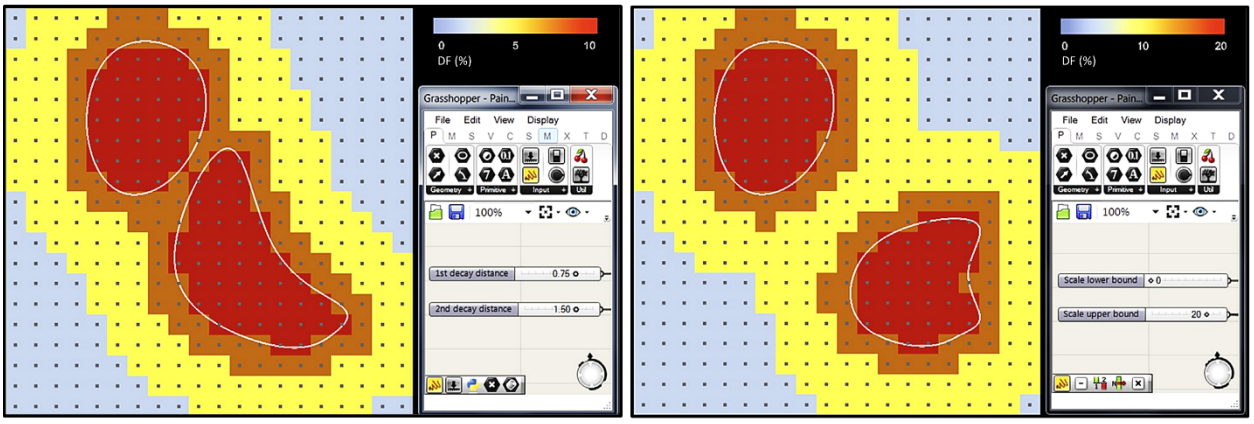

Figure 7-5. Controlling the light decay pattern (left) and changing performance targets by resetting the color scale values (right) using sliders.

Regarding the visualization of results, Painting with Light supports both visual and analytical tools. Visually, the interface pairs in the same viewport three heat maps: (i) the painted performance target in the sensor node grid mesh, (ii) the simulation result of the solution found by the system's search mechanism, and (iii) a difference map (Δ map) between simulation results and desired targets.

The tool automatically generates the difference map with a color scale that ranges from blue to white and white to red. Blue nodes indicate that the solution has a performance below the target, white nodes shows that the design achieved the target, and red nodes report that the daylight performance is higher than the painted targets. Figure 7-6 illustrates the three painted meshes in a Rhino viewport.

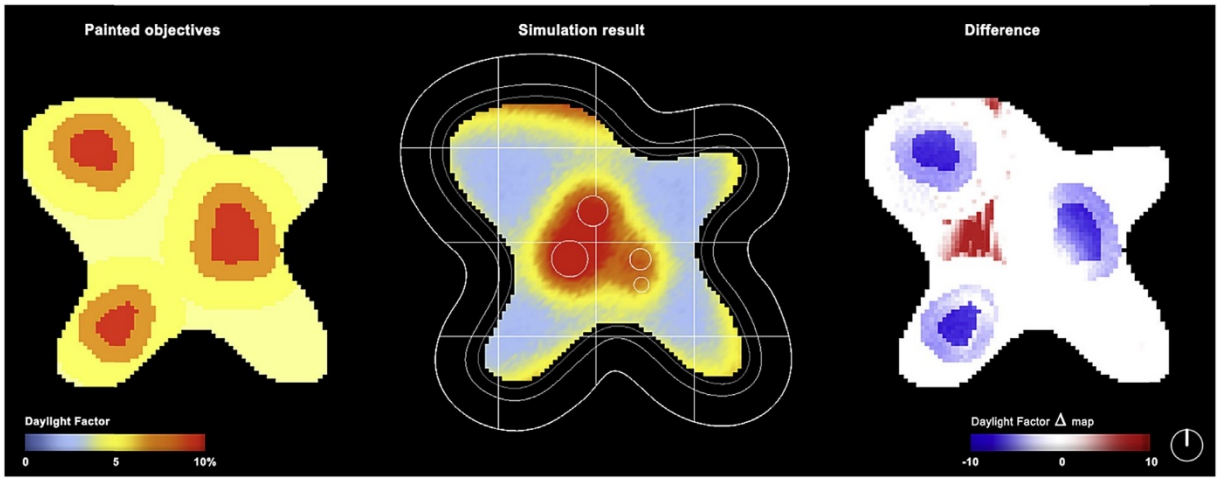

Figure 7-6. Visualization of results in the computational implementation of Strategy E - Painting with Light.

Finally, the system automatically computes and displays the different statistical metrics lacking in Audioptimization (Monks, Oh and Dorsey, 2000) and typically used in building performance simulation – NMBE, CVRMSE, and % of error. Regarding % of error, the tool measures its average across all nodes. The proposed implementation also includes other statistical indices, such as the percentage of area in the first quartile, and the absolute difference in average. Such metrics enable designers to quickly assess whether the simulation was successful or not. Figure 7-7 shows how Painting with Light presents the computed statistics indices. Section 7.3.2 – *Metrics used in simulation, calibration, and strategy validation* – further details the *statistical methods supported by the tool.*

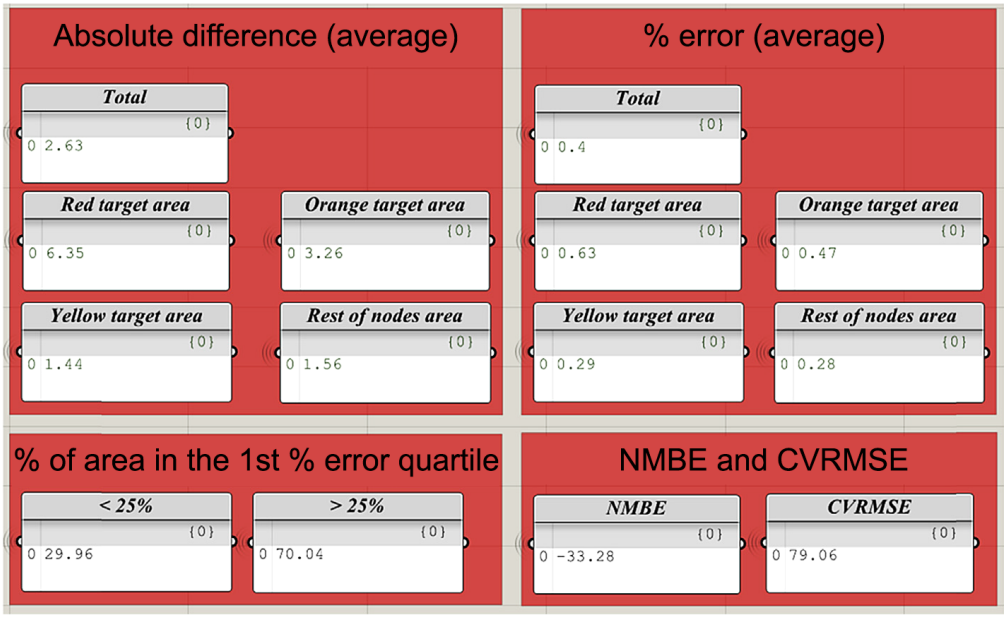

Figure 7-7. Statistic results dashboard in the proposed approach. The results measure the success of the optimization search in matching the spatially painted targets.

The next section introduces a set of experiments designed to assess the ability of the proposed approach in finding solutions that matched painted performance targets.

7.3.2 Design of experiments and strategy calibration

The development of the proposed PGDS entailed several experiments to both assess the accuracy of the system and progressively calibrate it. The method used to conduct those experiments contemplated three different steps: (i) parametric implementation of the building geometry used to perform the several optimization runs, (ii) selection of metrics used in simulation and result analysis, and (iii) Design of Experiments (DoE). The following section summarizes each step.

Implementation of the parametric model

To test the proposed modeling strategy for performance target definition, the authors implemented a parametric model of a free form open-plan building. The building assumes a blob form with an envelope that alternates between concave and convex shapes, therefore inducing self-shading surfaces. Figure 7-8 depicts two building examples, designed by renowned architectural offices, that inspired the hypothetical parametric building, particularly its convoluted roof shape and curvilinear curtain wall. The first building (Figure 7-8, left) is the Crematorium in Kakamigahara, Gifu, Japan, designed by Toyo Ito & Associates, Architects between 2004 and 2006 (Toyo Ito & Associates, 2006). The second example (Figure 7-8, right) is the 2009 Serpentine Gallery pavilion in London, UK, designed by the architectural office SANAA - Kazuyo Sejima + Ryue Nishizawa (SANAA, 2009).

Figure 7-8. Two examples that inspire the hypothetical parametric building used in Strategy E experiments. Left: Crematorium in Kakamigahara, Gifu, Japan. Image source: Toyo Ito & Associates (2006). Right: 2009 Serpentine Gallery pavilion, London, UK. Images adapted from: SANAA (2009).

The floor plan is fixed and oriented north-south in Figures 7-9 and 7-10 The floor plan is deep, particularly on the north side, to promote skylight use, as side lighting becomes insufficient to adequately daylight such deep spaces. The non-conventional building form challenges the designer's light prediction skills while supporting the generation of a wide variety of light distribution patterns, which are more difficult to obtain with more narrow and conventional layouts.

Roof shape, skylight radius, and skylight positioning are the primary parameters of the model. Four parametric interpolated NURBS curves generate the roof shape. The curves define the four

edges of an untrimmed NURBS surface, which is subsequently trimmed by the projection of the floor plan perimeter. Each curve has seven control points, the start and end points fixed at 3.5m height, and five intermediate points with variable z-axis coordinates. The parametric surface generated by these four curves enables the generation of a wide variety of roof designs and building curtain walls. Thus, the parametric roof allows the system to search for different roof designs and different façade height variation patterns to control the interior light levels. The roof can also generate an overhang for shading purposes, with a variable depth (*d*) between 2 and 6 m. The parametric model includes four circular skylights, with parametric radius (*r*) and position specified through their centroid point encoded in parametric surface coordinates *u* and *v*.

Figure 7-9 shows a plan of the implemented parametric model with the variable parameters marked in red. Figure 7-10 presents an axonometric view of the building showing the roof generating curves and their parametric control points.

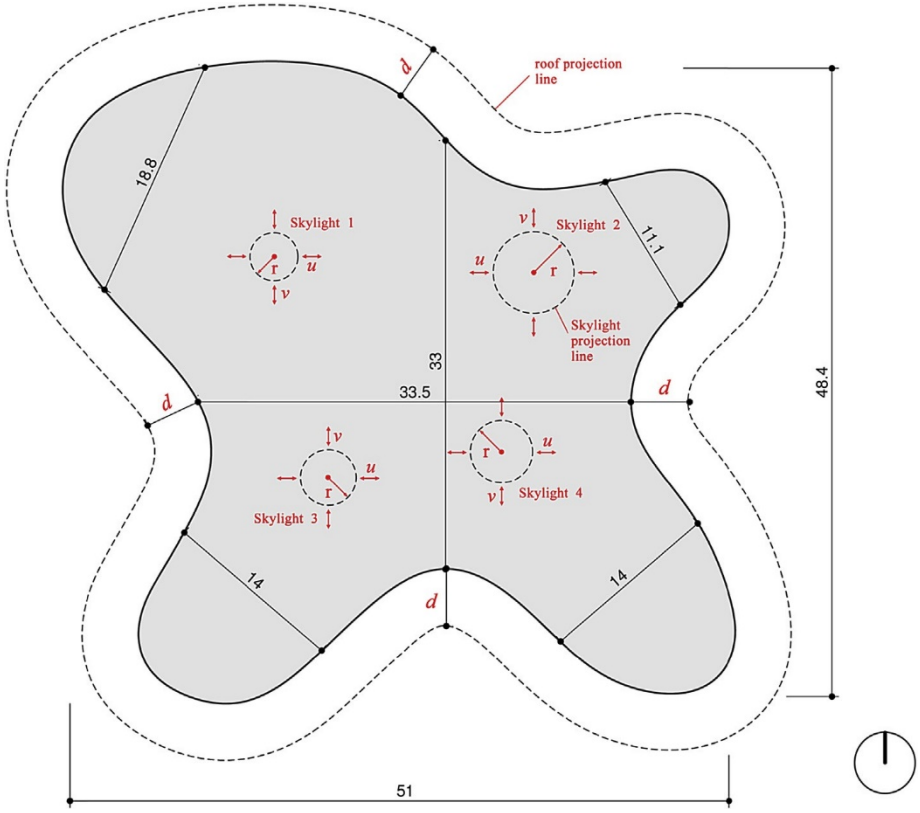

Figure 7-9. Plan of the parametric model. All variable parameters in red.

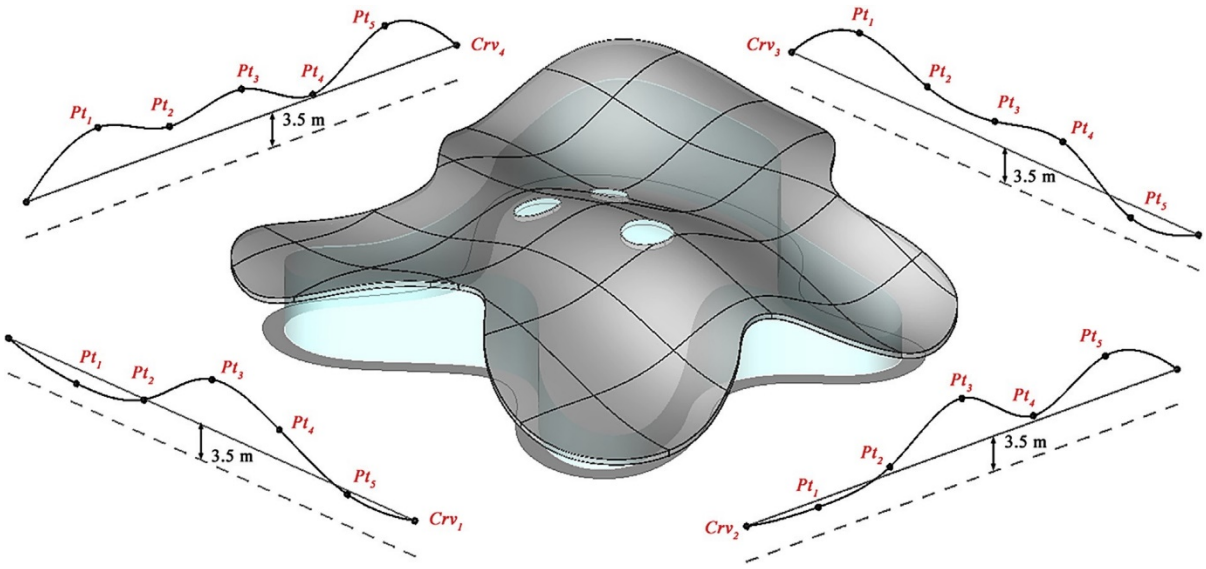

Figure 7-10. Axonometric of the parametric model showing the parametric curves that generate the roof. All variable parameters in red.

Table 7-1. Variable model parameters types and their respective domain.

Parameter	**Description**	**Range**
d	Depth of roof overhang	[2 m, 6 m]
r_n	Radius of each skylight (n)	[0 m, 2.5 m]
$Skylight_n u_n$	u coordinate (u_n) of each skylight center point ($Skylight_n$)	[0, 1]
$Skylight_n v_n$	v coordinate (v_n) of each skylight center point ($Skylight_n$)	[0, 1]
$Crv_n Ptz_n$	Move in the z-axis for each point (Ptz_n) of each generating roof curve (Crv_n)	[1.5 m, 5 m]

Table 7-2 describes the Radiance material properties, both for opaque and transparent surfaces, used in all experiments and simulations.

Table 7-2. Reflectance and Visual Light Transmittance (VLT) of Radiance materials used in the parametric model.

Surface	**Reflectance (%)**	**Visual Light Transmittance (%)**
Outside ground	20	N.A.
Roof cladding	50	N.A.
Curtain wall glass	N.A.	64
Skylight glass	N.A.	64
Interior floor	40	N.A.
Interior ceiling	80	N.A.

The ambient settings that control the calculation of inter-reflected light in Radiance's backward raytracing were the following:

- Ambient resolution (-ab) – four ambient bounces guarantees enough accuracy without a substantial computational burden, making it a suitable number for an optimization cycle which will run a large number of models
- Ambient resolution (-ar) – 300, a reasonable number for a point grid calculation with Radiance's subroutine *rtrace* and for a model of that size
- Ambient divisions (-ad) – 1000
- Ambient sampling (-as) – 500, typically half of -ad
- Ambient accuracy (-aa) – 0.1

Metrics used in simulation, calibration, and strategy validation

Strategy E and its computational implementation supports all current daylight metrics available through DAYSIM (Reinhart and Walkenhorst, 2001) and DIVA (Jakubiec and Reinhart, 2011), including climate-based metrics like Daylight Autonomy (DA), Useful Daylight Illuminance (UDI), and Continuous Daylight Autonomy (CDA). However, this investigation uses Daylight Factor (DF) because of two fundamental reasons:

1) **Computational time**. This work presents an initial prototype that computationally implements Strategy E in an interactive evolutionary generative system for daylight performance-based design. Considering the proof-of-concept nature of the research, the authors selected DF, a fast and easy to compute daylight index, to quickly run several optimization tests. Using more detailed metrics, such as climate-based ones, would entail calculation times incompatible with the phase of tool development and implementation.
2) **Generalized knowledge about DF**. DF is a well-known, non-point-in-time daylight metric, thus more intuitive for designers than more recently developed performance indices such as climate-based annual metrics. As this metric is more familiar to designers who are not daylight experts, it facilitates the use and initial deployment of Painting with Light. Since designers are more familiar with DF, they will be able to paint feasible objectives, a factor that is highly relevant in the quality of the system output.

This investigation used several statistical metrics to compare the different experiments, iteratively calibrate the proposed modeling strategy, and validate the resulting approach. The statistical indices used include CVRMSE, NMBE, absolute difference error (Δ error), absolute difference error average ($\overline{\Delta \text{ error}}$), percentage of error (% error), percentage of error ($\overline{\%\text{ error}}$) percentage of improvement (% of improvement), percentage of area ≤ 25 % error, percentage of area ≤ 10 % error.

Chapter 4, section 4.5.3, already introduced CVRMSE, NMBE, % error, and % of improvement. Nevertheless, it is necessary to contextualize such metrics in the particular scope of the research included in the present chapter.

Percentage of error (% error) is a simple metric commonly used in comparing the results of different simulations. It is a very useful metric in initial assessments because it is easy to

understand. In the following experiments, % error measures the relative deviation between performance targets and the simulated results of the solution found by the proposed system. Nevertheless, this index has often led to a compensation effect, whereby over-estimations cancel underestimations (Hubler, Tupper and Greensfelder, 2010; Coakley, Raftery and Keane, 2014). For that reason, this work uses more advanced statistical indices that better represent the performance of a model such as NMBE and CVRMSE. Chapter 4, section 4.5.3, equation (4-1) describes the % error calculation. The % error average, $\overline{\%\ \text{error}}$, is the arithmetic average of the % error calculated for all sensor nodes. Similarly to work presented in previous chapters, the acceptability threshold for % error is 10%.

CVRMSE and NMBE are indices commonly used in energy model calibration. In this study, both metrics determine how well the search results fit with the target data. CVRMSE does this by capturing offsetting errors between the defined target and simulated data while NMBE by analyzing the variation between the mean difference of the performance targets and the simulation results of the solution found by the system. As discussed in chapter 4, section 4.5.3, NMBE is susceptible to the cancelation effect but CVRMSE is not (Coakley, Raftery and Keane, 2014). Chapter 4, section 4.5.3, equation (4-3) describes CVRMSE, while equation describes (4-6) NMBE. Because there are no guidelines regarding the use of both metrics in daylight simulations, the acceptance criteria used for CVRMSE and NMBE was the same as advanced by ASHRAE guideline 14 for hourly based energy simulations (ASHRAE, 2002): 30% for CVRMSE and ± 10 for NMBE. The hourly threshold of guideline 14 was favored against the monthly one because the number of considered data points is clearly greater than 12, thus better approximating the array size of hourly-based building energy simulations.

The percentage of improvement (% of improvement) measures how much a system solution performance improved compared to a baseline case. In this chapter, this metric traces the evolution of the tool calibration process by comparing each calibration step with an initial calibration status. Chapter 4, section 4.5.3, equation (4-7) defines its calculation.

In the following experiments, the calculation of % error, CVRMSE, and NMBE considered the target performance data as the benchmark data, i.e., the accurate data component (D) of the equations presented in chapter 4, while the simulated data of the solution found by the proposed PGDS as the predicted component (S) of the same equations. Regarding % of improvement, the D and $S\ I$ term defined in chapter 4 corresponds to the comparison benchmark considered in this study and the calibrated version of the approach under study, respectively.

The three metrics used in the subsequent experiments that chapter 4 did not introduce are absolute difference error – Δ error –, its average, $\overline{\Delta\ \text{error}}$, percentage of area ≤ 25 % error, and percentage of area ≤ 10 % error.

The Δ error metric is useful to measure sensor-by-sensor differences in detail, and it is essential in the generation of the Δ map visualization. It constitutes the numerator of % error. Equation (7-1) defines its calculation as follows:

$$\Delta\ error_i = |S_i - T_i| \quad (7\text{-}1)$$

where S_i is the simulation result of the i^{th} sensor in the solution found by the system, and T_i is the objective value set by the user for the same sensor. Similarly to $\overline{\%\ \text{error}}$, $\overline{\Delta\ \text{error}}$ corresponds to the arithmetic average of Δ error across all sensors.

Percentage of area ≤ 25% error is a simple calculation that returns the percentage of area in the first % error quartile. The threshold of the % error is intentionally higher because of the limitation inherent to this index (cancellation effect), and because more accurate metrics (i.e., NMBE and CVRMSE) use a wider acceptance range. The measurement of the % error in the first quartile provides a rough idea of the overall spatial distribution of % error.

Percentage of area ≤ 10% error uses the same method described in percentage of area 25% error but with the typical acceptance threshold used in the early years of building simulation, 10%. Similar to the previous metric, the computation of this index delivers a preliminary estimation of the spatial distribution of % error distribution. Hence, this study does not consider this metric and percentage of area 25% error as the final metric on the deviation error assessment between the solution found by the system and the desired targets.

Design of Experiments (DoE)

The DoE set for calibrating Painting with Light emulates how a typical designer would use the system. In all DoE experiences, the fitness function used by the system applies the goal programming method (Coello, 1999; Aköz and Petrovic, 2007; Biswas and Pal, 2019). This technique is computationally efficient and, if the goals are in the feasible domain of the problem, always yields a dominated solution (Coello, 1999). To further improve the system's search procedure, the authors introduced penalties and weight factors to the goal programming method. Note that the fitness function is a general objective function encoded in the system, and the user does not have direct access to it. The user can only control the function that penalizes high deviations between simulated data and specified targets. The fitness function is agnostic to the daylight metric in use, and its purpose is to guide the optimization search towards the painted targets. For the reasons presented in chapter 2, section 2.3.2 - Metaheuristics, the optimization algorithms used in these experiments are GA-based. The implementation of the strategy in the Rhino+Grasshopper environment also determined the selection of optimization algorithms of the GA family. The Integrated Development Environment (IDE) of Rhino+Grasshopper provides easy access both to single- and multi-objective genetic algorithms. Nevertheless, the modular nature of the approach makes the strategy agnostic to the search approach adopted. Thus, it is possible to couple the strategy with different optimization algorithms.

The investigation entailed five testing experiments. The first four experiments consisted of progressive refinements on the formulation of the optimization algorithm objective function, by experimenting with methods for error computation as the primary way for improving Painting with Light prediction capabilities. After calibrating the system, the investigation entailed a final validation experiment to assess if Painting with Light could find a solution, for which the "optimum" value was already known. This validation experiment consisted of performing a DF calculation of an arbitrary building geometry and feed its results as the painted targets to the proposed tool. The following briefly describes the five experiments:

Experiment 1 - The first test used the SGA provided by Galapagos (Rutten, 2011). Galapagos' genetic algorithm is a standard, single-fitness GA. The fitness function applied in this experiment was a simple minimization of the sum of the averages of the absolute difference between simulation results (*S*) and performance targets (*T*). Equation (2-4) describes the search problem and its fitness function.

$$\min_{S_i,T_i \in \mathbb{R}^+} F(S_i,T_i) = \sum_{i=1}^{n} |S_i - T_i| \qquad (7\text{-}2)$$

where S_i is the simulation result of the i^{th} sensor in the solution found by the system, T_i is the objective value set by the user for the same sensor, and n is the number of sensors.

Experiment 2 - Still using Galapagos' SGA, the second experiment added penalties to the cost function defined in experiment 1 as a way to penalize significant deviations between the simulated results and their corresponding goals. The penalty attempts to force the system to find solutions that better match the painted objectives. Equation (2-7) defines the optimization problem and presents the penalized objective function.

$$\min_{S_i,T_i,p_i \in \mathbb{R}^+} F(S_i,T_i,p_i) = \sum_{i=1}^{n} |S_i - T_i| + p_i(S_i,T_i) \qquad (7\text{-}3)$$

where p_i is the penalty factor added to the absolute difference between S_i and T_i in the i^{th} sensor. The penalty value p_i calculation depends on the difference between S_i and T_i varying exponentially with it.

Experiment 3 - This experiment adds a weighting factor to the penalized fitness function. The goal was to minimize distortion effects in the computation of the overall cost. The weighting factor aimed to distribute the penalties better, balancing them according to the weight of the respective goal area. In this way, the system can smooth out significant deviations if they occur in a relatively small goal painted area. Equation (7-4) formulizes the optimization process and its fitness function.

$$\min_{S_i,T_i,p_{i,} \in \mathbb{R}^+, w_j \in]0,1[} F(w_j,S_i,T_i,p_i) = \sum_{j=1}^{m} \sum_{i=1}^{n_j} |S_i - T_i| + p_i(S_i,T_i) \ . w_j \qquad (7\text{-}4)$$

where w_j is the target area weighting factor, m is the number of target performance bins, i.e., the number of painted target areas, n is the number of nodes in each target area, Si is the simulation result, Ti the objective value, and p_i the penalty factor for the i^{th} sensor in the corresponding target area. The weighting scalar reflects the normalized area of each painted performance target bin (color) in the overall sensor grid. The function above shows that each performance target color has its own weighting factor that affects the penalized error in each of its sensors.

Experiment 4 - The fourth experiment used a slightly improved painted target (i.e., a more feasible one) and Octopus GA as the search mechanism. The reason for using a different GA was that Galapagos GA tends to find more local minima as the complexity of the problem increases (Rutten, 2011). Thus, the experiment tested the more robust Strength Pareto Evolutionary Algorithm 2 (SPEA 2) (Ziztler, Laumanns and Thiele, 2002) available through Octopus Grasshopper add-on.

The fitness function was the same as in experiment 3, but the penalty function that calculates the penalty factor was redefined to penalize less the sensor nodes that reported a performance closer to their corresponding target, and to penalize heavily the ones that register high deviations. To enable the system to use a Pareto GA to optimize a problem with a single cost function, the authors added genetic diversity as a neutral second optimization vector, i.e., as an objective that does not produce an effect on the search as recommended by Octopus user guidelines (Vierlinger, 2012).

Experiment 5 - After the approach calibration, the work entailed a final validation experiment. The fifth experiment used the results of a pre-defined design as painted goals, to assess if the system was able to find a solution similar both in performance and in design features. Considering that the painting goal interface depends on the user knowledge about light decay, which can be imprecise, this validation experiment also allowed to evaluate the impact of inputting a highly accurate, and therefore feasible, painted target space into the system. Nevertheless, since this experiment uses experiment 4 objective function, there was the need to discretize the target results by dividing their reported range into four bins.

7.3.3 Results

The following sections report the results for each experiment planned in the DoE.

Experiment 1

Figure 7-11 shows the geometry proposed by Painting with Light in experiment 1. Figure 7-12 shows the painted performance targets, the proposed solution DF performance, and the spatial mapping of their difference. The generated overhang (*d*) is 5 m deep.

The colors used in the painted targets were: Red: 10% DF; Orange: 7% DF; Yellow: 5% DF; Light yellow: 4% DF. Table 7-3 shows the values of the roof design variables, while Table 7-4 reports the skylights variables.

The system proposed a deep overhang of 5 m, to respond to the fact that the user did not predict in the painted targets that higher Daylight Factor levels usually occur closer to the facades. As for the four skylights, only one of them was wrongly positioned, but its radius was so small that it had little effect on the design performance. The other three are quite accurately positioned and have radiuses that vary from 1.24 m to 2.10 m. It is possible to observe that the system tried to aggregate two skylights in an attempt to match the elliptical red area painted in the southeast part of the building. The system also slightly elevated the northwest corner of the roof to increase the glazing area and achieve higher light levels close to the red spot painted in the northwest corner. However, as we can see in the difference map, the system missed most of the DF targets by underestimation. Painting with Light failed to meet the goals set for the northwest corner, which requested a skylight directly above them.

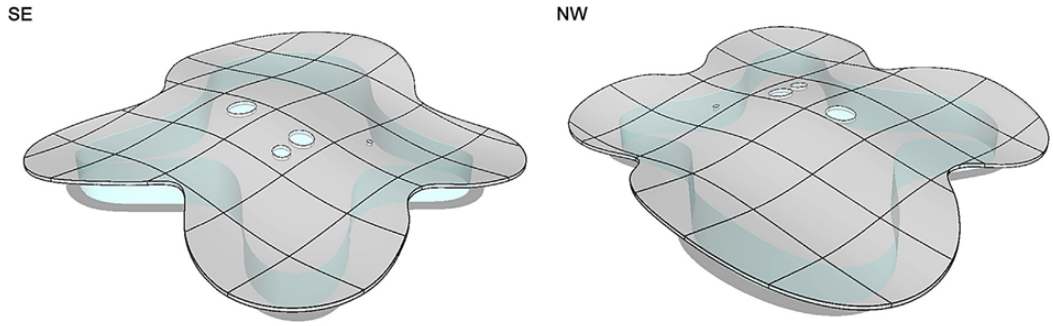

Figure 7-11. Views of experiment 1 solution. Left: southeast perspective. Right: northwest perspective.

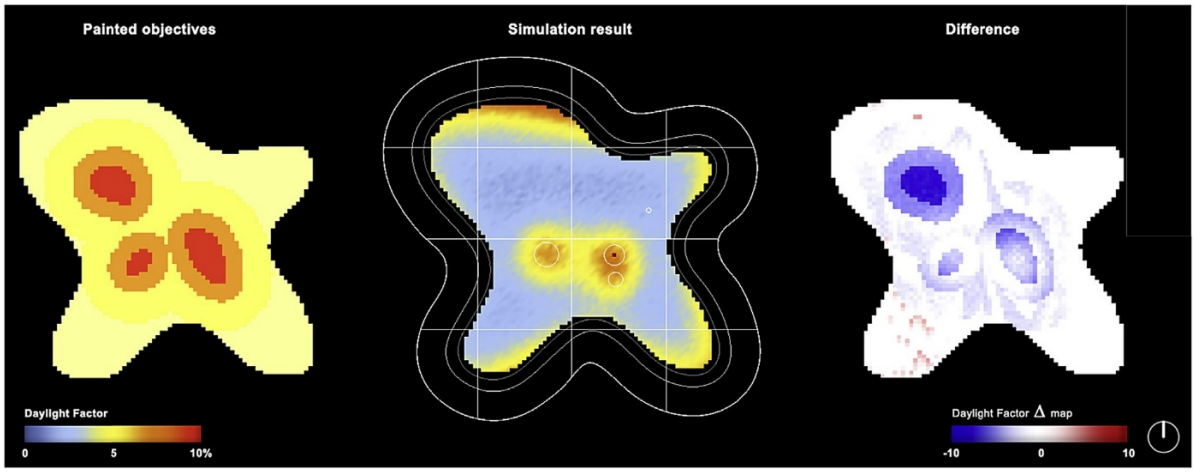

Figure 7-12. Experiment 1 visual results overview. Left: painted objectives. Center: daylight factor simulation results of the solution proposed by the system. Right: difference (Δ) heatmap between painted objectives and simulation results.

Table 7-5 shows the average of absolute difference and % error for each target color/DF levels and the overall space. It shows that the largest deviation between painted objectives and proposed solution performance is in the 10% and 7% DF target areas. The percentage of area ≤ 25% and ≤ 10% error are both small, 6.59% and 21.87%, respectively. NMBE of this experiment is 53.06%, and the CVRMSE is 77.46%, both very far for the acceptance criteria assumed for those metrics.

The poor results of this experiment are the result of two factors: the unfeasibility of the painted target solution that came about because of the user's lack of understanding of how DF works spatially in this experiment; and the distortion introduced by the necessary averaging on the fitness calculation for Galapagos GA.

Table 7-3. Experiment 1 roof design parameter results.

	PtZ_1 [m relative to 3.5 m]	**PtZ_2** [m relative to 3.5 m]	**PtZ_3** [m relative to 3.5 m]	**PtZ_4** [m relative to 3.5 m]	**PtZ_5** [m relative to 3.5 m]
Crv1 (South)	1.1	1.5	1.8	0.8	0.1
Crv2 (East)	2.7	2.9	3.9	1.4	3.8
Crv3 (North)	0.8	1.1	2.1	1.1	1.3
Crv4 (West)	2	0.2	2.1	1.4	3.3

Table 7-4. Experiment 1 Skylight design parameter results.

	U [0-1]	**V** [0-1]	**Radius** [m]
Skylight 1	0.54	0.48	2.1
Skylight 2	0.62	0.54	0.4
Skylight 3	0.57	0.44	1.24
Skylight 4	0.56	0.48	2.5

Table 7-5. Total and partial averages for absolute difference and percentage of error between desired goals and system output in Experiment 1.

Goal area	$\overline{\textbf{Δ error}}$ [DF]	$\overline{\textbf{\% error}}$
10% DF (red)	3.37	56.2
7% DF (orange)	2.08	48.1
5% DF (yellow)	1.1	41.6
4% DF (light yellow)	1.97	29
Total	2.2	44

Experiment 2

Figure 7-13 illustrates the design solution found by the system in this experiment. Figure 7-14 presents the performance of the solution and the painted objectives. Painting with Light modeled one overhang of 2.36 m. The painted targets are more feasible in this experiment, namely on the perimeter, where the user painted higher DF values. Table 7-6 and Table 7-7 report the design variable values for this experiment. 7-17 quantifies the average of absolute difference and % error between painted objectives and the design solution proposed by Painting with Light.

The system proposed a solution with an almost flat roof slightly tilted towards the East. The resulting glass facade has approximately the same height in all directions. The overhang is less deep than the one created in the first experiment, measuring 2.36 m. These results are consistent with the higher DF targets set for the perimeter in this experiment. The system produced a solution that is more compatible with the defined goals that depend on top lighting. The PGDS created four skylights: a group of two to match the elliptical red target area (10% DF) on the Southeast area of the building one for the Southwest red target values, and one for the Northwest red target area. Once again, Painting with light joins two circular skylights in an attempt to match the red target's elliptical shape.

However, the difference map shows that, although it did better than in the first experiment, the system was still unable to accurately locate the Northwest skylight, generate the correct skylight radius, and produce a balanced solution between the curtain glass height and the overhang. The result produced some over lit areas (the narrower convex areas of the building) and a large blue dim area, which does not correspond to the DF pattern target painted by the user.

In general, the average % error decreased in all the target areas for experiment 2. However, the average absolute difference increased as a result of some outlier data points. Although both the percentage of area ≤ 25% and ≤ 10% error increased, to 31.4% and 15.5% respectively, they still indicate that a large portion of the sensor node grid misses the target criteria. The NMBE and CVRMSE score confirm that preliminary indication. The NMBE scored 38.3%, and the CVRMSE 69.04%, both still far from their acceptance range criteria.

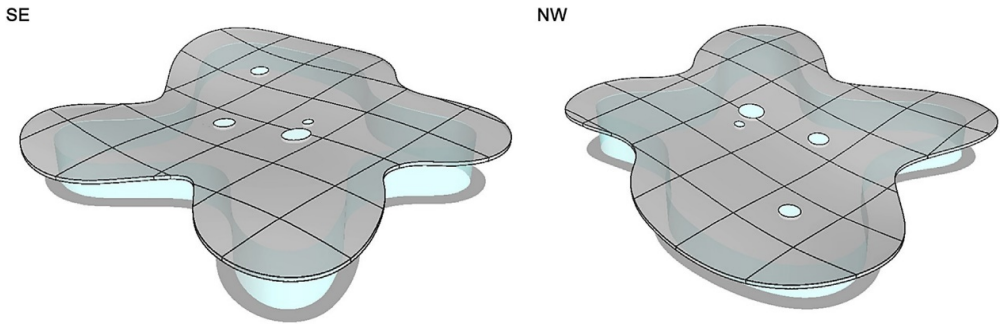

Figure 7-13. Views of experiment 2 solution. Left: southeast perspective. Right: northwest perspective.

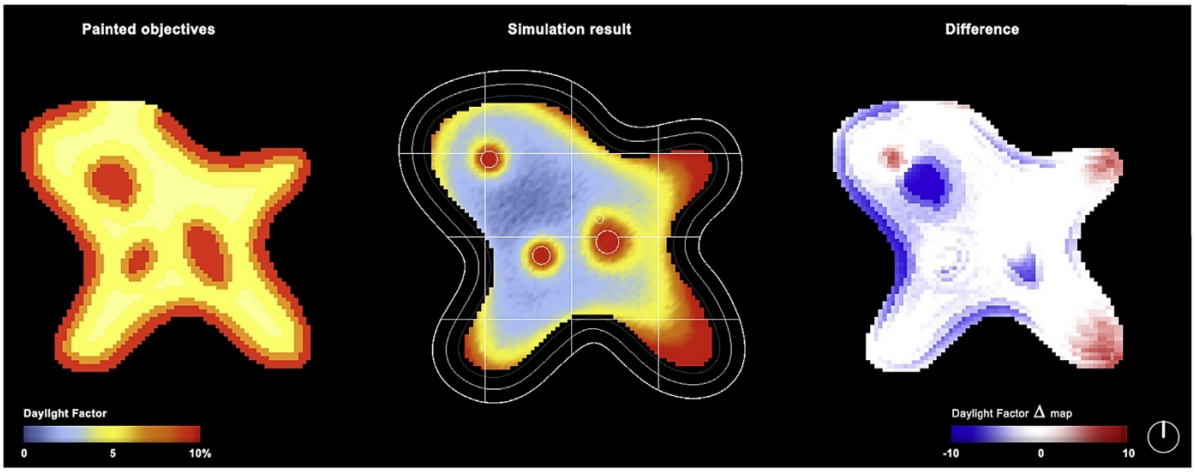

Figure 7-14. Experiment 2 visual results overview. Left: painted objectives. Center: daylight factor simulation results of the solution proposed by the system. Right: difference (Δ) heatmap between painted objectives and simulation results.

Table 7-6. Experiment 2 roof design parameter results.

	PtZ_1 [m relative to 3.5 m]	**PtZ_2** [m relative to 3.5 m]	**PtZ_3** [m relative to 3.5 m]	**PtZ_4** [m relative to 3.5 m]	**PtZ_5** [m relative to 3.5 m]
Crv1 (South)	0.3	0.5	1.2	2.2	1.1
Crv2 (East)	0.1	1.4	1.8	0.4	1.1
Crv3 (North)	1.2	2	1.8	1.5	1.1
Crv4 (West)	0.7	2.2	0.3	2	3.3

Table 7-7. Experiment 2 Skylight design parameter results.

	U [0-1]	**V** [0-1]	**Radius** [m]
Skylight 1	0.54	0.53	0.75
Skylight 2	0.38	0.62	1.42
Skylight 3	0.46	0.47	1.52
Skylight 4	0.55	0.49	1.95

Table 7-8. Total and partial averages for absolute difference and percentage of error between desired goals and system output in Experiment 2.

Goal area	**$\overline{\Delta}$ error** [DF]	**$\overline{\%}$ error**
10% DF (red)	4.15	41.5
7% DF (orange)	2.9	41.6
5% DF (yellow)	2	40
4% DF (light yellow)	1.43	38.9
Total	**2.65**	**40**

Experiment 3

Figures 7-15 and 7-16, and Tables 7-9 to 7-11 report experiment 3 results. The generated overhang (*d*) for this experiment is 2 m deep.

The design solution found by the system is very similar to that of experiment 2. However, the glass curtain wall is slightly higher, which improved the solution performance in the perimeter. The radiuses of the skylights are also slightly larger, further approximating DF criteria for inner areas. However, the proposed skylight locations are still inadequate, namely for the Northwest targets. This experiment reported a higher percentage of area in the first quartile of 25% error and 10% error: 44,77%, and 21.84%, respectively. Although NMBE improved to 17.2% and CVRMSE to 55.23%, they still did not meet their acceptance range.

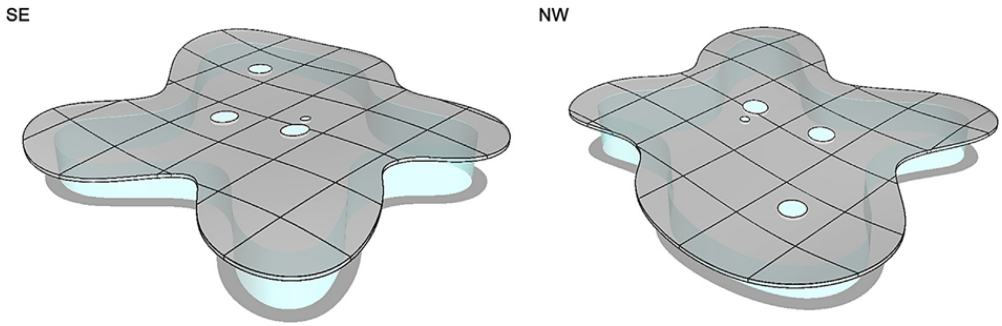

Figure 7-15. Views of experiment 3 solution. Left: southeast perspective. Right: northwest perspective.

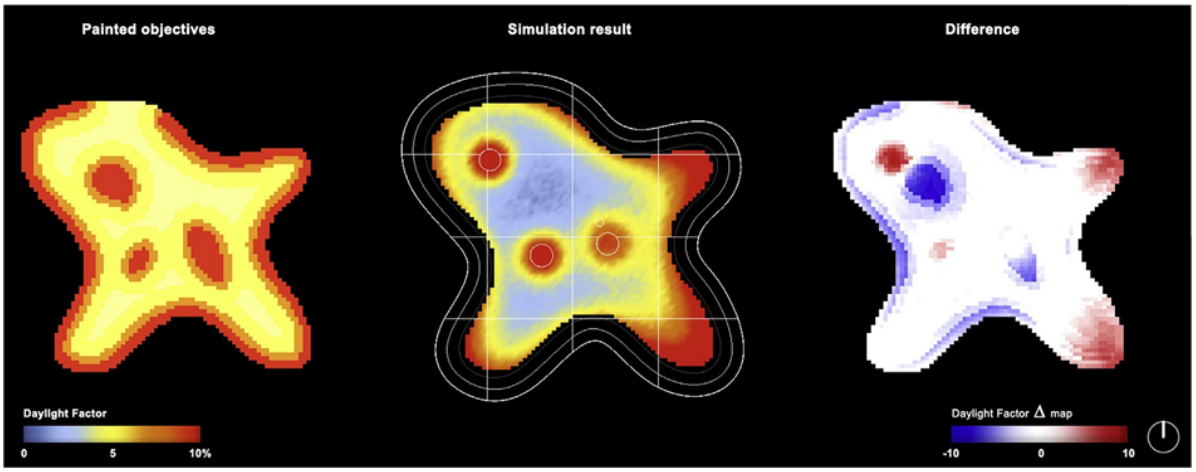

Figure 7-16. Experiment 3 visual results overview. Left: painted objectives. Center: daylight factor simulation results of the solution proposed by the system. Right: difference (Δ) heatmap between painted objectives and simulation results.

Table 7-9. Experiment 3 roof design parameter results.

	PtZ_1 [m relative to 3.5 m]	**PtZ_2** [m relative to 3.5 m]	**PtZ_3** [m relative to 3.5 m]	**PtZ_4** [m relative to 3.5 m]	**PtZ_5** [m relative to 3.5 m]
Crv1 (South)	0.2	0.5	1.2	2.1	1
Crv2 (East)	0	1.2	1.8	0.4	1.1
Crv3 (North)	1.1	2	1.7	1.5	1.1
Crv4 (West)	1	2.5	1.5	2	2.5

Table 7-10. Experiment 3 Skylight design parameter results.

	U [0-1]	**V** [0-1]	**Radius** [m]
Skylight 1	0.54	0.52	0.7
Skylight 2	0.38	0.62	1.85
Skylight 3	0.46	0.47	1.95
Skylight 4	0.55	0.49	1.9

Table 7-11. Total and partial averages for absolute difference and percentage of error between desired goals and system output in Experiment 3.

Goal area	**$\overline{\Delta}$ error** [DF]	**$\overline{\%}$ error**
10% DF (red)	3.6	35.8
7% DF (orange)	2.5	35.6
5% DF (yellow)	1.68	33.5
4% DF (light yellow)	1.4	38.1
Total	**2.3**	**36**

Experiment 4

Figures 7-17 and 7-18 show the solution found in the fourth experiment. Tables 7-12 and 7-13 show the design variables. The overhang depth (d) is 2.9 m. 7-13Table 7-14 reports the absolute deviation and the percentage of error between the painted targets and the design performance.

Building from the previous experiences, this experience used a more feasible painted target. All the perimeter nodes were set to higher values, and the inner red focus assumed a more circular shape since the parametric model could only generate circular skylights.

The solution found by the system generated a roof that achieves a good balance between facade height and overhang depth, better matching the painted objectives in the building perimeter. Thus, the system lowered the facade in the narrow southeast and southwest zones and raised it in the northwest quadrant, which has a deeper floor plan, generating a wavy rooftop with a central elevated bump area. Regarding the skylights, Painting with Light search mechanism only created three in this experiment, probably due to the approximation of the interior painted red spots to a circular shape. The skylights match the location of the inner red painted areas, and their radius are consistent with the defined target performance pattern. We can observe that the system located the largest skylights in the highest area of the rooftop. In contrast, the northwest skylight is smaller and placed in a location where the roof is relatively low, thus not needing to open as much to provide the required amount of light to meet the desired targets for that area. Overall, the difference map indicates that the solution met the vast majority of the desired results.

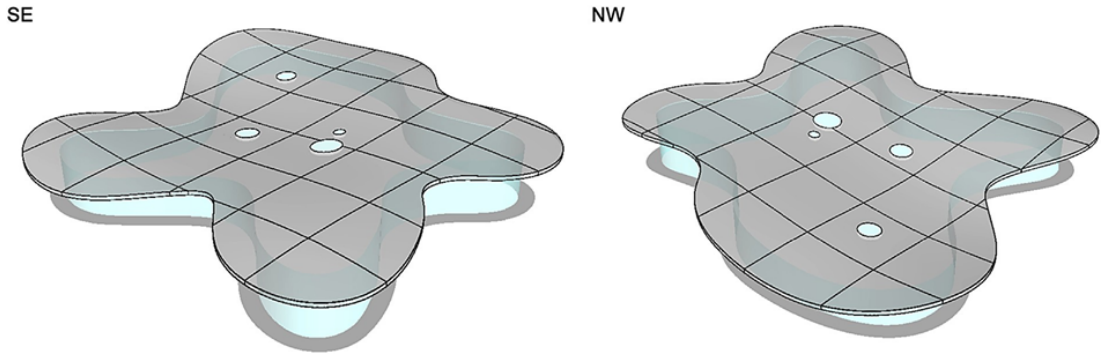

Figure 7-17. Views of experiment 4 solution. Left: southeast perspective. Right: northwest perspective.

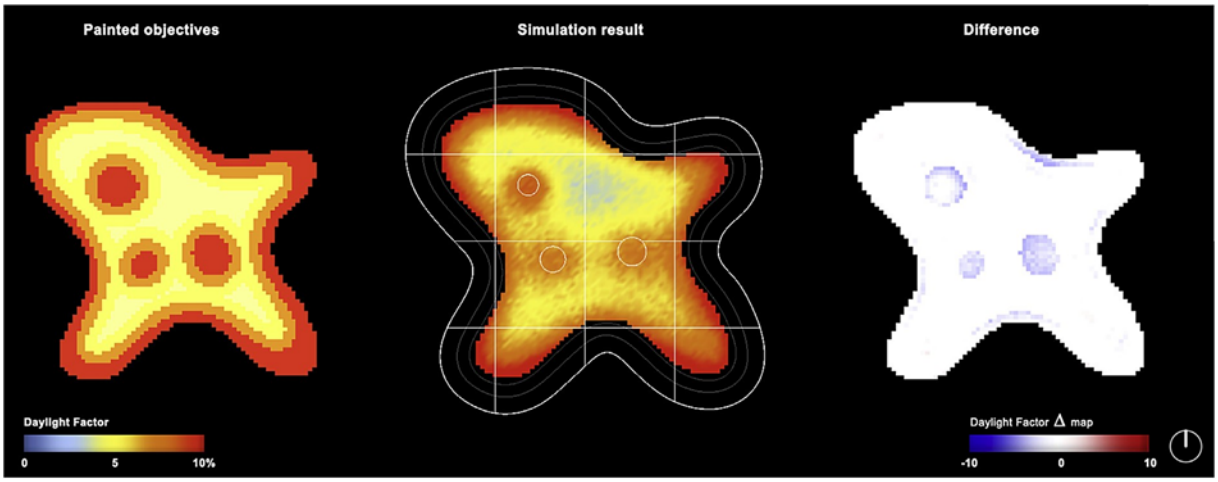

Figure 7-18. Experiment 4 visual results overview. Left: painted objectives. Center: daylight factor simulation results of the solution proposed by the system. Right: difference (Δ) heatmap between painted objectives and simulation results.

The % error average was kept below 20% ranging from 10.4% (for the 7% target areas) and 18,4% (for the 5% target zone). The percentage of area ≤ 25% error increased dramatically to 77.24%. The percentage of area ≤ 10% error is now 52.21%. The reported NMBE of 1.54% is significantly below the acceptance threshold of ± 10%. Similarly, the CVRMSE registered a value of 20.17%, almost 10% below the acceptance criterion used for this index, 30%.

Results for this experiment produced a pattern that matches well the painted DF target distribution, and statistical error measurements for NMBE and CVRMSE were acceptable. However, it is possible to further calibrate the system by manipulating the definition of the fitness function, e.g., redefining the fitness and penalty functions, or inputting an improved DF target.

Table 7-12. Experiment 4 roof design parameter results.

	PtZ_1 [m relative to 3.5 m]	**PtZ_2** [m relative to 3.5 m]	**PtZ_3** [m relative to 3.5 m]	**PtZ_4** [m relative to 3.5 m]	**PtZ_5** [m relative to 3.5 m]
Crv1 (South)	1.5	0.6	4.4	2.5	0.9
Crv2 (East)	1.2	0.2	4.4	0.1	3.4
Crv3 (North)	1.5	2.7	1.7	2.1	4.4
Crv4 (West)	4.3	1.8	2.9	0.2	4

Table 7-13. Experiment 4 Skylight design parameter results.

	U [0-1]	**V** [0-1]	**Radius** [m]
Skylight 1	0.42	0.58	1.75
Skylight 2	0.57	0.48	2.4
Skylight 3	0.59	0.34	0
Skylight 4	0.45	0.47	2.15

Table 7-14. Total and partial averages for absolute difference and percentage of error between desired goals and system output in Experiment 4.

Goal area	**$\overline{\Delta}$ error** [DF]	**$\overline{\%}$ error**
10% DF (red)	1.62	16.15
7% DF (orange)	0.76	10.8
5% DF (yellow)	0.92	18.4
4% DF (light yellow)	0.88	22
Total	**1.08**	**16.3**

Experiment 5

The top two images of Figure 7-19 show the pre-defined building design that Painting with Light was asked to find, which was the one that produced the DF target system input. The bottom two images of Figure 7-19 show the design found by the Painting with Light, which is very close to the original design. Figure 7-20 shows the performance of the solution generated by the system and compares it with the desired goals. Tables 7-15 and 7-16 report the design variables of the pre-defined building, while tables 7-177-17 and 7-18 show the values found by the implemented strategy. Table 7-19 shows the absolute deviation and the % error between the pre-defined test geometry and the Painting with Light solution results. The overhang (*d*) of both solutions is 0.5 m.

The overall shape of the roof that the system generated is very similar to that of the target building, which is particularly remarkable given the formal variation that the parametric model supports. As for the skylights, although the system generated only two skylights rather than the four skylights of the pre-shaped solution, it was capable of producing a solution whose performance is very close to the painted one.

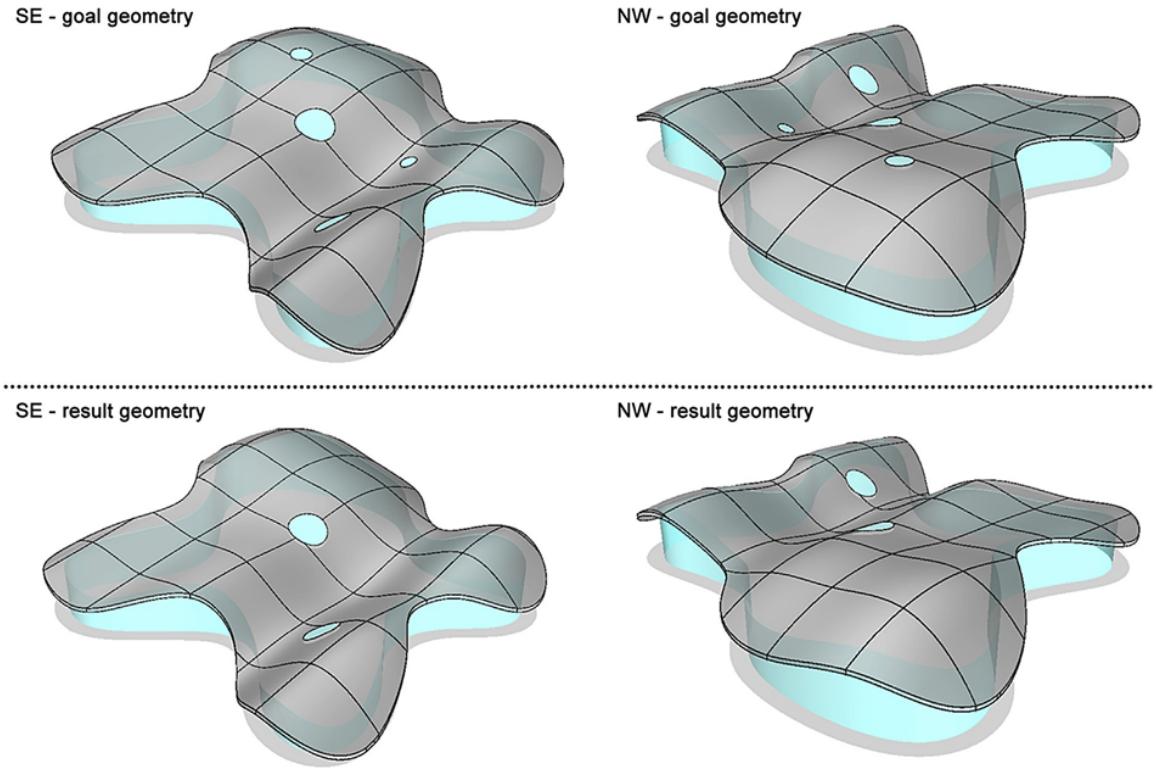

Figure 7-19. Perspective views of experiment 5 solutions. Top: pre-defined test solution, which DF simulated results served as painted targets for the system. Bottom: Solution found by painting with light.

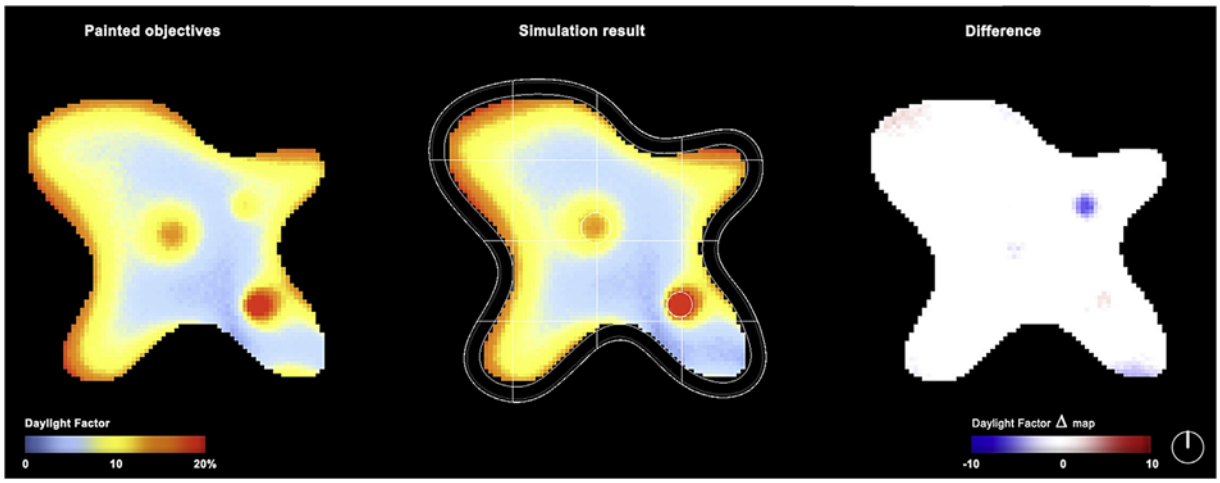

Figure 7-20. Experiment 5 results spatially mapped. Left: painted objectives, deriving from DF simulation of pre-determined geometry. Center: daylight factor simulation results of the solution proposed by painting with light. Right: difference (Δ) heatmap between painted objectives and simulation results.

Table 7-15. Experiment 5 pre-defined building roof design target values.

	PtZ_1 [m relative to 3.5 m]	**PtZ_2** [m relative to 3.5 m]	**PtZ_3** [m relative to 3.5 m]	**PtZ_4** [m relative to 3.5 m]	**PtZ_5** [m relative to 3.5 m]
Crv1 (South)	2.4	0.2	0.2	1.5	1.7
Crv2 (East)	1.5	1.5	1.5	1.4	1.4
Crv3 (North)	0.8	1.4	1.7	2.8	1.8
Crv4 (West)	1.5	1.5	0.2	1.5	0.4

Table 7-16. Experiment 5 pre-defined building skylight design target values

	U [0-1]	**V** [0-1]	**Radius** [m]
Skylight 1	0.62	0.41	2.0
Skylight 2	0.4	0.59	1.5
Skylight 3	0.6	0.55	1
Skylight 4	0.5	0.51	2.5

Table 7-17. Experiment 5 building roof design solution parameter results.

	PtZ_1 [m relative to 3.5 m]	**PtZ_2** [m relative to 3.5 m]	**PtZ_3** [m relative to 3.5 m]	**PtZ_4** [m relative to 3.5 m]	**PtZ_5** [m relative to 3.5 m]
Crv1 (South)	1.4	0.3	1.6	1.5	0.1
Crv2 (East)	1.5	1.5	1.5	1.4	1.3
Crv3 (North)	2	1.4	0.3	2.8	4.1
Crv4 (West)	1.5	1.5	0.2	1.5	0.4

Table 7-18. Experiment 5 skylight design parameter results.

	U [0-1]	**V** [0-1]	**Radius** [m]
Skylight 1	0.5	0.52	2.5
Skylight 2	0.72	0.34	0
Skylight 3	0.62	0.41	2.06
Skylight 4	0.73	0.6	0

Table 7-19. Total and partial averages for absolute difference and percentage of error between desired goals (pre-defined solution DF results) and system output in Experiment 5.

Goal area	$\overline{\textbf{Δ error}}$ [DF]	$\overline{\textbf{\% error}}$
15-20% DF (red)	1.5	8.3
10-15% DF (orange)	0.94	8.1
5-10% DF (yellow)	0.8	9.1
0-5% DF (light yellow)	0.5	9.5
Total	**0.8**	**8.8**

On average, the % error of the solution found by Painting with Light never goes beyond 10%. The difference map of Figure 7-20 shows minimal deviation, The difference map of Figure 7-20 shows minimal deviation, except for a NE area, which corresponds to a skylight of the predefined solution that the system did not generate. The percentage of area ≤ 25% error increased to 94.4%. The percentage of area ≤ 10% error increased to 67%. NMBE is 0.34% and CRMSE is 12.42%, yielding the best results of all the experiments.

The area weights used in the penalty function could be one of the reasons why Painting with Light did not find the two smaller skylights of the predefined solution. Because the area

affected by these skylights was quite small, they had little impact on the overall performance, thus making the system focus more on finding a better match to the larger areas of the painted goals. Figure 7-19 also shows that Painting with Light proposed minor differences on the facade, namely in the NW quadrant, to compensate for the absence of the NW skylight that contributed to higher DF values on that corner of the pre-calculated design.

This final validation experiment showed that Painting with Light is currently able to find solutions reasonably close to the optimum, giving a well painted, feasible solution space.

7.3.4 Discussion

The comparison of the different DoE experiments shows the impact of improving the definition of DF targets in system calibration. Figure 7-21 shows the progress of the percentage of area ≤ 25% error, and Figure 7-22 the incremental improvement of percentage of area ≤ 10% error. Figure 7-23 reports the evolution of the other metrics used in this study. The bar chart present in Figure 7-24 shows the percentage of improvement of all the experiments compared to experiment 1. However, because the first experiment was an initial trial that reflected the little knowledge the user had about DF spatial behavior, the analysis entails a second percentage of improvement study, which compares the experiments with a similar DF target pattern – experiment 2, 3, and 4. Figure 7-25 shows the pattern of improvement of experiment 3 and 4 when compared to experiment 2.

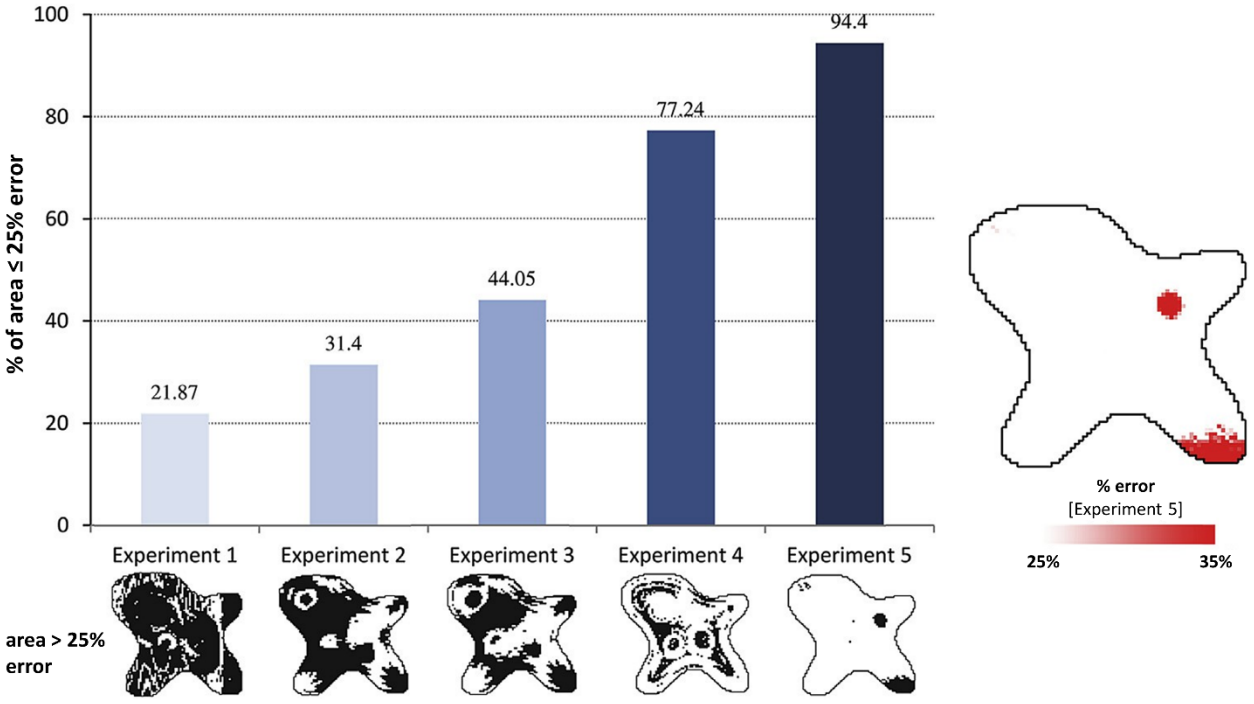

Figure 7-21. Total percentage of area ≤ 25% error between painted targets and simulation results on each experiment. Below each experiment bar there is a plan that locates the areas where percentage error is above 25%. On the right, a heatmap shows the nodes between 25% to 35% of error, to visualize the deviation pattern for the area above 25%.

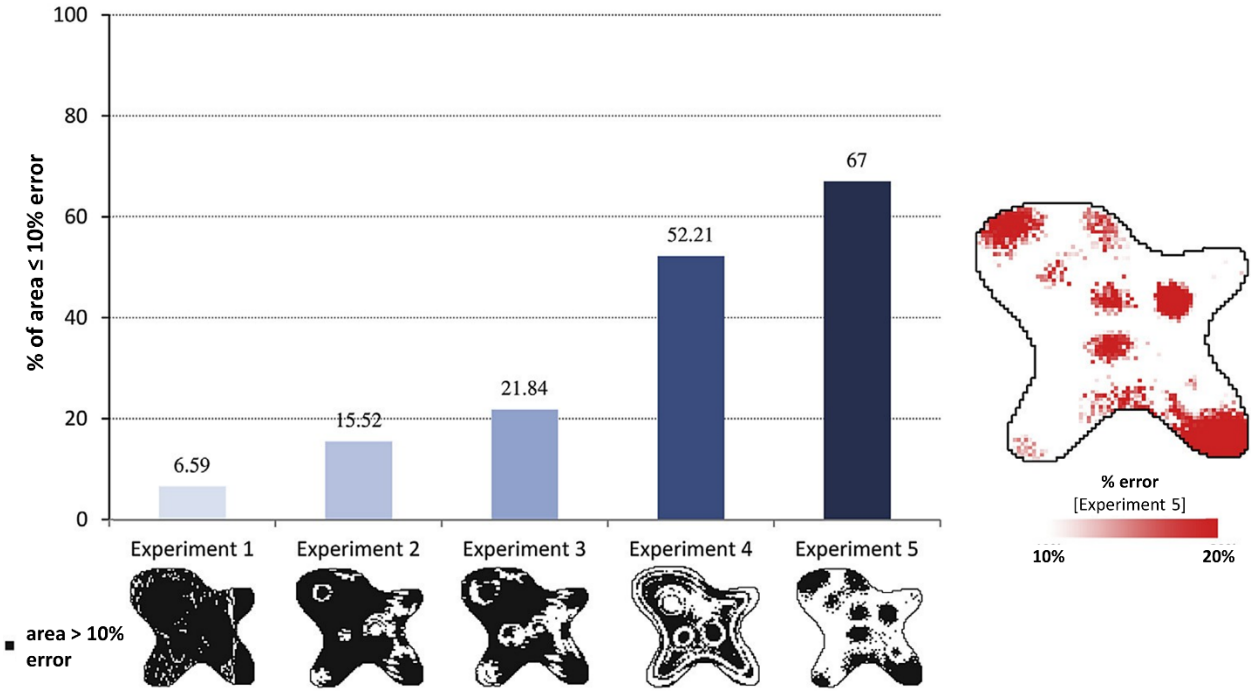

Figure 7-22. Total percentage of area ≤ 10% error between painted targets and simulation results on each experiment. Below each experiment bar, there is a plan that locates the areas in which % error is above 10%. On the right, a heatmap assesses the deviation pattern in the area above 10% of error by showing the nodes whose % error is between 10 and 20%.

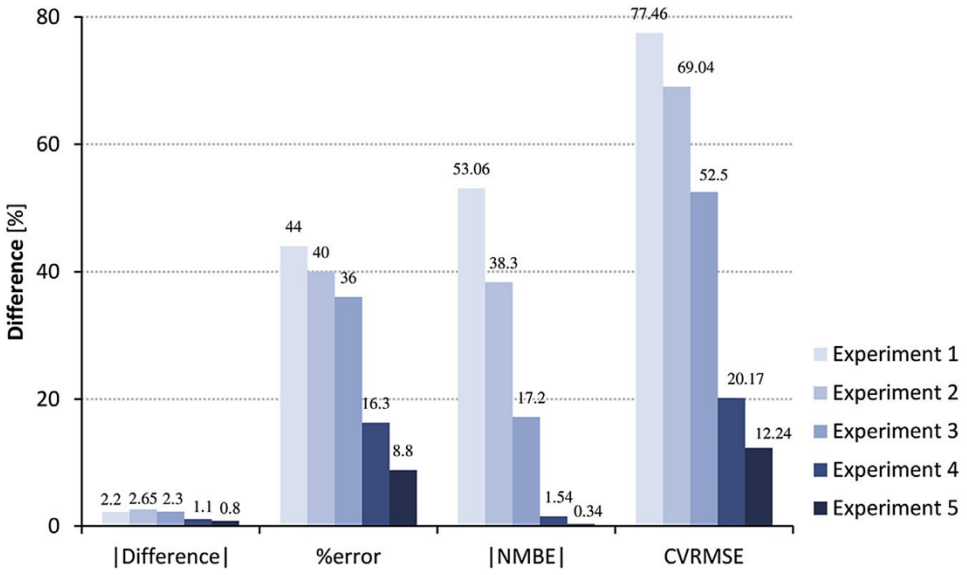

Figure 7-23. Difference between painted goal averages and DF results of the solutions found by the implemented strategy – Painting with Light – in the five experiments.

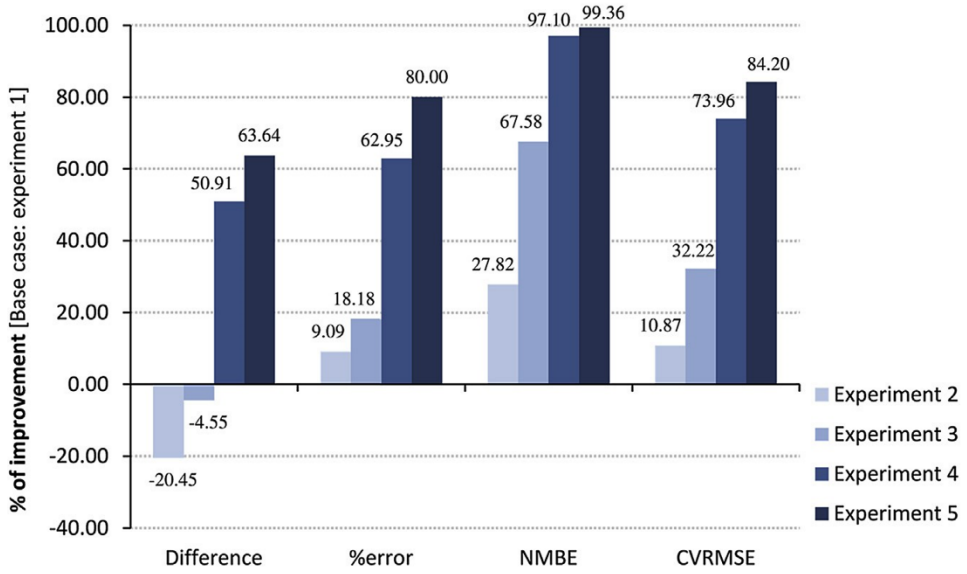

Figure 7-24. Percentage of improvement in the different error metrics of experiment 2, 3, and 4 when compared to experiment 1.

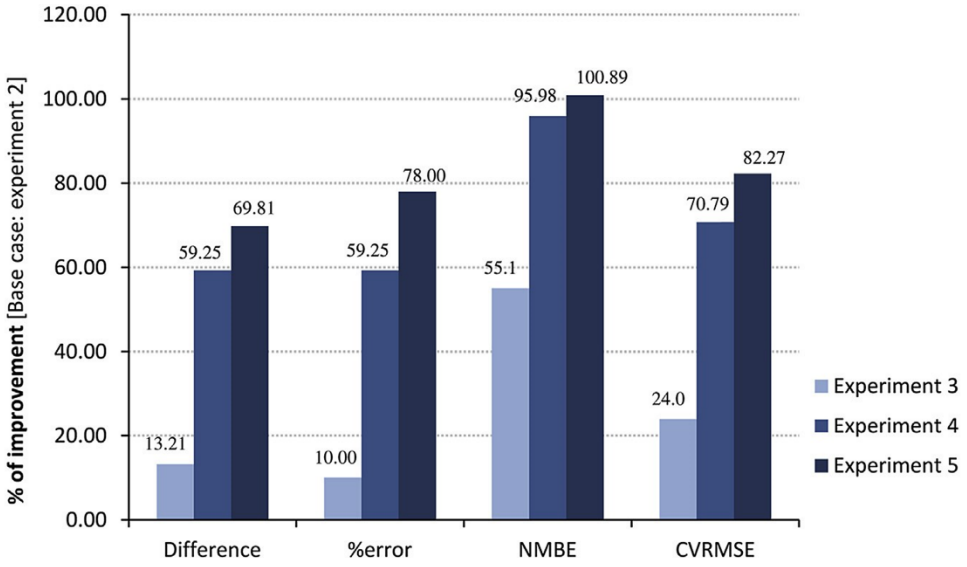

Figure 7-25. Percentage of improvement in the different error metrics of experiment 3, and 4 when compared to experiment 2.

The modifications introduced in experiment 2 only slightly improve the error reported in experiment 1. The percentage of area ≤ 25% error increased 9.53%, the percentage of area ≤ 10% error 8.93%, the global % error average decreased 4%, the NMBE 14.76%, and the CVRMSE only 8.42%. Those results indicate that while it provided a painted performance target with patterns closer to the real DF decay effect, the system still had difficulties in finding a good solution. This unsatisfying improvement is related to the averaging problems of the fitness function. Although the system uses a penalty function in experiment 2 the distribution

of the penalties did not consider the spatial weight of each target areas. Thus, the resulting fitness function could be biased by some outlier data points that had little relevance in the overall performance.

The introduction of weighting factors that express spatial bias in experiment 3 produced a noticeable improvement. However, those improvements were still far from the acceptance threshold assumed for NMBE and CVRMSE. Compared with the first experiment, experiment 3 improved 18.18% in % error, 67.58% in NMBE, and 32.22% in CVRMSE. The significant NMBE improvement is normal since this index is susceptible to the cancellation effect, where a positive bias compensates for a negative one. The high contrast between blue and red areas in experiment 3 solution DF results indicates that the system resorts to compensation mechanisms to smooth out the average error. In contrast, CVRMSE is not susceptible to the cancellation effect; thus, it reports a slight improvement. It is worth mentioning that the absolute difference average in experiment 2 and 3 appears to be worse than in experiment 1. However, outlier data points are biasing the absolute difference in experiment 1, thus distorting its average. In summary, when compared with experiment 1, experiment 3 indicates that the system could be further improved through calibration.

Nevertheless, the improvements introduced by experiment 3 are far from being relevant. For example, CVRMSE improved 24%, and the mean % error 10%. Those small improvements indicate that the search process could be hampered from the inherent limitations of the optimization algorithm, thus trapping the search in a local minimum. A comparison between the designs of the two solutions also supports this observation – the design solutions of experiments 2 and 3 were very similar.

Experiment 4 reports a considerable improvement in the system's performance in finding the painted goals. Steeping the penalty function curve but especially using a more robust GA (SPEA2) produced a significant impact on the quality of the system's outcome. The percentage of area $\leq$ 25% error was 77.24%, increasing 55.37%, 45.84%, and 33.19%, in relation to experiment 1, 2, and 3, respectively. Regarding the 10% threshold for % error, the percentage of area $\leq$ 10% surpassed 50%, registering 52.21%, which resulted in an increment of 45.62%, 36.7%, and 30.37% compared with experiment 1, 2 and 3, respectively. All the statistical indexes report significant improvements. When compared with experiment 1, the percentage of improvement raised to 97.1% in NMBE, and 73.96% in CVRMSE. When compared with experiment 2, this experience also shows remarkable progress, registering percentages of improvement that range from 53% (absolute difference) to 96% (NMBE). Both NMBE and CVRMSE, the most important indices in the calibration of the system, are comfortably in their acceptance range. Visually, the daylight performance pattern of the generated design is similar to the one painted by the user. This experiment demonstrates that it is possible to use goal-programming techniques to generate a solution that closely approximates a patterned performance target.

After the implementation and calibration experiments, experiment 5 validates the proposed strategy by testing if Painting with Light can find a predefined solution. The validation also assesses to what degree a realistic and accurately painted solution improves the system's prediction ability. This experiment showed that when the system receives a detailed feasible performance target – i.e., a painted target that is part of the design solution space and accurately conveys the granularity of light distribution and decay patterns – it is able to find design solutions whose

performance are very close to the desired targets. Experiment 5 yielded the best results in all statistic indexes. The experiment results show improvements ranging from 63.64% (absolute difference) to 99.36% (NMBE) when compared with experiment 1 results, and, when compared with experiment 2, improvement percentages of 69.81% (absolute difference) and 100.89% (NMBE). Even % error achieved the standard acceptable thresholds, below 10%. The more advanced statistical methods for building simulation calibration lie very comfortably in the acceptance range (NMBE registers 0.34% while CRMSE 12.24%). In terms of the design solution's architecture, the system was able to find the overall shape, with minor modifications on the northwest corner, and the two main skylights. The system did not find the two small skylights of the target (pre-calculated) design. However, those skylights affect a small area of the sensor grid plane, making them less relevant to the overall performance of the building. Because the fitness function prioritizes larger areas of painted goals, the low effect of those small skylights was probably neglected by the proposed computational implementation of Strategy E.

7.4 Concluding remarks

The research presented in this chapter discussed in detail Strategy E, which addresses the limitation that current goal-oriented design methods have in defining performance targets, particularly those that involve daylight metrics that entail a high level of spatial granularity.

The work discussed the strategy's implementation into a PGDS prototype for daylighting design – Painting with Light, which supports a visual description of the desired daylight patterns on a horizontal sensor grid. The implemented target editor directly addresses current limitations on goal definition of current PGDS for building performance metrics with a high spatial granularity by doing the following: (i) using brushing and linking techniques in Rhino through the drawing of polylines or closed NURBS curves; (ii) controlling light decay pattern with sliders; (iii) supporting diagnostic visualization techniques by automatically generating a difference heatmap between desired performance targets and simulation results; and (iv) computing and displaying different statistics indexes that inform the user about the quality of the system's output solution, in terms of its deviation from the painted objectives.

The experiments showed that by painting target patterns within the feasible region, and by progressively refining the fitness function, it is possible to calibrate the PGDS to produce high quality solutions. Experiment 4 demonstrated the tool's capability of generating solutions that meet the desired spatial daylight pattern, by producing a design with an NMBE of 1,54% and a CVRMSE of 20.17%, both in the range of acceptance typically used in hourly-based energy simulations: ±10% for NMBE, and 30% for CVRMSE.

Experiment 4 also showed that the robustness and quality of the search algorithm is crucial in the quality of the results. Whereas the initial experiments showed that Galapago's SGA search tended to get stuck in local minima as the complexity of the problem increased, the use of a more robust evolutionary optimization algorithm, SPEA2, in experiment 4 was more successful. The last experiment showed that when the system combines an efficient search mechanism with a realistically painted goal pattern, it can produce high-quality solutions that have a simulated performance close to the desired light values and their spatial distribution.

Despite the quality of the solutions that Strategy E implementation can generate, the approach still has some limitations related to the following:

- User handling

  • The user might poorly design the target space because of her or his lack of understanding of how different daylight metrics spatially behave, and consequently hamper the search ability of the system. Because the implementation of the strategy into a PGDS used goal programming, the imposition of an unfeasible goal makes the search method very inefficient (Coello, 1999).

  • A non-expert user might over constrain the parametric model, making it impossible for the optimization algorithm to search for solutions that meet the desired performance targets.

- Workflow

  • The system still requires some calibration of the fitness function to produce high-quality results. The need of this fine-tuning is a direct consequence of the main weakness of the goal programming method: the need to devise the appropriate weights (hyperparameters) to better steer the optimization search – a task that, depending on the problem, may require some iterations, an additional optimization procedure, and expert knowledge. Nevertheless, the system facilitates such calibration processes by enabling the designer to control the hyperparameters of the fitness function through sliders designed for that specific purpose. In that way, the architect does need to reformulate the entire objective function mathematically.

  • The experiments presented in this chapter only used Daylight Factor. There is a need to test the system with more complex daylight metrics, such as climate-based ones.

- Interface

  • To control light decay in the painting process, the system applies a simple linear strength factor implemented as a slider. This approach requires a deep intuition about light decay patterns from the user, thus making the system more prone to human error.

  • The implemented goal programming method uses hyperparameters, i.e., scalar factors related to the area of the different painted goals. This may lead the system to overlook small effects or light patterns that the designer might include in the goal space.

  • The statistical methods used in the assessment of the search output quality could benefit from adequate visualizations. Such visualization would improve diagnostic tasks throughout the design workflow.

Future work on the Painting with Light tool will address some of these limitations. To solve the current user limitations, it is necessary to develop an "expert" target editor that would steer the painting of performance patterns to more feasible regions or warn about the painting of unfeasible target areas. The development of this expert editor includes the investigation of special functions that compute patterns of light propagation and decay for different daylight metrics. To address the workflow limitations, further experiments will replace the goal-programming approach with Multi-Objective Optimization (MOO) methods that use evolutionary pareto-based optimization

metaheuristics such as the Non-dominated Standard Genetic Algorithm II (NSGA II) (Deb et al., 2002; Hamdy, Palonen and Hasan, 2012). Such experiments will assign to each target area an objective function for the multi-objective Pareto GA optimize. The goal is to remove any bias introduced by the weight area factors and possibly improve the system's ability to predict small pattern variations. Future experiences will also extend the daylight metrics used to annual climate-based metrics such as Daylight Autonomy and Useful Daylight Illuminance.

Additionally, the tool only used GA-based optimization algorithms. Recently, some authors have been challenging the efficiency of GA approaches in BPO (Wortmann et al., 2015, 2017; Wortmann, 2019). Belém and Leitão (2019) argue that no optimization algorithm outperforms all the others in every BPO problem. Thus, the authors recommend that selecting an optimization algorithm to solve a specific BPO problem should be supported by benchmark studies that compare the performance of several algorithms in similar problems. The modular nature of Strategy E allows such benchmarking studies, and future work will include them.

The requirement of both a feasible painted target and robust optimization algorithm indicates that this strategy is particularly useful in the refinement of initial building envelope designs. For example, an architect can use this strategy to evaluate the initial design performance of a roof design, re-arrange the simulation results to express the desired light distribution, and let the system search for non-disruptive solutions whose performance matches the desired light distribution. Similar design refinement approaches have been applied in the structural optimization of grid shells. The walkable roof of Fukuoka central "Grin Grin" Park in Japan designed by Toyo Ito and Associates used a similar approach using a Simulated Annealing as the optimization algorithm. The shell designed by Toyo Ito and Associates for Crematorium in Kakamigahara Crematorium applied the same approach but using a GA as the search mechanism (Pugnale and Sassone, 2007). Future experiments will include the test of the strategy in more constrained design settings and the examination of adequate search algorithms in such applications.

Although Strategy E promotes the design of diverse daylit environments, it is necessary to test the approach in more conventional designs that aim to obtain an even distribution of light levels, e.g., commercial buildings. An example of such an application includes the painting of adequate daylight goals in different programmatic areas of a commercial building and let the system optimize a shading system that seamlessly adapts to the several goals set by the designer.

Further developments will also focus on automating optimal simulation parameters. For example, to ensure accuracy in the simulation of parametric models that can drastically change size, the tool will automatically set the ambient resolution (-ar) parameter. In this way, the system avoids any possible error caused by the spacing of the model's surfaces; the literature reports that Radiance's simulation error begins to increase on surfaces spaced closer than the scene size divided by the ambient resolution (Ward, 1997).

Finally, to improve the simulation of the direct light component the authors plan to provide forward raytracing capabilities to the PGDS. Thus, future work will incorporate advanced Radiance-based simulation techniques such as the 3 and 5-Phase Method (McNeil and Lee, 2013; Geisler-Moroder, Lee and Ward, 2016) and the Photon Map extension to Radiance (Grobe, 2010; Schregle, Grobe and Wittkopf, 2015; Lars O. Grobe, 2019a; Lars Oliver Grobe, 2019), which overcomes the

limitations of Radiance's subroutine *mkillum* (Ward, 1995) in computing light reflections of curved specular reflectors.

Chapter 8:
Conclusion

8.1 Introduction

The intention of this research has been to contribute to the improvement of *Computational Design* (CD) approaches in the early stage design of high-performance buildings by facilitating feedback on their daylight, thermal, and building energy performance. Predicting the daylight, energy, and thermal behavior of buildings is paramount in producing designs that are simultaneously energy-efficient and thermally and visually comfortable. This investigation focused on improving the use of daylighting and whole-building energy simulation tools in *parametric* and *Building Performance Optimization* (BPO) workflows such as *Performance-based Generative Design Systems* (PGDS).

Based on this intention, the hypothesis of the research was the following: *The early integration of parametric, thermal, and daylight simulation tools is highly effective in the design, analysis, and optimization of high-performance buildings if it promotes model interoperability and provides performance feedback in useful time, regardless of the formal complexity of the design* (see chapter 1, section 1.3).

Chapter 3 discusses and critiques the current state-of-the-art in performance-based design approaches (see chapter 2) supported by Building Energy Simulation (BES) and daylighting analysis tools. The chapter concludes that current daylighting and BES tools pose critical challenges to the desirable use of efficient exploratory design methods such as *Parametric Design and Analysis* (PDA) and PGDS. These challenges arise from limitations regarding (i) tool interoperability, (ii) simulation processes, and (iii) problem and performance goal definition in BPO/PGDS. The following briefly summarizes them.

The obstacles posed by tool interoperability force designers to shift between modeling applications and "modes." The primary cause for the lack of a single modeling approach emerge from fundamental differences in geometric modeling capabilities between design and simulation tools, particularly in the case of BES. State-of-the-art BES tools have limitations in representing and simulating buildings with complex curved and double-curved envelopes or buildings with intricate architectural screens that are currently easy to model at early-stage design phases using algorithmic approaches.

Limitations related to simulation processes are primarily associated with run time. Detailed Building Energy Models (BEM) and advanced daylight simulations are computationally expensive and often result in unfeasible calculation times for PDA and BPO workflows.

The current limitations in defining building performance goals in BPO workflows result from the gap between PGDS and standard performance-based design approaches. The current mechanisms to define optimization problems and performance targets for BPO are non-trivial, particularly to non-experts in optimization such as architects. Additionally, it is difficult to include the spatial variation of building performance metrics such as those regarding daylighting ones.

The dissertation proposed five strategies to test the research hypothesis and address the current obstacles in integrating whole-building energy and daylighting simulations in PDA and BPO/PGDS workflows. The strategies are the following: (i) Strategy A – *Automatically generate valid building geometry for BES*, (ii) Strategy B – *Automatically simplify building geometry for BES*, (iii) Strategy C – *Abstract Complex Fenestration Systems (CFS) for BES*, (iv) Strategy D – *Assess glare potential of indoor spaces using a time and spatial sampling technique*, and (v) Strategy E – *Painting with Light - a novel method for spatially specify daylight goals in BPO*.

The research work showed that the strategies tackled the research problem and current limitations by (i) improving the interoperability between design and BES and daylighting simulation tools (Strategies A, B, and C); (ii) producing quick and adequate feedback on the daylight, thermal, and energy behavior of buildings (Strategies B, C, and D); and (iii) facilitating the spatial definition of performance goals in daylighting PGDS (Strategy E).

The investigation validated the proposed strategies using both external and internal validation procedures. The external validation consisted of inter-program and inter-modeling comparisons (see chapter 4, section 4.5.1) that compares the results produced by the modeling strategy with the ones delivered by simulation procedures currently used in design practice and research. The inter-modeling primarily validated Strategy A, B, and C. The validation approach was also used to support Strategy D and E. In the case of Strategy D, the work used external data produced by Santos, Leitão and Caldas (Santos, Leitão and Caldas, 2018) in developing a simplified predictive approach to signaling potential glare events in indoor spaces.

The internal validation of the strategies primarily consisted of requirement and face validity tests. Requirement tests examine whether a strategy complies with clearly defined requirements. This type of validation also provides meaningful answers to well-defined questions (see chapter 4.5, section 4.5.2). Strategy A, B, and C passed the requirement validity test: generate valid geometry for BEMs that do not produce any simulation errors in EnergyPlus. In Strategy B and C, the proposed approaches generated simplified models whose simulation deviation output compared with a benchmark model is within a pre-defined acceptable range. Strategy E utilizes pre-calculated Daylight Factor (DF) data as goals to the PGDS implemented by the strategy. The goal was to validate the form-finding capabilities of the proposed PGDS. The strategy passed the requirement validity test by generating a solution with a performance that is very close to the design that generated the pre-calculated DF data.

Face validity tests assess if the strategy provides plausible and useful feedback to a design process. Strategy A observes face validity because its application in a PGDS generates design candidates whose energy performance is better than that of initial design states. The sensitivity analysis conducted in Strategy B and C demonstrates that the strategies produced surrogate geometric descriptions for BEM that run quickly with minimal error deviations in simulation output. The case study application of Strategy D shows that the strategy produces meaningful and useful feedback both in spatially mapping glare potential and in identifying critical points-of-view (POVs) and time events regarding discomfort caused by glare. Thus, using fewer simulation resources, the strategy provides relevant information in useful time for early design stages. The experiment also demonstrates that a user can employ the feedback provided by Strategy D to perform detailed and advance glare simulations based on High Dynamic Range (HDR) images.

The summary of the strategies achievements and validation show that the proposed strategies were successful in attaining the primary research objective, which is *to develop a set of strategies that facilitate and improve the use of current thermal and daylight simulation tools in performance-based design supported by parametric and BPO workflows.*

Thus, and as hypothesized, the dissertation demonstrates that deploying the proposed strategies contributes to improving the efficiency of using daylight and BES tools in the design, analysis, and optimization of high-performance buildings. The strategies achieve such improvement by promoting tool interoperability, providing feedback on predicted building performance, and facilitating the definition of performance targets in PGDS.

The next section (8.2) answers the general research question (see chapter 1, section 1.3) and the more specific and refined questions posed in section 3.4 of chapter 3. The section examines how the proposed strategies provide valid answers to those questions. Section 8.3 reviews the merits and limitations of the modeling strategies. In section 8.4, the author presents recommendations for strategy application in computational performance-based design processes. Lastly, section 8.5 discusses further research and potential extensions to the proposed strategies.

8.2 Answers to Research Questions

Chapter 1 introduced the general research question that tests the formulated hypothesis and motivates the investigation conducted in this dissertation. The general research question stated below addresses the current limitations of using BES and daylight simulation tools in building design processes supported by computational approaches.

• ***How can we improve the design process of high-performance buildings using current digital design and analysis tools?***

After a thorough discussion about the research problem and its causes in chapter 3, the investigation concluded that to improve and better integrate current analysis tools in computational design workflows, it is necessary to achieve the following:

1) Enhance the interoperability between design and simulation tools by automating modeling procedures.
2) Propose alternative modeling methods that generate quick and adequate performance feedback on the thermal, energy, and daylight behavior of buildings.
3) Develop approaches that facilitate problem and performance targets in BPO.

To achieve these goals, the general question was further decomposed into four specific questions (see chapter 3, section 3.4). The next part of this section provides the answers to those questions.

• ***What type of geometric modeling strategies enable a better interoperability between parametric design and Building Energy Simulation (BES) tools?***

Currently, the geometric modeling capabilities of state-of-the-art BES programs, such as EnergyPlus, do not follow the formal expressiveness provided by current parametric and algorithmic approaches available in design tools, e.g., Rhino+Grasshopper, Revit+Dynamo. Such

design tools enable architects to explore, at the initial design stages, complex building forms, including curved and double-curved building envelopes and highly sophisticated building skins with intricate geometric patterns. Expressing such geometric complexity is a challenging task in BES since it requires a high level of expertise and time-consuming modeling processes that often result in detailed BEMs that are unfeasible to run in design times. This endeavor is even more challenging when it is necessary to automate the generation of simulation models from parametric or generative building descriptions. Thus, it is desirable to develop new methods that mediate and manage the geometric description of design and simulation models. Such methods should automatically and efficiently parse building geometry produced by parametric and generative tools, including complex curved and double-curved surfaces, for BES tools.

Strategy A answers this question by automating the generation of valid geometric descriptions for BEM from an initial set of surfaces that form a closed volume. The strategy automatically pre-processes any building surface, including those that are complex curved and double-curved, for whole-building energy simulation. Strategy B and C extend the capabilities of strategy A. Strategy B automatically simplifies the simulation models that result from the application of Strategy A to reduce calculation times. Strategy C generates surrogate descriptions of complex façade systems that architects might explore and study at the initial stages.

In sum, Strategies A, B, and C promote better interoperability between simulation tools and parametric and generative design approaches by automatically handling complex and time-consuming tasks of translating building geometry. For a detailed description of the implemented modeling steps of Strategy A, B, and C, please refer to chapter 5.

• ***Which modeling and analysis procedures generate quick and adequate feedback on energy and daylight performance of buildings at the early design stages?***

Considering that time-consuming calculations are accountable for hampering quick and useful feedback at the early design phases, it is necessary to develop modeling procedures that simplify simulation models and propose alternative prediction methods that are easy to use, run quickly, and produce meaningful outputs. BES is particularly susceptible to geometric complexity and to the number of thermal zones, whereas daylight simulations are sensitive to simulation type, particularly those supported by HDR images. Thus, the following is necessary: (i) develop approaches that simplify BEM geometry and multi-zone models without hampering the simulation output quality, (ii) daylight analysis workflows that avoid expensive calculations of HDR, and (iii) new visualizations that provide information on-demand to better support design analysis and exploratory tasks.

Strategy B, C, and D answer this question. Strategy B and C implement simplification procedures to reduce BEM run time without hindering simulation outcome. Strategy B implements and automates the following general procedure to single-zone models: (i) apply Strategy A to parse an initial building geometry into a BEM, (ii) simplify the resulting BEM geometry by reducing its mesh density (i.e., number of mesh faces) using a reduction factor, (iii) re-apply Strategy A to the resulting model to generate a valid BEM composed of triangular or quadrilateral planar faces that form an enclosed volume or set of enclosed volumes, and (iv) scale the resulting BEM uniformly to match the original volume of the initial BEM. In the case of multi-zone BEM, Strategy B samples the initial BEM and isolates representative parts of the model using a heuristic determined

by the user, e.g., orientation and solar exposure. It then applies Strategy B general procedure to generate single-zone BEMs, simulates them in parallel, and combines the results of the several single-zone BEMs weighted by the area of influence of each model.

Strategy C generates surrogates of complex façade systems, whose geometry is difficult to translate into BEM and which often results in time-consuming simulations. The modeling method uses a co-simulation process that generates surrogate representations of complex architectural screens and façade systems. The resulting surrogates abstract the façade systems to equivalent thermal and optical indices of glazing assemblies, namely Solar Heat Gain Coefficient (SHGC), U-factor (conductance), and Visual Light Transmission (VLT).

The models that result from Strategies B and C run much faster than current approaches, and the error deviation introduced by the simplifications is acceptable, particularly for early-design phases (see chapter 5, sections 5.4.4 and 5.5.4).

Strategy D illustrates how to avoid expensive time-series HDR simulations to predict annual glare. Using information produced by quicker and simpler daylight analysis – annual illuminance at the eye level (E_V) – the strategy automatically spatially maps glare potential over a grid of sensors and points-of-view (POVs) and provides information about critical events and POVs. A designer or a PGDS could use that information to conduct point-in-time, view-dependent, detailed glare simulations supported by HDR images. This strategy also advances an interactive visualization of spatial and temporal data based on radar graphs to qualify the visual comfort of indoor spaces (see chapter 6).

In sum, the techniques implemented by Strategies B and C support quick and useful feedback to design by automatically simplifying BES simulation models. Strategy D presents an alternative simulation method for studying visual comfort in indoor spaces. The strategy reduces the use of time-consuming simulations, and quickly provides adequate information for early design stages through a visualization that spatially maps glare potential and provides information about critical time events and POVs.

• How can we develop strategies that help architects and other non-experts in optimization to formulate inverse design problems?

As previously mentioned, the methods typically used in optimization formulation and target definition in PGDS and BPO are non-trivial and not easy for architects to utilize. Additionally, it is difficult to define a search procedure that spatially allocates different performance goals using an analytical formulation of objective functions. The spatial distribution of targets is particularly critical in the optimization of daylighting in buildings. As a result, designers often default to average-based processes, which are susceptible to the cancelation effect and do not support the search for designs with specific spatial performance patterns. To address these problems, it is necessary to advance strategies that mitigate the gap between common design approaches and techniques and facilitate the spatial definition of performance targets.

A way to mitigate the gap between the field of optimization and design in BPO is to develop procedures that help designers to visually define optimization problems and performance targets. Such procedures should process the architect's visual specified objectives and automatically

generate adequate objective functions for search and optimization in building design. Additionally, using visual methods to formulate and interface with BPO approaches provides architects with a "familiar environment," thus promoting the use of PGDS in building design.

Strategy E implements these types of procedures by proposing a painting-style interface that allows designers to easily set performance goals and define their spatial distribution in BPO workflows. Based on the painted performance goals, the strategy automatically generates an adequate objective function to be minimized or maximized by an optimization algorithm. By supporting the spatial definition of goals by drawing colored areas, Strategy E better resembles methods commonly used by designers in their workflows, thus being easier for them to use. The modeling approach captures the spatial granularity of daylight performance targets, thus avoiding the problems caused by averaging predicted daylight performance in daylight optimization of buildings.

• ***How effective are the proposed modeling strategies? What are their merits and limitations?***

The testing of the strategies in the several experiments conducted in this work shows that they effectively improve the use of BES and daylight simulations in early-stage performance-based design supported by parametric and BPO workflows. The general merits that make the strategies effective are the following:

1) Reduce the representational gap between design and simulation models – Strategy A.
2) Automate time-consuming modeling tasks that are prone to error for parametric and BPO processes – Strategies A, B, and C.
3) Reduce simulation time and therefore quickly provide feedback to design processes – Strategies B, C, and D.
4) Provide alternative analysis methods that are easy to handle and deploy. These analysis methods also produce meaningful and comprehensible information for design processes using fewer simulation resources – Strategy D.
5) Expedite the definition of performance goals in PGDS by deploying user-friendly approaches based on techniques known to architects – Strategy E.

The validation of the strategies briefly summarized in section 8.1 verify these benefits. These achievements are relevant contributions to the better use of BES and daylighting analysis tools in building design supported by computational approaches. They reduce (i) the user modeling effort in describing the design problem and its inputs and (ii) the time to obtain useful feedback from performance-driven parametric and optimization workflows.

There are two kinds of limitations: (i) those associated with inherent limitations of the simulation processes used by the strategies, and (ii) those related to the generalization of strategies application.

The development of the strategies is based on specific simulation procedures; therefore, the strategies carry the inherent limitations of such prediction methods. For example, the approximation of complex fenestration geometry to simple thermal, solar, and optical properties proposed in Strategy C is based on a steady-state simulation process. Thus, and although the cumulative error is small and acceptable, it does not precisely capture hourly variations.

Considering the unique nature of each design and the fact that the strategies are heuristic-based, it is difficult to ensure that they will be applicable to all design problems. For example, there is little benefit from applying Strategies A, B, and C in the analysis of box-like building geometries. Strategy D was specially crafted for side lit spaces, thus it has limited application in the analysis of designs that include top-lighting.

The following sections discuss the effectiveness of the proposed strategies by presenting each strategy's merits and limitations (section 8.3), determining guidelines for strategy application (section 8.4), and envisioning further research to address their limitations (section 8.5).

8.3 Merits and limitations of the proposed modeling strategies

The proposed modeling strategies focused on better integrating simulation models and analysis methods in PDA and BPO workflows. Regarding their overall merits, the previous sections demonstrate that the discussed strategies achieve the primary objective to a large extent. However, it is important to note that this research assumed that an adequate parametric or algorithmic description of a building would always be provided, which might not be the case in a real-world scenario.

Although parametric and algorithmic modeling methods are becoming more prevalent in architectural practice, architects may provide inefficient algorithmic descriptions of their designs, including under- and over-constrained parametric building models, and models with redundant or unnecessary parameters or modeling operations. Such design descriptions might also hinder the effectiveness of PDA and BPO approaches to design.

Developing efficient parametric descriptions for performance-based building design is non-trivial. The algorithmic description of a building is highly variable since it depends on the following aspects: (i) the specific design problem; (ii) the design team's approach to the project, e.g., a top-down approach, in which the design further details an initial idea, or a bottom-up approach where the design results from the summation of different parts; (iii) the generative approach used, i.e., whether the geometry is generated by a parametric model or by a generative system such as an L-system, a Cellular Automata, or a Shape-grammar, and (iv) the modeling techniques and operations involved.

Despite this complexity, there has been some progress on the generalization of algorithmic and parametric modeling processes for building design. Caetano, Santos, and Leitão (2015) and Caetano and Leitão (2016) advanced frameworks that generalize the implementation of typical parametric modeling strategies in building envelope design using a combination of functional operators. The algorithmic framework allows designers to describe a wide variation of design using and combining functional operators that control the form, scale, distribution, and articulation of different elements that compose a building envelope.

This parallel line of research complements the methods advanced in this dissertation. Both research lines concur for the effective deployment of computational-design methods in the design of high-performance buildings. However, the study of generalized methods to parametrize an open, overall building shape entails a level of complexity that requires a dedicated focus. Nevertheless, further

attention should be given to such methods in further applications developments of the proposed modeling approaches in this dissertation.

Sections 8.3.1 to 8.3.5 discuss the specific merits and limitations of the proposed modeling strategies. The discussion is based on the results of the application of the different strategies done in chapters 5, 6, and 7 and summarizes the findings presented for each strategy.

8.3.1 Strategy A: Automatically generate valid building geometry for BES

The primary merit of this strategy is the automatic production of valid geometry for BEM from initial parametric descriptions of curved and double-curved building geometries. The strategy uses planarization methods borrowed from the architectural computational geometry field to allow architects to automatically generate valid BEM geometry from a 3D CAD model. Hence the approach avoids time-consuming manual modeling tasks that are incompatible with BPO workflows. The strategy allows the user to control the degree of geometric detail in the generation of BEM models by managing the level of building envelope discretization. The application of the strategy in an optimization exercise (see chapter 5) demonstrated the importance of preserving the essential building form in BEM to capture self-shading and variable solar radiation distribution patterns. The same application also demonstrated that it is possible to handle free-form building geometries in optimizing predicted building energy use. The experiment showed that the PGDS that used this strategy found design alternatives that improved the building energy performance of initial designs by almost 70%.

The main limitation of the strategy is related to simulation time. The run time of the BEM produced by Strategy A depends heavily on the level of geometric detail described by the user: the greater the number of surface subdivisions, the higher the calculation time of its energy performance. Thus, the achievement of acceptable optimization times highly depends on initial settings for geometry discretization. Moreover, it is difficult to foresee whether a particular level of detail is adequate for all building geometries that a PGDS might generate during the optimization process. A level of surface discretization that results for a design candidate might not be suitable for another since they might not correspond to the overall desired level of detail.

Another limitation is that the strategy is unable to handle façade patterning and screen-based systems. This fact required that the author oversimplify glass fritting in the building envelope to generate simulation models that run quickly.

Lastly, the testing and validation of Strategy A focus on single-zone thermal models. Strategy B and C complement Strategy A by addressing those limitations.

8.3.2 Strategy B: Automatically simplify building geometry for efficient whole-building energy simulations

The principal merit of Strategy B is that it extends the scope of Strategy A to multi-zone models and improves the computational efficiency of the generated BEMs by automatically simplifying their geometry. Strategy B combines two approaches. The first automatically parses any curved enclosed building envelope and generates an equivalent low polygon BEM. The second approach samples a multi-zone BEM to isolate smaller and representative parts of the original model. Both approaches can be used separately or together.

The testing of Strategy B showed that both methods produce geometric surrogates for BEM that run quickly, with simulation output deviation within the acceptable range. The experiments demonstrate that it is possible to reduce by 80% the number of mesh faces in a BEM as long as it preserves the original volume of the single or sampled thermal zone (see chapter 6). As previously mentioned, Strategy B automatically applies a uniform scale to the low-resolution polygon BEM that it generates to preserve the original thermal zone volume.

Another merit is that the method implemented by Strategy B to handle multi-zone models automates several simplification tasks, including the sample of representative single-zone models, simulates them, and combines the results using a weighted sum. This approach also improved simulation time without producing significant deviations to simulation output. The research also showed that it is feasible and desirable to combine both approaches in addressing free-form buildings that comprise several thermal zones.

The following limitations constrain a generalized application of the recommendations that resulted from testing Strategy B: (i) the experiments used a commonly used Heating, Ventilation, and Air Conditioning (HVAC) at the early design stages (Ideal Loads Air System - ILAS), thus the results cannot be directly extrapolated to other HVAC systems; (ii) the strategy was tested only in narrow plan examples, thus requiring further research to examine acceptable levels of simplification for deep plan buildings; and (iii) the experiment used a limited range of climates, therefore limiting the generalization of findings to different climates.

8.3.3 Strategy C: Abstract Complex Fenestration Systems (CFS) for BES

Strategy C complements Strategy A by enabling the simulation of complex and sophisticated architectural screens and façade systems at the early design stages. The primary merit of the strategy is that it mitigates the existing gap between design and simulation tools by allowing architects to quickly assess the impact in building energy use of their façade designs.

Strategy C combines parametric design, statistical-learning techniques, window performance, and whole-building energy analysis tools in a single streamlined design workflow. The approach uses co-simulation to simplify the geometric features of complex fenestration systems (CFS) into thermal, solar, and optical indices. Because the strategy generates CFS surrogates based on a set of performance indices, it enables the generation of formally distinct solutions of similar performance. This ability is useful at initial stages of the design process, stages where architects examine different design alternatives.

The application of Strategy C in a parametric design and analysis (PDA) experiment showed that the surrogates that it produces run quickly and with acceptable accuracy, particularly in cumulative annual results (see chapter 5, section 5.5). These benefits make this strategy suitable for either parametric or goal-oriented design processes based on overall building energy performance.

Although Strategy C had a good performance in predicting annual building energy indices, it is less robust in producing surrogates that accurately capture building energy performance on an hourly basis. The experiments showed that strategy produced models with hourly deviations outside the acceptability range in heating energy use. This limitation might be the result of two factors. The first relates to the experimental setting and the statistical process applied. In the experiment, heating had a minimal weight in the overall energy performance. Thus, any small

deviation might have produced significant relative errors. The second factor lies in the co-simulation process itself. The simulation tool used to abstract the CFS geometry, WINDOW (Huizenga et al., 2017), is based on steady-state assumptions, making the resulting surrogates less capable of capturing granular hourly data on energy performance. Thus, it is necessary to conduct further research to determine the cause of that single error.

As argued in chapter 5, section 5.6, the annual accuracy presented by Strategy C makes the deployment of this strategy not only acceptable but desirable at early design phases, phases in which there is a need for quick feedback and architects are more concerned with global energy assessments than with hourly estimations.

8.3.4 Strategy D: Assess glare potential of indoor spaces using a time and spatial sampling technique

The primary merit of Strategy D is that it uses straightforward and easy-to-calculate methods to qualify entire spaces in terms of glare, thus mitigating the need to use sophisticated and time-consuming simulations in annual visual comfort studies. The approach advances a method for visual comfort studies that replaces computationally expensive annual *Daylight Glare Probability* (aDGP) simulations at the early design stages. The strategy maps glare potential in a space and helps architects to supplement that initial assessment with detailed and advance simulations. Thus, the strategy is a viable alternative analysis approach for early to intermediate design phases to those recommended by specific standards, e.g., EN17037 - Daylight in buildings (CEN, 2019).

The strategy uses annual *vertical illuminance at the eye level* (E_V) calculations to spatially map glare potential and find relevant points-of-view (POVs) and time events (hours-of-the-year, HOY) to conduct point-in-time DGP based on detailed HDR images.

The interactive visualization tool that spatially maps glare potential over a sensor grid also enables architects to (i) easily query E_V data for finding critical time events and POV in each sensor, (ii) examine daily and seasonal patterns of E_V distribution, and (iii) compare the glare potential of different design solutions.

The strategy automates the use of advanced bi-directional raytracing methods (3-phase method), thus facilitating the simulation of complex fenestration systems, an ability that standard simulation tools that compute aDGP – e.g., DAYSIM (Reinhart and Breton, 2009) – do not support. The approach also uses Typical Meteorological Year (TMY) data to hourly describe the sky conditions of a given location by using all-weather Perez sky models (Perez, Seals and Michalsky, 1993).

The primary limitation of Strategy D lies in its bias for low sun angles of bright and clear skies. This bias may be the result of using a single E_V threshold ($E_{V,Thr}$) to determine glare potential under different sky types and POV locations. The sensitivity analysis that supports the definition of the $E_{V,Thr}$ used by the strategy shows that an adaptive $E_{V,Thr}$ that responds to spatial location and sky type has the potential to outperform the use of a single general $E_{V,Thr}$. Finally, because DGP analysis supported the specification of $E_{V,Thr}$ the approach is constrained to the scope of DGP, which is limited to glare assessment in perimetral areas of side-lit offices

(Wienold and Christoffersen, 2006; Van Den Wymelenberg and Inanici, 2014; Wienold et al., 2018).

8.3.5 Strategy E: Painting with Light - a novel method for spatially specifying daylight goals in Building Performance Optimization

The main merit of Strategy E is that it enables architects to easily define spatial performance targets using a painting-like tool in a PGDS for daylighting design and optimization. The proposed PGDS advances an interactive approach that allows architects to use familiar techniques such as painting or drawing, to define performance targets in inverse design problems.

By enabling the spatial definition of different performance targets, the strategy also helps architects avoid averaging-based methods that condense the spatial variation of performance goals into a single value. Because averaging-based methods are susceptible to the *compensation effect*, their use to specify performance targets in BPO might negatively affect the quality of the search, particularly if the performance aspect to optimize entails a high level of spatial variability.

The definition of spatial performance target patterns also enhances the use and generative potential of daylighting PGDSs, since the spatial description of goals steers search procedures in a way that is impossible through averaging or cumulative-based approaches.

The iterative refinement of Strategy E and its application in a case study showed that the proposed PGDS is effective in finding solutions whose performance closely matches painted goal performance patterns.

Nevertheless, the approach presents some limitations. For example, the quality of the search output depends heavily on the user's knowledge about daylight behavior in buildings. The experiments show that the strategy could only generate interesting results if a precise goal pattern is provided. However, in the painting of the goals, the user controls daylight decay, thus constraining the quality of the inputted target to the user's expertise on the spatial variation of daylighting metrics. The *scalarization method* used by the strategy in defining the objective function also has limitations. Although the proposed PGDS automatically assigns weights depending on the area of painted goals, the weight distribution might still require some calibration from the user side to improve the search procedure. Moreover, the weight approach of the scalarization method might lead to the PGDS's search overlooking small light patterns included by the user in the performance goal pattern.

The implementation of the strategy is also limited to GA optimization algorithms. Despite the success of GA in daylighting and building energy optimization, GA approaches are still time consuming as they require the evaluation of a large number of design candidates. Considering that there is no universal optimization algorithm in BPO (Belém and Leitão, 2019), there is the need to test the Painting with Light interface with other optimization algorithms. The modular structure of the strategy implementation facilitated the testing of different optimization algorithms. Such benchmark studies will allow the mapping of adequate search methods for different daylighting optimization problems.

Finally, the experiments used only Daylight Factor (DF) as the daylight performance metric, limiting the generalization of the findings. Thus, there is a need to test the system with more complex daylight metrics, including climate-based metrics that capture the typical annual sky variations of a given location.

8.4 Recommendations for Strategy Application

After discussing the benefits and limitations of the proposed strategies, this section presents recommendations for their use in building design and analysis processes.

Strategy A is suitable for analyzing building forms that include curved or double-curved surfaces, particularly in cases that require a detailed geometric description of the building envelope for BES. Although Strategy A can parse box-like geometries, there are no benefits to using the strategy to do this, since box-like building geometry needs little pre-processing for energy simulation. Strategy A is also applicable only to single thermal zone BEMs.

Strategy B is recommended in cases where it is desirable to generate simplified and quick-to-run single or multi-zone BEMs of buildings with curved or double-curved envelopes. The multi-zone simplification approach of this strategy can also be applied to box-like multi-zone BEMs. The recommended level of BEM mesh face reduction in the simplification is between 75 to 85%. The experiments presented in chapter 5 show that this interval yields significant reductions in simulation time with a minimal impact on simulation output. Above 85%, the resulting simplified BEMs do not fully capture the overall shape of the design and therefore present higher error deviations in simulation output.

Strategy C is adequate in the initial assessments of complex façade systems, including CFS and light-redirecting systems in building energy performance. This strategy is recommended for conducting overall annual building energy estimations. As previously mentioned, this modeling approach has problems predicting hourly heating energy consumption. This strategy is also suitable in optimization scenarios in which the architect desires to compare different façade systems of similar performance.

It is appropriate to combine Strategy A with Strategy C. Combining Strategy B with C depends on the level of geometric simplification introduced by Strategy B, i.e., if the BEM geometry is too simplified, using Strategy C to generate CFS surrogates might result in significant cumulative deviations in simulation output.

Strategy D is suitable for early visual comfort assessments and to qualify the potential of visual discomfort caused by glare in indoor spaces. The strategy should be used only in designs dominated by side lighting. This strategy is able to provide useful information in façade design, including the design of shading systems and selection of glazed and opaque materials. The approach can also contribute to the optimization of automated dynamic shading controls, and the interior layout of furniture. The author recommends the following Radiance simulation parameters for assessing the glare potential of a space by using vertical eye illuminance calculations: 6 ambient bounces (-ab), ambient resolution (-ar) set to 300, ambient divisions (-ad) to 1000, ambient sampling (-as) to 500, ambient accuracy (-aa) to 0.1, and direct threshold to 0. In the case of detailed point-in-time DGP analysis -ad should be set

to 50,000. These parameters ensure simulation output quality in the examination of a wide range of fenestration systems. It is possible to use Strategy D either in single- or multi-objective BPO workflows. For example, in a single objective optimization the designer might minimize the number of potential glare events. In multi-objective optimization, the designer might minimize the number of potential glare events and the DGP levels in critical events and POVs found by the tool.

Strategy E is appropriate to daylight building optimization problems that require the spatial differentiation of daylight targets in the creation of variable light environments. The requirement of well-defined feasible performance targets makes Strategy E particularly suitable for refining an initial roof and building envelope design. A designer can use the system first to assess the performance of a well-defined design concept. Based on the analysis results, the designer can utilize the painting interface to adjust daylight levels and use them as goals to run an optimization procedure. The system will then search for similar design solutions that closely match the desired daylight targets.

Before using Strategy E, it is recommended to perform a small sensitivity analysis first. This analytical procedure would provide a useful insight into the specific daylight optimization problem at hand. Based on the sensitivity analysis results, the user will be better informed when painting performance targets, identifying the relevant parameters in the optimization problem, and assessing how sensitive the problem is too small lighting patterns.

Finally, the BES modeling strategies (Strategies A, B, and C) can be used in parallel with Strategy D and E in multi-criteria optimization workflows.

8.5 Future work

This section presents the research endeavors envisioned to tackle the shortcomings of the strategies. The section isolates and summarizes the primary future research tasks identified in the discussion conducted in chapters 5, 6, and 7.

Strategy B and C address the primary limitations of Strategy A. Hence, there is no pressing need for further refinements to Strategy A, only those that result from improving Strategies B and C.

Future work in Strategy B aims to extend its applicability. The author plans to study the application strategy in the design of a building with deep plans. That study would provide useful insights about the admissible degree of envelope simplification in that type of building. The hypothesis is that the reduction of BEM mesh density could be even greater in such cases and that the sampling of multi-zone thermal models should focus more on core zones. Additional research on Strategy B also includes testing the strategy in a wider range of climates and with other HVAC systems.

Regarding Strategy C, further research will focus on testing the strategy in different climates to assess whether the deviation found in hourly heating energy estimations is caused by a statistical procedure or by the steady-state nature of WINDOW simulations. Future work will also include the development of dynamic Solar Heat Gain Coefficients (SHGC), Visible Light

Transmission (VLT), and U-factor (i.e., thermal conductance) to generate surrogates of complex façade systems that better handle the transient nature of solar and heat transfer phenomena. The author envisions modeling those dynamic fenestration indices using a similar method to model electrochromic or thermochromic glazing units. Moreover, the dynamic description of SGGC, VLT, and U-factor will also extend the modeling abilities of Strategy C to dynamic CFS.

Future work on Strategy D will address the strategy limitations in signaling glare events caused by surface luminance contrast, and in using E_V thresholds for determining glare potential in the different daylit zones of the same space. The determination of an even more robust E_V threshold requires the inclusion of more annual skies of different latitudes and the formulation of a dynamic threshold. Such dynamic E_V threshold will depend on annual sky type, latitude, distance to the different glare sources, and their relative size. The strategy will also incorporate the 5-phase method as the primary simulation approach. The use of the 5-phase method will allow the decoupling of the direct and diffuse components of daylight, thus enable the user to distinguish glare events produced by the presence of the circumsolar region in the observer's field-of-view from those primarily produced by light reflections and surface luminance contrast.

As mentioned in chapter 7, section 7.4, future work on Strategy E will address current user limitations by developing an "intelligent" painting interface that helps designers to paint feasible performance targets. Such an interface should be able to automatically approximate light decay patterns from the specification of "hotspot" areas. The implementation of this expert editor requires the development of functions that calculate light propagation and decay for different daylight metrics. Further research will include a comparative study between the GA-based scalarization method currently used by the approach and other optimization approaches, including model-based optimization techniques and different multi-criteria optimization techniques such as Pareto-based methods. Such a comparative study aims to assess whether it is possible to remove the bias of the weighting-based approach applied by the scalarization method and whether there are more suitable search mechanisms to the proposed PGDS. The comparison between GA optimization techniques and model-based search mechanisms is especially relevant. Recent research shows that model-based optimization techniques based on the Radial Basis Function (RBF) can outperform GAs, particularly in optimization problems formulated using the scalarization method (Wortmann et al., 2017; Wortmann, 2019). The author also plans to extend Strategy E to other daylight performance indices, particularly climate-based daylight metrics.

Finally, further research efforts will include the combination of the different strategies in Multi-Objective Optimization (MOO) studies, particularly the combination of BES related strategies (Strategy A, B, and C) with Strategies D and E. These studies will further assess their combined effectiveness in current sustainable building design MOO workflows.

Bibliography

Abergel, T., Dean, B., Dulac, J. and Hamilton, I. (2018) *2018 Global Status Report - towards a zero-emission, efficient and resilient buildings and construction sector.* International Energy Agency, Global Alliance for Buildings and Construction, and the United Nations Environment Programme, p. 73. Available at: https://www.worldgbc.org/sites/default/files/2018%20GlobalABC%20Global%20Status%20Report.pdf (Accessed: 5 July 2020).

Abergel, T., Dulac, J., Hamilton, I., Jordan, M. and Pradeep, A. (2019) *2019 Global Status Report for Buildings and Construction - towards a zero-emissions, efficient and resilient buildings and construction sector.* International Energy Agency, Global Alliance for Buildings and Construction, and the United Nations Environment Programme, p. 41. Available at: http://wedocs.unep.org/bitstream/handle/20.500.11822/30950/2019GSR.pdf?sequence=1&isAllowed=y (Accessed: 10 July 2020).

Acosta, I., Navarro, J. and Sendra, J. J. (2011) 'Towards an analysis of daylighting simulation software', *Energies*. Molecular Diversity Preservation International, 4(7), pp. 1010–1024.

AEDAS (2012) *Al Bahar Towers Responsive Facade / Aedas*, *ArchDaily*. Available at: https://www.archdaily.com/270592/al-bahar-towers-responsive-facade-aedas (Accessed: 4 August 2020).

Agarwala, A., Dontcheva, M., Agrawala, M., Drucker, S., Colburn, A., Curless, B., Salesin, D. and Cohen, M. (2004) 'Interactive digital photomontage', in *ACM SIGGRAPH 2004 Papers*, pp. 294–302.

Aköz, O. and Petrovic, D. (2007) 'A fuzzy goal programming method with imprecise goal hierarchy', *European Journal of Operational Research*, 181(3), pp. 1427–1433. doi: 10.1016/j.ejor.2005.11.049.

Al-Homoud, M. S. (2005) 'A systematic approach for the thermal design optimization of building envelopes', *Journal of building physics*, 29(2), pp. 95–119.

Allegrini, J. and Carmeliet, J. (2018) 'Simulations of local heat islands in Zürich with coupled CFD and building energy models', *Urban climate*. Elsevier, 24, pp. 340–359.

Alnusairat, S., Hou, S. and Jones, P. (2017) 'Investigating spatial configurations of skycourts as buffer zones in high-rise office buildings', in *Proceedings of the 5th eCAADe Regional International Symposum. eCAADe RIS 2017: The Virtual and the Physical. Between the representation of space and the making of space.*, Welsh School of Architecture, Cardiff University, Wales, UK, pp. 83–92.

Al-Rabghi, O. M. and Al-Johani, K. M. (1997) 'Utilizing transfer function method for hourly cooling load calculations', *Energy Conversion and Management*. Elsevier, 38(4), pp. 319–332.

Amer, M., Hamdy, M., Wortmann, T., Mustafa, A. and Attia, S. (2020) 'Methodology for design decision support of cost-optimal zero-energy lightweight construction', *Energy and Buildings*, 223, p. 110170. doi: 10.1016/j.enbuild.2020.110170.

Amitrano, L. *et al.* (2014) *Building Energy End-use Study (BEES) Part 1: Final Report*. BRANZ Study Report SR297/1, BRANZ Ltd, Judgeford, New Zealand.

Andersen, M. (2015) 'Unweaving the human response in daylighting design', *Building and Environment*, 91, pp. 101–117.

Andersen, M., Gagne, J. M. and Kleindienst, S. (2013) 'Interactive expert support for early stage full-year daylighting design: a user's perspective on Lightsolve', *Automation in Construction*, 35, pp. 338–352.

Andersen, M., Kleindienst, S., Yi, L., Lee, J., Bodart, M. and Cutler, B. (2008) 'An intuitive daylighting performance analysis and optimization approach', *Building Research & Information*, 36(6), pp. 593–607.

Andjelković, A. S., Mujan, I. and Dakić, S. (2016) 'Experimental validation of a EnergyPlus model: Application of a multi-storey naturally ventilated double skin façade', *Energy and Buildings*. Elsevier, 118, pp. 27–36.

André, M., De Vecchi, R. and Lamberts, R. (2020) 'User-centered environmental control: a review of current findings on personal conditioning systems and personal comfort models', *Energy and Buildings*. Elsevier, 222, p. 110011.

Anton, I. and Tănase, D. (2016) 'Informed geometries. Parametric modelling and energy analysis in early stages of design', *Energy Procedia*. Elsevier, 85, pp. 9–16.

Aronson, J. E., Liang, T.-P. and MacCarthy, R. V. (2005) *Decision support systems and intelligent systems*. Pearson Prentice-Hall Upper Saddle River, NJ, USA:

Asadi, E., da Silva, M. G., Antunes, C. H., Dias, L. and Glicksman, L. (2014) 'Multi-objective optimization for building retrofit: A model using genetic algorithm and artificial neural network and an application', *Energy and Buildings*, 81, pp. 444–456.

Asadi, S. and Geem, Z. W. (2015) 'Sustainable building design: A review on recent metaheuristic methods', in *Recent Advances in Swarm Intelligence and Evolutionary Computation*. Springer, pp. 203–223. Available at: http://link.springer.com/chapter/10.1007/978-3-319-13826-8_11 (Accessed: 18 July 2016).

Ascione, F., Bellia, L. and Capozzoli, A. (2013) 'A coupled numerical approach on museum air conditioning: Energy and fluid-dynamic analysis', *Applied energy*. Elsevier, 103, pp. 416–427.

ASE (1989) 'Eclairage interieur par la lumicre du jour', *Association Suisse Des Electriciens, Zurich (CH)*.

ASHRAE (2002) 'Guideline 14-2002, Measurement of Energy and Demand Savings'.

ASHRAE (2013) 'ASHRAE Standard 90.1-2013 Determination of Energy Savings: Quantitative Analysis.'

Asl, M. R., Bergin, M., Menter, A. and Yan, W. (2014) 'BIM-based parametric building energy performance multi-objective optimization'. CUMINCAD.

Attia, S., Hamdy, M., O'Brien, W. and Carlucci, S. (2013) 'Assessing gaps and needs for integrating building performance optimization tools in net zero energy buildings design', *Energy and Buildings*, 60, pp. 110–124.

Autodesk (2019) *Insight | Building Performance Analysis Software | Autodesk*. Available at: https://www.autodesk.com/products/insight/overview (Accessed: 25 November 2019).

Autodesk (2020) *Dynamo Studio | Computational BIM Design | Autodesk*. Available at: https://www.autodesk.com/products/dynamo-studio/overview (Accessed: 23 February 2020).

Awbi, H. B. and Hatton, A. (1999) 'Natural convection from heated room surfaces', *Energy and buildings*. Elsevier, 30(3), pp. 233–244.

Azari, R., Garshasbi, S., Amini, P., Rashed-Ali, H. and Mohammadi, Y. (2016) 'Multi-objective optimization of building envelope design for life cycle environmental performance', *Energy and Buildings*, 126, pp. 524–534. doi: 10.1016/j.enbuild.2016.05.054.

Bäck, T. (2005) *modeFrontier 4.3 Users Manual: Evolution Strategies Module R1. 1 for modeFrontier*. Technical Report, May.

de Bakker, C., Aarts, M., Kort, H. and Rosemann, A. (2018) 'The feasibility of highly granular lighting control in open-plan offices: Exploring the comfort and energy saving potential', *Building and Environment*. Elsevier, 142, pp. 427–438.

de Bakker, C., Aries, M., Kort, H. and Rosemann, A. (2017) 'Occupancy-based lighting control in open-plan office spaces: A state-of-the-art review', *Building and Environment*. Elsevier, 112, pp. 308–321.

Baldassini, N., Pottmann, H., Raynaud, J. and Schiftner, A. (2010) 'New Strategies and Developments in Transparent Free-Form Design: From Facetted to Nearly Smooth Envelopes', *International Journal of Space Structures*, 25(3), pp. 185–197. doi: 10.1260/0266-3511.25.3.185.

Barrios, G., Huelsz, G. and Rojas, J. (2012) 'Thermal performance of envelope wall/roofs of intermittent air-conditioned rooms', *Applied Thermal Engineering*. Elsevier, 40, pp. 1–7.

Basbagill, J., Flager, F., Lepech, M. and Fischer, M. (2013) 'Application of life-cycle assessment to early stage building design for reduced embodied environmental impacts', *Building and Environment*. Elsevier, 60, pp. 81–92.

Basbagill, J. P., Flager, F. L. and Lepech, M. (2014) 'A multi-objective feedback approach for evaluating sequential conceptual building design decisions', *Automation in Construction*, 45, pp. 136–150.

Bauer, C. and Wittkopf, S. (2015) 'Annual daylight simulations with EvalDRC–Assessing the performance of daylight redirection components', *Journal of Facade Design and Engineering*. IOS Press, 3(3–4), pp. 253–272.

Bazjanac, V. (2008) 'IFC BIM-Based Methodology for Semi-Automated Building Energy Performance Simulation', p. 14.

Bazjanac, V., Maile, T., Rose, C., O'donnell, J., Mrazović, N., Morrissey, E. and Welle, B. (2011) 'An assessment of the use of building energy performance simulation in early design', *IBPSA Building Simulation*.

Becker, R. A. and Cleveland, W. S. (1987) 'Brushing scatterplots', *Technometrics*. Taylor & Francis, 29(2), pp. 127–142.

Belém, C. G. and Leitão, A. (2019) 'Conflicting Goals in Architecture: A study on Multi-Objective Optimization', in *Proceeding of the 24th CAADRIA Conference*. *CAADRIA*, Victoria Universtiy of Wellington, Wellington, New Zealand, pp. 453–461.

Belém, G. (2019) *Optimization of Time-Consuming Objective Functions. Derivative-Free Approaches and their Application in Architecture.* Instituto Superior Técnico - Universidade de Lisboa. Available at:

http://web.ist.utl.pt/antonio.menezes.leitao/ADA/documents/theses_docs/2019_OptimizationOfTime-ConsumingObjectiveFunctions.pdf (Accessed: 2 May 2020).

Bellia, L., Pedace, A. and Fragliasso, F. (2015) 'The impact of the software's choice on dynamic daylight simulations' results: A comparison between Daysim and 3ds Max Design®', *Solar Energy*, 122, pp. 249–263. doi: 10.1016/j.solener.2015.08.027.

Bichiou, Y. and Krarti, M. (2011) 'Optimization of envelope and HVAC systems selection for residential buildings', *Energy and Buildings*, 43(12), pp. 3373–3382.

BIG (2009) 'Astana National Library'. Available at: https://big.dk/#projects-anl (Accessed: 4 August 2020).

Big Ladder (2015) *Using Multipliers (Zone and/or Window): Tips and Tricks for Using EnergyPlus — EnergyPlus 8.3*, *Big Ladder Software*. Available at: https://bigladdersoftware.com/epx/docs/8-3/tips-and-tricks-using-energyplus/using-multipliers-zone-and-or-window.html (Accessed: 1 February 2020).

Biswas, P. and Pal, B. B. (2019) 'A fuzzy goal programming method to solve congestion management problem using genetic algorithm', *Decision Making: Applications in Management and Engineering*, 2(2), pp. 36–53.

Blum, C. and Roli, A. (2003) 'Metaheuristics in combinatorial optimization: Overview and conceptual comparison', *ACM Computing Surveys (CSUR)*, 35(3), pp. 268–308.

Bourgeois, D., Reinhart, C. F. and Ward, G. (2008) 'Standard daylight coefficient model for dynamic daylighting simulations', *Building Research & Information*. Routledge, 36(1), pp. 68–82. doi: 10.1080/09613210701446325.

Box, G. E. (1979) 'Robustness in the strategy of scientific model building', in *Robustness in statistics*. Elsevier, pp. 201–236.

Brembilla, E. and Mardaljevic, J. (2019) 'Climate-Based Daylight Modelling for compliance verification: Benchmarking multiple state-of-the-art methods', *Building and Environment*. Elsevier, 158, pp. 151–164.

Brooks, S. P. and Morgan, B. J. (1995) 'Optimization using simulated annealing', *The Statistician*, pp. 241–257.

Brown, N. C. and Mueller, C. T. (2016) 'Design for structural and energy performance of long span buildings using geometric multi-objective optimization', *Energy and Buildings*. Elsevier, 127, pp. 748–761.

BuHamdan, S., Alwisy, A. and Bouferguene, A. (2020) 'Generative systems in the architecture, engineering and construction industry: A systematic review and analysis':, *International Journal of Architectural Computing*. SAGE PublicationsSage UK: London, England. doi: 10.1177/1478077120934126.

Burke, D., Ghosh, A. and Heidrich, W. (2005) 'Bidirectional Importance Sampling for Direct Illumination.', *Rendering Techniques*. Citeseer, 5, pp. 147–156.

Caetano, I. and Leitão, A. (2016) 'DrAFT: an Algorithmic Framework for Facade Design.', in *eCAADe 16: Complexity & Simplicity, Proceedings of the 34th eCAADe Conference*. *eCAADe16*, Oulu, Finland, pp. 465–474.

Caetano, I., Santos, L. and Leitão, A. (2015) 'From Idea to Shape, from Algorithm to Design: A Framework for the Generation of Contemporary Facades', in Celani, G., Sperling, D. M., and

Franco, J. M. S. (eds) *Computer-Aided Architectural Design Futures. The Next City - New Technologies and the Future of the Built Environment*. Berlin, Heidelberg: Springer Berlin Heidelberg, pp. 527–546. doi: 10.1007/978-3-662-47386-3_29.

Caetano, I., Santos, L. and Leitão, A. (2020) 'Computational design in architecture: Defining parametric, generative, and algorithmic design', *Frontiers of Architectural Research*, 9(2), pp. 287–300. doi: 10.1016/j.foar.2019.12.008.

Cagan, J., Campbell, M. I., Finger, S. and Tomiyama, T. (2005) 'A framework for computational design synthesis: model and applications', *Journal of Computing and Information Science in Engineering*, 5(3), pp. 171–181.

Caicedo, D. and Pandharipande, A. (2016) 'Daylight and occupancy adaptive lighting control system: An iterative optimization approach', *Lighting Research & Technology*. SAGE Publications Ltd STM, 48(6), pp. 661–675. doi: 10.1177/1477153515587148.

Caldas, L. (2008) 'Generation of energy-efficient architecture solutions applying GENE_ARCH: An evolution-based generative design system', *Advanced Engineering Informatics*, 22(1), pp. 59–70.

Caldas, L. G. and Norford, L. K. (2002) 'A design optimization tool based on a genetic algorithm', *Automation in Construction*. (ACADIA '99), 11(2), pp. 173–184. doi: 10.1016/S0926-5805(00)00096-0.

Caldas, L. G. and Norford, L. K. (2003a) 'Genetic algorithms for optimization of building envelopes and the design and control of HVAC systems', *J. Sol. Energy Eng.*, 125(3), pp. 343–351.

Caldas, L. G. and Norford, L. K. (2003b) 'Shape generation using pareto genetic algorithms: integrating conflicting design objectives in low-energy architecture', *International journal of architectural computing*. SAGE Publications Sage UK: London, England, 1(4), pp. 503–515.

Caldas, L. and Norford, L. (1999) 'A genetic algorithm tool for design optimization'. Available at: https://www.mysciencework.com/publication/show/4a4831ffe3d3a9e80411d247f39d2772 (Accessed: 6 February 2017).

Caldas, L. and Santos, L. (2012) 'Generation of Energy-Efficient Patio Houses With GENE_ARCH: Combining an evolutionary generative design system with a shape grammar.', in *Digital Physicality: Proceedings of the 30th eCAADe Conference*. Prague, Czech Republic: Czech Technical University in Prague, Faculty of Architecture: eCAADe: Conferences, pp. 459–470. Available at: https://cumincad.architexturez.net/doc/oai-cumincadworks-id-ecaade2012-267 (Accessed: 6 February 2017).

Caldas, L. and Santos, L. (2016) 'Painting with light: An interactive evolutionary system for daylighting design', *Building and Environment*, 109, pp. 154–174. doi: 10.1016/j.buildenv.2016.07.023.

Carlucci, S., Causone, F., De Rosa, F. and Pagliano, L. (2015) 'A review of indices for assessing visual comfort with a view to their use in optimization processes to support building integrated design', *Renewable and Sustainable Energy Reviews*, 47, pp. 1016–1033. doi: 10.1016/j.rser.2015.03.062.

Celani, G. and Vaz, C. (2012) 'CAD scripting and visual programming languages for implementing computational design concepts: A comparison from a pedagogical point of view', *International Journal of Architectural Computing*, 10(1), pp. 121–138.

Cemesova, A., Hopfe, C. J. and Mcleod, R. S. (2015) 'PassivBIM: Enhancing interoperability between BIM and low energy design software', *Automation in Construction*, 57, pp. 17–32. doi: 10.1016/j.autcon.2015.04.014.

CEN, E. C. for S. (2019) 'EN17037 - Daylight in buildings'.

Challenge, L. B. (2016) *Living building challenge 3.0*.

Chamilothori, K., Chinazzo, G., Rodrigues, J., Dan-Glauser, E., Wienold, J. and Andersen, M. (2019) 'Subjective and physiological responses to facade and sunlight pattern geometry in virtual reality', *Building and Environment*, 150, pp. 144–155.

Chatzivasileiadi, A., Lannon, S., Jabi, W., Wardhana, N. M. and Aish, R. (2018) 'Addressing Pathways to Energy Modelling through Non-Manifold Topology', in *Proceedings of the Symposium on Simulation for Architecture and Urban Design*. San Diego, CA, USA: Society for Computer Simulation International (SIMAUD '18).

Chatzivasileiadi, A., Lila, A. M. H., Lannon, S. and Jabi, W. (2018) 'The Effect of Reducing Geometry Complexity on Energy Simulation Results', in *eCAADe 2018*. *eCAADe 2018*, pp. 559–568.

Chauvel, P., Collins, J. B., Dogniaux, R. and Longmore, J. (1982) 'Glare from windows: current views of the problem', *Lighting research and Technology*, 14(1), pp. 31–46.

Chen, Y., Zhou, J. and Spitler, J. D. (2006) 'Verification for transient heat conduction calculation of multilayer building constructions', *Energy and buildings*. Elsevier, 38(4), pp. 340–348.

Choi, J.-W. and Park, C.-S. (2016) 'Issues and limitations in BIM to BEM for Energy Simulation', *Journal of the Architectural Institute of Korea Planning & Design*, 32(2), pp. 223–230. doi: 10.5659/JAIK_PD.2016.32.2.223.

Chokhachian, A. (2014) *Studies on architecture design procedure: A framework for parametric design thinking*. PhD Thesis. Eastern Mediterranean University (EMU)-Doğu Akdeniz Üniversitesi (DAÜ).

Chronis, A., Dubor, A., Cabay, E. and Roudsari, M. S. (2017) 'Integration of CFD in computational design', *ShoCK*, pp. 601–610.

Clarberg, P., Jarosz, W., Akenine-Möller, T. and Jensen, H. W. (2005) 'Wavelet importance sampling: efficiently evaluating products of complex functions', in *ACM SIGGRAPH 2005 Papers*, pp. 1166–1175.

Clarke, J. A. (2001) *Energy simulation in building design*. Routledge. Available at: https://books.google.com/books?hl=pt-PT&lr=&id=WH0VCiF8jkoC&oi=fnd&pg=PR3&dq=Energy+Simulation+in+Building+Design&ots=c82C98zhty&sig=2VV8jPJSkOAqTP6nlvmd_U5jIv0 (Accessed: 13 February 2017).

Clarke, J. A. and McLean, D. (1988) 'ESP-A building and plant energy simulation system', *Strathclyde: Energy Simulation Research Unit, University of Strathclyde*.

Coakley, D., Raftery, P. and Keane, M. (2014) 'A review of methods to match building energy simulation models to measured data', *Renewable and sustainable energy reviews*, 37, pp. 123–141.

Coello, C. A. C. (1999) 'A comprehensive survey of evolutionary-based multiobjective optimization techniques', *Knowledge and Information systems*, 1(3), pp. 269–308.

Coello, C. C. (2006) 'Evolutionary multi-objective optimization: a historical view of the field', *IEEE computational intelligence magazine*, 1(1), pp. 28–36.

Cohen, M. F. and Wallace, J. R. (2012) *Radiosity and realistic image synthesis*. Elsevier.

Coley, D. A. and Schukat, S. (2002) 'Low-energy design: combining computer-based optimisation and human judgement', *Building and Environment*, 37(12), pp. 1241–1247.

Correia da Silva, P., Leal, V. and Andersen, M. (2013) 'Occupants interaction with electric lighting and shading systems in real single-occupied offices: Results from a monitoring campaign', *Building and Environment*, 64, pp. 152–168. doi: 10.1016/j.buildenv.2013.03.015.

Crawley, D. B. *et al.* (2001) 'EnergyPlus: creating a new-generation building energy simulation program', *Energy and buildings*, 33(4), pp. 319–331.

Crawley, D. B., Hand, J. W., Kummert, M. and Griffith, B. T. (2008) 'Contrasting the capabilities of building energy performance simulation programs', *Building and Environment*. (Part Special: Building Performance Simulation), 43(4), pp. 661–673. doi: 10.1016/j.buildenv.2006.10.027.

Cross, N. (2006) 'Design as a discipline', *Designerly Ways of Knowing*. Springer, pp. 95–103.

Cuvilliers, P. (2017) *gh-python-remote*. Available at: https://github.com/Digital-Structures/ghpythonremote (Accessed: 16 June 2020).

Daru, R. and Snijder, H. P. S. (1997) 'GACAAD or AVOCAAD? CAAD and Genetic Algorithms for an Evolutionary Design Paradigm'. Available at: http://cumincad.scix.net/cgi-bin/works/Show&_id=caadria2010_000&sort=DEFAULT&search=series:caadria/Show?6112 (Accessed: 1 July 2016).

David, M., Donn, M., Garde, F. and Lenoir, A. (2011) 'Assessment of the thermal and visual efficiency of solar shades', *Building and Environment*, 46(7), pp. 1489–1496.

Davila Delgado, J. M. (2014) *Building structural design generation and optimisation including spatial modification*. Doctoral Dissertation. Eindhoven University of Technology. Available at: https://research.tue.nl/en/publications/building-structural-design-generation-and-optimisation-including-.

Deb, K., Pratap, A., Agarwal, S. and Meyarivan, T. (2002) 'A fast and elitist multiobjective genetic algorithm: NSGA-II', *IEEE transactions on evolutionary computation*, 6(2), pp. 182–197.

Delaunay, J.-J., Wienold, J. and Sprenger, W. (1994) *GENDAYLIT*. Available at: https://floyd.lbl.gov/radiance/gendaylit.1.html (Accessed: 13 July 2020).

Deng, B., Bouaziz, S., Deuss, M., Kaspar, A., Schwartzburg, Y. and Pauly, M. (2015) 'Interactive design exploration for constrained meshes', *Computer-Aided Design*, 61, pp. 13–23.

Diakaki, C., Grigoroudis, E., Kabelis, N., Kolokotsa, D., Kalaitzakis, K. and Stavrakakis, G. (2010) 'A multi-objective decision model for the improvement of energy efficiency in buildings', *Energy*. Elsevier, 35(12), pp. 5483–5496.

Dino, I. G. and Üçoluk, G. (2017) 'Multiobjective design optimization of building space layout, energy, and daylighting performance', *Journal of Computing in Civil Engineering*. American Society of Civil Engineers, 31(5), p. 04017025.

DOE, E. (2018) *Daylighting Calculations: Engineering Reference — EnergyPlus 9.0*. Available at:

https://bigladdersoftware.com/epx/docs/9-0/engineering-reference/daylighting-calculations.html#daylighting-calculations (Accessed: 26 June 2020).

Dogan, T. and Reinhart, C. (2013) 'Automated conversion of architectural massing models into thermal 'shoebox'models', *Proceedings of BS2013*.

Dogan, T. and Reinhart, C. (2017) 'Shoeboxer: An algorithm for abstracted rapid multi-zone urban building energy model generation and simulation', *Energy and Buildings*, 140, pp. 140–153.

Dogan, T., Reinhart, C. and Michalatos, P. (2014) 'Automated multi-zone building energy model generation for schematic design and urban massing studies', in *IBPSA eSim Conference, Ottawa, Canada*.

Dogan, T., Reinhart, C. and Michalatos, P. (2016) 'Autozoner: an algorithm for automatic thermal zoning of buildings with unknown interior space definitions', *Journal of Building Performance Simulation*, 9(2), pp. 176–189.

Dols, W. S., Wang, L., Emmerich, S. J. and Polidoro, B. J. (2015) 'Development and application of an updated whole-building coupled thermal, airflow and contaminant transport simulation program (TRNSYS/CONTAM)', *Journal of Building Performance Simulation*. Taylor & Francis, 8(5), pp. 326–337.

Dorigo, M., Maniezzo, V. and Colorni, A. (1996) 'The ant system: Optimization by a colony of cooperative agents'. Available at: http://en.journals.sid.ir/ViewPaper.aspx?ID=111675 (Accessed: 6 February 2017).

Eberhart, R. and Kennedy, J. (1995) 'A new optimizer using particle swarm theory', in *Micro Machine and Human Science, 1995. MHS'95., Proceedings of the Sixth International Symposium on*. IEEE, pp. 39–43. Available at: http://ieeexplore.ieee.org/abstract/document/494215/ (Accessed: 6 February 2017).

Edelson, D. C. (2002) 'Design research: What we learn when we engage in design', *The Journal of the Learning sciences*. Taylor & Francis, 11(1), pp. 105–121.

Ehrgott, M. (2006) 'A discussion of scalarization techniques for multiple objective integer programming', *Annals of Operations Research*. Springer, 147(1), pp. 343–360.

Eigensatz, M., Deuss, M., Schiftner, A., Kilian, M., Mitra, N. J., Pottmann, H. and Pauly, M. (2010) 'Case studies in cost-optimized paneling of architectural freeform surfaces', *Advances in Architectural Geometry 2010*, pp. 49–72.

Einhorn, H. D. (1979) 'Discomfort glare: a formula to bridge differences', *Lighting Research & Technology*, 11(2), pp. 90–94.

El Daly, H. M. T. (2014) 'Automated fenestration allocation as complying with LEED rating system', *Alexandria Engineering Journal*, 53(4), pp. 883–890. doi: 10.1016/j.aej.2014.09.011.

Elango, M. and Devadas, M. D. (2014) 'Multi-criteria analysis of the design decisions in architectural design process during the pre-design stage', *Int. J. Eng. Technol*. Citeseer, 6, pp. 1033–1046.

Eltaweel, A. and Su, Y. (2017) 'Parametric design and daylighting: A literature review', *Renewable and Sustainable Energy Reviews*, 73, pp. 1086–1103. doi: 10.1016/j.rser.2017.02.011.

EnergyPlus (2017) 'EnergyPlus - features', *https://energyplus.net/features*, 8 February. Available at: https://energyplus.net/features (Accessed: 8 February 2017).

Ercan, B. and Elias-Ozkan, S. T. (2015) 'Performance-based parametric design explorations: A method for generating appropriate building components', *Design Studies*, 38, pp. 33–53. doi: 10.1016/j.destud.2015.01.001.

Evins, R. (2013) 'A review of computational optimisation methods applied to sustainable building design', *Renewable and Sustainable Energy Reviews*, 22, pp. 230–245. doi: 10.1016/j.rser.2013.02.004.

Fabrizio, E. and Monetti, V. (2015) 'Methodologies and Advancements in the Calibration of Building Energy Models', *Energies*. Multidisciplinary Digital Publishing Institute, 8(4), pp. 2548–2574. doi: 10.3390/en8042548.

FCC Arquitectura (2015) *CELLA BAR - FCC Arquitetura*. Available at: https://fc-arquitectura.com/projeto/cella-bar/ (Accessed: 21 February 2020).

Feng, M. and Staum, J. (2017) 'Green Simulation: Reusing the Output of Repeated Experiments', *ACM Transactions on Modeling and Computer Simulation*, 27(4), p. 23:1–23:28. doi: 10.1145/3129130.

Ferrara, M., Fabrizio, E., Virgone, J. and Filippi, M. (2014) 'A simulation-based optimization method for cost-optimal analysis of nearly Zero Energy Buildings', *Energy and Buildings*, 84, pp. 442–457.

Fesanghary, M., Asadi, S. and Geem, Z. W. (2012) 'Design of low-emission and energy-efficient residential buildings using a multi-objective optimization algorithm', *Building and environment*, 49, pp. 245–250.

Fisher, D. E. (1995) *An experimental investigation of mixed convection heat transfer in a rectangular enclosure*. PhD Thesis. University of Illinois at Urbana-Champaign.

Flager, F., Welle, B., Bansal, P., Soremekun, G. and Haymaker, J. (2009) 'Multidisciplinary process integration and design optimization of a classroom building', *Journal of Information Technology in Construction*, 14, pp. 595–612.

Foster and Partners (2000) *Great Glasshouse | Foster + Partners*. Available at: https://www.fosterandpartners.com/projects/great-glasshouse/ (Accessed: 21 February 2020).

Foster and Partners (2004) *Sage Gateshead | Architecture Projects | Foster + Partners*, *Foster and Partners*. Available at: https://www.fosterandpartners.com/projects/sage-gateshead/ (Accessed: 29 January 2020).

Foster and Partners (2014) *New International Airport Mexico City*. Available at: https://www.fosterandpartners.com/projects/new-international-airport-mexico-city/ (Accessed: 7 November 2019).

Foucquier, A., Robert, S., Suard, F., Stéphan, L. and Jay, A. (2013) 'State of the art in building modelling and energy performances prediction: A review', *Renewable and Sustainable Energy Reviews*, 23, pp. 272–288. doi: 10.1016/j.rser.2013.03.004.

Fraisse, G., Viardot, C., Lafabrie, O. and Achard, G. (2002) 'Development of a simplified and accurate building model based on electrical analogy', *Energy and buildings*. Elsevier, 34(10), pp. 1017–1031.

Fricke, G. (1996) 'Successful individual approaches in engineering design', *Research in Engineering Design*, 8(3), pp. 151–165. doi: 10.1007/BF01608350.

Friedman, K. (2003) ‘Theory construction in design research: criteria: approaches, and methods’, *Design studies*. Elsevier, 24(6), pp. 507–522.

Fritzson, P. and Engelson, V. (1998) ‘Modelica—A unified object-oriented language for system modeling and simulation’, in *European Conference on Object-Oriented Programming*. Springer, pp. 67–90.

Futrell, B. J., Ozelkan, E. C. and Brentrup, D. (2015a) ‘Bi-objective optimization of building enclosure design for thermal and lighting performance’, *Building and Environment*, 92, pp. 591–602.

Futrell, B. J., Ozelkan, E. C. and Brentrup, D. (2015b) ‘Optimizing complex building design for annual daylighting performance and evaluation of optimization algorithms’, *Energy and Buildings*, 92, pp. 234–245.

Geem, Z. W., Kim, J. H. and Loganathan, G. V. (2001) ‘A new heuristic optimization algorithm: harmony search’, *Simulation*, 76(2), pp. 60–68.

Gehry Technologies and others (2015) *Digital Project*.

Geisler-Moroder, D., Lee, E. and Ward, G. (2016) ‘Validation of the Radiance 5-Phase-Method against field measurements’, in *15th International Radiance Workshop, Padua, Italy*.

Georgescu, M. and Mezić, I. (2015) ‘Building energy modeling: A systematic approach to zoning and model reduction using Koopman Mode Analysis’, *Energy and Buildings*, 86, pp. 794–802. doi: 10.1016/j.enbuild.2014.10.046.

Gero, J. S., D’Cruz, N. and Radford, A. D. (1983) ‘Energy in context: a multicriteria model for building design’, *Building and Environment*, 18(3), pp. 99–107.

Giovannini, L., Favoino, F., Lo Verso, V., Pellegrino, A. and Serra, V. (2018) ‘A Simplified Approach for the Annual and Spatial Evaluation of the Comfort Classes of Daylight Glare Using Vertical Illuminances’, *Buildings*, 8(12), p. 171.

Glover, F. and Laguna, M. (2013) *Tabu Search∗*. Springer. Available at: http://link.springer.com/10.1007/978-1-4419-7997-1_17 (Accessed: 6 February 2017).

Goia, F., Chaudhary, G. and Fantucci, S. (2018) ‘Modelling and experimental validation of an algorithm for simulation of hysteresis effects in phase change materials for building components’, *Energy and Buildings*. Elsevier, 174, pp. 54–67.

Goldenberg, D. E. (1989) *Genetic algorithms in search, optimization and machine learning*. Addison Wesley, Reading: MA.

Gou, S., Nik, V. M., Scartezzini, J.-L., Zhao, Q. and Li, Z. (2018) ‘Passive design optimization of newly-built residential buildings in Shanghai for improving indoor thermal comfort while reducing building energy demand’, *Energy and Buildings*, 169, pp. 484–506. doi: 10.1016/j.enbuild.2017.09.095.

Gouda, M. M., Danaher, S. and Underwood, C. P. (2002) ‘Building thermal model reduction using nonlinear constrained optimization’, *Building and environment*. Elsevier, 37(12), pp. 1255–1265.

Granadeiro, V., Duarte, J. P., Correia, J. R. and Leal, V. M. (2013) ‘Building envelope shape design in early stages of the design process: Integrating architectural design systems and energy simulation’, *Automation in Construction*, 32, pp. 196–209.

Greenberg, D. P., Cohen, M. F. and Torrance, K. E. (1986) 'Radiosity: A method for computing global illumination', *The Visual Computer*. Springer, 2(5), pp. 291–297.

Grobe, L. O. (2010) 'The photon map extension for Radiance-Applications'.

Grobe, Lars O. (2019a) 'Photon mapping in image-based visual comfort assessments with BSDF models of high resolution', *Journal of Building Performance Simulation*. Taylor & Francis, 12(6), pp. 745–758.

Grobe, Lars O. (2019b) 'Photon mapping to accelerate daylight simulation with high-resolution, data-driven fenestration models', in *Journal of Physics: Conference Series*. IOP Publishing, p. 012154.

Grobe, Lars Oliver (2019) 'Photon-mapping in Climate-Based Daylight Modelling with High-resolution BSDFs', *Energy and Buildings*. Elsevier, 205, p. 109524.

Grobe, L. O., Wittkopf, S. and Kazanasmaz, Z. T. (2017) 'High-resolution data-driven models of Daylight Redirection Components'. TU Delft Open.

Grondzik, W. T. and Kwok, A. G. (2019) *Mechanical and electrical equipment for buildings*. John wiley & sons.

Guglielmetti, R., Macumber, D. and Long, N. (2011) *OpenStudio: an open source integrated analysis platform*. National Renewable Energy Lab.(NREL), Golden, CO (United States).

Guindon, R. (1990) 'Designing the Design Process: Exploiting Opportunistic Thoughts.', *Human-Computer Interaction*, 5, pp. 305–344.

Hamdy, M., Palonen, M. and Hasan, A. (2012) 'Implementation of pareto-archive NSGA-II algorithms to a nearly-zero-energy building optimisation problem', *BSO12 IBPSA-England*, pp. 10–11.

Harish, V. S. K. V. and Kumar, A. (2016) 'A review on modeling and simulation of building energy systems', *Renewable and Sustainable Energy Reviews*, 56, pp. 1272–1292. doi: 10.1016/j.rser.2015.12.040.

Hauer, M., Grobbauer, M., Holper, S. and PlÖrer, D. (2019) 'Thermal modeling of complex fenestration systems: Comparison with long-term measurements on an office façade mock-up', *Science and Technology for the Built Environment*, 0(0), pp. 1–14. doi: 10.1080/23744731.2019.1614863.

Haves, P., Ravache, B., Fergadiotti, A., Yazdanian, M. and Kohler, C. (2019) 'Accuracy of HVAC Load Predictions: Validation of EnergyPlus and DOE-2: Using an Instrumented Test Facility', *Proceedings of Building Simulation 2019*.

Hayter, S. J., Torcellini, P. A. and Judkoff, R. (1999) 'Optimizing building and HVAC systems', *ASHRAE journal*. American Society of Heating, Refrigeration and Air Conditioning Engineers, Inc., 41(12), p. 46.

Hemker, T., De Gersem, H., Von Stryk, O. and Weiland, T. (2008) 'Mixed-integer nonlinear design optimization of a superconductive magnet with surrogate functions', *IEEE transactions on magnetics*. IEEE, 44(6), pp. 1110–1113.

Henriques, G. C., Duarte, J. P. and Leal, V. (2012) 'Strategies to control daylight in a responsive skylight system', *Automation in Construction*, 28, pp. 91–105. doi: 10.1016/j.autcon.2012.06.002.

Hensen, J. L. and Lamberts, R. (2019) *Building performance simulation for design and operation*. Routledge.

Hirsch, J. J. (2006) *eQUEST*. Available at: http://www.doe2.com/equest/ (Accessed: 26 June 2020).

Hitchcock, R. J., Mitchell, R., Yazdanian, M., Lee, E. and Huizenga, C. (2008) 'COMFEN: A commercial fenestration/façade design tool', *Proceedings of SimBuild*, 3(1), pp. 246–252.

Hittle, D. C. (1981) 'BLAST-Building loads analysin and system thermodynamics program, version 3.0: User manual.', *Technical Report E-171*. US Army Construction Engineering Research Laboratory.

Hopkinson, R. G. (1972) 'Glare from daylighting in buildings', *Applied Ergonomics*, 3(4), pp. 206–215.

Hopkinson, R. G., Longmore, J. and Petherbridge, P. (1954) 'An empirical formula for the computation of the indirect component of daylight factor', *Transactions of the Illuminating Engineering Society*. SAGE Publications Sage UK: London, England, 19(7_IEStrans), pp. 201–219.

Hopkinson, R. G., Petherbridge, P. and Longmore, J. (1966) *Daylighting*. Heinemann.

Horváth, I. (2004) 'A treatise on order in engineering design research', *Research in engineering design*. Springer, 15(3), pp. 155–181.

Horváth, I. (2007) 'Comparison of three methodological approaches of design research', in *DS 42: Proceedings of ICED 2007, the 16th International Conference on Engineering Design, Paris, France, 28.-31.07. 2007*, pp. 361–362.

Horváth, I. (2008) 'Differences between'research in design context'and'design inclusive research'in the domain of industrial design engineering', *Journal of Design Research*. Inderscience Publishers, 7(1), pp. 61–83.

Hou, D., Liu, G., Zhang, Q., Wang, L. and Dang, R. (2017) 'Integrated Building Envelope Design Process Combining Parametric Modelling and Multi-Objective Optimization', *Transactions of Tianjin University*. Springer, 23(2), pp. 138–146.

Huang, Y. and Niu, J. (2016) 'Optimal building envelope design based on simulated performance: History, current status and new potentials', *Energy and Buildings*, 117, pp. 387–398.

Hubler, D., Tupper, K. and Greensfelder, E. (2010) 'AB-10-C028 Pulling the Levers on Existing Buildings: A Simple Method for Calibrating Hourly Energy Models', *ASHRAE Transactions*, 116(2), p. 261.

Huizenga, C. *et al.* (2017) *WINDOW 7.5*. Lawrence Berkeley National Laboratory.

Humppi, H. (2015) *Algorithm-Aided Building Information Modeling: Connecting Algorithm-Aided Design and Object-Oriented Design*. Master's Thesis.

Hussain, S. and Oosthuizen, P. H. (2012) 'A numerical study of the effect of thermal mass on the transient thermal performance of a simple three storied atrium building', in *Heat Transfer Summer Conference*. American Society of Mechanical Engineers, pp. 943–952.

Hviid, C. A., Nielsen, T. R. and Svendsen, S. (2008) 'Simple tool to evaluate the impact of daylight on building energy consumption', *Solar Energy*, 82(9), pp. 787–798.

IES, V. (2008) *Virtual Environment (VE) by Integrated Environmental Solutions (IES)*.

IESNA, I. (2012) 'LM-83-12 IES Spatial Daylight Autonomy (sDA) and Annual Sunlight Exposure (ASE)', *New York, NY, USA: IESNA Lighting Measurement*.

Immel, D. S., Cohen, M. F. and Greenberg, D. P. (1986) 'A radiosity method for non-diffuse environments', *Acm Siggraph Computer Graphics*. ACM New York, NY, USA, 20(4), pp. 133–142.

Jakica, N. (2018) 'State-of-the-art review of solar design tools and methods for assessing daylighting and solar potential for building-integrated photovoltaics', *Renewable and Sustainable Energy Reviews*, 81, pp. 1296–1328. doi: 10.1016/j.rser.2017.05.080.

Jakubiec, A. and Reinhart, C. (2010) 'The use of glare metrics in the design of daylit spaces: recommendations for practice', in *9th international Radiance workshop*, pp. 20–21.

Jakubiec, A. and Reinhart, C. (2011) 'DIVA-FOR-RHINO 2.0: environmental parametric modeling in rhinoceros/grasshopper using RADIANCE, Daysim and EnergyPlus', in *Conference proceedings of building simulation*.

Jeong, W. and Son, J. (2016) 'An Algorithm to Translate Building Topology in Building Information Modeling into Object-Oriented Physical Modeling-Based Building Energy Modeling', *Energies*, 9(1), p. 50.

Johnson, R., Sullivan, R., Selkowitz, S., Nozaki, S., Conner, C. and Arasteh, D. (1984) 'Glazing energy performance and design optimization with daylighting', *Energy and Buildings*, 6(4), pp. 305–317. doi: 10.1016/0378-7788(84)90014-8.

Jones, N. L. (2019) 'Fast Climate-Based Glare Analysis and Spatial Mapping', in *Proceedings of Building Simulation 2019: 16th Conference of IBPSA*.

Jones, N. L., Greenberg, D. P. and Pratt, K. B. (2012) 'Fast computer graphics techniques for calculating direct solar radiation on complex building surfaces', *Journal of Building Performance Simulation*, 5(5), pp. 300–312.

Jones, N. L., McCrone, C. J., Walter, B. J., Pratt, K. B. and Greenberg, D. P. (2013) 'Automated translation and thermal zoning of digital building models for energy analysis', in *Building Simulation Conference*. Available at: http://www.ibpsa.org/proceedings/BS2013/p_1027.pdf (Accessed: 1 July 2016).

Jones, Nathaniel L and Reinhart, C. F. (2015) 'Fast Daylight Coefficient Calculation Using Graphics Hardware', in *Proceedings of BS2015. 14th Conference of International Building Performance Simulation Association*, Hyderabad, India, p. 8.

Jones, Nathaniel L. and Reinhart, C. F. (2015) 'Validation of GPU lighting simulation in naturally and artificially lit spaces', in *Proceedings of the IBPSA Building Simulation Conference*.

Jones, N. L. and Reinhart, C. F. (2017) 'Experimental validation of ray tracing as a means of image-based visual discomfort prediction', *Building and Environment*, 113, pp. 131–150.

Jones, N. L. and Reinhart, C. F. (2019) 'Effects of real-time simulation feedback on design for visual comfort', *Journal of Building Performance Simulation*. Taylor & Francis, 12(3), pp. 343–361. doi: 10.1080/19401493.2018.1449889.

Jusselme, T., Cozza, S., Hoxha, E., Brambilla, A., Evequoz, F., Lalanne, D., Rey, E. and Andersen, M. (2016) 'Towards a pre-design method for low carbon architectural strategies', *Proceedings of PLEA 2016, 32th international Conference on Passive and Low Energy Architecture*. Available at: http://infoscience.epfl.ch/record/214876.

Kajiya, J. T. (1986) 'The rendering equation', in *Proceedings of the 13th annual conference on Computer graphics and interactive techniques*, pp. 143–150.

Kajiya, J. T. and Kay, T. L. (1989) 'Rendering fur with three dimensional textures', *ACM Siggraph Computer Graphics*. ACM New York, NY, USA, 23(3), pp. 271–280.

Kasinalis, C., Loonen, R. C., Cóstola, D. and Hensen, J. L. M. (2014) 'Framework for assessing the performance potential of seasonally adaptable facades using multi-objective optimization', *Energy and Buildings*. Elsevier, 79, pp. 106–113.

Kazanasmaz, T., Grobe, L. O., Bauer, C., Krehel, M. and Wittkopf, S. (2016) 'Three approaches to optimize optical properties and size of a South-facing window for spatial Daylight Autonomy', *Building and Environment*. Elsevier, 102, pp. 243–256.

Keller, A. I. (2005) *For Inspiration Only; Designer interaction with informal collections of visual material*.

Kensek, K. (2015) 'Visual programming for building information modeling: energy and shading analysis case studies', *College Publishing*, 10(4), pp. 28–43.

Kensek, K. and Noble, D. (2014) *Building information modeling: BIM in current and future practice*. John Wiley & Sons.

Keough, I. (2011) 'Dynamo: designing a visual scripting interface for the Revit API (notes)', *Also se e https://github. com/ikeough/Dynamo/wiki for more information about coding in Dynamo*.

Kharvari, F. (2020) 'An empirical validation of daylighting tools: Assessing radiance parameters and simulation settings in Ladybug and Honeybee against field measurements', *Solar Energy*. Elsevier, 207, pp. 1021–1036.

Khoroshiltseva, M., Slanzi, D. and Poli, I. (2016) 'A Pareto-based multi-objective optimization algorithm to design energy-efficient shading devices', *Applied Energy*, 184, pp. 1400–1410. doi: 10.1016/j.apenergy.2016.05.015.

Kim, J. B., Jeong, W., Clayton, M. J., Haberl, J. S. and Yan, W. (2015) 'Developing a physical BIM library for building thermal energy simulation', *Automation in construction*, 50, pp. 16–28.

Kim, J., Schiavon, S. and Brager, G. (2018) 'Personal comfort models–A new paradigm in thermal comfort for occupant-centric environmental control', *Building and Environment*. Elsevier, 132, pp. 114–124.

Kirimtat, A., Krejcar, O., Ekici, B. and Fatih Tasgetiren, M. (2019) 'Multi-objective energy and daylight optimization of amorphous shading devices in buildings', *Solar Energy*, 185, pp. 100–111. doi: 10.1016/j.solener.2019.04.048.

Kleindienst, S. and Andersen, M. (2009) 'The adaptation of daylight glare probability to dynamic metrics in a computational setting', in *Proceedings of Lux Europa 2009–11th European lighting conference*.

Kleindienst, S. and Andersen, M. (2012) 'Comprehensive annual daylight design through a goal-based approach', *Building Research & Information*, 40(2), pp. 154–173. doi: 10.1080/09613218.2012.641301.

Kleindienst, S., Bodart, M. and Andersen, M. (2008) 'Graphical representation of climate-based daylight performance to support architectural design', *Leukos*. Taylor & Francis, 5(1), pp. 39–61.

Klems, J. H. (1994a) 'New method for predicting the solar heat gain of complex fenestration systems- 2. Detailed description of the matrix layer calculation', *ASHRAE Transactions*, 100(1), pp. 1073–1086.

Klems, J. H. (1994b) 'New method for predicting the solar heat gain of complex fenestration systems- I. Overview and derivation of the matrix layer calculation', *ASHRAE Transactions*, 100(1), pp. 1065–1072.

Knippers, J. and Menges, A. (2010) *ICD/ITKE Research Pavilion 2010 | Institute for Computational Design and Construction | University of Stuttgart*. Available at: https://www.icd.uni-stuttgart.de/projects/icditke-research-pavilion-2010/ (Accessed: 24 February 2020).

Kolarevic, B. (2004) *Architecture in the digital age: design and manufacturing*. taylor & Francis.

Kolås, T. (2013) 'Performance of daylight redirecting venetian blinds for sidelighted spaces at high latitudes'. Norges teknisk-naturvitenskapelige universitet, Fakultet for arkitektur og ….

Konis, K. (2014) 'Predicting visual comfort in side-lit open-plan core zones: Results of a field study pairing high dynamic range images with subjective responses', *Energy and Buildings*, 77, pp. 67–79.

Konis, K., Gamas, A. and Kensek, K. (2016) 'Passive performance and building form: An optimization framework for early-stage design support', *Solar Energy*, 125, pp. 161–179.

Koskinen, I., Zimmerman, J., Binder, T., Redstrom, J. and Wensveen, S. (2013) 'Design research through practice: From the lab, field, and showroom', *IEEE Transactions on Professional Communication*. IEEE, 56(3), pp. 262–263.

Kota, S. and Haberl, J. S. (2009) 'Historical survey of daylighting calculations methods and their use in energy performance simulations'. Available at: http://oaktrust.library.tamu.edu/handle/1969.1/90845 (Accessed: 31 January 2017).

Kovacic, I., Oberwinter, L., Müller, C. and Achammer, C. (2013) 'The "BIM-sustain" experiment – simulation of BIM-supported multi-disciplinary design', *Visualization in Engineering*, 1(1), p. 13. doi: 10.1186/2213-7459-1-13.

Koziel, S., Ciaurri, D. E. and Leifsson, L. (2011) 'Surrogate-based methods', in *Computational optimization, methods and algorithms*. Springer, pp. 33–59.

Koziel, S. and Leifsson, L. (2013) *Surrogate-based modeling and optimization*. Springer.

Koziel, S. and Yang, X.-S. (2011) *Computational optimization, methods and algorithms*. Springer.

Krieg, O. D., Schwinn, T., Menges, A., Li, J.-M., Knippers, J., Schmitt, A. and Schwieger, V. (2015) 'Biomimetic lightweight timber plate shells: Computational integration of robotic fabrication, architectural geometry and structural design', in *Advances in Architectural Geometry 2014*. Springer, pp. 109–125. Available at: http://link.springer.com/10.1007/978-3-319-11418-7_8 (Accessed: 1 July 2016).

Kristensen, M. H. and Petersen, S. (2016) 'Choosing the appropriate sensitivity analysis method for building energy model-based investigations', *Energy and Buildings*. Elsevier, 130, pp. 166–176.

L+U (2015) *Facebook MPK 20 | LOISOS + UBBELOHDE | Architecture . Energy . Light*. Available at: http://www.coolshadow.com/consulting/MPK20.html (Accessed: 4 August 2020).

L+U (2018) *MPK 21 | LOISOS + UBBELOHDE | Architecture . Energy . Light*. Available at: http://www.coolshadow.com/consulting/MPK21.html (Accessed: 4 August 2020).

Lambda, R. C. (1994) *TracePro*. Lambda Research Corporation. Available at: https://lambdares.com/tracepro/.

Lange, B. (1994) 'The simulation of radiant light transfer with stochastic ray-tracing', in *Photorealistic rendering in computer graphics*. Springer, pp. 30–44.

Lartigue, B., Lasternas, B. and Loftness, V. (2014) 'Multi-objective optimization of building envelope for energy consumption and daylight', *Indoor and Built Environment*. SAGE Publications Ltd STM, 23(1), pp. 70–80. doi: 10.1177/1420326X13480224.

Lassance, G. (1999) 'A Pre-Design Aid Support for Architectural Daylighting', *Sharing Knowledge on Sustainable Buildings*, pp. 16–17.

Lauret, P., Boyer, H., Riviere, C. and Bastide, A. (2005) 'A genetic algorithm applied to the validation of building thermal models', *Energy and buildings*. Elsevier, 37(8), pp. 858–866.

LBNL (2015) *Complex Fenestration Daylighting Calculations: Engineering Reference — EnergyPlus 8.3*. Available at: https://bigladdersoftware.com/epx/docs/8-3/engineering-reference/complex-fenestration-daylighting-calculations.html#complex-fenestration-daylighting-calculations (Accessed: 25 November 2019).

Le Dréau, J. and Heiselberg, P. (2014) 'Sensitivity analysis of the thermal performance of radiant and convective terminals for cooling buildings', *Energy and Buildings*. Elsevier, 82, pp. 482–491.

Lee, Eleanor S., Geisler-Moroder, D. and Ward, G. (2018) 'Modeling the direct sun component in buildings using matrix algebraic approaches: Methods and validation', *Solar Energy*, 160, pp. 380–395. doi: 10.1016/j.solener.2017.12.029.

Lee, E. S., Geisler-Moroder, D. and Ward, G. (2018) 'Validation of the Five-Phase Method for Simulating Complex Fenestration Systems with Radiance against Field Measurements'.

Leitão, A. and Santos, L. (2011) 'Programming languages for generative design: visual or textual', *Proceedings of the 29th eCAADe*, pp. 549–557.

Leitão, A., Santos, L. and Lopes, J. (2012) 'Programming languages for generative design: A comparative study', *International Journal of Architectural Computing*, 10(1), pp. 139–162.

Li, N., Cheung, S. C. P., Li, X. and Tu, J. (2017) 'Multi-objective optimization of HVAC system using NSPSO and Kriging algorithms—A case study', *Building Simulation*, 10(5), pp. 769–781. doi: 10.1007/s12273-017-0352-5.

LightLouver LLC (2010) *LightLouver*, *LightLouver daylighting system*. Available at: http://lightlouver.com/design-information/cad-files/ (Accessed: 29 June 2017).

Lilis, G. N., Giannakis, G. I. and Rovas, D. V. (2017) 'Automatic generation of second-level space boundary topology from IFC geometry inputs', *Automation in Construction*, 76, pp. 108–124.

Lin, S.-H. and Gerber, D. J. (2014a) 'Designing-in performance: A framework for evolutionary energy performance feedback in early stage design', *Automation in Construction*, 38, pp. 59–73.

Lin, S.-H. and Gerber, D. J. (2014b) 'Evolutionary energy performance feedback for design: Multidisciplinary design optimization and performance boundaries for design decision support', *Energy and Buildings*, 84, pp. 426–441.

Liu, F. C. S., Lin, S. C., You, J.-Y., Chen, Y.-T. and Sun, J.-L. (2011) 'From Internal Validation to Sensitivity Test: How Grid Computing Facilitates the Construction of an Agent-Based Simulation in Social Sciences', in *Proceedings of The International Symposium on Grids and Clouds and the Open Grid Forum — PoS(ISGC 2011 & OGF 31)*. *The International Symposium on Grids and Clouds and the Open Grid Forum*, Academia Sinica, Taipei, Taiwan: Sissa Medialab, p. 002. doi: 10.22323/1.133.0002.

Living LLC, D. (2013) *WELL Building Standard_v1 with January 2017 addenda*. New York, NY 10014.

Longo, S., Montana, F. and Riva Sanseverino, E. (2019) 'A review on optimization and cost-optimal methodologies in low-energy buildings design and environmental considerations', *Sustainable Cities and Society*, 45, pp. 87–104. doi: 10.1016/j.scs.2018.11.027.

Luo, M., Arens, E., Zhang, H., Ghahramani, A. and Wang, Z. (2018) 'Thermal comfort evaluated for combinations of energy-efficient personal heating and cooling devices', *Building and Environment*. Elsevier, 143, pp. 206–216.

Machairas, V., Tsangrassoulis, A. and Axarli, K. (2014) 'Algorithms for optimization of building design: A review', *Renewable and Sustainable Energy Reviews*, 31, pp. 101–112.

Mackey, C., Roudsari, M. S., Subramaniam, S., Dao, A., Vasanthakumar, S. and Haider, A. (2015) *ladybug-tools/honeybee*. Ladybug Tools. Available at: https://github.com/ladybug-tools/honeybee (Accessed: 30 June 2020).

Mahmoud, A. H. A. and Elghazi, Y. (2016) 'Parametric-based designs for kinetic facades to optimize daylight performance: Comparing rotation and translation kinetic motion for hexagonal facade patterns', *Solar Energy*, 126, pp. 111–127. doi: 10.1016/j.solener.2015.12.039.

Makki, M., Showkatbakhsh, M. and Song, Y. (2020) *Wallacei V2.6*. Available at: https://www.wallacei.com (Accessed: 13 June 2020).

Mangkuto, R. A., Siregar, M. A. A. and Handina, A. (2018) 'Determination of appropriate metrics for indicating indoor daylight availability and lighting energy demand using genetic algorithm', *Solar Energy*. Elsevier, 170, pp. 1074–1086.

Manzan, M. (2014) 'Genetic optimization of external fixed shading devices', *Energy and Buildings*, 72, pp. 431–440. doi: 10.1016/j.enbuild.2014.01.007.

Manzan, M. and Clarich, A. (2017) 'FAST energy and daylight optimization of an office with fixed and movable shading devices', *Building and Environment*. (Advances in daylighting and visual comfort research), 113, pp. 175–184. doi: 10.1016/j.buildenv.2016.09.035.

Manzan, M. and Pinto, F. (2009) 'Genetic optimization of external shading devices', in *Proceedings: Building Simulation*. Available at: http://ibpsa.org/proceedings/BS2009/BS09_0180_187.pdf (Accessed: 2 February 2017).

Mara, T. A. and Tarantola, S. (2008) 'Application of global sensitivity analysis of model output to building thermal simulations', in *Building Simulation*. Springer, pp. 290–302.

March, J. S. and Simon, H. A. (1958) 'HA (1958) Organizations', *New York*.

Mardaljevic, J. (2000) 'Simulation of annual daylighting profiles for internal illuminance', *International Journal of Lighting Research and Technology*, 32(3), pp. 111–118.

Mardaljevic, J., Andersen, M., Roy, N. and Christoffersen, J. (2012) 'Daylighting metrics: is there a relation between useful daylight illuminance and daylight glare probability', in *Proceedings of the building simulation and optimization conference (BSO12), Loughborough, UK*.

Mardaljevic, J., Heschong, L. and Lee, E. (2009) 'Daylight metrics and energy savings', *Lighting Research and Technology*, 41(3), pp. 261–283.

Marin, P., Blanchi, Y. and Janda, M. (2015) 'Cost analysis and data based design for supporting programmatic phase'. CUMINCAD.

Martin, M., Afshari, A., Armstrong, P. R. and Norford, L. K. (2015) 'Estimation of urban temperature and humidity using a lumped parameter model coupled with an EnergyPlus model', *Energy and Buildings*. Elsevier, 96, pp. 221–235.

Mateus, N. M., Pinto, A. and da Graça, G. C. (2014) 'Validation of EnergyPlus thermal simulation of a double skin naturally and mechanically ventilated test cell', *Energy and Buildings*. Elsevier, 75, pp. 511–522.

MathWorks (2002) *Simulink - Simulation and Model-Based Design - MATLAB & Simulink*. Available at: https://www.mathworks.com/products/simulink.html (Accessed: 30 June 2020).

Matt, G., Brewer, A. and Sklar, M. (2010) 'External validity'. Elsevier.

McNeel, R. and others (2015) *Rhinoceros*.

McNeel, R. and others (2017) *Grasshopper*.

McNeil, A. (2010) 'The Three-Phase Method for Simulating Complex Fenestration with Radiance'. Available at: https://www.radiance-online.org/learning/tutorials/Tutorial-ThreePhaseMethod.pdf (Accessed: 8 July 2020).

McNeil, A., Jonsson, C. J., Appelfeld, D., Ward, G. and Lee, E. S. (2013) 'A validation of a ray-tracing tool used to generate bi-directional scattering distribution functions for complex fenestration systems', *Solar Energy*, 98, pp. 404–414.

McNeil, A. and Lee, E. S. (2013) 'A validation of the Radiance three-phase simulation method for modelling annual daylight performance of optically complex fenestration systems', *Journal of Building Performance Simulation*, 6(1), pp. 24–37.

Meerbeek, B. W., de Bakker, C., De Kort, Y. A. W., Van Loenen, E. J. and Bergman, T. (2016) 'Automated blinds with light feedback to increase occupant satisfaction and energy saving', *Building and Environment*. Elsevier, 103, pp. 70–85.

Menberg, K., Heo, Y. and Choudhary, R. (2016) 'Sensitivity analysis methods for building energy models: Comparing computational costs and extractable information', *Energy and Buildings*, 133, pp. 433–445. doi: 10.1016/j.enbuild.2016.10.005.

Menges, A. (2019) *Baden-Wuerttemberg Haus, World EXPO 2020, Dubai*. Available at: http://www.achimmenges.net/?p=21458 (Accessed: 21 February 2020).

Modest, M. F. (1982) 'A general model for the calculation of daylighting in interior spaces', *Energy and Buildings*, 5(1), pp. 69–79. doi: 10.1016/0378-7788(82)90030-5.

Monks, M., Oh, B. M. and Dorsey, J. (2000) 'Audioptimization: goal-based acoustic design', *IEEE computer graphics and applications*, 20(3), pp. 76–90.

Murphy/Jahn (2011) *Joe and Rika Mansueto Library*, *JAHN*. Available at: https://www.jahn-us.com/joe-and-rika-mansueto-library (Accessed: 21 February 2020).

Murray, S. N., Walsh, B. P., Kelliher, D. and O'Sullivan, D. T. J. (2014) 'Multi-variable optimization of thermal energy efficiency retrofitting of buildings using static modelling and genetic algorithms–A case study', *Building and Environment*, 75, pp. 98–107.

Nabil, A. and Mardaljevic, J. (2006) 'Useful daylight illuminances: A replacement for daylight factors', *Energy and buildings*, 38(7), pp. 905–913.

Nasruddin, Sholahudin, Satrio, P., Mahlia, T. M. I., Giannetti, N. and Saito, K. (2019) 'Optimization of HVAC system energy consumption in a building using artificial neural network and multi-objective genetic algorithm', *Sustainable Energy Technologies and Assessments*, 35, pp. 48–57. doi: 10.1016/j.seta.2019.06.002.

Navvab, M. and Altland, G. (1997) 'Application of CIE glare index for daylighting evaluation', *Journal of the Illuminating Engineering Society*, 26(2), pp. 115–128.

Nazzal, A. A. (2005) 'A new evaluation method for daylight discomfort glare', *International Journal of Industrial Ergonomics*, 35(4), pp. 295–306.

Negendahl, K. (2015) 'Building performance simulation in the early design stage: An introduction to integrated dynamic models', *Automation in Construction*, 54, pp. 39–53.

Nelder, J. A. and Mead, R. (1965) 'A simplex method for function minimization', *The computer journal*, 7(4), pp. 308–313.

Nguyen, A. T. (2013) *Sustainable housing in Vietnam: Climate responsive design strategies to optimize thermal comfort*. PhD Thesis. Université de Liège, Liège, Belgium.

Nguyen, A.-T. and Reiter, S. (2015) 'A performance comparison of sensitivity analysis methods for building energy models', in *Building simulation*. Springer, pp. 651–664.

Nguyen, A.-T., Reiter, S. and Rigo, P. (2014) 'A review on simulation-based optimization methods applied to building performance analysis', *Applied Energy*, 113, pp. 1043–1058.

Nielsen, T. R. and Svendsen, S. (2002) *Optimization of buildings with respect to energy and indoor environment*. Technical University of DenmarkDanmarks Tekniske Universitet, Department of Buildings and EnergyInstitut for Bygninger og Energi. Available at: http://orbit.dtu.dk/fedora/objects/orbit:83390/datastreams/file_5275664/content (Accessed: 7 February 2017).

Nocedal, J. and Wright, S. (2006) *Numerical optimization*. Springer Science & Business Media.

Ochoa, C. E., Aries, M. B. C. and Hensen, J. L. M. (2012) 'State of the art in lighting simulation for building science: a literature review', *Journal of Building Performance Simulation*. Taylor & Francis, 5(4), pp. 209–233. doi: 10.1080/19401493.2011.558211.

Olbina, S. and Beliveau, Y. (2009) 'Developing a transparent shading device as a daylighting system', *Building Research & Information*, 37(2), pp. 148–163.

Overbeeke, K. and Forlizzi, J. (2006) 'Creativity and Design: What the Established Teaches Us.' Baywood Publishing Co.

Oxman, R. (2008) 'Performance-based design: current practices and research issues', *International journal of architectural computing*, 6(1), pp. 1–17.

Oxman, R. (2017) 'Thinking difference: Theories and models of parametric design thinking', *Design studies*. Elsevier, 52, pp. 4–39.

Ozorhon, I. F. and Uraz, T. U. (2014) 'Natural light as a determinant of the identity of architectural space', *Journal of Architecture and Urbanism*, 38(2), pp. 107–119. doi: 10.3846/20297955.2014.916513.

Pachauri, R. K. *et al.* (2014) *Climate change 2014: synthesis report. Contribution of Working Groups I, II and III to the fifth assessment report of the Intergovernmental Panel on Climate Change*. IPCC. Available at: http://epic.awi.de/37530/ (Accessed: 13 February 2017).

Pan, Y., Li, Y., Huang, Z. and Wu, G. (2010) 'Study on simulation methods of atrium building cooling load in hot and humid regions', *Energy and Buildings*. Elsevier, 42(10), pp. 1654–1660.

Pan, Y., Yin, R. and Huang, Z. (2008) 'Energy modeling of two office buildings with data center for green building design', *Energy and Buildings*, 40(7), pp. 1145–1152. doi: 10.1016/j.enbuild.2007.10.008.

Parkinson, T. and De Dear, R. (2015) 'Thermal pleasure in built environments: physiology of alliesthesia', *Building Research & Information*. Taylor & Francis, 43(3), pp. 288–301.

Paule, B., Boutillier, J., Pantet, S., Sutter, Y. and Sa, E. (2018) 'A lighting simulation tool for the new European daylighting standard', in *International Building Simulation Association England: 4th Building Simulation and Optimization Conference*. *Building Simulation and Optimization Conference*, Cambridge, UK, pp. 32–37. Available at: http://www.ibpsa.org/proceedings/BSO2018/1A-5.pdf.

Peippo, K., Lund, P. D. and Vartiainen, E. (1999) 'Multivariate optimization of design trade-offs for solar low energy buildings', *Energy and Buildings*. Elsevier, 29(2), pp. 189–205.

Perez, R., Ineichen, P., Seals, R., Michalsky, J. and Stewart, R. (1990) 'Modeling daylight availability and irradiance components from direct and global irradiance', *Solar Energy*, 44(5), pp. 271–289. doi: 10.1016/0038-092X(90)90055-H.

Perez, R., Seals, R. and Michalsky, J. (1993) 'All-weather model for sky luminance distribution—preliminary configuration and validation', *Solar energy*, 50(3), pp. 235–245.

Peters, B. (2013) 'Computation works: the building of algorithmic thought', *Architectural design*, 2(83), pp. 8–15.

Petersen, S., Broholt, T., Christensen, L. and Purup, P. B. (2018) 'Thermal Performance Simulation of Complex Fenestration Systems in the Early Design Stage', in *Proceeding of BSO 2018*. *4th Building Simulation and Optimization Conference*, Cambridge UK, pp. 573–580.

Pharr, M., Jakob, W. and Humphreys, G. (2016) *Physically based rendering: From theory to implementation*. Morgan Kaufmann.

Phillips, D. A. and Soligo, M. J. (2019) 'Will CFD ever Replace Wind Tunnels for Building Wind Simulations?', *International Journal of High-Rise Buildings*. Council on Tall Building and Urban Habitat Korea, 8(2), pp. 107–116.

Piacentino, G. (2011) *GhPython*, *Food4Rhino*. Available at: https://www.food4rhino.com/app/ghpython (Accessed: 16 June 2020).

Picco, M., Lollini, R. and Marengo, M. (2014) 'Towards energy performance evaluation in early stage building design: A simplification methodology for commercial building models', *Energy and Buildings*, 76, pp. 497–505. doi: 10.1016/j.enbuild.2014.03.016.

Picco, M. and Marengo, M. (2015) 'On the impact of simplifications on building energy simulation for early stage building design', *Journal of Engineering and Architecture*, 3(1), pp. 66–78.

Piker, D. (2015) *Kangaroo 2 - Grasshopper Addon Reference*. Available at: https://rhino.github.io/addons/kangaroo-2.html (Accessed: 25 November 2019).

Pineda, J. (1988) 'A parallel algorithm for polygon rasterization', in *Proceedings of the 15th annual conference on Computer graphics and interactive techniques*, pp. 17–20.

Polak, E. and Wetter, M. (2003) 'Generalized pattern search algorithms with adaptive precision function evaluations'.

Pottmann, H., Eigensatz, M., Vaxman, A. and Wallner, J. (2015) 'Architectural geometry', *Computers & graphics*, 47, pp. 145–164.

Pugnale, A. and Sassone, M. (2007) 'Morphogenesis and structural optimization of shell structures with the aid of a genetic algorithm', *Journal of the International Association for Shell and Spatial Structures*. International Association for Shell and Spatial Structures (IASS), 48(3), pp. 161–166.

Qingsong, M. and Fukuda, H. (2016) 'Parametric office building for daylight and energy analysis in the early design stages', *Procedia-Social and Behavioral Sciences*. Elsevier, 216, pp. 818–828.

Rakha, T. and Nassar, K. (2010) 'Daylight as an evolutionary architectural form finder', in *The proceedings of the International Conference For Computing In Civil And Building Engineering–ICCCBE 2010*. Available at: http://www.engineering.nottingham.ac.uk/icccbe/proceedings/pdf/pf186.pdf (Accessed: 18 July 2016).

Rakha, T. and Nassar, K. (2011) 'Genetic algorithms for ceiling form optimization in response to daylight levels', *Renewable Energy*, 36(9), pp. 2348–2356. doi: 10.1016/j.renene.2011.02.006.

Reinhart, C. (2019) *Daylight performance predictions*, *Building Performance Simulation for Design and Operation*. Routledge. doi: 10.1201/9780429402296-7.

Reinhart, C. and Breton, P.-F. (2009) 'Experimental validation of Autodesk® 3ds Max® Design 2009 and DAYSIM 3.0', *Leukos*, 6(1), pp. 7–35.

Reinhart, C. F. (2014) *Daylighting handbook: fundamentals, designing with the sun*. Christoph Reinhart.

Reinhart, C. F. and Andersen, M. (2006) 'Development and validation of a Radiance model for a translucent panel', *Energy and Buildings*, 38(7), pp. 890–904.

Reinhart, C. F. and Herkel, S. (2000) 'The simulation of annual daylight illuminance distributions—a state-of-the-art comparison of six RADIANCE-based methods', *Energy and Buildings*, 32(2), pp. 167–187.

Reinhart, C. F., Mardaljevic, J. and Rogers, Z. (2006) 'Dynamic daylight performance metrics for sustainable building design', *Leukos*, 3(1), pp. 7–31.

Reinhart, C. F. and Walkenhorst, O. (2001) 'Validation of dynamic RADIANCE-based daylight simulations for a test office with external blinds', *Energy and buildings*, 33(7), pp. 683–697.

Reinhart, C. F. and Wienold, J. (2011) 'The daylighting dashboard–A simulation-based design analysis for daylit spaces', *Building and environment*. Elsevier, 46(2), pp. 386–396.

Reinhart, C. and Fitz, A. (2006) 'Findings from a survey on the current use of daylight simulations in building design', *Energy and Buildings*. Elsevier, 38(7), pp. 824–835.

Rodrigues, E., Soares, N., Fernandes, M. S., Gaspar, A. R., Gomes, Á. and Costa, J. J. (2018) 'An integrated energy performance-driven generative design methodology to foster modular lightweight steel framed dwellings in hot climates', *Energy for sustainable development*. Elsevier, 44, pp. 21–36.

Rogers, Z. (2006) 'Daylighting metric development using daylight autonomy calculations in the sensor placement optimization tool', *Boulder, Colorado, USA: Architectural Energy Corporation: http://www. archenergy. com/SPOT/SPOT_Daylight% 20Autonomy% 20Report. pdf*.

Rörig, T., Sechelmann, S., Kycia, A. and Fleischmann, M. (2015) 'Surface Panelization Using Periodic Conformal Maps', in *Advances in Architectural Geometry 2014*. Springer, pp. 199–214. Available at: http://link.springer.com/chapter/10.1007/978-3-319-11418-7_13 (Accessed: 1 July 2016).

Roth, S. (2014) 'Open green building XML schema: A building information modeling solution for our green world', *http://gbxml. org*, pp. 08–25.

Roudsari, M. S., Pak, M. and Smith, A. (2013) 'Ladybug: a parametric environmental plugin for grasshopper to help designers create an environmentally-conscious design', in *Proceedings of the 13th International IBPSA Conference Held in Lyon, France Aug*. Available at: http://www.ibpsa.org/proceedings/BS2013/p_2499.pdf (Accessed: 1 July 2016).

RPBW (2014) *RPBW - Jérôme Seydoux Pathé Foundation*. Available at: http://www.rpbw.com/project/pathe-foundation (Accessed: 21 February 2020).

RPBW (2019) *Academy Museum of Motion Pictures*. Available at: http://www.rpbw.com/project/academy-museum-of-motion-pictures (Accessed: 24 November 2019).

Rumianowski, P., Brau, J. and Roux, J. J. (1989) 'An adapted model for simulation of the interaction between a wall and the building heating system', in *Proceedings of the Thermal Performance of the Exterior Envelopes of Buildings IV Conference*, pp. 224–233.

Ruppertsberg, A. I. and Bloj, M. (2006) 'Rendering complex scenes for psychophysics using RADIANCE: How accurate can you get?', *JOSA A*. Optical Society of America, 23(4), pp. 759–768.

Rutten, D. (2011) 'Evolutionary Principles applied to Problem Solving', *I Eat Bugs For Breakfast*, 4 March. Available at: https://ieatbugsforbreakfast.wordpress.com/2011/03/04/epatps01/ (Accessed: 16 June 2020).

SANAA (2009) *Serpentine Gallery Pavilion 2009 by Kazuyo Sejima and Ryue Nishizawa of SANAA*, *Serpentine Galleries*. Available at: https://www.serpentinegalleries.org/whats-on/serpentine-gallery-pavilion-2009-kazuyo-sejima-ryue-nishizawa-sanaa-0/ (Accessed: 18 June 2020).

Santos, L. and Caldas, L. (2018) 'Assessing the Glare Potential of Complex Fenestration Systems: A Heuristic Approach Based on Spatial and Time Sampling', in *Passive Low Energy Architecture (PLEA) 2018: Smart and Healthy within the 2-degree Limit. PLEA 2018*, Hong Kong, pp. 446–451.

Santos, L. and Caldas, L. (2020) 'Assessing the glare potential of side-lit indoor spaces: a simulation-based approach', *Architectural Science Review*. Taylor & Francis, pp. 1–14. doi: https://doi.org/10.1080/00038628.2020.1758622.

Santos, L., Leitão, A. and Caldas, L. (2018) 'A comparison of two light-redirecting fenestration systems using a modified modeling technique for Radiance 3-phase method simulations', *Solar Energy*, 161, pp. 47–63.

Santos, L., Schleicher, S. and Caldas, L. (2017) 'Automation of CAD models to BEM models for performance based goal-oriented design methods', *Building and Environment*, 112, pp. 144–158. doi: 10.1016/j.buildenv.2016.10.015.

Santos, L., Schleicher, S. and Caldas, L. (2019) 'Automatic Simplification of Complex Building Geometry for Whole-building Energy Simulations', in *Proceedings of Building Simulation 2019: 16th Conference of IBPSA*. *Building Simulation 2019: 16th Conference of IBPSA*, Rome, Italy, pp. 2691–2697. doi: https//doi.org/10.26868/25222708.2019.210991.

Schleicher, S., Santos, L. and Caldas, L. (2018) 'Data-driven shading systems - Application for freeform glass facades', in *SKINS on Campus. Bridging Industry and Academia in Pursuit of Better Buildings and Urban Habitat. Facades Tectonics 2018 World Congress*, Tectonic Press, Los Angeles, pp. 3–14.

Schneider, S. and Donath, D. (2013) 'Topo-Metric Variations for Design Optimization: Introducing a Generative Model for simultaneously varying metric and topological properties of facade geometry', in *eCAADe 2013: Computation and Performance–Proceedings of the 31st International Conference on Education and research in Computer Aided Architectural Design in Europe, Delft, The Netherlands, September 18-20, 2013*. Faculty of Architecture, Delft University of Technology; eCAADe (Education and research in Computer Aided Architectural Design in Europe). Available at: http://repository.tudelft.nl/view/conferencepapers/uuid:bac05761-c9a8-4c99-91ab-d43b0b442fa3/ (Accessed: 19 July 2016).

Schregle, R. (2002) 'The RADIANCE Photon Map Manual Version 3.6', *Fraunhofer Institute for Solar Energy Systems*.

Schregle, R. (2003) 'Bias compensation for photon maps', in *Computer Graphics Forum*. Wiley Online Library, pp. 729–742.

Schregle, R. (2004) 'Daylight simulation with photon maps'.

Schregle, R., Bauer, C., Grobe, L. O. and Wittkopf, S. (2015) 'EvalDRC: A tool for annual characterisation of daylight redirecting components with photon mapping', in *Proceedings of International Conference CISBAT 2015 Future Buildings and Districts Sustainability from Nano to Urban Scale*. LESO-PB, EPFL, pp. 217–222.

Schregle, R., Grobe, L. O. and Wittkopf, S. (2016) 'An out-of-core photon mapping approach to daylight coefficients', *Journal of Building Performance Simulation*. Taylor & Francis, 9(6), pp. 620–632.

Schregle, R., Grobe, L. and Wittkopf, S. (2015) 'Progressive photon mapping for daylight redirecting components', *Solar Energy*, 114, pp. 327–336. doi: 10.1016/j.solener.2015.01.041.

Sechelmann, S., Rörig, T. and Bobenko, A. I. (2013) 'Quasiisothermic Mesh Layout', in Hesselgren, L., Sharma, S., Wallner, J., Baldassini, N., Bompas, P., and Raynaud, J. (eds)

Advances in Architectural Geometry 2012. Springer Vienna, pp. 243–258. doi: 10.1007/978-3-7091-1251-9_20.

Shea, K. (2000) 'EifForm: a generative structural design system', in *Proc. ACSA Technology Conference: The Intersection of Design and Technology*, pp. 87–92.

Shea, K., Aish, R. and Gourtovaia, M. (2005) 'Towards integrated performance-driven generative design tools', *Automation in Construction*. (Education and Research in Computer Aided Architectural Design in Europe (eCAADe 2003), Digital Design), 14(2), pp. 253–264. doi: 10.1016/j.autcon.2004.07.002.

Shea, K. and Cagan, J. (1997) 'Innovative dome design: applying geodesic patterns with shape annealing', *Artificial Intelligence for Engineering, Design, Analysis and Manufacturing*, 11(05), pp. 379–394.

Shea, K. and Cagan, J. (1999) 'The design of novel roof trusses with shape annealing: assessing the ability of a computational method in aiding structural designers with varying design intent', *Design Studies*, 20(1), pp. 3–23. doi: 10.1016/S0142-694X(98)00019-2.

Shi, X., Tian, Z., Chen, W., Si, B. and Jin, X. (2016) 'A review on building energy efficient design optimization from the perspective of architects', *Renewable and Sustainable Energy Reviews*, 65, pp. 872–884. doi: 10.1016/j.rser.2016.07.050.

Shirley, P. (1992) 'Physically based lighting calculations for computer graphics: A modern perspective', in *Photorealism in Computer Graphics*. Springer, pp. 73–83.

Shu-Hsien Liao (2005) 'Expert system methodologies and applications—a decade review from 1995 to 2004', *Expert Systems with Applications*, 28(1), pp. 93–103. doi: 10.1016/j.eswa.2004.08.003.

Si, B., Tian, Z., Chen, W., Jin, X., Zhou, X. and Shi, X. (2019) 'Performance assessment of algorithms for building energy optimization problems with different properties', *Sustainability*. Multidisciplinary Digital Publishing Institute, 11(1), p. 18.

Simpson, T. W., Poplinski, J. D., Koch, P. N. and Allen, J. K. (2001) 'Metamodels for computer-based engineering design: survey and recommendations', *Engineering with computers*. Springer, 17(2), pp. 129–150.

Smith, A., Skorupski, J. and Davis, J. (2008) 'Transient rendering'. Citeseer.

Sollema LLC (2020) *Climate Studio*. Available at: https://www.solemma.com/ClimateStudio.html (Accessed: 27 July 2020).

SOM (2015a) *BBVA Bancomer Operations Center*, *SOM*. Available at: https://www.som.com/projects/bbva_bancomer_operations_center (Accessed: 4 August 2020).

SOM (2015b) *The Christ Hospital*, *SOM*. Available at: https://www.som.com/projects/the_christ_hospital__environmental_graphics (Accessed: 4 August 2020).

SOM (2016) *U.S. Air Force Academy – Center for Character & Leadership Development – Sustainable Design*, *SOM*. Available at: https://www.som.com/projects/us_air_force_academy__center_for_character__leadership_development__sustainable_design (Accessed: 4 August 2020).

Song, Y. H., Chou, C. S. and Stonham, T. J. (1999) 'Combined heat and power economic dispatch by improved ant colony search algorithm', *Electric Power Systems Research*, 52(2), pp. 115–121.

Spitler, J. D. (2019) 'Thermal load and energy performance prediction', *Building performance simulation for design and operation*. Taylor & Francis, pp. 84–142.

Spitler, J. D., Fisher, D. E. and Pedersen, C. O. (1997) *The radiant time series cooling load calculation procedure*. American Society of Heating, Refrigerating and Air-Conditioning Engineers (ASHRAE).

Stiny, G. (1980) 'Introduction to shape and shape grammars', *Environment and planning B: planning and design*. SAGE Publications Sage UK: London, England, 7(3), pp. 343–351.

Strachan, P. A., Kokogiannakis, G. and Macdonald, I. A. (2008) 'History and development of validation with the ESP-r simulation program', *Building and Environment*. Elsevier, 43(4), pp. 601–609.

Strand, R., Buhl, F. W. F., Huang, J. and Taylor, R. (1999) 'Enhancing and extending the capabilities of the building heat balance simulation technique for use in EnergyPlus', in *in Proceedings of Building Simulation'99, Volume II*. Citeseer.

Studio Fuksas (2005) *New Milan Trade Fair Rho-Pero*. Available at: http://fuksas.com/?p=692 (Accessed: 7 November 2019).

Subramaniam, S. (2017) *Daylighting Simulations with Radiance using Matrix-based Methods*. Technical. Berkeley, CA: Lawrence Berkeley National Lab (LBNL).

Sudan, M., Mistrick, R. G. and Tiwari, G. N. (2017) 'Climate-Based Daylight Modeling (CBDM) for an atrium: An experimentally validated novel daylight performance', *Solar Energy*. Elsevier, 158, pp. 559–571.

Suk, J. Y., Schiler, M. and Kensek, K. (2013) 'Development of new daylight glare analysis methodology using absolute glare factor and relative glare factor', *Energy and Buildings*, 64, pp. 113–122.

Sullivan, R., Lee, E. S. and Selkowitz, S. E. (1992) 'A method of optimizing solar control and daylighting performance in commercial office buildings'.

Tabadkani, A., Valinejad Shoubi, M., Soflaei, F. and Banihashemi, S. (2019) 'Integrated parametric design of adaptive facades for user's visual comfort', *Automation in Construction*, 106, p. 102857. doi: 10.1016/j.autcon.2019.102857.

Tabares-Velasco, P. C., Christensen, C. and Bianchi, M. (2012) 'Verification and validation of EnergyPlus phase change material model for opaque wall assemblies', *Building and Environment*, 54, pp. 186–196.

Tian, W. (2013) 'A review of sensitivity analysis methods in building energy analysis', *Renewable and Sustainable Energy Reviews*, 20, pp. 411–419.

Tian, W., Han, X., Zuo, W. and Sohn, M. D. (2018) 'Building energy simulation coupled with CFD for indoor environment: A critical review and recent applications', *Energy and Buildings*. Elsevier, 165, pp. 184–199.

Tian, Z., Zhang, X., Jin, X., Zhou, X., Si, B. and Shi, X. (2018) 'Towards adoption of building energy simulation and optimization for passive building design: A survey and a review', *Energy and Buildings*, 158, pp. 1306–1316. doi: 10.1016/j.enbuild.2017.11.022.

Torres, S. and Sakamoto, Y. (2007) 'Facade design optimization for daylight with a simple genetic algorithm', in *Proceedings of Building Simulation*. Citeseer, pp. 1162–1167. Available at: http://citeseerx.ist.psu.edu/viewdoc/download?doi=10.1.1.526.1602&rep=rep1&type=pdf (Accessed: 2 February 2017).

Toyo Ito & Associates (2006) *Crematorium in Kakamigahara*, *Toyo Ito & Associates, Architects*. Available at: http://www.toyo-ito.co.jp/WWW/Project_Descript/2005-/2005-p_07/2005-p_07_en.html (Accessed: 18 June 2020).

Transsolar (2019) *Swatch Omega Headquarters | Transsolar | KlimaEngineering*. Available at: https://transsolar.com/projects/biel-swatch-omega-hauptquartier (Accessed: 4 August 2020).

Tregenza, P. R. and Waters, I. M. (1983) 'Daylight coefficients', *Lighting Research & Technology*. SAGE Publications, 15(2), pp. 65–71. doi: 10.1177/096032718301500201.

Trnsys, A. (2000) 'Transient System Simulation Program', *University of Wisconsin*.

Tuhus-Dubrow, D. and Krarti, M. (2010) 'Genetic-algorithm based approach to optimize building envelope design for residential buildings', *Building and environment*, 45(7), pp. 1574–1581.

Turrin, M., von Buelow, P., Kilian, A. and Stouffs, R. (2012) 'Performative skins for passive climatic comfort', *Automation in Construction*, 22, pp. 36–50. doi: 10.1016/j.autcon.2011.08.001.

Turrin, M., von Buelow, P. and Stouffs, R. (2011) 'Design explorations of performance driven geometry in architectural design using parametric modeling and genetic algorithms', *Advanced Engineering Informatics*, 25(4), pp. 656–675.

Ubbelohde, S. and Humann, C. (1998) 'Comparative evaluation of four daylighting software programs'. CUMINCAD.

UN Studio (2011) *Tour Bioclimatique*, *UNStudio*. Available at: http://www.unstudio.com/en/page/11997/tour-bioclimatique (Accessed: 4 August 2020).

UN Studio (2013) *Hanwha Headquarters Remodelling*, *UNStudio*. Available at: http://www.unstudio.com/en/page/11994/hanwha-headquarters-remodelling (Accessed: 4 August 2020).

UN Studio (2015) *Singapore University of Technology and Design*, *UNStudio*. Available at: http://www.unstudio.com/en/page/12103/singapore-university-of-technology-and-design (Accessed: 4 August 2020).

USGBC (2013) *LEED v4 for Building Design & Construction*.

Van Den Wymelenberg, K. and Inanici, M. (2014) 'A critical investigation of common lighting design metrics for predicting human visual comfort in offices with daylight', *Leukos*, 10(3), pp. 145–164.

Van Den Wymelenberg, K., Inanici, M. and Johnson, P. (2010) 'The effect of luminance distribution patterns on occupant preference in a daylit office environment', *Leukos*, 7(2), pp. 103–122.

Veach, E. and Guibas, L. J. (1995) 'Optimally combining sampling techniques for Monte Carlo rendering', in *Proceedings of the 22nd annual conference on Computer graphics and interactive techniques*, pp. 419–428.

Vermeeren, A. P., Roto, V. and Väänänen, K. (2016) 'Design-inclusive UX research: design as a part of doing user experience research', *Behaviour & Information Technology*. Taylor & Francis, 35(1), pp. 21–37.

Vierlinger, R. (2012) *Octopus*, *Food4Rhino*. Available at: https://www.food4rhino.com/app/octopus (Accessed: 2 August 2020).

Vierlinger, R. (2018) *Grasshopper3D - Octopus*. Available at: http://www.grasshopper3d.com/group/octopus (Accessed: 14 June 2020).

Wagdy, A. and Fathy, F. (2015) 'A parametric approach for achieving optimum daylighting performance through solar screens in desert climates', *Journal of Building Engineering*, 3, pp. 155–170. doi: 10.1016/j.jobe.2015.07.007.

Wallace, J. R., Cohen, M. F. and Greenberg, D. P. (1987) 'A two-pass solution to the rendering equation: A synthesis of ray tracing and radiosity methods', *ACM Siggraph Computer Graphics*. ACM New York, NY, USA, 21(4), pp. 311–320.

Walsh, J. W. (1951) 'The early years of illuminating engineering in Great Britain', *Lighting Research and Technology*, 16(3 IEStrans), pp. 49–60.

Wang, H. and Zhai, Z. (John) (2016) 'Advances in building simulation and computational techniques: A review between 1987 and 2014', *Energy and Buildings*, 128, pp. 319–335. doi: 10.1016/j.enbuild.2016.06.080.

Wang, J., Caldas, L., Huo, L. and Song, Y. (2016) 'Simulation-based Optimization Of Window Properties Based On Existing Products', in *Proceedings of BSO'16, International Conference on Building Simulation & Optimization 2016*. *IBPSA-BSO*, Newcastle, UK.

Ward, G. (1995) *MKILLUM*, *Radiance manual pages*. Available at: https://floyd.lbl.gov/radiance/man_html/mkillum.1.html (Accessed: 18 June 2020).

Ward, G. (1997) *RTRACE*, *Radiance manual pages*. Available at: https://floyd.lbl.gov/radiance/man_html/rtrace.1.html#EXAMPLES (Accessed: 18 June 2020).

Ward, G. (1999) *RPICT*, *Radiance manual pages*. Available at: http://radsite.lbl.gov/radiance/man_html/rpict.1.html (Accessed: 21 June 2017).

Ward, G. (2004a) *RVU*. Available at: https://floyd.lbl.gov/radiance/man_html/rvu.1.html (Accessed: 6 July 2020).

Ward, G. (2004b) 'The radiance synthetic imaging system', *University of California, Berkeley*.

Ward, G. (2010) *GENBSDF*, *Radiance manual pages*. Available at: http://radsite.lbl.gov/radiance/man_html/genBSDF.1.html (Accessed: 21 June 2017).

Ward, G. J. (1994) 'The RADIANCE lighting simulation and rendering system', in *Proceedings of the 21st annual conference on Computer graphics and interactive techniques*. ACM, pp. 459–472. Available at: http://dl.acm.org/citation.cfm?id=192286 (Accessed: 19 July 2016).

Ward, G. J. and Rubinstein, F. M. (1988) 'A new technique for computer simulation of illuminated spaces', *Journal of the Illuminating Engineering Society*, 17(1), pp. 80–91.

Ward, G. J., Rubinstein, F. M. and Clear, R. D. (1988) 'A ray tracing solution for diffuse interreflection', in *Proceedings of the 15th annual conference on Computer graphics and interactive techniques*, pp. 85–92.

Ward, G., Mistrick, R., Lee, E. S., McNeil, A. and Jonsson, J. (2011) 'Simulating the daylight performance of complex fenestration systems using bidirectional scattering distribution functions within Radiance', *Leukos*, 7(4), pp. 241–261.

Ward, G. and Shakespeare, R. (1998) 'Rendering with radiance', *Waltham: Morgan Kaufmann Publishers*.

Welle, B., Haymaker, J., Fischer, M. and Bazjanac, V. (2014) 'CAD-centric attribution methodology for multidisciplinary optimization environments: enabling parametric attribution for efficient design space formulation and evaluation', *Journal of Computing in Civil Engineering*. American Society of Civil Engineers, 28(2), pp. 284–296.

Welle, B., Haymaker, J. and Rogers, Z. (2011) 'ThermalOpt: A methodology for automated BIM-based multidisciplinary thermal simulation for use in optimization environments', in *Building Simulation*. Springer, pp. 293–313. Available at: http://link.springer.com/article/10.1007/s12273-011-0052-5 (Accessed: 1 July 2016).

Wensveen, S. A. (2005) *A tangibility approach to affective interaction*. Citeseer.

Westermann, P. and Evins, R. (2019) 'Surrogate modelling for sustainable building design – A review', *Energy and Buildings*, 198, pp. 170–186. doi: 10.1016/j.enbuild.2019.05.057.

Wetter, M. (2000) 'Design optimization with GenOpt', *Building Energy Simulation User News*, 21(19–28). Available at: https://www.researchgate.net/profile/Michael_Wetter/publication/228583322_Design_optimization_with_GenOpt/links/0c96052d025585f003000000.pdf (Accessed: 3 February 2017).

Wetter, M. (2001) 'GenOpt-A generic optimization program', in *Seventh International IBPSA Conference, Rio de Janeiro*, pp. 601–608.

Wetter, M. and Polak, E. (2004) 'A convergent optimization method using pattern search algorithms with adaptive precision simulation', *Building services engineering research and technology*, 25(4), pp. 327–338.

Wetter, M. and Wright, J. (2004) 'A comparison of deterministic and probabilistic optimization algorithms for nonsmooth simulation-based optimization', *Building and Environment*. (Building Simulation for Better Building Design), 39(8), pp. 989–999. doi: 10.1016/j.buildenv.2004.01.022.

Whitted, T. (1979) 'An improved illumination model for shaded display', in *Proceedings of the 6th annual conference on Computer graphics and interactive techniques*, p. 14.

Wienold, J. (2004) 'Evalglare–A new RADIANCE-based tool to evaluate daylight glare in office spaces', in *3rd International RADIANCE workshop 2004*. Available at: https://www.radiance-online.org:447/radiance-workshop3/cd/Wienold_extabs.pdf.

Wienold, J. (2009) 'Dynamic daylight glare evaluation', in *Proceedings of Building Simulation*, pp. 944–951. Available at: https://www.ibpsa.org/proceedings/BS2009/BS09_0944_951.pdf (Accessed: 31 January 2017).

Wienold, J. *et al.* (2018) 'Cross-validation and robustness of daylight glare metrics', *Lighting Research & Technology*, pp. 1–31.

Wienold, J. and Christoffersen, J. (2005) 'Towards a new daylight glare rating', *Lux Europa, Berlin*, pp. 157–161.

Wienold, J. and Christoffersen, J. (2006) 'Evaluation methods and development of a new glare prediction model for daylight environments with the use of CCD cameras', *Energy and buildings*, 38(7), pp. 743–757.

Wienold, J. and others (2007) 'Dynamic simulation of blind control strategies for visual comfort and energy balance analysis', in *Building Simulation*, pp. 1197–1204. Available at: http://ibpsa.org/proceedings/BS2007/p231_final.pdf (Accessed: 31 January 2017).

Winkelmann, F. C., Birdsall, B. E., Buhl, W. F., Ellington, K. L., Erdem, A. E., Hirsch, J. J. and Gates, S. (1993) *DOE-2 supplement: version 2.1 E*. Lawrence Berkeley Lab., CA (United States); Hirsch (James J.) and Associates ….

Winkelmann, F. and Selkowitz, S. (1984) 'Daylighting simulation in the DOE-2 building energy analysis program'.

Woodbury, R. (2010) 'Elements of parametric design'. Taylor & Francis Group.

Wortmann, T. (2017) 'Opossum-introducing and evaluating a model-based optimization tool for grasshopper'. CUMINCAD.

Wortmann, T. (2018) *Efficient, Visual, and Interactive Architectural Design Optimization with Model-based Methods*. Singapore University of Technology and Design.

Wortmann, T. (2019) 'Genetic evolution vs. function approximation: Benchmarking algorithms for architectural design optimization', *Journal of Computational Design and Engineering*. Oxford University Press, 6(3), pp. 414–428.

Wortmann, T., Costa, A., Nannicini, G. and Schroepfer, T. (2015) 'Advantages of surrogate models for architectural design optimization', *Artificial Intelligence for Engineering Design, Analysis and Manufacturing: AI EDAM*, 29(4), p. 471.

Wortmann, T., Waibel, C., Nannicini, G., Evins, R., Schroepfer, T. and Carmeliet, J. (2017) 'Are Genetic Algorithms Really the Best Choice for Building Energy Optimization?', in *SIMAUD'17: Symposium on Simulation for Architecture and Urban Design*. *SIMAUD*, Society for Computer Simulation International, pp. 1–8.

Wright, J. A., Brownlee, A., Mourshed, M. M. and Wang, M. (2014) 'Multi-objective optimization of cellular fenestration by an evolutionary algorithm', *Journal of Building Performance Simulation*, 7(1), pp. 33–51.

Wright, J. A. and Mourshed, M. (2009) 'Geometric optimization of fenestration'. Available at: https://dspace.lboro.ac.uk/dspace/handle/2134/6573 (Accessed: 6 February 2017).

Wright, J. and Alajmi, A. (2016) 'Efficient Genetic Algorithm sets for optimizing constrained building design problem', *International Journal of Sustainable Built Environment*, 5(1), pp. 123–131. doi: 10.1016/j.ijsbe.2016.04.001.

Xu, J., Kim, J.-H., Hong, H. and Koo, J. (2015) 'A systematic approach for energy efficient building design factors optimization', *Energy and Buildings*, 89, pp. 87–96.

Xuan, Q., Li, G., Lu, Y., Zhao, B., Zhao, X. and Pei, G. (2019) 'Daylighting characteristics and experimental validation of a novel concentrating photovoltaic/daylighting system', *Solar Energy*. Elsevier, 186, pp. 264–276.

Yang, Z., Li, X., Bowers, C. P., Schnier, T., Tang, K. and Yao, X. (2011) 'An efficient evolutionary approach to parameter identification in a building thermal model', *IEEE Transactions on Systems, Man, and Cybernetics, Part C (Applications and Reviews)*. IEEE, 42(6), pp. 957–969.

Yu, R., Gero, J. S., Ikeda, Y., Herr, C. M., Holzer, D., Kaijima, S., Kim, M. and Schnabel, A. (2015) 'An empirical foundation for design patterns in parametric design', in *Proceedings of the 20th International Conference of the Association for Computer-Aided Architectural Design Research in Asia CAADRIA*, pp. 1–9.

Zani, A., Andaloro, M., Deblasio, L., Ruttico, P. and Mainini, A. G. (2017) 'Computational Design and Parametric Optimization Approach with Genetic Algorithms of an Innovative Concrete Shading Device System', *Procedia Engineering*, 180, pp. 1473–1483. doi: 10.1016/j.proeng.2017.04.310.

Zeng, Z., Li, X., Li, C. and Zhu, Y. (2012) 'Modeling ventilation in naturally ventilated double-skin façade with a venetian blind', *Building and environment*. Elsevier, 57, pp. 1–6.

Zhang, A., Bokel, R., van den Dobbelsteen, A., Sun, Y., Huang, Q. and Zhang, Q. (2017) 'Optimization of thermal and daylight performance of school buildings based on a multi-objective genetic algorithm in the cold climate of China', *Energy and Buildings*, 139, pp. 371–384. doi: 10.1016/j.enbuild.2017.01.048.

Zhang, J., Chowdhury, S., Messac, A. and Castillo, L. (2011) 'A comprehensive measure of the energy resource potential of a wind farm site', in *Energy Sustainability*, pp. 2183–2192.

Zhang, Longwei, Zhang, Lingling and Wang, Y. (2016) 'Shape optimization of free-form buildings based on solar radiation gain and space efficiency using a multi-objective genetic algorithm in the severe cold zones of China', *Solar Energy*. Elsevier, 132, pp. 38–50.

Zhao, H. and Magoulès, F. (2012) 'A review on the prediction of building energy consumption', *Renewable and Sustainable Energy Reviews*, 16(6), pp. 3586–3592. doi: 10.1016/j.rser.2012.02.049.

Zhao, S. and de Angelis, E. (2019) 'Performance-based Generative Architecture Design: A Review on Design Problem Formulation and Software Utilization', *Journal of Integrated Design and Process Science*, 22(3), pp. 55–76. doi: 10.3233/JID190001.

Zhou, X., Hong, T. and Yan, D. (2014) 'Comparison of HVAC system modeling in EnergyPlus, DeST and DOE-2.1 E', in *Building Simulation*. Springer Berlin Heidelberg, pp. 21–33. Available at: https://www.researchgate.net/profile/Tianzhen_Hong/publication/257200602_Comparison_of_HVAC_Modeling_in_EnergyPlus_DeST_and_DOE-2.1E/links/00b7d528bfa102de23000000.pdf (Accessed: 13 February 2017).

Zimmerman, J. and Forlizzi, J. (2014) 'Research through design in HCI', in *Ways of Knowing in HCI*. Springer, pp. 167–189.

Ziztler, E., Laumanns, M. and Thiele, L. (2002) 'SPEA2: Improving the strength Pareto evolutionary algorithm for multiobjective optimization', *Evolutionary Methods for Design, Optimization, and Control*, pp. 95–100.

Znouda, E., Ghrab-Morcos, N. and Hadj-Alouane, A. (2007) 'Optimization of Mediterranean building design using genetic algorithms', *Energy and Buildings*, 39(2), pp. 148–153.

Zomorodian, Z. S. and Tahsildoost, M. (2019) 'Assessing the effectiveness of dynamic metrics in predicting daylight availability and visual comfort in classrooms', *Renewable Energy*. Elsevier, 134, pp. 669–680.

Zuo, W. and Chen, Q. (2010) 'Fast and informative flow simulations in a building by using fast fluid dynamics model on graphics processing unit', *Building and Environment*, 45(3), pp. 747–757. doi: 10.1016/j.buildenv.2009.08.008.

Zuo, W., McNeil, A., Wetter, M. and Lee, E. S. (2014) 'Acceleration of the matrix multiplication of Radiance three phase daylighting simulations with parallel computing on heterogeneous hardware of personal computer', *Journal of Building Performance Simulation*, 7(2), pp. 152–163.

Appendix A:
List of Daylight and Building Energy Metrics

This appendix summarizes the daylight and building energy metrics used or related to the work presented in the dissertation.

Daylight Metrics

Illuminance

Illuminance (E) is a local and point-in-time metric. The illuminance at a point P (E_P) of a given surface is a physical quantity, defined as the ratio between the luminous flux (ϕ) incident on an infinitesimal surface in the neighborhood of P and the area of that surface (A_{rec}). In the International System of Units (SI), E is measured in lux. In the Imperial System of Units (IP) it is measured in in foot-candles (fc). Illuminance basically measures how much the incident light illuminates a surface in terms of human brightness perception. The mathematical formula is as follows (Carlucci et al., 2015):

$$E_P = \frac{\mathrm{d}\phi}{\mathrm{d}A_{rec}} \quad \text{(lux or fc)} \qquad (1)$$

Because it is a local and point-in-time metric, its spatial and time scope is limited. E measurements or simulations are fast and deliver an accurate measurement in an instantaneous moment for a specific spatial location within a given luminous environment. Although it is typically simulated under pre-defined skies, such as the *Commission Internationale de l'Éclairage* (CIE) Clear Sky, E can be simulated using weather data to better approximate the actual conditions of a site. To achieve this a sky needs to be generated using weather data through RADIANCE's routines *gendaylit* or *gensky* (McNeil and Lee, 2013). It is possible to measure or predict E that falls in the horizontal plane (E_h), or in the vertical plane (E_V). Vertical illuminance predictions are paramount in visual comfort assessments since the calculation of Daylight Glare Probability (DGP) (see below) requires the estimation of the vertical illuminance at the observer's eye. To fully describe a luminous environment over time through E, the estimation of E needs to be taken in several points in space, typically organized in a horizontal sensor grid, at different occasions. The spatial and time granularity range from measurements performed in a couple of representative samples (e.g., for each analysis point, E is calculated at three different hours of the day for the equinox and solstices) to compact grids of analysis points with an hourly based time-series. The latter method leads to voluminous time-series, and it is the basis of dynamic daylight metrics.

Daylight Factor

First proposed by Trotter in 1895 (Walsh, 1951) and latter refined by Hopkins et al. (1954) the Daylight Factor (DF) at a point P (DF_P), is the ratio of the horizontal illuminance at P due to the presence of any type of barrier that obstructs the view of the sky ($E_{P,obs}$), to the horizontal illuminance measured at the same point if the view of the sky is unobstructed ($E_{P,unobs}$). Both obstructed and unobstructed conditions exclude direct sunlight. DF_P is calculated through the expression:

$$DF_P = \frac{E_{P,obs}}{E_{P,unobs}} \quad (2)$$

DF is based on a ratio to avoid the dependency of assessing daylight performance based on instantaneous sky conditions (Reinhart, Mardaljevic and Rogers, 2006). In DF, it is assumed that the sky has a uniform luminance, thus being modeled as an overcast sky. Although this assumption makes this metric quick to simulate and representative for an entire year, it also limits its application. As pointed out in (Mardaljevic, Heschong and Lee, 2009), DF cannot properly represent daylight illumination conditions that differ from the overcast sky model. The sky model also makes DF insensitive to building orientation (Kota and Haberl, 2009). Reinhart et al. (Reinhart, Mardaljevic and Rogers, 2006) highlight that maximizing DF leads to admitting as much daylight as possible through the building's envelope, potentially affect the thermal performance significantly. Finally, DF is also a local daylight metric forcing the measurement at different positions to understand its spatial behavior.

Daylight Autonomy

The Daylight Autonomy (DA) at a point *P* (DA_P) is the percentage of the occupied hours of the year that is above a specified illuminance threshold (E_{Limit}) only due to daylight. DA_P is calculated by applying the following expression (Carlucci et al., 2015):

$$DA_{E_{limit}P} = \frac{\sum_i Wf_i.t_i}{\sum_i t_i} \in [0,1] \quad \text{with, } Wf_i = \begin{cases} 1, \ if \ E_{Daylight} \geq E_{Limit} \\ 0, \ if \ E_{Daylight} < E_{Limit} \end{cases}, \quad (3)$$

where t_i is each occupied hour of the year; Wf_i is a discrete weighting factor that depends on: (i) the illuminance measure at t_i at point *P*, only due to daylight ($E_{Daylight}$); (ii) the illuminance threshold value (E_{Limit}). The *Association Suisse des Electriciens* (ASE, 1989) first proposed this metric, which was later refined by Reinhart and Walkenhorst (2001).

DA is a climate-based and local metric. It considers the weather conditions of the site and conveys the visual performance, at a specific point of the analysis plane, through a single value expressed as a percentage. Although it captures the variations of luminous environment through time, Nabil and Mardaljevic (2006) point the following limitations: (i) it excludes values that fall below the threshold, that could either be valued by the occupants or reduce electric lighting loads; (ii) considers values that largely exceed the threshold thus being oblivious to potential visual discomfort or excessive thermal gains due to an excess of daylight. The definition of DA also depends on the occupied schedule and the E_{Limit} threshold. Although this makes the metric versatile enough to be applied in a wide range of cases there is a lack of guidelines especially regarding the value of $E_{Limit.}$ Olbina and Beliveau (2009) proposed the E_{Limit} of 500 lux for a typical office environment, but 300 lux is also used both in practice and by standards (IESNA, 2012). Finally, being a local metric DA requires the evaluation of several analysis points to fully describe its spatial performance making the simulation of this metric computationally expensive.

Spatial Daylight Autonomy

Spatial Daylight Autonomy (sDA), as defined in (IESNA, 2012), is a measure of daylight illuminance sufficiency for a given area. It reports the percentage of floor area that exceeds a given illuminance level for a specified fraction of the operating hours per year. sDA is calculated by first assessing DA in each point of a spatial grid over the area of interest, and then summing all the areas affected to the points above a given DA reference value (DA_{Limit}). It is expressed in the following:

$$sDA_{x|y\%} = \frac{\sum_i Wf_i}{\sum_i P_i} \in [0,1] \quad \text{with, } Wf_i = \begin{cases} 1, & if\ DA_{x\,Pi} \geq DA_{Limit} \\ 0, & if\ DA_{x\,Pi} < DA_{Limit} \end{cases}, \tag{4}$$

where *x* is the illuminance threshold, *y%* is the time fraction, *Pi* are the points of the calculation grid.

Spatial Daylight Autonomy is a climate and a zonal based metric. The Illuminating Engineering Society (IES) recommends 300 lux as the illuminance threshold and 50% as time fraction limit: $sDA_{300/50\%}$ (IESNA, 2012). $sDA_{300/50\%}$ expresses the percentage of the analyzed area that is equal or over 300 lux for at least 50% of the operating hours (i.e., $DA_{300lux} \geq 50\%$). The approved method for the calculation of $sDA_{300/50\%}$ is described in the LM-83-12 standard (IESNA, 2012) which includes details and guidelines on performance criteria, analysis grids, blinds/shades operation, material properties, window groups, and other simulation parameters. The schedule for the occupied hours used in the calculation of $sDA_{300/50\%}$ is fixed at 10 hours per day, from 8am to 6pm, over a year. In the calculation of $sDA_{300/50\%}$ the standard enforces an hourly deployment of blinds/shades if specific criteria are not met, which can lead to an underestimation of the actual daylight performance of the building envelope. In sum, the main advantage that this metric has over DA is that it can describe the daylight performance of the analyzed area through a single value. However, this ability hinders the metric to provide more information about the daylight spatial variation if not paired with DA visualizations.

Useful Daylight Illuminance

Nabil and Mardaljevic proposed the Useful Daylight Illuminance (UDI) metric in (2006). Similar to DA, UDI is defined as the fraction of the time in a year when indoor horizontal daylight illuminance at a given point falls in a given range. Currently, the following three limits to illuminance are defined: a lower ($E_{L.L.}$), an autonomous ($E_{A.L.}$), and an upper ($E_{U.L.}$). Typically, these thresholds split the analyzed period into four bins: i) $UDI_{Overlit}$, which measures the percentage of time with excessive daylight levels which might lead to visual discomfort and/or overheating phenomena (Nabil and Mardaljevic, 2006), (ii) $UDI_{autonomous}$ that represents the ratio of time with appropriate autonomous daylight illuminance levels, i.e., daylight levels that dismiss the use of artificial lighting, (iii) UDI_{Useful} that gives the percentage of time of insufficient daylight levels that can be compensated with a partial use of an artificial lighting system, and (iv) $UDI_{Underlit}$ represents the percentage of time when there is too little daylight. UDI at a given point *P* (UDI_P) is expressed as follows:

$$UDI_P = \frac{\sum_i Wf_i . t_i}{\sum_i t_i} \in [0,1] \quad \begin{cases} UDI_{Overlit} & \text{with } Wf_i = \begin{cases} 1, & if\ E_{Daylight} > E_{U.L.} \\ 0, & if\ E_{Daylight} \leq E_{U.L.} \end{cases} \\ \text{UDI}_{Autonomous} & with \quad Wf_i = \begin{cases} 1, & if\ E_{A.L.} \leq E_{Daylight} \leq E_{U.L.} \\ 0, if\ \text{E}_{Daylight} < E_{A.L.} \vee E_{Daylight} > E_{U.L.} \end{cases} \\ \text{UDI}_{Useful} & with \quad Wf_i = \begin{cases} 1, & if\ E_{L.L.} \leq E_{Daylight} \leq E_{A.L.} \\ 0, if\ E_{Daylight} < E_{L.L.} \vee E_{Daylight} > E_{A.L.} \end{cases} \\ \text{UDI}_{Underlit} & with\ Wf_i = \begin{cases} 1, & if\ E_{Daylight} < E_{L.L.} \\ 0, & if\ E_{Daylight} > E_{U.L.} \end{cases} \end{cases} \quad (5)$$

UDI is a climate-based and local metric that resorts to upper and lower thresholds to report and qualify the annual quantity of daylight at a specific point in space. UDI aims to deliver information on useful illuminance levels caused by daylight and the frequency of excessive daylight levels that might lead to visual discomfort and unwanted solar gains. Nevertheless, there is no full agreement on the illuminance limit thresholds. Initially, Nabil and Mardaljevic proposed $E_{L.L}$= 100 lux, and $E_{U.L}$= 2000 lux (Nabil and Mardaljevic, 2006). Later, Mardaljevic et al. (2009) suggested increasing the upper *E* threshold to 2500 lux. In Olbina and Beliveau (2009), the lower threshold is set to 500 lux and the upper threshold to 2000 lux. David et al. (2011) proposed a very different range, 300 to 8000 lux. Currently, the most adopted thresholds, particularly by recent daylighting analysis tools, including Climate Studio (Sollema LLC, 2020), are the following: (i) $E_{L.L}$= 100 (ii) $E_{A.L}$= 300 lux, and (iii) $E_{U.L}$= 3000 lux.

Spatial Useful Daylight Illuminance

Spatial Useful Daylight Autonomy (sUDI), applies the sDA (see Spatial Daylight Autonomy) concept to the different bins of UDI. Hence, based on the UDI score of the different points (P_i), it is possible to determine sUDI for each UDI bin, *k*, as follows:

$$sUDI_{k|y\%} = \frac{\sum_i Wf_i}{\sum_i P_i} \in [0,1] \quad \text{with, } Wf_i = \begin{cases} 1, & if\ UDI_{k\,Pi} \in UDI_k \\ 0, & if\ UDI_{k\,Pi} \notin UDI_k \end{cases}, \quad (6)$$

where *k* is the UDI illuminance bin, *y%* is the time fraction, *Pi* are the points of the calculation grid.

Konis et al. (2016) used $\text{sUDI}_{autonomous}$ as one of building performance metrics in a multi-objective optimization application that aimed to simultaneously minimize building energy use and maximize comfortable daylight levels in commercial buildings. The authors used 50% as the time fraction for $\text{UDI}_{autonomous}$, $\text{sUDI}_{\text{autonomous}|50\%}$. Santos, Leitão, and Caldas (2018) also used also the time fraction of 50% to compare the performance of two Complex Fenestration Systems (CFS).

Annual Sun Exposure

The IES LM-83-12 standard (IESNA, 2012) defines Annual Sunlight Exposure (ASE) as the percent of an analysis area that exceeds a direct sunlight illuminance level ($E_{Direct\ Limit}$) for a specified number of hours per year.

$$ASE_{x,y} = \frac{\sum_i Wf_i}{\sum_i P_i} \in [0,1] \quad \text{with, } Wf_i = \begin{cases} 1, & if\ E_{Direct\ Pi} \geq E_{Direct\ Limit} \\ 0, & if\ E_{Direct\ Pi} < E_{Direct\ Limit} \end{cases}, \qquad (7)$$

where *x* is the direct illuminance threshold, *y i*s the absolute amount of time in hours, and *Pi* are the sensor nodes of the analysis grid.

ASE is a climate-based and zonal metric that describes the potential for visual discomfort in interior work environments. IES LM-83-12 standard recommends the analysis of $ASE_{1000,250h}$, i.e., the percentage of the analysis area exposed to more than 1000 lux of direct sunlight for more than 250 hours per year, before any shading device is deployed to block sunlight, considering the same analysis period as sDA. As stated in (IESNA, 2012), supporting research indicated that spaces with $ASE_{1000,250h} > 10\%$ have unsatisfactory visual comfort, while spaces with $ASE_{1000,250h} < 7\%$ were judge to be neutral, and spaces with $ASE_{1000,250h} < 3\%$ were considered acceptable. However, the same standard alerts that the research that led to these $ASE_{1000,250h}$ recommendations needs more information from field studies. The current metric does not include enough information on all variations of sun penetration, space types, shading devices, or climates (IESNA, 2012). Thus, it is recommended that this metric should be used in combination with DA and/or sDA.

Daylight Glare Probability

Although there are several glare metrics such as the Discomfort Glare Index (Hopkinson, 1972; Chauvel et al., 1982; Nazzal, 2005), the CIE Glare Index (Einhorn, 1979; Navvab and Altland, 1997) the dissertation focus on the Daylight Glare Probability (DGP) metric since it is the only glare-related metric that can handle large light sources including the sun. Proposed and validated by Wienold and Christoffersen (Wienold and Christoffersen, 2006) DGP is calculated as follows:

$$DGP = 5.87 \cdot 10^{-5} E_V + 0.0918 \cdot log_{10}\left[1 + \sum_{i=1}^{n}\left(\frac{L_{s,i}^2 \cdot \omega_{s,i}}{E_V^{1.87} \cdot P_i^2}\right)\right] + 0.16\,, \qquad (8)$$

where E_V is the vertical eye illuminance produced by the light sources at the observer's eye, $L_{s,i}$ is the luminance of a glare source, $\omega_{s,i}$ is the solid angle of the source seen by an observer in steradians (*sr*), and *Pi* is the position index, which expresses the change in experienced discomfort glare relative to the angular displacement of the source (azimuth and elevation) from the observer's line of sight. The formula is valid within the range of DGP between 0.2 and 0.8, and for vertical eye illuminance (E_V) above 380 lux.

Compared with other glare metrics, DGP includes the evaluation of vertical illuminance as perceived by the observer (E_V). Wienold and Christoffersen collected empirical data showing a stronger correlation of E_V with the observer's response towards glare (Wienold and Christoffersen, 2005). The discomfort of exceedingly bright environments can be predicted even without significant visual contrast (Jakubiec and Reinhart, 2011) (Wienold and Christoffersen, 2006) (Wienold and Christoffersen, 2005). The inclusion of E_V makes DGP the most sophisticated and appropriate metric in assessing absolute glare issues, as stated by Suk et al. (2013). Nevertheless, DGP is a metric that is computationally expensive to calculate when compared with other glare indexes (Andersen et al., 2008). To address the computation time problem, Wienold et al. (2007)

and Hviid et al. (2008) proposed simplifications to DGP. Both simplifications cannot be used if direct sun, or a specular reflection of it, hits the observer's eyes (Suk, Schiler and Kensek, 2013). Departing from the work conducted in Wienold et al. (2007), Wienold proposed the Enhanced Simplified Discomfort Glare Probability (*eDGPs*) (Wienold, 2009). The underlying idea is to split the initial definition of DGP into two simplified terms. The first term depends on the vertical eye illuminance and the second on the detected glare sources. The first term can be easily calculated while the second can be inferred by computing a simplified image that only renders the primary glare sources, neglecting the indirect ambient reflections. The results when compared to full DGP results, are acceptable (Wienold, 2009).

Although DGP is a local point-in-time metric, Jakubiec and Reinhart (2011) extended its temporal scope to a TMY by automating its simulation. The annual DGP (aDGP) is displayed as an annual heatmap that renders (i) intolerable glare (DGP $\geq$ 0.45), (ii) disturbing glare (0.45 > DGP $\geq$ 0.4), (iii) perceptible glare (0.4 > DGP $\geq$ 0.35), and (iv) imperceptible glare (0.35 $\geq$ DGP).

Visible Light Transmittance

The Visible Light Transmittance (VLT or Tvis) is a ratio that expresses the fraction of light in the visible portion of the spectrum that passes through a glazing material. Since it is a ratio, VLT varies between 0 and 1, or 0 % and 100%.

Building Energy Related Metrics

Building Energy Consumption

Building energy consumption refers to the cumulative of energy used to inhabit and operate a building during a specific period, usually the entire year. The energy that a building uses does not necessarily come from a single energy source. Buildings use different types of energy, from electricity, natural gas, biomass, to steam. It is possible to distinguish two types of energy in buildings, site, and source energy. Source energy represents the total amount of raw fuel that is required to operate the building. Thus, source energy incorporates all transmission, delivery, and energy production losses. Site energy is the energy consumed at the final destination of the power generation cycle, i.e., the energy consumed by the building without accounting for production and losses in transporting energy to the building. In other words, is the amount of energy shown on a utility bill. The dissertation uses site energy in the calculation of building energy consumption.

Building energy consumption can be expressed kilowatt-hour (kWh) or in British thermal units (Btu). One kWh is equivalent to 3600 kilojoules (kJ) and one Btu to approximately 1.06 kJ. The dissertation adopts the kWh, the international system (SI) unit.

The energy that a building uses in its operation can be further divided into different energy end-uses. The most commons ones are the following: heating, cooling, lighting, equipment, process loads, and ventilation. The heating energy end-use refers to the amount of energy required to heat the several spaces of a building to keep comfortable temperatures. Similar cooling energy is the energy spend by the building to cool down the several interior spaces to a comfortable temperature range. Lighting energy is the energy that a building spends in artificial lighting to provide adequate light levels to perform different activities and tasks. Equipment refers to the energy spend by typically electrical equipment. Process loads include the energy needed to operate processing

equipment, i.e., equipment that uses energy to process materials or other resources, including appliances. The energy used by a kitchen stove and oven is a good example of a process load. Finally, the ventilation energy end-use measures the amount of energy consumed by a mechanical ventilation system in providing an adequate amount of fresh air to the different spaces of a building.

Energy Use Intensity

Energy Use Intensity (EUI) is the normalization of building energy use (total or by different building energy end-uses) per unit area (EUI) or volume (EUI_V). When using EUI, energy use is either expressed as a function of a building's total area or volume. Hence, the calculation of EUI and EUI_V consists of dividing the predicted or measured energy consumption of a specific end-use by the total area (EUI) or volume of the building (EUI_V). In this dissertation, EUI is expressed in kWh/m^2 and EUI_V in kWh/m^3. In the absence of robust benchmarks or energy standards, EUI is critical to compare the measured or predicted energy performance between buildings or designs.

Solar Radiation

Solar Radiation (SR), also called solar irradiation or solar irradiance, is the radiant flux (power) received from the Sun per unit area. SR is often integrated over a given time period to express the radiant energy received into a specific surface or environment over time. The dissertation uses kWh/m^2 to express the time integration of SR.

The adding or decoupling of the direct and the diffuse components of solar irradiance commonly results in the following associated metrics:

- *Global Horizontal Irradiance* is the measure of the radiant flux over all wavelengths per unit area received on a horizontal surface.

- *Direct Normal Irradiance* or *Beam Radiation* measures the direct component of the radiant flux that falls in a surface that is perpendicular to the Sun. It excludes the diffuse component of SR (see below), thus considering only the radiation that comes from the *circumsolar* region, i.e., the sun and sun disk.

- *Diffuse Horizontal Irradiance* or *Diffuse Sky Radiation* corresponds to the diffuse component of solar radiation received by a horizontal surface. SR diffuse component includes the radiation that is scattered by the atmosphere and reflected by the surroundings from all directions, excluding the circumsolar radiation.

Solar Heat Gain Coefficient

Solar Heat Gain Coefficient (SHGC) is the fraction of incident solar radiation that enters a building through the glazed part of its envelope. This ratio is affected by glazing type and shading, and it is expressed as a dimensionless number from 0 to 1.

U-factor and R-value

U-factor is the heat transfer coefficient that measures the heat flow rate of a building envelope assembly. In other words, U-factor measures the capacity of a construction assembly to transfer

thermal energy across its several material layers. The U-factor reciprocal is the R-value, which measures the assembly's thermal resistance to heat flow driven by conduction. The inch-pound units (IP) for U-factor are degree British thermal unit per degree Fahrenheit square-foot hour (Btu/hr·ft^2·˚F), and the SI units are watts per square meter kelvin (W/m^2·K). The R-value IP units are degrees Fahrenheit square foot hour per British thermal unit (˚F·ft2·hr/Btu), and the SI units are kelvin square meter per watt (K· m2/W). The dissertation uses SI units for both U-factor and R-value.

References

Andersen, M., Kleindienst, S., Yi, L., Lee, J., Bodart, M., Cutler, B., 2008. An intuitive daylighting performance analysis and optimization approach. Building Research & Information 36, 593–607.

ASE, 1989. Eclairage interieur par la lumicre du jour. Association Suisse Des Electriciens, Zurich (CH).

Carlucci, S., Causone, F., De Rosa, F., Pagliano, L., 2015. A review of indices for assessing visual comfort with a view to their use in optimization processes to support building integrated design. Renewable and Sustainable Energy Reviews 47, 1016–1033. https://doi.org/10.1016/j.rser.2015.03.062

Chauvel, P., Collins, J.B., Dogniaux, R., Longmore, J., 1982. Glare from windows: current views of the problem. Lighting research and Technology 14, 31–46.

David, M., Donn, M., Garde, F., Lenoir, A., 2011. Assessment of the thermal and visual efficiency of solar shades. Building and Environment 46, 1489–1496.

Einhorn, H.D., 1979. Discomfort glare: a formula to bridge differences. Lighting Research & Technology 11, 90–94.

Hopkinson, R.G., 1972. Glare from daylighting in buildings. Applied Ergonomics 3, 206–215.

Hopkinson, R.G., Longmore, J., Petherbridge, P., 1954. An empirical formula for the computation of the indirect component of daylight factor. Transactions of the Illuminating Engineering Society 19, 201–219.

Hviid, C.A., Nielsen, T.R., Svendsen, S., 2008. Simple tool to evaluate the impact of daylight on building energy consumption. Solar Energy 82, 787–798.

IESNA, I., 2012. LM-83-12 IES Spatial Daylight Autonomy (sDA) and Annual Sunlight Exposure (ASE). New York, NY, USA: IESNA Lighting Measurement.

Jakubiec, A., Reinhart, C., 2011. DIVA-FOR-RHINO 2.0: environmental parametric modeling in rhinoceros/grasshopper using RADIANCE, Daysim and EnergyPlus, in: Conference Proceedings of Building Simulation.

Konis, K., Gamas, A., Kensek, K., 2016. Passive performance and building form: An optimization framework for early-stage design support. Solar Energy 125, 161–179.

Kota, S., Haberl, J.S., 2009. Historical survey of daylighting calculations methods and their use in energy performance simulations.

Mardaljevic, J., Heschong, L., Lee, E., 2009. Daylight metrics and energy savings. Lighting Research and Technology 41, 261–283.

McNeil, A., Lee, E.S., 2013. A validation of the Radiance three-phase simulation method for modelling annual daylight performance of optically complex fenestration systems. Journal of Building Performance Simulation 6, 24–37.

Nabil, A., Mardaljevic, J., 2006. Useful daylight illuminances: A replacement for daylight factors. Energy and buildings 38, 905–913.

Navvab, M., Altland, G., 1997. Application of CIE glare index for daylighting evaluation. Journal of the Illuminating Engineering Society 26, 115–128.

Nazzal, A.A., 2005. A new evaluation method for daylight discomfort glare. International Journal of Industrial Ergonomics 35, 295–306.

Olbina, S., Beliveau, Y., 2009. Developing a transparent shading device as a daylighting system. Building Research & Information 37, 148–163.

Reinhart, C.F., Mardaljevic, J., Rogers, Z., 2006. Dynamic daylight performance metrics for sustainable building design. Leukos 3, 7–31.

Reinhart, C.F., Walkenhorst, O., 2001. Validation of dynamic RADIANCE-based daylight simulations for a test office with external blinds. Energy and buildings 33, 683–697.

Santos, L., Caldas, L., 2018. Assessing the Glare Potential of Complex Fenestration Systems: A Heuristic Approach Based on Spatial and Time Sampling, in: Passive Low Energy Architecture (PLEA) 2018: Smart and Healthy within the 2-Degree Limit. Presented at the PLEA 2018, Hong Kong, pp. 446–451.

Sollema LLC, 2020. Climate Studio [WWW Document]. URL https://www.solemma.com/ClimateStudio.html (accessed 7.27.20).

Suk, J.Y., Schiler, M., Kensek, K., 2013. Development of new daylight glare analysis methodology using absolute glare factor and relative glare factor. Energy and Buildings 64, 113–122.

Walsh, J.W., 1951. The early years of illuminating engineering in Great Britain. Lighting Research and Technology 16, 49–60.

Wienold, J., 2009. Dynamic daylight glare evaluation, in: Proceedings of Building Simulation. pp. 944–951.

Wienold, J., Christoffersen, J., 2006. Evaluation methods and development of a new glare prediction model for daylight environments with the use of CCD cameras. Energy and buildings 38, 743–757.

Wienold, J., Christoffersen, J., 2005. Towards a new daylight glare rating. Lux Europa, Berlin 157–161.

Wienold, J., others, 2007. Dynamic simulation of blind control strategies for visual comfort and energy balance analysis, in: Building Simulation. pp. 1197–1204.

Appendix B:
Hourly Results of the Selected Vertical Eye illuminance Threshold to Predict Glare Events

In chapter 6, Figure 6-10 presents the matrix of the hourly performance of the selected $E_{V,Thr}$ in Strategy D ($E_{V,Thr}$ = 2300 lux) to signal glare events for all locations and points-of-view (POV). However, because of the layout of the page, the image does not show the full granularity of the results. Appendix B breakdowns Figure 6-10 results presented by location and POV in the heatmaps presented in the following pages.

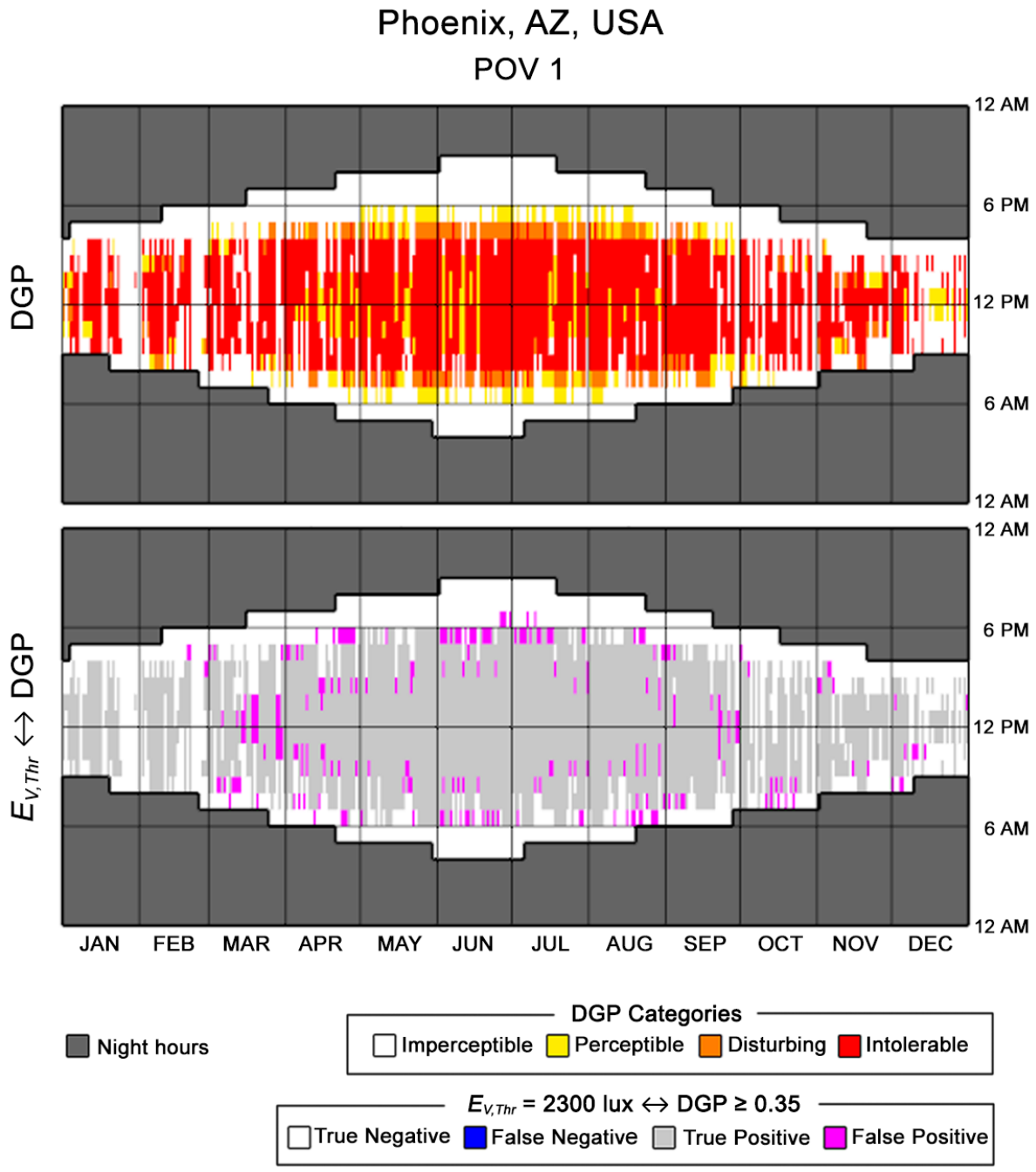

Figure Appendix B-1. Hourly results of using $E_{V,Thr}$ = 2300 lux to signal glare events in POV1 (see chapter 6, Figure 6-2) in Phoenix, AZ, USA.

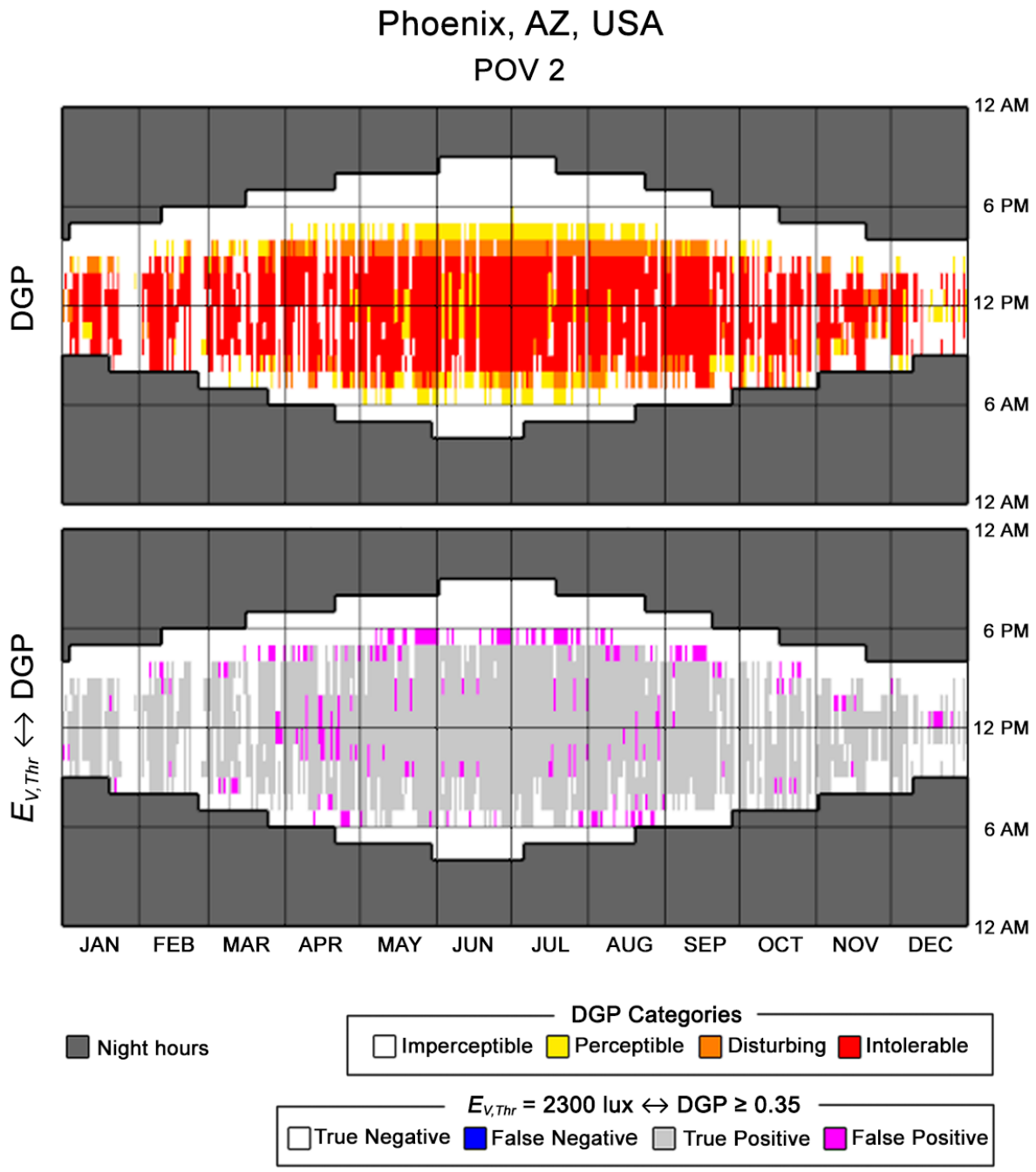

Figure Appendix B-2. Hourly results of using $E_{V,Thr}$ = 2300 lux to signal glare events in POV2 (see chapter 6, Figure 6-2) in Phoenix, AZ, USA.

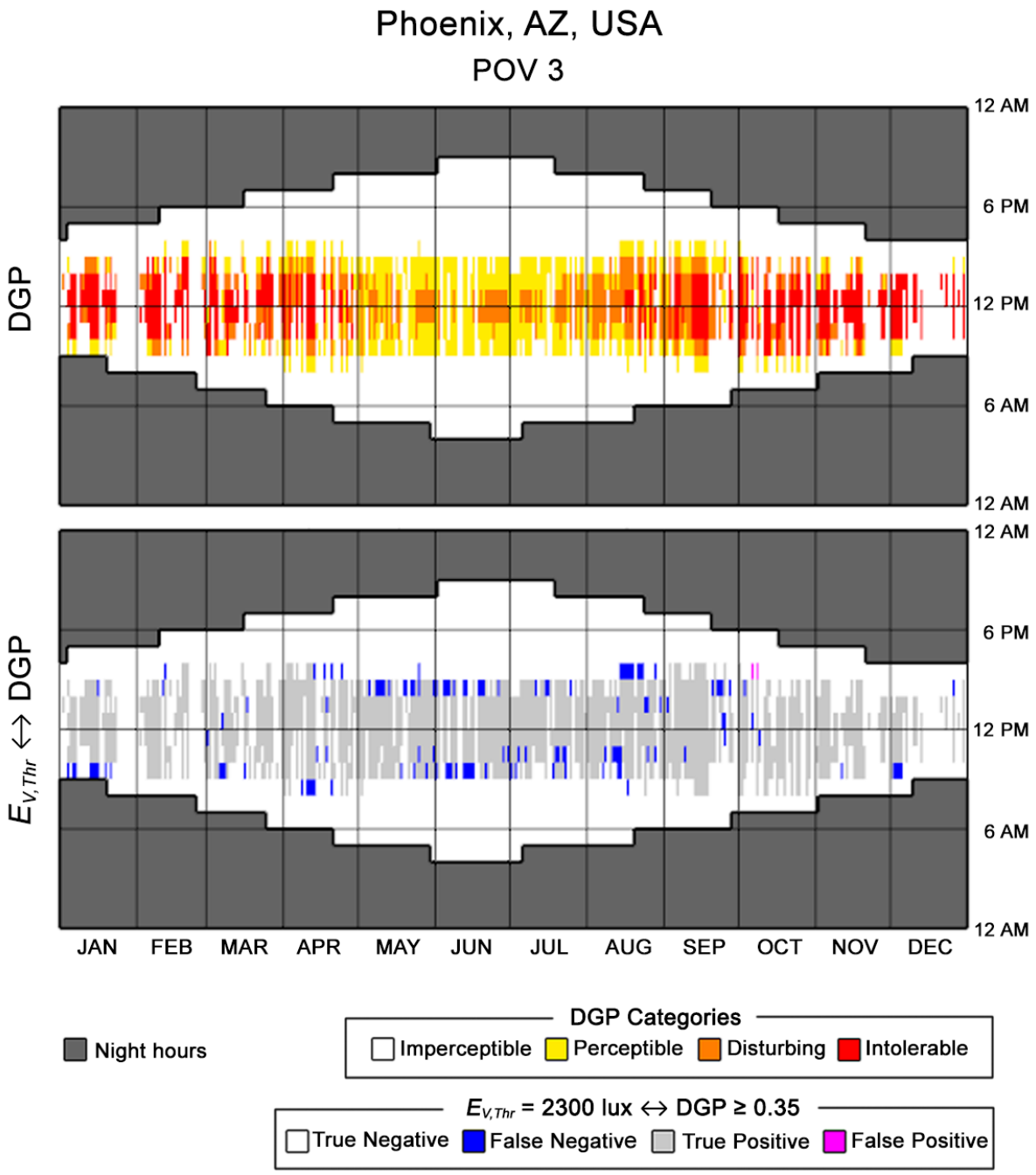

Figure Appendix B-3. Hourly results of using $E_{V,Thr}$ = 2300 lux to signal glare events in POV3 (see chapter 6, Figure 6-2) in Phoenix, AZ, USA.

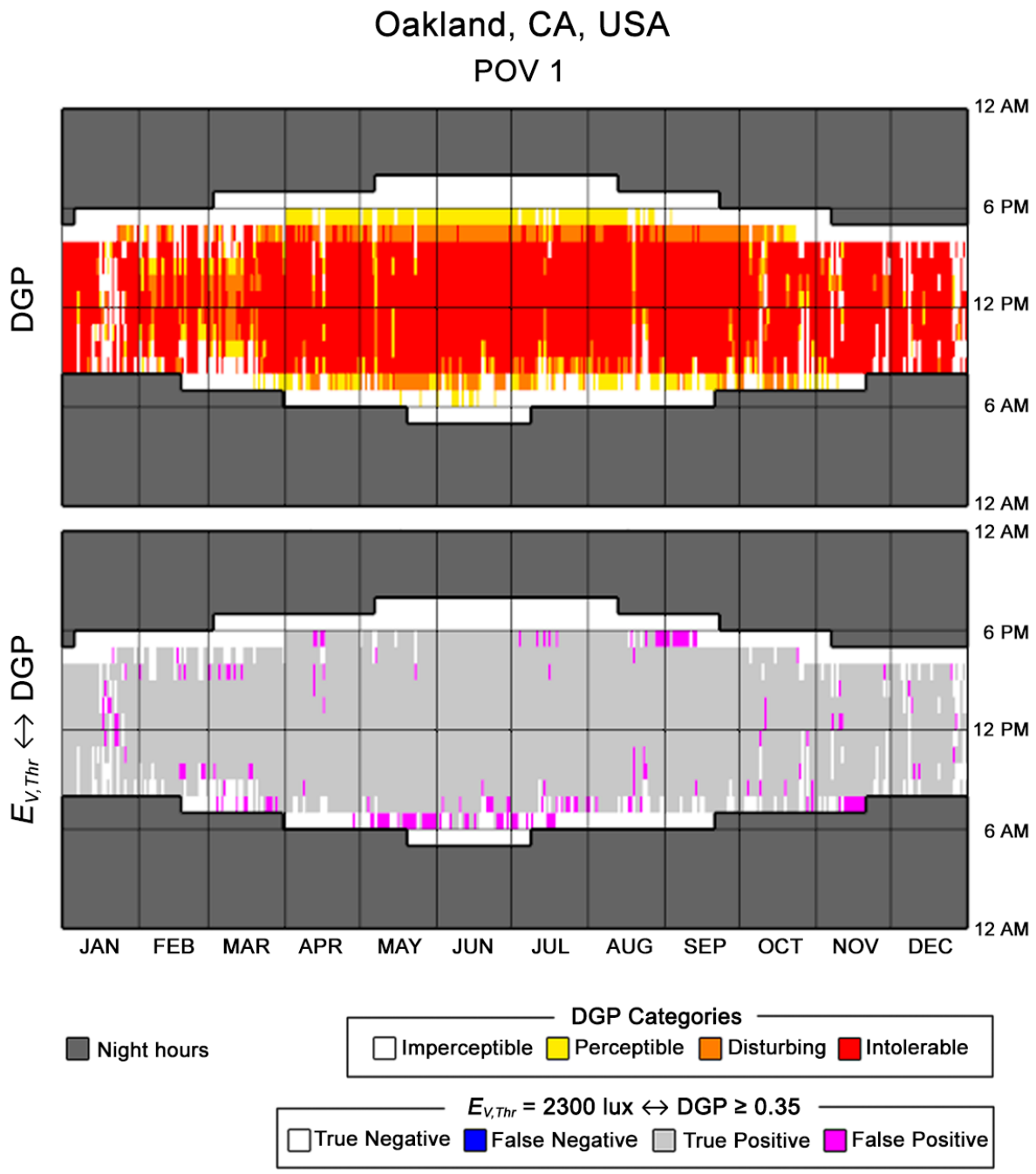

Figure Appendix B-4. Hourly results of using $E_{V,Thr}$ = 2300 lux to signal glare events in POV1 (see chapter 6, Figure 6-2) in Oakland, CA, USA.

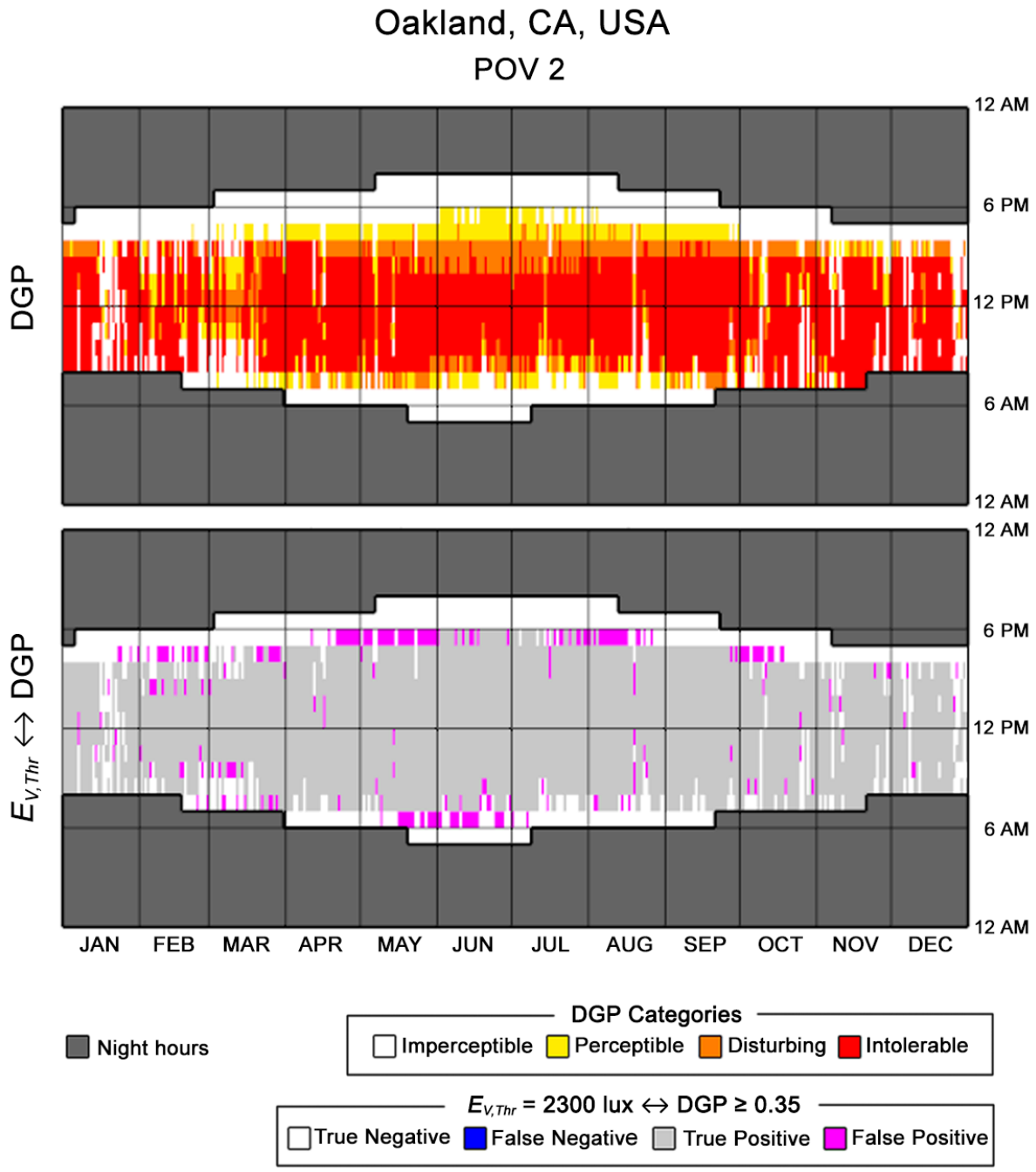

Figure Appendix B-5. Hourly results of using $E_{V,Thr}$ = 2300 lux to signal glare events in POV2 (see chapter 6, Figure 6-2) in Oakland, CA, USA.

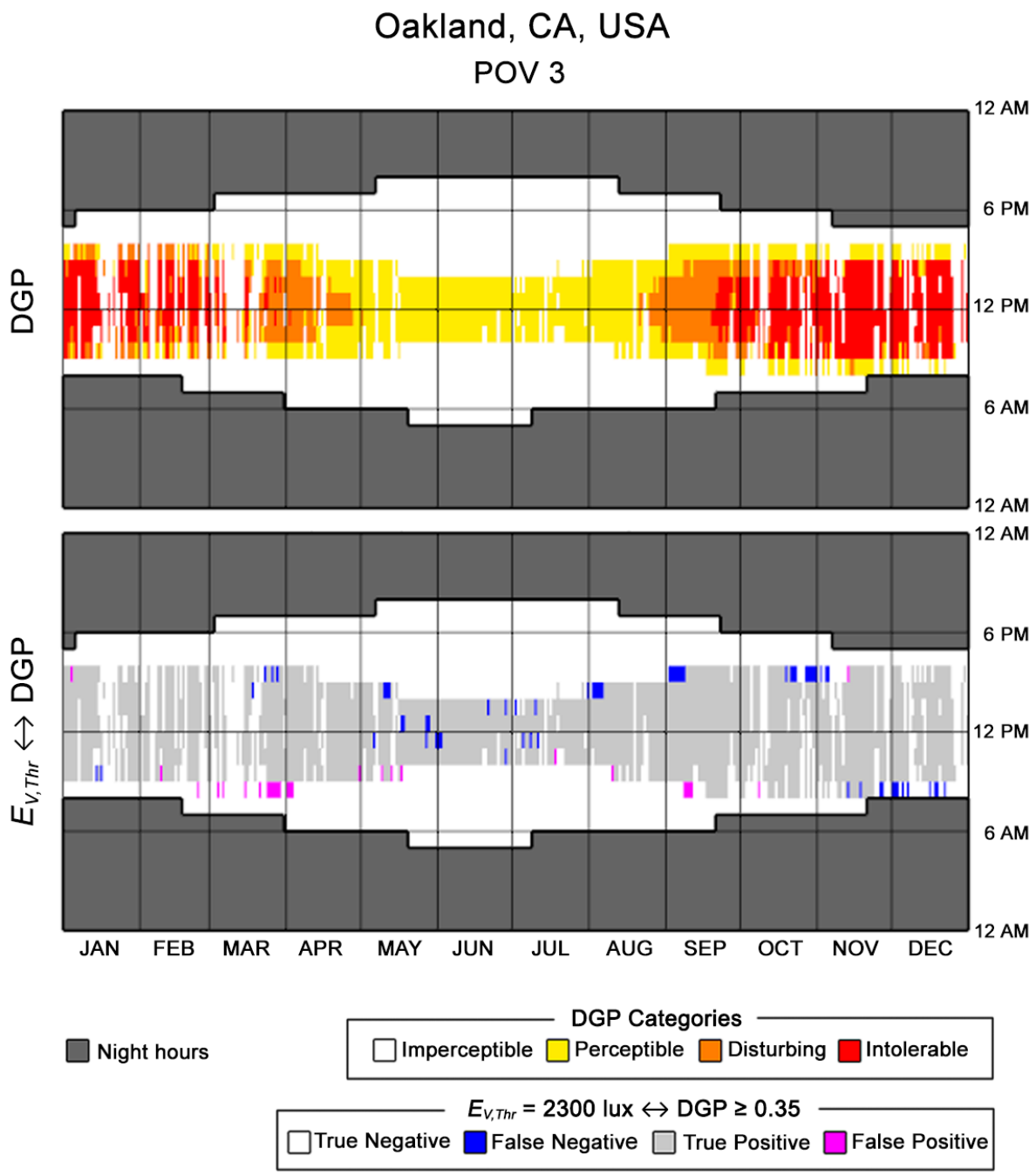

Figure Appendix B-6. Hourly results of using $E_{V,Thr}$ = 2300 lux to signal glare events in POV3 (see chapter 6, Figure 6-2) in Oakland, CA, USA.

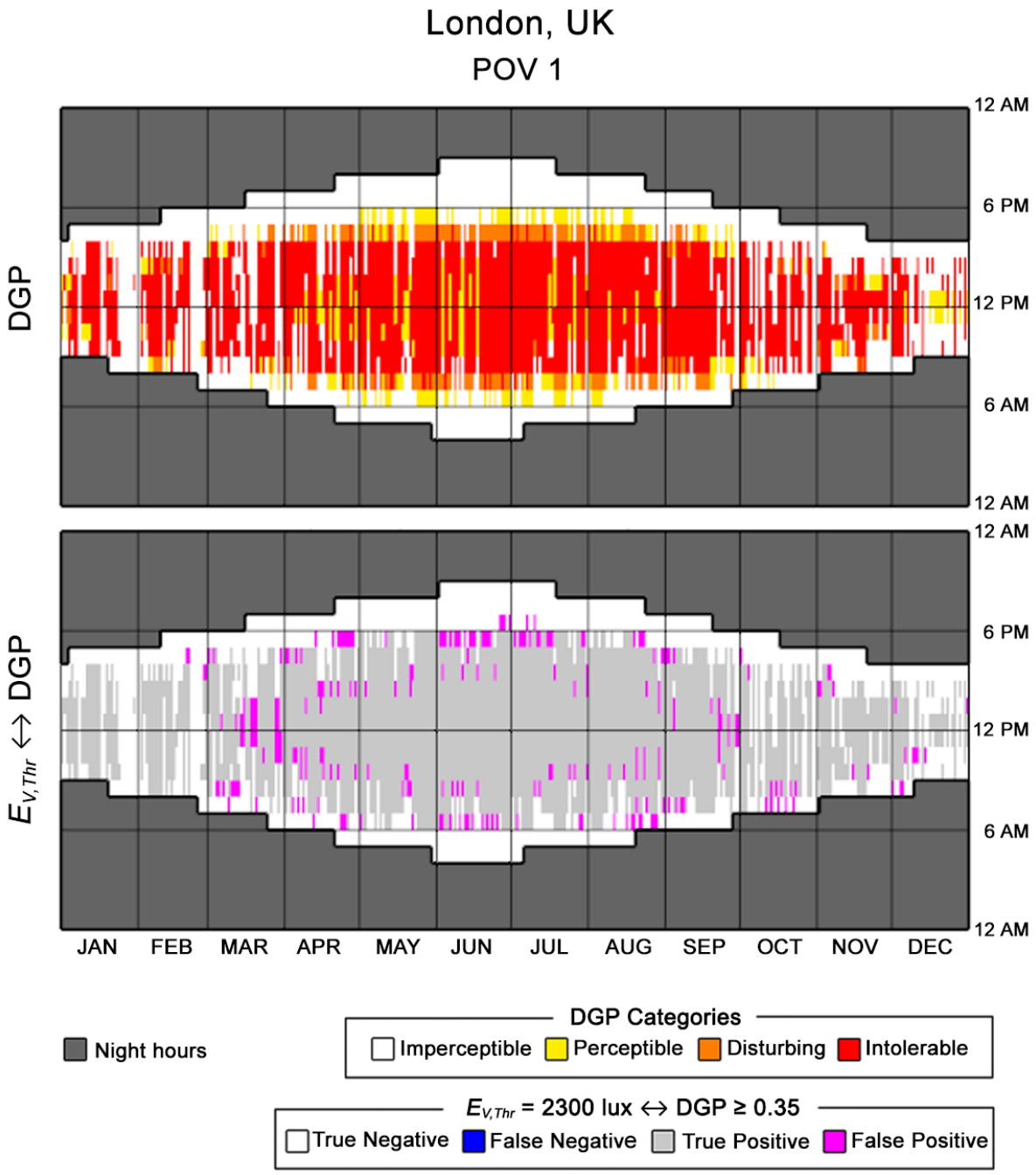

Figure Appendix B-7. Hourly results of using $E_{V,Thr}$ = 2300 lux to signal glare events in POV1 (see chapter 6, Figure 6-2) in London, UK.

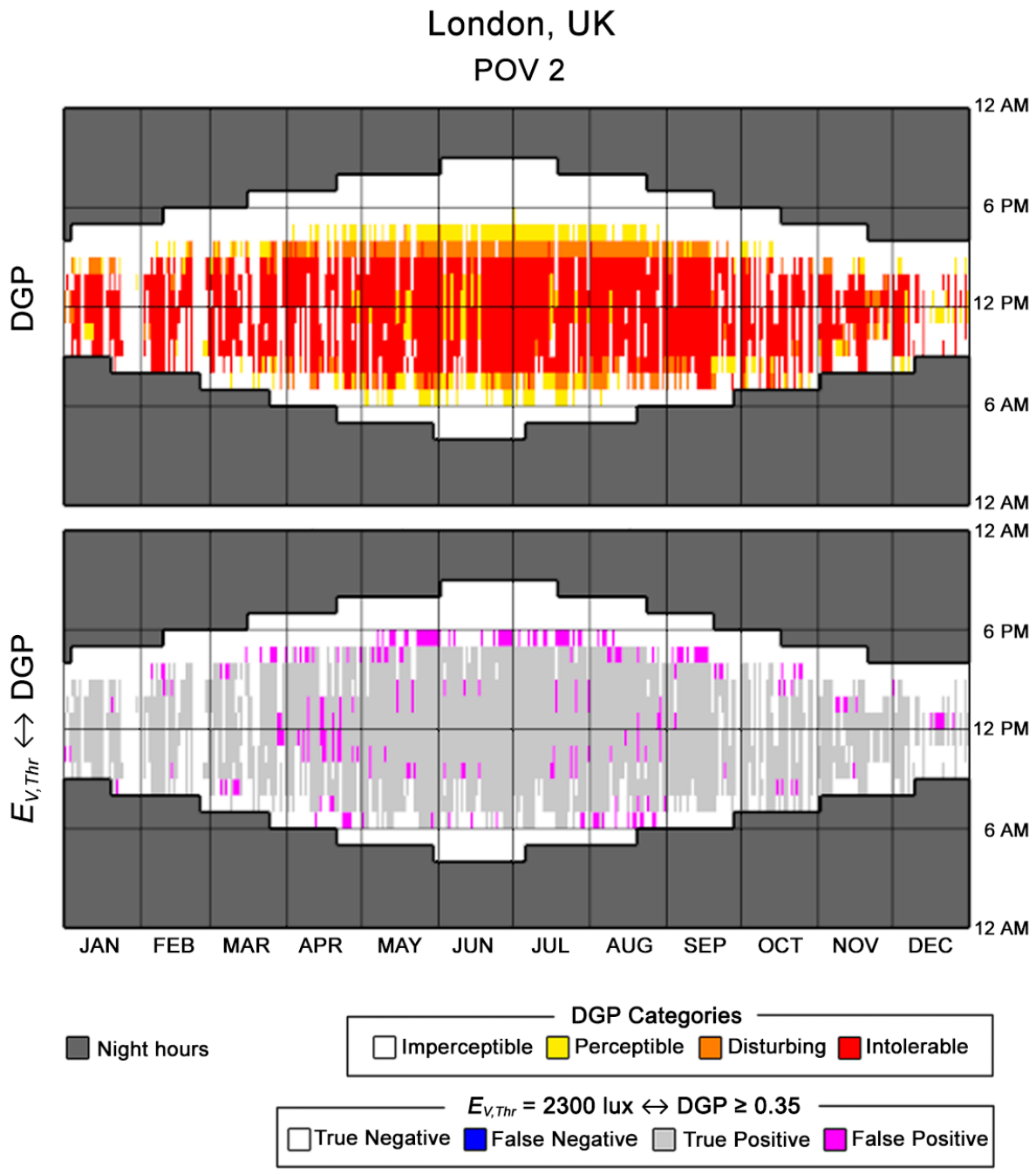

Figure Appendix B-8. Hourly results of using $E_{V,Thr}$ = 2300 lux to signal glare events in POV2 (see chapter 6, Figure 6-2) in London, UK.

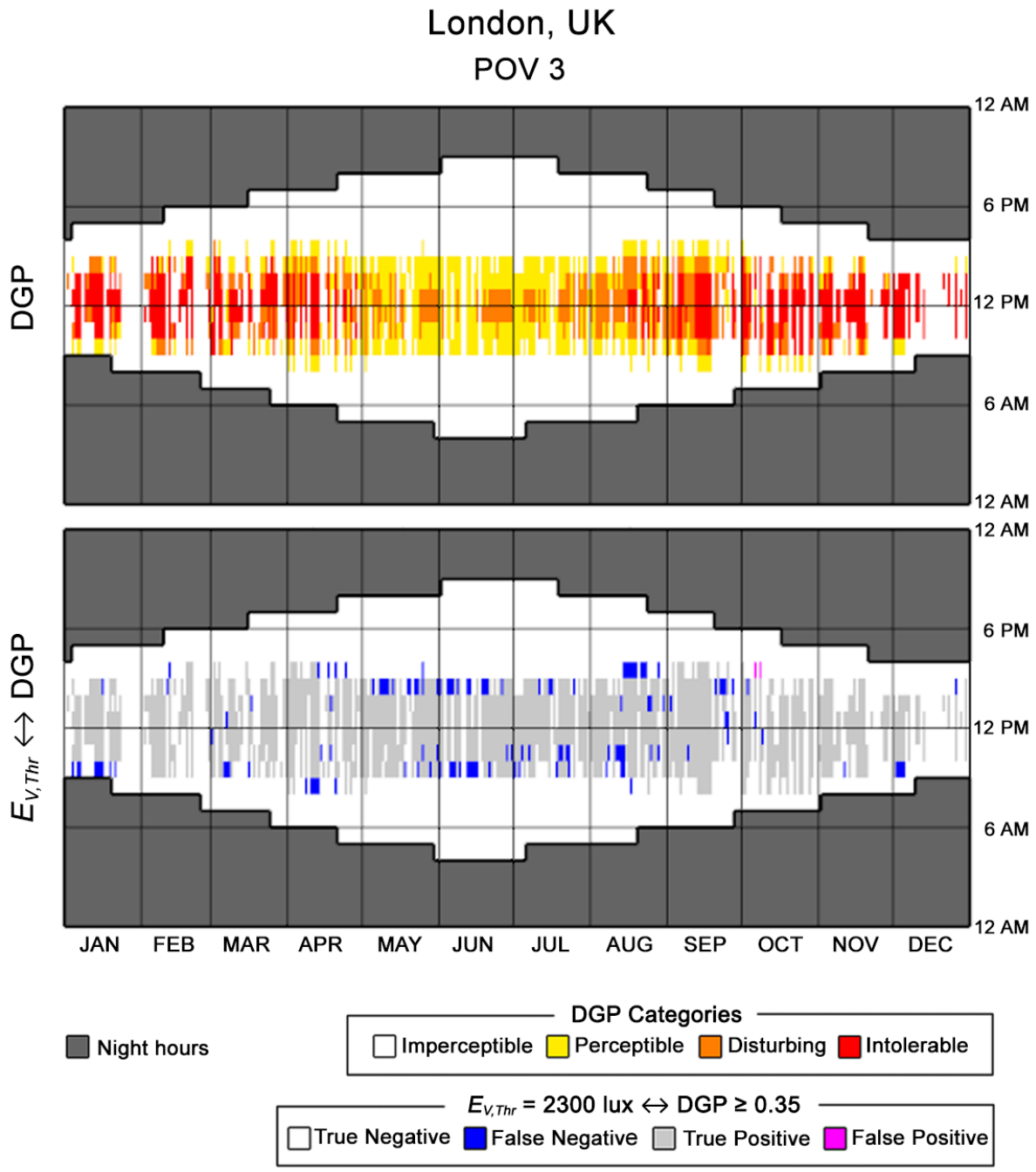

Figure Appendix B-9. Hourly results of using $E_{V,Thr}$ = 2300 lux to signal glare events in POV3 (see chapter 6, Figure 6-2) in London, UK.